



---

MARTIN-LUTHER-UNIVERSITÄT HALLE-WITTENBERG

---

**"The role of calcium signalling in  
innate immunity in *Arabidopsis thaliana*"**

**DISSERTATION**

zur Erlangung des akademischen Grades  
doctor rerum naturalium (Dr. rer. nat.)

vorgelegt der

NATURWISSENSCHAFTLICHEN FAKULTÄT I

BIOWISSENSCHAFTEN

DER MARTIN-LUTHER-UNIVERSITÄT HALLE-WITTENBERG

von

**Frau Stefanie Ranf**

geboren am 29.11.1978 in Augsburg

Gutachter /in

1. Prof. Dr. Dierk Scheel
2. Prof. Dr. Ingo Heilmann
3. Prof. Dr. Tina Romeis

Halle (Saale), den 28.07.2011

# LE CALCIUM, C'EST LA VIE

---

"Every reader ... knows that he or she started life as a single cell. Less familiar is the debt we owe to calcium in our earliest seconds. Penetration of the egg by the paternal sperm initiated an epigenetic calcium wave that moved quickly as a hollow band across the cytoplasm. In the wake of this calcium wave, processes were activated that led to cell division, differentiation, growth, and our eventual appearance as mature adults.

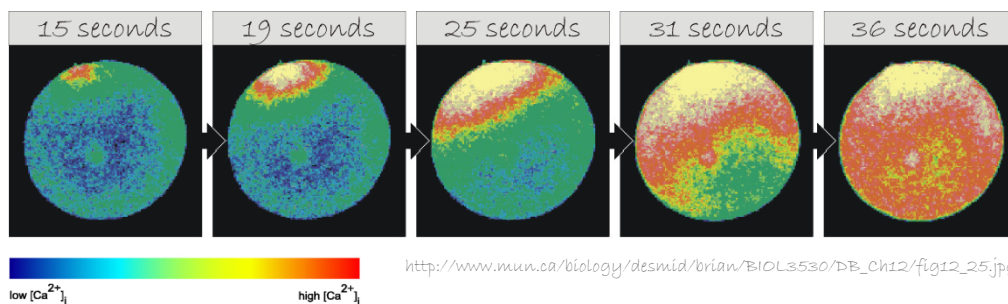
As it is said in France, "Le calcium, c'est la vie."

A calcium wave marked the onset of our existence, and will quite probably mark our demise: Irreversible failure of calcium-wave generation in the heart is the most common cause of death.

Therefore, calcium waves are a life-and-death issue."

Anthony Trewavas  
Plant Physiology, May 1999

A calcium wave initiated at fertilization results in egg activation:



---

**Parts of this work have been published in peer review journals:**

**Ranf S, Wünnenberg P, Lee J, Becker D, Dunkel M, Hedrich R, Scheel D, Dietrich P** (2008) Loss of the vacuolar cation channel, AtTPC1, does not impair Ca<sup>2+</sup> signals induced by abiotic and biotic stresses.

*Plant J* 53: 287-299

**Vadassery J, Ranf S, Drzewiecki C, Mithöfer A, Mazars C, Scheel D, Lee J, Oelmüller R** (2009) A cell wall extract from the endophytic fungus *Piriformospora indica* promotes growth of Arabidopsis seedlings and induces intracellular calcium elevation in roots.

*Plant J* 59: 193-206

**Gust AA, Biswas R, Lenz HD, Rauhut T, Ranf S, Kemmerling B, Gotz F, Glawischnig E, Lee J, Felix G, Nürnberger T** (2007) Bacteria-derived peptidoglycans constitute pathogen-associated molecular patterns triggering innate immunity in Arabidopsis.

*J Biol Chem* 282: 32338-32348

**Parts of this work have been submitted to peer review journals for publication:**

**Ranf S, Eschen-Lippold L, Pecher P, Lee J and Scheel D** (2011) Interplay between calcium signalling and early signalling elements during defence responses to microbe- or damage-associated molecular patterns.

Revised manuscript submitted to *Plant Journal*

**Ranf S, Grimmer J, Pöschl Y, Pecher P, Chinchilla D, Scheel D and Lee J** (2011) Defence-related calcium signalling mutants uncovered *via* a quantitative high-throughput screen in *Arabidopsis thaliana*.

Submitted to *Molecular Plant*

## SUMMARY

During infection of plants, pathogens betray themselves through conserved “pathogen/microbe-associated molecular patterns” (P/MAMPs) that are recognized by specific “pattern recognition receptors” (PRRs) and initiate intracellular signalling cascades leading to PAMP-triggered immunity (PTI). Rapid changes in the free cytosolic  $\text{Ca}^{2+}$  concentration ( $[\text{Ca}^{2+}]_{\text{cyt}}$ ) are prerequisite for establishment of downstream responses, such as accumulation of reactive oxygen species (ROS), activation of mitogen-activated protein kinases (MAPKs), and induction of defence gene expression. The bacterial MAMPs, flg22, a 22 amino-acid peptide of flagellin, and elf18, a 18 amino-acid peptide of elongation factor Tu, both induce a generally similar prolonged  $[\text{Ca}^{2+}]_{\text{cyt}}$  elevation in *Arabidopsis thaliana* although with distinct lag time and amplitude. Likewise, the oligosaccharide-containing MAMPs peptidoglycan, lipopolysaccharide (LPS) and chitinoligomers (ch8), the plant-derived “damage-associated molecular pattern” (DAMP), AtPep1, as well as a cell wall extract (CWE) from the root-colonizing fungus *Piriformospora indica* induce prolonged but characteristic  $[\text{Ca}^{2+}]_{\text{cyt}}$  changes in seedlings or roots, respectively. Interestingly, the residual  $[\text{Ca}^{2+}]_{\text{cyt}}$  elevations induced by flg22, elf18 and Pep1 were virtually identical in *bak1* despite distinct  $[\text{Ca}^{2+}]_{\text{cyt}}$  amplitudes in the wild type, suggesting a differential signal amplification by BAK1, a kinase associated with several receptors. In contrast, LPS-, ch8- or CWE-induced  $[\text{Ca}^{2+}]_{\text{cyt}}$  elevations were not dependent on BAK1. Further differences in defence gene expression and growth arrest responses to flg22 and elf18, were also, in part, controlled by BAK1.

Despite the pivotal role of  $\text{Ca}^{2+}$  as second messenger in MAMP signalling, little is known about the  $\text{Ca}^{2+}$ -permeable channels and transporters at the diverse  $\text{Ca}^{2+}$  stores shaping the  $[\text{Ca}^{2+}]_{\text{cyt}}$  elevations and their regulation. A putative role of the plasma membrane-resident  $\text{Ca}^{2+}$ -permeable channel defence-no-death 1 (DND1) or the vacuolar cation channel two-pore channel 1 (TPC1) in MAMP signalling, however, was disproved by direct aequorin-based measurement of stress-triggered  $[\text{Ca}^{2+}]_{\text{cyt}}$  elevations. In addition, a feedback impact on the  $[\text{Ca}^{2+}]_{\text{cyt}}$  elevation of signalling components acting concomitantly with  $\text{Ca}^{2+}$  signalling was analysed. Indeed, the  $\text{Ca}^{2+}$ -dependent and phosphatidic acid-regulated ROS accumulation leads to a subsequent additional  $[\text{Ca}^{2+}]_{\text{cyt}}$  elevation. Conversely, a prolonged ROS accumulation in *mpk3* had no impact on the  $\text{Ca}^{2+}$  response. A reduced inositol hexakisphosphate level did also not affect  $\text{Ca}^{2+}$  signalling but resulted in an enhanced flg22-mediated root growth arrest. Finally, the  $\text{Ca}^{2+}$ /CaM-dependent transcription factor CAMTA3 appears to regulate a subset of flg22-induced defence genes.

As a parallel approach, besides novel *fls2* and *bak1* alleles, mutants with *changed calcium elevation* (*cce*) in response to flg22 were isolated from reporter lines expressing cytosolic or vacuolar microdomain-localized aequorin. These *cce* mutants showed either reduced or enhanced  $[\text{Ca}^{2+}]_{\text{cyt}}$  elevations in response to flg22, elf18, Pep1 and some also to ch8 and LPS. Therefore, the *cce* mutants will be useful to unveil early signalling events in plant-microbe interactions.

## ZUSAMMENFASSUNG

Während der Besiedlung von Pflanzen verraten sich Pathogene durch konservierte Pathogen/Mikroben-assoziierte Molekülmuster (“pathogen/microbe-associated molecular patterns, P/MAMPs“), die von spezifischen Mustererkennungsrezeptoren (“pattern recognition receptors, PRRs”) erkannt werden und intrazelluläre Signalkaskaden auslösen, die zu PAMP-induzierter Immunität (“PAMP-triggered immunity, PTT”) führen. Schnell auftretende Veränderungen der zytosolischen  $\text{Ca}^{2+}$ -Konzentration ( $[\text{Ca}^{2+}]_{\text{zyt}}$ ) sind dabei Voraussetzung für die Aktivierung nachfolgender Antworten, wie die Akkumulation aktiver Sauerstoffspezies (AOS), die Aktivierung Mitogen-aktivierter Proteinkinasen (MAPKs) und die Induzierung von Abwehrgenexpression. Die bakteriellen MAMPs, flg22, ein 22 aminosäurenlanges Flagellinpeptid, und elf18, ein 18 aminosäuren-langes Peptid des Elongationsfaktor Tu, lösen beide generell ähnliche, anhaltende Erhöhungen der  $[\text{Ca}^{2+}]_{\text{zyt}}$  mit unterschiedlicher Verzögerung und Amplitude in *Arabidopsis thaliana* aus. Die Oligosaccharid-enthaltenden MAMPs Peptidoglykan, Lipopolysaccharid (LPS) und Chitinoligomere (ch8), das von Pflanzen stammende beschädigungsassoziierte Molekülmuster (“damage-associated molecular pattern, DAMP“), AtPep1, sowieso ein Zellwandextrakt (“cell wall extrakt, CWE“) des wurzelbesiedelnden Pilzes *Piriformospora indica* lösen gleichfalls anhaltende charakteristische Erhöhungen der  $[\text{Ca}^{2+}]_{\text{zyt}}$  in Keimlingen bzw. in Wurzeln aus. Interessanterweise sind die verbleibenden Erhöhungen der  $[\text{Ca}^{2+}]_{\text{zyt}}$  in *bak1*-Mutanten ausgelöst durch flg22, elf18 und Pep1 fast identisch ungeachtet der unterschiedlichen  $[\text{Ca}^{2+}]_{\text{zyt}}$ -Amplituden im Wildtyp und weisen auf eine differentielle Signalamplifizierung durch BAK1 hin, eine Kinase assoziiert mit mehreren Rezeptoren. Im Gegensatz dazu sind die Erhöhungen der  $[\text{Ca}^{2+}]_{\text{zyt}}$  ausgelöst durch LPS, ch8 oder CWE nicht abhängig von BAK1. Weitere Unterschiede in der Genexpression und der Wachstumsinhibierungsreaktion zwischen flg22 und elf18 sind teilweise ebenfalls durch BAK1 reguliert.

Trotz der herausragenden Rolle von  $\text{Ca}^{2+}$  als sekundärer Botenstoff in MAMP-Signalkaskaden ist nur wenig über die  $\text{Ca}^{2+}$ -Kanäle und Transporter an den unterschiedlichen  $\text{Ca}^{2+}$ -Speichern bekannt, die die Erhöhungen der  $[\text{Ca}^{2+}]_{\text{zyt}}$  formen, und ihre Regulation. Eine mögliche Beteiligung des plasmamembranständigen  $\text{Ca}^{2+}$ -Kanals “defence-no-death 1” (DND1) oder des vakuolären Kationenkanals “two-pore channel 1” (TPC1) an MAMP-Signalkaskaden wurde durch direkte Aequorin-basierte Messungen von stressinduzierten Erhöhungen der  $[\text{Ca}^{2+}]_{\text{zyt}}$  widerlegt. Weiterhin wurde ein Rückkopplungseffekt der parallel zu den  $\text{Ca}^{2+}$ -Signalen agierenden Signalkomponenten auf die Erhöhung der  $[\text{Ca}^{2+}]_{\text{zyt}}$  untersucht. Die  $\text{Ca}^{2+}$ -abhängige und durch Phosphatidylsäure regulierte Akkumulation von AOS führt in der Tat zu einer nachfolgenden weiteren Erhöhung der  $[\text{Ca}^{2+}]_{\text{zyt}}$ . Im Gegensatz dazu hat eine Verlängerung der AOS-Akkumulation in der *mpk3*-Mutante keinen Einfluss auf die  $[\text{Ca}^{2+}]_{\text{zyt}}$ -Antwort. Ein verringerter Inositolhexakisphosphat Spiegel hatte ebenfalls keinen Einfluss auf die Erhöhungen der  $[\text{Ca}^{2+}]_{\text{zyt}}$ , führte allerdings zu einer verstärkten flg22-vermittelten Wurzelwachstumsinhibierung. Der  $\text{Ca}^{2+}$ /CaM-abhängige Transkriptionsfaktor CAMTA3 schließlich reguliert scheinbar einen Teil der flg22-induzierten Abwehrgene.

In einem parallelen Ansatz wurden sowohl neue *fls*- und *bak1*-Allele als auch Mutanten mit einer veränderten Erhöhungen der  $[Ca^{2+}]$  (*changed calcium elevation, cce*) aus Reporterlinien isoliert, die Aequorin im Zytosol oder der vakuolären Mikrodomäne exprimieren. Diese *cce*-Mutanten zeigen entweder eine verringerte oder eine verstärkte Erhöhung der  $[Ca^{2+}]$  in Reaktion auf *flg22*, *elf18*, *Pep1* und einige ebenso auf *ch8* und LPS. Die *cce*-Mutanten werden sich daher nützlich für die Aufklärung der frühen Signaltransduktion in Pflanzen-Pathogen-Wechselwirkungen erweisen.

## ACKNOWLEDGEMENTS

Mein besonderer Dank gilt Herrn Prof. Dr. Dierk Scheel und Dr. Justin Lee, die mir diese spannenden Projekte zur Bearbeitung überlassen, mir dabei sehr viel Freiheit für meine Ideen eingeräumt und mir immer Vertrauen entgegengebracht haben. Außerdem möchte ich mich für die exzellente Betreuung, die stetige Unterstützung und die vielen bereichernden Diskussionen ganz herzlich bedanken.

Weiterhin möchte ich mich bei allen Gutachtern für die Übernahme der Gutachten bedanken.

Vielen Dank an alle Kooperationspartner, die uns diverse Materialien zur Verfügung gestellt haben und so die Bearbeitung der Projekte wesentlich erleichtert bzw. erst möglich gemacht haben.

Weiterhin möchte ich mich bei der ganzen Abteilung „Streß- und Entwicklungsbiologie“ am Leibniz-Institut für Pflanzenbiochemie in Halle für die gute Zusammenarbeit und die angenehme Arbeitsatmosphäre bedanken. Besonderer Dank gilt hierbei Lennart für sein Durchhaltevermögen bei den Protoplastenexperimenten, Pascal für seine immerwährende Unterstützung und Hilfsbereitschaft und allen anderen ehemaligen und aktuellen Mitgliedern unserer Arbeitsgruppe. Vielen Dank auch an Lore für ihre Beratung in allen genetischen Fragen.

Besonderer Dank gilt auch Christel und Nicole für die technischen Unterstützung und den Gärtnern Petra Jansen und Thomas Franz, die stetig und geduldig bemüht waren, Ordnung in mein (Samen-)Chaos zu bringen.

Meiner Familie danke ich für ihre Unterstützung und Hilfe in allen Lebenslagen. Besonders bedanken möchte ich mich bei meinem Lebenspartner Dirk, der mir immer den Rücken freigehalten, sich nie beschwert hat und einfach immer da war, auch wenn es im Labor mal wieder später wurde.

VIELEN DANK EUCH ALLEN

THANK YOU ALL

**TABLE OF CONTENTS**

<b>Summary</b> .....	<b>I</b>
Zusammenfassung.....	II
Acknowledgements.....	IV
Table of Contents.....	V
List of Figures.....	VII
List of Abbreviations.....	VIII
<b>1. Introduction</b> .....	<b>1</b>
1.1. Calcium as second messenger in plants.....	1
1.1.1. Ca <sup>2+</sup> fulfils diverse functions in plants.....	1
1.1.2. Ca <sup>2+</sup> homeostasis – a prerequisite for Ca <sup>2+</sup> signalling.....	2
1.1.3. Alternative concepts: “Ca <sup>2+</sup> signature“ <i>versus</i> “chemical on-off switch”.....	6
1.1.4. <i>In vivo</i> methods for measuring [Ca <sup>2+</sup> ].....	7
1.1.5. Deciphering the „Ca <sup>2+</sup> code“- Ca <sup>2+</sup> sensors.....	8
1.2. Innate immunity in <i>Arabidopsis thaliana</i> .....	10
1.2.1. The concept of “Microbe- or Damage-Associated Molecular Patterns” (M/DAMPs)..	10
1.2.2. Perception of MAMPs and DAMPs.....	13
1.2.3. MAMP-induced signalling downstream of the receptor (complex).....	15
1.2.4. Mechanisms of pathogens to interfere with MAMP and DAMP signalling.....	18
1.2.5. Ca <sup>2+</sup> in plant – microbe interactions: the role of Ca <sup>2+</sup> in MAMP signalling.....	18
1.3. Objectives.....	20
<b>2. Results</b> .....	<b>21</b>
2.1. Two-pore channel 1 - a putative Ca <sup>2+</sup> channel in stress responses.....	21
2.1.1. Aims and summary.....	21
2.1.2. Publication.....	22
2.2. Impact of different signalling components on MAMP-induced Ca <sup>2+</sup> signalling.....	35
2.2.1. Aims and summary.....	35
2.2.2. Manuscript.....	36
2.2.3. Additional results.....	54

---

2.3.	Screen for mutants with „ <i>changed calcium elevation</i> “ ( <i>cce</i> ) in MAMP signalling .....	57
2.3.1.	Aims and summary.....	57
2.3.2.	Manuscript.....	58
2.4.	Lipopolysaccharides induce $[Ca^{2+}]_{cyt}$ elevations in <i>Arabidopsis thaliana</i> seedlings.....	78
2.4.1.	Aims and summary.....	78
2.4.2.	Manuscript.....	79
2.5.	Peptidoglycans as MAMPs induce $Ca^{2+}$ signalling in <i>Arabidopsis thaliana</i> .....	93
2.5.1.	$[Ca^{2+}]_{cyt}$ elevations stimulated by peptidoglycans in <i>Arabidopsis</i> .....	93
2.5.2.	Summary of publication .....	93
2.6.	A cell wall extract from the endophytic fungus <i>Piriformospora indica</i> stimulates $Ca^{2+}$ signalling in <i>Arabidopsis thaliana</i> roots .....	94
2.6.1.	Aims and summary.....	94
2.6.2.	Publication.....	95
2.7.	Contribution to publications and manuscripts.....	109
<b>3.</b>	<b>Discussion and Perspectives.....</b>	<b>111</b>
3.1.	The role of $Ca^{2+}$ signalling in innate immunity in <i>Arabidopsis</i> .....	111
3.2.	Components shaping MAMP-induced $Ca^{2+}$ signatures in <i>Arabidopsis</i> .....	115
3.3.	Do MAMP-induced $Ca^{2+}$ signatures encode MAMP-specific information?.....	119
3.4.	$[Ca^{2+}]_{cyt}$ elevations as quantitative and kinetic read-out for early signalling events .....	124
3.5.	Conclusions .....	125
<b>4.</b>	<b>References .....</b>	<b>126</b>
<b>5.</b>	<b>Appendix .....</b>	<b>147</b>
5.1.	Supporting information to 2.2.2 .....	147
5.2.	Supporting information to 2.3.2 .....	153
5.3.	Publication and supporting information to 2.5.2 .....	158
5.4.	Supporting information to 2.6.2 .....	170

## LIST OF FIGURES

(if not part of a publication or manuscript)

<b>Figure 1–1.</b> Ca <sup>2+</sup> -permeable channels and transporters at the different Ca <sup>2+</sup> stores in Arabidopsis.....	5
<b>Figure 1–2.</b> Principle biochemical function of aequorin and cameleon Ca <sup>2+</sup> probes .....	8
<b>Figure 1–3.</b> Zigzag model .....	11
<b>Figure 1–4.</b> Evolutionary occurrence of MAMPs, DAMPs and effectors and their cognate perception systems.....	12
<b>Figure 1–5.</b> Perception of MAMPs, DAMPs and effectors as general “danger signals” activates a common set of defence responses.....	13
<b>Figure 1–6.</b> Overview of flagellin-stimulated early signalling in Arabidopsis.....	17
<b>Figure 2–1.</b> Flg22-induced ROS accumulation is reduced in <i>plda1</i> .....	54
<b>Figure 2–2.</b> Scheme of PA and InsP <sub>6</sub> synthesis pathways.....	55
<b>Figure 2–3.</b> Flg22-mediated root growth inhibition, but not [Ca <sup>2+</sup> ] <sub>cyt</sub> elevation, is enhanced in <i>ipk1</i> .....	55
<b>Figure 2–4.</b> Flg22-induced gene expression and root growth arrest is impaired in <i>camta3</i> .....	56
<b>Figure 2–5.</b> [Ca <sup>2+</sup> ] <sub>cyt</sub> elevations induced by <i>S. aureus</i> peptidoglycan in Arabidopsis leaf strips.....	93
<b>Figure 3–1.</b> Overview of early flg22-stimulated signalling steps in Arabidopsis.....	120
<b>Figure 3–2.</b> Comparison of different MAMP- and DAMP-induced [Ca <sup>2+</sup> ] <sub>cyt</sub> elevations in intact seedlings and isolated roots.....	123

## LIST OF ABBREVIATIONS

ABA	abscisic acid	CICR	Ca <sup>2+</sup> -induced Ca <sup>2+</sup> release
ACA	autoinhibited Ca <sup>2+</sup> -ATPase	CIPK	CBL-interacting protein kinase
Aeq <sup>cyt</sup>	cytosolic apoequorin (pMAQ2) expressing <i>Arabidopsis</i> Col-0	CML	calmodulin-like protein
Aeq <sup>vmd</sup>	vacuolar microdomain apoequorin (HVA1) expressing <i>Arabidopsis</i> C24	CNGC	cyclic nucleotide-gated channel
ANOVA	analysis of variance	cNMP	cyclic nucleotide monophosphate
AR	alkalinization response	Col-0	<i>Arabidopsis thaliana</i> accession Columbia-0
ATP	adenosine triphosphate	CRK	CDPK-related kinase
Avr	avirulence protein	CRT	calreticulin
Ax21	sulfated <i>Xanthomonas</i> peptide	CSP	cold shock protein
BAK1	BRI1-associated kinase 1	CTZ-n/h	coelenterazine native/h
BAPTA	1,2-bis(o-aminophenoxy)-ethane-N,N,N',N'-tetraacetic acid	DAG	diacylglycerin
BIK1	Botrytis-induced kinase 1	DAMP	damage-associated molecular pattern
BRI1	brassinosteroid insensitive 1	DGK	diacylglycerol (DAG) kinase
C24	<i>Arabidopsis thaliana</i> accession C24	DGPP	diacylglycerin pyrophosphate
[Ca <sup>2+</sup> ] <sub>cyt</sub>	free cytosolic Ca <sup>2+</sup> concentration	DNA	deoxyribonucleic acid
CaCA	Ca <sup>2+</sup> /cation antiporter	DND1	defence no death
cADPR	cyclic ADP-ribose	DPI	diphenylene iodonium chloride
CaM	calmodulin	<i>e. g.</i>	<i>exempli gratia</i> (for example)
CAMTA	Ca <sup>2+</sup> /CaM-binding transcriptional activator	ECA	ER-type Ca <sup>2+</sup> -ATPase
CAS	Ca <sup>2+</sup> -sensing receptor	EDS1	enhanced disease susceptibility 1
CAX	cation exchanger	EF hand	helix-loop-helix Ca <sup>2+</sup> -binding domain
CBL	calcineurin B-like protein	EFR	EF-Tu receptor
CCaMK	Ca <sup>2+</sup> -CaM-dependent kinase	EF-Tu	translational elongation factor Tu
CCE	changed calcium elevation	elf18	N-terminal EF-Tu peptide (acetyl-SKEKFERTKPHVNVGTIG)
CCX	cation calcium exchanger	EMS	ethylmethanesulfonate
cDNA	complementary DNA	EPS	extracellular polysaccharide
CDPK	Ca <sup>2+</sup> -dependent protein kinase	ER	endoplasmic reticulum
CERK1	chitin elicitor receptor kinase 1	<i>etc.</i>	<i>et cetera</i> (and so on)
chX	N-acetylchito-X-ose	ETI	effector-triggered immunity
		ETS	effector-triggered susceptibility

EZ	root elongation zone	OPS	O-polysaccharide
flg22	N-terminal flagellin peptide (QRLSTGSRINSAKDDAAGLQIA)	p.	page
FLS2	flagellin-sensitive 2	PAMP	pathogen-associated molecular pattern
FOU2	fatty acid oxygenation up- regulated 2	Pep13	<i>Phytophthora</i> transglutaminase peptide (VWNQPVRGFKVYE)
FRET	fluorescence resonance energy transfer	PEPR1/2	AtPep receptor 1/2
fwd	forward	PGN	peptidoglycan
GLR	glutamate receptor-like channel	PLC/PLD	phospholipase C/D
HR	hypersensitive response	PROPEP	AtPep peptide precursor
HrpZ	harpin elicitor protein	PRR	pattern recognition receptor
<i>i. e.</i>	<i>id est</i> (which means)	PTI	PAMP-triggered immunity
InsP <sub>3</sub> /IP <sub>3</sub>	inositol-(1,4,5)-trisphosphate	R	resistance protein
InsP <sub>6</sub> /IP <sub>6</sub>	inositolhexakisphosphate	Rboh	respiratory burst oxidase homolog
IPK1	inositolpolyphosphatekinase 1	rev	reverse
IPS1/2	inositolphosphate synthase 1/2	RLCK	receptor-like cytoplasmic kinase
ISR	induced systemic resistance	RLK	receptor-like kinase
JA	jasmonic acid	R-LPS	rough lipopolysaccharide
LOS	lipooligosaccharide	RNA	ribonucleic acid
LPS	lipopolysaccharide	ROS	reactive oxygen species
LRR	leucine-rich repeat	(RT-)PCR	(reverse transcriptase) polymerase chain reaction
LysM	lysine motif	SA	salicylic acid
MAMP	microbe-associated molecular pattern	SAR	systemic acquired resistance
MAP3K	MAPK kinase kinase	SERK	somatic embryogenesis receptor- like kinase
MAPK	mitogen-activated protein kinase	S-LPS	smooth lipopolysaccharide
min.	minute	SNP	single nucleotide polymorphism
MKK	MAPK kinase	SV	slow vacuolar
MS	Murashige-Skoog medium	T-DNA	transfer DNA
NAADP	nicotinic acid adenine dinucleotide phosphate	TLR	toll-like receptor
NADPH	nicotinamide adenine dinucleotide phosphate	TPC	two-pore channel
NO	nitric oxide	vmd	vacuolar microdomain
NPP1	necrosis-inducing protein 1	<i>vs.</i>	<i>versus</i> (against)
OGA	oligogalacturonide	WRKY	WRKY-domain-containing transcription factor

## 1. INTRODUCTION

Living organisms constantly need to adapt to numerous continuously changing environmental factors. This adaptation is of special importance for sessile organisms, such as plants, that cannot evade adverse conditions by relocation. To accomplish this, plant cells must be competent to perceive given stimuli and relay the external information into cellular responses through re-programming of gene expression and metabolic processes. To react appropriately to multiple different stimuli, the cell must also be able to integrate the information of these stimuli and compute a response in order to adapt to all stimuli adequately or “intelligently”. In addition to external stimuli, cells in multicellular associations need to integrate internal information from neighbouring or distant cells and tissues.

During the signal transduction process, a perceived stimulus is translated into the molecular and biochemical “language” of the cell using the different biochemical properties of proteins or enzymes and of non-proteinaceous molecules. The different classes of signalling components are often shared by diverse signalling pathways. For instance,  $\text{Ca}^{2+}$  is a ubiquitous second messenger involved in nearly all aspects of plant life. Whereas proteins, such as kinases or transcription factors, may comprise large gene families of several individuals with, for example, specific domain structures and expression patterns to determine specific outputs,  $\text{Ca}^{2+}$  is just a simple ion. This raises the question of how and to which extent signalling specificity is maintained during signal transduction by common signalling components and second messengers, and  $\text{Ca}^{2+}$  in particular.

### 1.1. Calcium as second messenger in plants

#### 1.1.1. $\text{Ca}^{2+}$ fulfils diverse functions in plants

Calcium is an important plant nutrient due to its structural function in membranes and the cell wall, as counteraction in (in)organic salts in the vacuole, and for biochemical processes, such as protein processing in the ER secretory pathway (Sanders *et al.*, 2002; White and Broadley, 2003). Within the plant,  $\text{Ca}^{2+}$  is mainly transported from roots to shoots *via* the apoplast/xylem by the transpiration stream, but symplastic transport accounts for the supply of intracellular compartments and possibly of tissues with a low transpiration rate, such as growing aerial parts, and phloem-fed tissues, such as fruits, seeds and tubers (White and Broadley, 2003). In addition, free  $\text{Ca}^{2+}$  plays a crucial role as second messenger in response to a wide variety of environmental and developmental factors. These range from abiotic stimuli, such as salt, drought (Knight *et al.*, 1997), cold (Knight *et al.*, 1991), heat (Gong *et al.*, 1998), oxidative stress (Price *et al.*, 1994; Clayton *et al.*, 1999) and accordingly regulation of stomatal aperture (McAinsh *et al.*, 1995; Allen *et al.*, 2001), mechanical stimuli (Knight *et al.*, 1991) and wounding (Moyen *et al.*, 1998) to biotic factors like bacterial or fungal pathogens (Stab and Ebel, 1987; Nürnberger *et al.*, 1994a; Tavernier *et al.*, 1995) but also beneficial interactions, for instance Rhizobium-legume (Ehrhardt *et al.*, 1996) or arbuscular mycorrhizal symbiosis (Navazio and Mariani, 2008). Concurrently,  $\text{Ca}^{2+}$  is involved in developmental processes, such as regulation of the circadian clock (Johnson *et al.*, 1995), photomorphogenesis (Shacklock *et al.*, 1992; Bowler *et al.*, 1994), pollen

tube (Franklin-Tong *et al.*, 1996; Malho and Trewavas, 1996) and root hair growth (Bibikova *et al.*, 1997; Monshausen *et al.*, 2008), self-incompatibility (Franklin-Tong *et al.*, 1993) and hormonal responses, for instance, to abscisic acid (ABA; McAinsh *et al.*, 1992), gibberellin (Chen *et al.*, 1997), auxin (Felle, 1988; Galon *et al.*, 2010a), ethylene (Zhao *et al.*, 2007), salicylic acid (SA; Du *et al.*, 2009) or jasmonic acid (JA; Walter *et al.*, 2007).

As second messenger  $\text{Ca}^{2+}$  needs to fulfil certain criteria: i) the “resting” concentration of free  $\text{Ca}^{2+}$ , i. e. in unstimulated condition, in the cytosol needs to be maintained at low level; ii) a rise in the free cytosolic  $\text{Ca}^{2+}$  concentration ( $[\text{Ca}^{2+}]_{\text{cyt}}$ ) must be transient; thus, appropriate attenuation mechanism are required for returning to resting levels; iii)  $\text{Ca}^{2+}$  needs to specifically bind to proteins or enzymes to further transduce the information. A unique feature of  $\text{Ca}^{2+}$  as second messenger is that the concentration of  $\text{Ca}^{2+}$  cannot be controlled *via* biosynthesis and degradation but  $\text{Ca}^{2+}$  rather needs to be stored in appropriate compartments and its abundance is regulated *via* release from and replenishing of these stores.

### 1.1.2. $\text{Ca}^{2+}$ homeostasis – a prerequisite for $\text{Ca}^{2+}$ signalling

Nutritional supply and structural cell wall integrity demand high  $[\text{Ca}^{2+}]$  levels in the apoplast (Conn *et al.*, 2011). On the contrary, owing to the low solubility of  $\text{Ca}^{2+}$ /phosphate compounds, an ATP-based energy metabolism in the cytosol necessitates maintenance of low free  $[\text{Ca}^{2+}]_{\text{cyt}}$  of  $< 100$  nM (Clapham, 1995; Malho *et al.*, 1998). Concurrently,  $\text{Ca}^{2+}$  is constantly supplied to intracellular compartments, some of which also function as  $\text{Ca}^{2+}$  stores, by symplastic transport (Figure 1–1, p. 5; Sanders *et al.*, 2002; Cheng *et al.*, 2003; White and Broadley, 2003; Cheng *et al.*, 2005). A balance of all requirements is attained by a tightly regulated  $[\text{Ca}^{2+}]_{\text{cyt}}$  homeostasis network, which was also a prerequisite for the evolution of  $[\text{Ca}^{2+}]_{\text{cyt}}$  signalling. Thus,  $\text{Ca}^{2+}$  influx into the cytosol through  $\text{Ca}^{2+}$ -permeable channels (Figure 1–1, p. 5; see below), some of which may also open at physiological “resting” conditions (White and Broadley, 2003), is antagonized by removal systems that export  $\text{Ca}^{2+}$  into the apoplastic space or intracellular compartments (Figure 1–1, p. 5; see below).

#### $\text{Ca}^{2+}$ extrusion systems

Due to the electrochemical gradient of  $\text{Ca}^{2+}$  across the plasma- and endomembranes (Figure 1–1, p. 5),  $\text{Ca}^{2+}$  extrusion from the cytosol is an active, energy-consuming transport process. Besides maintaining low  $[\text{Ca}^{2+}]_{\text{cyt}}$  in resting cells, the efflux transport is important for restoring resting  $[\text{Ca}^{2+}]_{\text{cyt}}$  after release of “signalling  $\text{Ca}^{2+}$ ”, and for loading  $\text{Ca}^{2+}$  into internal compartments and stores with regard to its biochemical and signalling function, such as ER, golgi-, endosome-, pre-vacuolar compartments, plastids or vacuoles (Figure 1–1, p. 5; Sanders *et al.*, 2002).

$\text{Ca}^{2+}$  efflux from the cytosol is achieved by the combined action of  $\text{Ca}^{2+}$ -ATPases and  $\text{Ca}^{2+}$ /cation antiporters (CaCA) that utilize ATP or electrochemical gradients of  $\text{H}^+$  or  $\text{Na}^+$  for  $\text{Ca}^{2+}$  transport, respectively. In plants, these are mainly  $\text{H}^+/\text{Ca}^{2+}$  antiporters of the cation exchanger family (CAX) with different  $\text{Ca}^{2+}$  specificities and capacities (Shigaki *et al.*, 2001; Shigaki and Hirschi, 2006). Of the six

Arabidopsis CAX antiporters, CAX1-4 reside in the vacuolar membrane but other CAXs may also localize to the plasma membrane (Figure 1–1, p. 5; Hirschi *et al.*, 2000; Cheng *et al.*, 2002a, 2003, 2005; Luo *et al.*, 2005). CAX antiporters are regulated by an N-terminal autoinhibitory domain, protein-protein interaction or heterodimerization (Pittman *et al.*, 2002; Cheng and Hirschi, 2003; Cheng *et al.*, 2003, 2004, 2005; Shigaki and Hirschi, 2006; Zhao *et al.*, 2009). Accordingly, expression of CAX1, a high capacity vacuolar antiporter, lacking the autoinhibitory domain, led to  $\text{Ca}^{2+}$  deficiency symptoms, despite an increased overall  $\text{Ca}^{2+}$  content, due to an increased vacuolar  $\text{Ca}^{2+}$  accumulation (Hirschi, 1999). A prominent role for CAX1 and its closest homolog, CAX3, in  $\text{Ca}^{2+}$  homeostasis is further illustrated by an increased free apoplasmic  $[\text{Ca}^{2+}]$  in the *cax1/cax3* double mutant, caused by compensatory changes in other  $\text{Ca}^{2+}$  antiporters and ATPases, with pleiotropic effects on plant growth and metabolism (Conn *et al.*, 2011). Furthermore, the authors highlight the importance of cell type-specific differences in the  $\text{Ca}^{2+}$  homeostasis, such as an overall low  $[\text{Ca}^{2+}] < 10$  mM in the epidermis vs.  $[\text{Ca}^{2+}] > 60$  mM in the mesophyll, which may also affect  $\text{Ca}^{2+}$  signalling processes (Conn *et al.*, 2011). Other, yet uncharacterized CaCA potentially involved in  $\text{Ca}^{2+}$  homeostasis are cation calcium exchangers (CCX), with similarity to mammalian  $\text{Na}^+/\text{Ca}^{2+}$  exchangers, and a group of antiporters with EF hand motifs, suggesting  $\text{Ca}^{2+}$ -dependent regulation (Shigaki *et al.*, 2006).

$\text{Ca}^{2+}$ -ATPases in plants either belong to the ER-type  $\text{Ca}^{2+}$ -ATPases (ECA; (phosphorylated)  $\text{P}_{\text{IIA}}$ -type ATPases) or the autoinhibited  $\text{Ca}^{2+}$ -ATPases (ACA;  $\text{P}_{\text{IIB}}$ -type ATPases; Sze *et al.*, 2000). While ACAs are activated by acidic phospholipids (Bonza *et al.*, 2001; Meneghelli *et al.*, 2008) or by  $\text{Ca}^{2+}/\text{CaM}$  binding to a regulatory domain to release the autoinhibitory domain (Harper *et al.*, 1998; Baekgaard *et al.*, 2006), they can be inhibited by phosphorylation, for instance by  $\text{Ca}^{2+}$ -dependent protein kinases (CDPKs; Hwang *et al.*, 2000). By contrast, no regulatory mechanisms were described so far for ECAs, which also display lower  $\text{Ca}^{2+}$  specificity than ACAs (Bonza and De Michelis, 2010). Both, ACAs and ECAs localize to the plasmamembrane or endomembranes of various compartments (Kudla *et al.*, 2010) (Figure 1–1, p. 5). According to their diverse localization,  $\text{Ca}^{2+}$ -ATPases probably fulfil multiple functions in  $\text{Ca}^{2+}$  homeostasis. Owing to their distinct  $\text{Ca}^{2+}$  affinity,  $\text{Ca}^{2+}$ -ATPases (high affinity but low capacity) and  $\text{Ca}^{2+}$  antiporters (low affinity but high capacity) are suggested to have complementary functions in  $\text{Ca}^{2+}$  homeostasis. While antiporters, such as CAX1, may account mainly for general restoration of the resting  $[\text{Ca}^{2+}]_{\text{cyt}}$  following high  $[\text{Ca}^{2+}]$  during signalling,  $\text{Ca}^{2+}$ -ATPases are thought to contribute to fine control of  $[\text{Ca}^{2+}]_{\text{cyt}}$  (Hirschi, 1999).

### ***Ca<sup>2+</sup>-permeable channels***

The  $[\text{Ca}^{2+}]$  difference between apoplast or intracellular compartments with a high  $[\text{Ca}^{2+}]$  and the cytosol with a low  $[\text{Ca}^{2+}]$ , allows passive influx of  $\text{Ca}^{2+}$  into the cytosol along the electrochemical gradient through channels residing in the plasma- or endomembranes (Figure 1–1, p. 5). In comparison to  $\text{Ca}^{2+}$ -specific channels in the mammalian system, plant channels are rather nonselective cation channels that are also  $\text{Ca}^{2+}$ -permeable (Demidchik *et al.*, 2002; Sanders *et al.*, 2002). These include, among others, the classes of cyclic nucleotide-gated channels (CNGCs), glutamate receptor-like channels (GLRs) or

two-pore channels (TPC) as deduced from genome analyses (Lacombe *et al.*, 2001; Maser *et al.*, 2001; Demidchik *et al.*, 2002; Very and Sentenac, 2002; Hetherington and Brownlee, 2004; Tapken and Hollmann, 2008). The characterized CNGCs all localize to the plasma membrane, as may GLRs, and are involved in a range of nutritional and developmental aspects and pathogen defence (Figure 1–1, p. 5; Balague *et al.*, 2003; Gobert *et al.*, 2006; Yoshioka *et al.*, 2006; Ali *et al.*, 2007; Frietsch *et al.*, 2007; Urquhart *et al.*, 2007; Guo *et al.*, 2008; Ma *et al.*, 2008). CNGCs are commonly activated by the cyclic nucleotides cAMP or cGMP and inhibited by overlapping  $\text{Ca}^{2+}$ /CaM binding, suggesting a negative feedback regulation of channel activity (Hua *et al.*, 2003; Ali *et al.*, 2006). GLRs are activated by glutamate, glycine and some other amino acids, and implicated in a range of physiological processes, such as nutrition, cold stress, aluminium toxicity, ABA biosynthesis and stomatal closure (Dennison and Spalding, 2000; Kim *et al.*, 2001; Kang and Turano, 2003; Sivaguru *et al.*, 2003; Kang *et al.*, 2004; Meyerhoff *et al.*, 2005; Qi *et al.*, 2006; Stephens *et al.*, 2008; Cho *et al.*, 2009). Additionally, electrophysiological studies reveal voltage-dependent, i. e. depolarization- or hyperpolarization-activated, and stretch-activated channels at the plasma membrane and possibly endomembranes that are yet to be identified (Demidchik *et al.*, 2002; Hetherington and Brownlee, 2004; Nakagawa *et al.*, 2007). Additionally, annexin proteins were suggested as further  $\text{Ca}^{2+}$  entry points in plants (Hofmann *et al.*, 2000; Cantero *et al.*, 2006; Mortimer *et al.*, 2008). Apparently, annexins can form  $\text{Ca}^{2+}$ -permeable channels or pores themselves or evoke  $[\text{Ca}^{2+}]_{\text{cyt}}$  elevations indirectly by activation of other  $\text{Ca}^{2+}$ -permeable channels (Hofmann *et al.*, 2000; Mortimer *et al.*, 2008; Laohavisit *et al.*, 2009; Laohavisit and Davies, 2011), but up to now their exact function in plants remains elusive.

The sole two-pore channel in Arabidopsis, TPC1, comprises the most abundant channel in the tonoplast where it is responsible for slow vacuolar (SV) currents (Figure 1–1, p. 5; Peiter *et al.*, 2005). As suggested by the two  $\text{Ca}^{2+}$ -binding EF hand motifs, a  $\text{Ca}^{2+}$ -dependent activation was reported for TPC1/SV channel, thereby making it a good candidate for a proposed direct  $\text{Ca}^{2+}$ -induced  $\text{Ca}^{2+}$  release (CICR) from the vacuole (Ward and Schroeder, 1994; Bewell *et al.*, 1999; Hetherington and Brownlee, 2004; Peiter *et al.*, 2005). Further information on TPC1 is provided in chapter 2.1. Furthermore, electrophysiological analyses suggest ligand-gated channels at vacuolar and ER endomembranes capable of mediating  $\text{Ca}^{2+}$  release into the cytosol. The second messenger nicotinic acid adenine dinucleotide phosphate (NAADP) is supposed to mediate  $\text{Ca}^{2+}$  release solely from the ER (Navazio *et al.*, 2000), while inositol-tris/hexakis-phosphate ( $\text{InsP}_3/\text{InsP}_6$ ) and cyclic ADP-ribose (cADPR) additionally seem to act at the tonoplast (Figure 1–1, p. 5; Allen *et al.*, 1995; Muir and Sanders, 1996; Martinec *et al.*, 2000; Navazio *et al.*, 2001; Lemtiri-Chlieh *et al.*, 2003). Several plant genome sequences, however, did not reveal the existence of  $\text{InsP}_3$  or cADPR/ryanodine receptors or any ADP-ribose cyclase with similarity to the mammalian counterparts in higher plants. Strikingly, an  $\text{InsP}_3$ -receptor homolog exists in the green algae *Chlamydomonas* (Wheeler and Brownlee, 2008). This finding raised the hypothesis that certain classes of ion channels were lost during evolution of higher plants, probably due to the absence of evolutionary pressure as a result of the different lifestyle of

sessile plants (Hetherington and Brownlee, 2004; Wheeler and Brownlee, 2008). Hence, plants may possess a different repertoire of channels than animals. Similar distinctions between the animal and plant system appear to exist in the phospholipase C (PLC)-mediated  $\text{InsP}_3$  generation, with evidence emerging for a role of  $\text{InsP}_6$ , rather than  $\text{InsP}_3$ , in ( $\text{Ca}^{2+}$ ) signalling (Munnik and Testerink, 2009). In conclusion,  $\text{Ca}^{2+}$  release mechanisms from internal stores in plants, such as vacuole and ER, remain speculative to date.

### $\text{Ca}^{2+}$ -binding proteins

In addition to the  $\text{Ca}^{2+}$ -permeable channels and  $\text{Ca}^{2+}$  transporters mentioned above,  $\text{Ca}^{2+}$ -binding proteins in the cytosol as well as intracellular compartments contribute to  $\text{Ca}^{2+}$  homeostasis. The ER contains various  $\text{Ca}^{2+}$ -binding proteins, such as molecular chaperone binding proteins, calnexin, calsequestrin and calreticulin (CRT; White and Broadley, 2003). Arabidopsis expressing anti-sense *CRT* are more sensitive to low external [ $\text{Ca}^{2+}$ ], while *CRT* over-expressing plants are less sensitive, suggesting a prominent role for the ER as exchangeable  $\text{Ca}^{2+}$  store in  $\text{Ca}^{2+}$  homeostasis (Persson *et al.*,

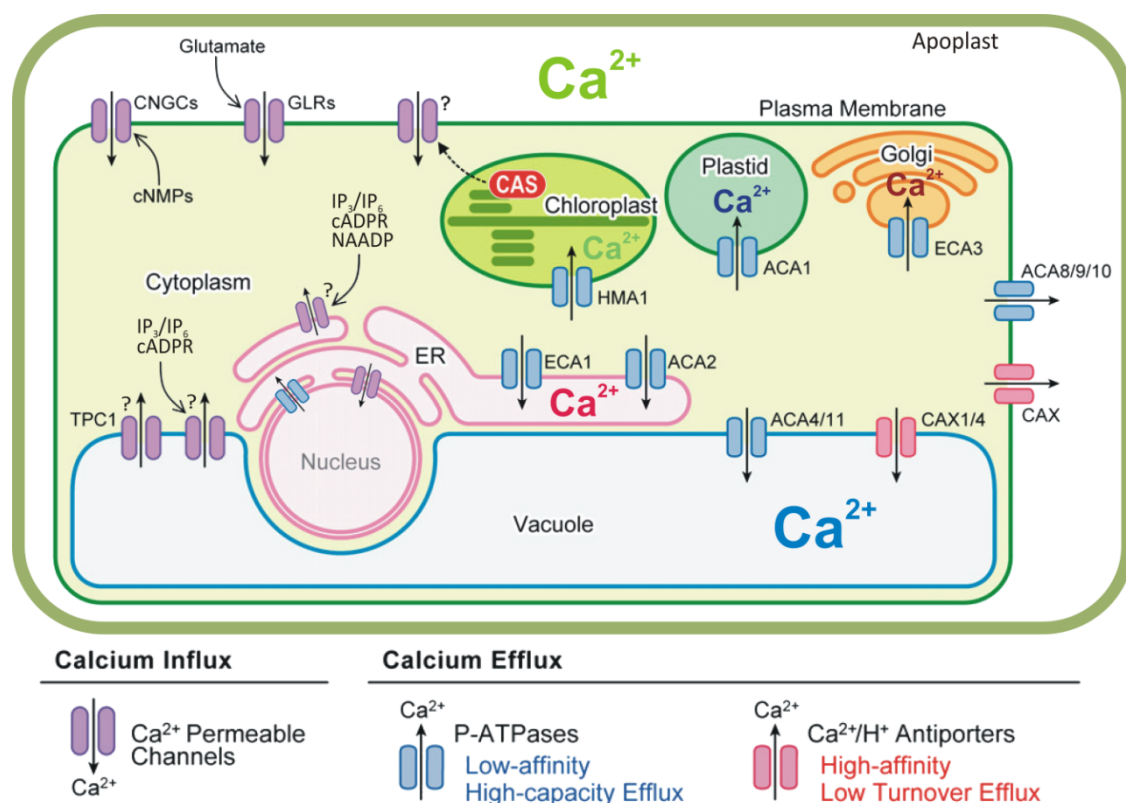


**Figure 1–1.  $\text{Ca}^{2+}$ -permeable channels and transporters at the different  $\text{Ca}^{2+}$  stores in Arabidopsis.**

Localization of the main classes of  $\text{Ca}^{2+}$ -permeable channels allowing  $\text{Ca}^{2+}$  influx into the cytosol and  $\text{Ca}^{2+}$  transporters responsible for  $\text{Ca}^{2+}$  efflux. While the 20 CNGC and 20 GLR channels constitute large protein families only one TPC channel exists in Arabidopsis.  $\text{Ca}^{2+}$  extrusion is achieved by P-class  $\text{Ca}^{2+}$ -ATPases, ten ACAs and four ECAs, and six  $\text{Ca}^{2+}/\text{H}^+$  antiporters of the CAX class. (Figure adapted from Kudla *et al.*, 2010)

**Abbreviations:** CNGC = cyclic nucleotide-gated channel; cNMP = cyclic nucleotide monophosphate; GLR = glutamate receptor-like channel; CAS =  $\text{Ca}^{2+}$ -sensing receptor; ECA = ER-type  $\text{Ca}^{2+}$ -ATPase; ACA = autoinhibited  $\text{Ca}^{2+}$ -ATPase; CAX = cation exchanger; TPC = two-pore channel; HMA1 =  $\text{Ca}^{2+}$ /heavy metal-ATPase; IP<sub>3/6</sub> = inositol-tris/hexakis-phosphate; cADPR = cyclic ADP-ribose; NAADP = nicotinic acid adenine dinucleotide phosphate; " $\text{Ca}^{2+}$ " symbols indicate  $\text{Ca}^{2+}$  stores.

2001; Wyatt *et al.*, 2002; Jia *et al.*, 2009). A high-capacity  $\text{Ca}^{2+}$ -binding protein, CAS ( $\text{Ca}^{2+}$ -sensing receptor), was recently found to localize to the thylakoid membrane in chloroplasts (Nomura *et al.*, 2008; Weinl *et al.*, 2008). Strikingly, *cas* mutant plants are affected in cytosolic  $[\text{Ca}^{2+}]$  homeostasis, show retarded growth under low  $\text{Ca}^{2+}$  conditions and are impaired in stomatal closure, probably due to altered  $\text{Ca}^{2+}$  signalling (Han *et al.*, 2003; Nomura *et al.*, 2008; Weinl *et al.*, 2008). Additionally,  $\text{Ca}^{2+}$ -binding proteins are found in the vacuole and also cytosolic  $\text{Ca}^{2+}$ -binding proteins have some capacity to buffer free cytosolic  $\text{Ca}^{2+}$  (Clapham, 1995; Malho *et al.*, 1998).

### 1.1.3. Alternative concepts: “ $\text{Ca}^{2+}$ signature” versus “chemical on-off switch”

In view of the ubiquitous employment of  $\text{Ca}^{2+}$  as second messenger, the question arises whether this simple cation can relay specific information. Real-time in vivo monitoring of cellular  $\text{Ca}^{2+}$  levels in plants provides evidence that different stimuli induce  $[\text{Ca}^{2+}]_{\text{cyt}}$  elevations with specific spatio-temporal patterns – the so-called “ $\text{Ca}^{2+}$  signature” (Webb *et al.*, 1996; Trewavas, 1999). This concept, adapted from the animal system, proposes that signal-specific information is encoded in certain parameters of the  $[\text{Ca}^{2+}]_{\text{cyt}}$  elevation, e. g. duration, amplitude, frequency in the case of oscillations, spatial distribution and source of the  $\text{Ca}^{2+}$ , and relayed to downstream  $\text{Ca}^{2+}$  sensors. Indeed, the various  $\text{Ca}^{2+}$ -permeable channels,  $\text{Ca}^{2+}$  transporters and  $\text{Ca}^{2+}$  sources described above, provide a whole toolkit for shaping such unique and specific  $[\text{Ca}^{2+}]_{\text{cyt}}$  elevations by precise control of concerted  $\text{Ca}^{2+}$  influx and efflux at the plasma- and endomembranes. Although this analogy to animal systems appears plausible, concerns have been raised about this concept in plants since for most stimuli no direct coupling between the  $\text{Ca}^{2+}$  signature and the end response has been proven, but most data are rather correlative (Plieth, 2001; Scrase-Field and Knight, 2003). An alternative notion is that  $\text{Ca}^{2+}$  may simply serve as a “chemical on-off switch”, i. e. that a  $[\text{Ca}^{2+}]$  rise above a certain threshold is sufficient to activate  $\text{Ca}^{2+}$ -dependent pathways, but components other than  $\text{Ca}^{2+}$  are causal for the response specificity (Scrase-Field and Knight, 2003). Moreover, some changes in  $[\text{Ca}^{2+}]_{\text{cyt}}$  may reflect indirect perturbations of the  $\text{Ca}^{2+}$ /ion homeostasis or nutritional  $\text{Ca}^{2+}$  fluxes (Plieth, 2001). To date, there are some examples with a definite  $\text{Ca}^{2+}$  signature - response coupling, but these might be the exception rather than the rule (Scrase-Field and Knight, 2003; Dodd *et al.*, 2010; Kudla *et al.*, 2010). Such a direct connection between the  $\text{Ca}^{2+}$  signature and the end response was illustrated in guard cells, where artificially imposed  $\text{Ca}^{2+}$  oscillations, with a frequency, duration and number resembling ABA-induced responses, evoked long-term stomatal closure in the absence of any stimulus. Remarkably, short-term stomatal closure was induced by any  $\text{Ca}^{2+}$  elevations above a certain threshold regardless of the pattern (Allen *et al.*, 2000, 2001). Thus,  $\text{Ca}^{2+}$  signalling in stomatal closure includes examples for both, threshold- and signature-mediated signalling. Actually, the contribution of  $[\text{Ca}^{2+}]_{\text{cyt}}$  elevations to specificity may vary for different stimuli between the two extreme positions of specific signature or simple chemical switch and thus needs to be carefully and critically assessed in each single case.

$\text{Ca}^{2+}$  is only poorly diffusible in the cytosol due to buffering by  $\text{Ca}^{2+}$ -binding proteins. Hence,  $[\text{Ca}^{2+}]_{\text{cyt}}$  elevations occur only spatially restricted but can rapidly reach high but short-lived concentrations locally (Clapham, 1995; Trewavas, 1999). However, an initial local  $[\text{Ca}^{2+}]_{\text{cyt}}$  elevation at, for instance, the plasma membrane, can either directly, through  $\text{Ca}^{2+}$ -activated channels, or indirectly, *via* generation of  $\text{Ca}^{2+}$ -releasing second messengers, induce a subsequent  $\text{Ca}^{2+}$  release, for example, from internal stores. This successive local release of  $\text{Ca}^{2+}$  at the plasma or endomembranes, referred to as “ $\text{Ca}^{2+}$ -induced  $\text{Ca}^{2+}$  release (CICR)”, thereby facilitates the formation of complex spatio-temporal patterns, such as oscillations or waves (Trewavas, 1999). As  $\text{Ca}^{2+}$  is involved in various pathways, concomitant signals converge at the level of  $\text{Ca}^{2+}$  signalling (Knight and Knight, 2001; Dodd *et al.*, 2010). Furthermore, previous stimuli can affect the response to further signals, e. g. owing to refractory states, depletion or up-regulation of  $\text{Ca}^{2+}$  signalling or decoding components (Knight *et al.*, 1998; Knight and Knight, 2000, 2001). Thus, repeated stimulation of cells with the same signal may lead to stimulus acclimation, observable, for instance, as decreasing  $[\text{Ca}^{2+}]_{\text{cyt}}$  amplitudes, providing cells with a basic “ $\text{Ca}^{2+}$  memory” (Knight *et al.*, 1996, 1998; Trewavas, 1999). Additional complexity arises from quantitative differences of stimuli and cell-type specificity of  $\text{Ca}^{2+}$  signals. In combination, all these features allow integration and concurrent processing of various stimuli at the level of  $\text{Ca}^{2+}$  signalling with characteristics of “scale-free networks” (Dodd *et al.*, 2010). In conclusion,  $\text{Ca}^{2+}$  is speculated to even enable “intelligent responses” in analogy to simple neural networks (Trewavas, 1999; Dodd *et al.*, 2010).

In addition to  $[\text{Ca}^{2+}]_{\text{cyt}}$  elevations, also intracellular organelles such as nucleus and chloroplasts are able to generate their own  $[\text{Ca}^{2+}]$  elevations. For instance, nuclear  $[\text{Ca}^{2+}]$  elevations ( $[\text{Ca}^{2+}]_{\text{nuc}}$ ) occur through  $\text{Ca}^{2+}$  influx from the nuclear envelope, and these  $[\text{Ca}^{2+}]_{\text{nuc}}$  elevations are coupled to cytosolic  $\text{Ca}^{2+}$  signals or even generated independently (Malho *et al.*, 1998; Pauly *et al.*, 2001; Lecourieux *et al.*, 2005; Mazars *et al.*, 2009). An example is the involvement of nuclear  $\text{Ca}^{2+}$  signals in nodulation during Rhizobium–legume symbiosis (Oldroyd and Downie, 2006).

#### 1.1.4. *In vivo* methods for measuring $[\text{Ca}^{2+}]$

The insights into cellular  $\text{Ca}^{2+}$  dynamics gained over the last years were facilitated by the development of sensitive  $\text{Ca}^{2+}$  reporters that allow non-invasive, quantitative and kinetic *in vivo* monitoring of even small changes in the  $\text{Ca}^{2+}$  concentration at whole-plant and single-cell level, and the corresponding sensitive detection equipment. The two prominent  $\text{Ca}^{2+}$  reporters used in plants to date are aequorin and cameleon probes that facilitate *in vivo*  $\text{Ca}^{2+}$  imaging and quantification (Allen *et al.*, 1999; Brownlee, 2000; Plieth, 2001; Rudd and Franklin-Tong, 2001). Both are  $\text{Ca}^{2+}$ -binding proteins that change their biochemical properties upon  $\text{Ca}^{2+}$  binding in a dose-dependent manner. The main advantage is that both proteins can be expressed ectopically in plants and even targeted to different cellular locations, e. g. cytosol, nucleus or “microdomains” adjacent to internal stores, such as the vacuole (Knight *et al.*, 1991, 1996; Sedbrook *et al.*, 1996; Brownlee, 2000; Mithöfer and Mazars, 2002). These  $\text{Ca}^{2+}$  reporters overcome the difficulties associated with loading of  $\text{Ca}^{2+}$ -sensitive fluorescent dyes regarding cell-wall

permeability, unequal distribution and lack of precise compartment targeting (Rudd and Franklin-Tong, 2001). Aequorin is a  $\text{Ca}^{2+}$ -sensitive luminescent protein that spontaneously reconstitutes with its luminophore coelenterazine (CTZ) or synthetic CTZ derivatives that confer distinct light emission properties (Figure 1–2, p. 8; Shimomura *et al.*, 1993; Mithöfer and Mazars, 2002). Aequorin with its high dynamic range is suitable for accurate quantification and whole plant or organ imaging, but due to a low light intensity, single-cell imaging is not feasible (Knight *et al.*, 1992; Sedbrook *et al.*, 1996; Allen *et al.*, 1999; Rentel and Knight, 2004). By contrast, ratiometric cameleon reporters are FRET (fluorescence resonance energy transfer)-based probes harbouring a  $\text{Ca}^{2+}$ -binding linker, which facilitate single-cell  $\text{Ca}^{2+}$  imaging (Figure 1–2, p. 8; Allen *et al.*, 1999; Brownlee, 2000).

### 1.1.5. Deciphering the „ $\text{Ca}^{2+}$ code“- $\text{Ca}^{2+}$ sensors

Since  $\text{Ca}^{2+}$  cations can coordinate six to eight uncharged oxygen atoms,  $\text{Ca}^{2+}$  binding to suitable protein domains can induce conformational changes (Sanders *et al.*, 1999). The most prominent of such  $\text{Ca}^{2+}$ -binding domains is the so-called helix-loop-helix “EF hand” motif, with up to 250 predicted EF hand-containing proteins encoded in the Arabidopsis genome (Day *et al.*, 2002). While a single EF hand can bind  $\text{Ca}^{2+}$  with high affinity, combination of several EF hand motifs confers cooperative  $\text{Ca}^{2+}$  binding (White and Broadley, 2003; Yang and Poovaiah, 2003; McCormack *et al.*, 2005). Other  $\text{Ca}^{2+}$ -binding domains are constituted by C2 domains, e. g. in phospholipases, or endonexin-folds, e. g. in annexins (Delmer and Potikha, 1997; Hofmann *et al.*, 2000; Wang, 2001). A conformational change induced by  $\text{Ca}^{2+}$ -binding can either affect the activity of the  $\text{Ca}^{2+}$ -binding protein itself, through intramolecular

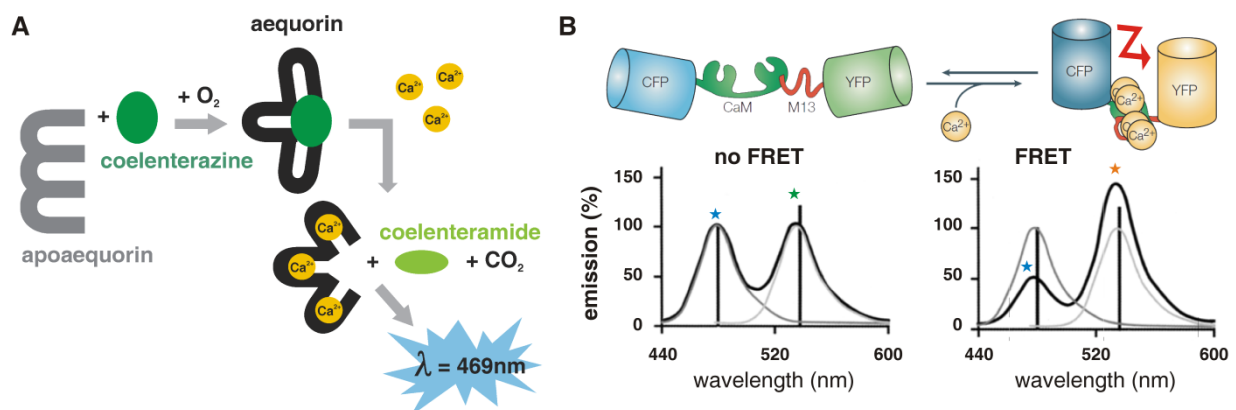


**Figure 1–2. Principle biochemical function of aequorin and cameleon  $\text{Ca}^{2+}$  probes**

A) Apoaequorin spontaneously reconstitutes with its luminophore coelenterazine to functional holoaequorin in the presence of oxygen. Upon binding of three  $\text{Ca}^{2+}$  ions coelenterazine is converted into coelenteramide accompanied by release of  $\text{CO}_2$  and emission of light in the visible range ( $\lambda = 469\text{ nm}$ ). The amount of emitted light correlates with the  $\text{Ca}^{2+}$  concentration. (Figure adapted from Mithöfer and Mazars, 2002)

B) Ratiometric cameleon probes are composed of two fluorescent proteins with different excitation and emission wavelengths, such as cyan- (CFP) and yellow-fluorescent proteins (YFP) in the “yellow cameleon”, separated by a flexible  $\text{Ca}^{2+}$ -binding linker consisting of a CaM and CaM-binding M13 domain. As the emission range of CFP overlaps with the excitation range of YFP, the fluorescence energy of CFP can excite YFP, so-called FRET (fluorescence resonance energy transfer), if both are in close proximity. Thus, without  $\text{Ca}^{2+}$  both, CFP and YFP, fluoresce independently, while upon  $\text{Ca}^{2+}$  binding a conformational change within the linker brings CFP and YFP close together and allows FRET to occur, thereby enhancing the emission of YFP compared to decreased CFP emission. According to this change in the emission ratio of CFP:YFP such probes are called ratiometric. The FRET efficiency corresponds to the  $\text{Ca}^{2+}$  concentration. (Figure adapted from Plieth, 2001; Rudolf *et al.*, 2003)

interactions, or the activity of an interacting protein partner, through intermolecular interaction. Whereas in the first case, the  $\text{Ca}^{2+}$ -binding protein itself is a  $\text{Ca}^{2+}$ -sensor and has response activity (sensor responder), the  $\text{Ca}^{2+}$ -binding protein in the latter case constitutes only a  $\text{Ca}^{2+}$ -sensor (sensor relay) that relays the information to a separate responder (Sanders *et al.*, 2002). Thus,  $\text{Ca}^{2+}$ -binding can be conveyed into various downstream activities, such as protein (de)phosphorylation (Kutuzov *et al.*, 2001; Cheng *et al.*, 2002b; Hrabak *et al.*, 2003; Takezawa, 2003; Luan, 2009; Weinl and Kudla, 2009; Boudsocq *et al.*, 2010) or transcriptional regulation (Galon *et al.*, 2010b), but also modulation of ion channel or transporter activity (Harper *et al.*, 1998; Hwang *et al.*, 2000; Hua *et al.*, 2003; Meneghelli *et al.*, 2008), metabolic or biosynthesis enzyme activity (Hsieh *et al.*, 2000; Kim *et al.*, 2002; Yang and Poovaiah, 2002; Du and Poovaiah, 2005; Kobayashi *et al.*, 2007; Ogasawara *et al.*, 2008), cytoskeleton-associated processes (Reddy and Reddy, 1999; Reddy *et al.*, 1999; Reddy, 2001b; Bouche *et al.*, 2005) *et cetera*.

Typical  $\text{Ca}^{2+}$ -binding sensor proteins are calmodulins (CaMs), calmodulin-like proteins (CMLs) or calcineurin B-like proteins (CBL; Kudla *et al.*, 1999; Shi *et al.*, 1999; McCormack *et al.*, 2005; DeFalco *et al.*, 2010). The existence of seven canonical CaMs and 50 CMLs with distinct expression patterns in Arabidopsis suggests diverse functions for these proteins, which are further increased by interaction with multiple target proteins (Yang and Poovaiah, 2003; McCormack *et al.*, 2005). While CaMs are merely considered as sensor proteins, a responder function for AtCAM7 as direct transcriptional regulator was recently reported (Kushwaha *et al.*, 2008). Otherwise, CaMs can regulate gene expression *via* interaction with  $\text{Ca}^{2+}$ /CaM-binding transcriptional activators (CAMTAs) and other transcription factors (Bouche *et al.*, 2002; Du and Poovaiah, 2004; Park *et al.*, 2005; Yoo *et al.*, 2005; Doherty *et al.*, 2009; Du *et al.*, 2009; Galon *et al.*, 2010b). Although CBLs exclusively interact with CBL-interacting protein kinases (CIPKs), the combinatorial possibilities of separated sensor (10 AtCBLs) and interacting responder (26 AtCIPKs) could accommodate diverse signals through the plethora of flexible combinable modules (Kudla *et al.*, 1999; Shi *et al.*, 1999; Kolukisaoglu *et al.*, 2004; Luan, 2009; Weinl and Kudla, 2009). By contrast, the 34 sensor responder Ca<sup>2+</sup>-dependent protein kinases (CDPKs) and eight CDPK-related kinases (CRKs) in Arabidopsis can only serve a comparatively limited number of signals (Reddy, 2001a; Cheng *et al.*, 2002b; Hrabak *et al.*, 2003). The third class of  $\text{Ca}^{2+}$ -regulated kinases in plants, the Ca<sup>2+</sup>-CaM-dependent kinases (CCaMKs), which play a crucial role in symbiosis, are absent in Arabidopsis (Hrabak *et al.*, 2003; Gleason *et al.*, 2006).

It is evident that “ $\text{Ca}^{2+}$  deciphering” mechanisms comprise another important layer in maintaining stimulus specificity. Only a cell that is competent to decode a certain stimulus can finally relay the signal into downstream responses. Additionally, differential expression and localization of decoding systems in distinct cell types or caused by acclimation to previous stimuli will substantially affect the end response. The local restriction of  $[\text{Ca}^{2+}]_{\text{cyt}}$  elevations further necessitates a close proximity of  $\text{Ca}^{2+}$  channels and  $\text{Ca}^{2+}$  sensors (Berridge, 2006). This can, for instance, be achieved by direct association of the  $\text{Ca}^{2+}$  sensor with a  $\text{Ca}^{2+}$  channel or through membrane tethering, which may further underlie dynamic regulation (Dammann *et al.*, 2003; Hua *et al.*, 2003; Yang and Poovaiah, 2003; Cheong *et al.*,

2007; Batistic *et al.*, 2008; Meneghelli *et al.*, 2008). Furthermore,  $\text{Ca}^{2+}$  sensors can recruit their target proteins to destined microdomains or protein complexes upon  $\text{Ca}^{2+}$  binding (Batistic *et al.*, 2010). Taken together, the cellular location of  $\text{Ca}^{2+}$  channels and  $\text{Ca}^{2+}$  sensors, as well as the flexibility of the  $\text{Ca}^{2+}$ -decoding network provide further levels of regulation and integration of diverse signals at the level of  $\text{Ca}^{2+}$  signalling (Cheong *et al.*, 2003; DeFalco *et al.*, 2010).

## 1.2. Innate immunity in *Arabidopsis thaliana*

As sessile organisms, plants are exposed to continuously changing environmental factors, like light, temperature, water and nutrient availability and mechanical stress. In addition to such abiotic factors, plant survival is permanently threatened by insect and vertebrate herbivores, as well as diverse classes of (phytopathogenic) microbes, such as bacteria, fungi, oomycetes, viruses and nematodes. Although some of the microbes are beneficial to the plant, particularly in the rhizosphere, the majority of (foliar) microbes constitute potential pathogens (Gomez-Gomez and Boller, 2002). Despite, plants are mostly healthy as they have evolved efficient survival strategies. These include preformed physical and chemical barriers, like cell wall, cuticle and antimicrobial compounds, aimed at hindering pathogen entry, as well as inducible defence responses (Hückelhoven, 2007). For inducible reactions it is crucial that pathogens are recognized immediately in order to rapidly mount appropriate defence mechanisms before pathogens proliferate to high numbers. Pathogens, in turn, try to evade recognition or suppress defence responses, while plants evolve new recognition strategies. Hence, a dynamic evolutionary arms-race exists between pathogenic microbes and their potential host plants (Boller and He, 2009).

### 1.2.1. The concept of “Microbe- or Damage-Associated Molecular Patterns” (M/DAMPs)

Plants have evolved diverse sensitive recognition mechanisms for “danger signals”. These range from perception of patterns characteristic for a whole class of microbes by a broad host range to pathovar-host-specific interactions, and also include detection of indirect microbe-induced perturbations (Boller and Felix, 2009). So-called “pathogen- or microbe-associated molecular patterns” (P/MAMPs, formerly named general elicitors), which are (i) characteristic for a certain class of microbes, (ii) indispensable for survival and therefore evolutionarily conserved and (iii) absent from the host, are detected by specific cell-surface “pattern recognition receptors” (PRRs; Boller and Felix, 2009). This is thought to provide a first layer of defence that, if successful, leads to PAMP-triggered immunity (PTI; Figure 1–3, p. 11). Pathogens, in turn, try to evade recognition by PAMP variation, which is often difficult due to essential PAMP function, or to suppress PAMP signal transduction. Most prominent are “effectors”, including avirulence (Avr) proteins, that are delivered into the host cell cytoplasm *via* the type III-secretion system to interfere with host signalling, thus causing “effector-triggered susceptibility” (ETS; Figure 1–3, p. 11). *Vice versa*, plants acquired intracellular “receptors”, named resistance (R) proteins, that either directly target the effector or detect effector-induced cellular manipulations (guard hypothesis), thereby resulting in “effector-triggered immunity” (ETI, Figure 1–3, p. 11; Jones and Dangl, 2006). In contrast to PTI, which confers immunity to a broad host

range, ETI is race-specific, i. e. only a plant cultivar carrying a certain *R* gene is resistant to a particular pathogen strain harbouring the corresponding *Avr* gene (Chisholm *et al.*, 2006; Jones and Dangl, 2006). Therefore, this hypothesis was originally named “gene-for-gene resistance” (Flor, 1942). Furthermore, ETI is assumed to generally induce stronger and more robust immune reactions than PTI, as illustrated by the hypersensitive response (HR), a programmed cell death reaction aimed at restricting growth of biotrophic pathogens (Tsuda and Katagiri, 2010). The dynamic co-evolutionary arms-race between PTI, ETS and ETI, is illustrated in the “Zig-Zag model” (Figure 1–3, p. 11) proposed by Dangl and Jones (2006). The molecular characterization

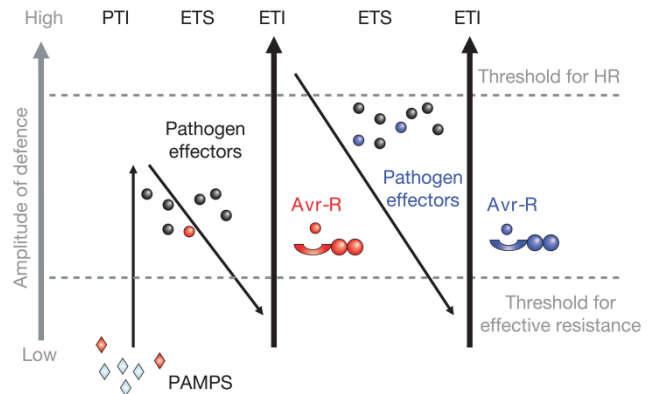


**Figure 1–3. Zigzag model**

The zigzag model illustrates the evolutionary arms-race between pathogen and host. A first layer of host defence constitutes the recognition of conserved pathogen-associated molecular patterns (PAMPs) leading to PAMP-triggered immunity (PTI). Pathogens try to suppress PTI with the help of effectors, including avirulence (*Avr*) proteins, thus resulting in effector-triggered susceptibility (ETS). Hosts, in turn, evolved perception mechanisms for effectors, resistance (*R*) proteins conferring effector-triggered immunity (ETI). While PTI often displays moderate reactions, effectors stimulate stronger responses, like the hypersensitive response (HR), a cell death reaction. (Figure from Jones and Dangl, 2006)

of several PAMP/PRR and *Avr/R* gene pairs, however, revealed that nature does not always fit this classification into PAMPs or effectors and PTI or ETI. For instance, common effectors and PAMPs with a limited host range exist (Figure 1–4, p. 12) and some PAMPs also induce HR (Elbaz *et al.*, 2002; Naito *et al.*, 2008; Thomma *et al.*, 2011).

In addition to PAMPs and effectors, plants are also able to sense direct mechanical damage or indirect herbivore- or microbe-induced damage through “damage-associated molecular patterns” (DAMPs or endogenous elicitors; Figure 1–5, p. 13; Boller and Felix, 2009). These are, for instance, cell wall fragments released by microbial cell wall-degrading enzymes (Figure 1–5, p. 13), such as oligogalacturonides (OGAs; D’Ovidio *et al.*, 2004; Denoux *et al.*, 2008; Brutus *et al.*, 2010) or cutin monomers (Schweizer *et al.*, 1996; Fauth *et al.*, 1998; Hüchelhoven, 2007). Additionally, some proteinaceous DAMPs are released from a precursor, e. g. upon wounding, such as systemin from prosystemin in tomato (McGurl *et al.*, 1992; Ryan and Pearce, 1998) or AtPep peptides from PROPEP precursor proteins in Arabidopsis (Huffaker *et al.*, 2006; Huffaker and Ryan, 2007). Since these DAMPs are also perceived by PRRs and induce similar defence responses, it was concluded that plants do not distinguish between PAMPs, DAMPs and effectors but these are rather generally sensed as “danger signals”, which, depending on the interaction strength, lead to defence responses of different intensity (Figure 1–5, p. 13; Boller and Felix, 2009; Thomma *et al.*, 2011). In principle, MAMPs, DAMPs and effectors can also be classified, in analogy to the animal innate immune system, as “non-self” (MAMPs and directly sensed effectors) and, intriguingly, “modified-self” (DAMPs and effectors sensed by “guard” *R* proteins; Matzinger, 2002).

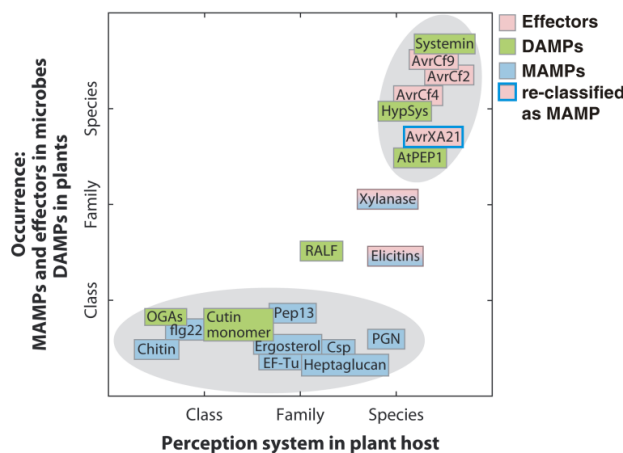


**Figure 1–4. Evolutionary occurrence of MAMPs, DAMPs and effectors and their cognate perception systems.**

Widespread distribution of MAMPs, DAMPs and effectors in whole pathogen or plant classes indicates evolutionary early occurrence, while evolutionary recent innovations are specific for certain species. Generally, MAMPs are considered as conserved patterns with widely distributed perception systems. In comparison, effectors are rather species-specific. Recent findings, however, led to the re-classification of certain narrow-distributed effectors, such as AvrXA21, as MAMPs. Thus, the classification into MAMPs, DAMPs or effectors may not be strictly maintained but may be replaced by the general term “danger signal”. (Figure adapted from Boller and Felix, 2009)

Csp = cold shock protein; PGN = peptidoglycan; HypSys = hydroxyproline-rich glyco-peptides; RALF = rapid alkalization inducing factor

Cell wall or other surface components are due to their exposed position to a potential host and their occurrence in whole microbial classes, predestined as PAMPs/MAMPs. Accordingly, fungal chitin (Felix *et al.*, 1993; Miya *et al.*, 2007; Wan *et al.*, 2008) and ergosterol (Granado *et al.*, 1995; Laquitaine *et al.*, 2006; Lochman and Mikes, 2006), oomycete  $\beta$ -glucans (Sharp *et al.*, 1984; Cheong *et al.*, 1991; Umemoto *et al.*, 1997), bacterial lipopolysaccharides (LPS; see 2.4; Silipo *et al.*, 2010), peptidoglycans (PGN; see 2.5; Gust *et al.*, 2007) and flagellin monomers (Felix *et al.*, 1999), act as MAMPs in diverse plant species. Likewise, secreted proteins/molecules can be easily sensed by host cells, such as fungal xylanase (Fuchs *et al.*, 1989; Ron and Avni, 2004), an oomycete transglutaminase, in particular, a highly conserved epitope of 13 amino acids (Pep13),

in parsley and potato (Nürnbergger *et al.*, 1994b; Brunner *et al.*, 2002; Halim *et al.*, 2004), or the quorum sensing signals acyl homoserine lactones in tomato (Schuhegger *et al.*, 2006). Intriguingly, also intracellular proteins can act as potent MAMPs, although it is yet unknown how they exactly get exposed to the host (Schwessinger and Zipfel, 2008). For instance, the translational elongation factor Tu (EF-Tu; Kunze *et al.*, 2004), the most abundant intracellular bacterial protein, is sensed as MAMP in *Arabidopsis*, and, likewise, bacterial cold shock protein (CSP) in tobacco (Felix and Boller, 2003).

Whereas perception systems for some MAMPs, such as chitin or flagellin, are evolutionarily “ancient” and thus widespread in the plant kingdom, others appear evolutionarily “young”, as their recognition is limited to certain plant species (Figure 1–4, p. 12; Boller and Felix, 2009). This is the case for EF-Tu, that, although it is a common and highly conserved protein in bacteria, is only sensed by Brassicaceae (Kunze *et al.*, 2004), or the secreted sulfated *Xanthomonas* Ax21 peptide (formerly AvrXA21) and its respective receptor Xa21, where both, the occurrence of the MAMP as well as the receptor is limited to certain species (*Xanthomonas oryzae* pv. *oryzae* in rice), which led to an initial classification as effector (Lee *et al.*, 2009). Likewise, OGAs and cutin monomers are quite “old” DAMPs, while systemin and the AtPep peptides are evolutionarily quite “new” (Figure 1–4, p. 12; Boller and Felix, 2009). Furthermore, several examples from plants and animals reveal that innate immunity, although relying on the recognition of microbial patterns in both kingdoms, has developed independently in plants and animals and is probably the result of convergent evolution (Zipfel and Felix, 2005). For instance, both,

plants and animals, are able to sense bacterial flagellin, albeit *via* distinct conserved epitopes (Gomez-Gomez and Boller, 2002).

### 1.2.2. Perception of MAMPs and DAMPs

In Arabidopsis, the most conserved N-terminal part of bacterial flagellin, represented by the 22-amino-acid peptide flg22, which corresponds to the active epitope of *Pseudomonas aeruginosa* flagellin and is by itself fully active as PAMP, is recognized by the receptor-like kinase (RLK) FLS2 (Flagellin-sensitive 2). FLS2 comprises a glycosylated extracellular domain, consisting of 28 leucine-rich repeats (LRRs), responsible for ligand binding, a transmembrane domain and an intracellular serine/threonine kinase domain (Felix *et al.*, 1999; Gomez-Gomez *et al.*, 1999; Gomez-Gomez and Boller, 2000; Chinchilla *et al.*, 2006). Within seconds of flg22 binding, FLS2 hetero-oligomerizes with another LRR-RLK, BAK1 (BRI1-associated kinase 1; Figure 1–6, p. 17; Chinchilla *et al.*, 2007; Heese *et al.*, 2007; Schulze *et al.*, 2010), which was originally identified as “co-receptor” of the brassinosteroid receptor

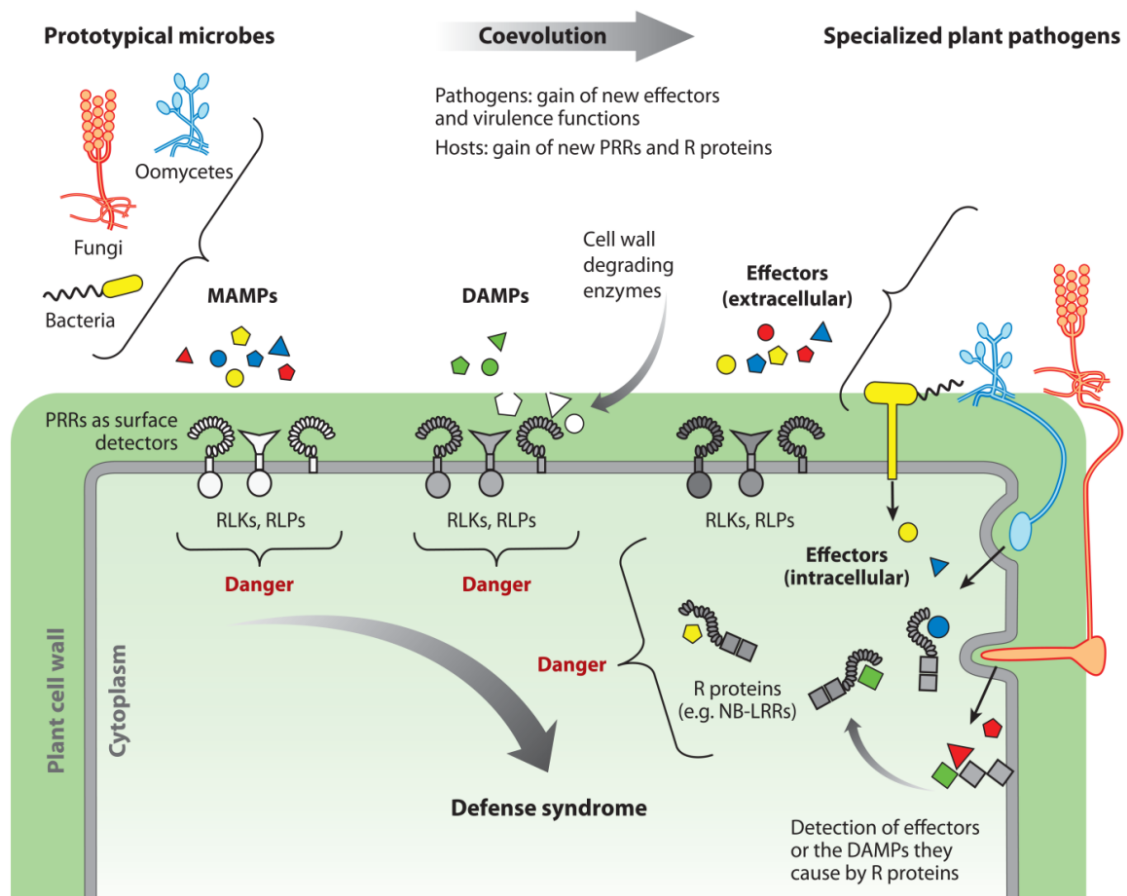


**Figure 1–5. Perception of MAMPs, DAMPs and effectors as general “danger signals” activates a common set of defence responses.**

MAMPs, DAMPs and effectors are commonly sensed as “danger signals” by plasma membrane-resident pattern recognition receptors (PRRs), such as receptor-like proteins (RPLs) or kinases (RLKs), or resistance (R) proteins. Co-evolution thereby continuously drives the requirement of new effectors on the pathogen and new PRRs and R proteins on the plant side. Thus, MAMPs, DAMPs and effectors and their respective receptors can be widely distributed among pathogens/plants or limited to certain species depending on their evolutionary occurrence. Principally, a common set of immune responses is activated but the defence reactions can vary in intensity and kinetics. (Figure from Boller and Felix, 2009)

BRI1 (Brassinosteroid insensitive 1; Li *et al.*, 2002; Nam and Li, 2002). Although BAK1, which contains only 4(-5) LRRs, is not involved in ligand binding, its interaction with FLS2 is required for full responsiveness (Chinchilla *et al.*, 2007; Heese *et al.*, 2007). Ligand binding (to LRRs 9–15) is proposed to induce a conformational change in FLS2 according to the “address-message concept”, where one part of the ligand mediates binding and another part receptor activation (Meindl *et al.*, 2000). Subsequently, the FLS2- and BAK1-kinase domains get into close proximity, thereby enabling trans-phosphorylation events that finally result in activation of the FLS2-BAK1 receptor complex (Figure 1–6, p. 17; Chinchilla *et al.*, 2009; Schulze *et al.*, 2010). Although plants sense the most conserved part of flagellin as MAMP, which is also crucial for flagellum assembly and therefore for motility, some bacterial strains can “afford” mutations in this region to evade recognition, such as *Agrobacterium tumefaciens* and *Sinorhizobium meliloti* (Felix *et al.*, 1999).

In analogy to flagellin/FLS2, EF-Tu and the respective peptide elf18, the conserved acetylated N-terminal fragment of EF-Tu, are perceived by the cognate receptor EFR (EF-Tu receptor; Kunze *et al.*, 2004; Zipfel *et al.*, 2006). Like FLS2, EFR is an LRR-RLK comprising 21 LRR domains that presumably also interacts with BAK1 (Chinchilla *et al.*, 2007). Furthermore, BAK1 is also involved in signalling induced by the plant-derived DAMP, AtPep1, as it associates with the two AtPep LRR-RLKs, PEPR1 and PEPR2 (Krol *et al.*, 2010; Postel *et al.*, 2010; Yamaguchi *et al.*, 2010). Arabidopsis contains seven AtPep peptides, which are released by processing of their respective precursors PROPEP1-7 upon stimulation, for instance, by wounding or pathogen attack. Processed AtPep peptides, in turn, also induce defence responses leading to sort of a feedforward amplification loop (Huffaker and Ryan, 2007). Due to specific expression patterns in distinct tissues and induced by different stimuli, such as the phytohormone JA, SA, ethylene, pathogens *etc.*, AtPep peptides probably exert multiple functions in stress signalling (Huffaker *et al.*, 2006; Huffaker and Ryan, 2007). Taken together, BAK1 acts as “partner” kinase for multiple MAMP- and DAMP-activated signalling pathways. Accordingly, a loss of BAK1 impairs not only responses to flg22, elf18 and AtPep1 but also PGN, LPS and harpin elicitor protein (HrpZ) in Arabidopsis (Shan *et al.*, 2008), as well as CSP and the oomycete infestin in tobacco (Heese *et al.*, 2007; Chaparro-Garcia *et al.*, 2011). The residual responses in *bak1* mutants may indicate partial redundancies with BAK1 homologs, as BAK1 belongs to the 5-membered somatic embryogenesis receptor-like kinase (SERK) group and is also named SERK3 (Hecht *et al.*, 2001; Albrecht *et al.*, 2008). In addition, BAK1 plays an important role in development, particularly as an interacting kinase for BRI1 (Li *et al.*, 2002; Nam and Li, 2002), and, together with its closest homolog SERK4, in cell death, although its exact function there remains yet elusive (He *et al.*, 2007; Kemmerling *et al.*, 2007; He *et al.*, 2008). However, signalling activated by other MAMPs, such as chitin or the necrosis-inducing protein from *Phytophthora sojae* (NPP1) is independent of BAK1 (Shan *et al.*, 2008). This is probably a consequence of the different structure of the chitin receptor, CERK1 (Chitin elicitor receptor kinase 1), an RLK containing three extracellular lysin-motifs (LysM; Miya *et al.*, 2007; Wan *et al.*, 2008; Iizasa *et al.*, 2010; Petutschnig *et al.*, 2010). LysM domains are supposed to generally bind carbohydrates (Knogge and Scheel, 2006; Buist *et al.*, 2008), such as chitin or the

lipochitooligosaccharide Nod factor, while LRR domains may commonly confer peptide- or protein-protein binding (Kobe and Kajava, 2001) but are also able to engage various other molecules including lipids and nucleic acids (Ronald and Beutler, 2010).

Receptor components are subjected to tight regulation. FLS2 is internalized by ligand-induced endocytosis, mediated by a PEST-like endocytosis motif and ubiquitination/proteasome function, which may represent not only catabolism or recycling of the activated receptor but may have specific intracellular signalling function (Robatzek *et al.*, 2006; Salomon and Robatzek, 2006). Likewise, EFR and other PRRs carry a C-terminal typical Yxx $\Phi$  endocytosis motif (Y is tyrosine, X any, and  $\Phi$  a bulky hydrophobic amino acid; Salomon and Robatzek, 2006). Two recent screens for reduced MAMP sensitivity revealed roles of ethylene in regulating transcriptional steady-state levels of *FLS2* (Boutrot *et al.*, 2010; Mersmann *et al.*, 2010). Similarly, various components of the ER secretory pathway and quality control were shown to be required for proper processing and export of functional EFR, but not FLS2, receptors to the plasma membrane (Li *et al.*, 2009; Lu *et al.*, 2009; Nekrasov *et al.*, 2009; Saijo *et al.*, 2009).

The vital contribution of PTI to innate immunity is highlighted by the enhanced susceptibility of several PRR receptor mutants (Zipfel *et al.*, 2004, 2006; Wan *et al.*, 2008) and, particularly, by cross-family transfer of PRRs, e. g. AtEFR into tobacco and tomato, that confers broad-spectrum resistance to otherwise adapted pathogens (Lacombe *et al.*, 2010).

### 1.2.3. MAMP-induced signalling downstream of the receptor (complex)

Generally, different MAMPs and DAMPs appear to activate a common set of signalling events and defence responses by sharing main signalling components (in addition to the adapter kinase BAK1). One of the earliest commonly observable signalling events after PRR activation are ion fluxes across the plasma membrane and concomitant membrane depolarization, which typically occur 30-60 seconds after MAMP application (Figure 1–6, p. 17). Thereby, an increased influx of H<sup>+</sup> and Ca<sup>2+</sup> into the cytosol is accompanied by an efflux of K<sup>+</sup> and anions like nitrate or Cl<sup>-</sup> (Jabs *et al.*, 1997; Blume *et al.*, 2000; Müller *et al.*, 2000; Lecourieux *et al.*, 2002; Ranf *et al.*, 2008; Jeworutzki *et al.*, 2010). These ion fluxes are easily detectable in suspension-cultured cells, as they lead to alkalinization of the growth medium (Granado *et al.*, 1995; Tavernier *et al.*, 1995; Felix *et al.*, 1999; Kunze *et al.*, 2004). The rapid change in the [Ca<sup>2+</sup>]<sub>cyt</sub> was shown to be a prerequisite for downstream responses (Figure 1–6, p. 17), due to the second messenger function of Ca<sup>2+</sup>, for instance, induced by Pep13 in parsley, cryptogein in tobacco or OGAs in soybean (Tavernier *et al.*, 1995; Jabs *et al.*, 1997; Lecourieux *et al.*, 2002; Navazio *et al.*, 2002). Furthermore, a production of the second messenger phosphatidic acid (PA) and its phosphorylated derivative diacylglycerol-pyrophosphate (DGPP) was demonstrated in tomato cell suspension cultures treated with the MAMPs flg22, xylanase or N-acetylchitotetraose (ch4) and was mainly accounted for by the combined activity of phospholipase C (PLC) and diacylglycerol (DAG) kinase (DGK; van der Luit *et al.*, 2000). Intriguingly, the second product of the PLC-mediated DAG

production is inositol-(1,4,5)-trisphosphate (InsP<sub>3</sub>), an established Ca<sup>2+</sup>-releasing second messenger in the animal system, which may also account for Ca<sup>2+</sup> release from plant vacuoles and ER (see 1.1.2).

Subsequently, generation of reactive oxygen species (ROS) may directly confine pathogen growth *via* toxic effects and cell wall strengthening or may exert signalling functions (Torres *et al.*, 2006; Hückelhoven, 2007). The Arabidopsis NADPH oxidases, RbohD and RbohF, contribute to ROS generation in response to pathogen attack (Torres *et al.*, 2002) but MAMP-induced ROS are mainly produced by RbohD in Arabidopsis (Figure 1–6, p. 17; Zhang *et al.*, 2007). Superoxide dismutases rapidly convert membrane-impermeant superoxide (O<sub>2</sub><sup>-</sup>), produced in the apoplast by NADPH oxidases, into H<sub>2</sub>O<sub>2</sub>, which can enter cytosol and nucleus to execute intracellular functions. Mitogen-activated protein kinase (MAPK) cascades are known to be activated upon elicitation with several MAMPs, such as Pep13 in parsley (Ligterink *et al.*, 1997) or flg22 in Arabidopsis (Asai *et al.*, 2002). MAPK cascades are combinatorial modules consisting of an upstream MAPK kinase kinase (MAP3K) that activates MAPK kinases (MKKs) by phosphorylation, while MKKs further activate MAPKs *via* dual phosphorylation of a conserved T-D/E-Y motif. Ultimately, MAPKs (in)activate multiple substrates to modulate metabolic processes or gene expression. In Arabidopsis flg22 elicitation activates MAP3K-MKK4/MKK5-MPK3/MPK6 and MEKK1-MKK1/MKK2-MPK4 (Figure 1–6, p. 17; Rodriguez *et al.*, 2010). While activation of MPK6 is involved in ethylene generation, which is activated within minutes of MAMP application, as well as ethylene signalling (Liu and Zhang, 2004; Bethke *et al.*, 2009), MPK4 seems to negatively regulate defence responses (Petersen *et al.*, 2000). Additionally, the Ca<sup>2+</sup>-dependent protein kinases CPK4, CPK5, CPK6 and CPK11 were shown to (partially) redundantly regulate flg22-induced gene expression re-programming, as well as ROS accumulation (Figure 1–6, p. 17; Boudsocq *et al.*, 2010; Rodriguez *et al.*, 2010).

Besides these “classical” signalling events, several receptor-like cytoplasmic kinases (RLCK), such as BIK1 (Botrytis-induced kinase 1) and its homologs PBL1 and PBL2, were recently reported to also be involved in signalling induced by several MAMPs like flg22, elf18 and chitin. While membrane-tethered BIK1 interacts with unstimulated FLS2 and BAK1, and probably also EFR and CERK1, it becomes phosphorylated upon ligand-induced FLS2-BAK1 interaction, in turn phosphorylates FLS2 and BAK1 and is subsequently released from the FLS2-BAK1 complex (Figure 1–6, p. 17; Lu *et al.*, 2010b; Zhang *et al.*, 2010). Thus, BIK1 and its homologs may attribute for activation of signalling components not directly associated with the receptor complex. Like BAK1, these RLCKs and many other signalling components like NADPH oxidases, MAPKs, CDPKs and several transcription factors (e. g. WRKYs) are shared not only between multiple MAMPs and DAMPs but also by other stimuli, such as abiotic stresses, hormones and developmental stimuli, and are thought to constitute convergence and integration points (Chinchilla *et al.*, 2009; Kudla *et al.*, 2010; Rodriguez *et al.*, 2010; Rushton *et al.*, 2010). Although these mostly comprise protein families with, for instance, distinct expression patterns or specific protein-interaction-domains, the common employment of transduction cascades raises the question of how signalling specificity is maintained.

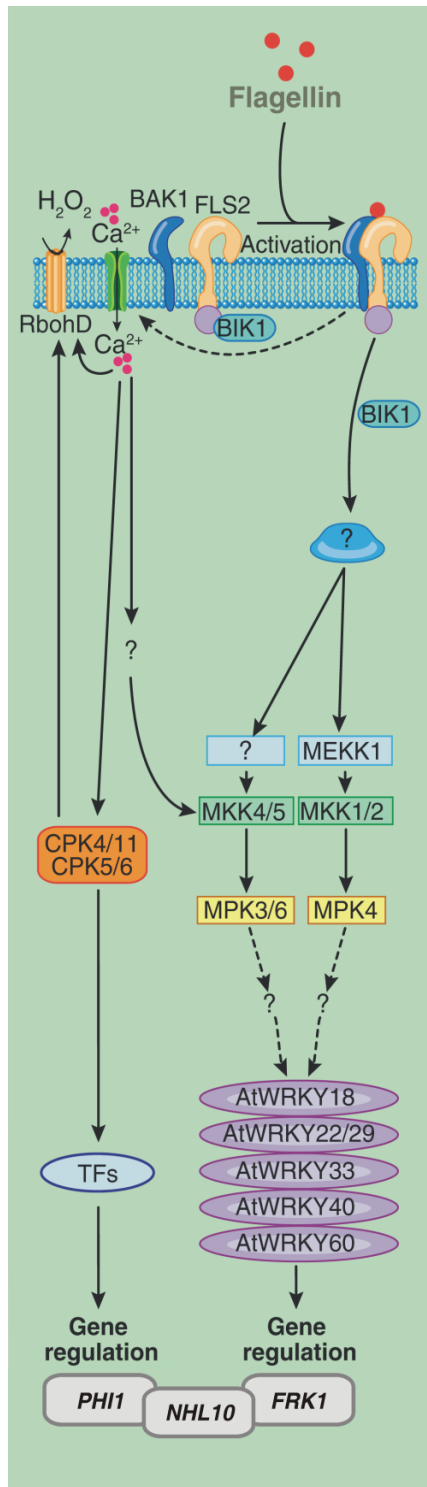


**Figure 1–6. Overview of flagellin-stimulated early signalling in Arabidopsis.**

Upon binding of flagellin/flg22 to its receptor kinase FLS2 this associates with the BAK1 kinase. Trans-phosphorylation is thought to activate the FLS2-BAK1 receptor complex. The receptor-like cytoplasmic kinase BIK1, associated with unstimulated FLS2, is released upon trans-phosphorylation with FLS2/BAK1 and may activate downstream targets in the cytosol. FLS2 activation triggers rapid ion fluxes across the plasma membrane, including influx of apoplasmic Ca<sup>2+</sup> into the cytosol, and concomitant membrane depolarization. Subsequently, Ca<sup>2+</sup> and Ca<sup>2+</sup>-dependent protein kinases (CDPKs) presumably activate the generation of ROS like H<sub>2</sub>O<sub>2</sub> by the plasma membrane-resident NADPH oxidase, RbohD. In parallel, activation of CDPKs and two mitogen-activated protein kinase (MAPK) cascades results in re-programming of gene expression, for instance via WRKY class transcription factors (TFs). While regulation of *PHI1* expression is dependent on CDPKs and *FRK1* expression on MAPKs, *NHL10* expression is regulated by both. The signalling steps leading from FLS2/BAK1 activation to Ca<sup>2+</sup> and MAPK signalling, however, remain yet elusive. (Figure adapted from Ronald and Beutler, 2010)

Gene expression re-modulation occurs already within 30 min after MAMP application (Ramonell *et al.*, 2002; Navarro *et al.*, 2004; Denoux *et al.*, 2008). A striking percentage of up-regulated genes are comprised by RLKs, several of which might have yet unknown function in immunity, and other MAMP-activated signalling components (Asai *et al.*, 2002; Navarro *et al.*, 2004; Zipfel *et al.*, 2006; Postel *et al.*, 2010). Only recently, the RLK BIR1 was identified that can associate with BAK1 and appears to negatively regulate defence responses and cell death (Gao *et al.*, 2009). Taken together, this suggests that MAMP perception generally alerts a plant of a potential danger and sets a “ready-to-defend” state. In agreement, MAMP perception in guard cells also triggers closure of stomata to prevent pathogen invasion, since stomata in their open state are potential entry points for many foliar pathogens (Melotto *et al.*, 2006; Zeng and He, 2010). Several hours after elicitation, MAMPs induce deposition of callose to fortify cell walls, which is dependent on ROS generation (Kohle *et al.*, 1985; Jacobs *et al.*, 2003; Zhang *et al.*, 2007; Luna *et al.*, 2011). Furthermore, MAMP perception not only induces local responses but also establishment of resistance in distant tissues through SA-mediated systemic acquired resistance (SAR; Mishina and Zeier, 2007; Vlot *et al.*, 2009) or potentially JA/ethylene-mediated induced systemic resistance (ISR), e. g. by LPS from rhizobacteria (Pieterse *et al.*, 1996, 1998). Long-term application of several MAMPs, such as flg22 and elf18, also leads to seedlings growth arrest, which is often used as a measure of MAMP responsiveness and applied for genetic screening (Gomez-Gomez *et al.*, 1999; Chinchilla *et al.*, 2007; Li *et al.*, 2009; Nekrasov *et al.*, 2009).

#### 1.2.4. Mechanisms of pathogens to interfere with MAMP and DAMP signalling

The central role of MAMP and DAMP signalling in innate immunity is further substantiated by the various effectors, with diverse biochemical functions, that target immune receptor complexes and downstream components to disrupt signalling (Göhre and Robatzek, 2008). *P. syringae*, for instance, is estimated to secrete up to 30 different effectors during infection (Chang *et al.*, 2005). Due to its shared function in several signalling pathways, BAK1 is a predestined object of effector manipulation (Lu *et al.*, 2010a). Indeed, the *Pseudomonas* effector AvrPto targets BAK1 (Shan *et al.*, 2008) or PRRs like FLS2 and EFR (Xiang *et al.*, 2008). AvrPto also impairs chitin signalling by a yet unknown mechanism (Shan *et al.*, 2008). Similarly, AvrPtoB ubiquitinates and therefore marks FLS2 and CERK1 for proteasome-mediated degradation (Göhre *et al.*, 2008; Gimenez-Ibanez *et al.*, 2009). Additionally, signalling events downstream of the receptor are subject to effector-mediated manipulation, such as MAPKs, which are irreversibly inactivated by the phosphothreonine lyase HopAI1 (Zhang *et al.*, 2007). While the majority of bacterial effectors act inside the host cell, fungal and oomycete effectors are probably mainly secreted into the apoplast but possibly may be taken up by host cells *via* endocytosis (Chisholm *et al.*, 2006). Fungal LysM effectors, for instance the secreted *Cladosporium fulvum* extracellular protein 6 (Ecp6), compete with chitin receptors for chitin binding to suppress signalling and mask the invading fungus (Bolton *et al.*, 2008; de Jonge *et al.*, 2010). Due to their widespread occurrence and functional conservation, LysM effectors may also qualify as PAMPs rather than effectors, thereby demonstrating again the difficulties of a strict MAMP–effector differentiation (Thomma *et al.*, 2011).

Plant stomata are not only central regulation points of plant catabolism but also entry points for many foliar pathogens and thus, subject to tight regulation from the plant side on the one hand, and targets for manipulation by the pathogen on the other hand. In agreement, some *Pseudomonas* strains secrete coronatine, an isoleucine-JA mimic, or syringolin A, an irreversible proteasome inhibitor, to gain access to the leaf interior by re-opening stomata that were closed upon MAMP perception (Melotto *et al.*, 2006; Melotto *et al.*, 2008; Schellenberg *et al.*, 2010).

Last but not least, a different strategy to the classical cytoplasmic bacterial effectors was recently reported. Pathogenic, but also symbiotic bacteria secrete extracellular polysaccharides (EPS) sequestering apoplastic  $\text{Ca}^{2+}$  to attenuate host MAMP signalling (Aslam *et al.*, 2008).  $\text{Ca}^{2+}$  chelation may, additionally, lead to weakening of the cell wall structure to facilitate access of bacteria to host cells, since  $\text{Ca}^{2+}$  mediates non-covalent cell wall cross-linking (Hückelhoven, 2007). This observation further reinforces the crucial role of  $\text{Ca}^{2+}$  and  $\text{Ca}^{2+}$  signalling in plant immunity.

#### 1.2.5. $\text{Ca}^{2+}$ in plant – microbe interactions: the role of $\text{Ca}^{2+}$ in MAMP signalling

The general requirement of a  $\text{Ca}^{2+}$  influx into the cytosol for activation of defence responses in plants has long been observed and is now well established (Stab and Ebel, 1987; Yang *et al.*, 1997; Scheel, 1998). Meanwhile, aequorin-based  $\text{Ca}^{2+}$  imaging revealed the characteristics of different MAMP-

induced  $[Ca^{2+}]_{cyt}$  elevations in various species (Knight *et al.*, 1991). The *Phytophthora* MAMP, Pep13, after a short lag phase, induces a characteristic biphasic  $[Ca^{2+}]_{cyt}$  elevation with a high transient primary peak that continues into a prolonged  $[Ca^{2+}]_{cyt}$  elevation of ~30 minutes (Blume *et al.*, 2000). A detailed pharmacological study revealed that the prolonged plateau phase mainly required influx of apoplastic  $Ca^{2+}$ , while the primary  $Ca^{2+}$  peak potentially involves  $Ca^{2+}$  release from internal stores. Apparently, all tested later responses, such as ROS accumulation, MAPK activation, defence gene expression and production of phytoalexins, are dependent on  $Ca^{2+}$ , in particular on the second sustained  $[Ca^{2+}]_{cyt}$  elevation (Nürnberg *et al.*, 1994b; Jabs *et al.*, 1997; Ligterink *et al.*, 1997; Blume *et al.*, 2000). Based on an electrophysiological characterization, the Pep13-induced  $[Ca^{2+}]_{cyt}$  elevation is mediated by a  $Ca^{2+}$ -permeable,  $La^{3+}$ -sensitive plasma membrane ion channel of large conductance, which is hardly voltage-dependent and reversibly activated upon receptor-mediated Pep13 perception (Zimmermann *et al.*, 1997). Similarly, biphasic  $[Ca^{2+}]_{cyt}$  elevations were elicited by fungal  $\beta$ -glucans in soybean cells, while chitinoligomers only induced a single  $Ca^{2+}$  peak (Mithöfer *et al.*, 1999). Likewise, biphasic  $Ca^{2+}$  responses were observed in suspension-cultured tobacco cells upon treatment with elicitors like cryptogein, OGAs, LPS, the linear  $\beta$ -1,3-glucan laminarin and N-acetylchitopentaose (ch5). Like in parsley, the  $[Ca^{2+}]_{cyt}$  elevations were necessary for downstream responses (Tavernier *et al.*, 1995; Lecourieux *et al.*, 2002). According to inhibitor studies, the biphasic  $[Ca^{2+}]_{cyt}$  elevations involve influx from extra- as well as intracellular  $Ca^{2+}$  stores mediated by  $O_2^-/H_2O_2$ , nitric oxide (NO) or PLC-derived  $InsP_3$  (Lecourieux *et al.*, 2002; Lamotte *et al.*, 2004). Moreover, the two TPC homologs, NtTPC1a and NtTPC1b, were reported to mediate  $Ca^{2+}$  influx across the plasma membrane in tobacco cells upon stimulation with the elicitor cryptogein but also cold shock, sucrose,  $H_2O_2$  or salicylic acid (Furuichi *et al.*, 2001; Kadota *et al.*, 2004; Kawano *et al.*, 2004; Lin *et al.*, 2005). Likewise, the rice OsTPC1 and wheat TaTPC1 homologs have been proposed to reside in the plasma membrane and to function in response to elicitors (Kurusu *et al.*, 2005) or abiotic stresses (Wang *et al.*, 2005), respectively. In strong contrast, AtTPC1 was found to localize to the tonoplast (Carter *et al.*, 2004; Peiter *et al.*, 2005). Another candidate  $Ca^{2+}$ -permeable channel contributing to MAMP-induced  $[Ca^{2+}]_{cyt}$  elevations is CNGC2, also known as defence-no-death (DND1; Clough *et al.*, 2000). DND1 shows constitutive defence responses and elevated SA levels but no HR upon inoculation with avirulent bacteria, demonstrating that DND1-mediated  $Ca^{2+}$  influx across the plasma membrane is crucial for establishment of HR-like cell death (Yu *et al.*, 1998; Clough *et al.*, 2000; Ali *et al.*, 2007; Ma *et al.*, 2009). Additionally, DND1 was reported to mediate LPS-induced  $[Ca^{2+}]_{cyt}$  elevations in Arabidopsis (Ali *et al.*, 2007; Ma *et al.*, 2009). The role of DND1 as well as TPC1 in stress-induced  $Ca^{2+}$  responses in Arabidopsis seedlings was examined as part of this work and will therefore be further discussed in chapter 2.1 (p. 21) and 2.4 (p. 78).

MAMP-induced  $Ca^{2+}$  signalling, however, is not restricted to pathogens, but also plays a central role in Rhizobium-legume as well as arbuscular mycorrhizal symbiosis (Müller *et al.*, 2000; Yokoyama *et al.*, 2000). While the pathogen-induced signalling activates innate immune responses to restrict pathogen growth and invasion, signalling events leading to beneficial symbiosis are characterized by events that

are favourable for both partners, which may include the active suppression of MAMP-induced defence responses (Dodd *et al.*, 2010).

### 1.3. Objectives

Although *Arabidopsis thaliana* is among the best studied model plants, particularly in innate immunity, the knowledge about MAMP-induced  $\text{Ca}^{2+}$  signalling is rather limited. To date, the majority of the  $\text{Ca}^{2+}$  signalling work in plant immunity has been performed in suspension-cultured cells. Although this system enables synchronous elicitation of mostly a single cell type, these cells might react substantially different compared to cells in whole plants. Moreover, studies in suspension-cultured cells are not easily amenable to genetical experimentation and heavily dependent on pharmacological manipulation, which – due to possible unspecific side effects – require critical assessment. Hence, this work aims at providing novel insights into MAMP-induced  $\text{Ca}^{2+}$  signalling in *Arabidopsis thaliana* on whole seedlings or plant level by using the available genetic tools. To this end,  $\text{Ca}^{2+}$  elevations induced by various MAMPs in *Arabidopsis* seedlings or leaf discs were characterised and genetically analysed as part of this work (published and unpublished results) as detailed below.

#### 1) **Analysis of the interplay between $\text{Ca}^{2+}$ signalling and other early signalling components.**

Therefore, mutants of established and potential MAMP-induced signalling components were analysed for a role in  $\text{Ca}^{2+}$  signalling by quantitative aequorin-based  $[\text{Ca}^{2+}]_{\text{cyt}}$  measurements.

#### 2) **Screen for mutants altered in MAMP-induced $\text{Ca}^{2+}$ signalling:**

##### ***Changed Calcium Elevation (CCE).***

This includes setting up a quantitative and high-throughput screening system using aequorin-based  $[\text{Ca}^{2+}]$  measurements and initial characterization of isolated *cce* mutants.

#### 3) **$[\text{Ca}^{2+}]$ elevations induced by yet uncharacterized or novel – pathogenic as well as beneficial – MAMPs in *Arabidopsis*.**

The  $[\text{Ca}^{2+}]$  elevations induced by the DAMP AtPep1, the MAMPs chitin, LPS (in collaboration with Ulrich Zähringer, Research Center Borstel) and PGN (in collaboration with Andrea Gust / Thorsten Nürnberger, ZMBP Tübingen), and a cell wall extract from the beneficial fungus *Piriformospora indica* (in collaboration with Jyothilakshmi Vadassery / Ralf Oelmüller, University of Jena) were examined.

## 2. RESULTS

The examination of early elicitor-activated signalling events, for instance, in tobacco, soybean and parsley cells, has demonstrated a crucial role of  $[Ca^{2+}]_{cyt}$  elevations for activation of defence responses, and this is assumed to be generally alike in most plant species. However, the underlying genetic components yet remain largely elusive. Despite its prominent role as model plant in innate immunity, MAMP-induced  $Ca^{2+}$  signalling in *Arabidopsis thaliana* has not yet been studied in great detail. The availability of the complete *Arabidopsis* Col-0 genome sequence, genetically defined mutants, tools for producing stable transgenics and the discovery of highly active peptide elicitors, such as flg22, elf18 and Pep1, provide a solid base for genetic dissection of MAMP-induced early signalling events, particularly  $Ca^{2+}$  signalling. Hence, the first part of this work aims at assessing the role of  $Ca^{2+}$  signalling in different mutant backgrounds by direct  $[Ca^{2+}]_{cyt}$  measurements and parallel analysis of downstream responses.

### 2.1. Two-pore channel 1 - a putative $Ca^{2+}$ channel in stress responses

#### 2.1.1. Aims and summary

Plasma membrane resident TPC channels in tobacco and rice were reported to contribute to biotic and abiotic stress responses (Kadota *et al.*, 2004; Kawano *et al.*, 2004; Kurusu *et al.*, 2005; Lin *et al.*, 2005). Due to their plasma membrane localization and their permeability to  $Ca^{2+}$ , TPC channels were therefore regarded as good candidates for the long-sought MAMP-activated  $Ca^{2+}$  influx channels. Re-evaluation of the localization by co-expression and electrophysiological studies, contrarily, proved a tonoplast localization for AtTPC1. The finding that TPC1 mediates the well-established SV currents at the vacuole (Peiter *et al.*, 2005) in combination with its  $Ca^{2+}$ -dependent activation and its permeability to mono- as well as divalent cations, suggested TPC1/SV channel to mediate CICR upon an initial  $[Ca^{2+}]_{cyt}$  elevation leading to mass influx of  $Ca^{2+}$  from the vacuole into the cytosol. However,  $[Ca^{2+}]_{cyt}$  elevations induced by diverse abiotic and biotic factors were not affected in *tpc1* knockout or TPC1-overexpressing *Arabidopsis* plants. The tested stimuli ranged from cold, hyperosmotic, salt and oxidative stress, elevation in extracellular  $Ca^{2+}$  concentration to the bacterial peptide MAMPs flg22 and elf18. Likewise, stress-induced gene expression was not altered in *tpc1* mutants or TPC1-overexpressors. Taken together, a putative role for TPC1 in stress-induced  $Ca^{2+}$  signalling in *Arabidopsis* could not be confirmed. Instead, the data obtained in this and other studies collectively suggest a function of TPC1 in  $Ca^{2+}$ -dependent  $K^+$  homeostasis.

### 2.1.2. Publication

*The Plant Journal* (2008) **53**, 287–299

doi: 10.1111/j.1365-313X.2007.03342.x

## Loss of the vacuolar cation channel, AtTPC1, does not impair Ca<sup>2+</sup> signals induced by abiotic and biotic stresses

Stefanie Ranf<sup>1,†</sup>, Petra Wünnenberg<sup>2,†</sup>, Justin Lee<sup>1</sup>, Dirk Becker<sup>3</sup>, Marcel Dunkel<sup>3</sup>, Rainer Hedrich<sup>3</sup>, Dierk Scheel<sup>1</sup> and Petra Dietrich<sup>2,\*</sup>

<sup>1</sup>Leibniz Institute of Plant Biochemistry, Stress and Developmental Biology, Weinberg 3, D-06120 Halle, Germany,

<sup>2</sup>University of Erlangen, Institute of Biology, Molecular Plant Physiology, Staudtstrasse 5, D-91058 Erlangen, Germany, and

<sup>3</sup>University of Würzburg, Julius-von-Sachs-Institute, Molecular Plant Physiology and Biophysics, Julius-von-Sachs-Platz 2, D-97082 Würzburg, Germany

Received 23 July 2007; accepted 27 September 2007.

\*For correspondence (fax +49 9131 28751; e-mail dietrich@biologie.uni-erlangen.de).

†These authors contributed equally to this paper.

### Summary

The putative two-pore Ca<sup>2+</sup> channel TPC1 has been suggested to be involved in responses to abiotic and biotic stresses. We show that AtTPC1 co-localizes with the K<sup>+</sup>-selective channel AtTPK1 in the vacuolar membrane. Loss of AtTPC1 abolished Ca<sup>2+</sup>-activated slow vacuolar (SV) currents, which were increased in AtTPC1-over-expressing *Arabidopsis* compared to the wild-type. A Ca<sup>2+</sup>-insensitive vacuolar cation channel, as yet uncharacterized, could be resolved in *tpc1-2* knockout plants. The kinetics of ABA- and CO<sub>2</sub>-induced stomatal closure were similar in wild-type and *tpc1-2* knockout plants, excluding a role of SV channels in guard-cell signalling in response to these physiological stimuli. ABA-, K<sup>+</sup>, and Ca<sup>2+</sup>-dependent root growth phenotypes were not changed in *tpc1-2* compared to wild-type plants. Given the permeability of SV channels to mono- and divalent cations, the question arises as to whether TPC1 *in vivo* represents a pathway for Ca<sup>2+</sup> entry into the cytosol. Ca<sup>2+</sup> responses as measured in aequorin-expressing wild-type, *tpc1-2* knockout and TPC1-over-expressing plants disprove a contribution of TPC1 to any of the stimulus-induced Ca<sup>2+</sup> signals tested, including abiotic stresses (cold, hyperosmotic, salt and oxidative), elevation in extracellular Ca<sup>2+</sup> concentration and biotic factors (elf18, flg22). In good agreement, stimulus- and Ca<sup>2+</sup>-dependent gene activation was not affected by alterations in TPC1 expression. Together with our finding that the loss of TPC1 did not change the activity of hyperpolarization-activated Ca<sup>2+</sup>-permeable channels in the plasma membrane, we conclude that TPC1, under physiological conditions, functions as a vacuolar cation channel without a major impact on cytosolic Ca<sup>2+</sup> homeostasis.

**Keywords:** SV channel, TPC1, *Arabidopsis thaliana*, vacuole, Ca<sup>2+</sup> signalling, K<sup>+</sup> homeostasis.

### Introduction

#### *AtTPC1*, a putative Ca<sup>2+</sup> channel

In plants, an array of plasma membrane and endomembrane Ca<sup>2+</sup>-permeable channels has been characterized electrophysiologically (Sanders *et al.*, 2002). In *Arabidopsis thaliana*, a sole member with homology to the voltage-dependent Ca<sup>2+</sup> channel (Ca<sub>v</sub>) family in animal systems exists (*Arabidopsis* Genome Initiative, 2000). In contrast to these four-domain-containing channels in animals, with a total of 24 transmembrane spans, the *Arabidopsis* singleton AtTPC1 is composed of only two domains with six transmembrane spans each. Two EF-hand motifs within

the cytosolic linker suggest Ca<sup>2+</sup>-dependent regulation of the protein.

Ca<sup>2+</sup> transport activity has been postulated for AtTPC1 and its homologs in tobacco (*NtTPC1a* and *NtTPC1b*), rice (*OsTPC1*) and wheat (*TaTPC1*), after heterologous expression in yeast (Furuichi *et al.*, 2001; Kadota *et al.*, 2004; Kurusu *et al.*, 2004; Wang *et al.*, 2005). NtTPC1s have been characterized as a pathway for Ca<sup>2+</sup> entry across the plasma membrane in tobacco cells in response to cold shock, sucrose, H<sub>2</sub>O<sub>2</sub>, salicylic acid, as well as elicitors (Kadota *et al.*, 2004; Kawano *et al.*, 2004; Lin *et al.*, 2005). OsTPC1 has been proposed to localize in the plasma membrane and

288 Stefanie Ranf et al.

to represent a key regulator of elicitor-induced defence responses (Kurusu *et al.*, 2005). TaTPC1 has been reported to reside in the plasma membrane and to function in response to abiotic stresses (Wang *et al.*, 2005). In strong contrast, a vacuolar localization of AtTPC1 was also found (Carter *et al.*, 2004; Peiter *et al.*, 2005). Careful electrophysiological analysis showed that patches excised from *tpc1-2* knockout vacuoles lack cation currents of the slow vacuolar (SV) type, while *AtTPC1*-over-expressing cells exhibited elevated SV channel activities (Peiter *et al.*, 2005).

#### SV channels in the vacuole

Slowly activating vacuolar (SV) channels open in response to depolarization in the presence of elevated cytosolic  $\text{Ca}^{2+}$  concentrations (Hedrich and Neher, 1987). Interestingly, in addition to  $\text{K}^+$  and  $\text{Na}^+$ , significant permeability for  $\text{Ca}^{2+}$  has been documented in the presence of  $\text{Ca}^{2+}$  as the major charge carrier (Allen and Sanders, 1996; Pottosin *et al.*, 2001; Ward and Schroeder, 1994), thus stimulating an ongoing discussion about the role of SV channels as a source for  $\text{Ca}^{2+}$ -induced  $\text{Ca}^{2+}$  release (CICR) across the vacuolar membrane, and subsequent elevation of cytosolic  $\text{Ca}^{2+}$  concentration (Barkla and Pantoja, 1996; Bewell *et al.*, 1999; Pottosin *et al.*, 1997; Sanders *et al.*, 2002; Ward and Schroeder, 1994, 1997). In guard cells, SV channels may also mediate  $\text{K}^+$  efflux during stomatal closure. Thus, the molecular identification of the SV channel as a distantly related member of the voltage-dependent  $\text{Ca}^{2+}$  channel family (Furuichi *et al.*, 2001) has re-opened the question of its physiological role in  $\text{K}^+$  and  $\text{Ca}^{2+}$  homeostasis.

In this study, we re-evaluated the localization of TPC1, and extended the electrophysiological analysis of *tpc1-2* mutants and *TPC1* over-expressors to the whole-vacuole level, supporting the finding that TPC1 causes SV-type currents in *Arabidopsis thaliana*. Germination and root growth assays, as well as gas exchange measurements, revealed no phenotype in *tpc1-2* mutants under the various conditions tested. The question of whether TPC1 transports  $\text{Ca}^{2+}$  into the cytosol was addressed using the aequorin  $\text{Ca}^{2+}$  reporter system. From a detailed comparison of  $\text{Ca}^{2+}$  responses and  $\text{Ca}^{2+}$ -dependent gene activation between wild-type, *tpc1-2* knockout and *TPC1*-over-expressing plants, a function in  $\text{Ca}^{2+}$  release from the vacuole or  $\text{Ca}^{2+}$  entry via the plasma membrane in response to various biotic and abiotic stresses can be excluded. Together, our results suggest that TPC1 functions as a cation channel without impact on cytosolic  $\text{Ca}^{2+}$  homeostasis.

#### Results

Transient co-expression of *AtTPC1* with the vacuolar  $\text{K}^+$  channel *AtTPK1* (Czempinski *et al.*, 2002; Schönknecht *et al.*, 2002) N-terminally fused to mRFP1 and mGFP4, respectively,

gave rise to fluorescence signals predominantly in the vacuolar membrane and not in the plasma membrane (Figure 1a). These data obtained in onion epidermal cells confirm the results from *Arabidopsis* mesophyll cells (Peiter *et al.*, 2005), and are in contrast to the localization of *AtTPC1*, *OsTPC1* and *TaTPC1* in the plasma membrane of BY-2 and onion epidermal cells (Kawano *et al.*, 2004; Kurusu *et al.*, 2005; Wang *et al.*, 2005).

#### Loss of TPC1 abolishes $\text{Ca}^{2+}$ -activated SV currents

We used the whole-vacuole configuration of the patch-clamp technique to enable the detection of possibly low numbers of active channels in the *tpc1-2* mutant, which could escape observation in excised patches. The results shown in Figure 1(b,c) completely confirm studies on excised patches by Peiter *et al.* (2005). In the wild-type, SV currents in the mesophyll vacuole are able to saturate the patch-clamp amplifier at 20 nA, while no SV currents were recorded in *tpc1-2* mutants under the same conditions. SV currents in *TPC1*-over-expressing vacuoles exceeded those obtained in the wild-type (Figure 1b,c), and emphasize the fact that, under reducing conditions,  $\text{K}^+$  release into the cytosol (inward currents in Figure 1b,c) can occur between  $-50$  mV and the Nernst potential for  $\text{K}^+$ , which is  $+17$  mV under the experimental conditions used (Figure 1b). In excised vacuolar side-in patches, single channels of about 43 pS could be resolved in membranes from wild-type and *TPC1*-over-expressing plants, but were absent from *tpc1-2* patches (Figure 1d). Instantaneous currents, probably due to the activity of fast vacuolar (FV) channels (Hedrich and Neher, 1987; Schönknecht *et al.*, 2002), were not affected by alterations in TPC1 expression (Figure 1e).

When cytosolic  $\text{Ca}^{2+}$  concentrations were reduced in wild-type samples using 10 mM EGTA in the absence of  $\text{Ca}^{2+}$ , SV channels remained silent due to their intrinsic  $\text{Ca}^{2+}$  sensitivity (Hedrich and Neher, 1987), but another time-dependent current component became visible at voltages  $>140$  mV (Figure 2a,c). The lack of SV channels in the *tpc1-2* mutant allowed us to show that the latter conductance is activated independently of the cytosolic  $\text{Ca}^{2+}$  concentration (Figure 2b,c). We therefore named this channel the  $\text{Ca}^{2+}$ -insensitive vacuolar channel (CIVC). A single channel conductance of 13 pS further distinguishes CIVC from the SV and FV channels (Figure 2d). Although how CIVC is activated *in vivo* remains unknown, its  $\text{Ca}^{2+}$  insensitivity, together with a significant  $\text{Na}^+$  permeability  $P_{\text{Na}:P_{\text{K}}}$  of  $1.06 \pm 0.02$  ( $n = 3$ ), as determined in the *tpc1-2* mutant, suggests that it may complement SV functions under conditions inhibiting  $\text{Ca}^{2+}$ -sensitive FV channels, i.e. elevated cytosolic  $\text{Ca}^{2+}$  concentrations (Allen and Sanders, 1996).

In contrast to the tonoplast localization shown here and elsewhere (Carter *et al.*, 2004; Peiter *et al.*, 2005), TPC1 has been proposed to represent a plasma membrane

**Figure 1.** TPC1 functions in the vacuolar membrane.

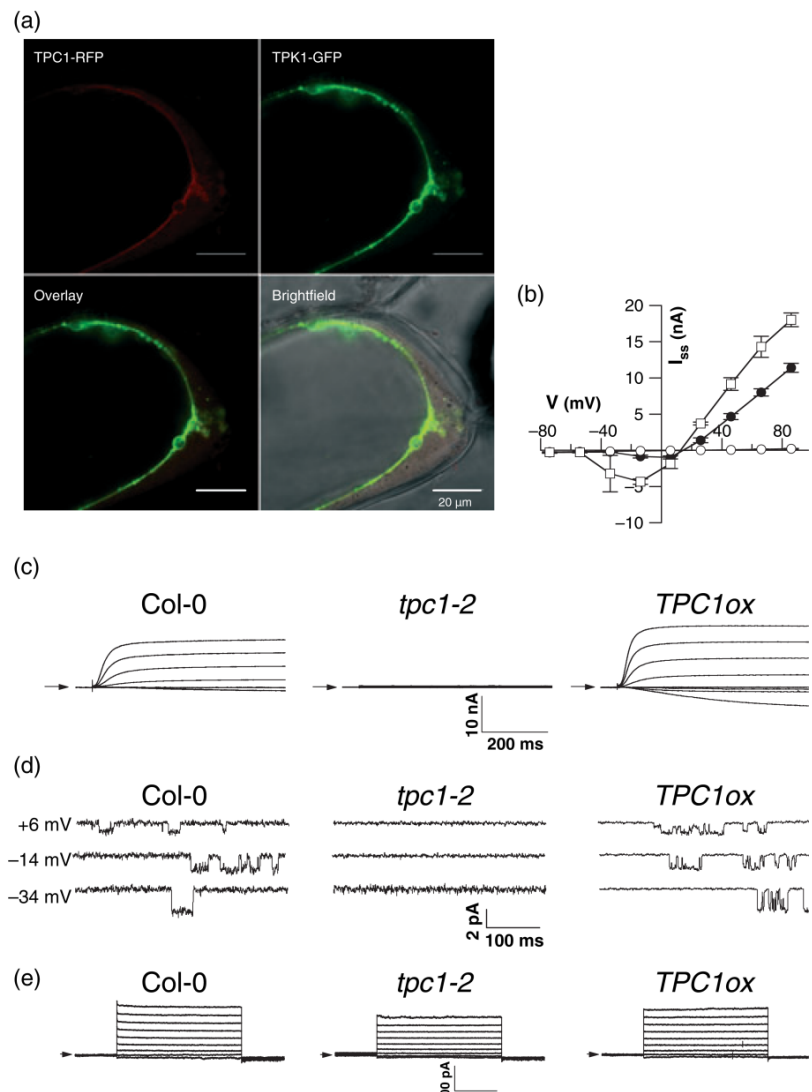
(a) TPC1-RFP1 (red) and TPK1-GFP (green) fluorescence after transient expression in onion epidermal cells. Bars = 20  $\mu$ m.

(b) Current–voltage relations of steady-state currents determined from traces as shown in (c), for wild-type (closed circles,  $n = 13$ ), *tpc1-2* mutants (open circles,  $n = 9$ ) and *TPC1*-over-expressing plants (open squares,  $n = 6$ ). Data represent means  $\pm$  SE.

(c) Whole-vacuolar currents from wild-type (left), *tpc1-2* knockout plants (middle) and *TPC1*-over-expressing plants (right). Currents were elicited by 600 msec test voltages between  $-74$  and  $+86$  mV in 20 mV increments. The presence of SV-type currents in wild-type and *TPC1*-over-expressing samples and their absence in *tpc1-2* were observed without exception.

(d) Single-channel fluctuations in vacuolar side-in patches from vacuoles derived from wild-type (left) and *TPC1*-over-expressing plants (right), but not in those from *tpc1-2* plants (middle). Currents were measured at the voltages indicated. The traces were selected to show openings of a single SV channel and could already be resolved at negative voltages (compare Figures 1b, 2a and 4a,b).

(e) Instantaneous currents in wild-type (left), *tpc1-2* knockout (middle) and *TPC1*-over-expressing plants (right). Currents were measured  $\leq 2$  min after whole-vacuolar access, before disappearance in Ca<sup>2+</sup>-containing solutions. Test pulses were applied between  $-74$  and  $+86$  mV in 20 mV increments, starting from a holding potential of  $-54$  mV. Traces are representative for 31 (Col-0), 15 (*TPC1* over-expressors) and 40 (*tpc1-2*) measurements.



Ca<sup>2+</sup>-permeable channel (Furuichi *et al.*, 2001; Hashimoto *et al.*, 2004; Kadota *et al.*, 2004; Kawano *et al.*, 2004; Kurusu *et al.*, 2004, 2005; Lin *et al.*, 2005; Wang *et al.*, 2005). The dominant plasma membrane Ca<sup>2+</sup>-permeable channel is activated by hyperpolarization (Grabov and Blatt, 1998; Pei *et al.*, 2000; Stoelzle *et al.*, 2003). In the mesophyll plasma membrane of wild-type and *tpc1-2* mutant plants, we resolved similar cation current amplitudes upon hyperpolarization (Figure 3), excluding the possibility that AtTPC1 mediates this type of Ca<sup>2+</sup> current.

#### Root growth and germination of *tpc1-2* mutants

SV channels in the tonoplast are Ca<sup>2+</sup>-permeable (Allen and Sanders, 1994; Peiter *et al.*, 2005; Pottosin *et al.*, 2001; Ward and Schroeder, 1994). In the species tested so far, SV channels are equally permeable to K<sup>+</sup> and Na<sup>+</sup>, and,

accordingly, a value of  $P_{Na}:P_K$  of  $0.96 \pm 0.06$  ( $n = 3$ ) was determined in Arabidopsis under bi-ionic conditions. However, elevated vacuolar Na<sup>+</sup>, Cs<sup>+</sup> or Ca<sup>2+</sup> concentrations shift the voltage dependence of the channel towards depolarized potentials, and reduce the possibility of cation release to the cytoplasm (Figure 4a,b) (Allen and Sanders, 1996; Ivashikina and Hedrich, 2005). Thus, any cation release function of TPC1 depends on the vacuolar and cytosolic cation composition. Under standard growth conditions, *tpc1-2* plants do not develop a characteristic phenotype, and a prediction concerning the exact role of TPC1 in K<sup>+</sup> and/or Ca<sup>2+</sup> homeostasis is therefore difficult. We tested a putative role of *TPC1* in germination and root growth under various cationic conditions. On agar plates containing K<sup>+</sup> concentrations between 50  $\mu$ M and 1 mM, germination rates were similar in the wild-type and the *tpc1-2* mutant (Figure 4c). Germination rates were also unaffected by changes in water

290 Stefanie Ranf et al.

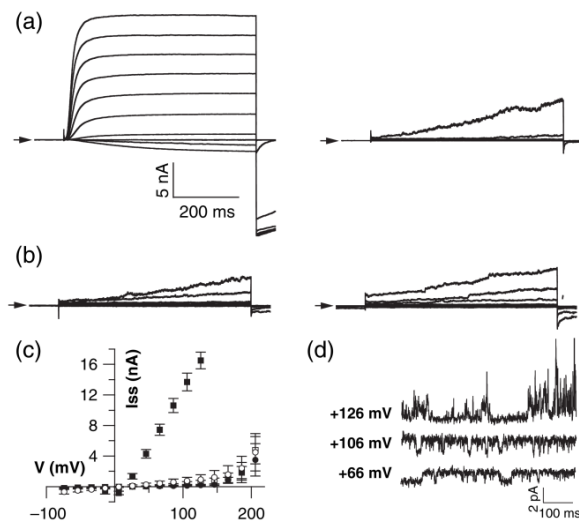


**Figure 2.** Comparison of  $\text{Ca}^{2+}$ -sensitive and -insensitive channels in wild-type and *tpc1-2* mutant plants.

(a) Whole-vacuolar currents from wild-type plants recorded before (left) and after (right) exchange of 1 mM  $\text{Ca}^{2+}$  against 10 mM EGTA in the bath solution. (b) Whole-vacuolar currents from *tpc1-2* mutants recorded as in (a).

(c) Corresponding current-voltage relations of whole-vacuolar currents in the presence (closed symbols) and in the absence (open symbols) of  $\text{Ca}^{2+}$  for wild-type (squares,  $n = 5$ ) and *tpc1-2* (circles,  $n = 3$ ). Data represent means  $\pm$  SE.

(d) Single-channel fluctuations for  $\text{Ca}^{2+}$ -insensitive channels in *tpc1-2* at the indicated voltages.

Currents were measured at test voltages between  $-74$  and  $+226$  mV in 20 mV increments, except for wild-type SV currents in the presence of  $\text{Ca}^{2+}$ , which were recorded between  $-74$  and  $+146$  mV only [left traces in (a); closed squares in (c)].

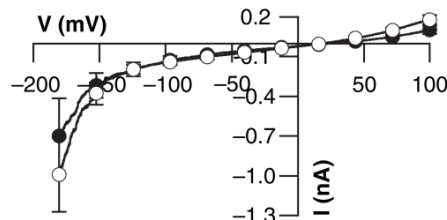


**Figure 3.** Hyperpolarization-activated  $\text{Ca}^{2+}$ -permeable channels in the plasma membrane are not affected in the *tpc1-2* mutant.

Current-voltage relations of hyperpolarization-activated channels in wild-type ( $n = 11$ , closed circles) and *tpc1-2* knockout plants ( $n = 20$ , open circles). Data represent means  $\pm$  SE. Currents were elicited in the whole-cell configuration by voltage ramps from  $+99.5$  to  $-181.5$  mV over 2000 msec. Pipette solution: 150 mM K-gluconate, 10 mM EGTA, 3 mM  $\text{MgCl}_2$ , 1 mM MgATP, 10 mM HEPES, pH 7.4/Tris; bath solution: 40 mM Ca-gluconate, 10 mM MES, pH 5.6/Tris.

potential (0, 5, 10 and 20% PEG 8000, data not shown). No difference in root growth between wild-type and mutant was observed at  $\text{K}^+$  concentrations between 5 and 105 mM (Figure 4d).  $\text{Ca}^{2+}$ -dependent effects on root growth were also equal in wild-type and *tpc1-2* mutant seedlings (Figure 4e). The phytohormone ABA inhibits root growth at 10–50  $\mu\text{M}$  in

the wild-type, and this did not differ in the *tpc1-2* mutant (Figure 4f).

#### Stomatal closure in the *tpc1-2* mutant

$\text{Ca}^{2+}$ -activated SV channels in the tonoplast have been proposed to fulfil a dual function, i.e.  $\text{K}^+$  homeostasis and CICR during stomatal responses to ABA and  $\text{CO}_2$ , for example (MacRobbie, 2000; Sanders *et al.*, 2002). We used gas exchange measurements in order to follow the kinetics of stomatal movement in the intact leaf. After feeding 100  $\mu\text{M}$  ABA via the petiole, stomatal closure was comparable between *tpc1-2* and wild-type plants (Figure 5a), in agreement with previous observations (Peiter *et al.*, 2005). In response to elevated  $\text{CO}_2$  concentration, which, like ABA, induces a rise in the cytoplasmic  $[\text{Ca}^{2+}]$  (Webb *et al.*, 1996), stomata of wild-type and *tpc1-2* leaves closed with the same kinetics (Figure 5b), indicating that the lack of TPC1 does not interfere with guard-cell  $\text{Ca}^{2+}$  signalling. The results furthermore show that, if TPC1 does play a role as a  $\text{K}^+$  channel, it is not rate-limiting for stomatal closure.

#### TPC1 does not contribute to $\text{Ca}^{2+}$ responses and gene expression induced by abiotic stresses

Cold, mannitol and high salinity, as well as oxidative stress, induce a transient rise in the cytosolic  $\text{Ca}^{2+}$  concentration, involving  $\text{Ca}^{2+}$  entry via the plasma membrane, as well as  $\text{Ca}^{2+}$  release from intracellular stores including the vacuole. Depending on the stimulus, the degree of vacuolar contribution to the  $\text{Ca}^{2+}$  signature varies, with mannitol and salt stress drawing on the vacuolar  $\text{Ca}^{2+}$  store to a larger extent than cold and  $\text{H}_2\text{O}_2$  (Knight *et al.*, 1996, 1997b). We used these abiotic stress stimuli in order to determine the role of TPC1 as a mediator of  $\text{Ca}^{2+}$  release into the cytosol. Changes in  $[\text{Ca}^{2+}]_{\text{cyt}}$  were resolved using  $\text{Ca}^{2+}$ -induced cytosolic aequorin luminescence, and showed no difference between wild-type, *tpc1-2* mutant and *TPC1*-over-expressing plants (Figure 6a–d). According to these results, TPC1 does not contribute to the  $\text{Ca}^{2+}$  release pathway involved in the elevation of  $[\text{Ca}^{2+}]_{\text{cyt}}$  in response to any of the stimuli tested. Elevation of the extracellular  $\text{Ca}^{2+}$  concentration has been shown to raise the cytosolic  $\text{Ca}^{2+}$  concentration by drawing on extra- and intracellular  $\text{Ca}^{2+}$  stores (Han *et al.*, 2003; McAinsh *et al.*, 1995). No difference in cytosolic  $\text{Ca}^{2+}$  concentration changes between wild-type, *tpc1-2* mutant and *TPC1*-over-expressing plants was measurable in response to 10 mM external  $\text{Ca}^{2+}$  (Figure 6e).

As a complementary approach, we determined stress-induced gene activation known to require an upstream  $\text{Ca}^{2+}$  signal. Expression of  $\Delta^1$ -pyrroline-5-carboxylate synthetase (*P5CS1*), the first enzyme of the proline biosynthesis pathway, was equally induced in wild-type, *tpc1-2* knockout and *TPC1*-over-expressing plants in response to mannitol and

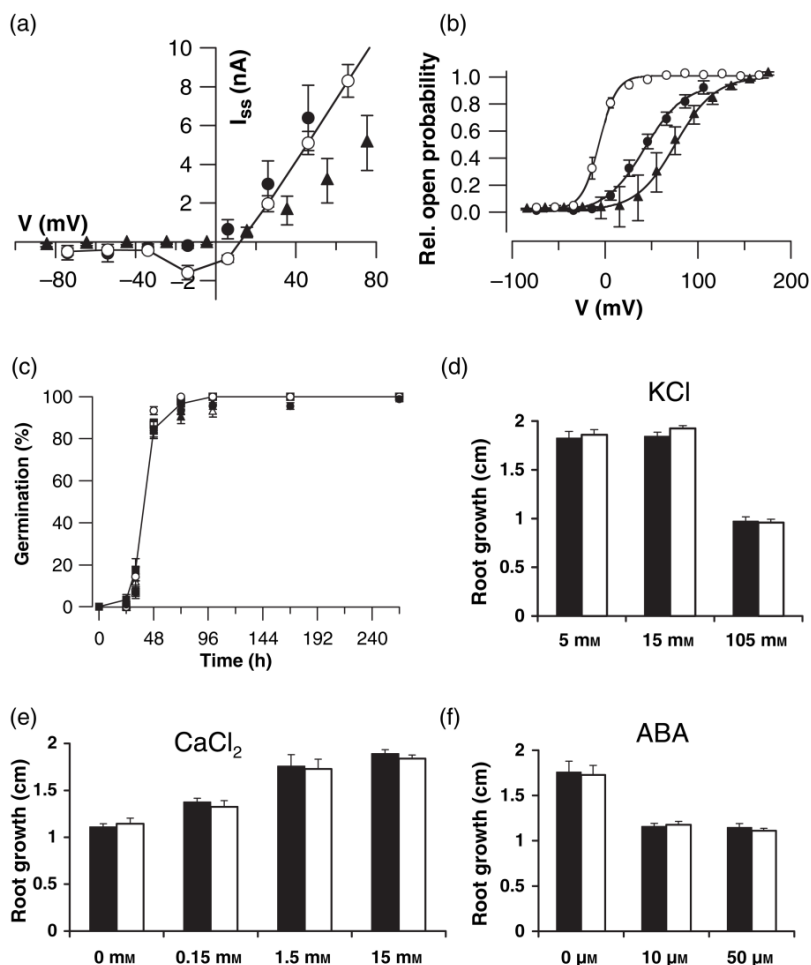
**Figure 4.** Regulation of wild-type TPC1 activity by cations, and lack of germination and root phenotype in *tpc1-2* mutants.

(a) Steady-state current–voltage relations of wild-type SV currents in the presence of 100 mM K<sup>+</sup> (open circles and line, *n* = 6), Na<sup>+</sup> (closed triangles, *n* = 3) or Cs<sup>+</sup> (closed circles, *n* = 5) on the vacuolar side.

(b) Relative open probabilities of SV channels in the presence of 100 mM K<sup>+</sup> (open circles), Cs<sup>+</sup> (closed circles) or Na<sup>+</sup> (closed triangles) on the vacuolar side. Data were fitted using the Boltzmann equation with half-maximal activation potentials ( $V_{1/2}$ ) of  $-6.2 \pm 2.6$  mV (*n* = 6) for K<sup>+</sup>,  $+42.6 \pm 5.6$  mV (*n* = 4) for Cs<sup>+</sup>, and  $+75.6 \pm 16$  mV (*n* = 5) for Na<sup>+</sup>.

Data in (a) and (b) represent means  $\pm$  SE. Whole-vacuolar currents were recorded at test pulses between  $-74$  and  $+126$  mV in 20 mV increments, starting from a holding potential of  $-54$  mV in standard external solution.

(c) Germination of *tpc1-2* (open symbols) versus wild-type seeds (closed symbols) in the presence of various K<sup>+</sup> concentrations. Data represent means  $\pm$  SE (*n* = 6; total of 90 seeds) for 50  $\mu$ M (triangle), 500  $\mu$ M (square) and 1 mM (circle) KCl. (d–f) Root growth within 4 days after transfer to various K<sup>+</sup> (d), Ca<sup>2+</sup> (e) and ABA (f) conditions. Data points for wild-type (black bars) and *tpc1-2* (white bars) represent means of seven ( $\pm$ SE; total of 70 plants). Note that 0 mM in (e) corresponds to 50  $\mu$ M Ca<sup>2+</sup>.



salt treatment (Figure 6f), confirming that the elevation in  $[Ca^{2+}]_{cyt}$  required for gene activation (Knight *et al.*, 1997b) was not altered in *tpc1-2* knockouts or *TPC1* over-expressors. Similarly, Ca<sup>2+</sup>-dependent induction of *RD29a* by osmotic/drought, cold and salt stresses (Cheong *et al.*, 2003; Kim *et al.*, 2003; Wu *et al.*, 1997) and induction of *GST1* by H<sub>2</sub>O<sub>2</sub> (Rentel and Knight, 2004) was comparable in *tpc1-2* knockout, *TPC1*-over-expressing and wild-type plants (Figure 6f).

#### *TPC1* does not contribute to Ca<sup>2+</sup> responses, oxidative burst or gene expression induced by biotic interactions

Induction of defence responses induced by pathogen-associated molecular patterns (PAMPs) was tested using the bacterial elongation factor Tu N-terminal peptide, elf18, as well as the peptide flg22 that corresponds to the conserved N-terminal part of bacterial flagellin. Both peptides have been shown to act as potent elicitors of the pathogen response, including extracellular alkalization, oxidative burst and defence gene activation (Felix *et al.*, 1999; Gomez-Gomez *et al.*, 1999; Kunze *et al.*, 2004; Zipfel *et al.*,

2006), while their role in Ca<sup>2+</sup> signalling during the defence response has not yet been documented. We show here that treatment of leaf discs with elf18 induced a prolonged Ca<sup>2+</sup> response after a lag phase of about 1 min (Figure 7a), indicating that the peptide is effective in elicitation of Ca<sup>2+</sup> responses as has been shown for other peptide/protein elicitors, such as pep13 in parsley (Blume *et al.*, 2000; Zimmermann *et al.*, 1997) and cryptogein in tobacco (Lecourieux *et al.*, 2002). A Ca<sup>2+</sup> signature of similar amplitude and kinetics was induced by treatment with flg22 (Figure 7a). Changes in  $[Ca^{2+}]_{cyt}$  are required for downstream defence reactions, including accumulation of reactive oxygen species during the plant–pathogen interaction (Nürnberg and Scheel, 2001). Treatment with the elicitors elf18 and flg22 induced the production of reactive oxygen species such as H<sub>2</sub>O<sub>2</sub> (Figure 7d, and data not shown), and this production could be completely blocked using the NADPH oxidase inhibitor diphenylene iodonium chloride (DPI, 25  $\mu$ M), or the Ca<sup>2+</sup> channel blocker LaCl<sub>3</sub> (10 mM), indicating Ca<sup>2+</sup> dependence of the oxidative burst via NADPH oxidase (data not shown). Accordingly, elf18 led to increased *FRK1*

292 Stefanie Ranf et al.

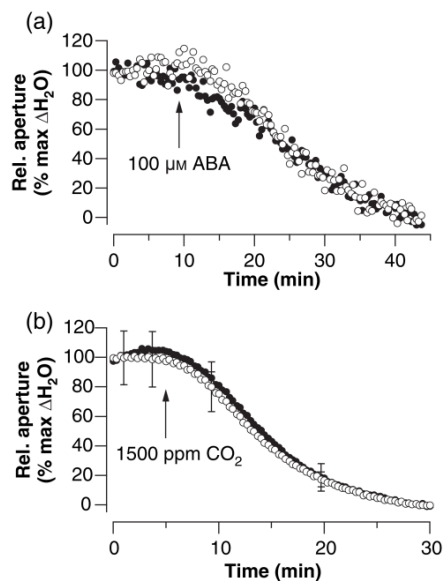


**Figure 5.** Kinetics of stomatal closure in wild-type and *tpc1-2* mutant plants. (a) Gas exchange in wild-type (closed circles) and *tpc1-2* knockout plants (open circles) before and after feeding 100 μM ABA (arrow) via the petiole of detached leaves. (b) Gas exchange in intact leaves of wild-type (closed circles) and *tpc1-2* knockout plants (open circles) after a shift from 50 to 1500 ppm CO<sub>2</sub> (arrow). Data represent means ± SE ( $n = 3$  for WT;  $n = 5$  for *tpc1-2*). Stomatal movement is expressed as the change in water loss relative to the maximum value.

and *GST1* expression in seedlings (Figure 7c), as was previously shown for the peptide elicitor flg22 (Asai *et al.*, 2002). No difference in the elf18- and flg22-induced Ca<sup>2+</sup> signature, oxidative burst and marker gene activation was observed between wild-type, *tpc1-2* knockout and *TPC1*-over-expressing plants (Figure 7a,c,d, and data not shown). flg22 induced a growth inhibition of the same extent in *tpc1-2* knockout, *TPC1*-over-expressing and wild-type seedlings (data not shown). H<sub>2</sub>O<sub>2</sub> accumulation in leaves infiltrated with an avirulent pathogen, *Pseudomonas syringae* pv. tomato (avrB), was also comparable between wild-type and *tpc1-2* knockout plants (Figure 7e).

We could not detect any Ca<sup>2+</sup> elevation following the addition of salicylate (Figure 7b), which accumulates during the plant defence response (Nürnberg and Scheel, 2001). It should be noted that the use of free salicylic acid caused some disturbance of the Ca<sup>2+</sup> homeostasis (data not shown), probably due to non-specific pH effects. However, salicylate induced *PR-1* expression to a similar extent in wild-type, mutant and over-expressing plants (Figure 7c). These results show that salicylate does not induce a rise in cytosolic Ca<sup>2+</sup> concentration, as has been previously reported using salicylic acid (Lin *et al.*, 2005). In conclusion, by probing for defence-related Ca<sup>2+</sup> signatures and oxidative burst, as well as downstream gene activation, we could

disprove any role of *TPC1* in these plant defence signal transduction pathways.

Finally, taken all together, our analyses covering electrophysiology, *in vivo* measurements of Ca<sup>2+</sup> signatures and Ca<sup>2+</sup>-dependent stress responses support our hypothesis that *AtTPC1* does not function as a Ca<sup>2+</sup> channel *in vivo*.

## Discussion

### *AtTPC1* function in pathogen responses

*TPC1* is considered to represent a key regulator of elicitor-induced hypersensitive cell death, activation of MAP kinases and defence-related genes in rice and tobacco cells (Kadota *et al.*, 2004; Kurusu *et al.*, 2005). As the elicitor-induced oxidative burst was not suppressed in *Ostpc1* knockout mutants, *TPC1* was suggested as a downstream candidate for H<sub>2</sub>O<sub>2</sub>-induced Ca<sup>2+</sup> entry. Our data strongly argue against this hypothesis, as Ca<sup>2+</sup> responses to H<sub>2</sub>O<sub>2</sub> at 10 mM (Figure 6d), 100 μM and 25 μM (data not shown) were identical, and downstream expression of *GST1* was not altered (Figure 6f) in wild-type, *tpc1-2* mutant and *TPC1*-over-expressing Arabidopsis plants. In response to the peptide elicitors elf18 and flg22, a transient rise in [Ca<sup>2+</sup>]<sub>cyt</sub> could be demonstrated. Its amplitude and kinetics were similar in wild-type, *tpc1-2* knockout and *TPC1*-over-expressing plants. No reduction or delay in MAPK activation was observed in *tpc1-2* mutant plants treated with either elf18 or flg22, compared to wild-type plants (data not shown). Pathogen-related gene expression and a pathogen-induced oxidative burst occurred independently of the *AtTPC1* expression level. In accordance with our results using bacterial pathogens and elicitors that predominantly induce salicylate signalling, Bonaventure *et al.* (2007) recently reported no difference between wild-type and *tpc1-2* knockout plants in response to infection with the necrotrophic fungus *Botrytis cinerea*, which induces the jasmonate pathway, or in MeJA-induced root growth inhibition. Instead, the effects that they did observe, such as enhanced resistance to *B. cinerea* and elevated oxylipin levels, were seen only in a gain-of-function mutation of *AtTPC1* (*fou2*) that probably leads to mis-regulation of its function – indicating that *AtTPC1 per se* is not involved in these defence processes.

Taken together, this leads us to conclude that *TPC1* does not play a crucial role in the signalling pathways of plant defence induced by bacterial or fungal pathogens, nor of the defence-related plant hormones salicylate and jasmonate.

### *AtTPC1* function in Ca<sup>2+</sup> homeostasis

In several reports, *TPC1* has been suggested to mediate Ca<sup>2+</sup> entry across the plant plasma membrane in response to cold shock, sucrose, oxidative stress, elicitors and salicylic acid (Furuichi *et al.*, 2001; Kadota *et al.*, 2004; Kawano *et al.*,

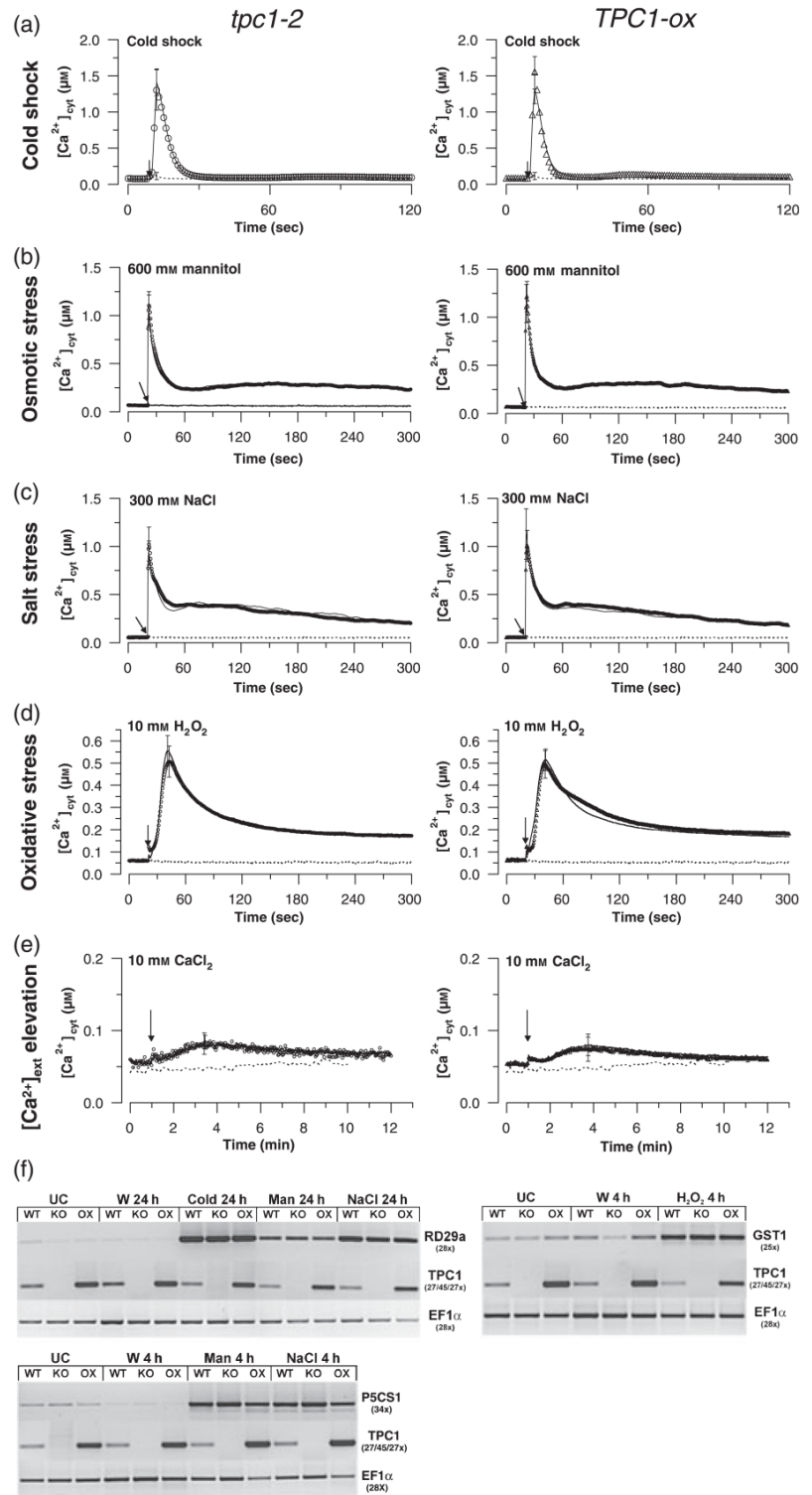
*Ca<sup>2+</sup> signals are not impaired by loss of AtTPC1* 293

**Figure 6.** Elevation of cytosolic  $Ca^{2+}$  concentration and gene activation induced by abiotic stresses are not altered in *tpc1-2* mutants and *TPC1* over-expressors.

- (a) Cold shock was applied by addition of 1 volume ice-cold water.  
 (b) Osmotic stress was simulated by the addition of 600 mM mannitol.  
 (c)  $Ca^{2+}$  response (300 mM NaCl).  
 (d) Oxidative stress was induced by 10 mM  $H_2O_2$ .  
 (e) External  $Ca^{2+}$  concentration was elevated to 10 mM.

(f) Results from RT-PCR analysis of four stress-related genes: *RD29a* induced by cold, mannitol and NaCl stress, *GST1* induced by oxidative stress, and *P5CS1* induced by mannitol and NaCl stress were visualized in wild-type (WT), *tpc1-2* (KO) and *TPC1*-over-expressing line 10.21 (OX). *EF1 $\alpha$*  was used as a constitutive control. Numbers of PCR cycles are indicated in parentheses. UC, untreated control; W, water control; Man, mannitol.

For (a), cytosolic  $Ca^{2+}$  concentrations were calculated from relative aequorin luminescence measured in leaf discs using 1 sec integration intervals, for (b)–(d) in seedlings using 0.5 sec integration intervals, and for (e) in leaf discs without lower epidermis using 2 sec integration intervals. Data represent means  $\pm$  SD,  $n \geq 5$ . Left graphs: pMAQ2/*TPC1* (WT) (solid lines), pMAQ2/*tpc1-2* (KO) (open circles). Right graphs: pMAQ2 (solid lines), pMAQ2/35S::*TPC1* (OX) (open triangles). Two independent controls were performed (see Experimental procedures for details). Dotted lines represent data obtained upon application of water as a control.



2004; Lin *et al.*, 2005), and across the plasma membrane of yeast cells after heterologous expression (Hashimoto *et al.*, 2004; Wang *et al.*, 2005). In contrast, our results obtained

from aequorin luminescence measurements strongly suggest that *TPC1* is not involved in the  $Ca^{2+}$  response to any of the tested stimuli (Figures 6 and 7). The discrepancy between

294 Stefanie Ranf et al.

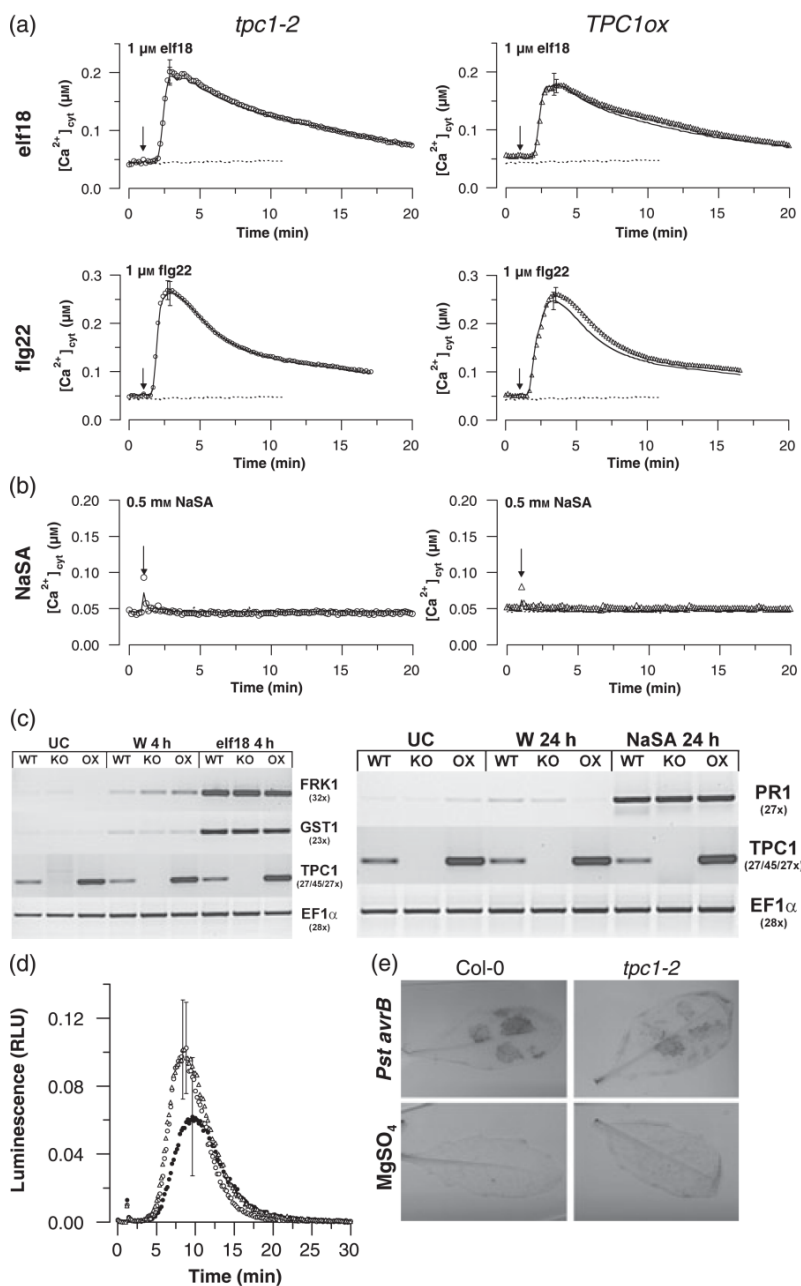


**Figure 7.** Elevation of cytosolic  $Ca^{2+}$  concentration, oxidative burst and gene activation in response to biotic stresses are not altered in  $tpc1-2$  mutants and  $TPC1$  over-expressors.

(a)  $Ca^{2+}$  response after challenge with the elicitors elf18 or flg22 ( $1 \mu M$ , leaf discs, 10 sec integration interval) following a lag phase of about 1 min in two independent wild-type controls (lines in left and right graphs, respectively),  $tpc1-2$  (open circles) and  $TPC1$ -over-expressing lines (open triangles). Data represent means  $\pm$  SD,  $n \geq 5$ .

(b) Lack of  $[Ca^{2+}]_{cyt}$  elevation after addition of  $500 \mu M$  sodium salicylate (seedlings, 10 sec integration interval). Data represent means  $\pm$  SD,  $n \geq 5$ . Symbols as in (a).

(c) Results from RT-PCR analysis of gene expression induced by biotic stresses: *FRK1* and *GST1* induced by elf18 ( $10 \mu M$ ) and *PR-1* by sodium salicylate ( $500 \mu M$ ). W, water control; NaSA, sodium salicylate

(d) Oxidative burst in response to treatment with  $1 \mu M$  elf18 in leaf slices from wild-type (closed circles),  $tpc1-2$  (open circles) and  $TPC1$ -over-expressing line 10.21 (open triangles), as determined using a luminol-based assay.

(e) Oxidative burst in response to infection by avirulent *Pseudomonas syringae* pv. tomato (*Pst avrB*) in wild-type (left) and  $tpc1-2$  knockout plants (right), as determined using DAB staining. Leaves were infiltrated with *Pst* DC 3000 *avrB* (upper images) or  $10 mM$   $MgSO_4$  (lower images).  $Ca^{2+}$  measurements and RT-PCR experiments were performed as described in Figure 6.

our results and those obtained for aequorin-expressing BY-2 wild-type and  $TPC1$ -co-suppressing and -over-expressing cell lines may be due to the sensitivity of the aequorin-based method to differences in total luminescence between the plant lines used for comparison. In particular, the free  $Ca^{2+}$  level is in a double logarithmic relationship to the aequorin luminescence. For proper quantification and comparability of  $[Ca^{2+}]_{cyt}$ , it is absolutely necessary to convert these luminescence values into actual  $[Ca^{2+}]$  (van Der Luit *et al.*, 1999; Knight *et al.*, 1996, 1997a; Rentel and Knight, 2004). For our

studies, we introgressed the pMAQ2 apoaequorin transgene into the  $tpc1-2$  mutant and  $TPC1$  over-expressor genetic background to ensure similar aequorin levels. However, we observed a strong reduction of the total aequorin luminescence in all progeny homozygous for the  $tpc1-2$  mutation. Thus, we carefully selected independent Arabidopsis wild-type lines from the crosses to pMAQ2 to serve as independent controls for knockouts and over-expressors, respectively (see Experimental procedures for details). Our data using lines with comparable total aequorin luminescence and calibrated

$[Ca^{2+}]_{\text{cyt}}$  show that, for the stimuli tested, TPC1 apparently does not contribute to  $Ca^{2+}$  entry into the cytosol, either from external or internal stores. We cannot, however, exclude a potential role in  $Ca^{2+}$  release from the vacuole in very local  $Ca^{2+}$  responses, which would escape observation by the cytosolic aequorin reporter.

We demonstrate that hyperpolarization-activated  $Ca^{2+}$  currents across the plasma membrane are independent of TPC1 expression. Instead, we confirm that TPC1 causes SV currents in the vacuolar membrane and show that it co-localizes with AtTPK1, a  $Ca^{2+}$ -activated vacuolar  $K^+$ -selective (VK) channel (Gobert *et al.*, 2007).

$Ca^{2+}$ -dependent activation and  $Ca^{2+}$  permeability have led to the hypothesis of the SV channel as mediator of CICR from vacuoles. Due to a small open probability in the physiological voltage range of  $-30$  to  $0$  mV, it has been questioned whether SV channel-mediated CICR occurs *in vivo* (Pottosin *et al.*, 1997). However, potentiation of the  $Ca^{2+}$ -dependent activation is induced by cytosolic  $Mg^{2+}$  (Pei *et al.*, 1999), revealing a  $K_d$  ( $Ca^{2+}$ ) that is similar to that reported initially in the presence of  $1$  mM  $Mg^{2+}$  (Hedrich and Neher, 1987) and allows gating around  $0$  mV. Further activating conditions, such as reducing agents and alkaline pH (Carpaneto *et al.*, 1999; Schulz-Lessdorf and Hedrich, 1995), could support channel opening and allow CICR to occur at physiological voltages. According to the results presented here, TPC1 cannot be the source for  $Ca^{2+}$  release during CICR, as wild-type-like  $Ca^{2+}$  signatures were observed in response to various biotic and abiotic stresses, including elevation of extracellular  $[Ca^{2+}]$  in TPC1 mutants and over-expressors. (Figures 6 and 7). The latter observation is in agreement with the very recent finding that an extracellular  $Ca^{2+}$ -induced  $Ca^{2+}$  increase exists in guard cells and mesophyll cells, and involves the  $Ca^{2+}$ -sensor receptor CAS, which triggers  $Ca^{2+}$  release from intracellular stores via second messenger ( $IP_3$ ) production, and therefore very likely requires ligand-gated rather than voltage-gated  $Ca^{2+}$  channel activity (Tang *et al.*, 2007). In guard cells, elevated external  $Ca^{2+}$  leads to  $Ca^{2+}$  inhibition of plasma membrane  $K^+$  channels (Dietrich *et al.*, 1998; Grabov and Blatt, 1999; Schroeder and Hagiwara, 1989). The  $Ca^{2+}$  insensitivity of stomata from the *tpc1-2* mutants (Peiter *et al.*, 2005) therefore does not necessarily indicate alterations in vacuolar  $Ca^{2+}$  release, but may suggest changes in cellular  $K^+$  homeostasis. Together, the data presented here strongly suggest that TPC1 functions in  $Ca^{2+}$  signalling as a target rather than as a source for  $Ca^{2+}$  release from the vacuole.

Under *in vivo* situations, the fractional  $Ca^{2+}$  current in the presence of competing  $K^+$  and  $Na^+$  ions has not yet been quantified. The relative  $Ca^{2+}$  permeability of TPC1 is only moderate compared to the high  $Ca^{2+}$  selectivity of related voltage-dependent  $Ca_v$  channels in animal systems (Pottosin *et al.*, 2001). In good agreement, a glutamate residue within the pore region that is responsible for high  $Ca^{2+}$

## $Ca^{2+}$ signals are not impaired by loss of AtTPC1 295

selectivity is conserved between  $Ca_v$  channels (Zagotta, 2006), but is missing in both pore domains of AtTPC1 and its homologs in other plant and animal species (Hashimoto *et al.*, 2004). Phylogenetic analyses of ion channel sequences suggest that the divergence of TPC1 from a common ancestor preceded that of  $Na^+$  and  $Ca^{2+}$  channels (Anderson and Greenberg, 2001). Given the absence of the latter four-domain  $Ca^{2+}$  and  $Na^+$  channels from the Arabidopsis genome, the enigmatic function of the two-pore channel singleton in cation homeostasis requires future research.

## Experimental procedures

### Plant material and growth conditions

The AtTPC1 T-DNA mutant line (SALK\_145413, *tpc1-2*) was either obtained from D. Sanders (York, UK) (Peiter *et al.*, 2005) or independently retrieved from the SALK collection (Alonso *et al.*, 2003), and plants homozygous for the insertion were identified by PCR, using primer pairs TPC1fw and TPC1rv for verification of the wild-type gene and Lba1 and TPC1rv for the T-DNA insertion (see Table 1). The absence of TPC1 mRNA in homozygous *tpc1-2* plants was confirmed by RT-PCR using the TPC1-specific primers TPC1fw and TPC1rv (see Table 1).

TPC1-over-expressing lines (numbers 5.6 and 10.21) were kindly provided by E. Peiter (York, UK), H. Knight (Durham, UK) and D. Sanders (Peiter *et al.*, 2005), and aequorin-expressing pMAQ2 plants by M. Knight (Durham, UK) and H. Knight. All plant lines used were in the Col-0 background. Seeds were stratified at  $4^\circ\text{C}$  for at least 2 days prior to germination. Plants were grown on soil in climate chambers under 8 h:16 h (short day) conditions, or on agar plates under constant light at  $22^\circ\text{C}$ .

### Electrophysiological recordings

Mesophyll tissue of leaves from 5–10-week-old plants was enzymatically digested (1% BSA, 0.05% pectolyase Y-23 (ICN; <http://www.mpbio.com>), 0.5% cellulase-R10 (Yakult <http://www.yakult.co.jp>), 0.5% macerozyme-R10 (Yakult), 1 mM  $CaCl_2$ , 10 mM MES, pH 5.6/Tris) at  $22^\circ\text{C}$  for 1 h, and washed twice with 400 mM  $D$ -sorbitol. Vacuoles were released from the protoplasts by osmotic lysis (10 mM EGTA, 10 mM HEPES, pH 7.4/Tris, sorbitol to 200 mOsm/kg). Vacuolar currents were studied in the whole-vacuolar and vacuolar side-in configuration using an EPC-7 patch-clamp amplifier (List Medical Electronics) and an LIH 1600 interface (HEKA Elektronik; <http://www.heka.com>). Patch-clamp recordings were performed as described previously (Dietrich and Hedrich, 1998; Hamill *et al.*, 1981). The external (cytoplasmic) solution consisted of 50 mM K-gluconate, 0.2 mM Ca-gluconate, 0.8 mM  $CaCl_2$ , 2 mM DTT, 10 mM HEPES pH 7.4/Tris. The pipette (luminal) solution was composed of 100 mM K-gluconate, 2 mM DTT, 10 mM EGTA, 10 mM HEPES pH 7.4/Tris. Solutions were adjusted to an osmolarity of 400 mOsm/kg using  $D$ -sorbitol. Any deviations from standard solutions are indicated in the figure legends.

### Gas exchange measurements

Wild-type and *tpc1-2* plants were analyzed using a gas exchange fluorescence system (GFS-3000, Heinz Walz GmbH ([© 2007 The Authors  
Journal compilation © 2007 Blackwell Publishing Ltd, \*The Plant Journal\*, \(2008\), 53, 287–299](http://</a></p></div><div data-bbox=)

296 Stefanie Ranf et al.

**Table 1** Primers used in this study

Gene	Length (bp)	Primer name	Sequence
AtP5CS1 (At2g39800)	560	P5CS1-F P5CS1-R	5'-GGAGGAGCTAGATCGTTCAC-3' 5'-TCAGTTCCAACGCCAGTAGA-3'
AtRD29a (At5g52310)	365	RD29a-F RD29a-R	5'-GAACACTCCGGTCTCTGTC-3' 5'-GCGAATCCTTACCGAGAACA-3'
AtGST1 (At1g02930)	364	GST1-F GST1-R	5'-TGTCGAGCTCAAAGATGGTG-3' 5'-GGACTCACCAGCCTGTGTT-3'
AtFRK1 (At2g19190)	340	FRK1-F FRK1-R	5'-TGAAGGAAGCGGTGAGATTT-3' 5'-CTGACTCATCGTTGGCCTCT-3'
AtPR1 (At2g14610)	480	PR1-F PR1-R	5'-AATTTTACTGGCTATTCTCG-3' 5'-GTATGGCTTCTCGTTCAC-3'
AtTPC1 (At4g03560)	269	tpc1-2 F2 tpc1-2 R2	5'-TGGGGAACAGCTACCTTCA-3' 5'-AGAGCTTTTGTCCCGACA-3'
AtEF1a (At1g07920)	653	EF1a-F EF1a-R	5'-TCACATCAACATTGTGGTCATTGGC-3' 5'-TTGATCTGGTCAAGAGCCCTCAAG-3'
Other primers used		LBa1 TPC1fw TPC1rv TPC1-fwd tpc1-2 rev Aeq-fwd Aeq-rev	5'-TGGTTCACGTAGTGGCCATCG-3' 5'-GGCAGGTTGCCGAGTTTGTGTC-3' 5'-GCAGTAGATACACAGCACGC-3' 5'-GAGAAGAATGTTGGAGAAGCCTTTGG-3' 5'-CGCAGAAAATGGTCCCTAAA-3' 5'-ATGAAATATGGTGTGAAACTGATT-3' 5'-GTTGTCTTGTCTCATCAACATC-3'

www.walz.com). Stomatal opening was promoted by superfusion of intact leaves with air containing 50 ppm CO<sub>2</sub>, and subsequent stomatal closure was induced by 1500 ppm CO<sub>2</sub>. For ABA-induced stomatal closure, detached leaves were opened in the presence of 100 ppm CO<sub>2</sub> in the light, and 100 μM ABA was fed via the petiole. Humidity and light intensities were 11 000 ppm H<sub>2</sub>O<sub>abs</sub>, and 250 μmol m<sup>-2</sup> sec<sup>-1</sup> PAR (photosynthetic active radiation), respectively.

#### Aequorin luminescence measurements

Plants expressing the aequorin apoprotein under control of the 35S promoter in the cytosol were used and were derived from the same homozygous pMAQ2 line (single insertion of aequorin, M. Knight, School of Biological and Biomedical Sciences, Durham University, UK, pers. comm.). Aequorin-expressing *tpc1-2* mutants and *TPC1*-over-expressing lines were generated by crossing of *tpc1-2* and *TPC10.21* with pMAQ2 plants. In case of the knockout, F<sub>2</sub> and F<sub>3</sub> progeny from pMAQ2 × *tpc1-2* crosses homozygous for the *tpc1-2* mutation (knockout) and progenies segregating for the wild-type *TPC1* genotype (as a control, see below) were used. Plants were screened by PCR using primers spanning the T-DNA insertion (*tpc1-2* F2/R2, see Table 1), as well as primers for the T-DNA insertion (LBa1) and the *TPC1* gene (*tpc1-2* rev), and primers specific for the aequorin cDNA (Aeq-fwd/rev), using genomic DNA. Genotypes were confirmed by RT-PCR using primers spanning the T-DNA insertion (*tpc1-2* F2/*tpc1-2* rev and *tpc1-2* R2) for all lines used. In case of the over-expressor, F<sub>1</sub> progeny from pMAQ2 × *TPC10.21* crosses heterozygous for the 35S::*TPC1* insertion were used, and original pMAQ2 plants were used as a control. Plants were screened by PCR using *TPC1*-specific primers (*TPC1* fwd/*tpc1-2* rev) spanning eight introns to discriminate between genomic *TPC1* and the inserted *TPC1* cDNA.

We observed a reduction in total aequorin luminescence in all F<sub>2</sub> and F<sub>3</sub> progeny from pMAQ2 × *tpc1-2* crosses tested, and therefore

used *TPC1* wild-type genotypes from the same generation as independent controls. Only plants with comparable amounts of total aequorin luminescence were selected for experiments, allowing comparison of the relative luminescence levels and calculated [Ca<sup>2+</sup>]<sub>cyt</sub> values.

Leaf discs (diameter 3 mm, 4–8-week-old plants) were cut from mature leaves and floated individually in wells of a 96-well plate on 100 μl H<sub>2</sub>O/10 μM native coelenterazine per well (5 mM stock in methanol, Molecular Probes/Invitrogen, <http://www.invitrogen.com/>) in darkness for at least 4 h for reconstitution. For treatment with external CaCl<sub>2</sub>, the lower epidermis was removed prior to reconstitution (1 mM MES-KOH, pH 5.7, 100 μM KCl, 10 μM coelenterazine) to allow direct contact of the CaCl<sub>2</sub> with the mesophyll tissue. Seedlings were grown axenically on MS agar plates (1 × MS, 1% sucrose, 1% agar), and used when 6–7 days old. Intact seedlings were placed individually in wells of a 96-well plate and reconstituted overnight as described above. Luminescence was measured using a Luminoskan Ascent 2.1 luminometer (Labsystems (<http://www.thermo.com/>)). After 30–60 sec recording, treatment was applied by addition of 50 μl of a threefold concentrated solution in water via an automatic dispenser, and measurements were continued for the indicated time. Controls were performed by addition of an equal volume of water. Remaining aequorin was discharged by automatic injection of 1 volume 2 M CaCl<sub>2</sub>/20% ethanol, and luminescence recorded for another 8–10 min until values were within 1% of the highest discharge value.

In the case of cold-shock treatment, luminescence was measured in a Lumat LB 9501/16 luminometer (Berthold; <http://www.berthold.com>). Reconstituted leaf discs were transferred individually to single tubes containing 200 μl H<sub>2</sub>O/10 μM coelenterazine, and allowed to recover for at least 15 min from the touch response. Tubes were placed individually into the luminometer chamber, and luminescence recorded at 1 sec integration intervals. After 30 sec, cold shock was applied by manual addition of 1 volume of ice cold water, and measurements were continued for 3 min. Remaining aequorin was discharged as described above.

Relative luminescence values were calculated and converted into actual  $\text{Ca}^{2+}$  concentrations using the calibration equation below as described in detail by Rentel and Knight (2004):

$$\text{pCa} = 0.332588(-\log k) + 5.5593$$

where  $k$  is the luminescence counts per sec/total luminescence counts remaining.

#### Oxidative burst in *Arabidopsis* leaves

**Luminol assay.** Reactive oxygen species were assayed by  $\text{H}_2\text{O}_2$ -dependent luminescence of luminol (Gomez-Gomez *et al.*, 1999). Mature *Arabidopsis* leaves were cut in 1 mm slices and floated overnight on  $\text{H}_2\text{O}$ . Slices were transferred to a 96-well plate (four slices per well) containing 200  $\mu\text{l}$  of  $\text{H}_2\text{O}$ , 200  $\mu\text{M}$  luminol, 2  $\mu\text{g}$  horseradish peroxidase. Luminescence was measured in the Luminoskan Ascent 2.1 luminometer with a 1 sec integration time at 12 sec intervals. After 60 sec, 1  $\mu\text{M}$  elf18 or an equal volume of water was added manually, and luminescence recorded for further 30 min. This assay is not quantifiable and allows only qualitative estimation of  $\text{H}_2\text{O}_2$  production.

**DAB staining.** Leaves of wild-type and *tpc1-2* plants were infiltrated with avirulent *P. syringae* pv. tomato Pst DC3000 *avrB* ( $\text{OD}_{600} = 0.2$ , washed twice in 10 mM  $\text{MgSO}_4$ ) and buffer control. Four hours after infection, leaves were transferred to diamino-benzidine solution (1 mg  $\text{ml}^{-1}$  DAB pH 3.8) and incubated in darkness for 18 h. Chlorophyll was cleared for 10 min in boiling 98% ethanol.

#### Semi-quantitative RT-PCR experiments

One-week-old seedlings grown as described above were transferred to liquid medium (1  $\times$  MS, 1% sucrose) in 24-well plates (two or three seedlings/1 ml per well). Seedlings that were 12–14 days old were treated by exchanging the medium with medium containing 10  $\mu\text{M}$  elf18, 0.5 mM NaSA, 10 mM  $\text{H}_2\text{O}_2$ , 0.6 M mannitol, 0.3 M NaCl or water as control. For cold treatment, the medium was exchanged with ice-cold medium, and seedlings were kept on ice. Whole seedlings were harvested at the time points indicated, frozen in liquid nitrogen and stored at  $-80^\circ\text{C}$ . Total RNA was prepared using RNeasy plant mini-preps (Qiagen, <http://www.qiagen.com/>). First-strand synthesis was performed with 1  $\mu\text{g}$  of total RNA (DNase I-treated, Fermentas; <http://www.fermentas.de>) using 200 U RevertAid M-MuLV reverse transcriptase (Fermentas), oligo(dT)<sub>18</sub> primer (MWG Biotech; <http://www.mwg-biotech.com>) and RiboLock RNase inhibitor (Fermentas) according to the manufacturers' instructions. A 0.5  $\mu\text{l}$  aliquot of cDNA was used in a 50  $\mu\text{l}$  PCR reaction containing 2.5 U Taq polymerase (New England Biolabs; <http://www.neb.com>), HiFi buffer (Fermentas), 1.5 mM  $\text{MgCl}_2$ , 200  $\mu\text{M}$  dNTPs and 200 nM primers (MWG Biotech). Amplification conditions were 1 min at  $94^\circ\text{C}$ ;  $x$  cycles of 15 sec at  $94^\circ\text{C}$ , 20 sec at  $50^\circ\text{C}$  and 45 sec at  $72^\circ\text{C}$ , followed by 5 min at  $72^\circ\text{C}$ . Optimal PCR cycle numbers determined to be in the non-saturated range have been established previously for each primer pair and are indicated in the text. PCR products were analyzed on 2% TAE agarose gels containing ethidium bromide. Primers were chosen to span at least one intron if possible.

#### Primers used

The primers used in this study are listed in Table 1.

© 2007 The Authors

Journal compilation © 2007 Blackwell Publishing Ltd, *The Plant Journal*, (2008), 53, 287–299

## $\text{Ca}^{2+}$ signals are not impaired by loss of AtTPC1 297

### Root growth measurements and germination assay

Wild-type and *tpc1-2* seedlings were grown on agar plates in climate chambers under a 16 h/8 h light/dark regimen at  $22^\circ\text{C}$ .  $\text{K}^+$ -dependent seed germination was observed for a period of 264 h on modified half-strength MS agar plates in which  $\text{KNO}_3$  and  $\text{KH}_2\text{PO}_4$  had been replaced by  $\text{NH}_4\text{NO}_3$  and  $\text{NH}_4\text{PO}_4$ . Final  $[\text{K}^+]$  was adjusted to 50  $\mu\text{M}$ , 500  $\mu\text{M}$  or 1 mM using  $\text{KNO}_3$ . The medium contained 1.8%  $\text{K}^+$ -depleted agar (Xu *et al.*, 2006). For root growth measurements, plants were grown on half-strength MS medium containing 1% sucrose and 0.8% agar for 4 days, and then transferred to plates with modified half-strength MS media containing 1% sucrose and 1% purified agar (A7921, Sigma, <http://www.sigmaaldrich.com/>). For variations in  $\text{Ca}^{2+}$  contents, 1.5 mM  $\text{CaCl}_2$  was replaced by 0, 0.15, 1.5 and 15 mM  $\text{CaCl}_2$ , respectively. Note that 0 mM corresponds to approximately 50  $\mu\text{M}$   $\text{Ca}^{2+}$ . For ABA-dependent root growth experiments, plants were transferred to half-strength MS plates containing 10 or 50  $\mu\text{M}$  ( $\pm$ ) *cis,trans*-ABA in 10 mM KCl and 1.5 mM  $\text{CaCl}_2$ . Root growth within 4 days after transfer was measured using IMAGEJ analysis software (<http://rsb.info.nih.gov/ij/>).

### TPC1-GFP construct, transient expression, and confocal fluorescence imaging

For localization of TPC1 in onion epidermal cells, *AtTPC1* cDNA lacking its stop codon was inserted in-frame with *mrfp1* (Campbell *et al.*, 2002) into pPily (Ferrando *et al.*, 2000), creating  $2 \times 35\text{S}$ -promotor:*TPC1-mrfp1*. In similar fashion, *AtTPK1* cDNA was inserted into pPily in-frame with *mgfp4* (Haseloff *et al.*, 1997), creating  $2 \times 35\text{S}$ -promotor:*TPK1-mgfp4*. Onion epidermal cells were then co-transfected by biolistic delivery of tungsten particles (tungsten M-17, Bio-Rad, <http://www.bio-rad.com/>) coated with equal amounts of both plasmids. After 1–2 days, transfected cells were imaged using a Zeiss LSM5 Pascal confocal microscope (<http://www.zeiss.com/>) in multi-track mode. mGFP4 fluorescence was measured using a 488 nm excitation wavelength and an emission band path of 505–530 nm, while mRFP1 was excited at 543 nm and fluorescence emission was detected using a longpass filter LP560 nm. Images were processed using ZEISS LSM software and ADOBE PHOTOSHOP Elements 2.0.

### Acknowledgements

We are grateful to Edgar Peiter (York, UK) Heather Knight (Durham, UK) and Dale Sanders (York, UK) for providing us with two independent *TPC1*-over-expressing lines and the *tpc1-2* mutant line, and Marc Knight (Durham, UK) and Heather Knight for providing the apoaequorin-expressing pMAQ2 line. We would like to thank Oliver Meyerhoff and Katharina Siebke (Heinz Walz GmbH, Effeltrich, Germany) for help with gas exchange equipment and measurements, and Uwe Sonnewald (Erlangen, Germany) for sharing the GFS-3000. We thank Elisabeth Dunkel for technical assistance and Heiner Busch for critical reading of the manuscript. This work was supported by grants from the Deutsche Forschungsgemeinschaft.

### References

Allen, G.J. and Sanders, D. (1994) Two voltage-gated, calcium release channels coreside in the vacuolar membrane of broad bean guard cells. *Plant Cell*, 6, 685–694.

298 *Stefanie Ranf et al.*

- Allen, G.J. and Sanders, D.** (1996) Control of ionic currents in guard cell vacuoles by cytosolic and luminal calcium. *Plant J.* **10**, 1055–1069.
- Alonso, J.M., Stepanova, A.N., Leisse, T.J. et al.** (2003) Genome-wide insertional mutagenesis of *Arabidopsis thaliana*. *Science*, **301**, 653–657.
- Anderson, P.A. and Greenberg, R.M.** (2001) Phylogeny of ion channels: clues to structure and function. *Comp. Biochem. Physiol. B.* **129**, 17–28.
- Arabidopsis Genome Initiative** (2000) Analysis of the genome sequence of the flowering plant *Arabidopsis thaliana*. *Nature*, **408**, 796–815.
- Asai, T., Tena, G., Plotnikova, J., Willmann, M.R., Chiu, W.L., Gomez-Gomez, L., Boller, T., Ausubel, F.M. and Sheen, J.** (2002) MAP kinase signalling cascade in *Arabidopsis* innate immunity. *Nature*, **415**, 977–983.
- Barkla, B.J. and Pantoja, O.** (1996) Physiology of ion transport across the tonoplast of higher plants. *Annu. Rev. Plant Physiol. Plant Mol. Biol.* **47**, 159–184.
- Bewell, M.A., Maathuis, F.J.M., Allen, G.J. and Sanders, D.** (1999) Calcium-induced calcium release mediated by a voltage-activated cation channel in vacuolar vesicles of red beet. *FEBS Lett.* **458**, 41–44.
- Blume, B., Nürnberg, T., Nass, N. and Scheel, D.** (2000) Receptor-mediated increase in cytoplasmic free calcium required for activation of pathogen defense in parsley. *Plant Cell*, **12**, 1425–1440.
- Bonaventure, G., Gfeller, A., Proebsting, W.M., Hortensteiner, S., Chetelat, A., Martinoia, E. and Farmer, E.E.** (2007) A gain-of-function allele of TPC1 activates oxylipin biogenesis after leaf wounding in *Arabidopsis*. *Plant J.* **49**, 889–898.
- Campbell, R.E., Tour, O., Palmer, A.E., Steinbach, P.A., Baird, G.S., Zacharias, D.A. and Tsien, R.Y.** (2002) A monomeric red fluorescent protein. *Proc. Natl Acad. Sci. U.S.A.* **99**, 7877–7882.
- Carpaneto, A., Cantu, A.M. and Gambale, F.** (1999) Redox agents regulate ion channel activity in vacuoles from higher plant cells. *FEBS Lett.* **442**, 129–132.
- Carter, C., Pan, S., Zouhar, J., Avila, E.L., Girke, T. and Raikhel, N.V.** (2004) The vegetative vacuole proteome of *Arabidopsis thaliana* reveals predicted and unexpected proteins. *Plant Cell*, **16**, 3285–3303.
- Cheong, Y.H., Kim, K.N., Pandey, G.K., Gupta, R., Grant, J.J. and Luan, S.** (2003) CBL1, a calcium sensor that differentially regulates salt, drought, and cold responses in *Arabidopsis*. *Plant Cell*, **15**, 1833–1845.
- Czempinski, K., Frachisse, J.M., Maurel, C., Barbier-Brygoo, H. and Mueller-Roeber, B.** (2002) Vacuolar membrane localization of the *Arabidopsis* ‘two-pore’ K<sup>+</sup> channel KCO1. *Plant J.* **29**, 809–820.
- van Der Luit, A.H., Olivari, C., Haley, A., Knight, M.R. and Trewavas, A.J.** (1999) Distinct calcium signaling pathways regulate calmodulin gene expression in tobacco. *Plant Physiol.* **121**, 705–714.
- Dietrich, P. and Hedrich, R.** (1998) Anions permeate and gate GCAC1, a voltage-dependent guard cell anion channel. *Plant J.* **15**, 479–487.
- Dietrich, P., Dreyer, I., Wiesner, P. and Hedrich, R.** (1998) Cation sensitivity and kinetics of guard cell potassium channels differ among species. *Planta*, **205**, 277–287.
- Felix, G., Duran, J.D., Volko, S. and Boller, T.** (1999) Plants have a sensitive perception system for the most conserved domain of bacterial flagellin. *Plant J.* **18**, 265–276.
- Ferrando, A., Farras, R., Jasik, J., Schell, J. and Koncz, C.** (2000) Intron-tagged epitope: a tool for facile detection and purification of proteins expressed in *Agrobacterium*-transformed plant cells. *Plant J.* **22**, 553–560.
- Furuichi, T., Cunningham, K.W. and Muto, S.** (2001) A putative two pore channel AtTPC1 mediates Ca<sup>2+</sup> flux in *Arabidopsis* leaf cells. *Plant Cell Physiol.* **42**, 900–905.
- Gobert, A., Isayenkov, S., Voelker, C., Czempinski, K. and Maathuis, F.J.** (2007) The two-pore channel TPK1 gene encodes the vacuolar K<sup>+</sup> conductance and plays a role in K<sup>+</sup> homeostasis. *Proc. Natl Acad. Sci. U.S.A.* **104**, 10726–10731.
- Gomez-Gomez, L., Felix, G. and Boller, T.** (1999) A single locus determines sensitivity to bacterial flagellin in *Arabidopsis thaliana*. *Plant J.* **18**, 277–284.
- Grabov, A. and Blatt, M.R.** (1998) Membrane voltage initiates Ca<sup>2+</sup> waves and potentiates Ca<sup>2+</sup> increases with abscisic acid in stomatal guard cells. *Proc. Natl Acad. Sci. U.S.A.* **95**, 4778–4783.
- Grabov, A. and Blatt, M.R.** (1999) A steep dependence of inward-rectifying potassium channels on cytosolic free calcium concentration increase evoked by hyperpolarization in guard cells. *Plant Physiol.* **119**, 277–288.
- Hamill, O.P., Marty, A., Neher, E., Sakmann, B. and Sigworth, F.J.** (1981) Improved patch-clamp techniques for high-resolution current recording from cells and cell-free membrane patches. *Pflügers Arch.* **391**, 85–100.
- Han, S., Tang, R., Anderson, L.K., Woerner, T.E. and Pei, Z.M.** (2003) A cell surface receptor mediates extracellular Ca<sup>2+</sup> sensing in guard cells. *Nature*, **425**, 196–200.
- Haseloff, J., Siemerling, K.R., Prasher, D.C. and Hodge, S.** (1997) Removal of a cryptic intron and subcellular localization of green fluorescent protein are required to mark transgenic *Arabidopsis* plants brightly. *Proc. Natl Acad. Sci. U.S.A.* **94**, 2122–2127.
- Hashimoto, K., Saito, M., Matsuoka, H., Iida, K. and Iida, H.** (2004) Functional analysis of a rice putative voltage-dependent Ca<sup>2+</sup> channel, *OstTPC1*, expressed in yeast cells lacking its homologous gene *CCH1*. *Plant Cell Physiol.* **45**, 496–500.
- Hedrich, R. and Neher, E.** (1987) Cytoplasmic calcium regulates voltage-dependent ion channels in plant vacuoles. *Nature*, **329**, 833–836.
- Ivashikina, N. and Hedrich, R.** (2005) K<sup>+</sup> currents through SV-type vacuolar channels are sensitive to elevated luminal sodium levels. *Plant J.* **41**, 606–614.
- Kadota, Y., Furuichi, T., Ogasawara, Y., Goh, T., Higashi, K., Muto, S. and Kuchitsu, K.** (2004) Identification of putative voltage-dependent Ca<sup>2+</sup>-permeable channels involved in cryptogin-induced Ca<sup>2+</sup> transients and defense responses in tobacco BY-2 cells. *Biochem. Biophys. Res. Commun.* **317**, 823–830.
- Kawano, T., Kadono, T., Fumoto, K., Lapeyrie, F., Kuse, M., Isobe, M., Furuichi, T. and Muto, S.** (2004) Aluminum as a specific inhibitor of plant TPC1 Ca<sup>2+</sup> channels. *Biochem. Biophys. Res. Commun.* **324**, 40–45.
- Kim, K.N., Cheong, Y.H., Grant, J.J., Pandey, G.K. and Luan, S.** (2003) CIPK3, a calcium sensor-associated protein kinase that regulates abscisic acid and cold signal transduction in *Arabidopsis*. *Plant Cell*, **15**, 411–423.
- Knight, H., Trewavas, A.J. and Knight, M.R.** (1996) Cold calcium signaling in *Arabidopsis* involves two cellular pools and a change in calcium signature after acclimation. *Plant Cell*, **8**, 489–503.
- Knight, H., Trewavas, A. and Knight, M.R.** (1997a) Recombinant aequorin methods for measurement of intracellular calcium in plants. In *Plant Molecular Biology Manual*. Dordrecht: Kluwer Academic Publishers, pp. 1–22.
- Knight, H., Trewavas, A.J. and Knight, M.R.** (1997b) Calcium signalling in *Arabidopsis thaliana* responding to drought and salinity. *Plant J.* **12**, 1067–1078.
- Kunze, G., Zipfel, C., Robatzek, S., Niehaus, K., Boller, T. and Felix, G.** (2004) The N terminus of bacterial elongation factor Tu elicits innate immunity in *Arabidopsis* plants. *Plant Cell*, **16**, 3496–3507.

- Kurusu, T., Sakurai, Y., Miyao, A., Hirochika, H. and Kuchitsu, K.** (2004) Identification of a putative voltage-gated  $\text{Ca}^{2+}$ -permeable channel (OsTPC1) involved in  $\text{Ca}^{2+}$  influx and regulation of growth and development in rice. *Plant Cell Physiol.* **45**, 693–702.
- Kurusu, T., Yagala, T., Miyao, A., Hirochika, H. and Kuchitsu, K.** (2005) Identification of a putative voltage-gated  $\text{Ca}^{2+}$  channel as a key regulator of elicitor-induced hypersensitive cell death and mitogen-activated protein kinase activation in rice. *Plant J.* **42**, 798–809.
- Lecourieux, D., Mazars, C., Pauly, N., Ranjeva, R. and Pugin, A.** (2002) Analysis and effects of cytosolic free calcium increases in response to elicitors in *Nicotiana plumbaginifolia* cells. *Plant Cell*, **14**, 2627–2641.
- Lin, C., Yu, Y., Kadono, T. et al.** (2005) Action of aluminum, novel TPC1-type channel inhibitor, against salicylate-induced and cold-shock-induced calcium influx in tobacco BY-2 cells. *Biochem. Biophys. Res. Commun.* **332**, 823–830.
- MacRobbie, E.A.C.** (2000) ABA activates multiple  $\text{Ca}^{2+}$  fluxes in stomatal guard cells, triggering vacuolar  $\text{K}^+$  ( $\text{Rb}^+$ ) release. *Proc. Natl Acad. Sci. U.S.A.* **97**, 12361–12368.
- McAinsh, M.R., Webb, A.A.R., Taylor, J.E. and Hetherington, A.M.** (1995) Stimulus-induced oscillations in guard cell cytosolic free calcium. *Plant Cell*, **7**, 1207–1219.
- Nürnbergger, T. and Scheel, D.** (2001) Signal transmission in the plant immune response. *Trends Plant Sci.* **6**, 372–379.
- Pei, Z.M., Ward, J.M. and Schroeder, J.I.** (1999) Magnesium sensitizes slow vacuolar channels to physiological cytosolic calcium and inhibits fast vacuolar channels in fava bean guard cell vacuoles. *Plant Physiol.* **121**, 977–986.
- Pei, Z.M., Murata, Y., Benning, G., Thomine, S., Klusener, B., Allen, G.J., Grill, E. and Schroeder, J.I.** (2000) Calcium channels activated by hydrogen peroxide mediate abscisic acid signalling in guard cells. *Nature*, **406**, 731–734.
- Peiter, E., Maathuis, F.J., Mills, L.N., Knight, H., Pelloux, J., Hetherington, A.M. and Sanders, D.** (2005) The vacuolar  $\text{Ca}^{2+}$ -activated channel TPC1 regulates germination and stomatal movement. *Nature*, **434**, 404–408.
- Pottosin, I.I., Tikhonova, L.I., Hedrich, R. and Schoenknecht, G.** (1997) Slowly activating vacuolar channels cannot mediate  $\text{Ca}^{2+}$ -induced  $\text{Ca}^{2+}$  release. *Plant J.* **12**, 1387–1398.
- Pottosin, I.I., Dobrovinskaya, O.R. and Muniz, J.** (2001) Conduction of monovalent and divalent cations in the slow vacuolar channel. *J. Membr. Biol.* **181**, 55–65.
- Rentel, M.C. and Knight, M.R.** (2004) Oxidative stress-induced calcium signaling in *Arabidopsis*. *Plant Physiol.* **135**, 1471–1479.
- Sanders, D., Pelloux, J., Brownlee, C. and Harper, J.F.** (2002) Calcium at the crossroads of signaling. *Plant Cell*, **14**, S401–S417.
- Schönknecht, G., Spoomaker, P., Steinmeyer, R., Brüggeman, L., Ache, P., Dutta, R., Reintanz, B., Godde, M., Hedrich, R. and Palme, K.** (2002) KCO1 is a component of the slow-vacuolar (SV) ion channel. *FEBS Lett.* **511**, 28–32.
- Schroeder, J.I. and Hagiwara, S.** (1989) Cytosolic calcium regulates ion channels in the plasma membrane of *Vicia faba* guard cells. *Nature*, **338**, 427–430.
- Schulz-Lessdorf, B. and Hedrich, R.** (1995) Protons and calcium modulate SV-type channels in the vacuolar-lysosomal compartment: channel interaction with calmodulin inhibitors. *Planta*, **197**, 655–671.
- Stoelzle, S., Kagawa, T., Wada, M., Hedrich, R. and Dietrich, P.** (2003) Blue light activates calcium-permeable channels in *Arabidopsis* mesophyll cells via the phototropin signaling pathway. *Proc. Natl Acad. Sci. U.S.A.* **100**, 1456–1461.
- Tang, R.H., Han, S., Zheng, H., Cook, C.W., Choi, C.S., Woerner, T.E., Jackson, R.B. and Pei, Z.M.** (2007) Coupling diurnal cytosolic  $\text{Ca}^{2+}$  oscillations to the CAS-IP3 pathway in *Arabidopsis*. *Science*, **315**, 1423–1426.
- Wang, Y.-J., Yu, J.-N., Chen, T., Zhang, Z.-G., Hao, Y.-J., Zhang, J.-S. and Chen, S.-Y.** (2005) Functional analysis of a putative  $\text{Ca}^{2+}$  channel gene *TaTPC1* from wheat. *J. Exp. Bot.* **56**, 3051–3060.
- Ward, J.M. and Schroeder, J.I.** (1994) Calcium-activated  $\text{K}^+$  channels and calcium-induced calcium release by slow vacuolar channels in guard cell vacuoles implicated in the control of stomatal closure. *Plant Cell*, **6**, 669–683.
- Ward, J.M. and Schroeder, J.I.** (1997) Roles of ion channels in initiation of signal transduction in higher plants. In *Molecular and Cell Biology Updates: Signal Transduction in Plants* (Aducci, P., ed.). Basel: Birkhäuser Verlag, pp. 1–22.
- Webb, A.A.R., McAinsh, M.R., Mansfield, T.A. and Hetherington, A.M.** (1996) Carbon dioxide induces increases in guard cell cytosolic free calcium. *Plant J.* **9**, 297–304.
- Wu, Y., Kuzma, J., Marechal, E., Graeff, R., Lee, H.C., Foster, R. and Chua, N.H.** (1997) Abscisic acid signaling through cyclic ADP-ribose in plants. *Science*, **278**, 2126–2130.
- Xu, J., Li, H.D., Chen, L.Q., Wang, Y., Liu, L.L., He, L. and Wu, W.H.** (2006) A protein kinase, interacting with two calcineurin B-like proteins, regulates  $\text{K}^+$  transporter AKT1 in *Arabidopsis*. *Cell*, **125**, 1347–1360.
- Zagotta, W.N.** (2006) Membrane biology: permutations of permeability. *Nature*, **440**, 427–429.
- Zimmermann, S., Nürnbergger, T., Frachisse, J.-M., Wirtz, W., Guern, J., Hedrich, R. and Scheel, D.** (1997) Receptor-mediated activation of a plant  $\text{Ca}^{2+}$ -permeable ion channel involved in pathogen defense. *Proc. Natl Acad. Sci. U.S.A.* **94**, 2751–2755.
- Zipfel, C., Kunze, G., Chinchilla, D., Caniard, A., Jones, J.D., Boller, T. and Felix, G.** (2006) Perception of the bacterial PAMP EF-Tu by the receptor EFR restricts Agrobacterium-mediated transformation. *Cell*, **125**, 749–760.

## 2.2. Impact of different signalling components on MAMP-induced $\text{Ca}^{2+}$ signalling

### 2.2.1. Aims and summary

While most downstream responses are crucially dependent on an initial  $[\text{Ca}^{2+}]_{\text{cyt}}$  elevation, they still may have a feedback impact on the  $\text{Ca}^{2+}$  response. ROS, for instance  $\text{H}_2\text{O}_2$ , are themselves capable of inducing  $[\text{Ca}^{2+}]_{\text{cyt}}$  alterations. Likewise, phospholipid signalling presumably is  $\text{Ca}^{2+}$ -dependent but in turn produces the putative  $\text{Ca}^{2+}$ -releasing second messengers  $\text{InsP}_3/\text{InsP}_6$ . To analyse the interplay between early signalling events and their possible impact on  $\text{Ca}^{2+}$  signalling, the second chapter of this thesis, consisting of a submitted manuscript and additional unpublished results, focussed on such signalling events that act in a similar time frame as  $\text{Ca}^{2+}$  signalling. Complete abrogation of the ROS production in the *rbohD* mutant indeed revealed a feedback impact of ROS on the  $[\text{Ca}^{2+}]_{\text{cyt}}$  elevation. This secondary ROS-induced  $[\text{Ca}^{2+}]_{\text{cyt}}$  elevation results in a second peak or prolonged plateau. Furthermore, a reduced ROS accumulation in *phospholipase D $\alpha$ 1* (*pld $\alpha$ 1*) suggests a role for phosphatidic acid (PA) upstream of ROS generation, while knockout of MPK3 led to a prolonged but not enhanced ROS production without affecting the  $[\text{Ca}^{2+}]_{\text{cyt}}$  elevations. Likewise, decreased  $\text{InsP}_6$  levels did not impair  $[\text{Ca}^{2+}]_{\text{cyt}}$  elevations but, intriguingly, resulted in an enhanced flg22-mediated root growth arrest. Last but not least,  $\text{Ca}^{2+}/\text{CaM}$  directly activate expression of early defence genes, such as *ZAT12*, via the transcription factor CAMTA3 in response to flg22.

Additionally, specificity within the signalling pathways stimulated by different MAMPs was observed. Although different MAMPs are thought to converge at early signalling steps and thus to induce a stereotypic defence program, the detailed comparison of flg22- and elf18-induced responses revealed qualitative and quantitative differences. While seedling growth on elf18-containing medium mainly resulted in strong reduction of shoot size, flg22 predominantly affected root growth. Since both MAMPs induced defence responses in shoots but only weak reactions in roots, the distinct growth inhibition phenotypes were not simply caused by tissue-specific perception. Moreover, flg22-induced gene expression kinetics were transient compared to a prolonged induction upon elf18 elicitation. Intriguingly, BAK1 differentially contributes to flg22- vs. elf18-mediated responses. Such, MAMP-induced  $[\text{Ca}^{2+}]_{\text{cyt}}$  amplitudes were virtually identical in *bak1* in contrast to significantly distinct peak heights in the wild type. Despite these comparable  $\text{Ca}^{2+}$  responses in *bak1*,  $\text{Ca}^{2+}$ -dependent defence gene expression and growth arrest were strongly dependent on BAK1 in response to flg22 but not elf18. However, other  $\text{Ca}^{2+}$ -dependent responses, such as ROS accumulation and MAPK activation were similarly reduced in *bak1* in response to both MAMPs. Unlike in *bak1*,  $[\text{Ca}^{2+}]_{\text{cyt}}$  elevations or ROS accumulation were neither reduced nor delayed in any of the other BAK1-homologous *serk* mutants. Moreover, loss of SERK2 or SERK4 resulted in an even opposite phenotype, an enhanced flg22-mediated root growth arrest. Thus, the role of BAK1 as “co-receptor” and the other SERK kinases appears more complex than initially assumed and may involve different regulation at distinct signalling levels. Taken together, early signalling elements are not strictly hierarchical organized but form a complex interrelated signalling network.

### 2.2.2. Manuscript

#### Interplay between calcium signalling and early signalling elements during defence responses to microbe- or damage-associated molecular patterns

Stefanie Ranf, Lennart Eschen-Lippold, Pascal Pecher, Justin Lee\* & Dierk Scheel

Leibniz Institute of Plant Biochemistry, Stress and Developmental Biology, Weinberg 3, D-06120 Halle

\*For correspondence: fax +49 34555821409; phone +49 34555821410; e-mail jlee@ipb-halle.de

Running title: Calcium signalling in Arabidopsis innate immunity

Keywords: *Arabidopsis thaliana*, MAMP, calcium, ROS, BAK1, SERK

#### SUMMARY

While diverse microbe- or damage-associated molecular patterns (MAMPs/DAMPs) typically trigger a common set of intracellular signalling events, comparative analysis between the MAMPs flg22 and elf18 revealed MAMP-specific differences in  $\text{Ca}^{2+}$  signalling, defence gene expression and MAMP-mediated growth arrest in *Arabidopsis thaliana*. Such MAMP-specific differences are, in part, controlled by BAK1, a kinase associated with several receptors. Whereas defence gene expression and growth inhibition mediated by flg22 were reduced in *bak1* mutants, BAK1 had no or minor effects on the same responses elicited by elf18. As the residual  $\text{Ca}^{2+}$  elevations induced by diverse MAMPs/DAMPs (flg22, elf18 and Pep1) were virtually identical in *bak1* mutants, a differential BAK1-mediated signal amplification to attain MAMP/DAMP-specific  $\text{Ca}^{2+}$  amplitudes in wild type plants may be hypothesized. Furthermore, abrogation of reactive oxygen species (ROS) accumulation, either in the *rbohD* mutant or through inhibitor application, led to loss of a second  $\text{Ca}^{2+}$  peak, demonstrating a feedback effect of ROS on  $\text{Ca}^{2+}$  signalling. Conversely, *mpk3* mutants showed a prolonged ROS accumulation but this did not significantly impinge on the overall  $\text{Ca}^{2+}$  response. Thus, fine-tuning of MAMP/DAMP responses involves interplay between diverse signalling elements functioning both up- or downstream of  $\text{Ca}^{2+}$  signalling.

#### INTRODUCTION

Plant defence is initiated through the recognition of conserved microbe/pathogen-associated molecular patterns (M/PAMPs) or plant-derived damage-associated molecular patterns (DAMPs) by specific pattern-recognition receptors (PRR). Activation of PRRs initiates a set of common defence responses eventually leading to immunity (reviewed in Boller and Felix, 2009). One of the earliest signalling events after MAMP/DAMP perception is a rapid change in the cytosolic  $\text{Ca}^{2+}$  concentration ( $[\text{Ca}^{2+}]_{\text{cyt}}$ ) and concomitant membrane depolarization (Blume *et al.*, 2000; Lecourieux *et al.*, 2002; Ranf *et al.*, 2008; Jeworutzki *et al.*, 2010). Subsequently, generation of reactive oxygen species (ROS) may directly confine pathogen growth *via* toxic effects and cell wall strengthening or may exert signalling functions (Torres *et al.*, 2006). The Arabidopsis NADPH oxidases, RbohD and RbohF, contribute to ROS generation in response to pathogen attack (Torres *et al.*, 2002). Superoxide dismutases rapidly convert membrane-impermeant superoxide ( $\text{O}_2^{\cdot-}$ ), produced in the apoplast by NADPH oxidases, into  $\text{H}_2\text{O}_2$ ,

which can enter cytosol and nucleus to execute intracellular functions. Activation of mitogen-activated protein kinase (MAPK) cascades (MAP3K-MKK4/MKK5-MPK3/MPK6 and MEKK1-MKK1/MKK2-MPK4) and  $\text{Ca}^{2+}$ -dependent kinases (CPK4/5/6/11) leads to gene expression re-programming (Boudsocq *et al.*, 2010; Rodriguez *et al.*, 2010).

The best studied PAMP/PRR pairs in Arabidopsis to date are flagellin/FLS2 (Flagellin sensitive 2) and EF-Tu/EFR (EF-Tu receptor), with the peptides flg22 and elf18 functioning as the elicitor-active PAMPs, respectively (Felix *et al.*, 1999; Gomez-Gomez *et al.*, 1999; Gomez-Gomez and Boller, 2000; Kunze *et al.*, 2004; Zipfel *et al.*, 2006). Upon flg22 binding, FLS2 hetero-oligomerizes with another receptor-like kinase (RLK), BRI1-associated kinase 1 (BAK1), which was originally found as interactor of the brassinosteroid receptor BRI1 (Brassinosteroid insensitive 1; Li *et al.*, 2002; Nam and Li, 2002). While sometimes referred to as a “co-receptor”, BAK1 is not involved in flg22 binding but its association with FLS2 is necessary for full responsiveness (Chinchilla *et al.*, 2007; Heese *et al.*, 2007). BAK1 also contributes to signalling pathways activated by several other PAMPs, as well as AtPep1, a plant-derived DAMP (Shan *et al.*, 2008; Krol *et al.*, 2010). Similarly, further signalling components like MAPKs, CDPKs and WRKY transcription factors are shared not only between multiple MAMPs/DAMPs but also by other stimuli, such as abiotic stresses, hormones and developmental cues (Kudla *et al.*, 2010; Rodriguez *et al.*, 2010; Rushton *et al.*, 2010). Moreover,  $\text{Ca}^{2+}$  is a ubiquitous second messenger involved in nearly all aspects of plant life (Dodd *et al.*, 2010; Kudla *et al.*, 2010). This raises the question of how and to which extent signal specificity is maintained by common signalling components. Whereas MAPKs, CDPKs and WRKY transcription factors comprise large gene families of several individuals with, for example, specific domain structures and expression patterns to determine specific outputs,  $\text{Ca}^{2+}$  is just a simple ion. A longstanding paradigm to explain stimulus-specific responses is the concept of the “ $\text{Ca}^{2+}$  signature” (Webb *et al.*, 1996), where duration, amplitude, frequency and spatial distribution are thought to encode stimulus-specific information that is decoded by various  $\text{Ca}^{2+}$ -binding proteins, like calmodulins (CaM),  $\text{Ca}^{2+}$ -dependent CaM-binding transcription factors (CAMTAs) and CDPKs. Alternatively,  $\text{Ca}^{2+}$  may act as a “chemical on-off switch”, where  $\text{Ca}^{2+}$  levels beyond a certain threshold are necessary and sufficient to trigger responses (Scrase-Field and Knight, 2003; Dodd *et al.*, 2010).

The relevance for these signalling components in immunity can be inferred from the strategies used by pathogens to interfere with their function. These include effector proteins delivered into host cells (Göhre and Robatzek, 2008) or secretion of extracellular polysaccharides that sequester apoplasmic  $\text{Ca}^{2+}$  to impair MAMP/DAMP signalling (Aslam *et al.*, 2008). Thus, changes in  $[\text{Ca}^{2+}]_{\text{cyt}}$  is one of the earliest and vital events for signalling. As the interaction and mutual relations of many early MAMP/DAMP signalling components in Arabidopsis are not well understood, these were analysed for a possible impact on  $\text{Ca}^{2+}$  signalling. We concentrated on such components that act in the same time frame as  $\text{Ca}^{2+}$  signalling, like BAK1 and homologous somatic embryogenesis receptor-like kinases (SERK), MAPKs and NADPH oxidases.

## RESULTS

### Different MAMPs and DAMPs induce specific $[Ca^{2+}]_{cyt}$ elevations in Arabidopsis seedlings.

As assessed by aequorin luminescence-based  $Ca^{2+}$  imaging, several MAMPs or DAMPs, such as bacterial flg22 and elf18, fungal *N*-acetylchitooctase (ch8), and the plant-derived DAMP, Pep1, elicit  $[Ca^{2+}]_{cyt}$  increases in Arabidopsis seedlings (Figure 1a). Specificity is demonstrated by the lack of  $[Ca^{2+}]_{cyt}$  increase in the controls, comprising either water or inactive forms of the MAMPs/DAMPs (Figure 1, S1; Felix *et al.*, 1999; Kunze *et al.*, 2004). Pre-treatment of seedlings with either  $LaCl_3$ , a  $Ca^{2+}$  channel blocker, or BAPTA, a membrane-impermeant  $Ca^{2+}$  chelator, completely abolished the MAMP/DAMP-induced  $[Ca^{2+}]_{cyt}$  elevations (Figure S2), showing that an initial influx of apoplastic  $Ca^{2+}$  across the plasma membrane is required for establishing the  $[Ca^{2+}]_{cyt}$  response.

Dose response curves showed that, with the exception of Pep1, the tested MAMPs/DAMPs reached apparent saturating concentrations for inducing  $[Ca^{2+}]_{cyt}$  elevations between 100 nM to 1  $\mu$ M (Figure S3). The MAMPs or DAMPs, which were applied at 1  $\mu$ M for general comparison, induced  $[Ca^{2+}]_{cyt}$  elevations with a typical pattern (Figure 1a): after a lag phase of about 40 sec (flg22/ch8) to 1 min (elf18/Pep1), the  $[Ca^{2+}]_{cyt}$  steeply increased, followed by a short plateau phase and a slow decline to resting level over 30-40 min. Maximum peak heights differed between the tested MAMPs/DAMPs, with flg22 having the highest  $[Ca^{2+}]_{cyt}$  amplitude (Figure 1a,c). Interestingly, two distinct peaks were detectable for flg22, whereas for elf18 and Pep1 the “twin peaks”, while regularly visible in individual plots (Figure S4), were merged to a prolonged plateau phase in the composite plot representing the average of more than 30 seedlings (Figure 1a).

### Root- and shoot-specific differences in response to MAMPs and DAMPs.

Since flagellin, EF-Tu and chitin are not specific for foliar microbes, their ability to induce  $[Ca^{2+}]_{cyt}$  responses in isolated roots was compared to the aerial seedling parts. No significant differences in amplitude or kinetics of MAMP/DAMP-induced  $[Ca^{2+}]_{cyt}$  elevations between intact and root-dissected seedlings (Figure 1c, S5) were found for flg22, elf18 and ch8. Pep1-induced  $[Ca^{2+}]_{cyt}$  amplitudes were slightly enhanced in root-dissected seedlings, probably due to wounding effects (Figure 1c, S5). Taken together, the detected flg22/elf18-induced  $[Ca^{2+}]_{cyt}$  elevations of intact seedlings represent that of the aerial tissues. Whereas ch8 and Pep1 induced rather similar responses in seedling shoots and roots, roots were insensitive to elf18 and showed only a minor response to flg22 (Figure 1b,c). The shape of the flg22-induced  $[Ca^{2+}]_{cyt}$  curve in roots resembled that in seedlings induced by lower flg22 concentrations (Figure S3a). Accordingly, the *FLS2* and *EFR* receptors are highly expressed in whole seedlings and rosette leaves but only marginally in roots, while *CERK1* (*Chitin elicitor receptor kinase 1*), *PEPR1/2* (*Pep receptor 1/2*) and *BAK1* are similarly expressed in roots and aerial parts (Figure 1d). Thus, the observed MAMP/DAMP-induced  $[Ca^{2+}]_{cyt}$  elevations in roots mirror the expression levels of the corresponding receptors.

Plant growth arrest in the presence of MAMPs/DAMPs is well documented, but there appear to be organ-specific differences e. g. for Pep1 (Krol *et al.*, 2010). We therefore re-evaluated growth inhibition of Col-0 seedlings on flg22- or elf18-containing agar plates. Seedlings on flg22-plates had short roots with many lateral roots, while the shoots were smaller, sometimes with slightly yellowish leaves, and very variable in size. By contrast, seedlings on elf18-plates had tiny, dark brown cotyledons and long, thin primary roots without lateral roots (Figure 2a). Thus, flg22 mainly inhibits root growth, whereas elf18 predominantly affects shoots (Figure 2b,c). Quantification, based on root length for flg22 and fresh weight for elf18 (Figure 2b,c), corroborates the  $[Ca^{2+}]_{cyt}$  elevation dose response data (Figure S3) that maximum inhibition is attained between 100 nM to 1  $\mu$ M. Hence, while at first sight, many MAMP-induced responses appear similar, detailed comparison based on flg22 and elf18 revealed that MAMP-specific differences exist in both “late” responses like MAMP-induced growth inhibition and “early” events such as  $[Ca^{2+}]_{cyt}$  elevations.

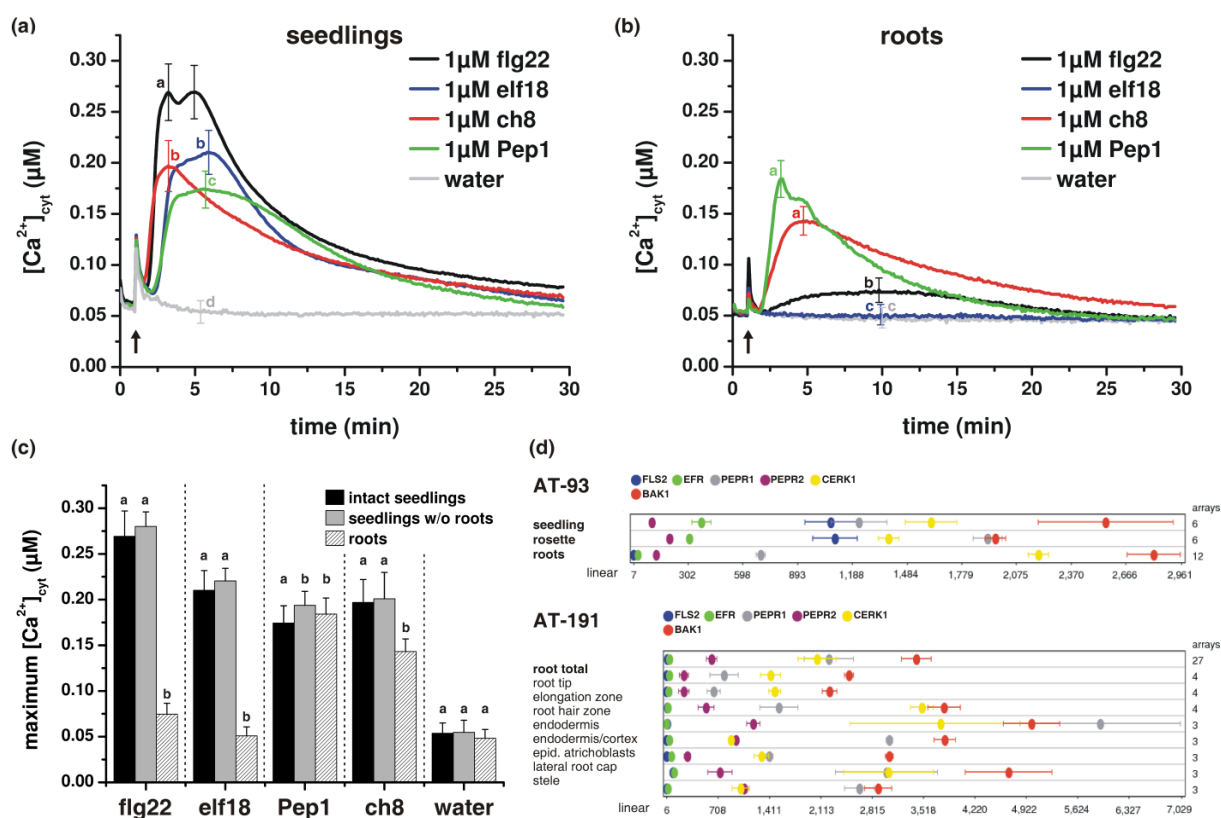


**Figure 1. MAMPs and DAMPs induce specific  $[Ca^{2+}]_{cyt}$  elevations in Arabidopsis seedlings and roots.**

(a,b)  $[Ca^{2+}]_{cyt}$  elevations upon application (marked by arrow) of the MAMPs/DAMPs flg22, elf18, ch8, Pep1 and water as control in (a) intact Col-0 seedlings or (b) isolated roots were monitored over time. Data represent mean  $\pm$  SD of  $\geq 4$  independent experiments ( $n \geq 30$ ). Letters indicate statistically significant differences between the  $[Ca^{2+}]_{cyt}$  amplitudes induced by the distinct MAMPs/DAMPs, with the statistically significant groups categorized by different letters (Kruskal-Wallis / Dunn's post test;  $p < 0.001$ ).

(c) Comparison of the maximum  $[Ca^{2+}]_{cyt}$  amplitudes in intact seedlings (black bars), root-dissected seedlings (without [w/o] roots; grey bars) or isolated roots (shaded bars) induced by the indicated MAMPs/DAMPs (all 1  $\mu$ M) or water as control. Letters indicate statistically significant differences between the  $[Ca^{2+}]_{cyt}$  amplitudes induced in the distinct tissues, separately calculated for each MAMP/DAMP, with the statistically significant groups categorized by different letters (Kruskal-Wallis / Dunn's post test;  $p < 0.001$ ).

(d) Expression of MAMP/DAMP receptors in Arabidopsis seedlings, rosettes and roots (upper panel; AT-93) or in distinct Arabidopsis root tissues (lower panel; AT-191). Data were obtained from public database (Genevestigator v3).

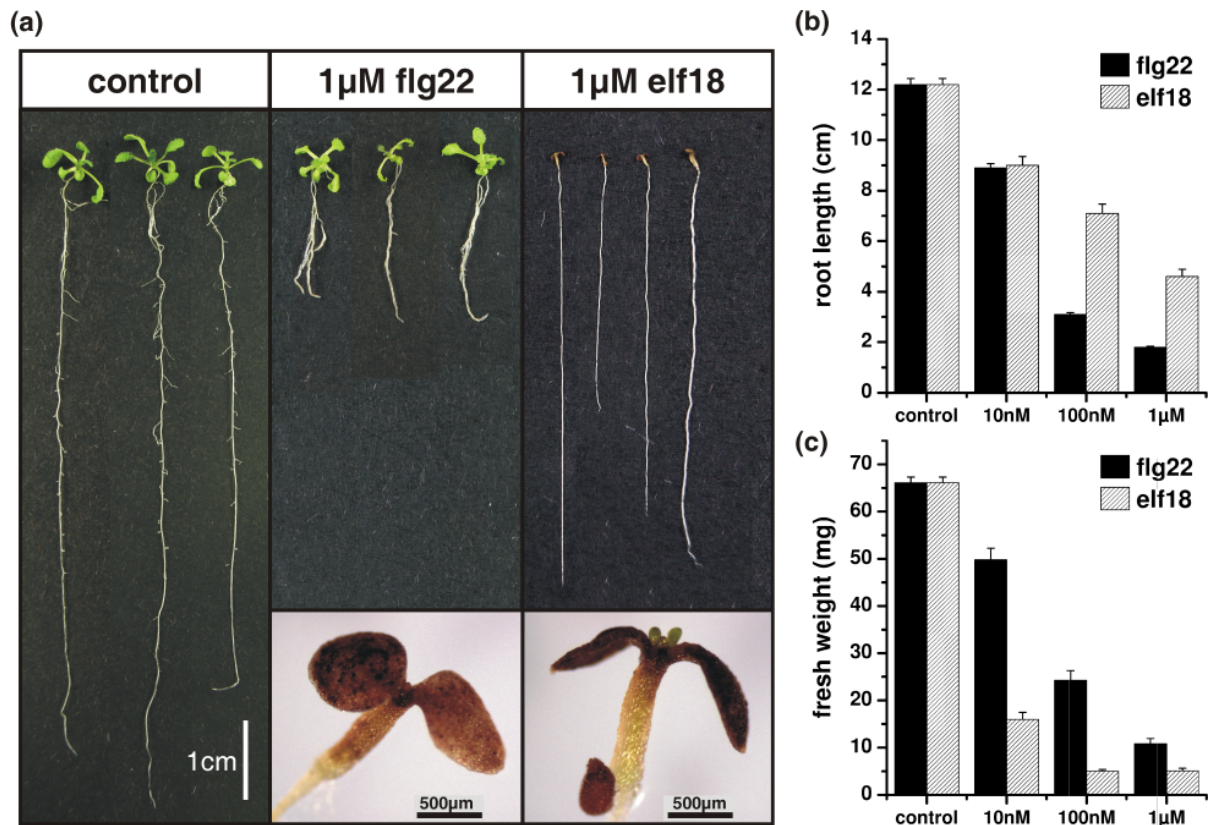


**Figure 2. Flg22- and elf18-induced growth inhibition reveals different phenotypes in Arabidopsis seedlings.**

(a) Col-0 seedlings were grown on agar plates  $\pm$  1  $\mu$ M flg22 or elf18 for 14 days and representative seedlings were photographed. Inserts show enlarged photographs of elf18-induced upper seedling parts. Identical results were obtained in  $\geq$  3 independent experiments.

(b) Root length of Col-0 seedlings grown for 14 days on agar plates containing the indicated concentrations of flg22 (black bars) or elf18 (shaded bars).

(c) Fresh weight of 5-days-old Col-0 seedlings grown for further 15 days in liquid medium containing the indicated concentrations of flg22 (black bars) or elf18 (shaded bars).

### **[Ca<sup>2+</sup>]<sub>cyt</sub> elevations induced by flg22, elf18 and Pep1, but not ch8 are delayed and reduced in *bak1* mutants.**

To investigate the role of Ca<sup>2+</sup> signalling, several signalling components were tested for their contribution to MAMP-induced [Ca<sup>2+</sup>]<sub>cyt</sub> elevations. The receptor mutants, *fls2*, *efr* and *cerk1*, were insensitive to their respective MAMPs, but reacted normally to other tested MAMPs/DAMPs (Figure S6). By contrast, mutants of the *BAK1* “co-receptor” did not show complete insensitivity, but delayed and reduced [Ca<sup>2+</sup>]<sub>cyt</sub> responses to flg22, elf18 and Pep1 (Figure 3a-c,e). Ch8-induced [Ca<sup>2+</sup>]<sub>cyt</sub> elevations in *bak1* mutants, in contrast, were essentially identical to wild type (Figure 3d). Similarly, MAPK activation, a downstream response of [Ca<sup>2+</sup>]<sub>cyt</sub> elevations, was clearly reduced and delayed (for flg22 and elf18) or slightly reduced (for Pep1) in *bak1-4* upon elicitation but not upon ch8 elicitation (Figure 3f). Hence, these findings are in agreement with the published role of BAK1 in early signalling for FLS2, EFR (Chinchilla *et al.*, 2007) and PEPR1/2 (Krol *et al.*, 2010), but not CERK1 (Shan *et al.*, 2008).

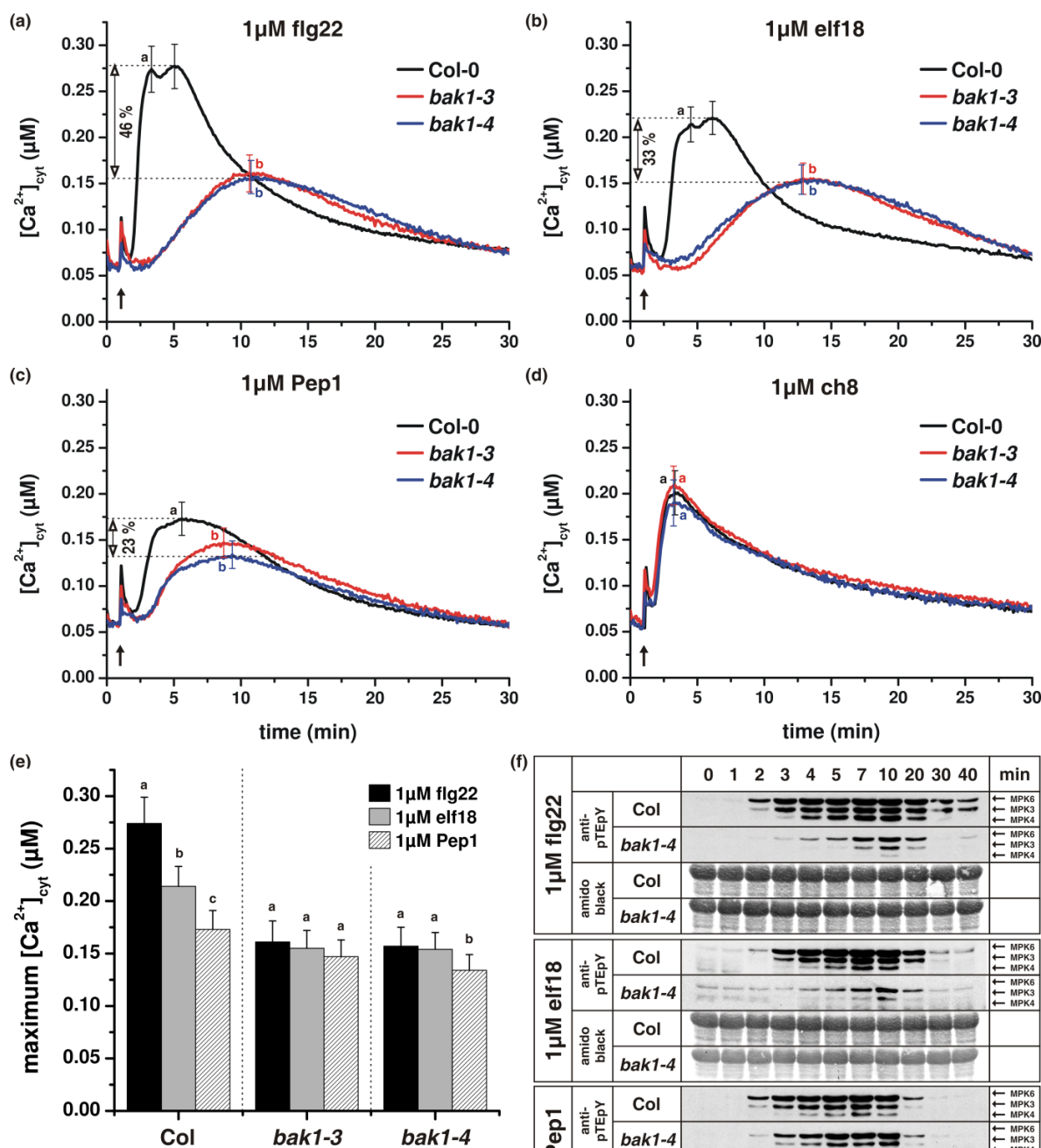


**Figure 3.  $[Ca^{2+}]_{cyt}$  elevation and MAPK activation is delayed and reduced in *bak1* seedlings upon flg22, elf18 and Pep1, but not ch8 elicitation.**

(a-d)  $[Ca^{2+}]_{cyt}$  elevations in *bak1* seedlings induced by the indicated MAMPs/DAMPs compared to Col-0. Dashed lines/arrows indicate reduction of peak height in *bak1-4* compared to Col-0. Black arrows mark time of MAMP/DAMP application. Data represent mean  $\pm$  SD of  $\geq 4$  independent experiments ( $n \geq 10$ ). Letters indicate statistically significant differences between the  $[Ca^{2+}]_{cyt}$  amplitudes in the distinct genotypes, separately calculated for each MAMP/DAMP, with the statistically significant groups categorized by different letters (Kruskal-Wallis / Dunn's post test;  $p < 0.001$ ). (e) Comparison of the maximum  $[Ca^{2+}]_{cyt}$  amplitudes in Col-0 or *bak1* mutants induced by 1 μM flg22 (black bars), 1 μM elf18 (grey bars) or 1 μM Pep1 (shaded bars). Letters indicate statistically significant differences between  $[Ca^{2+}]_{cyt}$  amplitudes induced by

the distinct MAMP/DAMPs, separately calculated for each genotype, with the statistically significant groups categorized by different letters (Kruskal-Wallis / Dunn's post test;  $p < 0.001$ ).

(f) MAPK activation upon application of the indicated MAMPs/DAMPs in *bak1-4* compared to Col-0 was analysed by anti-pTEpY Western blot at indicated time points. Amido-black-stained membranes show equal loading. Three independent experiments revealed comparable results.

Strikingly, the distinct flg22-, elf18- and Pep1-induced  $[Ca^{2+}]_{cyt}$  elevations in wild type were reduced in *bak1* mutants to virtually identical peak height (Figure 3e) and shape for all three MAMPs/DAMPs (Figure 3a-c). Different amplitudes for MAMP/DAMP-induced membrane depolarization have similarly been observed between *bak1-4* and wild type plants (Krol *et al.*, 2010). Thus, BAK1-receptor interaction determines the distinct amplitudes of  $[Ca^{2+}]_{cyt}$  elevation (Figure 3a-c,e) and membrane depolarization induced by different MAMPs/DAMPs in wild type plants, with BAK1 acting as signal amplifier to accelerate and boost the overall response. The residual responses observed in *bak1* mutants might originate from signalling solely *via* the receptors or from partially redundant BAK1 homologs (see below) or other receptor complex constituents.

**Other SERK family members do not show altered flg22/elf18-induced  $[Ca^{2+}]_{cyt}$  elevations and ROS accumulation, but enhanced flg22-mediated root growth arrest.**

BAK1 belongs to the five-membered family of somatic-embryogenesis receptor-like kinases (SERK) and is accordingly also named SERK3 (Hecht *et al.*, 2001). To assess if the other SERKs are involved in early MAMP and DAMP signalling, the aequorin transgene was introduced into *serk1-1*, *serk2-1*, *serk4-1* and *serk5-1*. All four mutants showed normal  $[Ca^{2+}]_{cyt}$  responses and ROS accumulation upon flg22 and elf18 elicitation (Figure 4a-d), thereby confirming earlier reports (Chinchilla *et al.*, 2007; Heese *et al.*, 2007). While ch8-induced  $[Ca^{2+}]_{cyt}$  responses were not altered in any of the other *serk* mutants, Pep1 induced wild-type-like  $[Ca^{2+}]_{cyt}$  elevations in *serk1-1*, *serk2-1* and *serk5-1*, but a slightly reduced  $[Ca^{2+}]_{cyt}$  increase in *serk4-1* (data not shown). Whereas none of the *bak1* or *serk* mutants showed any differential growth arrest to elf18 compared to the wild type (Figure S7), root growth of the *bak1* mutants was considerably less sensitive to flg22 (Figure 4e,f). Interestingly, flg22-mediated root growth inhibition was significantly enhanced in *serk2-1* and *serk4-1* mutants, while comparable to wild type for *serk1-1* and *serk5-1* (Figure 4e,f). As  $[Ca^{2+}]_{cyt}$  elevations (Figure 4a,b) and ROS accumulation (Figure 4c,d) were unaltered in both mutants, SERK2 and SERK4 probably do not exert their function in flg22 signalling at the early stages, but act further downstream in the pathway leading to growth arrest. Taken together, unlike *bak1*, none of the four *serk* mutants showed a phenotype with regard to  $[Ca^{2+}]_{cyt}$  responses or ROS accumulation. Nevertheless, it cannot be excluded that additional phenotypes might only become visible in higher order mutants. For instance, a role for SERK4 in cell death control only became evident in the *serk3serk4* double mutant (He *et al.*, 2007).

**BAK1 differentially contributes to responses induced by flg22 and elf18.**

To further elucidate the role of BAK1 in conferring MAMP- and DAMP-specific information, defence-related gene expression upon flg22 and elf18 elicitation was monitored. For better comparison, the protoplast-based *FRK1*-promoter-luciferase (*pFRK1-LUC*) expression assay, previously used to demonstrate differential roles of *BAK1* between flg22, elf18 and chitin (Shan *et al.*, 2008), was employed. *LUC*-expression driven by two additional defence-related promoters, *NHL10* and *PHI1*

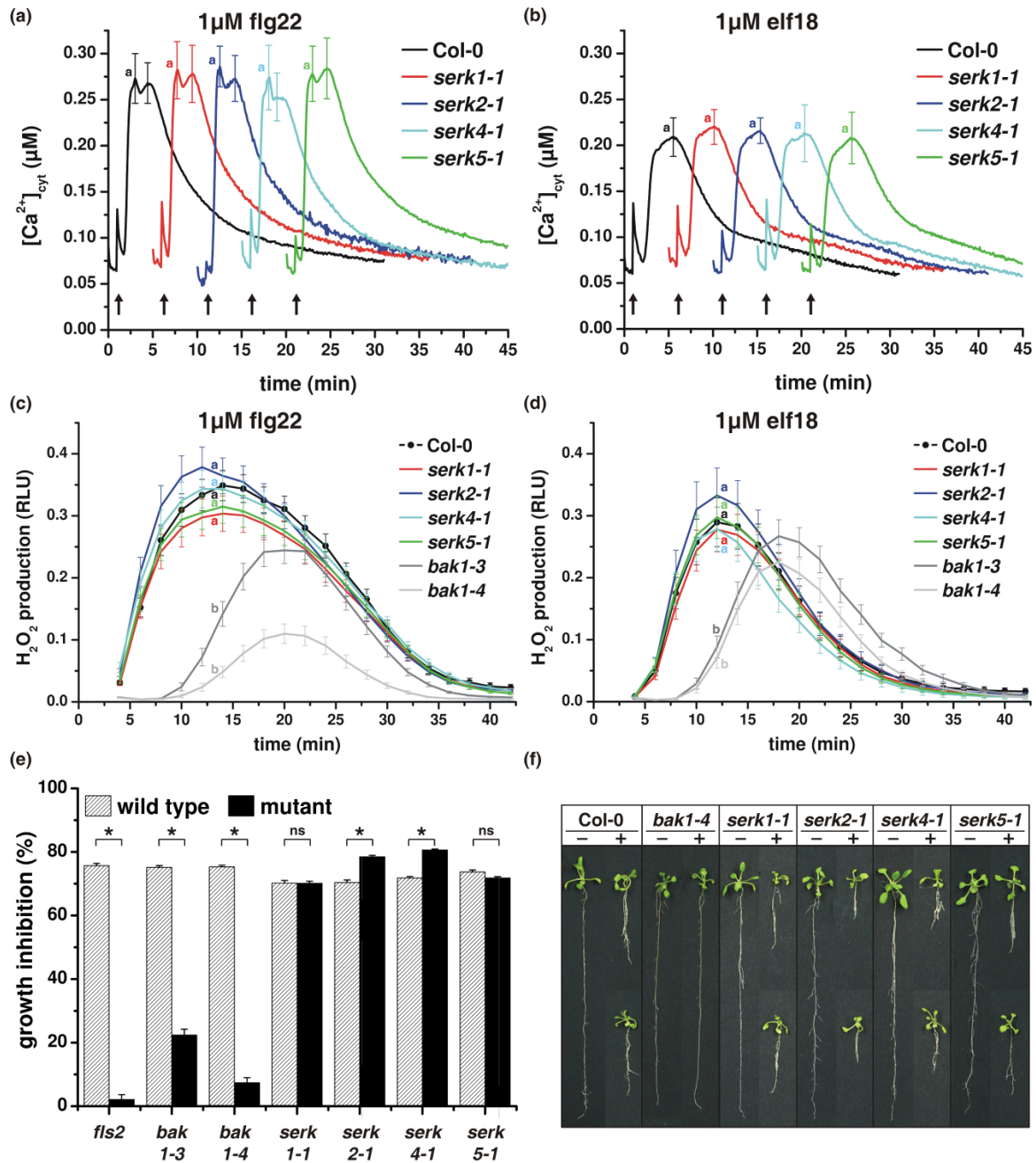


**Figure 4. Flg22-mediated root growth inhibition, but not  $[Ca^{2+}]_{cyt}$  elevation, is enhanced in *serk2-1* and *serk4-1*.**

(a,b)  $[Ca^{2+}]_{cyt}$  elevations in *serk* mutant seedlings induced by (a) 1  $\mu$ M flg22 or (b) 1  $\mu$ M elf18 compared to Col-0. For clarity, graphs are depicted offset. Arrows mark time of MAMP application. Data represent mean  $\pm$  SD of  $\geq 3$  independent experiments ( $n \geq 40$ ). Letters indicate statistically significant differences between the  $[Ca^{2+}]_{cyt}$  amplitude of the mutant compared to wild type, separately calculated for each mutant-wild type pair, with the statistically significant groups categorized by different letters (Student's t-test;  $p < 0.001$ ).

(c,d) ROS ( $H_2O_2$ ) production induced by (c) 1  $\mu$ M flg22 or (d) 1  $\mu$ M elf18 was monitored using a luminol-based assay in leaf discs of *bak1* and *serk* mutants compared to Col-0. Data are given as relative light units (RLU) and represent mean  $\pm$  SE of  $\geq 3$  independent experiments ( $n \geq 20$ ). Letters indicate statistically significant differences at the time of maximum ROS accumulation in the wild type, with the statistically significant groups categorized by different letters (Kruskal-Wallis / Dunn's post test;  $p < 0.05$ ).

(e) Root growth inhibition (1  $\mu$ M flg22) of different *serk* mutants (black bars) each compared to its respective wild-type control (shaded bars). Data are given as % inhibition compared to untreated control; mean  $\pm$  SE of  $\geq 3$  independent experiments ( $n \geq 60$ ); \* indicates statistically significant difference; ns = not significant (2-way ANOVA genotype x treatment;  $p < 0.001$ ).

(f) Photographs of representative Col-0 and *serk* mutant seedlings grown in the presence (+; two seedlings) or absence (-; one seedling) of 1  $\mu$ M flg22. Identical results were obtained in  $\geq 3$  independent experiments.

(Boudsocq *et al.*, 2010), was also included. Interestingly, by incorporating a time-course profiling aspect, different kinetics could already be detected between flg22- and elf18-induced expression of *pNHL10-LUC*, *pFRK1-LUC* and *pPHI1-LUC* in wild type protoplasts. Whereas expression of all three genes was generally more transient upon flg22 treatment, a long lasting response was observed after elf18 application within the tested time frame (Figure 5).

Moreover, BAK1 differentially contributed to flg22- and elf18-induced expression of *pNHL10-LUC*, *pFRK1-LUC* and *pPHI1-LUC*. In *bak1* mutants, all three constructs showed a loss of flg22-induced expression (Figure 5a-c), whereas elf18 activated all three promoter-constructs, although slightly delayed for *pNHL10* (Figure 5d-f). Two to three hours after elf18 elicitation, *pNHL10* and *pFRK1* activity in the *bak1* mutants was even higher than in wild type, whereas *pPHI1* activity did not reach wild-type levels (Figure 5d-f). Hence, BAK1 is not or only partially required for the early phase of elf18-induced *NHL10* and *FRK1* expression but is required to attenuate the expression of these two genes subsequently.

Like Chinchilla *et al.* (2007), we found that flg22-mediated growth inhibition is strongly reduced in *bak1* seedlings compared to wild type (Figure 4e,f), while no reduction was observed after elf18 treatment (Figure S7). In conclusion, besides the obvious distinct characteristics in the kinetics of defence gene expression and the growth inhibition phenotype upon flg22 vs. elf18 application, striking differences were noticed regarding the involvement of BAK1 in both responses.

### **Feedback effect of MAMP- and DAMP-induced RbohD-mediated ROS accumulation on $[Ca^{2+}]_{cyt}$ signalling.**

Another typical early response, occurring within minutes of MAMP and DAMP perception, is an accumulation of ROS. This is dependent on  $[Ca^{2+}]_{cyt}$  changes since pre-treatment with  $LaCl_3$ , to inhibit  $Ca^{2+}$  channels, also abrogates ROS accumulation in Arabidopsis leaf discs (Figure S8). Nevertheless, some ROS, like hydrogen peroxide ( $H_2O_2$ ), are themselves capable of inducing  $[Ca^{2+}]_{cyt}$  elevations (Pei *et al.*, 2000; Rentel and Knight, 2004; Ranf *et al.*, 2008). To test any possible feedback impact of ROS on  $[Ca^{2+}]_{cyt}$  elevations in response to different MAMPs and DAMPs, a pharmacological as well as a genetic approach were used. The NADPH oxidases, *rbohD* and *rbohF*, account for most of the pathogen-responsive oxidative burst (Torres *et al.*, 2002). In agreement with published results (Zhang *et al.*, 2007; Mersmann *et al.*, 2010), RbohD appears to be the major source of MAMP-induced ROS since the flg22/elf18-induced ROS accumulation was eliminated in the *rbohD* mutant (see Figure 7a,b), but not significantly altered in *rbohF* (Zhang *et al.*, 2007). Interestingly, when the flg22- and elf18-induced  $[Ca^{2+}]_{cyt}$  elevations in aequorin-transgenic *rbohD* mutant lines were analysed, the first  $Ca^{2+}$  peak was comparable to the wild type, while the second peak was abolished (Figure 6a,b). The plateau-phase of the Pep1-induced  $[Ca^{2+}]_{cyt}$  elevation was likewise reduced to a single maximum in *rbohD* (Figure 6c). A minor phenotype was observed after ch8 elicitation (Figure 6d). Similar results were obtained with the NADPH oxidase inhibitor diphenylene iodonium chloride (DPI; Figure 6e-h). Thus,

MAMP/DAMP-induced ROS indeed have a feedback effect on the  $[Ca^{2+}]_{\text{cyt}}$  response by inducing an additive  $[Ca^{2+}]_{\text{cyt}}$  elevation causing a second peak or prolonged plateau. However, flg22-mediated root growth arrest in *rbohD* was comparable to wild type (data not shown; Mersmann *et al.*, 2010). Thus, while ROS have a significant but overall minor feedback contribution to the “Ca<sup>2+</sup> signature”, the later growth inhibition response is independent of this rapid ROS generation.

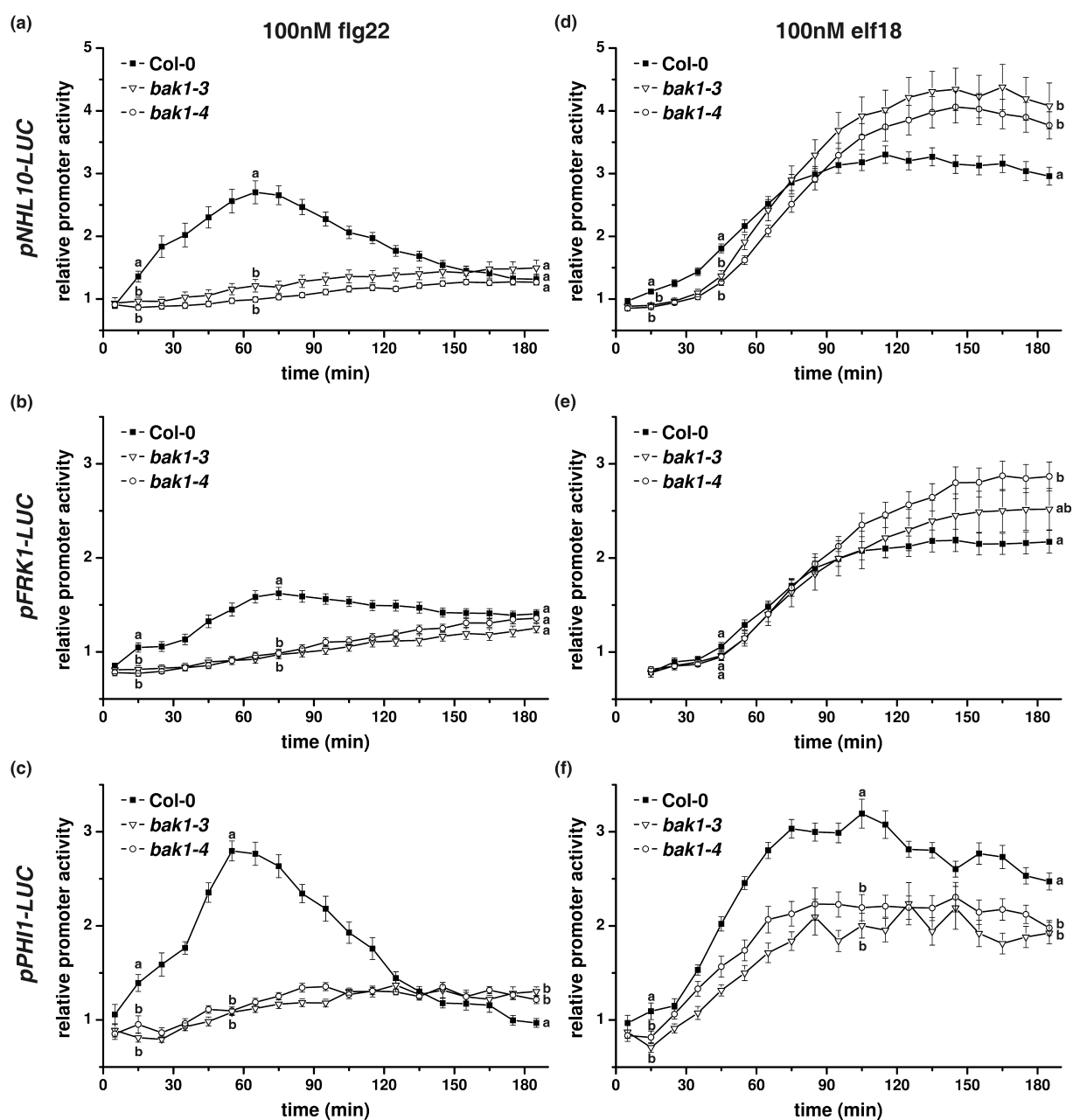


**Figure 5. Different patterns of defence gene promoter activity were observed in Col-0 and *bak1* protoplasts upon flg22 and elf18 elicitation.**

Promoter activities of the defence genes (a,d) *NHL10*, (b,e) *FRK1* and (c,f) *PHI1* were monitored in Col-0 and *bak1* protoplasts upon application of (a-c) 100 nM flg22 and (d-f) 100 nM elf18. Data are depicted as fold-induction compared to untreated control; mean  $\pm$  SE of  $\geq 4$  independent experiments ( $n \geq 20$ ). Letters indicate statistically significant differences at selected time points, with the statistically significant groups categorized by different letters (Kruskal-Wallis / Dunn's post test;  $p < 0.05$ ).

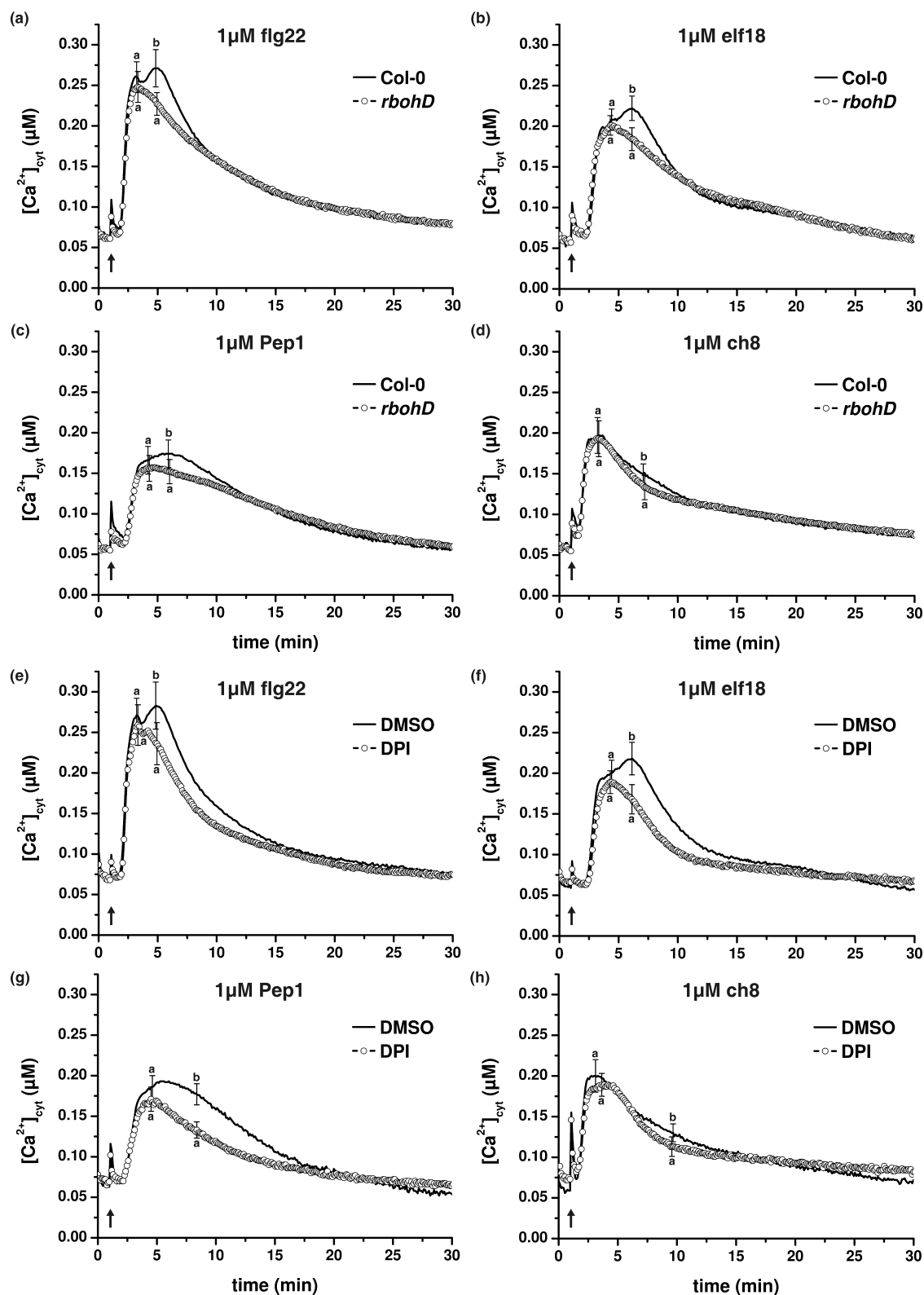


**Figure 6. Feedback effect of MAMP/DAMP-induced ROS accumulation on  $[Ca^{2+}]_{cyt}$  elevations.**

(a-d)  $[Ca^{2+}]_{cyt}$  elevations in *rbohD* seedlings induced by the indicated MAMPs/DAMPs compared to Col-0. Arrows mark time of MAMP/DAMP application. Data represent mean  $\pm$  SD of  $\geq 3$  independent experiments ( $n \geq 20$ ).

(e-h)  $[Ca^{2+}]_{cyt}$  elevations induced by the indicated MAMPs/DAMPs in Col-0 seedlings pre-treated with 25  $\mu M$  diphenylene iodonium chloride (DPI; in DMSO) or DMSO alone as control for 5 min. Arrows mark time of MAMP/DAMP application. Data represent mean  $\pm$  SD of  $\geq 2$  independent experiments ( $n \geq 15$ ).

Letters indicate statistically significant differences, separately calculated for each time point, with the statistically significant groups categorized by different letters (Student's t-test;  $p < 0.001$ ).

### Flg22 induces a wild type-like $[Ca^{2+}]_{cyt}$ elevation, but a prolonged ROS generation in *mpk3*.

MAPK activation is usually detectable two to three minutes after flg22 or elf18 elicitation (Figure 3f) and therefore occurs in the same time frame as the  $[Ca^{2+}]_{cyt}$  elevations. Although MAPK activation has been reported to be downstream of  $[Ca^{2+}]_{cyt}$  elevation in tobacco (Lecourieux *et al.*, 2002), LaCl<sub>3</sub> and BAPTA reduced but did not completely abolish MAPK activation in flg22-treated Arabidopsis suspension-cultured cells (Figure S9). Nevertheless, this demonstrates that MAPK activation is at least partially dependent on the  $[Ca^{2+}]_{cyt}$  elevation. Conversely, unlike the *rbohD* mutant shown above (Figure 6a,b), mutations in *MPK3* or *MPK6* did not significantly alter the flg22 or elf18-induced  $[Ca^{2+}]_{cyt}$  elevation (Figure 7c,d). By contrast, ROS accumulation in leaf discs of *mpk3*, but not *mpk6*, mutants was significantly prolonged upon flg22 and elf18 elicitation (Figure 7a,b). This correlates to a mild but statistically significant enhancement of the growth inhibition by flg22 in the *mpk3* mutants, while the *mpk6* mutant is slightly less sensitive to flg22 (Figure 7e).

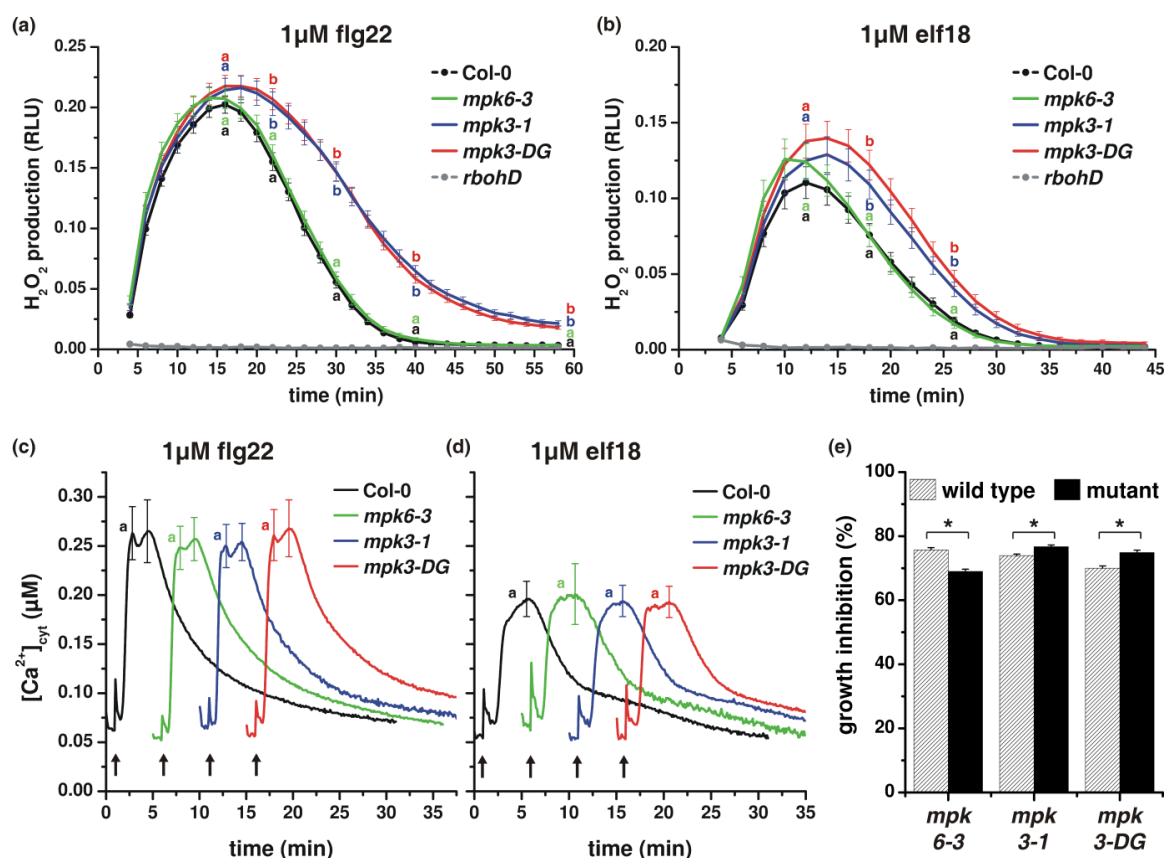


**Figure 7. MAMP-induced ROS accumulation, but not  $[Ca^{2+}]_{cyt}$  elevation, is prolonged in *mpk3*.**

(a,b) ROS (H<sub>2</sub>O<sub>2</sub>) production induced by (a) 1 μM flg22 or (b) 1 μM elf18 was monitored using a luminol-based assay in leaf discs of *mpk3* and *mpk6* mutants compared to Col-0 and *rbohD* as controls. While *mpk3-1* and *mpk6-3* are T-DNA insertion lines, *mpk3-DG* is a fast neutron deletion mutant (see table S1). Data are given as relative light units (RLU) and represent mean ± SE of ≥ 5 independent experiments (n ≥ 120). Letters indicate statistically significant differences, separately calculated for each time point, with the statistically significant groups categorized by different letters (Kruskal-Wallis / Dunn's post test; p < 0.05).

(c,d)  $[Ca^{2+}]_{cyt}$  elevations in *mpk3* and *mpk6* seedlings compared to Col-0 induced by (c) 1 μM flg22 or (d) 1 μM elf18. For clarity, graphs are depicted offset. Arrows mark time of MAMP application. Data represent mean ± SD of ≥ 4 independent experiments (n ≥ 20).

(e) Root growth inhibition (10 μM flg22) of *mpk3* and *mpk6* mutants (black bars) each compared to its respective wild-type control (shaded bars). Data are given as % inhibition compared to untreated control; mean ± SE of ≥ 4 independent experiments (n ≥ 40); \* indicates statistically significant difference (2-way ANOVA genotype x treatment; p < 0.001).

## DISCUSSION

### Response specificity encoding in $[Ca^{2+}]_{\text{cyt}}$ amplitude or signature.

A hallmark of MAMP- and DAMP-induced  $[Ca^{2+}]_{\text{cyt}}$  elevations, either in Arabidopsis shown here or in other systems, such as parsley, tobacco and soybean cell suspensions (Mithöfer *et al.*, 1999; Blume *et al.*, 2000; Lecourieux *et al.*, 2002), are  $[Ca^{2+}]_{\text{cyt}}$  elevations that are sustained as compared to the “spike-like” transient  $[Ca^{2+}]_{\text{cyt}}$  elevations induced by most abiotic stimuli (Knight *et al.*, 1996, 1997; Rentel and Knight, 2004; Ranf *et al.*, 2008). However, for valid comparison between different stimuli, nearly synchronous elicitation in the multicellular Arabidopsis seedlings should be attained. Thus, liquid-grown seedlings were used here, which due to direct contact of the complete surface with the surrounding medium and presumably due to a less developed cuticle, facilitated MAMP/DAMP accessibility. Additionally, near saturating MAMP concentrations were applied to further reduce accessibility variation and to compare the maximum  $[Ca^{2+}]_{\text{cyt}}$  elevation-inducing capacities of different MAMPs and DAMPs. Another advantage, over leaf discs, is that intact seedlings are not “primed” by or “refractory” from wounding.

Under the above-mentioned conditions, differences in lag phases and  $[Ca^{2+}]_{\text{cyt}}$  amplitudes were observed (Figure 1). Aslam and co-workers (2009), who also observed different  $[Ca^{2+}]_{\text{cyt}}$  amplitudes, suggested that this may be accounted by differential MAMP diffusion rates through the cell wall matrix. However, such diffusion rate differences for the relatively small peptide MAMPs or DAMPs being compared here are unlikely. Distinct lag phases for flg22 and elf18 were also observed for medium alkalization in Arabidopsis suspension-cultured cells (Zipfel *et al.*, 2006) and distinct MAMP/DAMP-induced membrane depolarization in leaves with the epidermis removed (Krol *et al.*, 2010). Thus, the differences are most probably intrinsic characteristics of the receptor-mediated perception of the distinct MAMPs.

Despite the overall similar  $[Ca^{2+}]_{\text{cyt}}$  kinetics, the lag phases and amplitudes differed between the tested MAMPs and DAMPs. It is conceivable that such qualitative, quantitative or kinetic differences in  $[Ca^{2+}]_{\text{cyt}}$  elevations encode information contributing to the MAMP-specific responses. On the contrary, *bak1* mutants show similar MAPK activation (Figure 3f) as well as distinct downstream responses, like gene expression (Figure 5) and growth arrest (Figure 4e, S7) to different MAMPs, despite virtually identical  $[Ca^{2+}]_{\text{cyt}}$  elevations (Figure 3a,b,e). This strongly argues against the concept that the “ $Ca^{2+}$  signatures” convey MAMP-specific information into downstream responses. The presented data therefore substantiate the notion of a “chemical on-off switch” or “threshold” function for  $Ca^{2+}$  in MAMP and DAMP signalling (Scrase-Field and Knight, 2003; Dodd *et al.*, 2010).

Concerning the question whether  $[Ca^{2+}]_{\text{cyt}}$  elevations encode and transmit MAMP-specific information, it should also be considered that aequorin-based  $[Ca^{2+}]$  imaging provides an average response of whole seedlings or tissues consisting of different cell types whose individual responses can differ substantially (see below). Hence, while it may reveal differences in some cases, as illustrated by the *rbohD* analysis,

the underlying single cell/tissue  $\text{Ca}^{2+}$  signatures may not always be deducible from aequorin-based  $[\text{Ca}^{2+}]$  imaging of whole seedlings (Dodd *et al.*, 2010).

### **Organ/tissue-specific differences in MAMP/DAMP responses.**

As the  $[\text{Ca}^{2+}]_{\text{cyt}}$  measurements show that both, flg22 and elf18, are effectively sensed in aerial parts and only marginally in roots (Figure 1), the distinct shoot and root growth arrest phenotypes cannot be simply explained by specific perception in these tissues. Based on callose deposition and reporter gene expression, Millet and co-workers (2010) also reported that roots are insensitive to elf18, but react strongly to chitin all over the mature zone, whereas flg22-induced responses were only detectable in the root elongation zone (EZ). By contrast, flg22-induced membrane depolarization was also detected in root hairs (Jeworutzki *et al.*, 2010). As *FLS2* is expressed throughout the entire root (Robatzek *et al.*, 2006) and no enhanced *FLS2* transcript level is observed in the EZ (Figure 1d), the minor flg22-induced  $[\text{Ca}^{2+}]_{\text{cyt}}$  elevation measured in whole roots is probably due to a weak response in the entire root rather than a localized response in the EZ.

Thus, in contrast to chitin, the bacterial MAMPs flg22 and elf18 apparently only have minor contributions to PTI in roots compared to shoots. However, as illustrated by the pivotal roles of  $\text{Ca}^{2+}$  signalling in roots during legume–rhizobia, arbuscular mycorrhizal symbiosis and beneficial interaction of Arabidopsis with the endophytic growth-promoting fungus *Piriformospora indica* (Harper and Harmon, 2005; Oldroyd and Downie, 2006; Navazio *et al.*, 2007; Vadassery *et al.*, 2009), perception of other MAMPs in roots is important for several other plant-microbe interactions.

### **The role of BAK1 in early and late signalling.**

The nearly identical  $[\text{Ca}^{2+}]_{\text{cyt}}$  kinetics (Figure 3a-c) and membrane-depolarization (Jeworutzki *et al.*, 2010) induced by flg22, elf18 and Pep1 in *bak1* mutants led to the hypothesis that a similar basal level of early signal transduction activation by these diverse MAMPs or DAMPs exists, and this is further differentially amplified and accelerated by the receptor-associated kinase BAK1. Using ROS accumulation and growth arrest as markers for early and late responses, respectively, Chinchilla and co-workers (2007) surmised that flg22-induced early and late responses are both altered in *bak1*, whereas BAK1 is only required for early signalling but not for late responses induced by elf18. Our current gene expression studies now suggest that BAK1 also has different regulatory functions in elf18-induced defence gene expression at early time points, well within the time frame of  $[\text{Ca}^{2+}]_{\text{cyt}}$  elevations and MAPK activation. Whereas  $[\text{Ca}^{2+}]_{\text{cyt}}$  elevations and MAPK activation revealed nearly identical phenotypes for both flg22 and elf18 in *bak1* (Figure 3), different phenotypes were observed regarding gene expression in *bak1* (Figure 5), although regulation of the analysed promoters was reported to be dependent on MAPK (*pFRK1*) or CDPK activity (*pPHI1*) or both (*pNHL10*; Boudsocq *et al.*, 2010). Taken together, a differential involvement of BAK1 can be observed at early and late signalling phases. One possible explanation for the diverse BAK1 regulatory roles at various signalling steps may be the

BAK1 association with receptors of numerous signalling pathways (Postel *et al.*, 2010), as well as several receptor-like cytoplasmic kinases (Lu *et al.*, 2010; Zhang *et al.*, 2010), which are connected with MAMP signalling pathways. For instance, BAK1 also interacts with the Pep receptors (PEPR1/2) and this is suggested to provide a feed-forward amplification loop of MAMP signals (Postel *et al.*, 2010). Thus, specificity in MAMP and DAMP signalling is, in part, determined by BAK1, possibly *via* differential amplification at distinct steps.

### The Ca<sup>2+</sup>/ROS feedback loop.

Inhibitor studies suggest that MAMP and DAMP-induced RbohD-mediated ROS generation is strictly dependent on an initial upstream [Ca<sup>2+</sup>]<sub>cyt</sub> elevation (Figure S8). This is supported by the Ca<sup>2+</sup>-dependent regulation of RbohD, either direct Ca<sup>2+</sup> activation by binding to the N-terminal EF-hand motifs in RbohD (Ogasawara *et al.*, 2008) or indirectly *via* Ca<sup>2+</sup>-activated CDPK-dependent phosphorylation (Kobayashi *et al.*, 2007; Boudsocq *et al.*, 2010). Nevertheless, ROS have a feedback effect on the [Ca<sup>2+</sup>]<sub>cyt</sub> response (Figure 6). Intriguingly, complete abrogation of MAMP-induced ROS generation in the *rbohD* mutant or by inhibition with DPI, did not result in an overall reduction of the [Ca<sup>2+</sup>]<sub>cyt</sub> elevations but rather affected solely the second peak or prolonged plateau. In tobacco cells, DPI similarly inhibited the second of two OGA-triggered [Ca<sup>2+</sup>]<sub>cyt</sub> peaks (Lecourieux *et al.*, 2002). The timing of the second [Ca<sup>2+</sup>]<sub>cyt</sub> peak, with a maximum at around five minutes after flg22 elicitation (Figure 1a), correlates with the kinetics of MAMP-induced ROS accumulation, which is measurable starting from three to four minutes after flg22 elicitation (Figure 4c,7a). Accordingly, the less pronounced second [Ca<sup>2+</sup>]<sub>cyt</sub> peaks for *elf18* or *Pep1* and particularly *ch8*, are generally associated with a lower, and in some cases delayed, ROS production (Figure 4d, 7b and data not shown). In any case, the secondary ROS-induced [Ca<sup>2+</sup>]<sub>cyt</sub> elevation is transient, which is comparable to a direct H<sub>2</sub>O<sub>2</sub>-induced [Ca<sup>2+</sup>]<sub>cyt</sub> elevation (Rentel and Knight, 2004). This may be due to saturation and refractory period of the H<sub>2</sub>O<sub>2</sub> perception system; and may also explain why the prolonged ROS response in *mpk3* mutants did not significantly alter the [Ca<sup>2+</sup>]<sub>cyt</sub> elevation induced by flg22 or *elf18* (Figure 7c,d). The “double Ca<sup>2+</sup> peak” reported here has so far not been reported by others for the Arabidopsis system (Jeworutzki *et al.*, 2010; Krol *et al.*, 2010; Qi *et al.*, 2010), which could be due to different experimental setup, in particular the integration intervals for luminescence measurement. Alternatively, leaf discs do not show an H<sub>2</sub>O<sub>2</sub>-induced [Ca<sup>2+</sup>]<sub>cyt</sub> elevation (data not shown). Hence, in line with a possible different H<sub>2</sub>O<sub>2</sub> refractory period speculated above, the use of wounded/excised plant material may lead to this second Ca<sup>2+</sup> peak being overlooked.

Although H<sub>2</sub>O<sub>2</sub> triggers [Ca<sup>2+</sup>]<sub>cyt</sub> elevations and H<sub>2</sub>O<sub>2</sub>-responsive plasma membrane Ca<sup>2+</sup>-permeable channels have been described (Pei *et al.*, 2000; Rentel and Knight, 2004), it is unclear from the current data whether RbohD-derived O<sub>2</sub><sup>•-</sup> or its dismutation product H<sub>2</sub>O<sub>2</sub> directly or indirectly activate Ca<sup>2+</sup>-permeable channels and if the ROS-triggered [Ca<sup>2+</sup>]<sub>cyt</sub> elevation involves Ca<sup>2+</sup> influx from the apoplast or release from internal stores. Moreover, apoplastically generated and membrane-permeant ROS like

H<sub>2</sub>O<sub>2</sub> are able to diffuse to or into neighbouring cells to activate signalling. Indeed, RbohD-derived ROS have been implicated in long-distance signalling in abiotic stress reactions (Miller *et al.*, 2009). In conclusion, although speculative, it appears plausible that the feedback effect between ROS and Ca<sup>2+</sup> signalling observed here, may similarly allow cell-to-cell propagation of MAMP/DAMP signals.

### **The role of MAPKs in early MAMP signalling.**

Loss of MPK3, but not MPK6, leads to a substantially prolonged ROS accumulation upon elicitation with flg22 or elf18, while the maximum ROS levels were not increased (Figure 7a,b). Although the ROS accumulation is strictly dependent on the [Ca<sup>2+</sup>]<sub>cyt</sub> elevation, this does not result from a prolonged [Ca<sup>2+</sup>]<sub>cyt</sub> increase. Surprisingly, a previous screen for components involved in the flg22-induced ROS response did not reveal a phenotype for *mpk3* (Mersmann *et al.*, 2010). This might result from the different conditions used: Mersmann and co-workers analysed ROS accumulation at lower flg22 concentrations in intact seedlings grown in liquid medium and pre-treated with 10 nM flg22. However, although such pre-treatment was designed to reduce variability of the ROS assay (Mersmann *et al.*, 2010), it may pre-stimulate the ROS catabolic pathway and mask the prolonged ROS accumulation in the *mpk3* mutant.

It has been proposed that MPK3 and MPK6 act upstream of the ROS production, as expression of constitutively active MKK5 leads to ROS-dependent callose formation without a MAMP stimulus and MPK3/6 inactivation *via* the effector protein HopA11 diminishes ROS accumulation (Zhang *et al.*, 2007). Such artificial over-expression of constitutively active MKKs or effector proteins lacks stimulus-specific regulation, and hence, the observed ROS accumulation may be due to indirect effects. Several lines of evidence rather point to MPK3/6-independent MAMP/DAMP-induced ROS production (Figure 7, S9): (i) loss of MPK3 is associated with a prolonged, rather than a reduced ROS accumulation, (ii) loss of MPK6 has no impact on ROS accumulation and (iii) activation of ROS production is strictly Ca<sup>2+</sup>-dependent, whereas MAPK-activation is only partially Ca<sup>2+</sup>-dependent. The prolonged ROS accumulation and the enhanced root growth inhibition phenotype in *mpk3* (Figure 7), instead, point to a possible role for MPK3 in down-regulating MAMP- and DAMP-induced signalling. Generally, all activated signalling components need to be eventually attenuated to prevent over-stimulation.

In conclusion, different MAMP- and DAMP-induced signalling pathways converge at very early stages by sharing main signalling components, like ion channels (Krol *et al.*, 2010), NADPH oxidase, MAPK cascades, several defence genes (Navarro *et al.*, 2004; Zipfel *et al.*, 2006; Denoux *et al.*, 2008), and, in some cases, the common signalling partner BAK1 (Chinchilla *et al.*, 2007; Krol *et al.*, 2010). While this is generally true, we show through kinetic analyses of [Ca<sup>2+</sup>]<sub>cyt</sub> elevations, MAPK activation, promoter activity and MAMP-induced growth arrest that there are specific differences between flg22- and elf18-induced responses. Moreover, BAK1 is differentially required in several signalling steps induced by

different MAMPs, but, in particular, in late as well as early elf18-induced responses. Hence, BAK1 participates in MAMP-specific response maintenance.

Finally, together with published data, the observations here accentuate the role of  $\text{Ca}^{2+}$  as a second messenger in MAMP and DAMP signalling and collectively support a threshold-dependent “on-off switch” function for  $\text{Ca}^{2+}$ .  $[\text{Ca}^{2+}]_{\text{cyt}}$  elevations are crucial for downstream responses such as ROS accumulation, which in turn, contributes to  $\text{Ca}^{2+}$  signalling in a positive feedback loop. Thus, the interplay between components acting up- or downstream of  $\text{Ca}^{2+}$  forms the complex MAMP/DAMP signalling network that awaits further discovery.

## SUPPORTING INFORMATION

Supporting information is available in the appendix 5.1 (p. 147).

**Figure S1.** Inactive MAMPs do not evoke  $[\text{Ca}^{2+}]_{\text{cyt}}$  elevations.

**Figure S2.** MAMP-induced  $[\text{Ca}^{2+}]_{\text{cyt}}$  elevations are abolished in  $\text{LaCl}_3$ - or BAPTA-treated seedlings.

**Figure S3.** Dose-dependent  $[\text{Ca}^{2+}]_{\text{cyt}}$  elevations.

**Figure S4.** Individual traces of MAMP/DAMP-induced  $[\text{Ca}^{2+}]_{\text{cyt}}$  elevations in seedlings.

**Figure S5.** MAMP/DAMP-induced  $[\text{Ca}^{2+}]_{\text{cyt}}$  elevations in root-dissected compared to intact seedlings.

**Figure S6.** MAMP/DAMP-induced  $[\text{Ca}^{2+}]_{\text{cyt}}$  elevations in receptor mutants.

**Figure S7.** Elf18-induced growth arrest in *bak1* and *serk* mutants.

**Figure S8.**  $\text{LaCl}_3$  pre-treatment inhibits MAMP-induced ROS accumulation.

**Figure S9.** Flg22-induced MAPK activation is reduced in  $\text{LaCl}_3$ - or BAPTA-treated Arabidopsis cells.

**Table S1.** Mutant lines.

**Table S2.** Primers for promoter cloning.

## EXPERIMENTAL PROCEDURES

### *Plant material and growth conditions*

All *Arabidopsis thaliana* lines were in Col-0 background (Table S1). Seeds were surface-sterilized if required and stratified at 4°C for  $\geq$  two days. Plants were grown on soil in climate chambers under short day or on ATS agar plates (Estelle and Somerville, 1987) or in liquid MS medium (0.5xMS, 0.25% sucrose, 1mM MES, pH5.7) in 24-well plates (10 seedlings / well) under long day conditions at 20-22°C.

### *Elicitors*

Flg22, elf18 and AtPep1 (Felix *et al.*, 1999; Kunze *et al.*, 2004; Huffaker *et al.*, 2006) were synthesized using an Abimed EPS221 ([www.abimed.de](http://www.abimed.de)) system. *N*-acetylchitooctose (ch8) was provided by N. Shibuya (Albert *et al.*, 2006).

### *Aequorin luminescence measurements*

For aequorin luminescence measurements, Col-0 plants expressing cytosolic p35S-apoaequorin were used (pMAQ2; Knight *et al.*, 1991). Mutant lines were generated by crossing or Agrobacterium-mediated transformation (Table S1). 8-days-old liquid-grown seedlings or roots of 10-days-old

seedlings from agar plates were placed individually in 96-well plates in 10  $\mu\text{M}$  coelenterazine /  $\text{H}_2\text{O}$  (native coelenterazine, P.J.K., [www.pjk-gmbh.com](http://www.pjk-gmbh.com)) in the dark over night. Luminescence was recorded by scanning each row in 6sec intervals (Luminoskan Ascent 2.1, Thermo Scientific, [www.thermo.com](http://www.thermo.com)). Remaining aequorin was discharged and  $\text{Ca}^{2+}$  concentrations were calculated according to Rentel and Knight (2004). In case of aequorin-transformation, for clarity only one of  $\geq$  three independent lines (Table S1) is shown, if all lines behaved similar. Statistical analysis was performed using GraphPad Prism 5.0 ([www.graphpad.com](http://www.graphpad.com)) as indicated in figure legends.

### ***Protoplast transient expression assay***

Protoplasts were isolated and transformed according to Yoo *et al.* (2007). *pFRK1*-, *pNHL10*- and *pPHI1*-promoter-luciferase constructs were used as reporters (Table S2; Asai *et al.*, 2002; Boudsocq *et al.*, 2010). *pUBQ10-GUS* was co-transfected for normalization (Sun and Callis, 1997). Luminescence of protoplast suspensions containing D-luciferin (200  $\mu\text{M}$ , Invitrogen, [www.invitrogen.com](http://www.invitrogen.com)) and treated with indicated MAMPs/DAMPs was recorded in 96-well plates at indicated intervals (Luminoskan Ascent 2.1). Results are expressed as LUC/GUS ratios relative to untreated controls. For statistical analysis a Kruskal-Wallis test with Dunn's post test ( $p < 0.05$ ) was performed using GraphPad Prism 5.0.

### ***Immunoblot analysis***

14-days-old liquid-grown seedlings were equilibrated in fresh MS for  $> 2\text{h}$ . Medium was discarded and after 30 min recovery seedlings were elicited with 1  $\mu\text{M}$  elicitor in MS. Seedlings were harvested at indicated time points. Protein extraction and immunoblot with anti-pTEpY ( $\alpha$ -phospho-p44/42-ERK; CST, [www.cellsignal.com](http://www.cellsignal.com)) were performed as described (Saijo *et al.*, 2009).

### ***ROS detection in Arabidopsis leaves***

ROS production was assayed as described (Gomez-Gomez *et al.*, 1999) using 3 mm leaf discs in 96-well plates measured in 2 min intervals (Luminoskan Ascent 2.1). For statistical analysis a Kruskal-Wallis test with Dunn's post test ( $p < 0.05$ ) was performed using GraphPad Prism 5.0.

### ***Root growth inhibition***

Seedlings were grown vertically on agar plates  $\pm 1 \mu\text{M}$  flg22 for 14 days or 5-days-old seedlings were transferred to plates  $\pm 10 \mu\text{M}$  flg22 for 20 days. Two-way ANOVA was performed on  $\log_2$ -transformed root length data (genotype x treatment;  $p < 0.001$ ; R statistical package; Delker *et al.*, 2010). Data were depicted as % root growth inhibition compared to control.

## **ACKNOWLEDGEMENTS**

We are grateful to Sacco de Vries, Birgit Kemmerling, Marc Knight, Naoto Shibuya, Gary Stacey and Cyril Zipfel for providing material, Frédéric Brunner and Malou Fraiture for help with protoplast assays and Carolin Delker, Yvonne Pöschl and Ivo Große for advice in statistics. We thank Christel Rülke and Nicole Bauer for technical assistance. This work is supported by a DFG grant (LE2321/1-2) within the priority project SPP1212. L. E.-L. and P. P. are financed by the BMBF project ProNet-T3 (03ISO2211B) and the DFG project SFB648-B1, respectively.

## **REFERENCES**

Due to high redundancy of references between the different chapters, the references are combined in the common REFERENCE section (chapter 4, p. 126).

### 2.2.3. Additional results

#### ROS generation is reduced in *pldα1* after elicitation with *flg22* and *elf18*.

Components of phospholipid signalling are proposed to be involved in MAMP and DAMP signalling in plants. Phospholipase C (PLC) generates diacylglycerol (DAG) that can be phosphorylated to phosphatidic acid (PA) by DAG-kinase (DGK), whereas phospholipase D (PLD) directly catalyses PA formation (Figure 2–2). PA accumulation has been shown for several MAMPs/DAMPs including *flg22*, N-acetylchitotetraose (*ch4*) and xylanase in tomato (van der Luit *et al.*, 2000). Recently, the requirement of PA for ABA-induced activation of RbohD and subsequent stomatal closure was proven genetically. In this case, PA was produced, at least in part, *via* PLD $\alpha$ 1 and activated RbohD by direct binding (Zhang *et al.*, 2009). Therefore, PLD $\alpha$ 1 and PLD $\delta$ , the two predominant PLD isoforms in Arabidopsis, were tested for involvement in early MAMP/DAMP signalling. Both, PLD $\alpha$ 1 and PLD $\delta$ , contain a C2-domain and require Ca<sup>2+</sup> for their activation (Qin and Wang, 2002), thus suggesting a role downstream of [Ca<sup>2+</sup>]<sub>cyt</sub> elevations. Accordingly, the *flg22*/*elf18*-induced ROS accumulation in leaf discs of the *pldα1-1* single as well as the *pldα1/δ* (*pldα1-1pldδ-1*) double mutant was consistently reduced (Figure 2–1a,b). The ROS production in the *pldδ-1* single mutant was too variable between independent experiments to draw reliable conclusions. Moreover, no additive effects on ROS accumulation were observed in *pldα1/δ*. As observed already for other mutants impaired in ROS production, the tested *pld* mutants showed no difference to wild type regarding root growth arrest (Figure 2–1c).

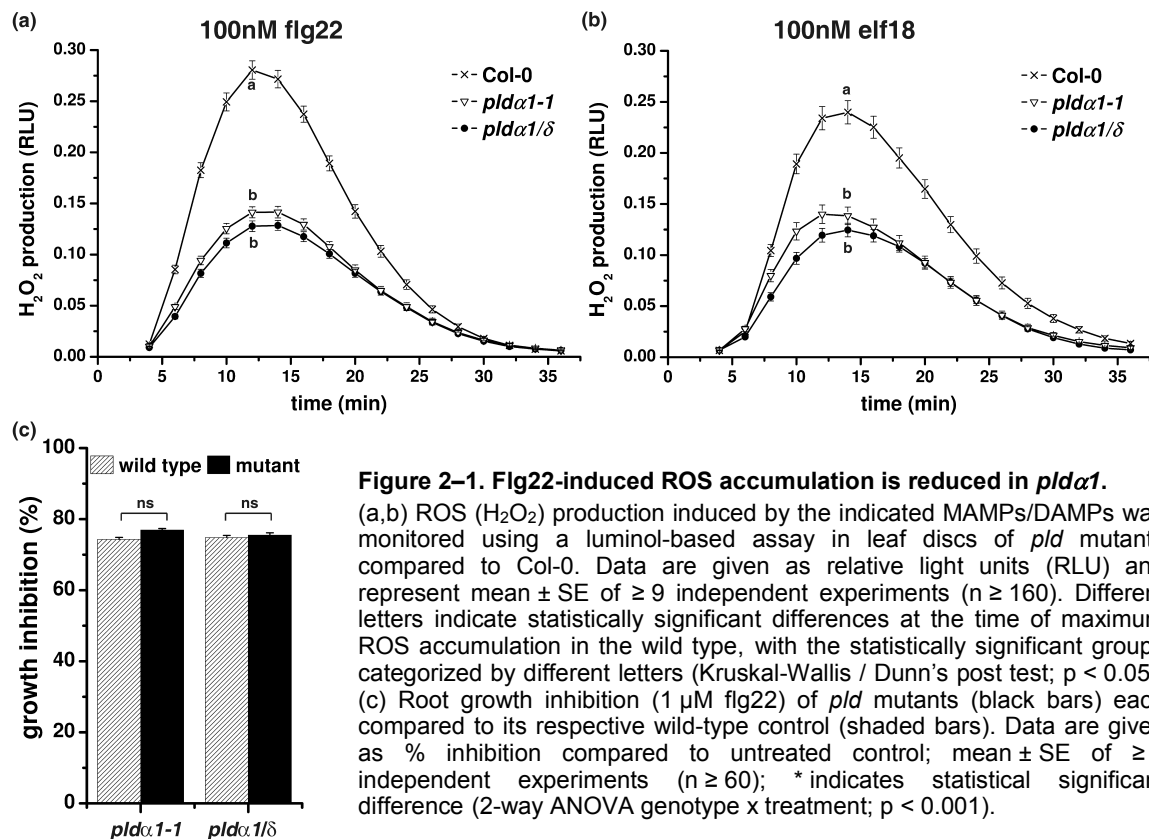


**Figure 2–1. Fig22-induced ROS accumulation is reduced in *pldα1*.**

(a,b) ROS (H<sub>2</sub>O<sub>2</sub>) production induced by the indicated MAMPs/DAMPs was monitored using a luminol-based assay in leaf discs of *pld* mutants compared to Col-0. Data are given as relative light units (RLU) and represent mean ± SE of ≥ 9 independent experiments (n ≥ 160). Different letters indicate statistically significant differences at the time of maximum ROS accumulation in the wild type, with the statistically significant groups categorized by different letters (Kruskal-Wallis / Dunn's post test; p < 0.05). (c) Root growth inhibition (1 μM *flg22*) of *pld* mutants (black bars) each compared to its respective wild-type control (shaded bars). Data are given as % inhibition compared to untreated control; mean ± SE of ≥ 3 independent experiments (n ≥ 60); \* indicates statistical significant difference (2-way ANOVA genotype x treatment; p < 0.001).

### An *ipk1* mutant shows an enhanced flg22-mediated root growth inhibition.

An initial apoplasmic  $\text{Ca}^{2+}$  influx *via* the plasma membrane is often necessary for  $\text{Ca}^{2+}$  release from internal stores, the so-called  $\text{Ca}^{2+}$ -induced  $\text{Ca}^{2+}$  release (CICR; Bewell *et al.*, 1999). In animal systems, the second messenger  $\text{InsP}_3$  mediates CICR by stimulating  $\text{InsP}_3$ -gated channels at internal stores (Navazio *et al.*, 2000; Navazio *et al.*, 2001; Lemtiri-Chlieh *et al.*, 2003). In contrast, the  $\text{Ca}^{2+}$ -releasing second messenger in plants may instead be  $\text{InsP}_6$  (Lemtiri-Chlieh *et al.*, 2003; Munnik and Testerink, 2009), which can be produced by a PLC/lipid-dependent or lipid-independent pathway involving inositolphosphate synthases (IPS) and inositolpolyphosphate kinase (IPK; Figure 2–2; Munnik and Vermeer, 2010). Inositol derivatives have been implicated in basal resistance to viral, bacterial and fungal pathogens (Murphy *et al.*, 2008).

However, mutants of IPK1 and two IPS (IPS1 and IPS2), with substantial decrease in the overall  $\text{InsP}_6$  content (Stevenson-Paulik *et al.*, 2005; Murphy *et al.*, 2008), were not affected in flg22-induced  $[\text{Ca}^{2+}]_{\text{cyt}}$  elevations (Figure 2–3a). Nevertheless, flg22-mediated root growth inhibition was significantly enhanced in the *ipk1* mutant compared to wild type (Figure 2–3b,c), although this is probably not mediated by  $\text{Ca}^{2+}$  signalling.

#### Lipid-dependent

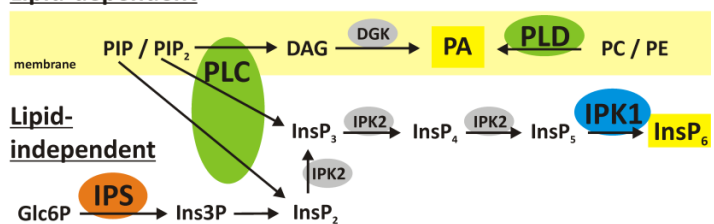


**Figure 2–2. Scheme of PA and  $\text{InsP}_6$  synthesis pathways.**

**PA synthesis:** phospholipase C (PLC) hydrolyses PtdIns4P (PIP) / PtdIns(4,5)P<sub>2</sub> (PIP<sub>2</sub>) to  $\text{InsP}_2/\text{InsP}_3$  and diacylglycerol (DAG), which can be phosphorylated by DAG kinase (DGK) to phosphatidic acid (PA). PA can also be directly produced from structural lipids like phosphatidylcholine (PC) or phosphatidylethanolamine (PE) by phospholipase D (PLD).

**$\text{InsP}_6$  synthesis:** a) lipid-dependent: PLC-mediated PIP/PIP<sub>2</sub>-hydrolysis yields  $\text{InsP}_2/\text{InsP}_3$ . b) lipid-independent:  $\text{InsP}_3$  synthesis from Glc6P by *myo*- $\text{InsP}_3$  synthase (IPS) followed by phosphorylation to  $\text{InsP}_2$  by IPK2. Both pathways converge at this step.  $\text{InsP}_2/\text{InsP}_3$  can be subsequently phosphorylated by inositolpolyphosphate kinase 2 (IPK2) to  $\text{InsP}_5$  and to  $\text{InsP}_6$  by IPK1.

Ptd = phosphatidyl, Ins = inositol, Glc = glucose, P = phosphate.

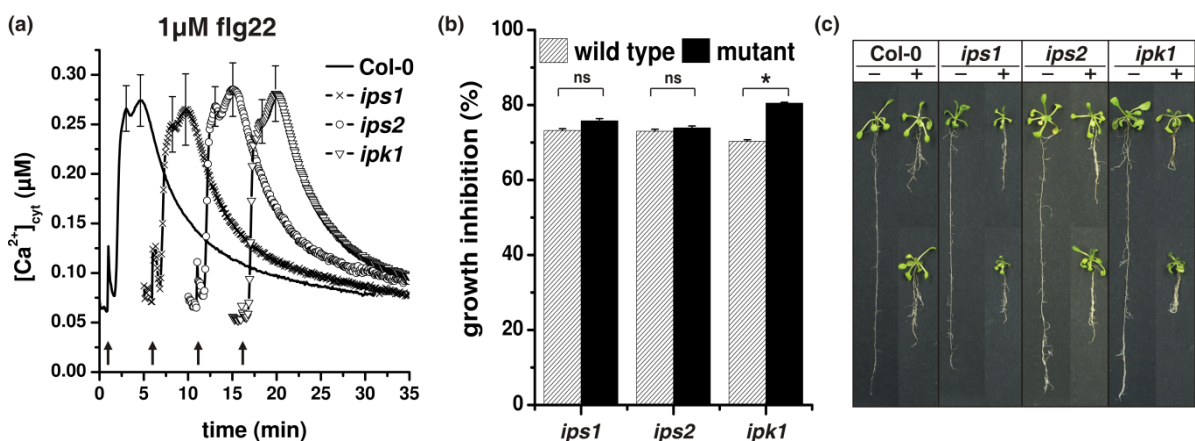


**Figure 2–3. Flg22-mediated root growth inhibition, but not  $[\text{Ca}^{2+}]_{\text{cyt}}$  elevation, is enhanced in *ipk1*.**

(a) Flg22-induced  $[\text{Ca}^{2+}]_{\text{cyt}}$  elevations in *ips1*, *ips2* and *ipk1* seedlings compared to Col-0. For clarity, graphs are depicted offset. Arrows mark time of MAMP/DAMP application. Data represent mean  $\pm$  SD of  $\geq 5$  independent experiments ( $n \geq 20$ ).

(b) Root growth inhibition (1  $\mu\text{M}$  flg22) of *ips1*, *ips2* and *ipk1* mutants (black bars) each compared to its respective wild-type control (shaded bars). Data are given as % inhibition compared to untreated control; mean  $\pm$  SE of  $\geq 3$  independent experiments ( $n \geq 60$ ). \* indicates statistical significant difference; ns = not significant (2-way ANOVA genotype  $\times$  treatment;  $p < 0.001$ ). (c) Photographs of representative Col-0 and mutant seedlings from (a) grown in the presence (+; two seedlings) or absence (-; one seedling) of 1  $\mu\text{M}$  flg22.

### *camta3* mutants show a reduced flg22-mediated root growth arrest and altered expression of the early defence gene *ZAT12*.

CAMTA transcription factors have been reported to play roles in abiotic and biotic stresses (Bouche *et al.*, 2002; Doherty *et al.*, 2009). CAMTA3 negatively regulates systemic acquired resistance (SAR) by direct binding to the promoter of *EDS1*, a gene required for pathogen-induced SA synthesis. This function is dependent on  $\text{Ca}^{2+}$ /CaM-binding (Galon *et al.*, 2008; Du *et al.*, 2009). To test putative contributions of CAMTA3 to MAMP signalling, gene expression was analysed in seedlings treated with flg22 for 30 minutes by quantitative RT-PCR (Figure 2–4a; performed by L. Eschen-Lippold). Two *camta3* mutants showed reduced *ZAT12* induction to a level comparable or even more pronounced to that seen in *bak1-4* (Figure 2–4a). Further evidence for CAMTA3 requirement in MAMP responses is shown by the reduced flg22-mediated root growth arrest in both *camta3* mutants (Figure 2–4b,c). As flg22-induced  $[\text{Ca}^{2+}]_{\text{cyt}}$  elevations in *camta3* were comparable to wild type (Figure 2–4d), CAMTA3 does not appear to regulate genes required for  $[\text{Ca}^{2+}]_{\text{cyt}}$  elevation but appears to regulate a subset of flg22-induced defence genes.

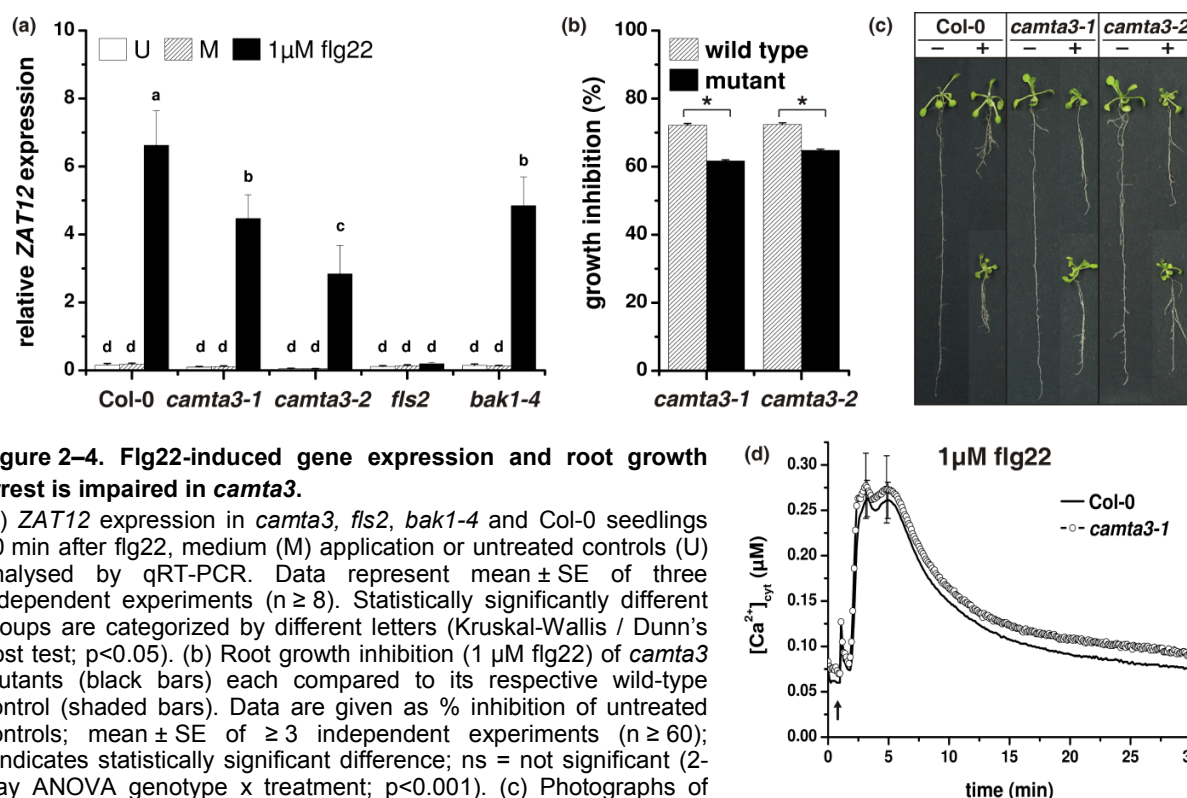


**Figure 2–4. Flg22-induced gene expression and root growth arrest is impaired in *camta3*.**

(a) *ZAT12* expression in *camta3*, *fls2*, *bak1-4* and Col-0 seedlings 30 min after flg22, medium (M) application or untreated controls (U) analysed by qRT-PCR. Data represent mean  $\pm$  SE of three independent experiments ( $n \geq 8$ ). Statistically significantly different groups are categorized by different letters (Kruskal-Wallis / Dunn's post test;  $p < 0.05$ ). (b) Root growth inhibition (1  $\mu\text{M}$  flg22) of *camta3* mutants (black bars) each compared to its respective wild-type control (shaded bars). Data are given as % inhibition of untreated controls; mean  $\pm$  SE of  $\geq 3$  independent experiments ( $n \geq 60$ ); \* indicates statistically significant difference; ns = not significant (2-way ANOVA genotype  $\times$  treatment;  $p < 0.001$ ). (c) Photographs of seedlings from (b) grown in the presence (+) or absence (-) of flg22. (d)  $[\text{Ca}^{2+}]_{\text{cyt}}$  elevations in *camta3*. Arrows mark time of flg22 application. Data represent mean  $\pm$  SD of  $\geq 4$  independent experiments ( $n \geq 40$ ).

#### **Additional experimental procedures: quantitative real-time RT-PCR**

14-days-old liquid-grown seedlings were equilibrated in fresh MS for 24h and elicited with flg22 (1  $\mu\text{M}$  final concentration) or MS as control. Total RNA was isolated using TRIZOL reagent according to standard protocols. First strand cDNA synthesis was performed with DNaseI-treated RNA according to

manuals (RevertAid<sup>TM</sup> Reverse Transcriptase; Fermentas, www.fermentas.com). Quantitative real-time PCR was performed with Maxima<sup>TM</sup> Probe qPCR Master Mix (Fermentas, www.fermentas.de) on an Mx3000P QPCR System (Agilent, www.agilent.com). For statistical analysis a Kruskal-Wallis with Dunn's post test ( $p < 0.05$ ) was performed with GraphPad Prism 5.0. Hydrolysis probes were Universal ProbeLibrary Probes (Roche, www.roche.de): *AtZAT12* (At5g59820) probe #66 (fwd: ctttgggaggacacatgagg; rev: caaagcgcgtgtaaccaac) and *AtPP2A* (reference gene; At1g13320; probe #29; (fwd: gaccggagccaactaggac; rev: aaaacttgtaactttccagca)

### 2.3. Screen for mutants with „*changed calcium elevation*“ (*cce*) in MAMP signalling

#### 2.3.1. Aims and summary

The discovery of several MAMPs and their cognate receptors in the recent years has resulted in significant progress in our understanding of innate immunity signalling in plants. Although several components of receptor complexes have been elucidated, the  $\text{Ca}^{2+}$ -permeable channels and pumps shaping the MAMP-induced  $\text{Ca}^{2+}$  signatures and their activation and regulation by upstream signalling components are yet unknown. To fill these gaps in our current knowledge, a quantitative high-throughput screening system was designed. Screening for mutants with “*changed calcium elevation*” (*cce*) upon flg22 elicitation was performed by applying quantitative [ $\text{Ca}^{2+}$ ] measurements on EMS-mutagenised aequorin-expressing Arabidopsis seedlings. In addition to the cytosolic aequorin line (Aeq<sup>cyt</sup>, Col-0 background), an Arabidopsis line expressing aequorin in the vacuolar microdomain (Aeq<sup>vmd</sup>, C24 background) was included in the screen that may yield mutants in  $\text{Ca}^{2+}$  release from the vacuole, which due to its size and capacity is a major  $\text{Ca}^{2+}$  store in plants. The screening concept was validated by the isolation of several novel *fls2* and *bak1* mutant alleles in both reporter lines.

Due to the different accession background, Aeq<sup>cyt</sup> in Col-0 and Aeq<sup>vmd</sup> in C24, the two aequorin reporter lines showed a different sensitivity to flg22 and elf18. Thus, while reacting more strongly to flg22 than Aeq<sup>cyt</sup>/Col-0, Aeq<sup>vmd</sup>/C24 was less sensitive towards elf18 treatment as assessed by seedling growth inhibition. Furthermore, Aeq<sup>vmd</sup>/C24 *bak1* mutants showed a reduced elf18-mediated growth arrest generally not observed in Aeq<sup>cyt</sup>/Col-0 *bak1* mutants, which may therefore directly correlate with the reduced elf18 sensitivity of Aeq<sup>vmd</sup>/C24.

Moreover, several other mutants with *changed calcium elevation* (*cce*) were isolated either showing a reduced or enhanced/prolonged [ $\text{Ca}^{2+}$ ] elevation in response to flg22 and elf18. The Aeq<sup>vmd</sup>/C24 *cce* mutants were all altered in the elf18- in addition to the flg22-mediated growth arrest. Generally, the reduced or enhanced growth inhibition reflected the corresponding reduced or enhanced [ $\text{Ca}^{2+}$ ] elevations, respectively. According to their response to the set of different MAMPs and DAMPs tested, i. e. flg22, elf18, Pep1 and ch8, the *cce* mutants can be further categorized in those only altered in flg22-, elf18- and Pep1-induced [ $\text{Ca}^{2+}$ ] elevations compared to those also altered in their response to ch8. This suggests that the *cce* mutants are all affected in components shared by different MAMP and DAMP signalling pathways. Hence, the *cce* mutants will be helpful to further define early signalling events in innate immunity in Arabidopsis in the future.

### 2.3.2. Manuscript

#### Defence-related calcium signalling mutants uncovered *via* a quantitative high-throughput screen in *Arabidopsis thaliana*

Stefanie Ranf, Julia Grimmer<sup>#</sup>, Yvonne Pöschl<sup>1</sup>, Pascal Pecher, Delphine Chinchilla<sup>2</sup>, Dierk Scheel & Justin Lee\*

Leibniz Institute of Plant Biochemistry, Stress and Developmental Biology, Weinberg 3, D-06120 Halle, Germany

<sup>1</sup>Institute of Computer Science, Martin Luther University Halle-Wittenberg, Von-Seckendorff-Platz 1, D-06120 Halle, Germany

<sup>2</sup>Zürich-Basel Plant Science Center, Botanical Institute, University of Basel, Hebelstrasse 1, 4056 Basel, Switzerland

<sup>#</sup>present address: Institute of Biochemistry and Biotechnology, Martin Luther University Halle-Wittenberg, Weinbergweg 22, D-06120 Halle, Germany

\*Corresponding author: Justin Lee; phone: +49 345 5582 1410 ; e-mail: jlee@ipb-halle.de

Running head: Screen for calcium signalling mutants

Keywords: Ca<sup>2+</sup> signalling, aequorin, MAMP, FLS2, BAK1, *Arabidopsis thaliana*

#### ABSTRACT

Calcium acts as a second messenger for signalling to a variety of stimuli including MAMPs (Microbe-Associated Molecular Patterns), such as flg22 and elf18 that are derived from bacterial flagellin and elongation factor Tu, respectively. Here, *Arabidopsis thaliana* mutants with *changed calcium elevation* (*cce*) in response to flg22 treatment were isolated and characterized. Besides novel mutant alleles of the flg22 receptor, *FLS2* (*Flagellin-Sensitive 2*), and the receptor-associated kinase, *BAK1* (*Brassinosteroid receptor 1-Associated Kinase 1*), the new *cce* mutants can be categorized into two main groups – those with a reduced or an enhanced calcium elevation. Moreover, *cce* mutants from both groups show differential phenotypes to different sets of MAMPs. Thus, these mutants will facilitate the discovery of novel components in early MAMP signalling and bridge the gaps in current knowledge of calcium signalling during plant-microbe interactions. Last but not least, the screening method is optimized for speed (covering 384 plants in three or ten hours) and can be adapted to genetically dissect any other stimuli that induce a change in calcium levels.

#### INTRODUCTION

Calcium is a crucial second messenger in diverse biotic and abiotic signalling pathways. How such a “simple” cation like Ca<sup>2+</sup> can encode specificity for signal transduction is a longstanding enigma. Possible answers to this question could be the so-called “Ca<sup>2+</sup> signature”, alterations in the magnitude, frequency and duration, as well as the cellular localization of the Ca<sup>2+</sup> changes, e. g. locally restricted cytosolic or organelle Ca<sup>2+</sup> changes, or the Ca<sup>2+</sup> sources, external or different internal stores (Webb *et al.*, 1996; McAinsh and Hetherington, 1998; Trewavas, 1999; Rudd and Franklin-Tong, 2001; White and Broadley, 2003). Alternatively, Ca<sup>2+</sup> may simply serve as a “chemical on-off switch” that activates downstream responses if it exceeds a certain threshold (Scrase-Field and Knight, 2003). In either scenario, the Ca<sup>2+</sup> signal is ultimately decoded and translated into downstream biochemical responses *via* diverse Ca<sup>2+</sup>-binding proteins, such as calmodulins (CaM) or calcineurin B-like (CBL) proteins, and Ca<sup>2+</sup>-regulated enzymes, e.g. calcium-dependent protein kinases (CDPKs; DeFalco *et al.*, 2010; Kudla *et al.*, 2010).

Due to their size and their capacity to store  $\text{Ca}^{2+}$  ( $[\text{Ca}^{2+}]_{\text{apo}} \sim 50\text{-}150 \mu\text{M}$ ,  $[\text{Ca}^{2+}]_{\text{vac}} > 10 \mu\text{M}$ ), the apoplast and the vacuole are likely the major plant  $\text{Ca}^{2+}$  stores (Allen and Sanders, 1997). Nevertheless, the nucleus, ER, chloroplasts and mitochondria are also capable of storing and releasing  $\text{Ca}^{2+}$  (Oldroyd and Downie, 2006; Nomura *et al.*, 2008; Weinl *et al.*, 2008; Kudla *et al.*, 2010). Using an aequorin- $\text{Ca}^{2+}$  reporter targeted to the cytoplasmic-face of the tonoplast, the so called “vacuolar microdomain” (vmd), a differential contribution of vacuolar  $\text{Ca}^{2+}$  was described for various abiotic stresses (Knight *et al.*, 1996). Peiter *et al.* (2005) reported a vacuolar cation channel, two-pore channel 1 (TPC1), potentially involved in  $\text{Ca}^{2+}$  signalling, but aequorin-based  $\text{Ca}^{2+}$  measurements revealed no contribution of TPC1 to stress-induced  $\text{Ca}^{2+}$  signalling (Ranf *et al.*, 2008). Nevertheless, a *TPC1* gain-of-function mutation, *fou2* (*fatty acid oxygenation up-regulated 2*), led to reduced sensitivity to luminal  $\text{Ca}^{2+}$  and a higher vacuolar  $\text{Ca}^{2+}$  accumulation (Bonaventure *et al.*, 2007a; Beyhl *et al.*, 2009), which indicates cation homeostasis function of TPC1.

An initial apoplastic  $\text{Ca}^{2+}$  influx *via* the plasmalemma is often necessary for  $\text{Ca}^{2+}$ -induced  $\text{Ca}^{2+}$  release (CICR) from internal stores either directly or mediated by second messengers, e. g. inositol trisphosphate or hexakisphosphate ( $\text{IP}_3/\text{IP}_6$ ), cyclic ADP-ribose (cADPR), nicotinic acid adenine dinucleotide phosphate (NAADP) or sphingosine-1-phosphate, that stimulate ligand-gated channels at internal stores, such as the vacuole and the ER (Bewell *et al.*, 1999; Navazio *et al.*, 2000, 2001; Ng *et al.*, 2001; Lemtiri-Chlieh *et al.*, 2003). For instance, TPC1 was shown to be the NAADP receptor in the animal system, but no comparable role has so far been reported for the plant TPC1 homolog (Calcraft *et al.*, 2009). Other second messengers or signals that can modulate  $\text{Ca}^{2+}$  fluxes include reactive oxygen species (ROS). In root hair tips, RbohC-mediated ROS stimulate hyperpolarization-activated  $\text{Ca}^{2+}$  channels to form a tip-focused  $\text{Ca}^{2+}$  gradient (Foreman *et al.*, 2003). Further, MAMP-induced  $\text{Ca}^{2+}$  elevations are partially dependent on the  $\text{Ca}^{2+}$ -dependent ROS production (Ranf *et al.*, submitted, figure 6, p. 46). Taken together, second messengers or other signals, such as ROS constitute a complex regulatory network in  $[\text{Ca}^{2+}]_{\text{cyt}}$  homeostasis.

Microbes activate intracellular signalling cascades in their potential hosts through recognition of conserved microbe- or damage-associated molecular patterns (MAMPs/DAMPs), which are perceived by specific pattern recognition receptors (PRRs; Boller and Felix, 2009). These are typically leucine-rich repeat (LRR) containing receptor-like kinases, such as FLS2 (Flagellin-sensitive 2), EFR (Elongation factor Tu receptor) or PEPR1/PEPR2 (AtPep receptor 1/2), which recognize the MAMPs, flg22 (N-terminal flagellin-derived peptide), elf18 (N-terminal fragment of elongation factor Tu) or the DAMP, AtPep1, respectively (Gomez-Gomez *et al.*, 1999; Gomez-Gomez and Boller, 2000; Kunze *et al.*, 2004; Chinchilla *et al.*, 2006; Huffaker *et al.*, 2006; Zipfel *et al.*, 2006; Krol *et al.*, 2010; Yamaguchi *et al.*, 2010). Within seconds of flg22 binding, FLS2 hetero-oligomerizes with BAK1 (BRI1-associated kinase 1; Chinchilla *et al.*, 2007), a kinase originally found as an interactor of the brassinosteroid hormone receptor, BRI1 (Li *et al.*, 2002). Similarly, BAK1 can also associate with PEPR1/PEPR2 (Postel *et al.*, 2010) and possibly with EFR, since BAK1 is rapidly phosphorylated *in*

*vivo* not only in response to flg22, but also elf18 and AtPep1 (Schulze *et al.*, 2010). Accordingly, loss of BAK1 impairs responses to these MAMPs/DAMPs (Ranf *et al.*, submitted, figure 3, p. 41; Krol *et al.*, 2010). Thus, BAK1 acts as protein partner for multiple pathways in plant immunity but also in development (Chinchilla *et al.*, 2009; Postel and Kemmerling, 2009). However, signalling induced by other MAMPs, such as chitin is independent of BAK1 (Shan *et al.*, 2008), which may be a consequence of the different structure of the potential receptor(s) required for perceiving chitin, CERK1 (Chitin elicitor receptor kinase 1), a LysM-containing receptor-like kinase in Arabidopsis (Miya *et al.*, 2007; Wan *et al.*, 2008; Iizasa *et al.*, 2010; Petutschnig *et al.*, 2010) and CeBiP (Chitin elicitor binding protein) in rice (Kaku *et al.*, 2006).

Generally, the earliest signalling events after MAMP or DAMP perception are ion fluxes across the plasma membrane including influx of  $\text{Ca}^{2+}$  into the cytosol (Blume *et al.*, 2000; Lecourieux *et al.*, 2002; Ranf *et al.*, 2008; Jeworutzki *et al.*, 2010), which is a prerequisite for most downstream responses. For instance, ROS are generated in a  $\text{Ca}^{2+}$ -dependent manner by the NADPH oxidase RbohD in Arabidopsis (Torres *et al.*, 2002). Subsequently, activation of mitogen-activated protein kinase (MAPK) cascades and CDPKs leads to gene expression re-programming (Boudsocq *et al.*, 2010; Rodriguez *et al.*, 2010). Phytopathogenic bacteria can suppress host immunity by secretion of extracellular polysaccharides to sequester apoplastic  $\text{Ca}^{2+}$  and attenuate host MAMP signalling (Aslam *et al.*, 2008) – an observation that supports the pivotal role of  $\text{Ca}^{2+}$  signalling in plant immunity.

In plants, little is known about the molecular identity of the  $\text{Ca}^{2+}$ -permeable channels and  $\text{Ca}^{2+}$  transporters controlling the various  $\text{Ca}^{2+}$  stores and their regulation by upstream components (Kudla *et al.*, 2010; Verret *et al.*, 2010). Here, we report an optimized high-throughput screening system aimed at identifying components regulating MAMP-induced  $[\text{Ca}^{2+}]$  elevations by quantitative  $[\text{Ca}^{2+}]$  measurements. As proof of concept numerous novel alleles of the upstream receptor *FLS2* and the receptor-associated kinase *BAK1* were identified. Additionally, this screen revealed several other mutants with *changed calcium elevation (cce)* that either show a reduced or enhanced  $[\text{Ca}^{2+}]$  elevation in response to a set of different MAMPs and DAMPs.

## RESULTS

### **Flg22 and elf18 induce $\text{Ca}^{2+}$ elevations in Arabidopsis $\text{Aeq}^{\text{cyt}}$ and $\text{Aeq}^{\text{vmd}}$ seedlings.**

Alterations in the  $\text{Ca}^{2+}$  concentration ( $[\text{Ca}^{2+}]$ ) can be monitored *in vivo* with the bioluminescent  $\text{Ca}^{2+}$ -binding protein aequorin (Knight *et al.*, 1991). Apoaequorin can be expressed ectopically in plants and spontaneously reconstitutes to functional holoaequorin upon addition of the native luminophore coelenterazine (CTZ-n) or chemically modified derivatives, such as coelenterazine-h (CTZ-h), for enhanced sensitivity (Shimomura *et al.*, 1993; Mithöfer and Mazars, 2002). In this study, two established Arabidopsis aequorin-transgenic lines were used, which either express apoaequorin in the cytosol ( $\text{Aeq}^{\text{cyt}}$ , pMAQ2, Col-0 background) or targeted to the so-called vacuolar microdomain (vmd), the cytoplasmic-face of the tonoplast, as a pyrophosphatase ( $\text{H}^+$ -PPase)-apoaequorin fusion protein

(Aeq<sup>vmd</sup>, HVA1, C24 background; Knight *et al.*, 1996). Thus, the Aeq<sup>vmd</sup> line serves as a reporter for Ca<sup>2+</sup> fluxes occurring at the vacuole.

The total amount of reconstituted aequorin in a sample can be estimated by disrupting the cells and discharging the released aequorin with excess Ca<sup>2+</sup>. The Ca<sup>2+</sup> level correlates with the light emission from aequorin and is depicted as L/L<sub>max</sub> ratio, where the actual aequorin luminescence (L) at any measurement point is normalized to the total remaining aequorin (L<sub>max</sub>; Figure 1A left). In the case of the cytosolic aequorin (Aeq<sup>cyt</sup>) reconstituted with CTZ-n, L/L<sub>max</sub> can be further converted into actual [Ca<sup>2+</sup>]<sub>cyt</sub> using an empirical calibration that takes into account the double-logarithmic relationship between aequorin luminescence and [Ca<sup>2+</sup>] (Figure 1A right; Knight *et al.*, 1996). By contrast, absolute calibration of [Ca<sup>2+</sup>]<sub>vmd</sub> is not feasible and is shown only as L/L<sub>max</sub> ratio, as in the Aeq<sup>vmd</sup> line not all aequorin molecules are exclusively targeted to the tonoplast (Knight *et al.*, 1997) and CTZ-h, which confers a different (i. e. higher) quantum yield, was used (Shimomura *et al.*, 1993). Furthermore, only qualitative but not quantitative comparisons should be made between the Aeq<sup>cyt</sup> and Aeq<sup>vmd</sup> lines.

The bacterial MAMPs, flg22 and elf18, the fungal *N*-acetylchitooctose (ch8), as well as the plant-derived DAMP, AtPep1 (Pep1), induce a prolonged increase of [Ca<sup>2+</sup>]<sub>cyt</sub> in Arabidopsis Aeq<sup>cyt</sup> seedlings (Figure 1A; depicted as L/L<sub>max</sub> ratio (left) or after calibration (right)). [Ca<sup>2+</sup>] elevations were also observed in the Aeq<sup>vmd</sup> line for all tested MAMPs and DAMPs (Figure 1B). Although a quantitative comparison of the [Ca<sup>2+</sup>] elevations between the Aeq<sup>cyt</sup> and Aeq<sup>vmd</sup> lines is not possible, the [Ca<sup>2+</sup>] elevations were qualitatively very similar for the tested stimuli (Figure 1). In both cases, after a MAMP/DAMP-specific lag phase, a rapid rise and a prolonged decline of [Ca<sup>2+</sup>] that lasted for around 30 minutes is observed. The different MAMPs and DAMPs thereby induced [Ca<sup>2+</sup>] elevations with specific [Ca<sup>2+</sup>] peak heights, peak patterns and slightly different lag phases. Taken together, the observed [Ca<sup>2+</sup>] elevations in both aequorin reporter lines, Aeq<sup>cyt</sup> and Aeq<sup>vmd</sup>, point to a potential involvement of vacuolar Ca<sup>2+</sup> in MAMP signalling.

To uncover new components in early MAMP signalling, we screened for an altered [Ca<sup>2+</sup>] response (*changed calcium elevation, cce*) to flg22 in two ethylmethanesulfonate (EMS)-mutagenised populations of the Aeq<sup>cyt</sup> and the Aeq<sup>vmd</sup> lines. Potentially, the Aeq<sup>vmd</sup> line may yield mutants impaired in second messenger-evoked Ca<sup>2+</sup> release from the vacuole. For the mutant screen flg22 was used, as in both lines, Aeq<sup>cyt</sup> and Aeq<sup>vmd</sup>, the flg22-induced [Ca<sup>2+</sup>] elevations were strongest and most consistent (Figure 1).

### Setup of a quantitative high-throughput Ca<sup>2+</sup>-based screening system in 384 well plates.

To maximize throughput and minimize screening costs, e.g. for CTZ-n/h and flg22 peptide, 384-well plates were used in combination with a plate-reader luminometer equipped with an automatic injection system. Details of the protocol are provided in supplemental information (Protocol 2A). A complete 384 well-plate, containing M2 seedlings corresponding to 32 individual M1 lines (12 segregating M2 seedlings per M1 line), was measured automatically including discharge in less than 10 hours without

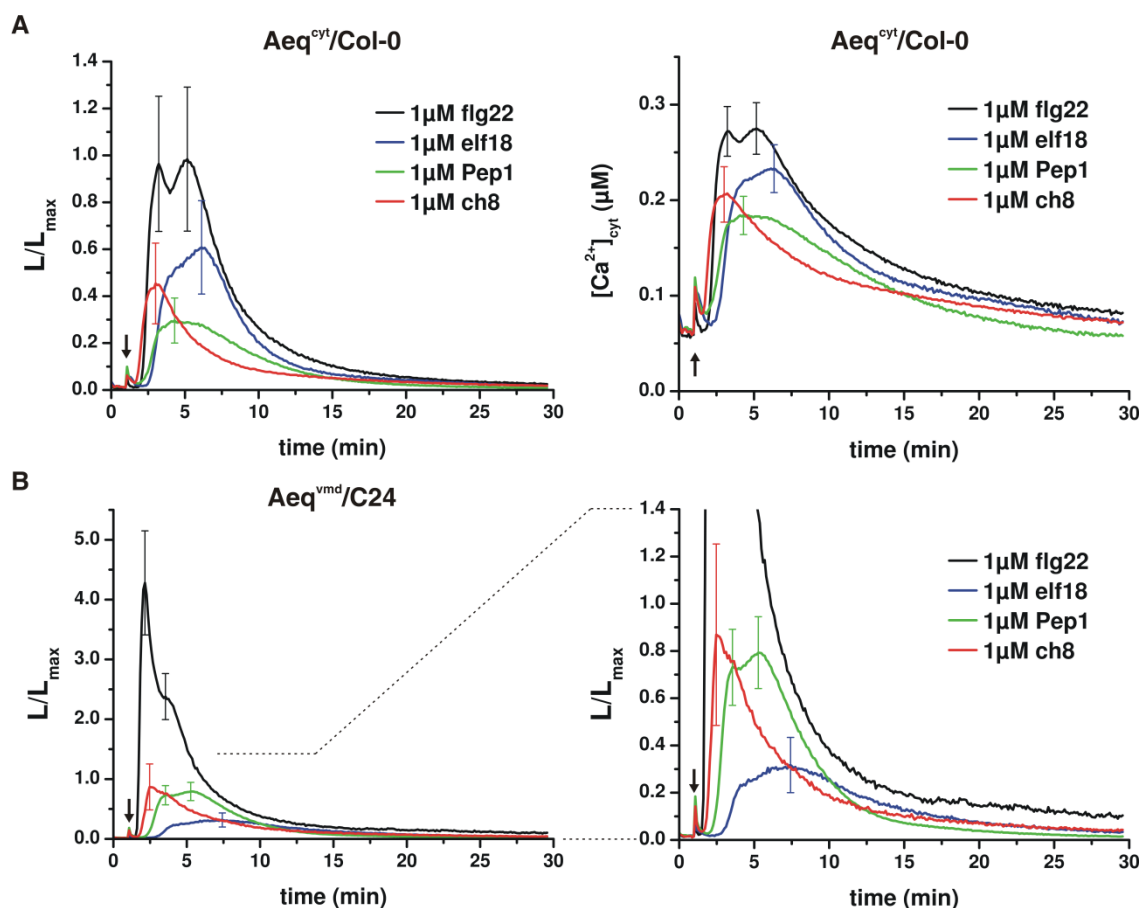


**Figure 1. MAMPs and DAMPs induce specific  $[Ca^{2+}]_{\text{cyt}}$  elevations and potentially release of vacuolar  $Ca^{2+}$  in Arabidopsis seedlings.**

(A)  $[Ca^{2+}]_{\text{cyt}}$  elevations in  $Aeq^{\text{cyt}}/\text{Col-0}$  seedlings induced by the indicated MAMPs/DAMPs. Data are shown as  $L/L_{\text{max}}$ -normalized values in the left graph and after conversion to  $[Ca^{2+}]_{\text{cyt}}$  in the right graph.

(B)  $[Ca^{2+}]_{\text{cyt}}$  elevations in  $Aeq^{\text{vmd}}/\text{C24}$  seedlings induced by the indicated MAMPs/DAMPs. Data are shown as  $L/L_{\text{max}}$ -normalized values. To facilitate visualization, the lower part of the left graph is shown enlarged in the right graph.

Arrows mark time of MAMP/DAMP application and data represent mean  $\pm$  SD of  $\geq 3$  independent experiments ( $n \geq 30$ ) for both (A) and (B).

any additional hands-on time. However, such quantitative measurements required discharging of the sample and thereby sacrificing the putative mutant seedlings. Alternatively, in a qualitative screen (without discharge), candidate seedlings can be rescued from 384 well-plates after flg22 elicitation if the phenotype is already visible without quantification. This way, a complete 384 well-plate was measured automatically in less than 3 hours. In any case, the phenotype of putative mutants was confirmed in the next generation by analyzing 8-12 offspring seedlings in 384 well-plates in the same way (Figure S1).

### High-throughput screening requires high-throughput sample preparation and data calibration techniques.

Most quantitative high-throughput screens of plant mutant populations are logistically challenging in terms of manpower and space requirement. To obtain most consistent results, sterile plant growth in liquid medium was preferred over growth on soil for several reasons: the use of 8-10 days-old seedlings

significantly lowered (i) growth time, (ii) space-requirements in often space-limited environmentally controlled growth chambers and (iii) costs and time for plant maintenance compared to use of adult plants; sterile growth in liquid medium further (iv) limited environmental variability, (v) allowed more even growth of mutants in sucrose-supplemented medium, e.g. those suffering from growth defects and (vi) allowed direct and synchronized access of the applied MAMPs to the whole seedling, due to a poorly developed cuticle and direct contact with the surrounding medium.

In order to significantly shorten hands-on labour time in preparation of sterile seedlings, an optimized and modified high-throughput vapour-phase sterilization technique was developed (Clough and Bent, 1998; see Protocol 1 in supplemental information). This enabled M2 seeds of 192 individual M1 lines to be sterilized in a single run and grown with optimized time and space utilization.

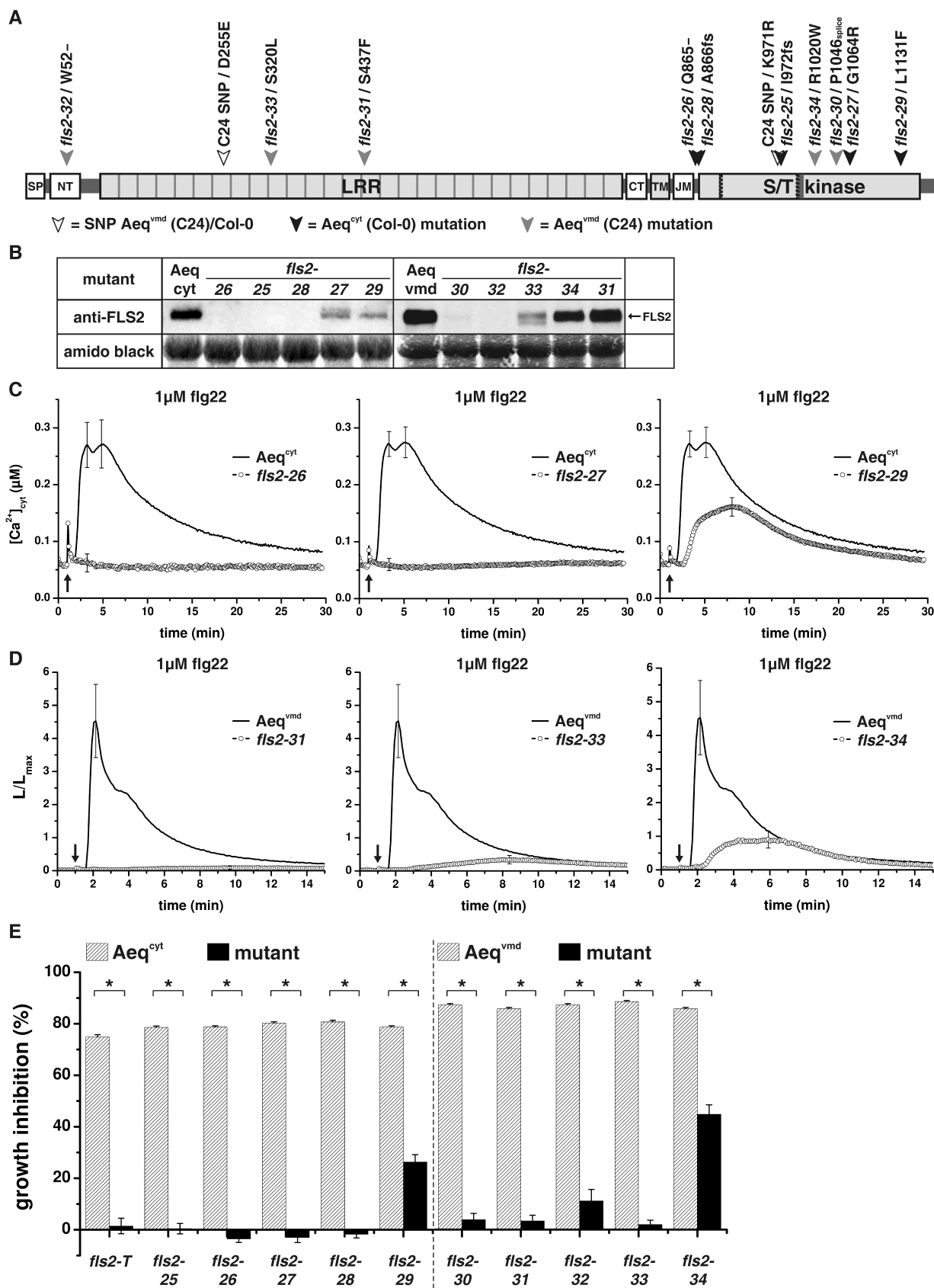
To facilitate processing of the large data files obtained from quantitative measurements of 384 well-plates, an R-based script was written to convert data into  $L/L_{\max}$  or  $[Ca^{2+}]_{\text{cyt}}$ , respectively, and to graphically plot the quantified data against a wild-type control for easy data examination in pdf format (Figure S1). Thus, data calibration did not require any specialized software or hardware and could be run on an average computer system by the sole use of free available software (“freeware”).

### Isolation of new *fls2* alleles.

Screening of EMS-mutagenised populations of the  $Aeq^{\text{cyt}}/Aeq^{\text{vmd}}$  lines for an altered  $[Ca^{2+}]$  response was performed with flg22. Currently, M2 seedlings corresponding to 2300  $Aeq^{\text{vmd}}$  and 2800  $Aeq^{\text{cyt}}$  individual M1 lines have been analysed, which resulted in 19 mutants in the  $Aeq^{\text{vmd}}$  line and 16 mutants in the  $Aeq^{\text{cyt}}$  background. Characterizing the obtained mutants against other MAMPs such as elf18, rapidly distinguished those that are flg22-specific, i. e. likely affected in the FLS2 receptor, or showed altered responses to several MAMPs. Through sequencing of *FLS2* and allelism analysis (data not shown), ten novel *fls2* alleles were uncovered (Figure 2A; table SI). These included mutations of exon-intron borders, single nucleotide insertions/deletions causing frame shifts, nonsense mutations, as well as missense mutations leading to non-conservative amino acid exchanges. The different mutations and their location within the FLS2 receptor protein are summarized in figure 2A. Additionally, two single nucleotide polymorphisms (SNPs) between  $Aeq^{\text{cyt}}/Col-0$  and  $Aeq^{\text{vmd}}/C24$  are also shown in figure 2A.

#### Figure 2. $Ca^{2+}$ -based screening reveals novel *fls2* alleles.

- (A) Schematic illustration of the *fls2* mutations. Mutations in the  $Aeq^{\text{cyt}}$  (Col-0) background are marked with black and mutations in the  $Aeq^{\text{vmd}}$  (C24) background with gray arrowheads. Open arrowheads mark SNPs between  $Aeq^{\text{vmd}}/C24$  and Col-0. Abbreviations: fs = frame shift; splice = mutation of exon-intron border; “-” = nonsense mutation; SP = signal peptide; LRR = leucine-rich repeat domain; NT/CT = N/C-terminal LRR domain; TM = transmembrane domain; JM = juxtamembrane domain; S/T kinase = serine/threonine kinase domain (gray bar = catalytic loop, dashed lines = proton and ATP binding sites)
- (B) FLS2 protein accumulation was analysed by immunoblot using anti-FLS2 antibodies. Amido-black-stained membranes show equal loading. Three independent experiments revealed identical results.
- (C)  $[Ca^{2+}]_{\text{cyt}}$  elevations in  $Aeq^{\text{cyt}}$  *fls2* mutant seedlings induced by 1  $\mu\text{M}$  flg22 each compared to its respective wild-type control. Arrows mark time of flg22 application. Data represent mean of calibrated  $[Ca^{2+}]_{\text{cyt}} \pm \text{SD}$  of  $\geq 4$  independent experiments ( $n \geq 30$ ).
- (D)  $[Ca^{2+}]$  elevations in  $Aeq^{\text{vmd}}$  *fls2* mutant seedlings induced by 1  $\mu\text{M}$  flg22 each compared to its respective wild-type control. Arrows mark time of flg22 application.  $L/L_{\max}$ -normalized data are shown as mean  $\pm$  SD of  $\geq 6$  independent experiments ( $n \geq 45$ ).
- (E) Root growth inhibition (1  $\mu\text{M}$  flg22) of different *fls2* mutants (black bars) each compared to its respective wild-type control (shaded bars). Data are given as % inhibition compared to untreated control; mean  $\pm$  SE of  $\geq 3$  independent experiments ( $n \geq 45$ ); \* indicates statistically significant difference ( $p < 0.001$ ).



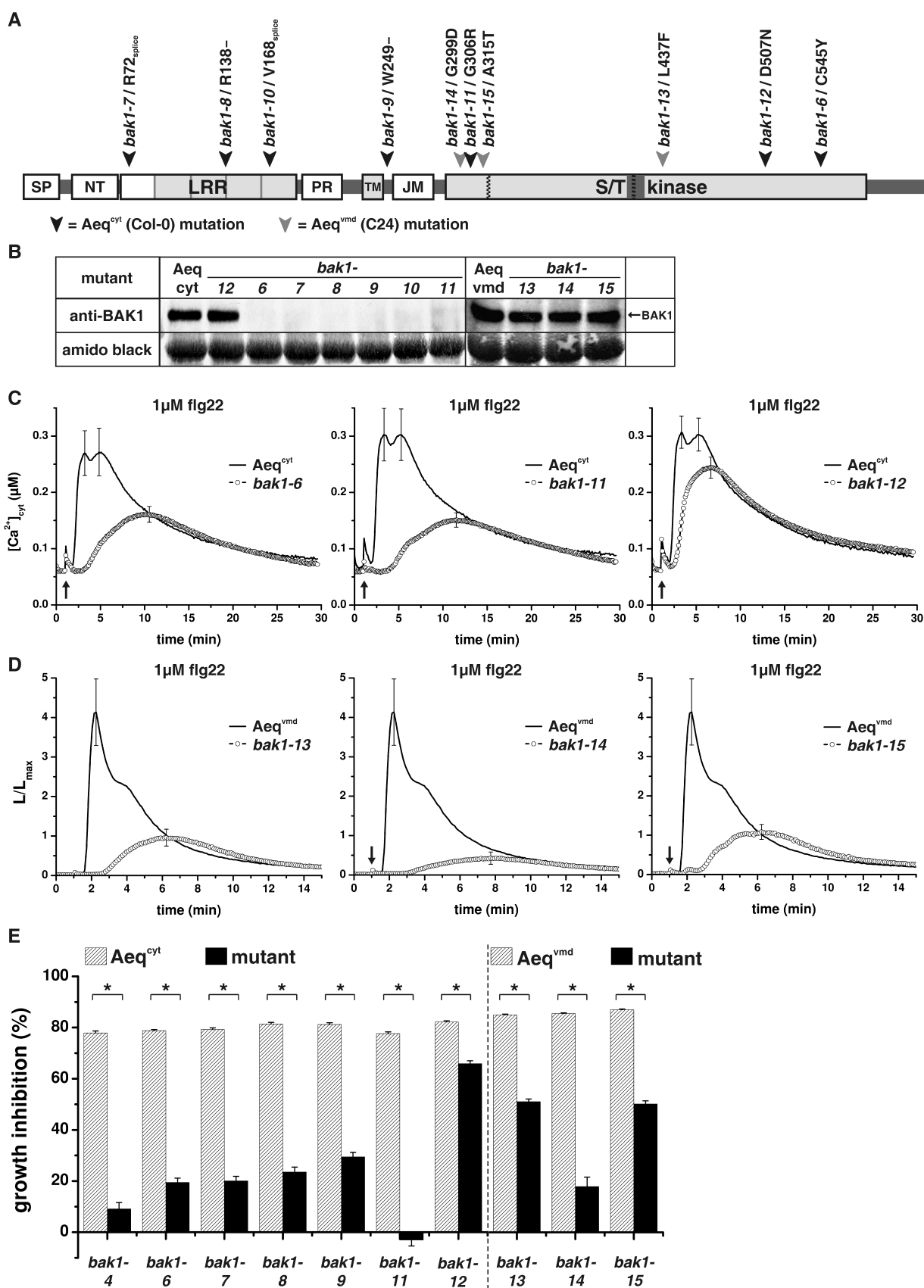
The presence of FLS2 receptor protein was analysed by immunoblot with anti-FLS2 antibodies (Schulze *et al.*, 2010). Generally, mutations of exon-intron borders, frame shifts or nonsense mutations resulted in complete loss of FLS2 receptor protein and flg22 responsiveness (Figure 2B-E). In addition to analysis of  $[Ca^{2+}]_{\text{cyt}}$  elevations, MAMP-induced growth arrest was examined routinely to evaluate MAMP responsiveness. Due to the strong effect of flg22 on roots (Ranf *et al.*, submitted, figure 2, p. 40), flg22-induced growth arrest was determined by root length measurements. In accordance to the loss of FLS2 receptor, *fls2-25*, *-26*, *-28*, *-30* and *-32* were insensitive or strongly impaired in sensitivity to flg22 regarding  $[Ca^{2+}]_{\text{cyt}}$  elevation (Figure 2C/D) and root growth arrest (Figure 2E) as observed for *fls2-T*, a T-DNA insertion null mutant (Ranf *et al.*, submitted, figure 4, p. 43).

Mutants with amino acid exchanges still contained FLS2 receptor protein, although in variable amounts. As reported for the *fls2-17* allele with an identical mutation but in the Landsberg-erecta background (Gomez-Gomez and Boller, 2000), a glycine1064 to arginine mutation within the *fls2-27* kinase domain (Figure 2A) not only caused a strong reduction of the FLS2 protein level (Robatzek *et al.*, 2006) but also a second band with slightly larger apparent mass on immunoblot (Figure 2B). Nevertheless, *fls2-27* was completely flg22-insensitive regarding  $[Ca^{2+}]_{\text{cyt}}$  elevation (Figure 2C middle) and root growth arrest (Figure 2E). Similarly, the exchange of serine320 to leucine within the LRR domain (LRR10) of *fls2-33* (Figure 2A) led to strong reduction of FLS2 protein and a faint second band with slightly lower apparent mass on immunoblot (Figure 2B). Accordingly, the flg22-induced  $[Ca^{2+}]$  elevation in *fls2-33* was almost abolished (Figure 2D middle). Furthermore, despite normal FLS2 protein levels (Figure 2B), the mutation of serine437 to phenylalanine within the LRR domain (LRR16) in *fls2-31* (Figure 2A) also completely abrogated  $[Ca^{2+}]$  elevation (Figure 2D left) and root growth inhibition (Figure 2E). By contrast, two amino acid exchanges within the kinase domain of *fls2-29* and *fls2-34* (Figure 2A) resulted in a more or less pronounced reduction in FLS2 protein content (Figure 2B) that was accompanied by only a partial reduction of flg22-induced  $[Ca^{2+}]$  elevations (Figure 2C/D right) and root growth inhibition (Figure 2E). Taken together, depending on the mutation, residual  $[Ca^{2+}]$  elevations were observed in some *fls2* mutants and this correlated with the degree of root growth inhibition caused by growing them on flg22-containing medium (Figure 2).

### Isolation of new *bak1* alleles.

As BAK1 associates not only with the FLS2 receptor, but is also involved in elf18 and Pep1 signalling (Chinchilla *et al.*, 2007; Krol *et al.*, 2010; Ranf *et al.*, submitted, figure 3, p. 41), those mutants with altered responses to flg22 and elf18 possibly comprise mutations in *BAK1*. Accordingly, sequencing of *BAK1* and allelism analysis revealed 10 novel *bak1* alleles (Figure 3A; table SII). The different mutations ranged from mutations of exon-intron borders and nonsense mutations to missense mutations leading to non-conservative amino acid exchanges and are, together with their location within the BAK1 protein, indicated in figure 3A. Using antibodies directed against BAK1 (Schulze *et al.*, 2010), the BAK1 protein content in different mutants was analysed by immunoblot (Figure 3B). Most of the

*bak1* mutants in the *Aeq<sup>cyt</sup>* background showed no detectable BAK1 protein, including the *bak1-6* and *bak1-11* mutants that both contain amino acid exchanges within the kinase domain (Figure 3A/B).



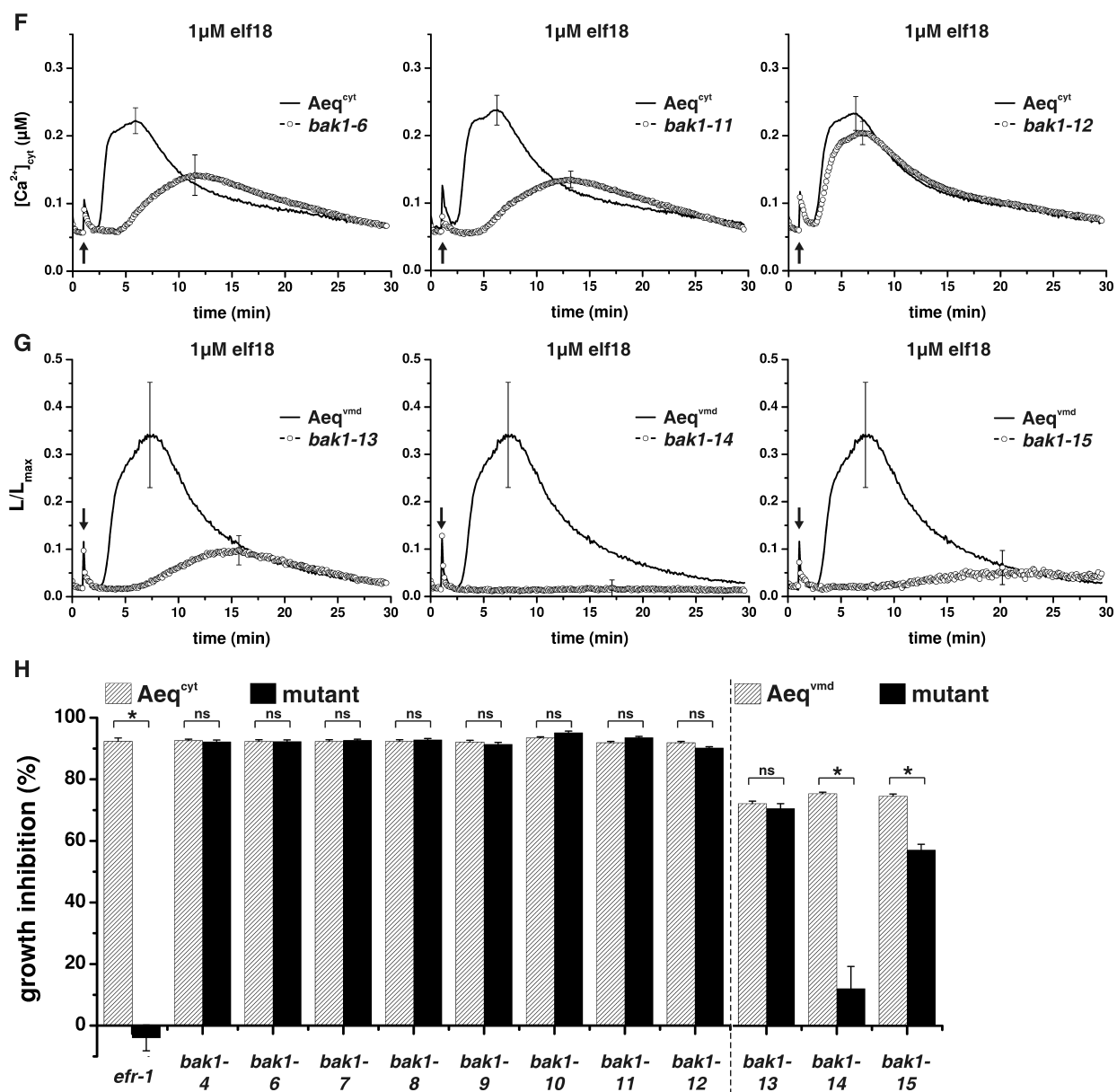


**Figure 3. Ca<sup>2+</sup>-based screening reveals novel *bak1* alleles.**

(A) Schematic illustration of the *bak1* mutations. Mutations in the  $\text{Aeq}^{\text{cyt}}$  (Col-0) background are marked with black and mutations in the  $\text{Aeq}^{\text{vmd}}$  (C24) background with gray arrowheads.

Abbreviations: splice = mutation of exon-intron border; “-” = nonsense mutation; SP = signal peptide; LRR = leucine-rich repeat domain; NT = N-terminal LRR domain; PR = proline-rich domain; TM = transmembrane domain; JM = juxtamembrane domain; S/T kinase = serine/threonine kinase domain (gray bar = catalytic loop, dashed lines = proton and ATP binding sites)

(B) BAK1 protein accumulation was analysed by immunoblot using anti-BAK1 antibodies. Amido-black-stained membranes show equal loading. Three independent experiments revealed identical results.

(C/F) [Ca<sup>2+</sup>]<sub>cyt</sub> elevations in  $\text{Aeq}^{\text{cyt}}$  *bak1* mutant seedlings induced by (C) 1  $\mu\text{M}$  flg22 and (F) 1  $\mu\text{M}$  elf18 each compared to its respective wild-type control. Arrows mark time of MAMP application. Data represent mean of calibrated [Ca<sup>2+</sup>]<sub>cyt</sub>  $\pm$  SD of  $\geq 3$  independent experiments ( $n \geq 45$ ).

(D/G) [Ca<sup>2+</sup>] elevations in  $\text{Aeq}^{\text{vmd}}$  *bak1* mutant seedlings induced by (D) 1  $\mu\text{M}$  flg22 and (G) 1  $\mu\text{M}$  elf18 each compared to its respective wild-type control. Arrows mark time of MAMP application. L/L<sub>max</sub>-normalized data are shown as mean  $\pm$  SD of  $\geq 5$  independent experiments ( $n \geq 20$ ).

(E/H) Growth inhibition of different *bak1* mutants (black bars) each compared to its respective wild-type control (shaded bars) was analysed by (E) root length (1  $\mu\text{M}$  flg22) or (H) fresh weight (100 nM elf18) examination. Data are given as % inhibition compared to untreated control; mean  $\pm$  SE of  $\geq 3$  independent experiments ( $n \geq 24$ ); \* indicates statistically significant difference, ns = not significant ( $p < 0.001$ ).

As illustrated for *bak1-6* and *bak1-11*, all these *bak1* null mutants showed a similar delay and strong reduction of the flg22- or the elf18-induced  $[Ca^{2+}]_{\text{cyt}}$  elevation (Figure 3C/F) as observed for the T-DNA insertion line *bak1-4* (Ranf *et al.*, submitted, figure 3, p. 41). In addition, these *bak1* null mutants more or less resembled the flg22-mediated root growth arrest phenotype of *bak1-4* (Figure 3E). Due to a growth phenotype with very short roots, flg22-induced root growth inhibition could not be assessed in *bak1-10*. Remarkably, *bak1-11* was completely insensitive to flg22 regarding growth arrest despite a virtually identical  $[Ca^{2+}]_{\text{cyt}}$  elevation to *bak1-6* (Figure 3E). Since EMS mutants without back crosses were analysed here, it is not clear if this growth inhibition phenotype is caused by the *bak1* mutation or a second site mutation. Alternatively, as brassinosteroid signalling was not investigated here, some of the growth phenotype might be due to altered brassinolide signalling.

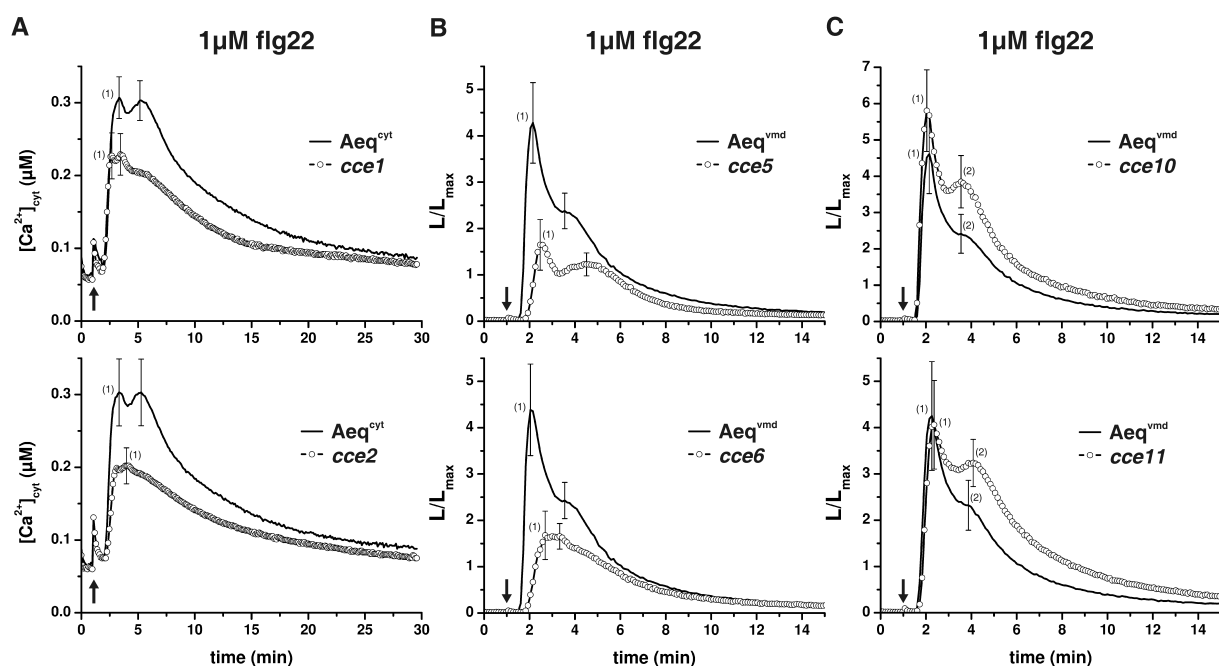
The Aeq<sup>cyt</sup> *bak1* mutant exhibiting normal BAK1 protein level, *bak1-12*, with a conservative exchange of aspartate507 to asparagine within the kinase domain (Figure 3A/B), showed only a weak reduction in  $[Ca^{2+}]_{\text{cyt}}$  elevations (Figure 3C/F right) and growth arrest (Figure 3E) compared to *bak1* null mutants. By contrast, all three *bak1* mutants in Aeq<sup>vm</sup> background, with non-conservative amino acid exchanges in the kinase domain, contained normal amounts of BAK1 protein (Figure 3A/B). For these mutants, the different levels of reduction in the flg22- and elf18-induced  $[Ca^{2+}]$  elevations (Figure 3D/G) were well reflected in the distinct flg22-mediated root growth arrest (Figure 3E). As reported for *bak1-4* (Chinchilla *et al.*, 2007), the newly isolated *bak1* mutants in Aeq<sup>cyt</sup>/Col-0 background also did not show an altered growth inhibition in response to elf18 (Figure 3H). However, two out of the three *bak1* mutants in Aeq<sup>vm</sup>/C24 background – in particular, the *bak1-14* allele – showed reduced sensitivity to elf18 regarding growth arrest (Figure 3H), which correlated with the distinct elf18-induced  $[Ca^{2+}]$  elevations (Figure 3G). This unexpected finding may be attributed to the different accession background (see Discussion).

### Quantitative screening reveals potentially novel components in MAMP signalling.

In addition to the *fls2* and *bak1* mutants described above, *cce* mutants with reduced or enhanced  $[Ca^{2+}]$  elevations were isolated. Characterizations for six of these mutants are presented below. None of these *cce* mutants were specific for a single MAMP, but all showed altered  $[Ca^{2+}]$  elevations to flg22 and elf18 (Figure 4A-C/G-I). Sequence analysis revealed no mutations in *FLS2* or *BAK1*. Accordingly, the *cce* mutants contained normal levels of FLS2 and BAK1 proteins with the exception of *cce2* that showed reduced FLS2 levels (Figure 4F). However, like all other *cce* mutants, *cce2* also showed a reduced  $[Ca^{2+}]$  response to elf18 (Figure 4G). Thus, *cce2* is not simply an *fls2* mutant, but shows a complex phenotype.

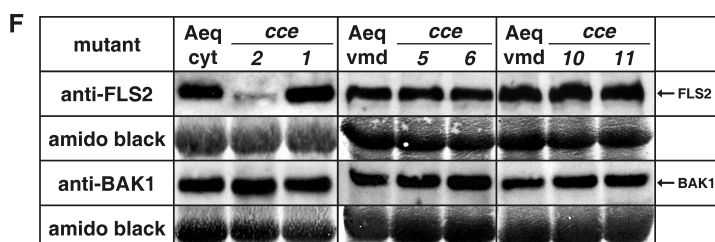
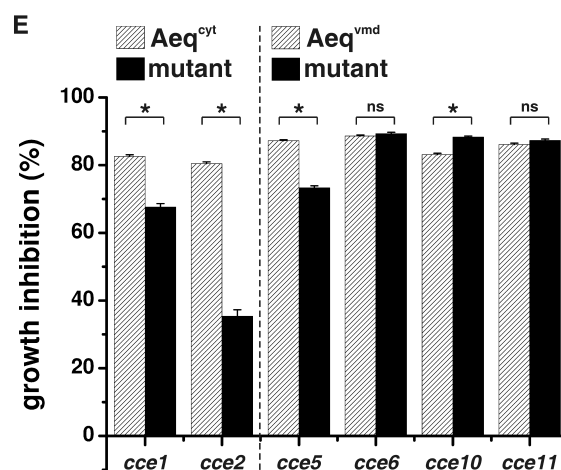
To further evaluate the *cce* mutants, the maximum peak height and total sum of the  $[Ca^{2+}]$  alterations induced by flg22 and elf18 were analysed statistically (Figure 4D/J). Two examples from *cce* mutants with reduced  $[Ca^{2+}]$  elevation in the Aeq<sup>cyt</sup> or Aeq<sup>vm</sup> background are illustrated in figure 4A/G and 4B/H, respectively. The  $[Ca^{2+}]$  amplitudes were reduced by about 20% in response to flg22 or elf18 in

*cce1* and by about 35% in *cce2* (Figure 4D/J). While the  $[Ca^{2+}]$  elevations in *cce1* were only reduced, a slight delay was observed in *cce2* (Figure 4A/G). The flg22-induced root growth arrest of *cce1* and *cce2* reflected the reduction observed in the  $[Ca^{2+}]$  amplitude, while the elf18-induced growth arrest was comparable to wild type (Figure 4E/K). In both  $Aeq^{vmd}$  *cce* mutants, *cce5* and *cce6*, the  $[Ca^{2+}]$  elevations were similarly reduced, by about 60%, and delayed upon flg22, as well as elf18 elicitation (Figure 4B/H). However, the flg22-induced root growth inhibition was only reduced in *cce5*, whereas no reduction was observed for *cce6* (Figure 4E), despite the virtually identical  $[Ca^{2+}]$  amplitudes



**D**

mutant	$[Ca^{2+}]$ max (% WT)	$[Ca^{2+}]$ sum (% WT)
<i>cce1</i>	(1) $74.5 \pm 9.3^*$	$77.9 \pm 12.6^*$
<i>cce2</i>	(1) $66.8 \pm 8.8^*$	$77.1 \pm 10.1^*$
<i>cce5</i>	(1) $38.5 \pm 12.8^*$	$50.1 \pm 8.6^*$
<i>cce6</i>	(1) $38.2 \pm 11.9^*$	$62.7 \pm 12.4^*$
<i>cce10</i>	(1) $127.2 \pm 24.6^*$	$145.0 \pm 20.7^*$
	(2) $158.3 \pm 29.6^*$	
<i>cce11</i>	(1) $95.8 \pm 22.8^{ns}$	$143.4 \pm 22.4^*$
	(2) $138.9 \pm 21.8^*$	



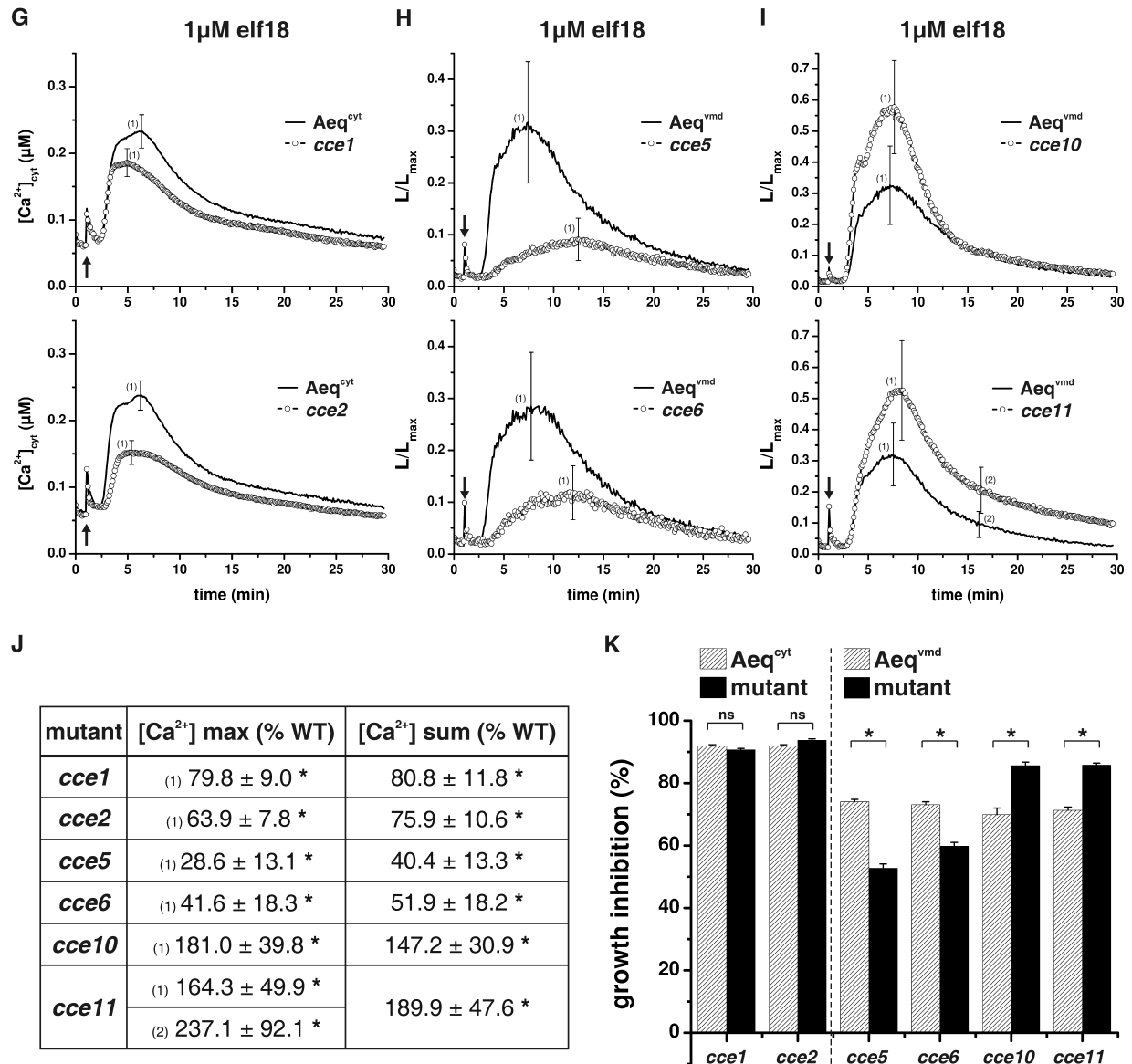


**Figure 4. *cce* mutants show reduced or enhanced responses to flg22 and elf18.**

(A/G) [Ca<sup>2+</sup>]<sub>cyt</sub> elevations in Aeq<sup>cyt</sup> *cce* mutant seedlings induced by (A) 1  $\mu$ M flg22 and (G) 1  $\mu$ M elf18 each compared to its respective wild-type control. Arrows mark time of MAMP application. Data represent mean of calibrated [Ca<sup>2+</sup>]<sub>cyt</sub>  $\pm$  SD of  $\geq$  3 independent experiments ( $n \geq 45$ ). [Ca<sup>2+</sup>]<sub>cyt</sub> peaks chosen for calculation (D/J) are marked with (1) or (2).

(B/C, H/I) [Ca<sup>2+</sup>]<sub>cyt</sub> elevations in Aeq<sup>vmd</sup> *cce* mutant seedlings induced by (B/C) 1  $\mu$ M flg22 and (H/I) 1  $\mu$ M elf18 each compared to its respective wild-type control. Arrows mark time of MAMP application. L/L<sub>max</sub>-normalized data are shown as mean  $\pm$  SD of  $\geq$  3 independent experiments ( $n \geq 26$ ). [Ca<sup>2+</sup>]<sub>cyt</sub> peaks chosen for calculation (D/J) are marked with (1) or (2).

(D/J) Statistical analysis of MAMP-induced [Ca<sup>2+</sup>]<sub>cyt</sub> elevations in *cce* mutants. Amplitudes of the [Ca<sup>2+</sup>]<sub>cyt</sub> peaks ([Ca<sup>2+</sup>]<sub>max</sub>) or the overall sum of the [Ca<sup>2+</sup>]<sub>cyt</sub> elevation ([Ca<sup>2+</sup>]<sub>sum</sub>) induced by (D) 1  $\mu$ M flg22 or (J) 1  $\mu$ M elf18 were calculated for each *cce* mutant line and are given as % of the respective wild-type control. Data represent mean  $\pm$  SD of  $\geq$  3 independent experiments ( $n \geq 26$ ). \* indicates statistically significant difference, ns = not significant ( $p < 0.001$ ). [Ca<sup>2+</sup>]<sub>cyt</sub> peaks chosen for calculation are marked with (1) or (2) in (A-C) and (G-I).

(E/K) Growth inhibition of different *cce* mutants (black bars) each compared to its respective wild-type control (shaded bars) was analysed by (E) root length (1  $\mu$ M flg22) or (K) fresh weight (100 nM elf18) examination. Data are given as % inhibition compared to untreated control; mean  $\pm$  SE of  $\geq$  3 independent experiments ( $n \geq 24$ ); \* indicates statistically significant difference, ns = not significant ( $p < 0.001$ ).

(F) FLS2 and BAK1 protein accumulation was analysed by immunoblot using anti-FLS2 and anti-BAK1 antibodies. Amido-black-stained membranes show equal loading. Three independent experiments revealed identical results.

(Figure 4B). In contrast to the  $Aeq^{cyt}$  mutants, *cce1* and *cce2*, both  $Aeq^{vmd}$  mutants, *cce5* and *cce6*, showed reduced sensitivity to elf18 regarding growth arrest that reflected the respective  $[Ca^{2+}]$  amplitudes (Figure 4H/K). Furthermore, *cce* mutants with enhanced  $[Ca^{2+}]$  elevations upon flg22 or elf18 application were isolated (Figure 4C/I). While the overall shape of the  $[Ca^{2+}]$  elevations induced by flg22 or elf18 were similar between *cce10* and *cce11*, both mutants showed clearly distinct characteristics in response to both MAMPs (Figure 4C/I). The second

$[Ca^{2+}]$  peak induced by flg22 and the subsequent decline of the  $[Ca^{2+}]$  elevation were significantly enhanced in both mutants (Figure 4C/D). The first flg22-induced  $[Ca^{2+}]$  peak, on the contrary, was only increased in *cce10*, while comparable to wild type in *cce11* (Figure 4C/D). This difference in the first  $[Ca^{2+}]$  peak, that also determines the absolute maximum of the  $[Ca^{2+}]$  elevation, is reflected in the flg22-induced root growth arrest, which is enhanced in *cce10* but not *cce11* (Figure 4E). Although the  $[Ca^{2+}]$  elevation upon flg22 elicitation was increased and prolonged in *cce10*, the elf18-induced  $[Ca^{2+}]$  response showed nearly a duplication of the maximum  $[Ca^{2+}]$  peak but quickly returned to wild type  $[Ca^{2+}]$  levels (Figure 4I/J). *Vice versa*, unlike the normal flg22-induced  $[Ca^{2+}]$  maximum, the elf18-induced  $[Ca^{2+}]$  amplitude was strongly enhanced in *cce11* and, furthermore, persisted into a sustained elevated  $[Ca^{2+}]$  level (Figure 4I/J). In agreement with the increase in the absolute maximum of the elf18-induced  $[Ca^{2+}]$  elevations in *cce10* and *cce11*, both mutants were significantly more sensitive to elf18-mediated growth arrest (Figure 4K).

In order to expand the potential phenotypes beyond flg22 and elf18, the *cce* mutants were further tested against the fungal MAMP ch8 and the Arabidopsis-derived DAMP Pep1. This led to two different phenotype categories in the *cce* mutants (summarized in table I). One group (*cce5*, *cce6* and *cce10*) comprises mutants that showed altered  $[Ca^{2+}]$  elevations to flg22, elf18 and Pep1 but no change in their response to ch8, whereas the second group contains mutants with altered  $[Ca^{2+}]$  responses to all four tested MAMPs and DAMPs (*cce1*, *cce2* and *cce11*).

In summary, the current screen for *cce* mutants resulted not only in the identification of additional alleles of *fls2* and *bak1* but also of potentially novel signalling components. These showed distinct and characteristic  $[Ca^{2+}]$  responses and growth arrest phenotypes to flg22 and elf18 that were either reduced or enhanced in comparison to the wild type. Moreover, some *cce* mutants from both groups, reduced or enhanced response, could be sub-categorized into those that showed additional phenotype to Pep1 and/or ch8. Thus, all *cce* mutants obtained so far are affected in common rather than MAMP- or DAMP-specific signalling components.

**Table I:  $[Ca^{2+}]$  response of *cce* mutants to different MAMPs and DAMPs<sup>a</sup>**

<i>cce-</i>	flg22	elf18	Pep1	ch8
<b>1</b>	↓	↓	↓	↓
<b>2</b>	↓↓	↓↓	↓↓	↓
<b>5</b>	↓↓	↓↓	↓↓	—
<b>6</b>	↓↓	↓	↓	—
<b>10</b>	↑↑	↑↑	↑↑	—
<b>11</b>	↑	↑↑	↑↑	↑↑

<sup>a</sup>) the reduced or increased  $[Ca^{2+}]_{cyt}$  response to the MAMPs and DAMPs are depicted by the number of corresponding arrows.

## DISCUSSION

### The power of high-throughput $\text{Ca}^{2+}$ -based screening

Despite the crucial role of  $\text{Ca}^{2+}$  as second messenger in MAMP/DAMP signalling, little is known about the molecular components involved in  $\text{Ca}^{2+}$  signalling and the upstream connection to the receptor. As a very early response occurring within minutes after stimulus application,  $[\text{Ca}^{2+}]$  measurements are linked to MAMP/DAMP-induced receptor complex activities and reflect early upstream signalling events in a quantitative and kinetic manner. Here a high-throughput  $\text{Ca}^{2+}$ -based screening system aimed at elucidating the missing links in early MAMP/DAMP-stimulated  $\text{Ca}^{2+}$  signalling is presented.

Optimization of the screening system minimized hands-on labour time in sample preparation and data evaluation, as well as screening costs while maintaining quantitative and kinetic analyses in a high-throughput manner. Using this setup to screen for *cce* mutants in response to flg22 resulted in several novel alleles of *fls2*, the flagellin receptor, as well as *bak1*, a receptor-associated kinase (Table SI/II). Besides serving as proof of principle for the  $\text{Ca}^{2+}$ -based screening, the rapid isolation of novel *fls2* and *bak1* alleles will be instrumental for further functional characterization of distinct domains within FLS2 and BAK1. Moreover, several potentially novel *cce* mutants were isolated with either reduced or enhanced responses to different sets of MAMPs/DAMPs (Table I). These also included mutants that did not show an altered growth arrest induced either by flg22 or elf18, which could be potentially useful for uncoupling signal transduction pathways linking and distinguishing between defence and developmental processes. Although the growth response is regularly used to isolate MAMP signalling mutants due to the fast and facile screening of huge mutant pools (Chinchilla *et al.*, 2007; Nekrasov *et al.*, 2009), it may not be suitable for all mutants (e.g. *cce6* and *cce11*; Figure 4E) and may not be applicable for all MAMPs. The elf18-induced growth inhibition in Col-0, for instance, is impaired in mutants with reduced EFR receptor levels (Li *et al.*, 2009; Nekrasov *et al.*, 2009; Saijo *et al.*, 2009) but not in *bak1-4* (Figure 3H; Chinchilla *et al.*, 2007) or other potential signalling mutants downstream of the receptor (e.g. *cce1* and *cce2*; Figure 4K). Additionally, not only whole seedlings, but also excised tissues, such as isolated roots or mature leaf discs, can be used for  $[\text{Ca}^{2+}]$  measurements to analyse specific responses in such tissues.

A drawback in  $\text{Ca}^{2+}$ -based screening is the need of aequorin-transgenic mutant pools, which excludes the use of established pools like T-DNA insertion or transposon lines. Such aequorin-transgenic mutant pools are mainly generated by EMS mutagenesis or similar techniques, where identification of mutants requires intensive mapping. However, this might be easily overcome through the advance in current deep sequencing technologies that have reached acceptable genome coverage to permit rapid mutation identification (Schneeberger *et al.*, 2009).

In conclusion, the  $\text{Ca}^{2+}$ -based screening system provided here is highly suitable for identification of receptor complex constituents as well as early signalling components activated by any MAMP and DAMP inducing  $[\text{Ca}^{2+}]$  elevations in a single screen. As  $\text{Ca}^{2+}$  is a ubiquitous second messenger involved in diverse signalling pathways,  $\text{Ca}^{2+}$ -based screening is not restricted to MAMP and DAMP

signalling but is generally applicable for any stimulus involving  $\text{Ca}^{2+}$  signalling and in intact seedlings as well as specific tissues.

***cce* mutants comprise potentially novel components in MAMP signalling.**

Overall, the obtained *cce* mutants were not specific for a single MAMP or DAMP, but all showed altered  $[\text{Ca}^{2+}]$  elevations to several MAMPs and DAMPs that were either reduced or enhanced. Furthermore, all mutants showed distinct characteristics in their responses. For instance, the mutants *cce10* and *cce11* differed in their response pattern to flg22 and elf18, i. e. the  $[\text{Ca}^{2+}]$  elevations were either increased or prolonged or a combination of both depending on the applied MAMP (Figure 4C/I). In the different mutants distinct phenotype patterns were observed to the set of tested MAMPs/DAMPs (summarized in table I). Besides the different flg22- and elf18-induced phenotypes described above, some *cce* mutants also showed an altered response to Pep1 but not to ch8 (Table I). The signalling pathways activated by the three MAMPs/DAMPs, flg22, elf18 and Pep1, share the common kinase component BAK1 (Chinchilla *et al.*, 2007; Krol *et al.*, 2010). Thus, these *cce* mutants are probably affected in similarly shared signalling components like BAK1, which are specific for a certain class of receptors. However, these are unlikely to be from the *SERK* family of *BAK1* homologs since *serk* mutants do not have any impact on MAMP-induced  $[\text{Ca}^{2+}]$  elevations (Ranf *et al.*, submitted, figure 4, p. 43). Interestingly, one of the mutants with an enhanced  $[\text{Ca}^{2+}]$  response (*cce11*) as well as two mutants with a reduced  $[\text{Ca}^{2+}]$  elevation (*cce1* and *cce2*), showed altered responses not only to flg22, elf18 and Pep1 but also to ch8 (Table I). As responses to these MAMPs and DAMPs are mediated by two completely different classes of receptors, i. e. LRR- or LysM-containing receptors (Gomez-Gomez *et al.*, 1999; Gomez-Gomez and Boller, 2000; Zipfel *et al.*, 2006; Miya *et al.*, 2007; Wan *et al.*, 2008), the broad spectrum of phenotypes of these mutants potentially indicate that unknown common components are affected.

Most of the *cce* mutants also showed normal levels of FLS2 and BAK1 protein (Figure 4F), suggesting that components downstream of the receptor but upstream of or involved in  $\text{Ca}^{2+}$  signalling are causal for the observed phenotypes. An exception is the *cce2* mutant that contained less FLS2 protein (Figure 4F). As *FLS2* is not mutated in *cce2*, the reduced protein level might be due to alterations in the molecular machinery controlling FLS2 receptor level. Steady-state FLS2 levels, for instance, are regulated by ethylene signalling (Boutrot *et al.*, 2010; Mersmann *et al.*, 2010), whereas the EFR receptor, and to a lesser extent the FLS2 receptor, are subject to a strict and specific ER-mediated quality control (Li *et al.*, 2009; Nekrasov *et al.*, 2009; Saijo *et al.*, 2009). Nevertheless, *cce2* also shows a reduced  $[\text{Ca}^{2+}]$  response to elf18, Pep1 and ch8 (Table I) and thus, potentially, immune receptors in general are affected, thereby causing the observed broad-spectrum phenotype. Taken together, all *cce* mutants obtained so far are affected in common signalling components shared by diverse MAMPs and DAMPs.

### **C24 seedlings reveal accession-specific differences in MAMP sensitivity and a potential role for BAK1 in late elf18-induced growth arrest.**

As the two aequorin reporter lines used in this screen, Aeq<sup>cyt</sup> and Aeq<sup>vmd</sup>, are in different Arabidopsis accessions, Col-0 and C24 respectively, accession-specific differences in MAMP responses were observed during evaluation of the obtained mutants. This is particularly well illustrated by the different sensitivities to flg22 and elf18 regarding growth arrest in the two accessions (Figure 2E/3H). While C24 seedlings were more sensitive to flg22 than Col-0 (Figure 2E), they were remarkably less affected by elf18 compared to Col-0 (Figure 3H). Although the [Ca<sup>2+</sup>] elevations in Aeq<sup>cyt</sup> and Aeq<sup>vmd</sup> cannot be compared directly, the [Ca<sup>2+</sup>] amplitudes evoked by the different MAMPs/DAMPs within each accession show a comparatively distinct pattern (Figure 1). The [Ca<sup>2+</sup>] amplitude induced by elf18 in Col-0 lies between the flg22- and the ch8-induced response (Figure 1A), while in C24 seedlings elf18 induced the lowest and flg22 an exceptionally high [Ca<sup>2+</sup>] amplitude (Figure 1B). In good agreement to public gene expression profiling data, *EFR* expression is significantly reduced in C24 in comparison to Col-0, while *FLS2* expression appears slightly enhanced (Figure S2B). Moreover, the *FLS2* receptor level in Aeq<sup>vmd</sup>/C24 was much higher than in Col-0 as detected by immunoblot analysis with anti-*FLS2* antibodies, while *BAK1* levels were comparable (Figure S2A).

Concerning the distinct growth arrest sensitivity, receptor expression and *FLS2* protein level, the specific [Ca<sup>2+</sup>] amplitude patterns appear to reflect general differences in sensitivity towards flg22 vs. elf18 in Col-0 and Aeq<sup>vmd</sup>/C24. This is further supported by SNPs detected in *FLS2*, *EFR* and *BAK1* in Aeq<sup>vmd</sup>/C24 compared to Col-0. Three SNPs in *BAK1* are located in intron regions, while sequencing of Aeq<sup>vmd</sup>/C24 *FLS2* revealed two conservative amino acid exchanges in comparison to Col-0, one within the leucine-rich repeat domain (LRR7, D255E) and one within the kinase domain (K971R) quite close to the proton acceptor site (D997; Figure 2A). Moreover, one of three SNPs in C24 *EFR* is a synonymous substitution, while the other two lead to non-conservative lysine to glutamate (K116E) and glutamate to valine (E134V) exchanges in LRR1 and LRR2, respectively, which can potentially affect ligand binding. Remarkably, only the *FLS2* SNP leading to the D255E exchange and the *EFR* SNP leading to the E134V exchange are annotated in public database (<http://polymorph-clark20.weigelworld.org>; Clark *et al.*, 2007; Zeller *et al.*, 2008), whereas the K971R exchange within the *FLS2* kinase domain and the K116E exchange in the *EFR* LRR1 domain appear to be specific for Aeq<sup>vmd</sup>. As the two *FLS2* and the two *EFR* SNPs in Aeq<sup>vmd</sup> are located in regions important for activity, i. e. ligand binding LRR or kinase domain, they might, either directly or indirectly, e. g. *via* protein stability, be relevant for the observed differences in sensitivity towards flg22 and elf18, respectively. Taken together, several different aspects, such as expression of receptor genes, receptor protein accumulation and SNPs leading to amino acid exchanges, may account for the difference in sensitivity of the accessions Col-0 and Aeq<sup>vmd</sup>/C24 towards flg22 and elf18 regarding [Ca<sup>2+</sup>] elevations and MAMP-mediated growth arrest.

In addition to this general difference in elf18 sensitivity, also a differential role of BAK1 in the late elf18-induced growth arrest was observed between Col-0 and Aeq<sup>vmd</sup>/C24. As reported, the null T-DNA insertion mutants *bak1-3* and *bak1-4*, both in Col-0 background, are only impaired in flg22- but not elf18-induced growth arrest, while BAK1 is involved in the early accumulation of reactive oxygen species in response to both MAMPs (Chinchilla *et al.*, 2007). Accordingly, also none of the *bak1* mutants in the Aeq<sup>cyt</sup>/Col-0 background were impaired in elf18-mediated growth arrest (Figure 3H) and, similarly, none of the Aeq<sup>cyt</sup> *cee* mutants (Figure 4K), while all of them were clearly reduced in the flg22-induced growth inhibition (Figure 3E/4E). By contrast, two of the three *bak1* mutants and all *cee* mutants in the Aeq<sup>vmd</sup>/C24 background showed an altered growth arrest to elf18 (Figure 3H/4K), which also reflected the reduction in the elf18-induced [Ca<sup>2+</sup>] elevations (Figure 3G/4H-I). Whether these point mutation *bak1* mutants might differ from the *bak1* null mutants by interfering with normal BAK1 signalling, for instance *via* the four other *BAK1*-homologs, or alternatively, whether brassinosteroid signalling might be affected in these mutants, remains to be determined. Bearing these constraints in mind, BAK1, and similarly the yet-to-be-identified CCEs, play a role not only in the early [Ca<sup>2+</sup>] elevation but also the late growth inhibition induced by elf18 in Aeq<sup>vmd</sup>/C24 seedlings. As both accession show a differential sensitivity towards elf18, the observed role of BAK1 in the elf18-induced growth arrest in Aeq<sup>vmd</sup>/C24 may be directly linked to the reduced elf18-sensitivity. In conclusion, the analysis of MAMP and DAMP responses in different *Arabidopsis* accessions potentially reveals additional phenotypes not discovered in standard accessions used in routine laboratory experiments such as Col-0. Exploring natural diversity to uncover potential components in MAMP and DAMP signalling should also receive more consideration in the future.

## SUPPLEMENTAL DATA

Supplemental data are available in the appendix 5.2 (p. 153).

**Figure S1.** Output examples of R-based data calibration.

**Figure S2.** Col-0 and C24 seedlings show differential expression and accumulation of immune receptors.

**Table SI.** *fls2* mutants.

**Table SII.** *bak1* mutants.

**Table SIII.** Primers for PCR and sequencing.

**Protocol 1.** Seed sterilization.

**Protocol 2.** [Ca<sup>2+</sup>] measurements in 96/384 well plates.

## METHODS

### *Plant material and growth conditions*

The *Arabidopsis thaliana* line Aeq<sup>cyt</sup>/pMAQ2 in Col-0 background and Aeq<sup>vmd</sup>/HVA1 in C24 background were obtained from M. and H. Knight (Knight *et al.*, 1991, 1996). Mutagenesis was performed using EMS at two concentrations (0.2% and 0.4%, w/v) according to standard protocol

(*Arabidopsis*: A laboratory manual, ISBN: 0-87969-573-0) and M1 plants were harvested individually. T-DNA insertion lines *fls2-T* (At5g46330, SALK\_062054) and *bak1-4* (At4g33430, SALK\_116202; Chinchilla *et al.*, 2007) were obtained from B. Kemmerling and *efr-1* (At5g20480, SALK\_044334; Zipfel *et al.*, 2006) from C. Zipfel. Seeds were surface-sterilized, if required (see protocol 1 in supplemental information), and stratified at 4°C for  $\geq 2$  days. Plants were grown on soil in climate chambers under short day or on ATS agar plates (Estelle and Somerville, 1987) or in liquid MS medium (0.5 x MS, 0.25 % sucrose, 1 mM MES, pH 5.7) in 24-well plates (10 seedlings / well) under long day conditions at 20-22°C.

### **Sequencing**

For sequence analysis *FLS2*, *EFR* and *BAK1* were amplified from genomic DNA by PCR with gene-specific primers (Table SIII) using Phusion<sup>®</sup> Hot Start High-Fidelity DNA Polymerase (Finnzymes, Espoo, Finland). Purified PCR products were sequenced using the indicated primers (Table SIII).

### **Elicitors**

Flg22, elf18 and AtPep1 (Pep1; Gomez-Gomez *et al.*, 1999; Kunze *et al.*, 2004; Huffaker *et al.*, 2006) were synthesized using an Abimed EPS221 (Abimed, Langenfeld, Germany) system. N-acetylchitooctose (ch8) was provided by N. Shibuya (Albert *et al.*, 2006).

### **Aequorin luminescence measurements**

For aequorin luminescence measurements Col-0 plants expressing p35S-apoaequorin (pMAQ2) in the cytosol (Aeq<sup>cyt</sup>) or C24 plants expressing p35S-apoaequorin as cytoplasmic-faced H<sup>+</sup>-PPase-fusion (HVA1) in the tonoplast (Aeq<sup>vm</sup>) were used (Knight *et al.*, 1991, 1996). 8-days-old liquid-grown seedlings were placed individually in 96- or 384-well plates in 10  $\mu$ M CTZ / dH<sub>2</sub>O (CTZ native/h, P.J.K., Kleinblittersdorf, Germany) in the dark over night. Luminescence was recorded by scanning each row in 6 sec (96-wells) or two rows in 10 sec intervals (384-wells) using a Luminoskan Ascent 2.1 luminometer (Thermo Scientific, Schwerte, Germany). Detailed protocols are available as supporting information (protocol 2). Remaining aequorin was discharged and Ca<sup>2+</sup> concentrations were calculated according to Rentel and Knight (2004):  $pCa = 0.332588(-\log(L/L_{max})) + 5.5593$

$L/L_{max}$  = luminescence counts per sec/total luminescence counts remaining

Amplitudes of the [Ca<sup>2+</sup>] peaks and the overall sum of the [Ca<sup>2+</sup>] elevation were calculated for each cce mutant line and are given as % of the respective wild-type control. For statistical analysis Student's t-test ( $p < 0.001$ ) was performed using GraphPad Prism 5.0.

### **Immunoblot analysis**

Seedlings were grown for 14 days in MS medium. Total protein and membrane proteins were solubilized in 25 mM Tris-HCl pH 8.0, 150 mM NaCl, 1% (w/v) octylphenoxypolyethoxyethanol (Nonidet P-40) and Serva inhibitor mix HP (www.serva.de). Immunoblot was performed with anti-FLS2 and anti-BAK1 antibodies (Chinchilla *et al.*, 2006; Schulze *et al.*, 2010).

### **Growth inhibition**

For root growth analysis seedlings were grown vertically on agar plates  $\pm 1 \mu$ M flg22 for 14 days. For fresh weight examination 5-days-old seedlings from agar plates were transferred individually into 48-well plates  $\pm 100$  nM elf18 (1ml / well / seedling) for 15 days. To distinguish between growth differences due to treatment *vs.* genotype effects, two-way ANOVA was performed on log<sub>2</sub>-transformed

root length or fresh weight data (genotype x treatment;  $p < 0.001$ ; R statistical package; Delker *et al.*, 2010). Data were depicted as % growth inhibition compared to control.

### **FUNDING**

This work is supported by a Deutsche Forschungsgemeinschaft (DFG) grant (LE2321/1-2) within the priority project SPP1212. P.P. is financed by the DFG grant (SFB648/TP-B1) to J.L. and D.S., while D.C. is financed by the Swiss National Science Foundation grant (31003A-120655).

### **ACKNOWLEDGEMENTS**

We are grateful to Birgit Kemmerling, Marc and Heather Knight and Cyril Zipfel for providing material and Carolin Delker and Ivo Große for advice in statistics. We thank Christel Rülke and Nicole Bauer for technical assistance.

### **REFERENCES**

Due to high redundancy of references between the different chapters, the references are combined in the common REFERENCE section (chapter 4, p. 126).

## 2.4. Lipopolysaccharides induce $[Ca^{2+}]_{cyt}$ elevations in *Arabidopsis thaliana* seedlings

### 2.4.1. Aims and summary

The third objective of this thesis is the characterization of the  $Ca^{2+}$  responses induced by different MAMPs and DAMPs. While the well-established MAMPs and DAMPs flg22, elf18, Pep1 and ch8 are covered in the previous section, the following chapter will focus on the less-studied MAMPs lipopolysaccharide (LPS) and peptidoglycan (PGN). Since the peptide MAMPs can be synthetically produced and their cognate perception systems have been discovered, the specificity of their MAMP activity was genetically and biochemically demonstrated. In contrast, LPS and PGN need to be purified from bacterial cultures and thus may contain MAMP-active contaminants if not properly purified. Indeed, in animal systems, such highly active contaminants in LPS and PGN preparations led to contradictory reports about their perception. Since in most plants studies very high concentrations of LPS were applied, this raised concerns about the specificity of the observed phenotypes for LPS and potential MAMP-active contaminants in the LPS preparations used. Furthermore, inter-strain differences between distinct bacterial species, as well as intra-strain variability of LPS further hinders comparability of different studies.

Here, analysis of the  $[Ca^{2+}]_{cyt}$  elevation in *Arabidopsis* seedlings induced by a widely used commercial source of *Pseudomonas aeruginosa* LPS preparation pointed to a substantial contamination with bacterial EF-Tu protein, which is highly active as MAMP. Re-evaluation of the  $Ca^{2+}$ -releasing activity of *P. aeruginosa* LPS using preparations from different strains, as well as provided by different laboratories all resulted in comparable  $[Ca^{2+}]_{cyt}$  elevations. Several *Xanthomonas campestris* LPS preparations, tested in comparison, also induced comparable but lower  $[Ca^{2+}]_{cyt}$  elevations. Furthermore, the purified LPS preparations still induced significant  $[Ca^{2+}]_{cyt}$  elevations at 100-fold lower concentrations as regularly used in plant studies, pointing to a sensitive perception system. In general, the LPS-induced  $Ca^{2+}$  response resembled the typical characteristics observed with other MAMPs, such as a prolonged  $[Ca^{2+}]_{cyt}$  elevation. Intriguingly, in contrast to published results (Shan *et al.*, 2008), LPS-induced  $[Ca^{2+}]_{cyt}$  elevations were independent of BAK1. Moreover, neither LPS- nor flg22- or elf18-induced  $[Ca^{2+}]_{cyt}$  elevations were altered by loss of DND1, thus disproving the purported role for this cyclic nucleotide-gated channel in MAMP-induced  $Ca^{2+}$  signalling as suggested (Ali *et al.*, 2007; Ma *et al.*, 2009). In conclusion, purified LPS acts as MAMP in *Arabidopsis*, even at low concentrations. The data further illustrate the importance of critical assessment of the purity and specificity of MAMP preparations used to study innate immunity.

## 2.4.2. Manuscript

### Lipopolysaccharides induce calcium elevations in *Arabidopsis thaliana* independent of the adapter kinase BAK1 and the calcium permeable channel DND1

Stefanie Ranf<sup>1</sup>, Lennart Eschen-Lippold<sup>1</sup>, Ulrich Zähringer<sup>2</sup>, Justin Lee<sup>1</sup> & Dierk Scheel<sup>1</sup>

<sup>1</sup>Leibniz Institute of Plant Biochemistry, Stress and Developmental Biology, Weinberg 3, D-06120 Halle, Germany

<sup>2</sup>Division of Immunochimistry, Research Center Borstel, Leibniz-Center for Medicine and Biosciences, Parkallee 1-40, 23845 Borstel, Germany

Keywords: Ca<sup>2+</sup> signalling, MAMP, lipopolysaccharide, *Pseudomonas*, *Xanthomonas*, *Arabidopsis thaliana*

#### SUMMARY

Cell wall components, due to their exposed location, are predestined as pathogen/microbe-associated molecular patterns (P/MAMPs) that are perceived by a potential host to induce defence responses. The glyco-conjugate lipopolysaccharide (LPS) is the main component in the outer cell envelope of Gram-negative bacteria and belongs to the most potent MAMPs in mammalian systems. By contrast, comparatively high LPS concentrations (50-100 µg/ml) are necessary to elicit defence responses in plants, thereby raising concerns about the purity of the applied preparations. Using a sensitive system for monitoring changes in cytosolic Ca<sup>2+</sup> ([Ca<sup>2+</sup>]<sub>cyt</sub>), a wide collection of purified LPS preparations from *Pseudomonas* and *Xanthomonas* was found to induce [Ca<sup>2+</sup>]<sub>cyt</sub> elevations in *Arabidopsis thaliana* at concentrations (~0.5 µg/ml) that are > 100-fold lower than those reported previously. Hence, this points to a sensitive perception system for LPS in *Arabidopsis*. Moreover, [Ca<sup>2+</sup>]<sub>cyt</sub> elevations induced by the purified LPS preparations were independent of the adapter kinase BAK1 (Brassinosteroid receptor 1-associated kinase 1), which associates with several MAMP receptors, including EFR (Elongation factor Tu (EF-Tu) receptor). Conversely, a commercial LPS preparation showed reduced [Ca<sup>2+</sup>]<sub>cyt</sub> elevations in *bak1* but also in *efr* mutant seedlings compared to wild type seedlings, pointing to a contamination with bacterial EF-Tu protein. Furthermore, LPS-induced [Ca<sup>2+</sup>]<sub>cyt</sub> elevations in *Arabidopsis* were not mediated by the Ca<sup>2+</sup>-permeable plasma membrane channel CNGC2/DND1 (Cyclic nucleotide-gated channel 2/defence no death 1). Taken together, previous reports on roles of BAK1 and CNGC2/DND1 in LPS signalling need to be re-evaluated.

#### INTRODUCTION

Specific pattern recognition receptors (PRRs) perceive conserved microbe/pathogen-associated molecular patterns (M/PAMPs) to initiate defence responses. One of the earliest signalling events observable is a rapid change in the cytosolic Ca<sup>2+</sup> concentration ([Ca<sup>2+</sup>]<sub>cyt</sub>), which is a prerequisite for most downstream responses, such as accumulation of reactive oxygen species (ROS), activation of mitogen-activated and Ca<sup>2+</sup>-dependent protein kinases and defence gene expression (Blume *et al.*, 2000; Boller and Felix, 2009; Boudsocq *et al.*, 2010; Ranf *et al.*, submitted, see 2.2).

Currently, the best studied MAMP/PRR pairs in *Arabidopsis thaliana* are flagellin/FLS2 (Flagellin-sensitive 2) and EF-Tu/EFR (Elongation factor Tu receptor), with the peptides flg22 and elf18

functioning as the respective MAMPs (Felix *et al.*, 1999; Gomez-Gomez *et al.*, 1999; Gomez-Gomez and Boller, 2000; Kunze *et al.*, 2004; Chinchilla *et al.*, 2006; Zipfel *et al.*, 2006). Upon ligand binding, FLS2 associates with the adapter kinase BAK1 (Brassinosteroid receptor 1-associated kinase 1), and this is required for full responsiveness to flg22 (Chinchilla *et al.*, 2007; Heese *et al.*, 2007). Meanwhile, BAK1 was also found to act in signalling pathways activated by several other MAMPs/elicitors like elf18, harpin elicitor protein (HrpZ), peptidoglycan (PGN) and lipopolysaccharides (LPS), but not chitin in *Arabidopsis* (Shan *et al.*, 2008) and infestin and bacterial cold-shock protein in tobacco (Heese *et al.*, 2007; Chaparro-Garcia *et al.*, 2011).

Due to their exposed position to any potential host, cell wall components are predestined as MAMPs. Indeed, PGN from *Staphylococcus aureus* acts as MAMP in *Arabidopsis* (Gust *et al.*, 2007) and chitin-oligomers from fungal cell walls are sensed by the *Arabidopsis* RLK CERK1 (Chitin elicitor receptor kinase 1; Miya *et al.*, 2007; Wan *et al.*, 2008; Petutschnig *et al.*, 2010). These cell wall components fit the definition of MAMPs as they are representative for a whole class of microbes and indispensable for survival. Another such typical MAMP could be LPS. This common glyco-conjugate is the main component in the outer cell envelope of Gram-negative bacteria. The common structure of these tripartite amphiphilic macromolecules consists of lipid A, which functions as membrane anchor and is linked to a saccharide part consisting of a conserved oligosaccharide core region and a variable O-polysaccharide moiety (OPS). LPS lacking the OPS is also referred to as lipo-oligosaccharide (LOS) or rough (R-)LPS due to the rough appearance of the bacterial colonies in contrast to smooth wild type colonies (S-LPS; reviewed in Molinaro, 2009).

Besides its structural function as cell wall component, LPS plays a role in adhesion and as a protective barrier to antimicrobial compounds while allowing nutrient uptake (Kingsley *et al.*, 1993; Dow *et al.*, 1995; Titarenko *et al.*, 1997; Deng *et al.*, 2010). LPS therefore enables bacteria to survive in harsh environments including those inside the host. Due to its cell surface localization, LPS is also highly suited for interaction with the host. In mammals, LPS/lipid A is recognized by the innate immune system after association with an LPS-binding protein *via* a CD14/MD-2/TLR4 receptor complex leading to inflammatory responses and possibly septic shock (Miyake, 2004). The lipid A part of LPS therefore acts as typical PAMP in the mammalian innate immune system and belongs to the endotoxins, whereas the OPS component comprises strong antigenic activity in the adaptive immune system (Zipfel and Felix, 2005; Knirel *et al.*, 2006).

LPS also acts as MAMP in different dicotyledonous plants species, including *Arabidopsis thaliana* (Coventry and Dubery, 2001; Meyer *et al.*, 2001; Newman *et al.*, 2001; Newman *et al.*, 2002; Gerber and Dubery, 2004; Zeidler *et al.*, 2004; Braun *et al.*, 2005; Silipo *et al.*, 2005; Deng *et al.*, 2010), and in rice (Desaki *et al.*, 2006). However, LPS from diverse bacteria showed differential activities in different plant species in their ability to induce defence responses. LPS from different bacteria, as well as purified lipid A, for example, induce NO production in an *Arabidopsis* cell suspension culture and leaves (Zeidler *et al.*, 2004). Whereas *Escherichia coli* and *Ralstonia solanacearum*-derived LOS are

inactive, LOS from *Xanthomonas* induces pathogenesis-related (PR) gene expression in a biphasic manner. Interestingly, the core oligosaccharide only induces the first phase, whereas the lipid A only induces the second phase, suggesting that both parts can be recognized separately (Silipo *et al.*, 2005). The LPS of many phytopathogenic bacteria like *Pseudomonas*, *Xanthomonas* and *Erwinia* contain OPS consisting of a rhamnose backbone. Synthetic nona-rhamnans, probably due to a specific coiled structure, strongly induce PR gene expression (Bedini *et al.*, 2005). LPS of endophytic bacteria, on the contrary, prevalently contain monosaccharides other than rhamnose in their OPS (Molinaro, 2009). LPS also plays a role in induced systemic resistance by plant growth-promoting rhizobacteria (van Loon *et al.*, 1998; Bakker *et al.*, 2007) and in nodule formation/colonization in the Rhizobium-legume symbiosis (Niehaus and Becker, 1998; Albus *et al.*, 2001; Scheidle *et al.*, 2005; Tellstrom *et al.*, 2007). Thus, LPS is involved in pathogenic as well as symbiotic plant-microbe interactions.

In summary, both plants and animals have the ability to sense different parts of LPS, namely the lipid A component, the core oligosaccharide, as well as the OPS. The underlying perception mechanisms for the different LPS components in plants, however, are yet unknown. Recently, Shan and co-workers (2008) suggested an involvement of BAK1 in several MAMP-receptor complexes, including LPS from *Pseudomonas aeruginosa*, and the Ca<sup>2+</sup>-permeable plasma membrane channel CNGC2/DND1 was reported to mediate LPS signalling in Arabidopsis (Ali *et al.*, 2007; Ma *et al.*, 2009).

The data reported here show that *Arabidopsis thaliana* Col-0 seedlings respond very sensitively to treatment with various *Pseudomonas* and *Xanthomonas* LPS preparations with typical [Ca<sup>2+</sup>]<sub>cyt</sub> elevations reminiscent of other MAMP-induced [Ca<sup>2+</sup>]<sub>cyt</sub> changes in Arabidopsis. However, the obtained data further demonstrate that the LPS-induced [Ca<sup>2+</sup>]<sub>cyt</sub> responses are independent of BAK1 and CNGC2/DND1.

## RESULTS

### LPS as MAMP – is it really LPS?

An elevation of the cytosolic Ca<sup>2+</sup> concentration, [Ca<sup>2+</sup>]<sub>cyt</sub>, belongs to the very first responses activated after binding of a MAMP ligand to its receptor. Alterations in [Ca<sup>2+</sup>]<sub>cyt</sub> therefore reflect the activity of the receptor complex in a quantitative and kinetic manner. Arabidopsis Col-0 seedlings expressing apoaequorin in the cytosol were used to assess the capability of different LPS preparations to induce [Ca<sup>2+</sup>]<sub>cyt</sub> elevations. This included several LPS preparations from different *Pseudomonas* strains and *Xanthomonas campestris* pathovars provided by different laboratories, as well as different batches of a widely used commercial *Pseudomonas aeruginosa* preparation.

Remarkably, the three different batches of the commercial *P. aeruginosa* (LPS<sub>com</sub>) preparation showed different efficacies in inducing [Ca<sup>2+</sup>]<sub>cyt</sub> elevations (Figure 1a). While LPS-1<sub>com</sub> and LPS-2<sub>com</sub> induced reproducible but distinct [Ca<sup>2+</sup>]<sub>cyt</sub> elevations, LPS-3<sub>com</sub> did not show any activity in this assay. Moreover, analysis of LPS-2<sub>com</sub> revealed a substantial reduction of the [Ca<sup>2+</sup>]<sub>cyt</sub> amplitude in the *efr-1* and *efr-2* mutant background (Figure 1b). These T-DNA insertion mutants are both null mutants of the

EFR receptor and hence completely insensitive to elf18 (Figure 1c), whereas both lines react normally to treatment with other MAMPs like flg22 (Figure 1d). As the EFR receptor is specific for sensing the bacterial EF-Tu protein, the reduction of the  $[Ca^{2+}]_{\text{cyt}}$  elevation in the *efr* mutants appears to be caused by a substantial contamination of LPS-2<sub>com</sub> with EF-Tu protein. The residual  $[Ca^{2+}]_{\text{cyt}}$  elevation in the *efr* mutant background, of less than 25% of the wild type response, might be due to LPS.

### LPS do induce $Ca^{2+}$ elevations in Arabidopsis seedlings.

The results obtained with the commercial LPS preparations raised the necessity to re-evaluate if LPS indeed acts as a MAMP and induces  $[Ca^{2+}]_{\text{cyt}}$  elevations in plants. Thus, purified LPS preparations from different *Pseudomonas* strains, namely *P. aeruginosa*, *P. alcaligenes*, *P. syringae*, and *P. fluorescens* were tested. These LPS preparations all induced  $[Ca^{2+}]_{\text{cyt}}$  elevations with amplitudes and kinetics (Figure 2a-d) that are comparable to those obtained with LPS-1<sub>com</sub> (c.f. Figure 1a/8c). Additionally, several LPS preparations of different *X. campestris* pathovars induced similar although lower  $[Ca^{2+}]_{\text{cyt}}$  elevations in Col-0 seedlings (Figure 2e). More importantly, these LPS preparations, including LPS-1<sub>com</sub>, also induced normal  $[Ca^{2+}]_{\text{cyt}}$  responses in *efr-1* and *efr-2* mutant seedlings (Figure 3).

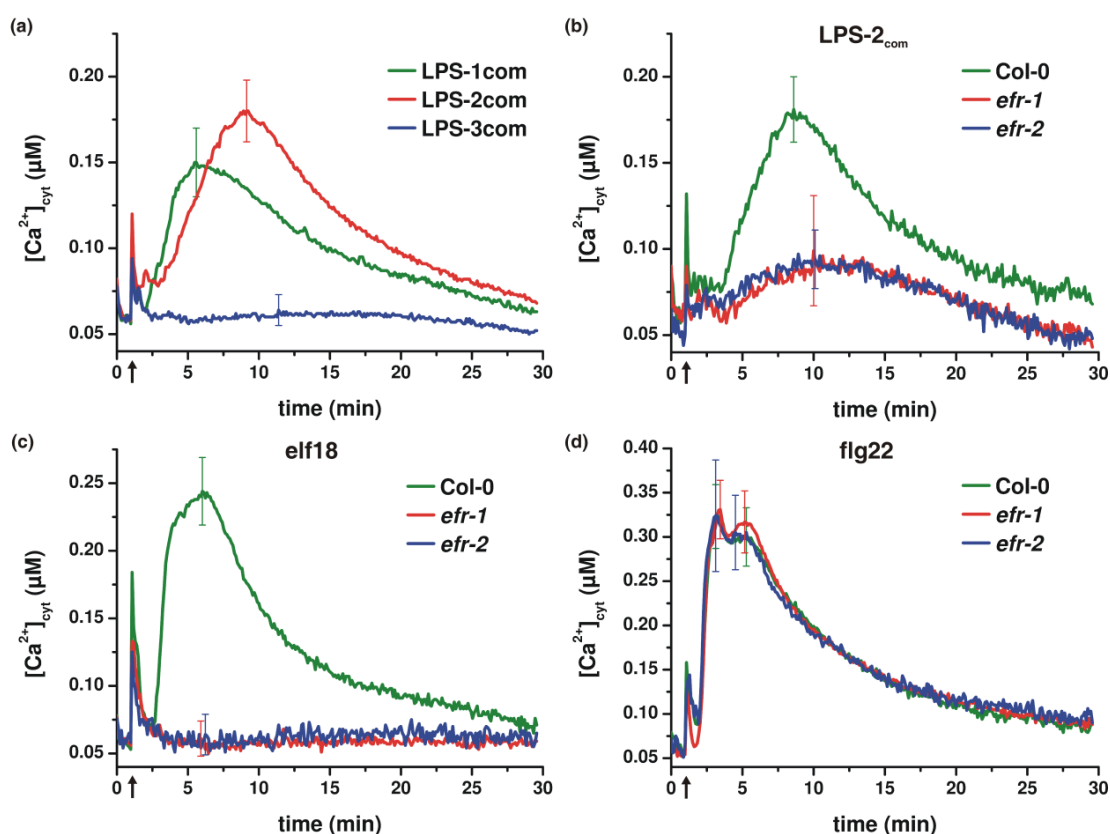


**Figure 1. Commercial LPS preparations induce distinct  $[Ca^{2+}]_{\text{cyt}}$  elevations in Col-0 and a reduced  $[Ca^{2+}]_{\text{cyt}}$  elevation in *efr* reveals a potential contamination.**

(a)  $[Ca^{2+}]_{\text{cyt}}$  elevations in Col-0 seedlings induced by three different batches of a commercial *P. aeruginosa* LPS preparation (50  $\mu\text{g/ml}$ ). Arrows mark time of LPS application. Data represent mean  $\pm$  SD of  $\geq 3$  independent experiments ( $n \geq 10$ ).

(b-d)  $[Ca^{2+}]_{\text{cyt}}$  elevations in *efr* seedlings induced by (b) 50  $\mu\text{g/ml}$  LPS-2<sub>com</sub>, (c) 1  $\mu\text{M}$  elf18 or (d) 1  $\mu\text{M}$  flg22 compared to Col-0. Arrows mark time of MAMP application. Data represent mean  $\pm$  SD of  $\geq 2$  independent experiments ( $n \geq 6$ ).

Most of the reported LPS-induced responses in *Arabidopsis*, as well as other plant species required high LPS concentrations in the range of 50-100  $\mu\text{g/ml}$ . The requirement of such high LPS levels generally questions the specificity of the analysed responses for LPS. To further examine the concentration range of LPS sufficient for the induction of  $[\text{Ca}^{2+}]_{\text{cyt}}$  elevations, dilution series of the different purified LPS preparations were examined. Strikingly, 10-fold lower LPS concentrations of 5-10  $\mu\text{g/ml}$  still induced nearly maximum  $[\text{Ca}^{2+}]_{\text{cyt}}$  amplitudes, although with a slight delay compared to higher concentrations (Figure 4a-c). A further > 10-fold dilution (0.5-0.2  $\mu\text{g/ml}$ ) still stimulated significant and reproducible

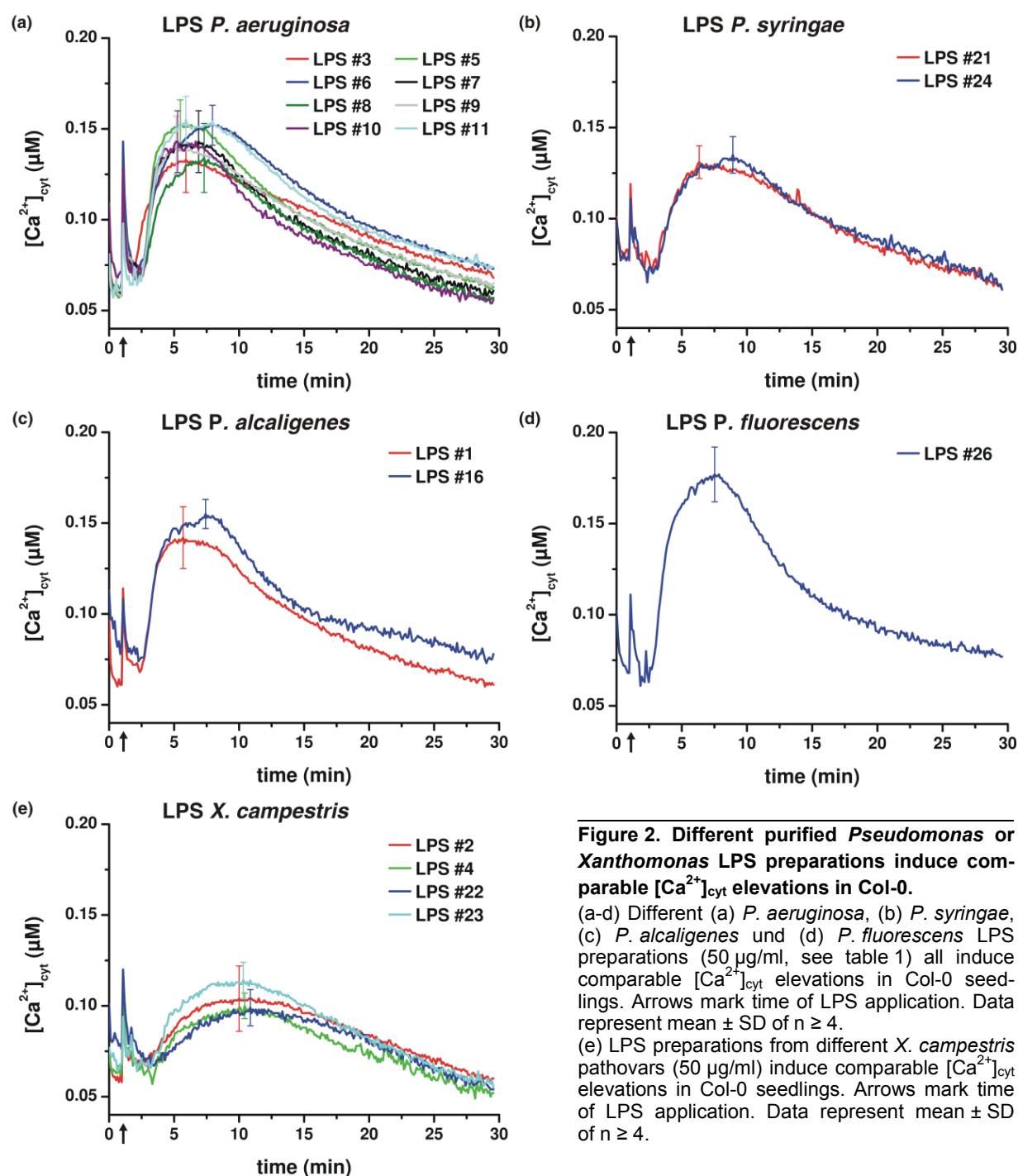
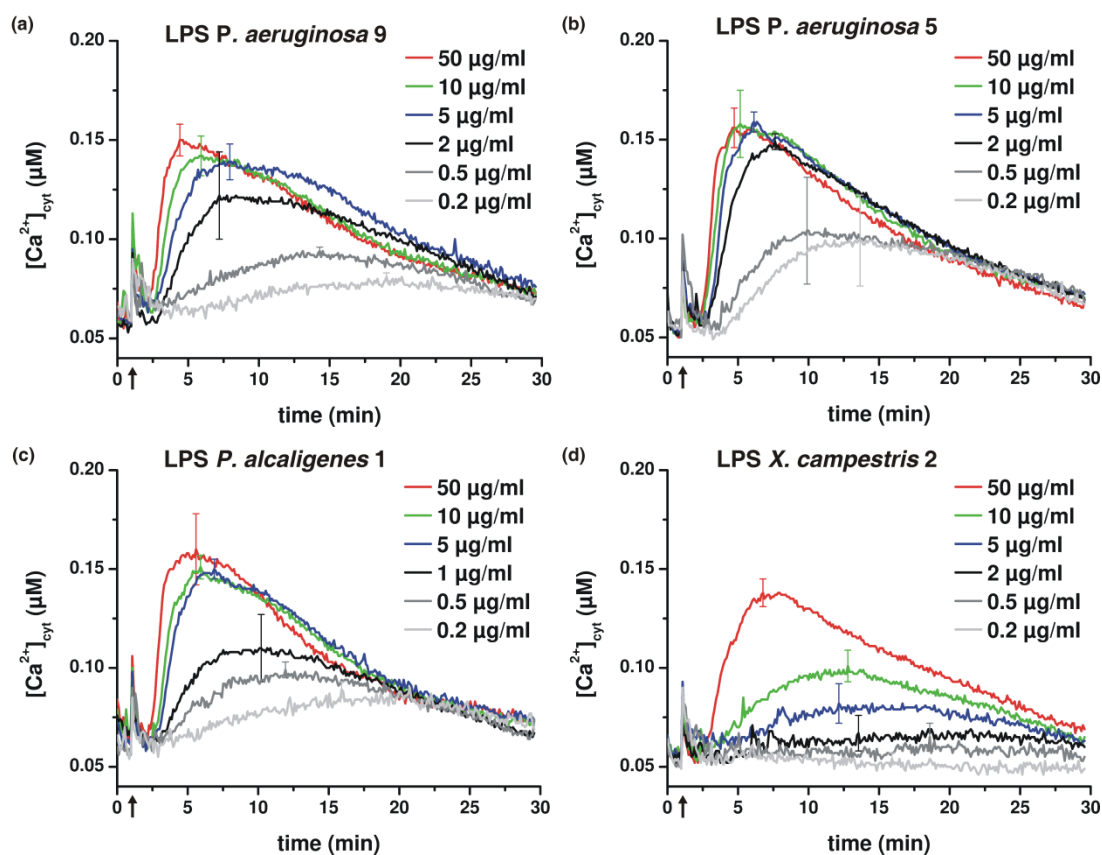
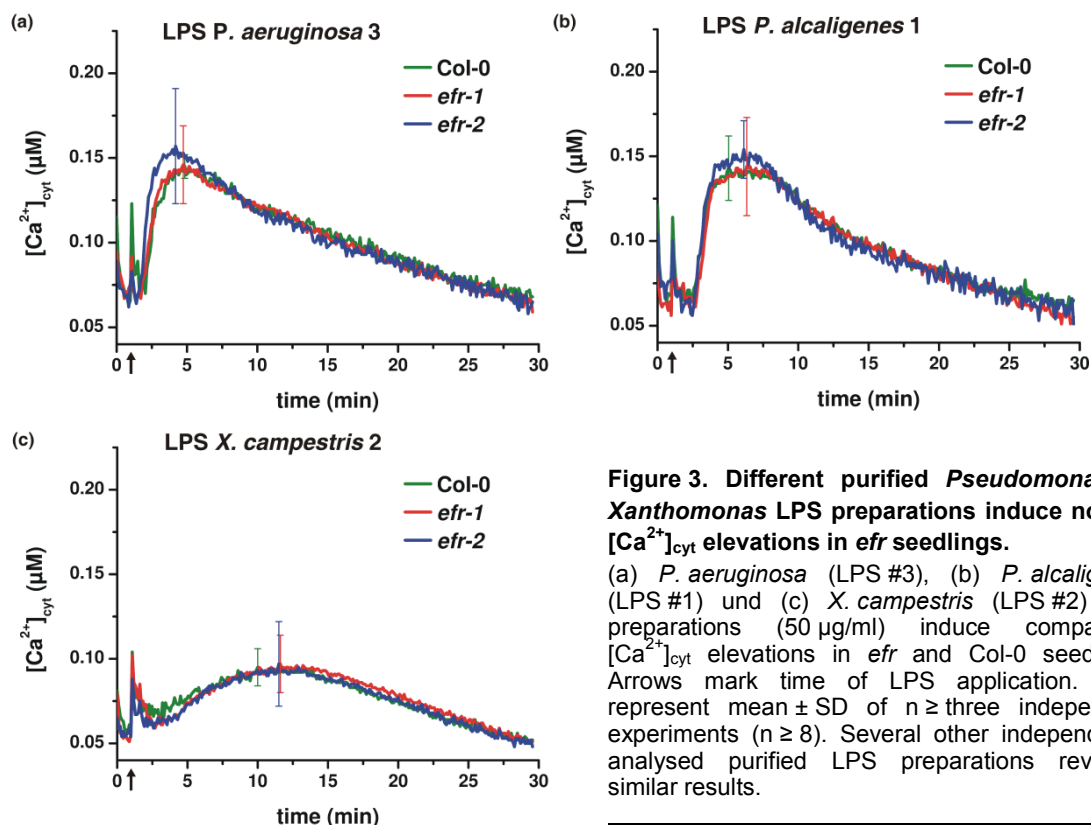


**Figure 2. Different purified *Pseudomonas* or *Xanthomonas* LPS preparations induce comparable  $[\text{Ca}^{2+}]_{\text{cyt}}$  elevations in Col-0.**

(a-d) Different (a) *P. aeruginosa*, (b) *P. syringae*, (c) *P. alcaligenes* and (d) *P. fluorescens* LPS preparations (50  $\mu\text{g/ml}$ , see table 1) all induce comparable  $[\text{Ca}^{2+}]_{\text{cyt}}$  elevations in Col-0 seedlings. Arrows mark time of LPS application. Data represent mean  $\pm$  SD of  $n \geq 4$ .

(e) LPS preparations from different *X. campestris* pathovars (50  $\mu\text{g/ml}$ ) induce comparable  $[\text{Ca}^{2+}]_{\text{cyt}}$  elevations in Col-0 seedlings. Arrows mark time of LPS application. Data represent mean  $\pm$  SD of  $n \geq 4$ .



$[Ca^{2+}]_{\text{cyt}}$  elevations albeit with decreased amplitudes and slower kinetics. *X. campestris* LPS preparations generally stimulated lower  $[Ca^{2+}]_{\text{cyt}}$  elevations compared to *Pseudomonas* LPS preparations (Figure 4d). Accordingly, LPS concentrations of 5-10  $\mu\text{g/ml}$  still induced lower but significant  $[Ca^{2+}]_{\text{cyt}}$  elevations, whereas concentrations  $< 2 \mu\text{g/ml}$  were ineffective. Thus, analysis of  $[Ca^{2+}]_{\text{cyt}}$  elevations induced by different LPS preparations reveals a sensitive perception system for *Pseudomonas*- and *Xanthomonas*-derived LPS in Arabidopsis Col-0 seedlings.

In addition, *P. aeruginosa* (LPS #3) and *P. alcaligenes* (LPS #1) LPS induced an accumulation of reactive oxygen species in Arabidopsis Col-0 leaf discs comparable to N-acetylchitooctaoase (ch8) (Figure 5). Taken together, these data demonstrate that *Pseudomonas* and *Xanthomonas* LPS indeed have MAMP/elicitor activity in Arabidopsis.

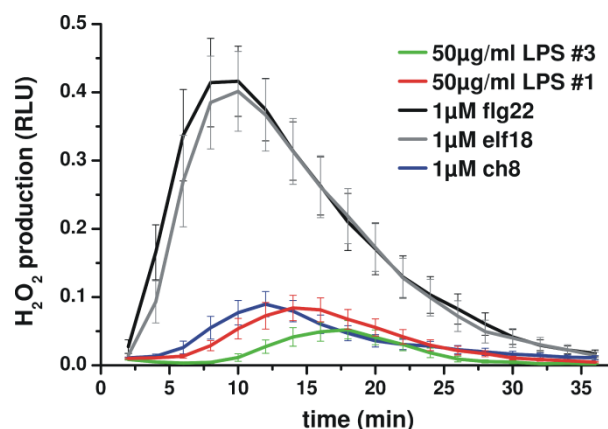


**Figure 5. Purified *Pseudomonas* LPS preparations induce ROS accumulation in Col-0 leaf discs comparable to ch8.**

ROS ( $H_2O_2$ ) production induced by the indicated MAMPs was monitored in Col-0 leaf discs using a luminol-based assay. Data are given as relative light units (RLU) and represent mean  $\pm$  SE ( $n \geq 16$ ). Two independent experiments revealed similar results.

### LPS-induced $Ca^{2+}$ elevations are inhibited by $La^{3+}$ and protein kinase inhibitor.

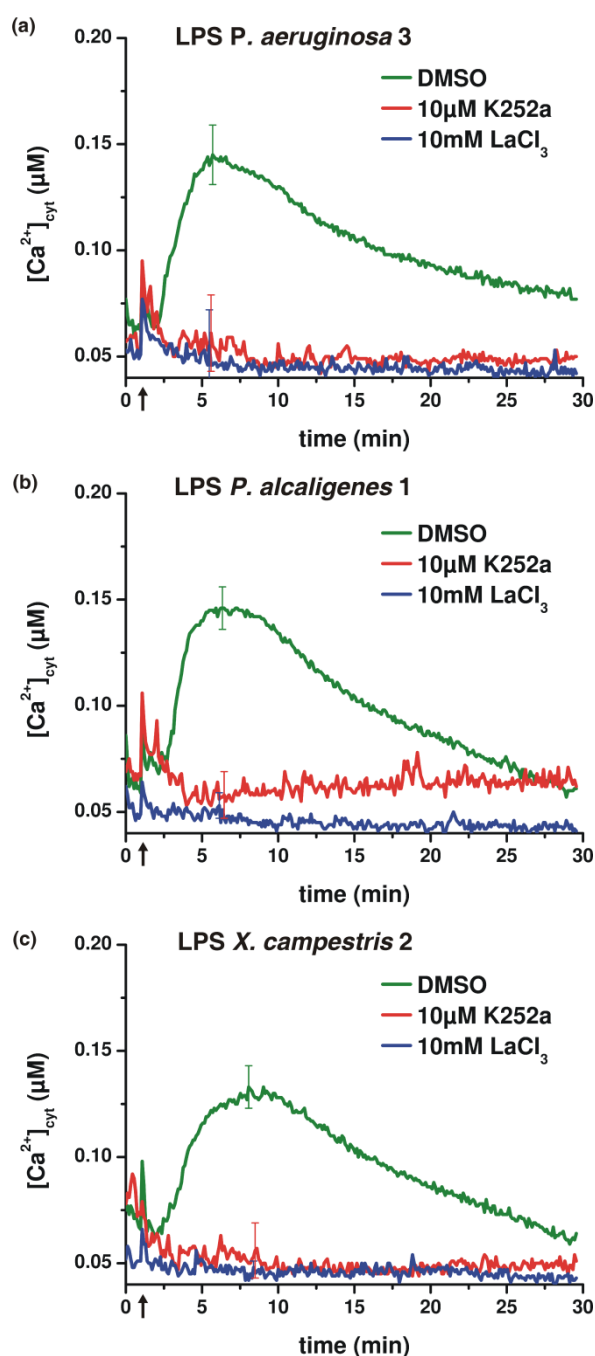
Pre-treatment of Col-0 seedlings with 10 mM  $LaCl_3$ , a  $Ca^{2+}$  channel inhibitor, completely abolished the  $[Ca^{2+}]_{\text{cyt}}$  elevations induced by different *Pseudomonas* and *X. campestris* LPS preparations (Figure 6). Thus, the LPS-induced  $[Ca^{2+}]_{\text{cyt}}$  elevations appear to be mediated by specific  $La^{3+}$ -sensitive  $Ca^{2+}$ -permeable channels. A possible  $Ca^{2+}$ -permeable plasma membrane channel is CNGC2/DND1, which is reported to be responsible for LPS-induced  $[Ca^{2+}]_{\text{cyt}}$  elevations (Ali *et al.*, 2007; Ma *et al.*, 2009). However,  $[Ca^{2+}]_{\text{cyt}}$  elevations induced by several different *Pseudomonas* and *X. campestris* LPS preparations, as well as the established MAMPs, flg22 and elf18, were not reduced in *dnd1* null mutant seedlings (Figure 7).

Additionally, pre-treatment of seedlings with the general protein kinase inhibitor K252a abrogated  $[Ca^{2+}]_{\text{cyt}}$  elevations in response to different *Pseudomonas* and *X. campestris* LPS preparations (Figure 6). This points to phosphorylation events upstream of the  $[Ca^{2+}]_{\text{cyt}}$  elevations. In analogy to the FLS2 or CERK1 receptors being protein kinases, such phosphorylation events could imply protein kinase activities of the LPS receptor or receptor-associated kinases.

### LPS-induced $Ca^{2+}$ elevations are independent of BAK1.

As suggested by Shan *et al.* (2008), signalling induced by many different MAMPs involves BAK1 as a “co-receptor”. This includes not only flg22, elf18 and HrpZ but also *P. aeruginosa* LPS, as well as

*S. aureus* PGN. All these MAMPs induced lower expression of the MAMP-responsive gene, *FRK1*, in protoplasts derived from *bak1* compared to Col-0, whereas, chitin stimulated normal *FRK1* expression in the *bak1* background. Accordingly, *bak1-3* and *bak1-4* seedlings show a delayed and reduced  $[Ca^{2+}]_{cyt}$  response to flg22 and elf18, but not to ch8 (Figure 8f; Ranf *et al.*, submitted, figure 3, p. 41). Likewise,  $[Ca^{2+}]_{cyt}$  elevations induced by the presumably contaminated LPS-2<sub>com</sub> were delayed and reduced in *bak1* seedlings (Figure 8d). By contrast, the different purified *Pseudomonas* and *X. campestris* LPS preparations, as well as LPS-1<sub>com</sub> stimulated  $[Ca^{2+}]_{cyt}$  peaks in *bak1* seedlings comparable to the wild type response (Figure 8a-c,e). Thus, the same LPS preparation, LPS-2<sub>com</sub>, that exhibited a reduced  $[Ca^{2+}]_{cyt}$  elevation in *efr* mutants (Figure 1b), also elicited an attenuated response in



*bak1* mutants (Figure 8d), whereas all purified preparations stimulated wildtype-like  $[Ca^{2+}]_{cyt}$  peaks in both mutant backgrounds (Figure 3/8). In conclusion, the reduced  $[Ca^{2+}]_{cyt}$  elevation in *efr* and *bak1* seedlings induced by LPS-2<sub>com</sub> can be attributed to a contamination with EF-Tu protein, which requires BAK1 for full signalling. In addition, reduced  $[Ca^{2+}]_{cyt}$  peaks were observed in *efr* and *bak1* mutants upon application of commercial *S. aureus* PGN preparations, thereby pointing to similar (EF-Tu) contaminations (data not shown). Taken together, the data provided here demonstrate that purified *Pseudomonas* and *X. campestris* LPS preparations act as MAMPs in Arabidopsis in terms of their ability to induce  $[Ca^{2+}]_{cyt}$  elevations and that LPS-induced  $Ca^{2+}$  signalling is independent of BAK1.

**Figure 6. Pre-treatment with  $LaCl_3$  or the protein kinase inhibitor K252a abolishes  $[Ca^{2+}]_{cyt}$  elevations induced by *Pseudomonas* or *Xanthomonas* LPS preparations.**

Pre-treatment of Col-0 seedlings with 10 mM  $LaCl_3$  or 10  $\mu$ M K252a for 30 min inhibits  $[Ca^{2+}]_{cyt}$  elevations induced by LPS preparations (50  $\mu$ g/ml) from (a) *P. aeruginosa* (LPS #3), (b) *P. alcaligenes* (LPS #1) and (c) *X. campestris* (LPS #2). Arrows mark time of MAMP application. Data represent mean  $\pm$  SD of  $n \geq 4$ .

## DISCUSSION

The exposed position on the cell surface, the abundant presence in all Gram-negative bacteria and the complete absence in the host, as well as the generally conserved structure of the lipid A-core component, warrant the classification of LPS as a MAMP. In mammalian systems, indeed, LPS belongs to the most potent MAMPs - being active in apparently trace amounts (< 1ng/ml; Miyake, 2004). In plants, knowledge of LPS signalling is more fragmentary, with some growing evidence in the last years that LPS can act as a MAMP in different plant species. Such activated responses include an  $[Ca^{2+}]_{cyt}$  increase and ROS accumulation in tobacco (Meyer *et al.*, 2001; Braun *et al.*, 2005), as well as NO production and defence gene expression in Arabidopsis (Zeidler *et al.*, 2004; Silipo *et al.*, 2005; Livaja *et al.*, 2008). Nevertheless, comparatively high LPS concentrations of 50-100  $\mu\text{g/ml}$  were necessary to

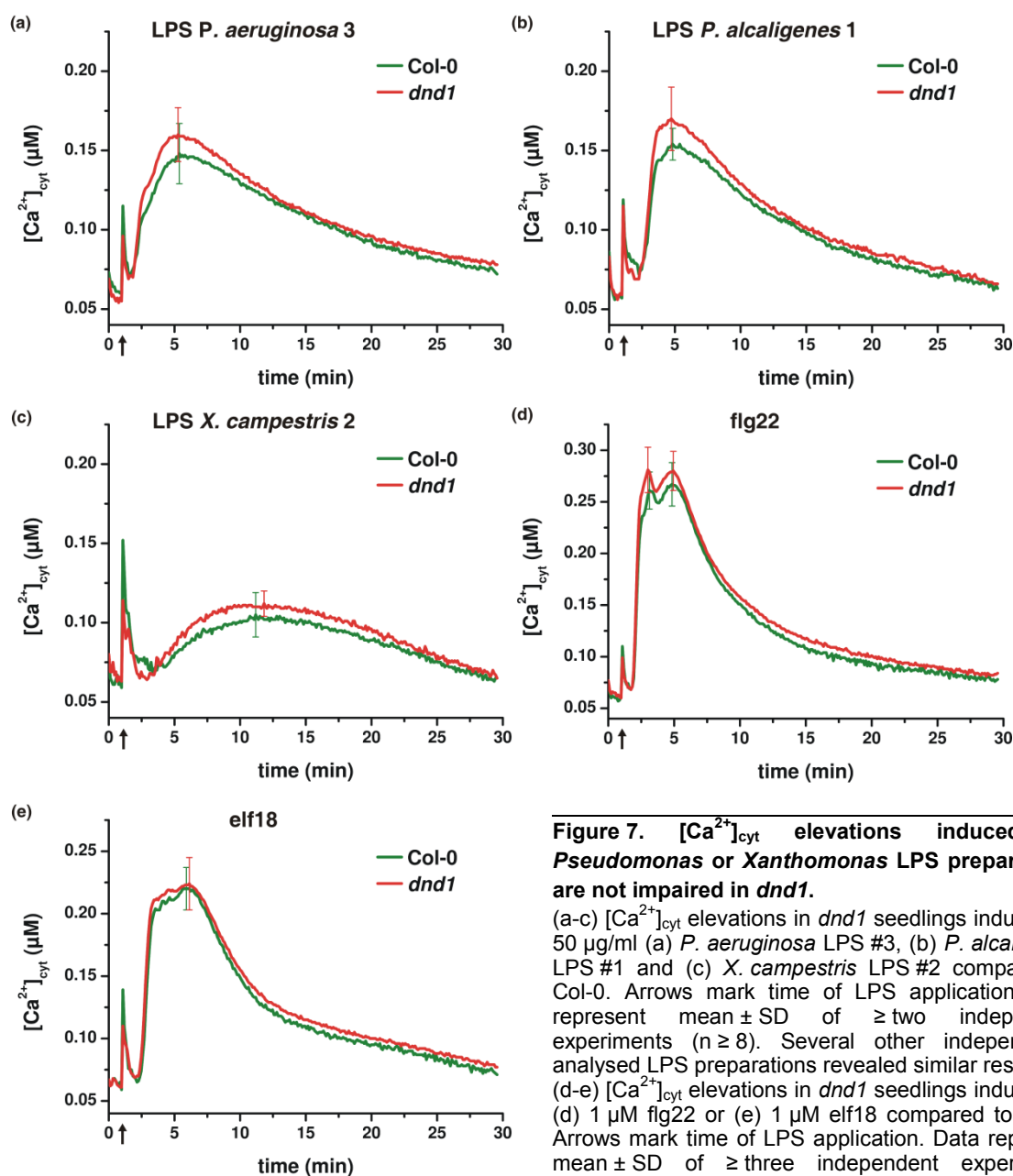


**Figure 7.  $[Ca^{2+}]_{cyt}$  elevations induced by *Pseudomonas* or *Xanthomonas* LPS preparations are not impaired in *dnd1*.**

(a-c)  $[Ca^{2+}]_{cyt}$  elevations in *dnd1* seedlings induced by 50  $\mu\text{g/ml}$  (a) *P. aeruginosa* LPS #3, (b) *P. alcaligenes* LPS #1 and (c) *X. campestris* LPS #2 compared to Col-0. Arrows mark time of LPS application. Data represent mean  $\pm$  SD of  $\geq$  two independent experiments ( $n \geq 8$ ). Several other independently analysed LPS preparations revealed similar results. (d-e)  $[Ca^{2+}]_{cyt}$  elevations in *dnd1* seedlings induced by (d) 1  $\mu\text{M}$  flg22 or (e) 1  $\mu\text{M}$  elf18 compared to Col-0. Arrows mark time of LPS application. Data represent mean  $\pm$  SD of  $\geq$  three independent experiments ( $n \geq 20$ ).

elicit plant defence responses (Molinaro, 2009). This is in strong contrast to the situation in mammalian systems and to other MAMPs in plants, most of which are active in the nano- to picomolar range. Therefore, it was suggested that plants may possess only a low affinity perception system for LPS (Zeidler *et al.*, 2004; Silipo *et al.*, 2010). Alternatively, aggregation of the amphiphilic LPS might hinder its access through the cell wall matrix and binding to its receptor(s) (Braun *et al.*, 2005; Zähringer *et al.*, 2008). On the contrary, LPS preparations used in this study were capable of inducing significant  $[Ca^{2+}]_{cyt}$  elevations in Arabidopsis seedlings at 100-fold lower concentrations of  $\sim 0.5 \mu\text{g/ml}$  (Figure 4). Hence, this points to a sensitive perception system for LPS in Arabidopsis. The low affinity NO-inducing (Zeidler *et al.*, 2004) and the sensitive  $[Ca^{2+}]_{cyt}$  elevation-inducing perception, however, might originate from recognition of distinct LPS moieties, as observed for *Xanthomonas* lipid A and core oligosaccharide (Silipo *et al.*, 2005). Furthermore, the LPS-induced  $[Ca^{2+}]_{cyt}$  elevations resembled the typical kinetics observed for other MAMPs, which include a lag phase of  $< 1$  minute, a rapid increase to a short plateau of MAMP-specific  $[Ca^{2+}]_{cyt}$  amplitude, and a slow decline lasting over  $\sim 30$  minutes (*c. f.* Figure 1c,d /Figure 2a-d; Ranf *et al.*, submitted, figure 1, p. 39).

The complex structure of LPS differs substantially between bacterial strains, but even a single bacterium comprises a mixture of structural LPS variants. *Pseudomonas*, for example, contains in parallel R-LPS and S-LPS, which carry either linear oligo-rhamnans or complex OPS (Kannenberg and Carlson, 2001; Zipfel and Felix, 2005; Knirel *et al.*, 2006). The complex LPS composition is apparently also subject to dynamic regulation; for instance with bacteria adapting to environmental conditions through modulation of lipid A acylation or changes in the ratio of R- and S-type glycoforms (Kannenberg and Carlson, 2001; Knirel *et al.*, 2006; Silipo *et al.*, 2008). In this respect, *P. aeruginosa* isolates of cystic fibrosis patients contain modified LPS and PGN to evade detection by the innate immune system (Knirel *et al.*, 2001; Knirel *et al.*, 2006; Cigana *et al.*, 2009). Similarly, phytobacteria can alter their LPS structures during symbiotic interactions (Kannenberg and Carlson, 2001). Thus, plant pathogens have been speculated to alter the LPS composition after plant host invasion to avoid recognition (Silipo *et al.*, 2008). Besides the LPS structural variants showing different biological activities as MAMPs in plants, the purification conditions can have further impact on the LPS activity through the loss or modification of critical moieties (Knirel *et al.*, 2006). The phosphoramidate group in the *Xanthomonas* core oligosaccharide, for example, is sensitive to hydrolysis and loss of negative phosphate or galacturonic acid residues impedes LOS activity, as interaction with putative receptors is supposed to depend on electrostatic interactions (Silipo *et al.*, 2005). Thus, structural differences due to culture or purification conditions might explain the inactivity of LPS-3<sub>com</sub> and the very low residual activity of LPS-2<sub>com</sub> (Figure 1a).

Eventually, it cannot be excluded that the observed activities are not caused by LPS itself but might potentially be due to the presence of minor, highly-active contaminants in the LPS preparations (Zipfel and Felix, 2005). In this regard, several reports from the animal field have raised the suspicion of misinterpretation of results due to contamination of PAMP preparations. Highly active

lipoprotein/lipopeptide contaminants in PGN preparations are suggested as the *bona fide* TLR2 (toll-like receptor 2) ligands rather than PGN (Travassos *et al.*, 2004; Zähringer *et al.*, 2008). Indeed, re-purification of such PGN preparations completely abolished TLR2 activation (Travassos *et al.*, 2004). Likewise, Hirschfeld *et al.* (2000) demonstrated that LPS signalling *via* TLR2 was due to highly active contaminants in commercially available LPS preparations, while purified LPS only activates TLR4. *Drosophila* can distinguish between Gram-negative and -positive bacteria on the basis of specific

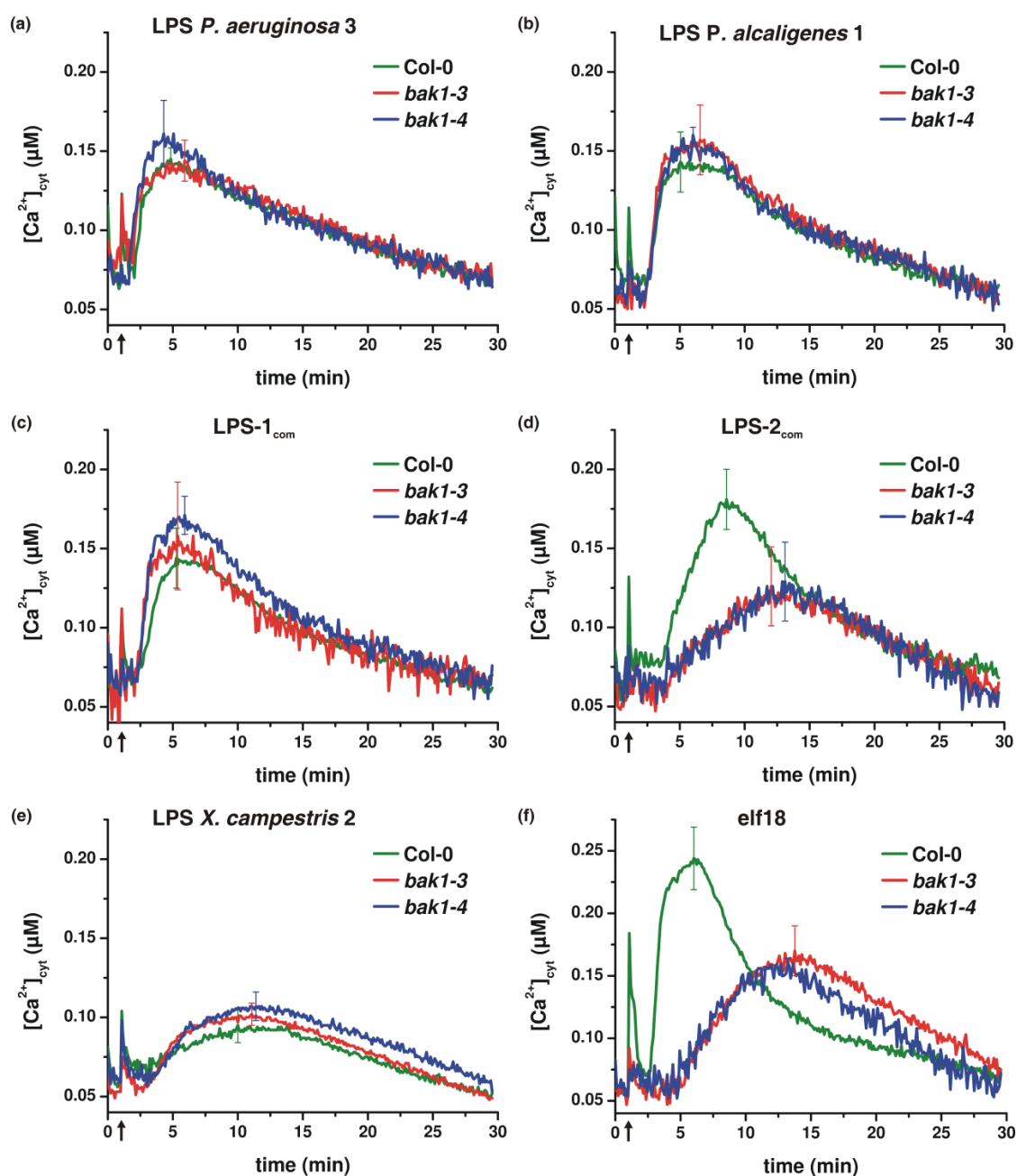


**Figure 8. Different purified *Pseudomonas* LPS preparations induce normal  $[Ca^{2+}]_{cyt}$  elevations in *bak1* seedlings in contrast to a commercial preparation.**

$[Ca^{2+}]_{cyt}$  elevations induced by 50  $\mu\text{g/ml}$  (a) *P. aeruginosa* LPS #3, (b) *P. alcaligenes* LPS #1, (c) *P. aeruginosa* LPS-1<sub>com</sub>, (d) *P. aeruginosa* LPS-2<sub>com</sub>, (e) *X. campestris* LPS #2 or (f) 1  $\mu\text{M}$  elf18 in *bak1* compared to Col-0 seedlings. Arrows mark time of MAMP application. Data represent mean  $\pm$  SD of  $\geq$  two independent experiments ( $n \geq 3$ ). Several other independently analysed purified LPS preparations revealed similar results as in (a-c) and (e).

PGN forms and not, as earlier reported, by recognition of LPS (Leulier *et al.*, 2003). It is also noteworthy, that several plant PAMPs were found serendipitously when bacterial culture preparations were analysed for other PAMP activities. Flagellin, for instance, was the actual active component in an harpin preparation from *Pseudomonas syringae* pv. *tabaci* (Felix *et al.*, 1999), EF-Tu in boiled extracts from an *E. coli* mutant lacking flagellin (Boller and Felix, 2009) and bacterial cold-shock protein (CSP) in an *S. aureus* PGN preparation (Felix and Boller, 2003). Along this line, it should be noted, that the core oligosaccharide of *Pseudomonas* LPS is extensively phosphorylated (Knirel *et al.*, 2006). Such highly negative phosphate charges can build strong interactions with undesirable contaminants. However, applying harsh purification conditions might diminish the PAMP activity of the purified product due to chemical modifications. This study based on different – both purified and commercial – *Pseudomonas* LPS preparations pointed to significant contaminations in commercially available PAMP preparations. Analysis based on the *efr* mutants revealed that bacterial EF-Tu protein was probably the predominant component in LPS-2<sub>com</sub> (Figure 1b), as well as in commercially available PGN preparations (data not shown). Such EF-Tu contaminations in commercial LPS and PGN preparations could also explain the BAK1-dependent *FRK1*-expression observed by Shan and co-workers (2008). In support of this, the purified *Pseudomonas* LPS preparations did not significantly induce *FRK1* or *NHL10* expression in Col-0-derived protoplast, while both genes were strongly up-regulated by flg22 or elf18 elicitation (data not shown). Likewise, published gene expression data reveal only weak and delayed LPS-induced gene expression in comparison to other MAMPs (Zeidler *et al.*, 2004; Livaja *et al.*, 2008). For instance, a set of typically MAMP-responsive WRKY transcription factors was unaffected by LPS (Livaja *et al.*, 2008), suggesting substantial differences in “late” gene expression responses between LPS and other MAMPs. However, using purified LPS preparations and examining a very early LPS response, namely  $[Ca^{2+}]_{cyt}$  elevation, no evidence was found for a BAK1 involvement in initial receptor complex activation as seen with other well-established MAMPs like flg22 and elf18 (Figure 8).

In contrast to earlier reports in adult *dnd1* leaves (Ali *et al.*, 2007; Ma *et al.*, 2009),  $[Ca^{2+}]_{cyt}$  elevations induced by purified LPS preparations were not reduced in *dnd1* seedlings (Figure 7a-c). This discrepancy in the results may be due to the growth conditions employed; for instance, the young *dnd1* seedlings grown in sterile liquid culture used here, neither showed a dwarf phenotype nor any other visible phenotypes typical for *dnd1* grown on soil. Constitutive defence activation observed for the *dnd1* dwarfed plants might lead to pleiotropic secondary effects on MAMP responses. Additionally, neither flg22- or elf18-stimulated  $[Ca^{2+}]_{cyt}$  elevations nor flg22-mediated root growth arrest were reduced in *dnd1* (Figure 7d-e; data not shown). In agreement, flg22-induced membrane depolarization in mesophyll cells was also not impaired in *dnd1* (Jeworutzki *et al.*, 2010). In conclusion, CNGC2/DND1 does not appear to mediate MAMP-induced  $Ca^{2+}$  influx in general.

In conclusion, LPS, even in low concentrations, is active as a MAMP in Arabidopsis with respect to the capacity to induce  $[Ca^{2+}]_{cyt}$  elevations and this is independent of BAK1 and CNGC2/DND1.

However, only the elucidation of the exact structural components causing the different activities within the LPS and their respective receptors will clarify the role of LPS in plant-microbe interactions. Most of the characterized PAMPs, in either mammalian or plant systems, are active at very low concentrations. Therefore, special care has to be taken to ensure that elicitor preparations of microbial origins are free of potent contaminants, such that the observed activity is indeed caused by the enriched/purified component. Unfortunately, commercial PAMP preparations do not always fulfil such criteria and hence should be used with caution.

## EXPERIMENTAL PROCEDURES

### *Plant material and growth conditions*

The *Arabidopsis thaliana* line pMAQ2 in Col-0 background was obtained from M. Knight (Knight *et al.*, 1991, 1996). T-DNA insertion lines *bak1-3* (At4g33430, SALK\_034523) and *bak1-4* (At4g33430, SALK\_116202; Chinchilla *et al.*, 2007) were obtained from B. Kemmerling and *efr-1* (At5g20480, SALK\_044334) and *efr-2* (At5g20480, SALK\_068675; Zipfel *et al.*, 2006) from C. Zipfel. Aequorin-transgenic lines were described in Ranf *et al.* (submitted, see 2.2). Seeds were surface-sterilized, if required and stratified at 4°C for  $\geq 2$  days. Plants were grown on soil in climate chambers under short day or in liquid MS medium (0.5 x MS, 0.25 % sucrose, 1 mM MES, pH 5.7) in 24-well plates (10 seedlings / well) under long day conditions at 20-22°C.

### *Elicitors*

Flg22 and elf18 (Felix *et al.*, 1999; Kunze *et al.*, 2004) were synthesized on an Abimed EPS221 (www.abimed.de) system. N-acetylchitooctose (ch8) was provided by N. Shibuya (Albert *et al.*, 2006). LPS preparations (see table 1) were provided by U. Zähringer LG/Immunchemie (Research Center Borstel) and Y. A. Knirel (N.D. Zelinsky Institute of Organic Chemistry in Moscow, Russia)

**Table 1**

LPS #	Bacterial strain	provided by
1	<i>P. alcaligenes</i> strain 537	LG Immunchemie
2	<i>X. campestris</i> pv. <i>malvacearum</i> GSPB 1386	Y.A. Knirel
3	<i>P. aeruginosa</i> H4	LG Immunchemie
4	<i>X. campestris</i> pv. <i>malvacearum</i> HVS GSPB 2388	Y.A. Knirel
5	<i>P. aeruginosa</i> mutant H4	LG Immunchemie
6	<i>P. aeruginosa</i> R5	LG Immunchemie
7	<i>P. aeruginosa</i> PAC 1R- $\Delta$ algC mutant	LG Immunchemie
8	<i>P. aeruginosa</i> mutant PAN1	LG Immunchemie
9	<i>P. aeruginosa</i> PA01wt	LG Immunchemie
10	<i>P. aeruginosa</i> PA01- $\Delta$ algC mutant	LG Immunchemie
11	<i>P. aeruginosa</i> F1 (Habs 6)	LG Immunchemie
16	<i>P. alcaligenes</i> strain 537	LG Immunchemie
21	<i>P. syringae</i> pv. <i>Porri</i> NCPPB 3365	Y.A. Knirel
22	<i>X. campestris</i> pv. <i>phaseoli</i> var. <i>Fuscan</i> GSPB 271	Y.A. Knirel
23	<i>X. campestris</i> pv. <i>begoniae</i> GSPB 525	Y.A. Knirel
24	<i>P. syringae</i> pv. <i>atrofaciens</i> IMV 2399	Y.A. Knirel
26	<i>P. fluorescens</i> strain ATCC 49271	LG Immunchemie
1 com	<i>P. aeruginosa</i> 10 (LOT 100K4063)	Sigma Aldrich (L8643)
2 com	<i>P. aeruginosa</i> 10 (LOT 019K4065)	Sigma Aldrich (L8643)
3 com	<i>P. aeruginosa</i> 10 (LOT 010M4055)	Sigma Aldrich (L8643)

### ***Aequorin luminescence measurements***

For aequorin luminescence measurements, Col-0 plants expressing p35S-apoaequorin (pMAQ2) in the cytosol (Knight *et al.*, 1991, 1996) were used. 8-days-old liquid-grown seedlings were placed individually in 96-well plates in 10  $\mu$ M coelenterazine / H<sub>2</sub>O (native coelenterazine, P.J.K., www.pjk-gmbh.com) in the dark over night. Luminescence was recorded by scanning each row in 6 sec intervals using a Luminoskan Ascent 2.1 luminometer (Thermo Scientific, www.thermo.com) as described (Ranf *et al.*, submitted, protocol 2B, p. 157). Remaining aequorin was discharged and Ca<sup>2+</sup> concentrations were calculated according to Rentel and Knight (2004).

### ***ROS detection in Arabidopsis leaves***

ROS production was assayed as described (Gomez-Gomez *et al.*, 1999) using 3 mm leaf discs in 96-well plates measured in 2 min intervals (Luminoskan Ascent 2.1).

### **ACKNOWLEDGEMENTS**

We are grateful to B. Kemmerling, M. Knight, Y. A. Knirel and C. Zipfel for providing material. We thank C. Rülke and N. Bauer for technical assistance. This work is supported by a DFG grant (LE2321/1-2) within the priority project SPP1212. L. E.-L. is financed by the BMBF project ProNet-T3 (03ISO2211B).

### **REFERENCES**

Due to high redundancy of references between the different chapters, the references are combined in the common REFERENCE section (chapter 4, p. 126).

## 2.5. Peptidoglycans as MAMPs induce $\text{Ca}^{2+}$ signalling in *Arabidopsis thaliana*

### 2.5.1. $[\text{Ca}^{2+}]_{\text{cyt}}$ elevations stimulated by peptidoglycans in *Arabidopsis*

The results obtained with commercial peptidoglycan (PGN) preparations from the Gram-positive bacterium *Staphylococcus aureus* also point to contaminants causal for the observed  $[\text{Ca}^{2+}]_{\text{cyt}}$  elevations. Thus, the  $[\text{Ca}^{2+}]_{\text{cyt}}$  elevation-inducing activity of PGN in *Arabidopsis* was tested with purified *S. aureus* PGN preparations provided by Andrea Gust (Tübingen). Since the macromolecular PGN preparations are not water soluble, PGN was dispersed in water by sonication. To facilitate access of the PGN suspension into the leaf interior, thin-cut leaf strips instead of seedlings or leaf discs were used for measuring  $[\text{Ca}^{2+}]_{\text{cyt}}$  elevations. The purified PGN preparations reproducibly induced a prolonged  $[\text{Ca}^{2+}]_{\text{cyt}}$  elevation after a lag phase of two to three minutes in leaf strips at a concentration of 100  $\mu\text{g}/\text{ml}$ . Application of 500  $\mu\text{g}/\text{ml}$  PGN increased the  $[\text{Ca}^{2+}]_{\text{cyt}}$  amplitude, but it was still significantly lower than the flg22-induced  $[\text{Ca}^{2+}]_{\text{cyt}}$  peak, and probably not yet in the saturating range. However, higher PGN concentrations were not applied due to the low solubility, since the insoluble particles induce a significant touch response. For the same reason, mixing of the PGN suspension with the leaf strips was not feasible. Thus, only a small portion of the PGN may have reached the leaf interior and the kinetics and amplitudes of PGN-induced  $[\text{Ca}^{2+}]_{\text{cyt}}$  elevations can not be directly compared to those induced by small soluble peptide elicitors like flg22 using leaf strips. Nevertheless, PGN-induced  $[\text{Ca}^{2+}]_{\text{cyt}}$  elevations generally resemble the typical prolonged MAMP-induced  $[\text{Ca}^{2+}]_{\text{cyt}}$  response observed for other MAMPs.

### 2.5.2. Summary of publication

The PGN  $[\text{Ca}^{2+}]_{\text{cyt}}$  measurements were published in collaboration with Andrea Gust under my co-authorship. Due to space limitations, here only the data obtained as part of this work are shown in detail but the complete publication is available in the appendix 5.3 (p. 158). In summary, the authors provide evidence that PGN indeed acts as a PAMP in *Arabidopsis*, which, in addition to  $[\text{Ca}^{2+}]_{\text{cyt}}$  elevations, induces medium alkalization in suspension-cultured cells, activates MAPK cascades and production of the phytoalexin camalexin. PGN treatment further results in expression of pathogenesis-related protein 1 (PR1) as illustrated by GUS staining in PR1-transgenic plants and activates a set of typical defence genes as assessed by microarray analysis. While muramyl dipeptides activate immune responses in animals, they are inactive in *Arabidopsis*. Instead, PGN is apparently sensed *via* its

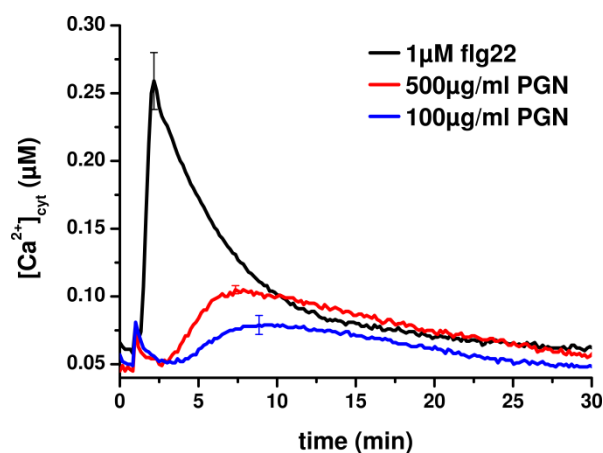


**Figure 2-5.  $[\text{Ca}^{2+}]_{\text{cyt}}$  elevations induced by *S. aureus* peptidoglycan in *Arabidopsis* leaf strips.**

$[\text{Ca}^{2+}]_{\text{cyt}}$  elevations induced by the indicated concentrations of *S. aureus* PGN in *Arabidopsis* leaf strips or flg22 as control. MAMPs were applied after one minute. Data represent mean  $\pm$  SD of  $n \geq 3$  independent experiments ( $n \geq 3$ ).

polysaccharide backbone. Comparison of the PGN activity to the structurally related polysaccharide PAMP chitin, furthermore, revealed independent perception mechanisms for both PAMPs. Taken together, this suggests that PGN is specifically sensed by *Arabidopsis* with the PAMP-active epitope residing in the sugar backbone. This suggests convergent evolution of the perception systems in plants and animals.

## **2.6. A cell wall extract from the endophytic fungus *Piriformospora indica* stimulates $\text{Ca}^{2+}$ signalling in *Arabidopsis thaliana* roots**

### **2.6.1. Aims and summary**

$\text{Ca}^{2+}$  is not only a pivotal second messenger in plant-pathogen interactions, but also plays a key role in the Rhizobium-legume and arbuscular mycorrhizal symbiosis. The endophytic fungus *Piriformospora indica* can colonize roots of many plant species including *Arabidopsis*. *P. indica* colonization thereby leads to plant growth promotion and enhanced resistance towards various abiotic and biotic stresses. Remarkably, a cell wall extract (CWE) from the fungus also promoted growth of *Arabidopsis* seedlings, although to a lower extent. Mutants insensitive to the fungus also did not react to the CWE and both, fungus and CWE, stimulated the expression of a similar set of genes. Moreover, the CWE can be used to study a putative role of  $\text{Ca}^{2+}$  signalling in the beneficial *P. indica*-plant interaction. Indeed, the CWE stimulated a  $[\text{Ca}^{2+}]_{\text{cyt}}$  elevation in the roots of aequorin-transgenic *Arabidopsis* and tobacco plants, as well as in suspension-cultured tobacco BY-2 cells. The  $[\text{Ca}^{2+}]_{\text{cyt}}$  elevation was significantly more pronounced in roots than in shoots. Likewise,  $\text{Ca}^{2+}$ -dependent activation of MAPKs by the CWE was much stronger in roots than in leaves compared to flg22, which strongly activates MAPKs in leaves but only weakly in roots. Furthermore, loss of MPK6 impaired the *P. indica*-stimulated growth promotion. Inhibitor studies with  $\text{La}^{3+}$  and BAPTA point to an initial  $\text{Ca}^{2+}$  influx from the apoplastic space. A tobacco BY-2 cell line expressing nuclear-targeted aequorin additionally revealed nuclear CWE-stimulated  $[\text{Ca}^{2+}]$  elevations. A protein kinase inhibitor completely abrogated the  $[\text{Ca}^{2+}]_{\text{cyt}}$  elevation, indicating upstream phosphorylation events. Together with the refractory nature of the  $\text{Ca}^{2+}$  response to repeated CWE application, this suggests a receptor-mediated perception of the CWE. Apparently, the CWE did not stimulate ROS production or activation of defence gene expression. Taken together,  $\text{Ca}^{2+}$  signalling appears to contribute crucially to the beneficial interaction of *Arabidopsis* or tobacco with *P. indica*.

Supporting information is available in the appendix 5.4 (p. 170).

## 2.6.2. Publication

*The Plant Journal* (2009) **59**, 193–206

doi: 10.1111/j.1365-313X.2009.03867.x

# A cell wall extract from the endophytic fungus *Piriformospora indica* promotes growth of *Arabidopsis* seedlings and induces intracellular calcium elevation in roots

Jyothilakshmi Vadassery<sup>1</sup>, Stefanie Ranf<sup>2</sup>, Corinna Drzewiecki<sup>1</sup>, Axel Mithöfer<sup>3</sup>, Christian Mazars<sup>4</sup>, Dierk Scheel<sup>2</sup>, Justin Lee<sup>2</sup> and Ralf Oelmüller<sup>1,\*</sup>

<sup>1</sup>Friedrich-Schiller-Universität Jena, Institut für Allgemeine Botanik und Pflanzenphysiologie, Dornburger Street 159, D-07743 Jena, Germany,

<sup>2</sup>Leibniz-Institut für Pflanzenbiochemie, Abt. Stress- und Entwicklungsbiologie, Weinberg 3, D-06120 Halle/Saale, Germany,

<sup>3</sup>Max Planck Institute for Chemical Ecology, Department Bioorganic Chemistry, Hans-Knöll-Straße 8, D-07745 Jena, Germany, and

<sup>4</sup>Signaux et Messages Cellulaires chez les Végétaux, UMR CNRS/UPS 5546; BP 42617 Auzeville, 31326 Castanet-Tolosan, France

Received 26 November 2008; revised 5 February 2009; accepted 12 February 2009; published online 24 April 2009.

\*For correspondence (fax +49 3641 949232; e-mail b7oera@uni-jena.de).

## SUMMARY

Calcium (Ca<sup>2+</sup>), as a second messenger, is crucial for signal transduction processes during many biotic interactions. We demonstrate that cellular [Ca<sup>2+</sup>] elevations are early events in the interaction between the plant growth-promoting fungus *Piriformospora indica* and *Arabidopsis thaliana*. A cell wall extract (CWE) from the fungus promotes the growth of wild-type seedlings but not of seedlings from *P. indica*-insensitive mutants. The extract and the fungus also induce a similar set of genes in *Arabidopsis* roots, among them genes with Ca<sup>2+</sup> signalling-related functions. The CWE induces a transient cytosolic Ca<sup>2+</sup> ([Ca<sup>2+</sup>]<sub>cyt</sub>) elevation in the roots of *Arabidopsis* and tobacco (*Nicotiana tabacum*) plants, as well as in BY-2 suspension cultures expressing the Ca<sup>2+</sup> bioluminescent indicator aequorin. Nuclear Ca<sup>2+</sup> transients were also observed in tobacco BY-2 cells. The Ca<sup>2+</sup> response was more pronounced in roots than in shoots and involved Ca<sup>2+</sup> uptake from the extracellular space as revealed by inhibitor studies. Inhibition of the Ca<sup>2+</sup> response by staurosporine and the refractory nature of the Ca<sup>2+</sup> elevation suggest that a receptor may be involved. The CWE does not stimulate H<sub>2</sub>O<sub>2</sub> production and the activation of defence gene expression, although it led to phosphorylation of mitogen-activated protein kinases (MAPKs) in a Ca<sup>2+</sup>-dependent manner. The involvement of MAPK6 in the mutualistic interaction was shown for an *mpk6* line, which did not respond to *P. indica*. Thus, Ca<sup>2+</sup> is likely to be an early signalling component in the mutualistic interaction between *P. indica* and *Arabidopsis* or tobacco.

**Keywords:** *Arabidopsis*, *Piriformospora indica*, plant/microbe interaction, calcium, aequorin.

## INTRODUCTION

An important aspect in plant survival is the early detection of and rapid response to specific stimuli. Calcium (Ca<sup>2+</sup>) signalling, which can be activated within seconds (or minutes) in response to quite diverse sets of stimuli (Carafoli, 2002; Harper and Harmon, 2005), is an important part of the early signalling system. Changes in cytosolic free Ca<sup>2+</sup> ([Ca<sup>2+</sup>]<sub>cyt</sub>) occur in response to many biotic and abiotic signals (Sanders *et al.*, 2002), such as light (Lewis *et al.*, 1997; Baum *et al.*, 1999; Sai and Johnson, 2002), low

and high temperature (Plieth *et al.*, 2000), touch (Knight *et al.*, 1991) or drought (Knight *et al.*, 1997). The biotic signals include phytohormones such as abscisic acid (ABA) and gibberellins (Gilroy and Jones, 1992; McAinsh *et al.*, 1992), fungal/oomycete elicitors (Knight *et al.*, 1991; Mithöfer *et al.*, 1999; Blume *et al.*, 2000; Lecourieux *et al.*, 2002) or nodulation (Nod) factors (Ehrhardt *et al.*, 1996; Müller *et al.*, 2000). Ca<sup>2+</sup> acts as a secondary messenger in plant cells and links different input signals to many diverse

and specific responses. The specificity in the  $\text{Ca}^{2+}$  signalling system is based on multifactorial processes, which start with a specific  $\text{Ca}^{2+}$  signature and the availability of a specific set of  $\text{Ca}^{2+}$  sensors and end with target genes and proteins that activate precise downstream events (Sanders *et al.*, 2002; Lecourieux *et al.*, 2006). The source of the  $\text{Ca}^{2+}$  contributing to the rise in  $[\text{Ca}^{2+}]_{\text{cyt}}$  (apoplasts or internal stores or both) is thought to be important for the physiological response (Knight *et al.*, 1991, 1997; van der Luit *et al.*, 1999).

In symbiotic interactions a rapid  $\text{Ca}^{2+}$  influx and an oscillation in nuclear  $\text{Ca}^{2+}$  levels ( $[\text{Ca}^{2+}]_{\text{nuc}}$ ), termed  $\text{Ca}^{2+}$  spiking, are some of the earliest responses to Nod factors (Ehrhardt *et al.*, 1996; Shaw and Long, 2003) and mutant analyses have demonstrated that the  $\text{Ca}^{2+}$  signalling is central to rhizobial and arbuscular mycorrhizal symbiosis (Harrison, 2005). Genetic studies have demonstrated that a single  $\text{Ca}^{2+}$ /calmodulin-dependent protein kinase, DMI3/CCaMK, is responsible for decoding both Nod and possible Myc-factor-induced  $\text{Ca}^{2+}$  oscillations (Lévy *et al.*, 2004; Mitra *et al.*, 2004; Kanamori *et al.*, 2006). It is located in or at the nucleus, suggesting that besides changes in the cytosol, nuclear  $\text{Ca}^{2+}$  levels are also important for a proper response in the symbiosis (Oldroyd and Downie, 2006).

The endophyte *Piriformospora indica* colonises the roots of many plant species including *Arabidopsis thaliana* and promotes their growth, development and seed production. The fungus stimulates nutrient uptake and confers resistance to various biotic and abiotic stresses (cf. Verma *et al.*, 1998; Sahay and Varma, 1999; Varma *et al.*, 1999, 2001; Peřkan-Berghöfer *et al.*, 2004; Pham *et al.*, 2004; Shahollari *et al.*, 2005, 2007; Sheraleti *et al.*, 2005, 2008a,b; Waller *et al.*, 2005). *Piriformospora indica* is a cultivatable fungus and can grow on synthetic or complex media without a host (Varma *et al.*, 2001; Peřkan-Berghöfer *et al.*, 2004). Since *P. indica* can colonise the roots of many plant species including trees, agricultural, horticultural and medicinal plants, monocots and dicots and even mosses (Varma *et al.*, 2001; Glen *et al.*, 2002; Peřkan-Berghöfer *et al.*, 2004; Weiss *et al.*, 2004; Barazani *et al.*, 2005, 2007; Shahollari *et al.*, 2005, 2007; Sheraleti *et al.*, 2005; Waller *et al.*, 2005), the interaction between the symbiotic partners should be based on general recognition and signalling processes.

In this paper we report the isolation of a fraction from the cell wall (CW) of *P. indica*, which can mimic the presence of the fungus in the initial stages and induce growth promotion. This fraction is also able to induce an elevation of  $[\text{Ca}^{2+}]_{\text{cyt}}$  in plant roots stably expressing the  $\text{Ca}^{2+}$  bioluminescent indicator aequorin. This may point to a role for  $\text{Ca}^{2+}$  in the early signalling events between *P. indica* and *A. thaliana*, similar to the well-characterised legume–rhizobia and arbuscular mycorrhizal symbiosis.

## RESULTS

### A cell wall extract (CWE) from *P. indica* promotes growth in *Arabidopsis* seedlings

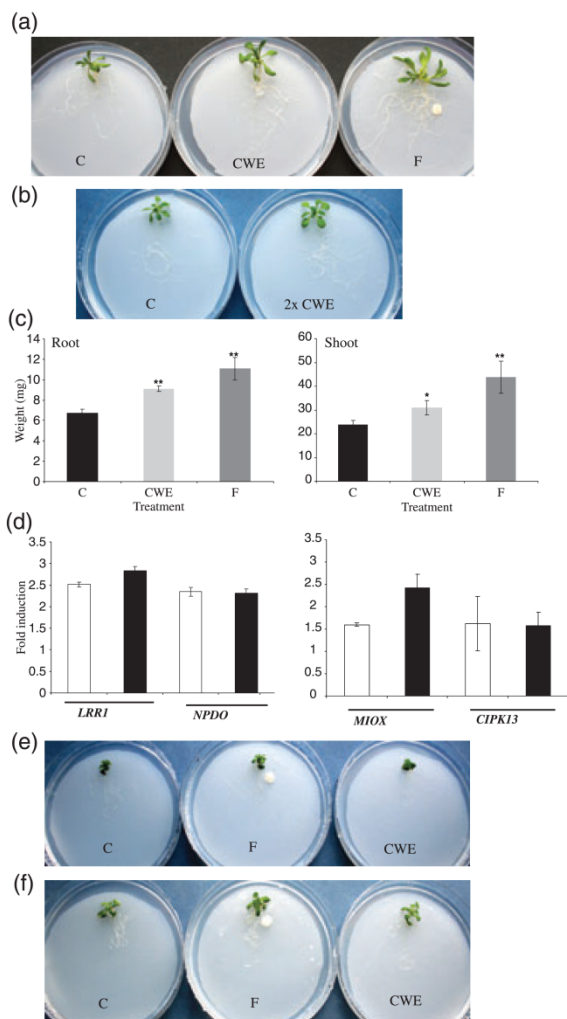
We have previously reported that the endophytic fungus *P. indica* interacts with *Arabidopsis* roots and promotes growth and seed production (Shahollari *et al.*, 2007). Here we demonstrate that components extracted from the fungal cell wall (CW) are also effective in stimulating growth in *Arabidopsis* seedlings. The active fraction was obtained from *P. indica* grown in liquid medium. Fungal CW was isolated and autoclaved to release CW-associated factors. A heat-stable fraction is able to stimulate root and shoot growth when applied to the roots (Figure 1a–c). The overall growth promotion after 10 days was in the range of  $18 \pm 1\%$ , and root growth ( $21 \pm 1\%$ ) was more promoted by the extract than shoot growth ( $15 \pm 1\%$ ). The stimulatory effect on growth is weaker when compared with the growth promotion induced by the fungus, which is  $36 \pm 1\%$  (Figure 1c). Furthermore, no more growth stimulation could be detected 12 days after the application of the CWE, while the fungus still promotes growth (Figure S1 in Supporting Information). A second application of 50  $\mu\text{l}$  of CWE 6 days after the first application resulted in prolonged growth promotion for 14 days and more (Figure 1b) but could not reach the fungal growth promotion levels.

The transcript levels for a leucine-rich repeat protein (LRR1; Shahollari *et al.*, 2007) and for 2-nitro-propane-dioxygenase (NPDO; Sheraleti *et al.*, 2005) are up-regulated in colonised *Arabidopsis* roots compared with the non-colonised controls. The same genes are also up-regulated after the application of the CWE (Figure 1d). Furthermore, microarray analysis with roots exposed to either the fungus or the CWE for 2 days demonstrated that a subset of the regulated genes responded to both treatments. This includes *MIOX* for an enzyme involved in ascorbate biosynthesis (Lorence *et al.*, 2004; Kanter *et al.*, 2005) and *CIPK13* (for a  $\text{Ca}^{2+}$  sensor) (Figure 1d).

To further test the specificity of the growth-promoting effect of the CWE, the *P. indica*-insensitive mutants (*pii*)-3 and -4, which grow like uncolonised plants in the presence of the fungus, were tested for their response to the CWE. The two mutants also failed to respond to the CWE (Figure 1e,f) and the *P. indica* inducible genes were not up-regulated (Figure S2). This suggests that the molecular mechanism for CWE-mediated growth promotion is similar to that obtained during *P. indica* colonisation.

### The CWE from *P. indica* induces cytosolic $\text{Ca}^{2+}$ elevation in *Arabidopsis* roots

In transgenic *Arabidopsis* plants expressing the  $\text{Ca}^{2+}$  sensor aequorin, changes in  $[\text{Ca}^{2+}]_{\text{cyt}}$  can be monitored by aequorin-mediated light emission (Knight *et al.*, 1997). A resting  $[\text{Ca}^{2+}]_{\text{cyt}}$  of  $80 \pm 10 \text{ nM}$  was measured in transgenic

Fungal cell wall extract promotes seedling growth and  $Ca^{2+}$  elevation 195

**Figure 1.** The effect of a cell wall extract (CWE) from *Piriformospora indica* on Arabidopsis growth and gene expression.

(a) The effect of *P. indica*, co-cultivated with Arabidopsis seedlings for 10 days (F) or of 65  $\mu$ l CWE, applied to the seedlings for 10 days (CWE), on growth. C, untreated control.

(b) The effect of two applications (50  $\mu$ l each) of the CWE at days 1 and 6 on growth (2  $\times$  CWE). C, untreated control.

(c) Quantified data for shoots and roots. Sixty-five microlitres of CWE or a fungal plug (F) was added to the seedlings after 1 day of growth on PNM medium. The figure shows root and shoot fresh weights from seedlings 10 days after the treatments. They were identical in sizes and weights at the beginning of the experiments (i.e. 0 days). Bars represent SE. Asterisks indicate statistically significant differences between treated and non-treated plants (unpaired Student's *t*-test: \* $P$  < 0.05, \*\* $P$  < 0.01).

(d) The response of various genes to treatments with *P. indica* or the CWE in Arabidopsis roots. Arabidopsis seedlings were grown in the absence or presence of the fungus, or treated with the CWE for 2 days on PNM medium. Relative transcript abundance in roots was determined by real-time PCR analysis and normalised to the plant *GAPDH* mRNA level. The graph shows fold induction of the mRNA levels by the fungus (white) or CWE (black) relative to the levels in the untreated control roots. The values represent the means of three independent experiments and error bars indicate the SE.

(e, f) The *P. indica*-insensitive mutants *pii-3* (e) and *pii-4* (f) do not respond to the CWE. For details see (a).

Arabidopsis lines. When the CWE was added to Arabidopsis roots after 1 min of measurement, a rapid and transient elevation of the intracellular  $Ca^{2+}$  concentration was observed (Figure 2a). After a lag phase of  $20 \pm 5$  sec, the level of  $[Ca^{2+}]_{cyt}$  begins to rise and a sharp  $Ca^{2+}$  peak of  $207 \pm 14$  nM at  $55 \pm 5$  sec was observed. This was followed by a sustained increase that declined gradually and showed a  $[Ca^{2+}]_{cyt}$  of  $100 \pm 4$  nM at 20 min, reaching background values 40 min after the application of the CWE (Figure 2c). The  $[Ca^{2+}]_{cyt}$  response is concentration-dependent: increasing the amount of the CWE also increases the  $Ca^{2+}$  peak (Figure 2b). No response was observed with water or 4 nM *cis*-zeatin, which were used as controls. *cis*-Zeatin was used because *P. indica* produces this phytohormone in large amounts, although this has no direct role in growth promotion (Vadassery *et al.*, 2008). Surprisingly, the  $[Ca^{2+}]_{cyt}$  response was mainly observed in Arabidopsis roots. Only a minor response was observed with leaf discs or hypocotyls and the  $[Ca^{2+}]_{cyt}$  increased only to  $100 \pm 21$  nM for leaf discs (Figure 2a). This response in leaves can be slightly raised by increasing the amount of CWE (100  $\mu$ l) but it is still less compared than the root response (Figure S3).

Previously, we have shown that *Nicotiana tabacum* is an excellent host for *P. indica* (Sherameti *et al.*, 2005). Transgenic aequorin tobacco seedlings showed the same response to the CWE as Arabidopsis seedlings: the increase in the  $[Ca^{2+}]_{cyt}$  was high in roots (Figure 2c) and only marginal in leaf discs (not shown). Thus, the CWE contains a signal that is recognised by at least two *P. indica*-responsive plant species. However, the  $Ca^{2+}$  signature obtained with tobacco CWE differs from that of Arabidopsis in that two peaks can be detected, the first after 60 sec and the second after 355 sec, and the response does not reach background levels within 40 min (Figure 2c). Navazio *et al.* (2007) reported that a diffusible signal from arbuscular mycorrhizal fungi elicits a transient  $[Ca^{2+}]_{cyt}$  elevation in cell suspension cultures from soybean. Using the same culture, we did not observe any  $Ca^{2+}$  response with our CWE (Figure 2c). Since the culture was generated from green hypocotyls, these results are consistent with the observation that the response induced by the CWE from *P. indica* is predominantly root-specific.

#### Nuclear $Ca^{2+}$ elevation induced by the *P. indica* CWE

$Ca^{2+}$ -dependent signalling is distributed between different cell organelles (Pauly *et al.*, 2001). Nuclear  $Ca^{2+}$  ( $[Ca^{2+}]_{nuc}$ ) elevations are important in symbiotic signalling: for instance the nuclear localised DMI3 is a sensor for  $Ca^{2+}$  signals of the Nod and postulated Myc factors (Kaló *et al.*, 2005; Smit *et al.*, 2005). Since nuclear localised Arabidopsis aequorin plants are not available, the effect of the *P. indica* CWE on  $[Ca^{2+}]_{nuc}$  was tested using BY-2 tobacco cell cultures expressing apoaequorin either in the cytoplasm or

196 Jyothilakshmi Vadassery et al.

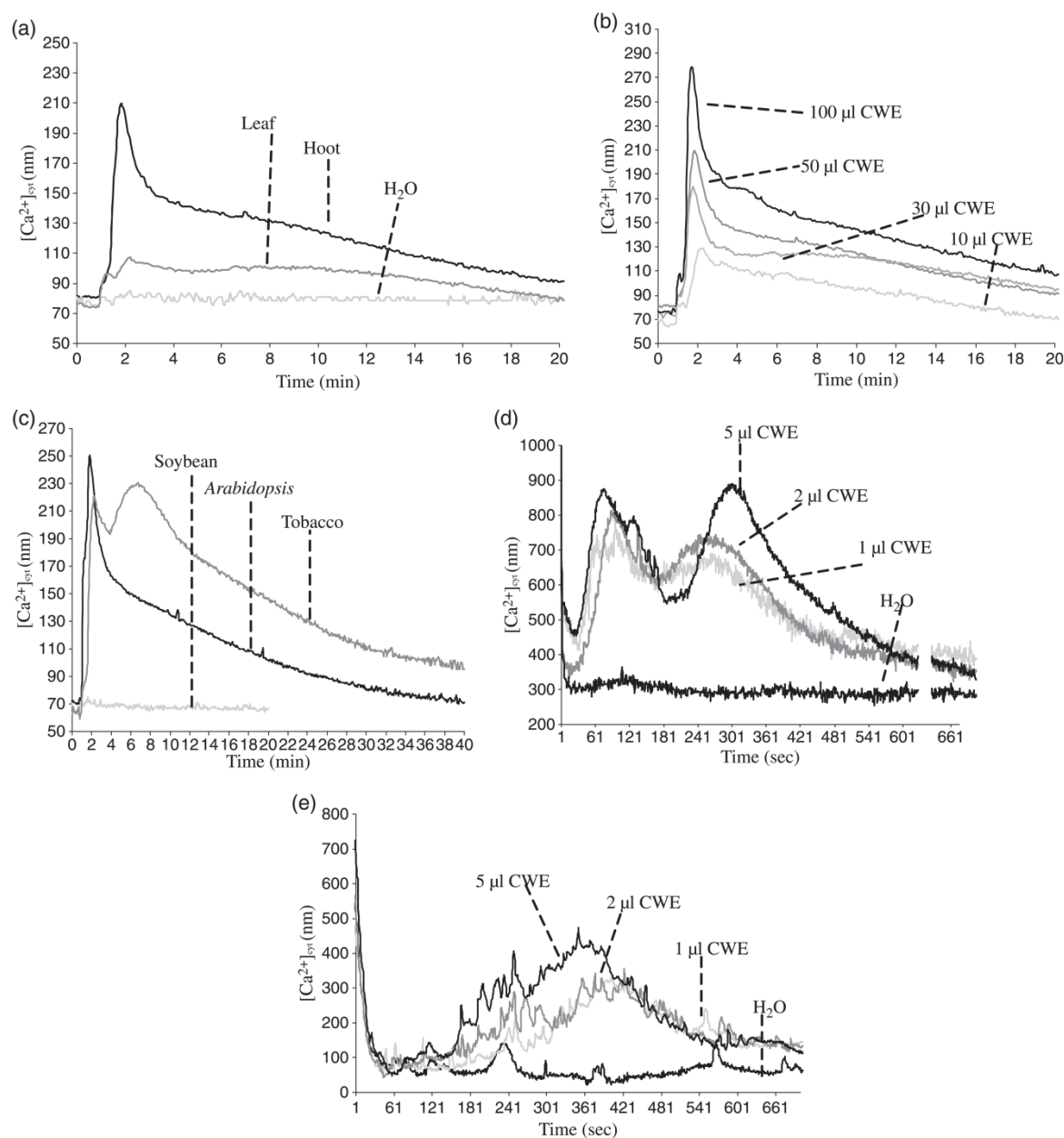


**Figure 2.** *Piriformospora indica* cell wall extract (CWE) induces changes in cytosolic  $Ca^{2+}$  ( $[Ca^{2+}]_{cyt}$ ) in apoaquorin-transformed Arabidopsis seedlings. All curves represent averages of four independent experiments.

(a) Application of 50 μl CWE to Arabidopsis roots and leaves with H<sub>2</sub>O on roots as a control. The  $[Ca^{2+}]_{cyt}$  was calculated from the relative light units (RLU) measured in various tissues at 5-sec integration time for 20 min. In all the experiments, water was used as control and gave background readings.

(b) Application of various doses (10, 30, 50 and 100 μl) of CWE to the roots.

(c) Effect of 50 μl CWE on Arabidopsis or tobacco roots or soybean cell cultures derived from green hypocotyls. The relative aequorin luminescence was measured for 40 min for Arabidopsis and tobacco until the signal returns to background level.

(d, e) *Piriformospora indica* CWE induces changes in  $[Ca^{2+}]_{cyt}$  and nuclear  $Ca^{2+}$  levels ( $[Ca^{2+}]_{nuc}$ ) in apoaquorin-transformed tobacco BY-2 cells. (d) Application of various doses of the CWE (1, 2 and 5 μl) to BY-2 cell cultures to measure  $[Ca^{2+}]_{cyt}$  elevation. (e)  $[Ca^{2+}]_{nuc}$  elevation analyzed with different doses of *P. indica* CWE.

the nucleus (Pauly *et al.*, 2001). The  $[Ca^{2+}]_{cyt}$  response with the tobacco cell cultures resembles that shown with tobacco plants (Figure 2d). The CWE also gave a specific  $Ca^{2+}$  signature in the nucleus, with  $[Ca^{2+}]_{nuc}$  reaching a

peak at 6 min (Figure 2e). A much lower concentration of the CWE was sufficient to induce these responses in the BY-2 cell cultures, when compared to the transgenic plant/seedlings.

### Source for $\text{Ca}^{2+}$ elevation

Inhibitors were used to study the source of  $\text{Ca}^{2+}$  influx. Lanthanum chloride ( $\text{LaCl}_3$ ) is used to inhibit import of  $\text{Ca}^{2+}$  across the plasma membrane and addition of 1 mM  $\text{LaCl}_3$  to the roots 15 min prior to the application of the CWE completely blocked the  $[\text{Ca}^{2+}]_{\text{cyt}}$  elevation (both the rapid peak and the gradual decline) (Figure 3a). Exogenous application of the  $\text{Ca}^{2+}$  chelator 1,2-bis(*o*-aminophenoxy)ethane-*N,N,N',N'*-tetraacetic acid (BAPTA) also completely blocked the  $[\text{Ca}^{2+}]_{\text{cyt}}$  elevation (Figure 3a).

Application of staurosporine, a protein kinase inhibitor, also abolishes *P. indica*-induced  $\text{Ca}^{2+}$  elevation (Figure 3a). Cells often do not respond to consecutive treatments with the same stimulus within a certain time frame ('refractory behaviour'), but remain sensitive to a different stimulus (Müller *et al.*, 2000). To test if the *P. indica*-derived extract follows this rule, it was applied to the roots at the beginning of the experiment and 20 min later when the  $[\text{Ca}^{2+}]_{\text{cyt}}$  induced by the first application is in decline. A second application of the CWE did not induce a strong  $[\text{Ca}^{2+}]_{\text{cyt}}$  elevation in roots (Figure 3b). In contrast, a different stimulus, 10 mM  $\text{H}_2\text{O}_2$ , applied instead of the second CWE, induced a much stronger  $[\text{Ca}^{2+}]_{\text{cyt}}$  elevation indicating that the system is still competent. Additionally, 10 mM  $\text{H}_2\text{O}_2$  applied alone also produced a peak of similar intensity (Figure S4). Thus, both stimuli use different input pathways and probably activate two different receptors and/or channels (Figure 3b). The CWE-desensitised roots regained  $\text{Ca}^{2+}$  responsiveness again after 2 h and the  $\text{Ca}^{2+}$  signature was comparable to the one recorded after the first  $\text{Ca}^{2+}$  application, although the overall signal intensities were lower (cf. Figure 3c,b).

### *P. indica* CWE neither induces $\text{H}_2\text{O}_2$ production nor activates defence responses in roots

Interaction with pathogens or microbe-associated molecular patterns (MAMPs) often induces the production of  $\text{H}_2\text{O}_2$ , which contributes to the activation of defence genes and the hypersensitive response (Grant *et al.*, 2000). Application of the chitotetraose (CH4, 1  $\mu\text{M}$ ) derived from pathogens, for instance, induced production of  $\text{H}_2\text{O}_2$  in the roots. The same was observed for the flg22 elicitor in the leaves (data not shown). However, the CWE of *P. indica* did not induce  $\text{H}_2\text{O}_2$  accumulation that was stronger than observed for the control (Figure 4a). Staining can only be observed at the tips of the main and lateral roots, for which  $\text{H}_2\text{O}_2$  production has been shown previously (Dunand *et al.*, 2007). Furthermore, stimulation of defence responses by pathogenic fungus is associated with a rapid up-regulation of the mRNA levels for many defence-related genes such as *phenylalanine ammonia lyase* (PAL), *pathogenesis-related protein-1* (PR-1), *enhanced disease susceptibility* (EDS1) and *lipoxygenase* (LOX) (Schenk *et al.*, 2000). Transcript levels for these four

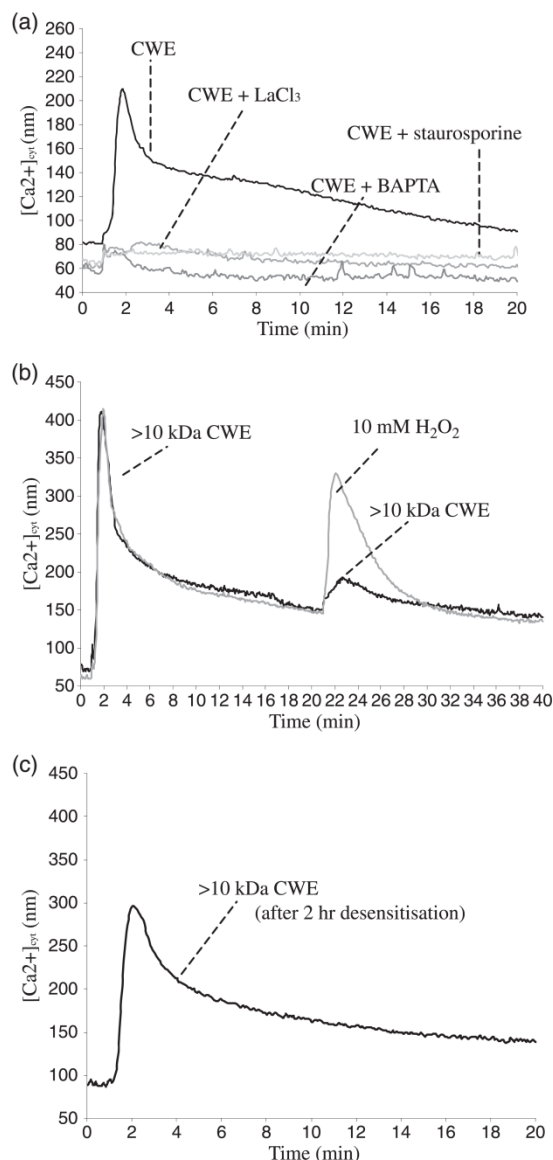


**Figure 3.** Properties of cell wall extract (CWE)-induced cytosolic  $\text{Ca}^{2+}$  ( $[\text{Ca}^{2+}]_{\text{cyt}}$ ) elevation in Arabidopsis roots.

(a) The effect of inhibitors blocking  $\text{Ca}^{2+}$  influx across the plasma membrane and protein phosphorylation in CWE-induced cellular responses. Fifteen minutes prior to the measurement 1 mM  $\text{LaCl}_3$  and 4 mM 1,2-bis(*o*-aminophenoxy)ethane-*N,N,N',N'*-tetraacetic acid (BAPTA) dissolved in water were added. Staurosporine (10  $\mu\text{M}$ ) was pre-incubated with the roots for 15 min.

(b) The CWE-induced  $\text{Ca}^{2+}$  change is refractory to consecutive applications of CWE. Fifty microliters of a >10 kDa CWE subfraction was applied twice to a single root after 1 min and 20 min and luminescence measured over 40 min at 5-sec integration time. Black, application of CWE followed by 10 mM  $\text{H}_2\text{O}_2$ ; grey, a second application of water did not induce a response.

(c) Application of a >10-kDa CWE subfraction 2 h after initial application (desensitisation).

genes did not increase in response to the *P. indica* CWE after 2-days of treatment when *P. indica*-responsive genes like *LRR1* and *MIOX* are up-regulated (Figure 4b).

198 Jyothilakshmi Vadassery et al.

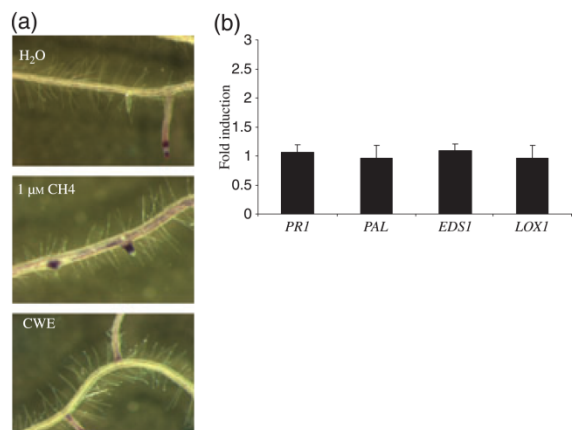


**Figure 4.** Detection of H<sub>2</sub>O<sub>2</sub> production in Arabidopsis roots and defence gene expression upon cell wall extract (CWE) treatment.

(a) Nitrobluetetrazolium (NBT) staining was performed with 9-day-old seedlings treated for 20 min with 1 μM chitinase-4 (CH<sub>4</sub>), or 60 μl *Piriformospora indica* CWE. H<sub>2</sub>O, untreated control. Note that the root tips are stained in all cases. Representative of three independent experiments.

(b) Defence gene expression was determined by real-time PCR analysis and normalised to the plant *GAPDH* mRNA level on treatment of roots with 60 μl CWE for 48 h. The values represent means of three independent experiments and error bars indicate the SE.

#### Ca<sup>2+</sup> signalling genes are regulated by the *P. indica* CWE

Microarray data for Arabidopsis roots treated with the CWE for 1 h were determined to uncover the early signalling events. They were compared with roots co-cultivated with the fungus for 2 days (data not shown as the experiment had no replicates). We observed a substantial overlap among genes associated with Ca<sup>2+</sup> signal transduction. Regulation of a few of them was confirmed by real-time PCR: a glutamate receptor gene, *GLR2.5*, was up-regulated two- to three-fold by both treatments, the cyclic nucleotide gated channel (*CNGC*)-13 and -10 genes were up-regulated 5.6- and 2.4-fold, respectively, by the CWE (Figure 5). Interestingly, *CNGC2* and *CNGC11*, which are implicated in defence signalling (Ali *et al.*, 2007) and *CNGC20* with unknown function were down-regulated by the CWE treatment. Calmodulin-like genes (*CML*) present in Arabidopsis were up-regulated by both stimuli and the strongest response was observed for *CML42*, followed by *CML30* and *CML38*. Finally, a calmodulin-binding protein, *CBP20*, was up-regulated by both treatments (Figure 5).

#### Ca<sup>2+</sup>-dependent mitogen-activated protein kinase (MAPK) activation and its role in the interaction

Many pathogen-derived elicitors and MAMPs, including flg22, activate MAPKs to regulate defence responses (Asai *et al.*, 2002). Activation of three MAPKs (most likely including the flg22-activated MAPK3 and MAPK6) was also observed after the application of the CWE from *P. indica*

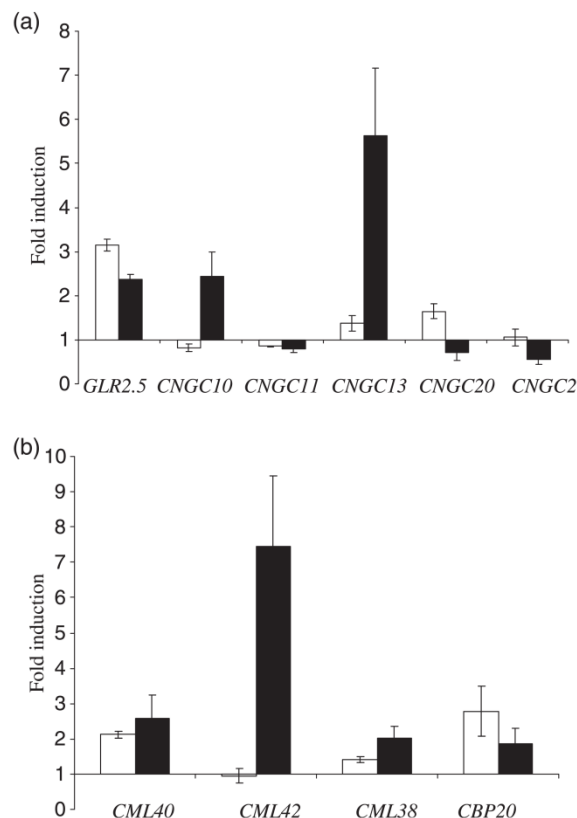


**Figure 5.** The response of Ca<sup>2+</sup> signalling genes on treatment with *Piriformospora indica* and cell wall extract (CWE) in Arabidopsis roots.

Arabidopsis seedlings were grown in the absence or presence of the fungus for 2 days on PNM medium, or treated with the CWE for 1 h. Relative transcript abundance in roots was determined by real-time PCR analysis and normalised to the plant *GAPDH* mRNA level. The graph shows the fold induction of the mRNA levels by the fungus (white) or CWE (black) relative to the levels in the untreated control roots. The values represent means of three independent experiments and error bars indicate the SE.

(a) The Ca<sup>2+</sup> permeable channel (cyclic nucleotide gated channel, *CNGC*) and glutamate receptor (*GLR*) genes.

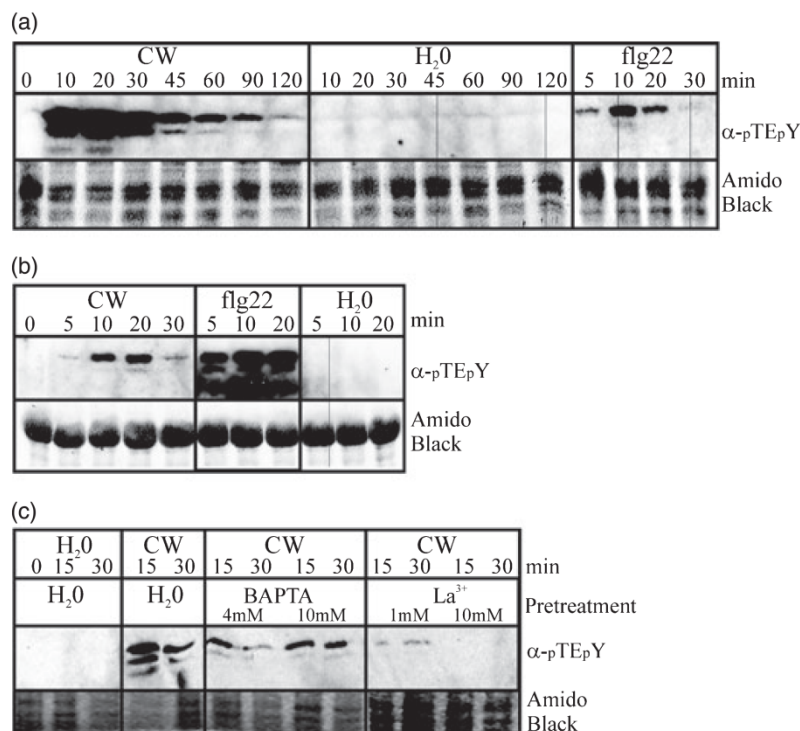
(b) Ca<sup>2+</sup> sensor (calmodulin like gene, *CML*) and calmodulin binding protein (*CBP*) genes.

to the roots, which is much stronger than the activation of MAPKs by flg22 in roots (Figure 6a). In contrast, the reciprocal results were obtained in leaves, where MAPK activation is much stronger when treated with flg22 compared with CWE (Figure 6b). This indicates that MAPK activation is either involved in both beneficial and pathogenic responses, or that defence responses downstream of MAPK activation are repressed by other components, present in the CWE. Furthermore, the crude CWE does not contain high levels of MAMPs that can activate MAPKs in leaves.

To test if MAPK activation in response to the CWE is Ca<sup>2+</sup>-dependent, roots were pre-treated with the Ca<sup>2+</sup> chelator BAPTA (4 and 10 mM), or the Ca<sup>2+</sup> antagonist LaCl<sub>3</sub> (1 and

**Figure 6.** Mitogen-activated protein kinase (MAPK) activation.

Mitogen-activated protein kinase activation was monitored by western blot with antibodies that recognise the dual phosphorylations of the activation loop of MAPKs ( $\alpha\text{-pTEpY}$ ), in roots (a) or in leaves (b). Amido black staining was used to gauge equal loading of proteins in each sample. (c) Pre-treatment with  $\text{Ca}^{2+}$  chelator (1,2-bis(*o*-aminophenoxy)ethane-*N,N,N',N'*-tetraacetic acid; BAPTA) or antagonist ( $\text{LaCl}_3$ ) was used to show the requirement of  $\text{Ca}^{2+}$  transients for MAPK activation in roots.



10 mM), prior to the application of the CWE.  $\text{LaCl}_3$  and BAPTA blocked or strongly reduced MAPK activation, respectively (Figure 6c). Application of BAPTA (4 mM) to the seedlings also blocks the growth promotion response (Figure 7a), the induction of *P. indica* marker genes (Figure 7b) and  $\text{Ca}^{2+}$  signalling genes (Figure 7c).  $\text{LaCl}_3$  was toxic in these long-term assays (data not shown). Finally, a *MAPK6* knock-out mutant failed to respond to *P. indica*: while the fungus stimulated growth of wild-type roots by >60%, no significant difference between colonised and uncolonised *MAPK6* roots could be detected (Figure 7d). Taken together, these results suggest that MAPK and their activation via  $\text{Ca}^{2+}$  signals play a role in the mutualistic interaction.

#### Characterisation of the chemical nature of the CWE-derived active compound

The growth-promoting extract isolated from the fungal CW was heat stable (20 min–3 h at 121°C) and autoclaving appears to be required for the release of the factor(s) from the CW preparation. Fungal CWs are mainly composed of polysaccharides (chitin, glucan) and proteins (Montesano *et al.*, 2003). Thus, initial size-based separations and enzyme treatments of the CWE were performed to learn more about the nature of the active compound(s) in the CWE.

Separation of the CWE into <10 kDa and >10 kDa fractions demonstrated that the active compound is enriched in the

>10 kDa fraction (Figure 8a). The >10 kDa fraction was used for enzyme digestions. Treatment with chitinase (Figure 8b) had no significant effect on the  $\text{Ca}^{2+}$  signature monitored in the roots. Glucanase treatment slightly affected the second phase of the  $\text{Ca}^{2+}$  response but the difference was not significant (at 10 min CWE + inactive glucanase gave a value of  $160 \pm 19$  nM, while CWE + glucanase was  $140 \pm 3.5$  nM; Figure 8c). However, trypsin treatment attenuated the response, with the  $[\text{Ca}^{2+}]_{\text{cyt}}$  peak at 2 min reduced from  $218 \pm 14$  nM to  $146 \pm 12$  nM. The subsequent sustained increase does not change upon trypsin treatment (Figure 8d).

#### DISCUSSION

We report that a CWE from *P. indica* is able to promote root and shoot growth in *A. thaliana* and induces a  $[\text{Ca}^{2+}]_{\text{cyt}}$  increase in root cells and a  $[\text{Ca}^{2+}]_{\text{nuc}}$  increase in tobacco BY-2 cell cultures. To our knowledge, a root cell elevation of intracellular  $\text{Ca}^{2+}$  levels in Arabidopsis induced by a beneficial fungus has not been reported before.

#### *P. indica* CW-derived molecules trigger $\text{Ca}^{2+}$ signalling

$\text{Ca}^{2+}$  is a key component of plant signal transduction and the 'Ca<sup>2+</sup> signature' characterised by its amplitude, duration, frequency and location is responsible for the induction of a specific physiological response (McAinsh and Hetherington, 1998; Sanders *et al.*, 2002). We obtained a signature with a transient increase in  $[\text{Ca}^{2+}]_{\text{cyt}}$  after a lag phase of 55 sec in

200 Jyothilakshmi Vadassery et al.

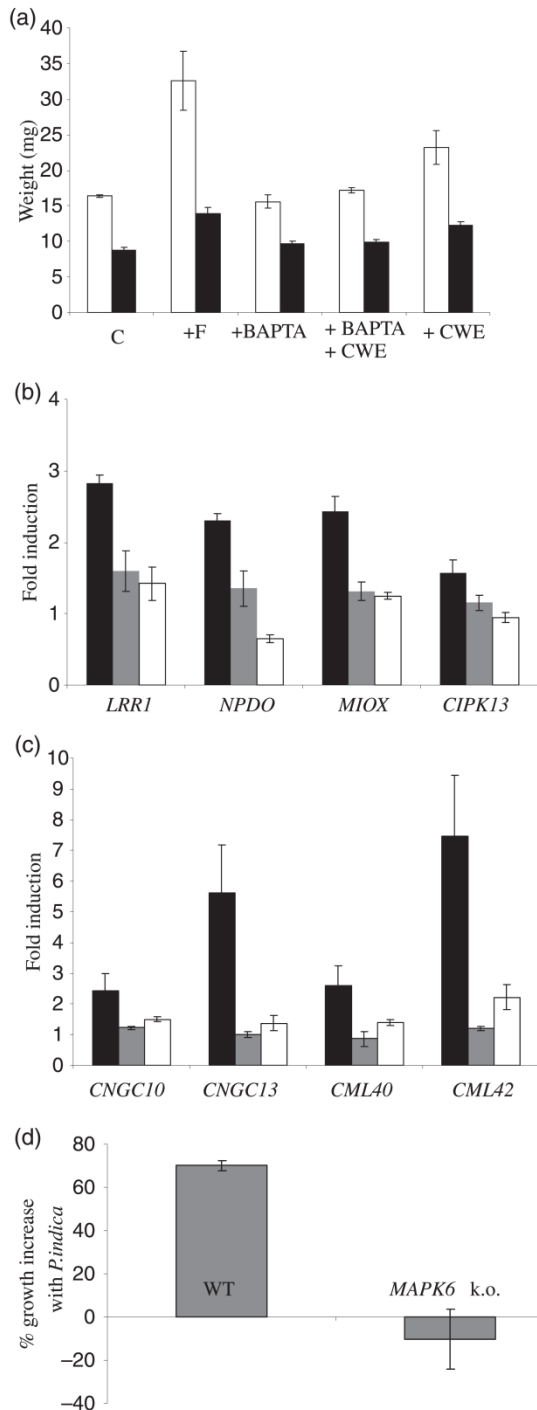


**Figure 7.** The effect of inhibitors blocking  $\text{Ca}^{2+}$  influx and MAPK6 on the *Piriformospora indica*/Arabidopsis interaction.

(a) Shoot (white) and root (black) weights from seedlings 10 days after the treatments with the fungus (F), 1,2-bis(*o*-aminophenoxy)ethane-*N,N,N,N*-tetraacetic acid (BAPTA; 4 mM) and/or the cell wall extract (CWE). C, untreated control. Values represent the mean of four independent experiments and error bars represent the SE.

(b) The response of the *LRR1*, *NPDO*, *MIOX* and *CIPK13* mRNA levels to treatments with the CWE (black), BAPTA (4 mM, grey) and BAPTA + CWE (white) in Arabidopsis roots. Relative transcript abundance in roots was determined by real-time PCR analysis and normalised to the plant *GAPDH* mRNA level. The graph shows the fold induction of the mRNA levels relative to the levels in the untreated control roots 2 days after the treatments. The values represent means of three independent experiments and error bars indicate SE.

(c) The response of the *CNGC10*, *-13* and *CML40*, *-42* mRNA levels to 1 h of treatment with the CWE. For details see (b).

(d) Percentage increase in fresh weight of wild-type and *MAPK6* knock-out roots, after co-cultivation with *P. indica* for 8 days. Values represent the mean of three independent experiments and error bars represent the SE.

colonise aerial parts of plants as reported for *Populus* (Kaldorf *et al.*, 2005). The  $[\text{Ca}^{2+}]_{\text{cyt}}$  elevation observed in tobacco roots has a significantly different signature from the one observed in Arabidopsis tissue, since two  $\text{Ca}^{2+}$  peaks at 60 and 355 sec could be detected. Different  $\text{Ca}^{2+}$  signatures have been reported depending on the organ, tissue, cell type or developmental stages of cells (McAinsh and Hetherington, 1998; Kiegle *et al.*, 2000; Reddy, 2001; Moore *et al.*, 2002) and the results show how a single stimulus can result in unique  $\text{Ca}^{2+}$  signatures in two different plant species.

$\text{Ca}^{2+}$  elevations have been reported, for instance, for the oligopeptide elicitor pep-13 in parsley cell cultures (Blume *et al.*, 2000), flg22 in Arabidopsis leaf discs,  $\beta$ -glucan fragments in soybean cell cultures (Mithöfer *et al.*, 1999) and for many proteinaceous elicitors (like cryptogein) and oligosaccharide elicitors (Lecourieux *et al.*, 2002). The induction of a biphasic response with a second, long-lasting plateau seems to be necessary for phytoalexin synthesis (Blume *et al.*, 2000). We also observed a biphasic  $[\text{Ca}^{2+}]_{\text{cyt}}$  elevation in leaf discs with the MAMP lipopolysaccharide (Figure S5). Similar to these pathogenic elicitors, Navazio *et al.* (2007) reported that diffusible factors released by *Gigaspora margarita* (a fungus involved in arbuscular mycorrhizal symbiosis) induce a  $\text{Ca}^{2+}$  response that dissipates in 30 min. But such an elevation did not activate defence, but instead activated the symbiotic *DMI* genes. In our case, the lag phase (1 min), peak time ( $\sim 2$  min), duration of the  $\text{Ca}^{2+}$  response (40 min) and tissue specificity differ from other elicitors and this may be one of the factors contributing to its specificity.

Using the  $\text{Ca}^{2+}$  chelator, BAPTA, and the  $\text{Ca}^{2+}$  channel blocker,  $\text{LaCl}_3$ , we showed that CWE-induced  $[\text{Ca}^{2+}]_{\text{cyt}}$  increase was strongly reduced. Since  $\text{LaCl}_3$  and BAPTA pre-treatment, prior to CWE addition, were relatively short, it is unlikely that these inhibitors affected endogenous  $\text{Ca}^{2+}$  pools. Hence, it is likely that the external medium is the primary source for the  $\text{Ca}^{2+}$  influx. The CWE-induced

Arabidopsis roots. A maximum was observed about 1.5 min after the application of the CWE and dissipated in 40 min. Consistent with the observation that *P. indica* is a root-colonising fungus (Varma *et al.*, 1999) the CWE stimulates only a low response in leaves. This can be attributed to the fact that prolonged incubation also stimulated the fungus to

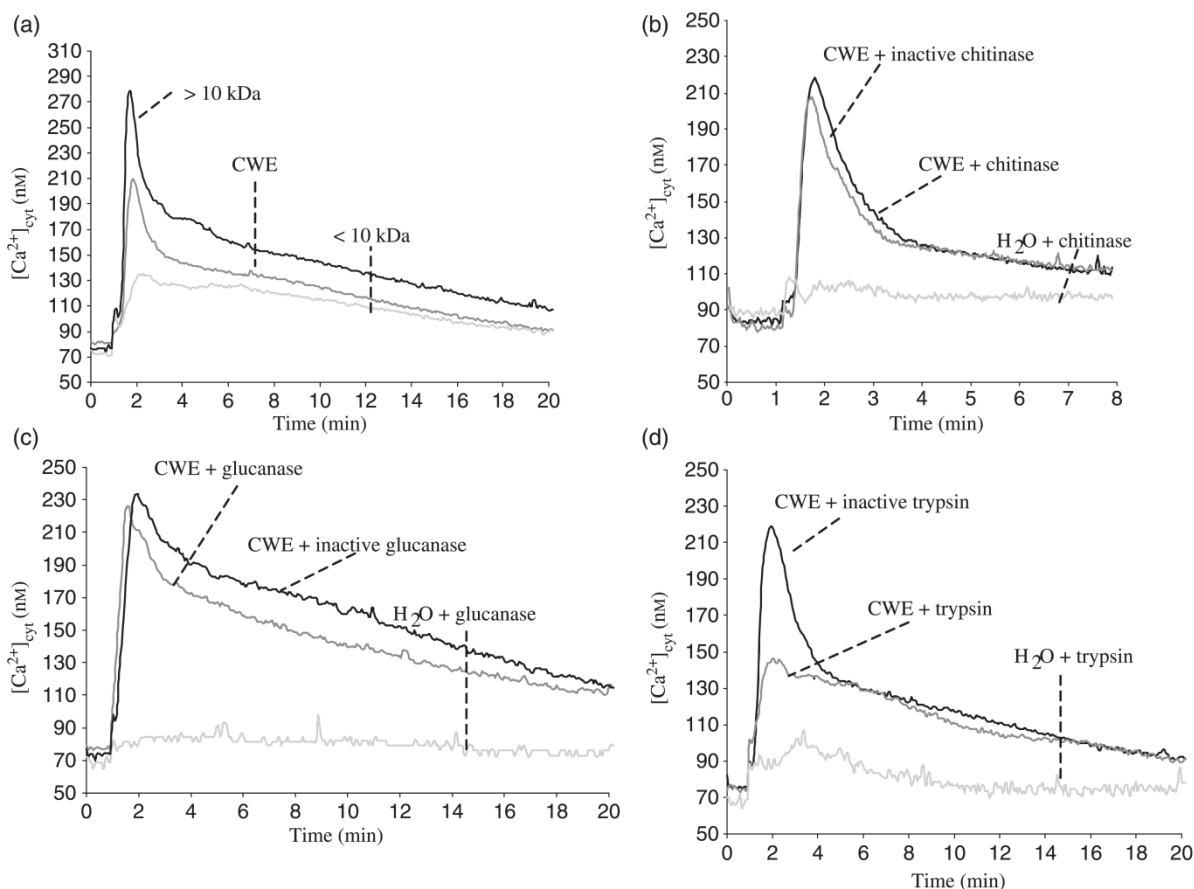


**Figure 8.** Analysis of the size of the active signal in the cell wall extract (CWE) and enzyme treatments to determine the chemical nature of the active compound. (a) Separation of the CWE into  $<10$  kDa and  $>10$  kDa subfractions. Most of the activity is in the  $>10$  kDa fraction.

(b–d) The CWE was treated with chitinase (b) ( $5 \mu\text{g}/100 \mu\text{l}$ ), glucanase (c) ( $5 \mu\text{g}/100 \mu\text{l}$ ) or trypsin (d) ( $1 \mu\text{g}/100 \mu\text{l}$ ) before measuring the cytosolic  $\text{Ca}^{2+}$  ( $[\text{Ca}^{2+}]_{\text{cyt}}$ ) elevation in roots. Heat-inactivated enzymes were used as the control. The  $>10$  kDa fraction was used for the treatment. All curves represent averages of three independent experiments.

The luminescence readings were taken for 10 min (b) or 20 min (a, c, d).

response also shows a refractive behaviour, since a second application of CWE after the dissipation of a first  $[\text{Ca}^{2+}]_{\text{cyt}}$  elevation results in a strongly reduced response (Figure 3b,c). This is reminiscent of the desensitisation of the putative receptors for chitooligosaccharides in tomato and for pep-13 in parsley (Felix *et al.*, 1998; Blume *et al.*, 2000). Finally, the sensitivity of the  $\text{Ca}^{2+}$  elevation to the protein kinase inhibitor staurosporine indicates that protein phosphorylation is involved upstream to the response, probably at the receptor level. Thus, these observations are compatible with the notion that the  $\text{Ca}^{2+}$  response induced by *P. indica* is receptor-mediated.

#### Nuclear $\text{Ca}^{2+}$ elevation by *P. indica* CWE

Compartmentalisation of the  $\text{Ca}^{2+}$  signal is an important parameter in encoding response specificity (Pauly *et al.*, 2001; Walter *et al.*, 2007).  $[\text{Ca}^{2+}]_{\text{nuc}}$  can be regulated sepa-

rately from  $[\text{Ca}^{2+}]_{\text{cyt}}$  and this can also affect the specificity of the response, or they can also act in cooperation (Allen and Schroeder, 2001). Using aequorin targeted to the nucleus in a tobacco cell culture system, we could detect an elevation of  $[\text{Ca}^{2+}]_{\text{nuc}}$  with the *P. indica* CWE. The  $[\text{Ca}^{2+}]_{\text{nuc}}$  elevation peaks at 361 sec and  $[\text{Ca}^{2+}]_{\text{cyt}}$  has two peaks at 60 and 355 sec. Since the nuclear signals are delayed by 6 min, they can be independent of the cytoplasmic signals or one signal can follow the other. Because imaging or detecting the  $\text{Ca}^{2+}$  spikes is not possible with the aequorin system, we cannot rule out that they also occur in our system, as described in other symbiotic interactions. Several  $\text{Ca}^{2+}$  sensors like CAM and CAM-binding proteins or DMI3 are localised in the nucleus (Oldroyd and Downie, 2006). Hence the  $[\text{Ca}^{2+}]_{\text{nuc}}$  elevation is of importance and *P. indica*-induced  $[\text{Ca}^{2+}]_{\text{nuc}}$  elevation points to a role for the nucleus in signal processing.

### The CWE is involved in growth promotion and not in defence

An interesting observation was that the CWE is capable of promoting plant growth. This indicates that growth promotion can be uncoupled from the colonisation of the roots, although the CWE cannot completely replace the fungus *per se*, since even repeated applications of CWEs do not induce a growth promotion comparable to the fungus. The CWE activates a signalling cascade that initiates growth promotion, as blocking  $\text{Ca}^{2+}$  signalling pathway by BAPTA also blocked growth promotion. Also it is possible that not all factors provided by the fungus are present in the CWE. The staining of the roots for  $\text{H}_2\text{O}_2$  production and the absence of defence gene activation support the idea that the CWE does not result in prolonged activation of defence responses. We propose that the fungus colonises and propagates in roots and the amount of the active compound(s) depends on the harmony of the symbiosis and the degree of colonisation. In a natural system, the release of MAMPs would be regulated such that defence signalling is not activated via controlled colonisation. A study with alfalfa roots exposed to both Nod factors and pathogen-derived oligochitin elicitors has shown that activation of defence-related reactions might require elevation of  $[\text{Ca}^{2+}]_{\text{cyt}}$  above a hypothetical threshold level, which is reached by oligochitin elicitors but not by Nod factors (Felle *et al.*, 2000). Similar results have also been described for *P. indica* and Arabidopsis where PYK10 restricts root colonisation, which results in repression of defence responses and increase in mutualistic interaction (Sherameti *et al.*, 2008a).

### MAPK6 is crucial for the growth promotion response and MAPK activation is $\text{Ca}^{2+}$ dependent

Similar to the activation of the MAPKs SIMK and SAMK in the roots of *Lupinus albus* after infection by *Bradyrhizobium* sp., a symbiotic bacterium that forms nodules in lupines (Fernandez-Pascual *et al.*, 2006), the *P. indica*-derived CWE also activated MAPKs. Although signalling events leading to symbiotic and pathogenic interactions should be different, common strategies have been found in the early plant responses, encouraging the idea that pathogenesis and symbiosis are variations on a common theme (Parniske, 2000, 2004; Hérouart *et al.*, 2002). It has been suggested that general defence responses become activated during early symbiosis events (Carden and Felle, 2003). The MAPK cascade might be involved in plant–pathogen infections as well as in plant–symbiont interactions. The latter is supported by the observation that plant growth is not promoted in the *mapk6* mutant, and hence MAPK6 is essential for the symbiotic interaction. MAPK6 is activated by various microbial elicitors (Nühse *et al.*, 2000) and synthesis of camalexin, a major phytoalexin in Arabidopsis, is regulated by the

MAPK3/MAPK6 cascade (Ren *et al.*, 2008). Silencing of MAPK6 compromised both gene-for-gene and basal resistance in Arabidopsis (Menke *et al.*, 2004; Takahashi *et al.*, 2007) and hence is a common element in plant resistance. Furthermore, it has been shown that  $\text{Ca}^{2+}$  influx-dependent activation of MAPK is common in elicitor-treated cells (Lecourieux *et al.*, 2002), comparable to the results shown here (Figure 6c). Thus, activation of MAPK6 and its role in growth promotion are dependent on the elevation of  $[\text{Ca}^{2+}]_{\text{cyt}}$ .

### Specificity of the response

The temporal and spatial nature as well as the amplitude of the  $\text{Ca}^{2+}$  signal caused by a given stimulus contributes to the specificity of the response (McAinsh and Hetherington, 1998; Knight, 2000). Specificity to the CWE is demonstrated by several observations: the CWE promotes growth of the wild type but not of *pji* seedlings. The CWE and the fungus appear to up-regulate a common set of genes. *Piriformospora indica*-specific marker genes are not up-regulated by the CWE in *pji* mutants. It induces a transient  $[\text{Ca}^{2+}]_{\text{cyt}}$  elevation in an organ-specific manner. The growth promotion response is blocked when the  $\text{Ca}^{2+}$  elevation is inhibited by adding BAPTA. In contrast to the common signalling cascade shared by rhizobium and arbuscular mycorrhizal symbiosis, inactivation of the Arabidopsis *DML-1* homologue does not affect the interaction with *P. indica* (Shahollari *et al.*, 2007).

### $\text{Ca}^{2+}$ -regulated genes in the interaction

The cyclic nucleotide-gated ion channels (CNGCs) maintain the cation homeostasis essential for a wide range of physiological processes in plant cells. It has been reported that *CNGC10*, which is up-regulated by CWE, codes for a protein that localises to the plasma membrane and influences growth responses and starch accumulation. *CNGC10* is highly expressed in dividing root cells and controls growth (Borsics *et al.*, 2007; Christopher *et al.*, 2007). *CNGC13* is most responsive to the CWE and is closely related to *CNGC10*. Down-regulation of *CNGC2/DND1*, which is involved in the generation of NO and the innate immune response to pathogens (Ali *et al.*, 2007), and *CNGC11*, which is a regulator of resistance against fungal pathogens (Yoshioka *et al.*, 2006), supports the idea that they are suppressed by the CWE to prevent defence gene activation. Many diverse stimuli result in increases of  $[\text{Ca}^{2+}]_{\text{cyt}}$  in plant cells, and  $\text{Ca}^{2+}$  sensors play a major role in defining the specificity. The Arabidopsis genome has seven calmodulin (*CAM*) and 50 *CML* genes that encode potential  $\text{Ca}^{2+}$  sensors (McCormack *et al.*, 2005). Gene expression analysis revealed that *CML42* is the most up-regulated by the CWE. It is known that a closely related gene, *CML43*, is rapidly induced in disease-resistant Arabidopsis leaves following inoculation with *Pseudomonas syringae* pv. tomato. Overexpression of *CML43* in Arabidopsis accelerated the hypersensitive response (Chiasson *et al.*, 2005). The role of the *P. indica*-

inducible *CML42*, *CML40*, *CML38* and *CBP20*, which are up-regulated by both the fungus and the CWE, is unknown. The up-regulation of  $\text{Ca}^{2+}$  signalling genes supports the important role of  $\text{Ca}^{2+}$  in the interaction.

#### Chemical nature of the CWE

The active compound could be a protein, peptide, glycoprotein, lipid, oligosaccharide (Veit *et al.*, 2001) or other CW component such as a chitin or glucan which constitute the main skeletal polysaccharides of basidiomycetes (Wolski *et al.*, 2005). It is known that the Nod factors released by nodule-forming rhizobia in symbiotic interactions are lipochitooligosaccharides and the perception of the Nod factors has evolved from the perception of more general elicitors like lipopolysaccharides or chitins (Boller, 1995; Cullimore *et al.*, 2001; Montesano *et al.*, 2003). It is unlikely that the active compound in the *P. indica* CWE is a chitin since corresponding enzyme treatments had no significant effect on the  $\text{Ca}^{2+}$  response. Observations that the chitin oligomers, CH4 and CH5, did not induce a transient increase in  $\text{Ca}^{2+}_{\text{cyt}}$  in Arabidopsis roots support the data. The CWE might contain an active proteinaceous factor since trypsin treatments partially inhibited the activity of the CWE. But the lack of change in the sustained increase phase of  $[\text{Ca}^{2+}]_{\text{cyt}}$  on trypsin treatment hints at the involvement of additional factors.

The role of  $\text{Ca}^{2+}$  signalling in the *P. indica*/Arabidopsis interaction has many parallels with the arbuscular mycorrhizal symbiosis and rhizobium/legume symbiotic systems. The identification of the active compound in the CWE, its receptor and  $\text{Ca}^{2+}$  sensor(s) might shed light on this symbiosis.

### EXPERIMENTAL PROCEDURES

#### Growth conditions of plant and fungus

Wild-type and mutant (*pri-3* and *pri-4*) *A. thaliana* seeds (ecotype Columbia) were surface-sterilised and placed on petri dishes containing MS nutrient medium (Murashige and Skoog, 1962). After cold treatment at 4°C for 48 h, plates were incubated for 7 days at 22°C under continuous illumination ( $100 \mu\text{mol m}^{-2} \text{sec}^{-1}$ ). *Piriformospora indica* was cultured as described previously (Verma *et al.*, 1998; Peřkan-Berghöfer *et al.*, 2004) on *Aspergillus*-minimal medium. For solid medium 1% (w/v) agar was included.

#### Preparation of the CWE from *P. indica*

The CWE was prepared using the protocol of Anderson-Prouty and Albersheim (1975) with modifications. Mycelia from 14-day-old liquid cultures were homogenised using mortar and pestle in 5 ml water  $\text{g}^{-1}$  mycelia. The homogenate was filtered using a coarse sintered glass funnel. The residue was washed three times with water, once with chloroform/methanol (1:1) and finally in acetone. This preparation was air dried for 2 h and the mycelial CW material was recovered. Elicitor fractions were prepared from mycelial CWs by suspending 1 g of CW in 100 ml water and autoclaving for 20 min at 121°C. Autoclaving releases the active fraction. The suspension was centrifuged at 28 000 g for 10 min, filter-sterilised using a 0.22- $\mu\text{m}$  filter and concentrated to half and used for further assay.

#### Co-cultivation experiments and estimation of plant growth

Ten days-after the growth of seedlings on MS media, *A. thaliana* seedlings were transferred to nylon discs (mesh size 70  $\mu\text{m}$ ) and placed on top of a modified plant nutrient medium (Vadassery *et al.*, 2008), in petri dishes. One seedling was used per petri dish. After 24 h, fungal plugs with a diameter of approximately 5 mm were placed at a distance of 1 cm from the roots. Seventy microlitres of the prepared CWE was added directly onto the roots of a seedling. The plates were incubated at 22°C under continuous illumination from the side ( $80 \mu\text{mol m}^{-2} \text{sec}^{-1}$ ). Fresh weights were determined separately for shoots and roots at 6, 10 and 14 days after application of the CWE.

#### $\text{Ca}^{2+}$ measurements

Transgenic *A. thaliana* (Col) and *N. tabacum* expressing cytosolic apoaequorin were used for  $\text{Ca}^{2+}$  measurements (Knight *et al.*, 1997). Plants were grown vertically in Hoagland's medium with 1% agar for 14 days (Arabidopsis) or 30 days (*N. tabacum*). For  $\text{Ca}^{2+}$  measurements the roots were dissected from 14-day-old seedlings and reconstituted in 5  $\mu\text{M}$  coelenterazine (P.J.K. GmbH, <http://www.pjk-gmbh.de/>) in the dark overnight at 21°C. The luminescence counts obtained with a microplate luminometer (Luminoscan Ascent, version 2.4; Thermo Fisher Scientific, <http://www.thermofisher.com/>) were calibrated using the equation by Rentel and Knight (2004). For experimental details see Appendix S1.

#### Enzyme treatments

Fractionation of CWE was done using Amicon Ultra centrifugal devices with a 10-kDa MW cut-off (Millipore, <http://www.millipore.com/>). The CWE was treated with trypsin (1  $\mu\text{g}/100 \mu\text{l}$ ), glucanase (5  $\mu\text{g}/100 \mu\text{l}$ ) or chitinase (5  $\mu\text{g}/100 \mu\text{l}$ ) using the appropriate buffers at 37°C for 30–40 min. The reaction with trypsin was stopped using trypsin inhibitor. At the end of all reactions four volumes of cold methanol (–20°C) was added to stop the reactions. The supernatant after centrifugation was lyophilised, resuspended in water and used for  $\text{Ca}^{2+}$  measurements. All enzymes were from Sigma Aldrich (<http://www.sigmaaldrich.com/>), except for Sequencing Grade Trypsin (Promega, <http://www.promega.com/>). Boiled inactive enzymes were used as controls. The buffers used for enzyme treatments were also tested for  $\text{Ca}^{2+}$  activities.

#### Inhibitor treatments

Roots were pre-incubated with  $\text{LaCl}_3$  (1 mM) and BAPTA (4 mM), 15 min prior to the start of the readings.  $\text{LaCl}_3$  and BAPTA were from Sigma Aldrich and dissolved in water. Protein phosphorylation inhibitor, staurosporine (10  $\mu\text{M}$ ), dissolved in DMSO, was from Alexis (<http://www.alexis-biochemicals.com/>). The final DMSO concentration in the assay was 0.1%.

#### MAPK assay

Roots from 14-day-old Arabidopsis seedlings grown in Hoagland's medium were used. For inhibitor studies,  $\text{LaCl}_3$  (1 and 10 mM) and BAPTA (4 and 10 mM) were applied 2 h before the experiments and the CWE was applied to the roots at the time points given in figure 6. The *mpk6* (*At2g43790*) line is the *mpk6-3* allele described in Liu and Zhang (2004) but independently isolated from the SALK collection (SALK\_127507).

#### $\text{H}_2\text{O}_2$ measurements

The whole seedlings were used for  $\text{H}_2\text{O}_2$  measurements 15–20 days after germination. Roots were stained for 5 min in a

204 *Jyothilakshmi Vadassery et al.*

solution containing 2 mM nitrobluetetrazolium (NBT; Sigma Aldrich) in 20 mM phosphate buffer pH 6.1. The reaction was stopped by washing the seedlings with water. The elicitor or CW preparations were added for 10–20 min on the seedlings before the staining with NBT. Experiments were repeated five times with comparable results. Roots were observed under the stereomicroscope SV 6 with an AxiomCam HRc color camera (Carl Zeiss, <http://www.zeiss.com/>). The chitin oligomer CH4 was obtained from Seikagaku Corporation (<http://www.seikagaku.co.jp/english/>).

**Real-time PCR and microarrays**

Real-time quantitative RT-PCR was performed using an iCycler iQ real-time PCR detection system and iCYCLER software version 2.2 (Bio-Rad, <http://www.bio-rad.com/>). Total RNA was isolated from three independent replicates of Arabidopsis roots, treated with *P. indica* CWE for 1 h or 48 h. Complementary DNA was synthesised using the Omniscript cDNA synthesis kit (Qiagen, <http://www.qiagen.com/>) using 1 µg RNA. Microarray hybridisation was performed with the Arabidopsis Genome Array ATH1 from Affymetrix (<http://www.affymetrix.com/>) and the data were analysed with gcOS1.4 software (Affymetrix). The microarrays were performed at the Kompetenzzentrum für Fluoreszenz Bioanalytik (KFB), Regensburg, Germany. For the amplification of the RT-PCR products, iQ SYBR Green Supermix (Bio-Rad) was used according to the manufacturer's protocol in a final volume of 25 µl. The iCYCLER was programmed to 95°C 2 min, 40 × (95°C 30 sec, 57°C 40 sec, 72°C 45 sec), 72°C 10 min, followed by a melting curve program 55°C to 95°C in increasing steps of 0.5°C. All reactions were performed in triplicate. The mRNA levels for each cDNA probe were normalised with respect to the *GAPDH* mRNA level. Fold induction values of target genes were calculated with the  $\Delta\Delta CP$  equation of Pfaffl (2001) and related to the mRNA level of target genes in control roots, which were defined as 1.0. The following primer pairs, with product sizes between 150 and 170 bp were used: *MIOX2* (*At2g19800*), 5'-TTGGCAAGGTTCTCCTTCTG-3', 5'-TTGGCTGAGTCGAAGGTACA-3'; *LRR1* (*At5g16590*), 5'-CTCGTTCCGTGACATCAGA-3', 5'-GACCCGACTCACATTGGACT-3'; *NPDO* (*At5g64250*), 5'-GAAGCAGGTGGGCATGTTAT-3', 5'-GTGCCAGACAGACCCCTTG-3'; *CIPK13* (*At2g34180*), 5'-GTTGATTCAATGCGAGACC-3', 5'-CCAATCCTTCTCTCACCA-3'; *GAPDH* (*At3g04120*), 5'-GAGCTGACTACGTTGTTGAG-3', 5'-GGAGACAATGTCAAGGTCGG-3'; *CNGC10* (*At1g01340*), 5'-GGATCCTGACCACAAGGAAA-3', 5'-AAGACAGTGCCTTGCGCTAT-3'; *CNGC11* (*At2g46440*), 5'-TGCTAGGACATCCGACTG-3', 5'-TAGGACCCTGACTTCAACG-3'; *CNGC13* (*At4g01010*), 5'-GCAGAGCAATGGATGTCTCA-3', 5'-ATGGCGTTTGATGTCTCTCC-3'; *CNGC20* (*At3g17700*), 5'-GCTTTCACCTCCAGGAGTCG-3', 5'-GGAGGACGTCTGTGAGTTCCG-3'; *CNGC2* (*At5g15410*), 5'-CATCTTCTGGGGCCTAATGA-3', 5'-TAACCTCGAGCCAGTTGCTT-3'; *GLR2.5* (*At5g11210*), 5'-TTCGGAGGAGAAGAGCTGAA-3', 5'-GATAGAGCAACGCCGAGTTC-3'; *CML40* (*At3g01830*), 5'-TAAGTCTGGCAAACGTGCAG-3', 5'-TCCTCTCCTTCTTCCACCA-3'; *CML42* (*At4g20780*), 5'-CGTCGAAGAGCTAAGCCAAG-3', 5'-CCGAAGAAAGAAATCGTCGAG-3'; *CML38* (*At1g76650*), 5'-TCAGCCGGAGAGATACAACA-3', 5'-GCAGCTACGGCTTTCATC-3'; *CBP20* (*At5g26920*), 5'-TCGAAGCTGAGGATGGTTCT-3', 5'-TAAATCCCTCAACGGTCCAG-3'; *PAL* (*At3g53260*), 5'-CCTCAATGCTAGGTCCTCA-3', 5'-ACTCCGATTGGTGTCTCTTG-3'; *EDS1* (*At3g48090*), 5'-CCTCGTTGTGTGACATTTGG-3', 5'-AATTGGCAAGAACATGAGG-3'; *PR-1* (*At2g14610*), 5'-TTCTTCCCTCGAAAGCTCAA-3', 5'-AAGGCCACAGAGTGTATG-3'; *LOX1* (*At1g55020*), 5'-GATGGCTTGGGTTTGTA-3', 5'-GTTCTTCCAGGTTTGCAAT-3'.

**ACKNOWLEDGEMENTS**

We thank Dr Mark Knight (University of Durham, UK) for the gift of the apoaquorin-expressing pMAQ2 lines of Arabidopsis and tobacco and Dr Margit Leitner (MPI Chemical Ecology, Jena, Germany) for help in H<sub>2</sub>O<sub>2</sub> measurements. Work was supported by the IMPRS Jena, SPP 1212, the SFB 604 and DFG (Oe133/19-1).

**SUPPORTING INFORMATION**

Additional Supporting Information may be found in the online version of this article:

**Figure S1.** The effect of the cell wall extract (CWE) on Arabidopsis growth.

**Figure S2.** Genes which are up-regulated in the wild-type roots after the application of the cell wall extract (CWE) are not up-regulated in the *Piriformospora indica*-insensitive mutant *pii-3*.

**Figure S3.** *Piriformospora indica* cell wall extract (CWE) induces changes in cytosolic Ca<sup>2+</sup> ([Ca<sup>2+</sup>]<sub>cyt</sub>) in apoaquorin-transformed Arabidopsis seedlings.

**Figure S4.** Changes in cytosolic Ca<sup>2+</sup> ([Ca<sup>2+</sup>]<sub>cyt</sub>) in Arabidopsis roots on treatment with 10 mM H<sub>2</sub>O<sub>2</sub>.

**Figure S5.** Tissue specific 'Ca<sup>2+</sup> signatures' of various biotic elicitors in Arabidopsis.

**Appendix S1.** Supplementary data on Ca<sup>2+</sup> measurements and comparison of the *Piriformospora indica* cell wall extract (CWE) activity with known elicitors.

Please note: Wiley-Blackwell are not responsible for the content or functionality of any supporting materials supplied by the authors. Any queries (other than missing material) should be directed to the corresponding author for the article.

**REFERENCES**

- Ali, R., Ma, W., Lemtiri-Chlieh, F., Tsaltas, D., Leng, Q., von Bodman, S. and Berkowitz, G.A. (2007) Death don't have no mercy and neither does calcium: *Arabidopsis* CYCLIC NUCLEOTIDE GATED CHANNEL2 and innate immunity. *Plant Cell*, **19**, 1081–1095.
- Allen, G.J. and Schroeder, J.I. (2001) Combining genetics and cell biology to crack the code of plant cell calcium signalling. *Sci STKE*, **102**, 1–7.
- Anderson-Prouty, A.J. and Albersheim, P. (1975) Host-pathogen interactions. VIII. Isolation of a pathogen-synthesized fraction rich in glucan that elicits a defense response in the pathogen's host. *Plant Physiol.* **56**, 286–291.
- Asai, T., Tena, G., Plotnikova, J., Willmann, M.R., Chiu, W.L., Gomez-Gomez, L., Boller, T., Ausubel, F.M. and Sheen, J. (2002) MAP kinase signalling cascade in Arabidopsis innate immunity. *Nature*, **415**, 977–983.
- Barazani, O., Benderoth, M., Groten, K., Kuhlemeier, C. and Baldwin, I.T. (2005) *Piriformospora indica* and *Sebacina vermifera* increase growth performance at the expense of herbivore resistance in *Nicotiana attenuata*. *Oecologia*, **146**, 234–243.
- Barazani, O., von Dahl, C.C. and Baldwin, I.T. (2007) *Sebacina vermifera* promotes the growth and fitness of *Nicotiana attenuata* by inhibiting ethylene signaling. *Plant Physiol.* **144**, 1223–1232.
- Baum, G., Long, J.C., Jenkins, G.I. and Trewavas, A.J. (1999) Stimulation of the blue light phototropic receptor NPH1 causes a transient increase in cytosolic Ca<sup>2+</sup>. *Proc. Natl Acad. Sci. USA*, **96**, 13554–13559.
- Blume, B., Nürnberger, T., Nass, N. and Scheel, D. (2000) Receptor-mediated increase in cytoplasmic free calcium required for activation of pathogen defense in parsley. *Plant Cell*, **12**, 1425–1440.
- Boller, T. (1995) Chemoperception of microbial signals in plant cells. *Annu. Rev. Plant Physiol. Plant Mol. Biol.* **46**, 189–214.
- Borsics, T., Webb, D., Andeme-Ondzighi, C., Staehelin, L.A. and Christopher, D.A. (2007) The cyclic nucleotide-gated calmodulin-binding channel At-CNGC10 localizes to the plasma membrane and influences numerous growth responses and starch accumulation in Arabidopsis thaliana. *Planta*, **225**, 563–73.
- Carafoli, E. (2002) Calcium signalling: a tale for all seasons. *Proc. Natl Acad. Sci. USA*, **99**, 1115–1122.

Fungal cell wall extract promotes seedling growth and Ca<sup>2+</sup> elevation 205

- Carden, D.E. and Felle, H.H. (2003) The mode of action of cell wall-degrading enzymes and their interference with Nod factor signalling in *Medicago sativa* root hairs. *Planta*, **216**, 993–1002.
- Chiasson, D., Ekengren, S.K., Martin, G.B., Dobney, S.L. and Snedden, W.A. (2005) Calmodulin-like proteins from *Arabidopsis* and tomato are involved in host defense against *Pseudomonas syringae* pv. tomato. *Plant Mol. Biol.* **58**, 887–897.
- Christopher, D.A., Borsics, T., Yuen, C.Y., Ullmer, W., Andème-Ondzighi, C., Andres, M.A., Kang, B.H. and Staehelin, L.A. (2007) The cyclic nucleotide gated cation channel AtCNGC10 traffics from the ER via Golgi vesicles to the plasma membrane of *Arabidopsis* root and leaf cells. *BMC Plant Biol.* **19**, 7.
- Cullimore, J.V., Ranjeva, R. and Bono, J.-J. (2001) Perception of lipochitoooligosaccharidic nod factors in legumes. *Trends Plant Sci.* **6**, 24–30.
- Dunand, C., Crèvecoeur, M. and Penel, C. (2007) Distribution of superoxide and hydrogen peroxide in *Arabidopsis* root and their influence on root development: possible interaction with peroxidases. *New Phytol.* **174**, 332–341.
- Ehrhardt, D.W., Wais, R. and Long, S.R. (1996) Calcium spiking in plant root hairs responding to Rhizobium nodulation signals. *Cell*, **85**, 673–681.
- Felix, G., Baureithel, K. and Boller, T. (1998) Desensitization of the perception system for chitin fragments in tomato cells. *Plant Physiol.* **117**, 643–650.
- Felle, H.H., Kondorosi, É., Kondorosi, Á. and Schultze, M. (2000) How alfalfa root hairs discriminate between nod factors and oligochitin elicitors. *Plant Physiol.* **124**, 1373–1380.
- Fernandez-Pascual, M., Lucas, M., Rosario de Felipe, M., Bosca, L., Hirt, H. and Pilar Golvano, M. (2006) Involvement of mitogen-activated protein kinases in the symbiosis *Bradyrhizobium-Lupinus*. *J. Exp. Bot.* **57**, 2735–2742.
- Gilroy, S. and Jones, R.L. (1992) Gibberellic acid and abscisic acid coordinately regulate cytoplasmic calcium and secretory activity in barley aleurone protoplasts. *Proc. Natl Acad. Sci. USA*, **89**, 3591–3595.
- Glen, M., Tommerup, I.C., Bougher, N.L. and O'Brien, P.A. (2002) Are Sebacinaceae common and widespread ectomycorrhizal associates of *Eucalyptus* species in Australian forests? *Mycorrhiza*, **12**, 243–247.
- Grant, M., Brown, I., Adams, S., Knight, M., Ainslie, A. and Mansfield, J. (2000) The *RPM1* plant disease resistance gene facilitates a rapid and sustained increase in cytosolic calcium that is necessary for the oxidative burst and hypersensitive cell death. *Plant J.* **23**, 441–450.
- Harper, J.F. and Harmon, A. (2005) Plants, symbiosis and parasites: a calcium signalling connection. *Nature Rev.* **6**, 555–567.
- Harrison, M.G. (2005) Signaling in the arbuscular mycorrhizal symbiosis. *Annu. Rev. Microbiol.* **59**, 19–42.
- Hérouart, D., Badouin, E., Frenedo, P., Harrison, J., Santos, R., Jamet, A., Van de Sype, G., Touati, D. and Puppo, A. (2002) Reactive oxygen species, nitric oxide and glutathione: a key role in the establishment of the legume – *Rhizobium* symbiosis? *Plant Physiol. Biochem.* **40**, 619–624.
- Kaldorf, M., Koch, B., Rexer, K.H., Kost, G. and Varma, A. (2005) Patterns of interaction between *Populus Esch5* and *Piriformospora indica*: a transition from mutualism to antagonism. *Plant Biol.* **7**, 210–218.
- Kaló, P., Gleason, C., Edwards, A. et al. (2005) Nodulation signaling in legumes requires NSP2, a member of the GRAS family of transcriptional regulators. *Science*, **308**, 1749–1750.
- Kanamori, N., Madsen, L.H., Radutoiu, S. et al. (2006) A nucleoporin is required for induction of Ca<sup>2+</sup> spiking in legume nodule development and essential for rhizobial and fungal symbiosis. *Proc. Natl Acad. Sci. USA*, **103**, 359–364.
- Kanter, U., Usadel, B., Guerineau, F., Li, Y., Pauly, M. and Tenhaken, R. (2005) The inositol oxygenase gene family of *Arabidopsis* is involved in the biosynthesis of nucleotide sugar precursors for cell-wall matrix polysaccharides. *Planta*, **221**, 243–254.
- Kiegle, E., Moore, C.A., Haseloff, J., Tester, M.A. and Knight, M.R. (2000) Cell-type-specific calcium responses to drought, salt and cold in the *Arabidopsis* root. *Plant J.* **23**, 267–278.
- Knight, H. (2000) Calcium signaling during abiotic stress in plants. *Int. Rev. Cytol.* **195**, 269–324.
- Knight, M.R., Campbell, A.K., Smith, S.M. and Trewavas, A.J. (1991) Transgenic plant aequorin reports the effects of touch and cold-shock and elicitors on cytoplasmic calcium. *Nature*, **352**, 524–526.
- Knight, H., Trewavas, A.J. and Knight, M.R. (1997) Calcium signalling in *Arabidopsis thaliana* responding to drought and salinity. *Plant J.* **12**, 1067–1078.
- Lecourieux, D., Mazars, C., Pauly, N., Ranjeva, R. and Pugin, A. (2002) Analysis and effects of cytosolic free calcium increases in response to elicitors in *Nicotiana plumbaginifolia* cells. *Plant Cell*, **14**, 2627–2641.
- Lecourieux, D., Ranjeva, R. and Pugin, A. (2006) Calcium in plant defence-signalling pathways. *New Phytol.* **171**, 249–269.
- Lévy, J., Bres, C., Geurts, R. et al. (2004) A putative Ca<sup>2+</sup> and calmodulin dependent protein kinase required for bacterial and fungal symbioses. *Science*, **303**, 1361–1364.
- Lewis, B.D., Karlin-Neumann, G., Davis, R.W. and Spalding, E.P. (1997) Ca<sup>2+</sup>-activated anion channels and membrane depolarizations induced by blue light and cold in *Arabidopsis* seedlings. *Plant Physiol.* **114**, 1327–1334.
- Liu, Y. and Zhang, S. (2004) Phosphorylation of 1-aminocyclopropane-1-carboxylic acid synthase by MPK6, a stress-responsive mitogen-activated protein kinase, induces ethylene biosynthesis in *Arabidopsis*. *Plant Cell*, **16**, 3386–3399.
- Lorence, A., Chevone, B.I., Mendes, P. and Nessler, C.L. (2004) *myo*-inositol oxygenase offers a possible entry point into plant ascorbate biosynthesis. *Plant Physiol.* **134**, 1200–1205.
- van der Luit, A.H., Olivari, C., Haley, A., Knight, M.R. and Trewavas, A.J. (1999) Distinct signaling pathways regulate calmodulin gene expression in tobacco. *Plant Physiol.* **121**, 705–714.
- McAinsh, M.R. and Hetherington, A.M. (1998) Encoding specificity in Ca<sup>2+</sup> signalling systems. *Trends Plant Sci.* **3**, 32–36.
- McAinsh, M.R., Brownlee, C. and Hetherington, A.M. (1992) Visualizing changes in cytosolic Ca<sup>2+</sup> during the response of stomatal guard cells to abscisic acid. *Plant Cell*, **4**, 1113–1122.
- McCormack, E., Tsai, Y.C. and Braam, J. (2005) Handling calcium signaling: *Arabidopsis* CaMs and CMLs. *Trends Plant Sci.* **10**, 383–389.
- Menke, F.L., van Pelt, J.A., Pieterse, C.M. and Klessig, D.F. (2004) Silencing of the mitogen-activated protein kinase MPK6 compromises disease resistance in *Arabidopsis*. *Plant Cell*, **16**, 897–907.
- Mithöfer, A., Ebel, J., Bhagwat, A.A., Boller, T. and Neuhaus-Url, G. (1999) Transgenic aequorin monitors cytosolic calcium transients in soybean cells challenged with β-glucan or chitin elicitors. *Planta*, **207**, 566–574.
- Mitra, R.M., Gleason, C.A., Edwards, A., Hadfield, J., Downie, J.A., Oldroyd, G.E. and Long, S.R. (2004) A Ca<sup>2+</sup>/calmodulin-dependent protein kinase required for symbiotic nodule development: gene identification by transcript-based cloning. *Proc. Natl Acad. Sci. USA*, **101**, 4701–4705.
- Montesano, M., Brader, G. and Palva, E.T. (2003) Pathogen derived elicitors: searching for receptors in plants. *Mol. Plant Pathol.* **4**, 73–79.
- Moore, C.A., Bowen, H.C., Scrase-Field, S., Knight, M.R. and White, P.J. (2002) The deposition of suberin lamellae determines the magnitude of cytosolic Ca<sup>2+</sup> elevations in root endodermal cells subjected to cooling. *Plant J.* **30**, 457–465.
- Müller, J., Staehelin, C., Xie, Z.-P., Neuhaus-Url, G. and Boller, T. (2000) Nod factors and chitoooligomers elicit an increase in cytosolic calcium in aequorin-expressing soybean cells. *Plant Physiol.* **124**, 733–740.
- Murashige, T. and Skoog, F. (1962) A revised medium for rapid growth and bioassays with tobacco tissue cultures. *Physiol. Plant.* **15**, 473–497.
- Navazio, L., Moscattello, R., Genre, A., Novero, M., Baldan, B., Bonfante, P. and Mariani, P. (2007) A diffusible signal from arbuscular mycorrhizal fungi elicits a transient cytosolic calcium elevation in host plant cells. *Plant Physiol.* **144**, 673–681.
- Nühse, T.S., Peck, S.C., Hirt, H. and Boller, T. (2000) Microbial elicitors induce activation and dual phosphorylation of the *Arabidopsis thaliana* MAPK 6. *J. Biol. Chem.* **275**, 7521–7526.
- Oldroyd, G.E.D. and Downie, J.A. (2006) Nuclear calcium changes at the core of symbiosis signalling. *Curr. Opin. Plant Biol.* **9**, 351–357.
- Parniske, M. (2000) Intracellular accommodation of microbes by plants: a common developmental program for symbiosis and disease? *Curr. Opin. Plant Biol.* **3**, 320–328.
- Parniske, M. (2004) Molecular genetics of the arbuscular mycorrhizal symbiosis. *Curr. Opin. Plant Biol.* **7**, 414–421.
- Pauly, N., Knight, M.R., Thuleau, P., Graziana, A., Muto, S., Ranjeva, R. and Mazars, R. (2001) The nucleus together with the cytosol generates patterns of specific cellular calcium signatures in tobacco suspension culture cells. *Cell Calcium*, **30**, 413–421.

- Peškan-Berghöfer, T., Shahollari, B., Giong, P.H., Hehl, S., Markert, C., Blanke, V., Varma, A.K. and Oelmüller, R. (2004) Association of *Piriformospora indica* with *Arabidopsis thaliana* roots represents a novel system to study beneficial plant-microbe interactions and involves early plant protein modifications in the endoplasmic reticulum and at the plasma membrane. *Physiol. Plant.* **122**, 465–477.
- Pfaffl, M.W. (2001) A new mathematical model for relative quantification in real-time RT-PCR. *Nucleic Acids Res.* **29**, 2002–2007.
- Pham, G.H., Kumari, R., Singh, An. et al. (2004) Axenic cultures of *Piriformospora indica*. In *Plant Surface Microbiology* (Varma, A., Abbott, L., Werner, D. and Hampf, R., eds). Germany: Springer-Verlag, pp. 593–616.
- Plieth, C., Sattelmacher, B. and Knight, M.R. (2000) Ammonium uptake and cellular alkalisation in roots of *Arabidopsis thaliana*: the involvement of cytoplasmic calcium. *Physiol. Plant.* **110**, 518–523.
- Reddy, A.S.N. (2001) Calcium: silver bullet in signalling. *Plant Sci.* **160**, 381–404.
- Ren, D., Liu, Y., Yang, K.Y., Han, L., Mao, G., Glazebrook, J. and Zhang, S. (2008) A fungal-responsive MAPK cascade regulates phytoalexin biosynthesis in *Arabidopsis*. *Proc. Natl. Acad. Sci. USA*, **105**(14), 5638–5643.
- Rentel, M.C. and Knight, M.R. (2004) Oxidative stress-induced calcium signalling in *Arabidopsis*. *Plant Physiol.* **135**, 1471–1479.
- Sahay, N.S. and Varma, A. (1999) *Piriformospora indica*: a new biological hardening tool for micropropagated plants. *FEMS Microbiol. Lett.* **181**, 297–302.
- Sai, J. and Johnson, C.H. (2002) Dark-stimulated calcium ion fluxes in the chloroplast stroma and cytosol. *Plant Cell*, **14**, 1279–1291.
- Sanders, D., Pelloux, J., Brownlee, C. and Harper, J.F. (2002) Calcium at the crossroads of signaling. *Plant Cell*, **14**, S401–S417.
- Schenk, P.M., Kazan, K., Wilson, I., Anderson, J.P., Richmond, T., Somerville, S.C. and Manners, J.M. (2000) Coordinated plant defense responses in *Arabidopsis* revealed by microarray analysis. *Proc. Nat. Acad. Sci. USA*, **97**, 11655–11660.
- Shahollari, B., Varma, A. and Oelmüller, R. (2005) Expression of a receptor kinase in *Arabidopsis* roots is stimulated by the basidiomycete *Piriformospora indica* and the protein accumulates in Triton X-100 insoluble plasma membrane microdomains. *J. Plant Physiol.* **162**, 945–958.
- Shahollari, B., Vadassery, J., Varma, A. and Oelmüller, R. (2007) A leucine-rich repeat protein is required for growth promotion and enhanced seed production mediated by the endophytic fungus *Piriformospora indica* in *Arabidopsis thaliana*. *Plant J.* **50**(1), 1–13.
- Shaw, S.L. and Long, S.R. (2003) Nod factor elicit two separable calcium responses in *Medicago truncatula* root hair cells. *Plant Physiol.* **131**, 976–984.
- Sherameti, I., Shahollari, B., Venus, Y., Altschmied, L., Varma, A. and Oelmüller, R. (2005) The endophytic fungus *Piriformospora indica* stimulates the expression of nitrate reductase and the starch-degrading enzyme glucoamylase in tobacco and *Arabidopsis* roots through a homeodomain transcription factor which binds to a conserved motif in their promoters. *J. Biol. Chem.* **280**, 2641–2647.
- Sherameti, I., Venus, Y., Drzewiecki, C., Tripathi, S., Dan, V.M., Nitz, I., Varma, A., Grundler, F.M. and Oelmüller, R. (2008a) PYK10, a beta-glucosidase located in the endoplasmic reticulum, is crucial for the beneficial interaction between *Arabidopsis thaliana* and the endophytic fungus *Piriformospora indica*. *Plant J.* **54**, 428–439.
- Sherameti, I., Tripathi, S., Varma, A. and Oelmüller, R. (2008b) The root-colonizing endophyte *Piriformospora indica* confers drought tolerance in *Arabidopsis* by stimulating the expression of drought stress-related genes in leaves. *Mol. Plant Microbe Interact.* **21**, 799–807.
- Smit, P., Raedts, J., Portyanko, V., Debellé, F., Gough, C., Bisseling, T. and Geurts, R. (2005) NSP1 of the GRAS protein family is essential for rhizobial Nod factor-induced transcription. *Science*, **308**, 1749–1750.
- Takahashi, F., Yoshida, R., Ichimura, K., Mizoguchi, T., Seo, S., Yonezawa, M., Maruyama, K., Yamaguchi-Shinozaki, K. and Shinozaki, K. (2007) The mitogen-activated protein kinase cascade MKK3–MPK6 is an important part of the jasmonate signal transduction pathway in *Arabidopsis*. *Plant Cell*, **19**(3), 805–818.
- Vadassery, J., Ritter, C., Venus, Y., Camehl, I., Varma, A., Shahollari, B., Novák, O., Strnad, M., Ludwig-Müller, J. and Oelmüller, R. (2008) The role of auxins and cytokinins in the mutualistic interaction between *Arabidopsis* and *Piriformospora indica*. *Mol. Plant Microb. Interact.* **21**, 1371–1383.
- Varma, A., Verma, S., Sudha, Sahay, N.S., Butehorn, B. and Franken, P. (1999) *Piriformospora indica*, a cultivable plant growth promoting root endophyte. *Appl. Environ. Microbiol.* **65**, 2741–2744.
- Varma, A., Singh, A., Sudha et al. (2001) *Piriformospora indica*: a cultivable mycorrhiza-like endosymbiotic fungus. In *Mycota IX*. Germany: Springer Series, pp. 123–150.
- Veit, S., Wörle, J.M., Nürnberger, T., Koch, W. and Seitz, H.U. (2001) A novel protein elicitor (PaNie) from *Pythium aphanidermatum* induces multiple defense responses in carrot, *Arabidopsis*, and tobacco. *Plant Physiol.* **127**, 832–841.
- Verma, S.A., Varma, A., Rexer, K.-H., Hassel, A., Kost, G., Sarbhoy, A., Bisen, P., Butehorn, B. and Franken, P. (1998) *Piriformospora indica*, gen. et sp. nov., a new root-colonizing fungus. *Mycologia*, **90**, 898–905.
- Waller, F., Achatz, B., Baltruschat, H. et al. (2005) The endophytic fungus *Piriformospora indica* reprograms barley to salt-stress tolerance, disease resistance, and higher yield. *Proc. Natl. Acad. Sci. USA*, **102**, 13386–13391.
- Walter, A., Mazars, C., Maitrejean, M., Hopke, J., Ranjeva, R., Boland, W. and Mithöfer, A. (2007) Structural requirements of jasmonates and synthetic mimetics as inducers of Ca<sup>2+</sup> signals in the nucleus and the cytosol of plant cells. *Angew Chem – Int. Ed.* **46**, 4783–4785.
- Weiss, M., Selosse, M.A., Rexer, K.H., Urban, A. and Oberwinkler, F. (2004) Sebaciales: a hitherto overlooked cosm of heterobasidiomycetes with a broad mycorrhizal potential. *Mycol. Res.* **108**, 1003–1010.
- Wolski, E.A., Lima, C., Agusti, R., Daleo, G.R., Andreu, A.B. and de Lederkremer, R.M. (2005) An  $\alpha$ -glucan elicitor from the cell wall of a biocontrol binucleate *Rhizoctonia* isolate. *Carbohydr. Res.* **340**, 619–627.
- Yoshioka, K., Moeder, W., Kang, H.-G., Kachroo, P., Masmoudi, K., Berkowitz, G. and Klessig, D.F. (2006) The chimeric *Arabidopsis* cyclic nucleotide-gated ion channel 11/12 activates multiple pathogen resistance responses. *Plant Cell*, **18**, 747–763.

## 2.7. Contribution to publications and manuscripts

**Chapter 2.1.2: Ranf S\***, Wünnenberg P\*, Lee J, Becker D, Dunkel M, Hedrich R, Scheel D and Dietrich P (2008) Loss of the vacuolar cation channel, AtTPC1, does not impair Ca<sup>2+</sup> signals induced by abiotic and biotic stresses.

*Plant J*, 53, 287-299

\* these authors contributed equally to this paper

### Own contributions:

*Experimentation:* introgression of aequorin transgene into TPC1 knockout and overexpressing lines, design and performance of [Ca<sup>2+</sup>] measurements, gene expression studies and ROS luminol assay (45 %)

*Data analysis:* analysis of the above data (45 %)

*Writing:* design and preparation of figures for above data (45 %); strong participation in writing of the manuscript (30 %)

Other contributions: M. Dunkel, D. Becker and R. Hedrich performed co-expression studies; P. Wünnenberg and P. Dietrich performed all other assays; P. Dietrich wrote the manuscript.

**Chapter 2.2.2: Ranf S**, Eschen-Lippold L, Pecher P, Lee J and Scheel D (2011) Interplay between calcium signalling and early signalling elements during defence responses to microbe- or damage-associated molecular patterns.

**Revised manuscript submitted to *Plant Journal***

### Own contributions:

*Experimentation:* preparation of aequorin transgenic mutant lines; design and performance of most experiments; protoplast assay was performed in cooperation with L. Eschen-Lippold (90 %)

*Data analysis:* data analysis including statistical analysis (100 %)

*Writing:* design and preparation of figures (100 %); writing of the manuscript (90 %).

Other contributions: L. Eschen-Lippold cloned the promoter luciferase constructs; P. Pecher performed the *mpk* root growth assays.

**Chapter 2.3.2: Ranf S**, Grimmer J, Pöschl Y, Pecher P, Chinchilla D, Scheel D and Lee J (2011) Defence-related calcium signalling mutants uncovered via a quantitative high-throughput screen in *Arabidopsis thaliana*.

**Submitted to *Molecular Plant***

### Own contributions:

*Experimentation:* design and performance of complete mutant screen; isolation of all *cee* mutants; design of all experiments; performance of Aeq<sup>vmd</sup> mutant experiments; design and supervision of Aeq<sup>cyt</sup> mutant experiments (90 %)

*Data analysis:* data analysis including statistical analysis (95 %)

*Writing:* design and preparation of figures (100 %); writing of the manuscript (90 %)

Other contributions: J. Grimmer characterized the Aeq<sup>cyt</sup> mutants as part of a diploma thesis under my supervision; Y. Pöschl wrote the R script for analysis of 384 well-plate [Ca<sup>2+</sup>] measurements. D. Chinchilla provided the anti-FLS2 and -BAK1 antibodies.

**Chapter 2.4.2:** **Ranf S**, Eschen-Lippold L, Zähringer U, Lee J and Scheel D (2011) Lipopolysaccharides induce calcium elevations in *Arabidopsis thaliana* independent of the adapter kinase BAK1 and the calcium permeable channel DND1.

**Manuscript in preparation**

Own contributions:

*Experimentation:* design and performance of experiments (90 %)

*Data analysis:* complete data analysis (100 %)

*Writing:* design and preparation of figures (100 %); writing of the manuscript (90 %)

Other contributions: U. Zähringer provided the purified LPS preparations; protoplast assay was performed in cooperation with L. Eschen-Lippold.

**Chapter 2.5.2:** Gust AA, Biswas R, Lenz HD, Rauhut T, **Ranf S**, Kemmerling B, Gotz F, Glawischnig E, Lee J, Felix G and Nürnberger T. (2007) Bacteria-derived peptidoglycans constitute pathogen-associated molecular patterns triggering innate immunity in Arabidopsis.

*J Biol Chem*, 282, 32338-32348

Own contribution:

*Experimentation:* design and performance of [Ca<sup>2+</sup>] measurements with PGN (10 %)

*Data analysis:* analysis of above data (10 %)

*Writing:* critical reading of manuscript; experimental procedures for [Ca<sup>2+</sup>] measurements (10 %)

**Chapter 2.6.2:** Vadassery J, **Ranf S**, Drzewiecki C, Mithöfer A, Mazars C, Scheel D, Lee J and Oelmüller R. (2009) A cell wall extract from the endophytic fungus *Piriformospora indica* promotes growth of Arabidopsis seedlings and induces intracellular calcium elevation in roots.

*Plant J*, 59, 193-206

Own contributions:

*Experimentation:* design and performance of analysis of MAPK activation by anti-pTEpY immunoblot; initial CWE-induced [Ca<sup>2+</sup>] measurements in Arabidopsis roots/leaf discs and training and supervision of J. Vadassery in aequorin-based [Ca<sup>2+</sup>] measurements in Arabidopsis; J. Vadassery subsequently performed all [Ca<sup>2+</sup>] measurements in the paper (30 %)

*Data analysis:* analysis of MAPK activation and training and supervision of J. Vadassery in analysis of aequorin-based [Ca<sup>2+</sup>] measurements (20 %)

*Writing:* critical reading and corrections of manuscript (20 %)

### 3. DISCUSSION AND PERSPECTIVES

#### 3.1. The role of $\text{Ca}^{2+}$ signalling in innate immunity in *Arabidopsis*

##### *MAMPs and DAMPs induce $\text{Ca}^{2+}$ signalling in *Arabidopsis*.*

Pioneering work, mainly performed in suspension-cultured parsley, tobacco and soybean cells, has demonstrated a crucial role for  $\text{Ca}^{2+}$  as second messenger in MAMP and DAMP signalling (see 1.2.5; p. 18). Likewise, several MAMPs, such as flg22, elf18, ch8, LPS and PGN, and the DAMP Pep1 induce  $[\text{Ca}^{2+}]_{\text{cyt}}$  elevations in *Arabidopsis* seedlings and leaves as has been shown as part of this work (summarized in Figure 3–2; p. 123) and in part also by other groups (Aslam *et al.*, 2009; Ma *et al.*, 2009; Jeworutzki *et al.*, 2010; Krol *et al.*, 2010; Qi *et al.*, 2010). To facilitate discussion, the major points, indicated by the numbers ① to ⑩, are summarized in an updated signalling scheme in figure 3–1 (p. 120). In general, the  $[\text{Ca}^{2+}]_{\text{cyt}}$  elevations, also in *Arabidopsis*, belong to the first observable responses after receptor activation (Figure 3–1 ①, p. 120), occurring mostly within one minute after MAMP and DAMP addition (Figure 3–2; p. 123). Based on inhibitor studies with the  $\text{Ca}^{2+}$  channel blocker  $\text{La}^{3+}$  and the  $\text{Ca}^{2+}$  chelator BAPTA, these  $[\text{Ca}^{2+}]_{\text{cyt}}$  elevations result from an initial influx of  $\text{Ca}^{2+}$  from the apoplast (Figure S2, p. 147; Figure 3–1 ②<sup>a</sup>, p. 120) but subsequently  $\text{Ca}^{2+}$  release from internal stores may occur (Figure 1, p. 62; Figure 3–1 ②<sup>b</sup>, p. 120). Furthermore, these  $[\text{Ca}^{2+}]_{\text{cyt}}$  elevations are prerequisite for most, if not all, later responses. Electrophysiological studies show that  $\text{Ca}^{2+}$  is tightly coupled with or even upstream of plasma membrane depolarization, which likely involves  $\text{Ca}^{2+}$ -activated anion (Cl) channels (Figure 3–1 ③, p. 120; Jeworutzki *et al.*, 2010).

##### *ROS accumulation is strictly $\text{Ca}^{2+}$ -dependent.*

Inhibition of  $[\text{Ca}^{2+}]_{\text{cyt}}$  elevations with  $\text{La}^{3+}$  suggests that the MAMP-stimulated ROS generation, which is mainly catalysed by the plasma membrane-resident NADPH oxidase, RbohD (Zhang *et al.*, 2007; Mersmann *et al.*, 2010), is strictly dependent on  $\text{Ca}^{2+}$  (Figure S8, p. 150; Figure 3–1 ⑤, p. 120). This is corroborated by the various means of  $\text{Ca}^{2+}$ -dependent regulation mechanisms of RbohD. First of all,  $\text{Ca}^{2+}$  directly regulates RbohD activity by binding to two EF hand motifs located in the cytoplasmic N-terminal extension inducing conformational changes (Figure 3–1 ⑤, p. 120; Ogasawara *et al.*, 2008). RbohD is synergistically activated by phosphorylation. In potato, StCPK4 and StCPK5, phosphorylate, and thereby activate, StRbohB at two N-terminal serine residues (Kobayashi *et al.*, 2007). In *Arabidopsis* CPK4, 5, 6 and 11, are implicated to act partially redundantly in activation of RbohD, since the quadruple mutant is strongly impaired in MAMP-induced ROS accumulation (Figure 3–1 ⑤, p. 120; Boudsocq *et al.*, 2010). All four CDPKs localize to the cytoplasm as well as the nucleus. A majority of the *Arabidopsis* CDPKs, however, contain potential sites for myristoylation and palmitoylation conferring membrane tethering (Cheng *et al.*, 2002b; Hrabak *et al.*, 2003). While CPK4 and CPK11 do not harbour myristoylation sites according to *in silico* analysis, CPK5 and potentially CPK6 are myristoylated *in vitro* and may also be partially membrane-associated *in vivo* (Hrabak *et al.*, 2003).

Thus, membrane tethering of CPK5 and CPK6 may bring them into close proximity to plasma membrane resident  $\text{Ca}^{2+}$ -permeable channels for activation, as well as to their substrate RbohD for phosphorylation.

A link to phospholipid signalling is indicated by the recent demonstration that ABA-induced ROS generation in guard cells and subsequent stomatal closure requires production of PA by PLD $\alpha$ 1 and that PA directly activates RbohD by binding to the N-terminal extension (Zhang *et al.*, 2009). PA accumulates, for instance, also in suspension-cultured tomato cells upon elicitation with flg22, xylanase or chitin (van der Luit *et al.*, 2000). PLD $\alpha$ 1 and PLD $\delta$ , the most prominent of the twelve PLD isoforms in Arabidopsis, are both implicated in response to high salt, dehydration and wounding, where they have partially redundant functions (Bargmann *et al.*, 2009a, 2009b). Unlike PLD $\alpha$ 1, which was shown to be crucial for ROS generation (Sang *et al.*, 2001; Zhang *et al.*, 2009), PLD $\delta$  may be activated by ROS rather than involved in its production (Zhang *et al.*, 2003). In accordance with a potential PA activation of RbohD upon MAMP application, flg22- and elf18-induced ROS accumulation was significantly impaired in *pld $\alpha$ 1* and *pld $\alpha$ 1/ $\delta$*  mutant leaf discs and, on average, no additive effects on ROS accumulation were observed for *pld $\delta$*  (Figure 2–1, p. 54; Figure 3–1 ④, p. 120). Quantification of the PA species produced in *pld* mutants upon elicitation will give clearer insight into the role of PLD $\alpha$ 1, and possibly PLD $\delta$  in MAMP and DAMP signalling. Further investigations are needed to confirm a putative direct PA activation of RbohD in analogy to ABA signalling.

The  $\alpha$ - and  $\delta$ -class PLDs, in turn, appear to be under  $\text{Ca}^{2+}$ -dependent regulation as is suggested by the presence of  $\text{Ca}^{2+}$ -binding C2 domains and shown through *in vitro* activity assays (Qin and Wang, 2002). Unfortunately, aequorin-based quantification of the flg22- and elf18-induced  $[\text{Ca}^{2+}]_{\text{cyt}}$  elevations in the *pld $\alpha$ 1* and *pld $\alpha$ 1/ $\delta$*  mutants attempted within this work were not consistent between independently transformed lines (data not shown). Examination of independent *pld* mutant alleles may therefore help to clarify the role of  $\text{Ca}^{2+}$  in PA signalling (Figure 3–1 ④, p. 120).

Remarkably, most of the reported biotic stimuli (ch4-7, flg22, xylanase, Avr4 and Nod factor) in different systems accumulated PA *via* the PLC-DGK pathway (Figure 2–2, p. 55) with the exception of xylanase/tomato, ch7/rice and Nod factor/alfalfa that additionally activated a PLD pathway (van der Luit *et al.*, 2000; Laxalt *et al.*, 2001; den Hartog *et al.*, 2003; Yamaguchi *et al.*, 2003; de Jong *et al.*, 2004; Yamaguchi *et al.*, 2005). The reduced flg22-induced ROS accumulation in *pld $\alpha$ 1* and *pld $\alpha$ 1/ $\delta$*  observed in this work (Figure 2–1, p. 54; Figure 3–1 ④, p. 120), points to a significant role for PLD in MAMP/DAMP signalling in Arabidopsis. The residual ROS accumulation in the *pld $\alpha$ 1* and *pld $\alpha$ 1/ $\delta$*  mutant might be due to additional PA production *via* other PLD isoforms or PLC-DGK or additional RbohD activation mechanisms as discussed above (Kobayashi *et al.*, 2007; Ogasawara *et al.*, 2008; Boudsocq *et al.*, 2010). Moreover, PA probably has additional roles in MAMP/DAMP signalling, for instance in ethylene signalling (Testerink *et al.*, 2007). Additionally, ABA-induced and possibly also MAMP-induced stomatal closure is promoted by PA, since it activates not only RbohD-mediated ROS

accumulation but also inhibits the protein phosphatase ABI1 by membrane recruitment in guard cells (Zhang *et al.*, 2004; Melotto *et al.*, 2006; Zhang *et al.*, 2009; Mersmann *et al.*, 2010).

### ***MAPK activation is partially $Ca^{2+}$ -dependent.***

In tobacco, cryptogein-induced MAPK activation is strictly dependent on the  $[Ca^{2+}]_{\text{cyt}}$  elevation, since it is abrogated by  $La^{3+}$  (Lebrun-Garcia *et al.*, 1999; Lecourieux *et al.*, 2002). Likewise, Pep13-induced MAPK activation in suspension-cultured parsley cells is completely abolished by pre-treatment with  $La^{3+}$  or BAPTA (Scheel and Lee, unpublished results). By contrast, under the same conditions MAPK activation upon flg22 elicitation is only diminished in suspension-cultured Arabidopsis cells or mesophyll protoplasts (Figure S9, p. 150; Boudsocq *et al.*, 2010). This may indicate a partially  $Ca^{2+}$ -independent pathway of MAPK activation in Arabidopsis (Figure 3–1 ⑥, p. 120). Alternatively, this may be a secondary effect of the inhibitor treatment.

Several reports in Arabidopsis and tobacco suggested a role for MAPKs upstream of ROS production (Zhang *et al.*, 2007; Asai *et al.*, 2008). MPK3 and MPK6 inactivation *via* the ectopically over-expressed effector protein HopA11 diminished flg22-induced ROS accumulation, while constitutively active MKK5 induced ROS-dependent callose deposition without MAMP stimulus (Zhang *et al.*, 2007). Since MAPKs are also involved in various other signalling pathways (Rodriguez *et al.*, 2010), such as ethylene biosynthesis (Liu and Zhang, 2004) and signalling (Bethke *et al.*, 2009), and ethylene in turn regulates FLS2 expression (Boutrot *et al.*, 2010) and ROS generation (Mersmann *et al.*, 2010), the strong disturbance of the otherwise strictly regulated MAPK activation and ROS accumulation by over-expression of effectors or constitutively active MKKs, may lead to pleiotropic perturbations and may therefore not be necessarily indicative for their physiological function. In contrast, loss of MPK6 did not affect MAMP-induced ROS accumulation, while loss of MPK3 resulted in a prolonged ROS response (Figure 7, p. 47; Figure 3–1 ⑥, p. 120). Together with the enhanced flg22-induced root growth inhibition in *mpk3* mutants this may indicate a role for MPK3 in signalling attenuation. Activated signalling components generally need to be down-regulated at a certain stage to prevent overreaction but also to allow re-stimulation (Schwessinger and Zipfel, 2008). ROS levels are particularly strictly controlled as illustrated by the diverse scavenging systems, since an excessive ROS accumulation has direct detrimental effects and may lead to cell death (Davletova *et al.*, 2005; de Pinto *et al.*, 2006; Miller *et al.*, 2007).

### ***$Ca^{2+}$ -dependent defence gene expression.***

While there has been significant progress in the identification of  $Ca^{2+}$  sensor modules implicated in abiotic stress signalling in the recent years (Kudla *et al.*, 2010), comparably little is known about  $Ca^{2+}$  sensors in biotic signalling pathways. Besides regulating RbohD activity, CPK4, 5, 6, and 11, and partially also MPK3 and MPK6, contribute to MAMP-induced  $Ca^{2+}$ -dependent defence gene expression (Figure 3–1 ⑦, p. 120; Asai *et al.*, 2002; Boudsocq *et al.*, 2010). All four CDPKs localize also to the

nucleus (Boudsocq *et al.*, 2010), explaining how they can serve such distinct functions as regulation of plasma membrane-resident RbohD and nuclear gene expression. In comparison to protein kinases, the employment of  $\text{Ca}^{2+}$ - or  $\text{Ca}^{2+}/\text{CaM}$ -dependent transcription factors provides a rather direct route for  $\text{Ca}^{2+}$  regulation of gene expression (Figure 3–1 ⑦, p. 120). Accordingly, a prominent role in stress-regulated gene expression has emerged for the CAMTA-class of  $\text{Ca}^{2+}/\text{CaM}$ -dependent transcription factors. Auxin-regulated gene expression, for instance, is partially controlled by CAMTA1 (Galon *et al.*, 2010a) and cold-stimulated gene expression by CAMTA1 and CAMTA3 (Doherty *et al.*, 2009). Microarray analysis of *camta3* mutants further suggests that defence gene expression upon biotic stresses is negatively controlled by CAMTA3 (Galon *et al.*, 2008). In agreement, CAMTA3 inhibits expression of *EDSI*, a central regulator of SA-mediated defence signalling and SAR, by direct binding to the *EDSI* promoter in a  $\text{Ca}^{2+}/\text{CaM}$ -dependent manner (Du *et al.*, 2009). Since *EDSI* expression was only modestly induced upon flg22 application, a role for CAMTA3 in MAMP signalling was tested by analysing expression of *ZATI2*, which is rapidly and strongly induced by abiotic and biotic signals including flg22 (Rizhsky *et al.*, 2004; Davletova *et al.*, 2005; Miller *et al.*, 2009). Indeed, flg22-stimulated *ZATI2* expression and flg22-mediated root growth arrest were significantly reduced in *camta3* mutants (Figure 2–4, p. 56). Since *ZATI2* carries canonical CAMTA-binding motifs (vCGCGb) in its promoter (Doherty *et al.*, 2009), CAMTA3 probably binds the *ZATI2* promoter directly. Taken together, this suggests a dual role of CAMTA3 in gene regulation – as transcriptional activator, e. g. of *ZATI2* expression, or as negative regulator, e. g. of *EDSI* expression.

It remains to be shown, however, if the activation of nuclear-localized CDPKs and CAMTAs is conferred by nuclear  $[\text{Ca}^{2+}]$  changes or by translocation to the nucleus upon activation in the cytosol as reported for parsley MAPKs (Figure 3–1 ⑦, p. 120; Lee *et al.*, 2004). Although direct evidence for nuclear MAMP-induced  $[\text{Ca}^{2+}]$  changes in Arabidopsis is missing, it seems plausible in analogy to tobacco, where specific cytosolic and nuclear  $[\text{Ca}^{2+}]$  changes can occur independently and can induce distinct responses (van Der Luit *et al.*, 1999; Pauly *et al.*, 2001; Lecourieux *et al.*, 2005). In tobacco, indeed, flg22 induces nuclear  $[\text{Ca}^{2+}]$  elevations (Lecourieux *et al.*, 2005).

#### ***MAMP- and DAMP-induced $\text{Ca}^{2+}$ signalling in roots.***

Although the majority of innate immunity studies focus on leaf tissues, roots are, as well, able to sense MAMPs and DAMPs, although with different efficiencies (summarized in Figure 3–2; p. 123; Millet *et al.*, 2010). While ch8- and Pep1-induced  $[\text{Ca}^{2+}]_{\text{cyt}}$  elevations in seedling shoots and roots were similar, roots reacted only weakly to flg22 and were even insensitive to elf18 and LPS (Figure 3–2; p. 123; data not shown). The different sensitivities to the tested MAMPs and DAMPs in roots compared to shoots appear to correlate directly with the distinct expression patterns of the respective PRRs in roots, with very low expression levels of *FLS2* and *EFR* (Figure 1, p. 39). Thus, apparently, the bacterial MAMPs flg22, elf18 and LPS, in contrast to ch8, only have minor contribution to PTI in roots. Nevertheless,  $\text{Ca}^{2+}$  signalling in roots, for instance, is crucial for Rhizobium-legume and arbuscular

mycorrhizal symbiosis (Harper and Harmon, 2005; Oldroyd and Downie, 2006; Navazio *et al.*, 2007). Nod factors, for instance, induce a rapid  $\text{Ca}^{2+}$  influx and subsequent nuclear  $\text{Ca}^{2+}$  oscillations, which are decoded by a single  $\text{Ca}^{2+}$ /calmodulin-dependent protein kinase (CCaMK), DMI3 (Mitra *et al.*, 2004; Gleason *et al.*, 2006). However, Arabidopsis does not contain CCaMKs (Hrabak *et al.*, 2003; Gleason *et al.*, 2006).

$\text{Ca}^{2+}$  signalling also takes place during the beneficial interaction with the growth-promoting fungus *Piriformospora indica* that, among other species, also associates with Arabidopsis by root-colonization (Verma *et al.*, 1998; Varma *et al.*, 1999; Barazani *et al.*, 2005; Sherameti *et al.*, 2008). Root-colonization, nevertheless, needs to be strictly regulated, since excess colonization, for instance in some ethylene signalling mutants, leads to activation of defence responses (Camehl and Oelmüller, 2010; Camehl *et al.*, 2010). Thus, the maintenance of a beneficial interaction between both symbiotic partners is regulated by ethylene. Intriguingly, a crude *P. indica* cell wall extract (CWE) itself was sufficient to induce growth promoting effects, although to a lower extent than the living fungus (Figure 1, p. 97). Moreover, this CWE triggered  $[\text{Ca}^{2+}]_{\text{cyt}}$  elevations, resulting from an initial influx of apoplastic  $\text{Ca}^{2+}$ , quite specifically in Arabidopsis roots and only weakly in shoots (Figure 2, p. 98). Furthermore, the kinetics were reminiscent of other MAMP-induced  $[\text{Ca}^{2+}]_{\text{cyt}}$  elevations in Arabidopsis seedlings, regarding lag phase,  $[\text{Ca}^{2+}]_{\text{cyt}}$  amplitude and the typical subsequent prolonged decrease to resting level (Figure 3–2; p. 123). The data based on inhibitor studies and refractory behaviour point to a receptor-mediated but BAK1-independent perception of the CWE (data not shown). In addition to the cytosolic  $[\text{Ca}^{2+}]$  response, the CWE also stimulated prolonged nuclear  $[\text{Ca}^{2+}]$  changes in tobacco (Figure 2, p. 98). As these occur several minutes delayed compared to the cytosolic  $[\text{Ca}^{2+}]$  response, they may be independently generated by a nuclear  $\text{Ca}^{2+}$  release system (Figure 3–1 ⑦, p. 120; Lecourieux *et al.*, 2005; Mazars *et al.*, 2009). The identification of the underlying molecular structure will determine if the CWE-active epitope qualifies as a *bona fide* MAMP, since the fungus, and therefore presumably also the CWE, is recognized by different plant species.

### 3.2. Components shaping MAMP-induced $\text{Ca}^{2+}$ signatures in Arabidopsis

#### ***The $\text{Ca}^{2+}$ -permeable channel DND1 does not mediate MAMP-induced $\text{Ca}^{2+}$ signalling.***

The cyclic nucleotide-gated channel 2 / defence-no-death 1 (CNGC2/DND1) plays not only a crucial role in establishment of HR but is also handled as a candidate mediating the instantaneous MAMP-induced  $\text{Ca}^{2+}$  influx across the plasma membrane based on the observation that LPS- and AtPep3-induced  $[\text{Ca}^{2+}]_{\text{cyt}}$  elevations were strongly reduced in *dnd1* leaves (Ali *et al.*, 2007; Ma *et al.*, 2009; Qi *et al.*, 2010). On the contrary,  $[\text{Ca}^{2+}]_{\text{cyt}}$  elevations induced by several MAMPs, such as flg22, elf18 and several purified LPS preparations (Figure 7, p. 87), as well as flg22-induced plasma membrane depolarization, which is tightly coupled with  $\text{Ca}^{2+}$  influx, were not diminished in *dnd1* seedlings (grown in sterile medium) or mesophyll cells, respectively (Jeworutzki *et al.*, 2010). In accordance, downstream flg22-mediated root growth arrest was not impaired in *dnd1* seedlings (data not shown).

AtPep1 also induced comparable  $[Ca^{2+}]_{\text{cyt}}$  elevations in *dnd1* and wild type (data not shown). Moreover, a reduced ROS accumulation upon flg22 elicitation was reported for *dnd1* seedlings (Mersmann *et al.*, 2010). These contrasting results may be explained by the different growth conditions used, which ranged from sterile grown seedlings used here or pre-treated with flg22 (Mersmann *et al.*, 2010) to adult leaves from soil-grown plants (Jeworutzki *et al.*, 2010; Qi *et al.*, 2010). Since *dnd1* mutants constitutively express defence genes and accumulate high SA levels (Yu *et al.*, 1998), the growth conditions may lead to pleiotropic effects. Thus, soil-grown plants are dwarfed and partially show lesion-mimic phenotypes (Clough *et al.*, 2000), while seedlings in liquid culture appear healthy and have wild-type size (data not shown). In conclusion, taking the negative results obtained in this work and by others into account, a role of DND1 in early MAMP-induced  $Ca^{2+}$  signalling as reported appears very questionable.

***The vacuolar cation channel TPC1 does not contribute to stress-induced  $Ca^{2+}$  signalling.***

Two-pore channel 1 (TPC1), originally reported as plasma membrane channel mediating abiotic and biotic stress-induced  $[Ca^{2+}]_{\text{cyt}}$  elevations in tobacco (Furuichi *et al.*, 2001; Kadota *et al.*, 2004) and biotic defence responses in rice (Kurusu *et al.*, 2005), is, contrarily, located in the tonoplast in Arabidopsis and mediates slow-vacuolar (SV) currents (Figure 1, p. 24; Figure 3–1 ⑧, p. 120; Carter *et al.*, 2004; Peiter *et al.*, 2005). A proposed role for TPC1/SV channel in  $Ca^{2+}$ -induced  $Ca^{2+}$  release (CICR) from the vacuole, *via* direct  $Ca^{2+}$ -regulation of TPC1 by its two EF hand motifs (Ward and Schroeder, 1994; Bewell *et al.*, 1999; Hetherington and Brownlee, 2004; Peiter *et al.*, 2005), however, could not be confirmed by aequorin-based  $[Ca^{2+}]_{\text{cyt}}$  quantification upon application of several (SA-inducing) biotic (Figure 7, p. 29) or abiotic stimuli (Figure 6, p. 28; Figure 3–1 ⑧, p. 120). Intriguingly, loss of TPC1, the most abundant tonoplast channel in Arabidopsis encoded by a single gene, does not have obvious detrimental growth effects (own observations; Peiter *et al.*, 2005; Bonaventure *et al.*, 2007a). While loss of TPC1 reduced expression of some JA-induced defence genes, the gain-of-function mutation *fou2*, that renders the channel hyperactive, results in enhanced defence gene expression and resistance upon infection with necrotrophic pathogens and resembles  $K^+$  starvation-induced gene expression patterns (Bonaventure *et al.*, 2007a, 2007b). While not affected in ABA- or  $CO_2$ -induced stomatal closure, *tpc1* is impaired in the response to external  $Ca^{2+}$  without affecting  $[Ca^{2+}]_{\text{cyt}}$  oscillations (Figure 6, p. 28; Peiter *et al.*, 2005; Islam *et al.*, 2010). Moreover, this phenotype may be due to the enhanced expression and  $Ca^{2+}$  sensitivity of TPC1 in guard compared to mesophyll cells (Rienmuller *et al.*, 2010). Meanwhile, in the animal system, TPCs were identified as receptors for the second messenger NAADP that stimulates  $Ca^{2+}$  release from lysosomal and endosomal stores through TPC1 (Brailoiu *et al.*, 2009; Calcraft *et al.*, 2009) but so far, no function for TPC1 in plant NAADP signalling has been reported. The lack of the two EF hand motifs in animal TPCs further suggests a different,  $Ca^{2+}$ -independent mode of regulation (Ishibashi *et al.*, 2000). In conclusion, a role in stress-induced or guard cell  $Ca^{2+}$  release for TPC1 was disproved. Instead, the data collectively

suggest a role for TPC1 as downstream  $\text{Ca}^{2+}$  sensor in cation homeostasis, particularly in  $\text{K}^+$  homeostasis (Bonaventure *et al.*, 2007b; Pottosin and Schonknecht, 2007; Beyhl *et al.*, 2009).

### ***Interplay between $\text{Ca}^{2+}$ and other early signalling elements.***

A major objective of the current work is to identify components involved in regulating and shaping MAMP-induced  $[\text{Ca}^{2+}]_{\text{cyt}}$  elevations. Since the roles of two purported  $\text{Ca}^{2+}$  channels, DND1 and TPC1, are questionable, a combined approach to search for such components was applied: (i) mutant pools, produced by EMS mutagenesis, were screened for *changed calcium elevation (cce)* mutants (see 2.3) and (ii) known or potential early signalling components were analysed for their impact on MAMP-induced  $[\text{Ca}^{2+}]_{\text{cyt}}$  elevations (see 2.2). The latter approach included signalling components such as the NADPH oxidase, RbohD, or MPK3 and MPK6 that are themselves, strictly or at least partially, dependent on the  $[\text{Ca}^{2+}]_{\text{cyt}}$  elevation, respectively. Whereas loss of MPK3 or MPK6 did not significantly impinge on flg22- or elf18-induced  $[\text{Ca}^{2+}]_{\text{cyt}}$  elevations (Figure 7, p. 47), a feedback effect of RbohD-derived ROS on  $[\text{Ca}^{2+}]_{\text{cyt}}$  elevations was observed for flg22, elf18 and Pep1 and to a lesser extent also for ch8 (Figure 6, p. 46). Intriguingly, complete abrogation of MAMP-induced ROS generation in the *rbohD* mutant or by inhibition with DPI, did not result in an overall dramatic reduction of the  $[\text{Ca}^{2+}]_{\text{cyt}}$  elevations but rather affected specifically the second peak. This second peak is well visible in response to flg22, but in the case of elf18 and Pep1 often merges with the first peak to a prolonged plateau (Figure 6, p. 46; figure S4, p. 148). Thus, in the latter case the plateau was reduced to a single peak in *rbohD*. Thus, MAMP- or DAMP-induced ROS trigger an additive  $[\text{Ca}^{2+}]_{\text{cyt}}$  elevation visible as second peak or prolonged plateau (Figure 3–1 ⑨, p. 120). In tobacco cells, ROS similarly induced a second OGA-triggered  $[\text{Ca}^{2+}]_{\text{cyt}}$  peak and enhanced the cryptogein-induced  $[\text{Ca}^{2+}]_{\text{cyt}}$  response (Lecourieux *et al.*, 2002). The timing of the second  $[\text{Ca}^{2+}]_{\text{cyt}}$  peak, with a maximum at around five minutes after flg22 elicitation (Figure 6, p. 46), thereby correlates with the ROS production kinetics, starting three to four minutes after flg22 elicitation (Figure 4, p. 43). Accordingly, the second  $[\text{Ca}^{2+}]_{\text{cyt}}$  peak, as well as the ROS production are around one or two minutes delayed upon elf18 or Pep1 treatment due to the longer lag phase (~1 minute) in comparison to flg22 (~40 seconds) and the lower ROS accumulation (Figure 4, p. 43; data not shown). Ch8, in contrast, with a similar  $[\text{Ca}^{2+}]_{\text{cyt}}$  elevation lag phase as flg22 (~40 seconds) but only a delayed (~4 minutes) and significantly lower ROS accumulation than flg22 and elf18 (Figure 5, p. 85), accordingly, shows only a minor secondary  $[\text{Ca}^{2+}]_{\text{cyt}}$  elevation at around 7 minutes (Figure 6, p. 46). Regardless of the duration of the ROS accumulation (~30 minutes for flg22), the secondary ROS-induced  $[\text{Ca}^{2+}]_{\text{cyt}}$  elevation appears to only last a few minutes, comparable to a directly  $\text{H}_2\text{O}_2$ -triggered  $[\text{Ca}^{2+}]_{\text{cyt}}$  elevation (Figure 6, p. 28; Rentel and Knight, 2004), maybe owing to saturation and refractory period of the  $\text{H}_2\text{O}_2$  perception system. This is further indicated by the unaltered secondary  $[\text{Ca}^{2+}]_{\text{cyt}}$  elevation induced by flg22 in *mpk3* mutants despite the significantly prolonged ROS response (Figure 7, p. 47). Although  $\text{H}_2\text{O}_2$ -responsive  $\text{Ca}^{2+}$ -permeable channels in the plasma membrane have been described (Pei *et al.*, 2000; Rentel and Knight, 2004), it can not be

concluded from the current data whether apoplastic RbohD-derived  $O_2^{\cdot-}$  or its dismutation product  $H_2O_2$  directly or indirectly activate  $Ca^{2+}$ -permeable channels and whether the ROS-triggered  $[Ca^{2+}]_{cyt}$  elevation is caused by  $Ca^{2+}$  influx from the apoplast or internal stores (Figure 3–1 ⑨, p. 120). Since  $H_2O_2$  is membrane-permeant it can not only activate signalling in the cell interior but also at or in neighbouring cells (Figure 3–1 ⑩, p. 120). Indeed, in abiotic stress reactions, RbohD-derived ROS trigger long-distance signalling (Miller *et al.*, 2009). Although the authors concluded from inhibitor studies with  $La^{3+}$  and BAPTA that ROS-mediated cell-to-cell signalling does not require  $Ca^{2+}$  (Miller *et al.*, 2009), this appears rather unlikely with regard to the multiple  $Ca^{2+}$ -dependent regulation modes of RbohD. The inhibitor concentration or distribution may not have been sufficient to suppress  $H_2O_2$ -triggered  $Ca^{2+}$  signalling completely, since the  $Ca^{2+}$ -ROS signalling loop may be self-sustaining and may only require an initial local trigger. Alternatively,  $H_2O_2$  may release  $Ca^{2+}$  from internal stores, which is not inhibited by  $La^{3+}$  or BAPTA. In conclusion, it appears plausible that the feedback effect between ROS and  $Ca^{2+}$  signalling observed here, may also allow cell-to-cell propagation of MAMP and DAMP signals (Figure 3–1 ⑩, p. 120).

#### ***MAMP-induced $Ca^{2+}$ release from internal stores.***

While a primary influx of apoplastic  $Ca^{2+}$  across the plasma membrane appears to be crucial to initiate MAMP-induced  $Ca^{2+}$  signalling (Figure 3–1 ②<sup>a</sup>, p. 120), this does not exclude subsequent release of  $Ca^{2+}$  from internal stores (Figure 3–1 ②<sup>b</sup>, p. 120). In the majority of cases, the distinction between  $Ca^{2+}$  release from external and internal stores is based on pharmacological studies. Thus, using the classical inhibitors successfully used for animal models, it was proposed that plants rely on the same  $Ca^{2+}$  release mechanisms, namely  $InsP_3$ - and cADPR/ryanodine-responsive  $Ca^{2+}$  channels residing in the vacuolar and ER endomembrane systems (see 1.1.2; Figure 1–1, p. 5), albeit genetic evidence is yet missing. On the contrary, the examination of several plant genomes revealed no homologs to these animal channels in higher plants (Wheeler and Brownlee, 2008). Moreover, assessing the phospholipid composition and the repertoire of the corresponding enzymes in plants suggests that PA and  $InsP_6$  may constitute the actual second messengers in plants (Munnik and Testerink, 2009).

Most inhibitors have been adapted from animal systems without evaluation of their effectiveness and specificity in plants. Noteworthy, often enormously high concentrations are required for effects in plants, which may lead to unspecific or even toxic side effects. Hence, conclusions based on pharmacological studies need to be carefully and critically assessed. In case of the interplay between  $Ca^{2+}$  and ROS signalling, the data obtained from experiments with the NADPH oxidase inhibitor DPI could be confirmed by a genetic approach using *rbohD* knockouts (Figure 6, p. 46). Inhibitor manipulations of flg22-induced  $[Ca^{2+}]_{cyt}$  and  $[Ca^{2+}]_{vmd}$  elevations, performed in *Arabidopsis* seedlings, further suggested a contribution of PLC-derived  $InsP_3/InsP_6$  (Figure 2–2, p. 55) to  $Ca^{2+}$  release from internal stores (data not shown). Due to the quite high inhibitor concentrations required, however, this was not further followed up but, instead, tested genetically. Genetic analysis may, however, be

hampered by functional redundancies, since *Arabidopsis* comprises nine PLC genes. Flg22-induced  $[Ca^{2+}]_{\text{cyt}}$  elevations were unaltered in several *plc* single as well as a *plc3plc6plc9* triple mutant (data not shown). Likewise, a knockdown of the last enzyme in the  $InsP_6$  synthesis pathway, IPK1, did not affect flg22-induced  $[Ca^{2+}]_{\text{cyt}}$  elevations (Figure 2–3, p. 55). Although the overall  $InsP_6$  content was substantially reduced in *ipk1* (Stevenson-Paulik *et al.*, 2005; Murphy *et al.*, 2008), the residual enzyme activity may still have been sufficient for signalling. Thus, further independent knockout alleles, also in combination with knockout of IPK2 $\alpha/\beta$  (Figure 2–2, p. 55), need to be examined for MAMP-induced  $[Ca^{2+}]_{\text{cyt}}$  elevations. Until now, there is no genetic evidence for a contribution of PLC-derived  $InsP_3/InsP_6$  in MAMP-induced  $Ca^{2+}$  signalling. Furthermore, PLD $\alpha 1$ , which apparently is causal for about 50% of the flg22-induced ROS accumulation (Figure 2–1, p. 54), directly produces PA from structural phospholipids without generation of  $InsP_3$  or  $InsP_6$  (Figure 2–2, p. 55).

Nevertheless, inositol derivatives have been implicated in plant immunity. For instance, *ips2* and *ipk1* are impaired in basal resistance and nuclear localized IPS1 contributes to programmed cell death (Murphy *et al.*, 2008; Meng *et al.*, 2009). Intriguingly, flg22-mediated root growth inhibition was enhanced in *ipk1* but not *ips1* or *ips2* compared to wild type (Figure 2–3, p. 55). The flg22-mediated root growth phenotype in *ipk1* is probably not mediated by  $Ca^{2+}$  signalling. Instead,  $InsP_6$  may, for example, act through gene expression regulation as shown in yeast and animals (York, 2006; Alcazar-Roman and Went, 2008; Michell, 2008; Shears, 2009) or through its function in auxin signalling.  $InsP_6$  is required for auxin binding to the auxin receptors TIR1 (transport inhibitor response 1), AFB2, and AFB3 (auxin signalling F-box proteins 2 and 3), which are targeted by the flg22-induced microRNA393 (Navarro *et al.*, 2006; Tan *et al.*, 2007), thereby providing a speculative but plausible link between flg22 and auxin signalling involving  $InsP_6$ . It will be interesting to examine the role of auxin and  $InsP_6$  in MAMP responses, since the underlying mechanism for growth inhibition, which is regularly analysed as measure of MAMP responsiveness, is not identified. It is not known yet if the growth arrest is caused by specific hormonal-regulated processes or is a simple trade-off of the energy consuming defence responses. Intriguingly, seedlings growth arrest has so far been only reported for the peptides flg22, elf18 and Pep1 requiring BAK1 for full responsiveness, a crucial co-receptor in brassinosteroid signalling (Felix *et al.*, 1999; Nam and Li, 2002; Chinchilla *et al.*, 2007; Krol *et al.*, 2010).

To further address the potential involvement of  $Ca^{2+}$  release from internal stores in MAMP signalling, a genetic screen was performed using the  $Aeq^{vmd}$  reporter line with aequorin localized to the vacuolar microdomain (see 2.3). This screen may potentially result in mutants altered in  $Ca^{2+}$  release from the vacuole, the major internal  $Ca^{2+}$  store of plants.

### 3.3. Do MAMP-induced $Ca^{2+}$ signatures encode MAMP-specific information?

An intriguing question in  $Ca^{2+}$  signalling in general concerns the information transmitted by the  $Ca^{2+}$  signals. Does the MAMP-induced “ $Ca^{2+}$  signature” encode and relay MAMP-specific information or do MAMP-induced  $[Ca^{2+}]_{\text{cyt}}$  elevations merely act as “ $Ca^{2+}$  switches” in a threshold-dependent manner?

### MAMP- and DAMP-induced $[Ca^{2+}]_{cyt}$ elevations show some common characteristics.

The analysis of several MAMP- and DAMP-induced  $[Ca^{2+}]_{cyt}$  elevations in Arabidopsis seedlings revealed typical common characteristics (summarized in Figure 3–2; p. 123): after a lag phase of mostly one minute or less, the  $[Ca^{2+}]_{cyt}$  steeply increases to the maximum amplitude. In some cases, a biphasic response is visible with two distinct peaks but often the peaks merge to a prolonged “plateau” phase. Subsequently, the  $[Ca^{2+}]_{cyt}$  declines slowly back to resting level over 30–40 minutes. All in all, similar

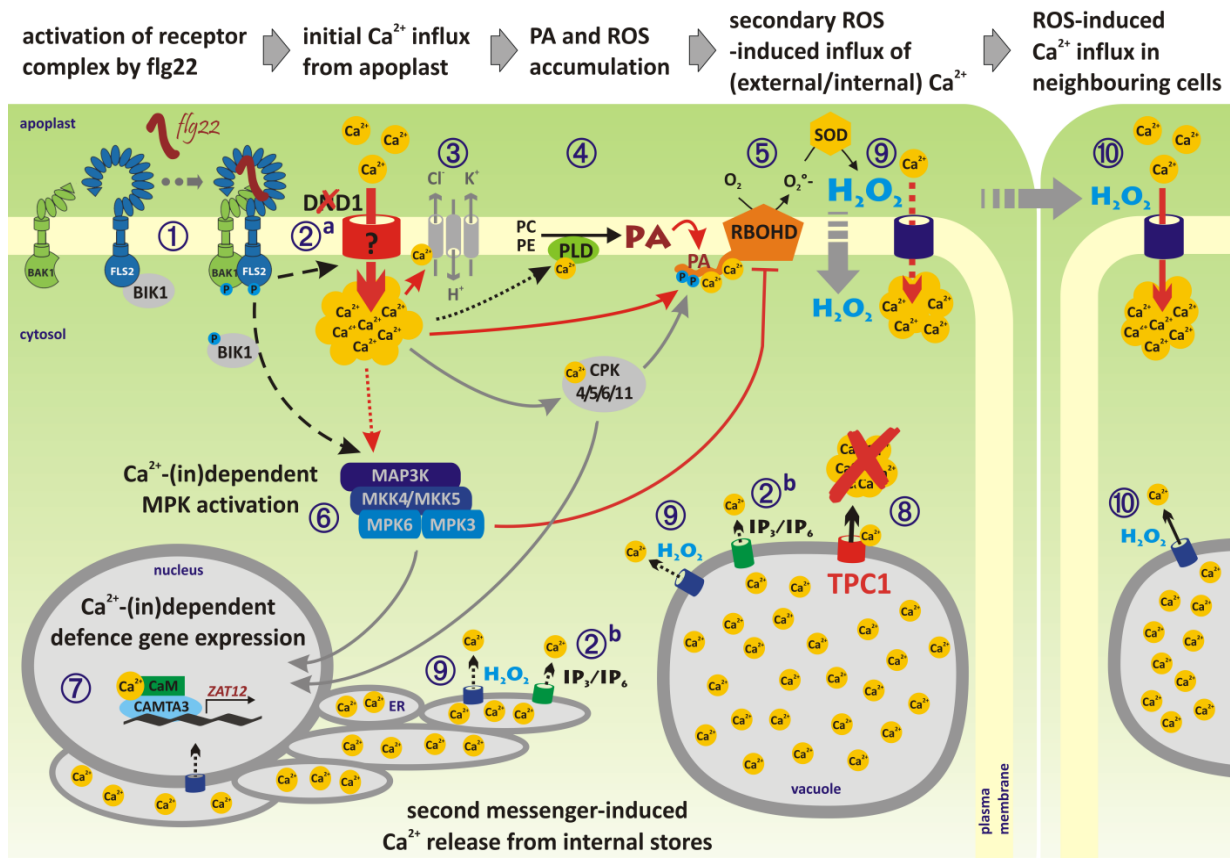


**Figure 3–1. Overview of early flg22-stimulated signalling steps in Arabidopsis.**

① Upon flg22 binding, the FLS2 receptor kinase associates with the BAK1 kinase and trans-phosphorylation is thought to activate the FLS2-BAK1 receptor complex. The cytoplasmic kinase BIK1 is presumably released from the receptor complex upon trans-phosphorylation with FLS2/BAK1. ② FLS2 activation triggers a rapid influx of apoplastic  $Ca^{2+}$  into the cytosol, which is not mediated by the cyclic nucleotide-gated  $Ca^{2+}$ -permeable channel DND1. Subsequently,  $Ca^{2+}$  may also be released from internal stores, e. g. through second-messenger-activated channels. ③ Concomitant ion fluxes, e. g. through  $Ca^{2+}$ -activated anion channels, lead to plasma membrane depolarization. ④ Activation of PLD $\alpha$ 1, presumably in a  $Ca^{2+}$ -dependent manner, generates PA. ⑤  $Ca^{2+}$ , CDPKs and PA synergistically activate the plasma membrane-resident NADPH oxidase RbohD that generates apoplastic  $O_2^{\cdot-}$ , which is rapidly converted to  $H_2O_2$  by superoxide dismutases (SOD). ⑥ The (partially)  $Ca^{2+}$ -dependent activation of MPK3, in parallel, appears to attenuate ROS accumulation. Activation of CDPKs and MAPK cascades further results in gene expression re-modulation. ⑦ Gene expression is also directly controlled via  $Ca^{2+}$ - or  $Ca^{2+}$ /CaM-dependent transcription factors, such as CAMTA3 that, for instance, activates expression of the early defence gene ZAT12. This may involve nuclear  $[Ca^{2+}]$  elevations. ⑧ The tonoplast cation channel TPC1 does not, in contrast to earlier predictions, mediate  $Ca^{2+}$ -induced  $Ca^{2+}$  release from the vacuole. ⑨ The  $Ca^{2+}$ -dependent generation of  $H_2O_2$  feeds back on the  $[Ca^{2+}]_{cyt}$  elevations since membrane-permeant  $H_2O_2$  triggers a subsequent additional  $[Ca^{2+}]_{cyt}$  elevation either through  $Ca^{2+}$  influx from the apoplast or  $Ca^{2+}$  release from internal stores. ⑩ The diffusible  $H_2O_2$  may also trigger  $[Ca^{2+}]_{cyt}$  elevations in neighbouring cells.

**Abbreviations:** CDPK =  $Ca^{2+}$ -dependent protein kinase; DND1 = defence-no-death; IP<sub>3/6</sub> = inositol-tris/hexakis-phosphate; MAPK = mitogen-activated protein kinase; PA = phosphatidic acid; PLD = phospholipase D; ROS = reactive oxygen species; TPC1 = two-pore channel 1

to MAMP-induced  $[Ca^{2+}]_{cyt}$  responses observed, for instance, in parsley or tobacco cells (Blume *et al.*, 2000; Lecourieux *et al.*, 2002; Lecourieux *et al.*, 2005), MAMP-induced  $[Ca^{2+}]_{cyt}$  elevations in Arabidopsis appear to be generally sustained (Figure 3–2; p. 123). In most cases, a primary influx of apoplastic  $Ca^{2+}$  across the plasma membrane is required to initiate the  $[Ca^{2+}]_{cyt}$  response, as illustrated by the complete inhibition with  $La^{3+}$  or BAPTA (Figure 6, p. 86; figure S2, p. 147). However, a secondary  $Ca^{2+}$  influx from external or release from internal stores may account for the different “fine structures” observed for the responses to distinct MAMPs, for instance the ROS-induced second peaks induced by flg22 in Arabidopsis (Figure 6, p. 46) or OGAs in tobacco (Lecourieux *et al.*, 2002).

### ***MAMP- and DAMP-induced $[Ca^{2+}]_{cyt}$ elevations – what can be compared?***

Since the PGN preparations are hardly soluble in water, this may account for the delayed and low  $[Ca^{2+}]_{cyt}$  response observed upon application of PGN suspensions (Figure 2–5, p. 93). Likewise the solubility of LPS correlates with its molecular structure with S-LPS being more soluble than R-LPS forms. Additionally, it is unlikely, that the macromolecular forms of PGN, LPS and chitin constitute the physiologically elicitor-active forms. Instead, plant-derived apoplastic enzymes, such as chitinases, glucanases and proteases, are likely necessary to release elicitor-active fragments that subsequently can be perceived by cell wall-associated or plasma membrane-resident PRRs (Zipfel and Felix, 2005; Hückelhoven, 2007; Göhre and Robatzek, 2008). This is, for instance, illustrated by the fungal *C. fulvum* effector protein Avr4 that binds long-chain chitin oligosaccharides to protect fungal hyphae from chitinase attack (van den Burg *et al.*, 2004; van den Burg *et al.*, 2006; de Jonge *et al.*, 2010). Furthermore, cell-wall localised or plasma membrane-associated binding proteins may be required to assist perception and transduction of certain MAMP signals, as is, for example, the case for the chitin-binding protein CeBIP in rice or the glucan-binding protein GPB from soybean that also has an intrinsic endoglucanase activity (Zipfel, 2009). Since these binding proteins lack intracellular (kinase) domains for signal transduction, they need to interact with another transmembrane transducer containing intracellular signalling domains (Zipfel, 2009). Moreover, LPS perception in the mammalian system is conferred by an LPS-binding protein (LBP), a lipid transferase that catalyzes LPS transfer from the bacterial membrane to CD14 and finally TLR4 for signal transduction (Miyake, 2004). Thus, the enzymatic activity of LBP is crucial for processing and exposing LPS to the host perception system, since membrane-bound LPS is inactive as PAMP (Miyake, 2004). The peptide MAMPs, flg22 and elf18, instead directly bind their cognate RLK-PRRs (Chinchilla *et al.*, 2006; Zipfel *et al.*, 2006). Nevertheless, recognition of the respective full-length proteins flagellin and EF-Tu may also require processing by host enzymes to facilitate perception, since, for instance, the flg22 epitopes are not surface exposed within the flagellum and thus not directly accessible for receptor binding (Zipfel and Felix, 2005). Optimized small synthetic peptides that are easily accessible for receptor binding, such as flg22, elf18 and Pep1 and fully active as MAMPs or DAMPs are regularly used in innate immunity studies. They were also preferentially used in this work not only because of the advantages in handling

and availability but also to avoid potential contaminations in MAMP preparations from cultures (see also 2.4). Likewise, the water soluble chitin oligosaccharide ch8 was used instead of an undefined mixture of chitin fragments derived from ground crab shells. It is, however, generally difficult to compare  $\text{Ca}^{2+}$  responses induced by small synthetic peptides on the one hand, and poorly soluble macromolecules on the other hand, since host processing may account for different kinetics.

***MAMP- and DAMP-specific differences in  $[\text{Ca}^{2+}]_{\text{cyt}}$  elevations are partially controlled by BAK1.***

To achieve synchronous elicitation, which is a prerequisite for resolving kinetic characteristics in a multicellular system, apparent saturating MAMP concentrations and liquid-grown seedlings were used to overcome the variation caused by different cell wall accessibility and to compare the maximum  $[\text{Ca}^{2+}]_{\text{cyt}}$  elevation-inducing capacities of different MAMPs and DAMPs (Figure 3–2; p. 123). Nevertheless, all MAMPs used were also active at low concentrations (Figure 4, p. 84; figure S3, p. 148). Under saturating conditions, MAMP-specific differences in lag phases and  $[\text{Ca}^{2+}]_{\text{cyt}}$  amplitudes were observed that most probably are intrinsic characteristics of the distinct MAMPs and their respective receptor complexes rather than simple differences in diffusion rate through the cell wall matrix as suggested (Figure 3–2; p. 123; Aslam *et al.*, 2009). In medium alkalization assays in suspension-cultured Arabidopsis cells, which are more readily accessible to peptides compared to intact tissues or organs, also distinct lag phases for flg22 and elf18 were observed (Zipfel *et al.*, 2006). LPS-induced  $[\text{Ca}^{2+}]_{\text{cyt}}$  amplitudes, for instance, all were in the same range of maximum  $\sim 150$  nM regardless of the different molecular weight and steric conditions, i. e. smooth or deep rough LPS forms (Figure 2, p. 83). Furthermore, the three peptide MAMPs/DAMPs, flg22, elf18 and Pep1, showed highly reproducible and characteristic  $[\text{Ca}^{2+}]_{\text{cyt}}$  amplitudes throughout all experiments (Figure 3–2; p. 123). While flg22 induced  $[\text{Ca}^{2+}]_{\text{cyt}}$  amplitudes of up to 300 nM, elf18 reached a maximum amplitude of  $\sim 200$  nM and Pep1 only  $\sim 170$  nM (Figure 1, p. 39). Strikingly, the  $[\text{Ca}^{2+}]_{\text{cyt}}$  amplitudes were almost identical in *bak1* mutants under the same conditions,  $\sim 150$  nM for all three MAMPs or DAMPs (Figure 3, p. 41). This suggests that flg22, elf18 and Pep1 are generally quantitatively similarly perceived but the signal is differentially amplified by the receptor-associated kinase BAK1 thereby resulting in the MAMP-specific  $[\text{Ca}^{2+}]_{\text{cyt}}$  amplitudes. Ch8- and LPS-triggered  $[\text{Ca}^{2+}]_{\text{cyt}}$  elevations, conversely, are not altered in *bak1*. Moreover, BAK1 also accelerates early flg22, elf18 and Pep1 responses, as the lag phases of the  $[\text{Ca}^{2+}]_{\text{cyt}}$  responses are severely delayed in *bak1* mutants (Figure 3, p. 41). Taken together, although MAMP- and DAMP-induced  $[\text{Ca}^{2+}]_{\text{cyt}}$  elevations share some characteristics, at the same time MAMP- and DAMP-specific variations in certain parameters are observable (Figure 3–2; p. 123). Similarly, different MAMPs and DAMPs induce generally a common set of defence responses, but these often differ in a qualitative, quantitative or kinetic manner. For instance, both, flg22 and elf18, induce the same defence genes, albeit with distinct kinetics (Figure 5, p. 45), and both mediate a prominent seedling growth arrest but with obviously different phenotypes (Figure 2, p. 40). Hence, it appears possible and also plausible that the distinct  $[\text{Ca}^{2+}]_{\text{cyt}}$  elevations

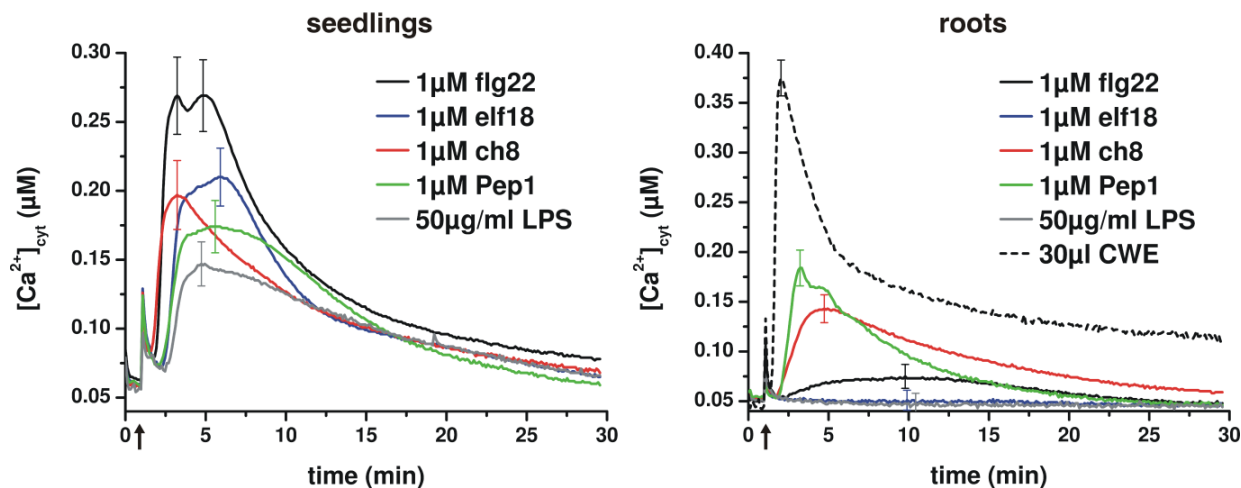


**Figure 3–2. Comparison of different MAMP- and DAMP-induced  $[Ca^{2+}]_{\text{cyt}}$  elevations in intact seedlings and isolated roots.**

$[Ca^{2+}]_{\text{cyt}}$  elevations upon application (marked by arrow) of the indicated MAMPs and DAMPs in intact Col-0 seedlings (left panel) or isolated roots (right panel) were monitored over time by aequorin-based  $[Ca^{2+}]_{\text{cyt}}$  measurements.

encode information contributing to the MAMP-specific responses. On the contrary, *bak1* mutants show similar as well as distinct downstream responses to different MAMPs, despite nearly identical  $[Ca^{2+}]_{\text{cyt}}$  elevations (Figure 3, p. 41). This strongly argues against the conception that the  $[Ca^{2+}]_{\text{cyt}}$  elevations (alone) are sufficient to convey MAMP-specific information into downstream responses. Taken together, the obtained data support a threshold function for  $Ca^{2+}$  in MAMP and DAMP signalling, as has also been suggested by Dodd and co-authors (2010).

#### **Limitations of aequorin-based $Ca^{2+}$ reporters.**

Regarding the question whether  $[Ca^{2+}]_{\text{cyt}}$  elevations encode and transmit MAMP-specific information it needs to be considered that aequorin-based  $[Ca^{2+}]$  imaging always gives an average response of whole seedlings/tissues consisting of different cell types whose individual responses can differ substantially. For instance, the different  $Ca^{2+}$  content between guard and mesophyll cells (Conn *et al.*, 2011) may influence MAMP-induced  $Ca^{2+}$  signatures in these cell types. Distinct root cell types, for instance, react differentially to salt but equally to cold stress (Kiegle *et al.*, 2000). Hence, the underlying single cell  $Ca^{2+}$  signatures can not be simply deduced from aequorin-based  $[Ca^{2+}]$  imaging of whole seedlings. Aequorin-based measurements, for example, can not reveal if the MAMP-induced  $[Ca^{2+}]_{\text{cyt}}$  elevations are based on sustained  $Ca^{2+}$  influx or are an overlay of asynchronous oscillations. While  $Ca^{2+}$  imaging upon elicitation with Pep13 in suspension-cultured parsley cells point to a sustained elevated  $[Ca^{2+}]$  level rather than oscillations (Blume *et al.*, 2000), this question could not be addressed in Arabidopsis by aequorin-based measurements of whole seedlings.

Nevertheless, the data provided here demonstrate that aequorin-based  $[Ca^{2+}]$  measurements are applicable for mutant analysis. Thus, synchronous elicitation revealed “fine structures” of the  $[Ca^{2+}]_{\text{cyt}}$  response as illustrated in *rbohD*. Though, it can not be concluded if these secondary ROS-induced

$\text{Ca}^{2+}$  release/influx occurs in the same or in neighbouring cells or from external or internal stores. Resolution of  $[\text{Ca}^{2+}]_{\text{cyt}}$  elevations at the single cell level is so far only feasible in single cell systems such as guard cells or root hairs but even there the resolution of the intracellular locations of the  $[\text{Ca}^{2+}]$  elevations is limited. In the case of mesophyll cells, direct cell access is difficult in intact tissues and thus protoplasting is required, which, in turn, might alter the  $\text{Ca}^{2+}$  signatures. While suspension-cultured cells are highly applicable for synchronous elicitation and often comprise only a single but re-differentiated cell type, their analysis is mostly limited to pharmacological studies. Bearing these constraints in mind, the presented work, demonstrates that aequorin-based  $[\text{Ca}^{2+}]$  quantification is indeed applicable for diagnostic purposes in reverse as well as forward genetic screening.

#### **3.4. $[\text{Ca}^{2+}]_{\text{cyt}}$ elevations as quantitative and kinetic read-out for early signalling events**

Measuring alkalinization of the growth medium of suspension-cultured cells is a well-established assay to assess the putative elicitor activity of a test substance by an early, sensitive and quantifiable response (Felix *et al.*, 1993; Tavernier *et al.*, 1995; Felix *et al.*, 1999). Since the ion fluxes causal for the medium alkalinization response (AR) occur temporally close to the receptor activation and constitute a defined biochemical response, the medium alkalinization reflects the activity of the receptor complex. Stimulus-induced  $[\text{Ca}^{2+}]_{\text{cyt}}$  elevations, which are tightly coupled to ion fluxes and AR (Jeworutzki *et al.*, 2010), likewise resemble the activity of upstream receptor complex and signalling components. Moreover,  $[\text{Ca}^{2+}]$  measurements are applicable to distinct tissues, such as whole seedlings, leaf discs, roots or epidermal strips. Currently, mutant analysis of MAMP-induced defence responses is mainly performed by analysing ROS accumulation or MAMP-mediated seedling growth arrest. While the growth arrest response is well quantifiable, it is a “late” response whose biochemical mechanism is yet unresolved. As a “late” response, seedling growth arrest assays are not only time-consuming but also suffer from various unpredictable developmental or environmental cues leading to pleiotropic side effects. ROS accumulation, on the other hand, is a well-defined early response. However, ROS accumulation cannot be accurately quantified and is very variable in leaf discs and particularly in seedlings between different but even within a single experiment. Pre-treatment of seedlings with low MAMP concentrations has been reported to reduce variability between the responses of individual seedlings (Mersmann *et al.*, 2010). However, such pre-treatment with MAMPs, in turn, or wounding, during leaf discs preparation, may have “priming” effects altering the end response.  $[\text{Ca}^{2+}]$  measurements, either based on aequorin or ratiometric cameleon technology, instead, yield very accurate quantification due to the internal normalization, which is well reproducible even between independent experiments, thus allowing robust statistical evaluation. Additionally, the  $[\text{Ca}^{2+}]$  response yields high temporal resolution in single cells as well as multicellular tissues if the stimulus is applied synchronously. This can, for instance be achieved by using liquid-grown seedlings or thinly-cut leaf strips. Hence, like the AR,  $[\text{Ca}^{2+}]$  measurements are highly applicable for assessing early upstream MAMP-induced activities, including receptor complex components, in the whole seedling system and, most importantly, are highly suited for rapid and

sensitive high-throughput mutant screens (see 2.3). Moreover,  $\text{Ca}^{2+}$  reporters can be targeted to (i) distinct cell types (Kiegle *et al.*, 2000) or (ii) distinct intracellular locations (Knight *et al.*, 1996; Mithöfer and Mazars, 2002), thus allowing dissection of signalling processes at sub-tissue and even sub-cellular level in combination with mutant analysis. The efficacy of  $\text{Ca}^{2+}$  screening was demonstrated in this work by the isolation of several additional *fls2* and *bak1* alleles, as well as several novel *cce* mutants (see 2.3). Intriguingly, one subset of *cce* mutants shows only altered responses to flg22, elf18 and Pep1, while the other mutants additionally show altered  $[\text{Ca}^{2+}]$  elevations upon ch8 and LPS elicitation (Table 1, p. 71; data not shown). Thus, all isolated *cce* mutants are common components of signalling pathways shared by several MAMPs.

### 3.5. Conclusions

The detailed comparison of  $[\text{Ca}^{2+}]_{\text{cyt}}$  elevations triggered by diverse MAMPs and DAMPs, such as the peptides flg22, elf18 and Pep1 and the polysaccharide-containing ch8, LPS and PGN, revealed common as well as MAMP/DAMP-specific characteristics. Distinct MAMPs and DAMPs further stimulate a common set of defence responses by sharing several signalling components. Nevertheless, early and late responses have been shown to differ quantitatively as well as qualitatively in response to certain MAMPs or DAMPs.  $\text{Ca}^{2+}$  signalling plays a pivotal role in all studied MAMP and DAMP signalling pathways. Although the MAMP/DAMP-specific characteristics of the  $[\text{Ca}^{2+}]_{\text{cyt}}$  elevations may contribute to the MAMP/DAMP specificity of some downstream responses, it is, based on the presented data, unlikely that the  $[\text{Ca}^{2+}]_{\text{cyt}}$  elevations are by themselves sufficient to convey MAMP/DAMP specificity. Instead, BAK1 appears to differentially regulate certain early as well as late MAMP/DAMP responses. Furthermore, feedback effects between different early signalling components were uncovered. In conclusion, MAMP- and DAMP-stimulated signalling pathways are not hierarchical but multilayered and manifold interrelated which may result in differential signal amplification or attenuation at several levels leading to distinct end responses. The novel isolated *cce* mutants, which are also commonly involved in signalling by several MAMPs, will be useful to further unveil the early signalling events in innate immunity. Taken together, the various signalling components acting in, up- and downstream of  $\text{Ca}^{2+}$  signalling form a complex and versatile signalling network.

#### 4. REFERENCES

- Albert, P, Miya, A, Hiratsuka, K, Kawakami, N and Shibuya, N** (2006) A high-throughput evaluation for Arabidopsis mutants for defense signaling. *Plant Biotechnology* **23**: 459-466
- Albrecht C, Russinova E, Kemmerling B, Kwaaitaal M, de Vries SC** (2008) Arabidopsis SOMATIC EMBRYOGENESIS RECEPTOR KINASE proteins serve brassinosteroid-dependent and -independent signaling pathways. *Plant Physiol* **148**: 611-619
- Albus U, Baier R, Holst O, Pühler A, Niehaus K** (2001) Suppression of an elicitor-induced oxidative burst reaction in *Medicago sativa* cell cultures by *Sinorhizobium meliloti* lipopolysaccharides. *New Phytologist* **151**: 597-606
- Alcazar-Roman AR, Wentz SR** (2008) Inositol polyphosphates: a new frontier for regulating gene expression. *Chromosoma* **117**: 1-13
- Ali R, Ma W, Lemtiri-Chlieh F, Tsaltas D, Leng Q, von Bodman S, Berkowitz GA** (2007) Death don't have no mercy and neither does calcium: Arabidopsis CYCLIC NUCLEOTIDE GATED CHANNEL2 and innate immunity. *Plant Cell* **19**: 1081-1095
- Ali R, Zielinski RE, Berkowitz GA** (2006) Expression of plant cyclic nucleotide-gated cation channels in yeast. *J Exp Bot* **57**: 125-138
- Allen GJ, Chu SP, Harrington CL, Schumacher K, Hoffmann T, Tang YY, Grill E, Schroeder JI** (2001) A defined range of guard cell calcium oscillation parameters encodes stomatal movements. *Nature* **411**: 1053-1057
- Allen GJ, Chu SP, Schumacher K, Shimazaki CT, Vafeados D, Kemper A, Hawke SD, Tallman G, Tsien RY, Harper JF, Chory J, Schroeder JI** (2000) Alteration of stimulus-specific guard cell calcium oscillations and stomatal closing in Arabidopsis *det3* mutant. *Science* **289**: 2338-2342
- Allen GJ, Kwak JM, Chu SP, Llopis J, Tsien RY, Harper JF, Schroeder JI** (1999) Cameleon calcium indicator reports cytoplasmic calcium dynamics in Arabidopsis guard cells. *Plant J* **19**: 735-747
- Allen GJ, Muir SR, Sanders D** (1995) Release of Ca<sup>2+</sup> from individual plant vacuoles by both InsP<sub>3</sub> and cyclic ADP-ribose. *Science* **268**: 735-737
- Allen GJ, Sanders D** (1997) Vacuolar ion channels of higher plants. In DS R.A. Leigh, JA Callow, eds, *Advances in Botanical Research*, Volume 25. Academic Press, pp 217-252
- Asai S, Ohta K, Yoshioka H** (2008) MAPK signaling regulates nitric oxide and NADPH oxidase-dependent oxidative bursts in *Nicotiana benthamiana*. *Plant Cell* **20**: 1390-1406
- Asai T, Tena G, Plotnikova J, Willmann MR, Chiu WL, Gomez-Gomez L, Boller T, Ausubel FM, Sheen J** (2002) MAP kinase signalling cascade in Arabidopsis innate immunity. *Nature* **415**: 977-983
- Aslam SN, Erbs G, Morrissey KL, Newman MA, Chinchilla D, Boller T, Molinaro A, Jackson RW, Cooper RM** (2009) Microbe-associated molecular pattern (MAMP) signatures, synergy, size and charge: influences on perception or mobility and host defence responses. *Mol Plant Pathol* **10**: 375-387
- Aslam SN, Newman MA, Erbs G, Morrissey KL, Chinchilla D, Boller T, Jensen TT, De Castro C, Ierano T, Molinaro A, Jackson RW, Knight MR, Cooper RM** (2008) Bacterial polysaccharides suppress induced innate immunity by calcium chelation. *Curr Biol* **18**: 1078-1083
- Baekgaard L, Luoni L, De Michelis MI, Palmgren MG** (2006) The plant plasma membrane Ca<sup>2+</sup> pump ACA8 contains overlapping as well as physically separated autoinhibitory and calmodulin-binding domains. *J Biol Chem* **281**: 1058-1065
- Bakker PAHM, Pieterse CMJ, van Loon LC** (2007) Induced systemic resistance by fluorescent *Pseudomonas* spp. *Phytopathology* **97**: 239-243
- Balague C, Lin B, Alcon C, Flottes G, Malmstrom S, Kohler C, Neuhaus G, Pelletier G, Gaymard F, Roby D** (2003) HLM1, an essential signaling component in the hypersensitive response, is a member of the cyclic nucleotide-gated channel ion channel family. *Plant Cell* **15**: 365-379

- Barazani O, Benderoth M, Groten K, Kuhlemeier C, Baldwin IT** (2005) *Piriformospora indica* and *Sebacina vermifera* increase growth performance at the expense of herbivore resistance in *Nicotiana attenuata*. *Oecologia* **146**: 234-243
- Bargmann BO, Laxalt AM, ter Riet B, Testerink C, Merquiol E, Mosblech A, Leon-Reyes A, Pieterse CM, Haring MA, Heilmann I, Bartels D, Munnik T** (2009a) Reassessing the role of phospholipase D in the Arabidopsis wounding response. *Plant Cell Environ* **32**: 837-850
- Bargmann BO, Laxalt AM, ter Riet B, van Schooten B, Merquiol E, Testerink C, Haring MA, Bartels D, Munnik T** (2009b) Multiple PLDs required for high salinity and water deficit tolerance in plants. *Plant Cell Physiol* **50**: 78-89
- Batistic O, Sorek N, Schultke S, Yalovsky S, Kudla J** (2008) Dual fatty acyl modification determines the localization and plasma membrane targeting of CBL/CIPK  $Ca^{2+}$  signaling complexes in Arabidopsis. *Plant Cell* **20**: 1346-1362
- Batistic O, Waadt R, Steinhorst L, Held K, Kudla J** (2010) CBL-mediated targeting of CIPKs facilitates the decoding of calcium signals emanating from distinct cellular stores. *Plant J* **61**: 211-222
- Bedini E, De Castro C, Erbs G, Mangoni L, Dow JM, Newman MA, Parrilli M, Unverzagt C** (2005) Structure-dependent modulation of a pathogen response in plants by synthetic O-antigen polysaccharides. *J Am Chem Soc* **127**: 2414-2416
- Berridge MJ** (2006) Calcium microdomains: organization and function. *Cell Calcium* **40**: 405-412
- Bethke G, Unthan T, Uhrig JF, Pöschl Y, Gust AA, Scheel D, Lee J** (2009) Flg22 regulates the release of an ethylene response factor substrate from MAP kinase 6 in *Arabidopsis thaliana* via ethylene signaling. *Proc Natl Acad Sci U S A* **106**: 8067-8072
- Bewell MA, Maathuis FJ, Allen GJ, Sanders D** (1999) Calcium-induced calcium release mediated by a voltage-activated cation channel in vacuolar vesicles from red beet. *FEBS Lett* **458**: 41-44
- Beyhl D, Hortensteiner S, Martinoia E, Farmer EE, Fromm J, Marten I, Hedrich R** (2009) The *fou2* mutation in the major vacuolar cation channel TPC1 confers tolerance to inhibitory luminal calcium. *Plant J* **58**: 715-723
- Bibikova TN, Zhigilei A, Gilroy S** (1997) Root hair growth in *Arabidopsis thaliana* is directed by calcium and an endogenous polarity. *Planta* **203**: 495-505
- Blume B, Nürnberger T, Nass N, Scheel D** (2000) Receptor-mediated increase in cytoplasmic free calcium required for activation of pathogen defense in parsley. *Plant Cell* **12**: 1425-1440
- Boller T, Felix G** (2009) A renaissance of elicitors: perception of microbe-associated molecular patterns and danger signals by pattern-recognition receptors. *Annu Rev Plant Biol* **60**: 379-406
- Boller T, He SY** (2009) Innate immunity in plants: an arms race between pattern recognition receptors in plants and effectors in microbial pathogens. *Science* **324**: 742-744
- Bolton MD, van Esse HP, Vossen JH, de Jonge R, Stergiopoulos I, Stulemeijer IJ, van den Berg GC, Borrás-Hidalgo O, Dekker HL, de Koster CG, de Wit PJ, Joosten MH, Thomma BP** (2008) The novel *Cladosporium fulvum* lysin motif effector Ecp6 is a virulence factor with orthologues in other fungal species. *Mol Microbiol* **69**: 119-136
- Bonaventure G, Gfeller A, Proebsting WM, Hortensteiner S, Chetelat A, Martinoia E, Farmer EE** (2007a) A gain-of-function allele of TPC1 activates oxylipin biogenesis after leaf wounding in Arabidopsis. *Plant J* **49**: 889-898
- Bonaventure G, Gfeller A, Rodriguez VM, Armand F, Farmer EE** (2007b) The *fou2* gain-of-function allele and the wild-type allele of Two Pore Channel 1 contribute to different extents or by different mechanisms to defense gene expression in Arabidopsis. *Plant Cell Physiol* **48**: 1775-1789
- Bonza MC, De Michelis MI** (2010) The plant  $Ca^{2+}$ -ATPase repertoire: biochemical features and physiological functions. *Plant Biology*: 421-430
- Bonza MC, Luoni L, De Michelis MI** (2001) Stimulation of plant plasma membrane  $Ca^{2+}$ -ATPase activity by acidic phospholipids. *Physiol Plant* **112**: 315-320
- Bouche N, Scharlat A, Snedden W, Bouchez D, Fromm H** (2002) A novel family of calmodulin-binding transcription activators in multicellular organisms. *J Biol Chem* **277**: 21851-21861

- Bouche N, Yellin A, Snedden WA, Fromm H** (2005) Plant-specific calmodulin-binding proteins. *Annu Rev Plant Biol* **56**: 435-466
- Boudsocq M, Willmann MR, McCormack M, Lee H, Shan L, He P, Bush J, Cheng SH, Sheen J** (2010) Differential innate immune signalling via  $Ca^{2+}$  sensor protein kinases. *Nature* **464**: 418-422
- Boutrot F, Segonzac C, Chang KN, Qiao H, Ecker JR, Zipfel C, Rathjen JP** (2010) Direct transcriptional control of the Arabidopsis immune receptor FLS2 by the ethylene-dependent transcription factors EIN3 and EIL1. *Proc Natl Acad Sci U S A* **107**: 14502-14507
- Bowler C, Neuhaus G, Yamagata H, Chua NH** (1994) Cyclic GMP and calcium mediate phytochrome phototransduction. *Cell* **77**: 73-81
- Brailoiu E, Churamani D, Cai X, Schrlau MG, Brailoiu GC, Gao X, Hooper R, Boulware MJ, Dun NJ, Marchant JS, Patel S** (2009) Essential requirement for two-pore channel 1 in NAADP-mediated calcium signaling. *J Cell Biol* **186**: 201-209
- Braun SG, Meyer A, Holst O, Puhler A, Niehaus K** (2005) Characterization of the *Xanthomonas campestris* pv. *campestris* lipopolysaccharide substructures essential for elicitation of an oxidative burst in tobacco cells. *Mol Plant Microbe Interact* **18**: 674-681
- Brownlee C** (2000) Cellular calcium imaging: so, what's new? *Trends Cell Biol* **10**: 451-457
- Brunner F, Rosahl S, Lee J, Rudd JJ, Geiler C, Kauppinen S, Rasmussen G, Scheel D, Nürnberger T** (2002) Pep-13, a plant defense-inducing pathogen-associated pattern from *Phytophthora* transglutaminases. *EMBO J* **21**: 6681-6688
- Brutus A, Sicilia F, Macone A, Cervone F, De Lorenzo G** (2010) A domain swap approach reveals a role of the plant wall-associated kinase 1 (WAK1) as a receptor of oligogalacturonides. *Proc Natl Acad Sci U S A* **107**: 9452-9457
- Buist G, Steen A, Kok J, Kuipers OP** (2008) LysM, a widely distributed protein motif for binding to (peptido)glycans. *Mol Microbiol* **68**: 838-847
- Calcraft PJ, Ruas M, Pan Z, Cheng X, Arredouani A, Hao X, Tang J, Rietdorf K, Teboul L, Chuang KT, Lin P, Xiao R, Wang C, Zhu Y, Lin Y, Wyatt CN, Parrington J, Ma J, Evans AM, Galione A, Zhu MX** (2009) NAADP mobilizes calcium from acidic organelles through two-pore channels. *Nature* **459**: 596-600
- Camehl I, Oelmüller R** (2010) Do ethylene response factors-9 and -14 repress PR gene expression in the interaction between *Piriformospora indica* and Arabidopsis? *Plant Signal Behav* **5**: 932-936
- Camehl I, Sherameti I, Venus Y, Bethke G, Varma A, Lee J, Oelmüller R** (2010) Ethylene signalling and ethylene-targeted transcription factors are required to balance beneficial and nonbeneficial traits in the symbiosis between the endophytic fungus *Piriformospora indica* and Arabidopsis thaliana. *New Phytol* **185**: 1062-1073
- Cantero A, Barthakur S, Bushart TJ, Chou S, Morgan RO, Fernandez MP, Clark GB, Roux SJ** (2006) Expression profiling of the Arabidopsis annexin gene family during germination, de-etiolation and abiotic stress. *Plant Physiol Biochem* **44**: 13-24
- Carter C, Pan S, Zouhar J, Avila EL, Girke T, Raikhel NV** (2004) The vegetative vacuole proteome of *Arabidopsis thaliana* reveals predicted and unexpected proteins. *Plant Cell* **16**: 3285-3303
- Chang JH, Urbach JM, Law TF, Arnold LW, Hu A, Gombar S, Grant SR, Ausubel FM, Dangl JL** (2005) A high-throughput, near-saturating screen for type III effector genes from *Pseudomonas syringae*. *Proc Natl Acad Sci U S A* **102**: 2549-2554
- Chaparro-Garcia A, Wilkinson RC, Gimenez-Ibanez S, Findlay K, Coffey MD, Zipfel C, Rathjen JP, Kamoun S, Schornack S** (2011) The receptor-like kinase SERK3/BAK1 is required for basal resistance against the late blight pathogen *Phytophthora infestans* in *Nicotiana benthamiana*. *PLoS One* **6**: e16608
- Chen X, Chang M, Wang B, Wu B** (1997) Cloning of a  $Ca^{2+}$ -ATPase gene and the role of cytosolic  $Ca^{2+}$  in the gibberellin-dependent signaling pathway in aleurone cells. *Plant J* **11**: 363-371
- Cheng NH, Hirschi KD** (2003) Cloning and characterization of CXIP1, a novel PICOT domain-containing Arabidopsis protein that associates with CAX1. *J Biol Chem* **278**: 6503-6509

- Cheng NH, Liu JZ, Nelson RS, Hirschi KD** (2004) Characterization of CXIP4, a novel Arabidopsis protein that activates the  $H^+/Ca^{2+}$  antiporter, CAX1. *FEBS Lett* **559**: 99-106
- Cheng NH, Pittman JK, Barkla BJ, Shigaki T, Hirschi KD** (2003) The Arabidopsis *cax1* mutant exhibits impaired ion homeostasis, development, and hormonal responses and reveals interplay among vacuolar transporters. *Plant Cell* **15**: 347-364
- Cheng NH, Pittman JK, Shigaki T, Hirschi KD** (2002a) Characterization of CAX4, an Arabidopsis  $H^+$ /cation antiporter. *Plant Physiol* **128**: 1245-1254
- Cheng NH, Pittman JK, Shigaki T, Lachmansingh J, LeClere S, Lahner B, Salt DE, Hirschi KD** (2005) Functional association of Arabidopsis CAX1 and CAX3 is required for normal growth and ion homeostasis. *Plant Physiol* **138**: 2048-2060
- Cheng SH, Willmann MR, Chen HC, Sheen J** (2002b) Calcium signaling through protein kinases. The Arabidopsis calcium-dependent protein kinase gene family. *Plant Physiol* **129**: 469-485
- Cheong JJ, Birberg W, Fugedi P, Pilotti A, Garegg PJ, Hong N, Ogawa T, Hahn MG** (1991) Structure-activity relationships of oligo-beta-glucoside elicitors of phytoalexin accumulation in soybean. *Plant Cell* **3**: 127-136
- Cheong YH, Kim KN, Pandey GK, Gupta R, Grant JJ, Luan S** (2003) CBL1, a calcium sensor that differentially regulates salt, drought, and cold responses in Arabidopsis. *Plant Cell* **15**: 1833-1845
- Cheong YH, Pandey GK, Grant JJ, Batistic O, Li L, Kim BG, Lee SC, Kudla J, Luan S** (2007) Two calcineurin B-like calcium sensors, interacting with protein kinase CIPK23, regulate leaf transpiration and root potassium uptake in Arabidopsis. *Plant J* **52**: 223-239
- Chinchilla D, Bauer Z, Regenass M, Boller T, Felix G** (2006) The Arabidopsis receptor kinase FLS2 binds flg22 and determines the specificity of flagellin perception. *Plant Cell* **18**: 465-476
- Chinchilla D, Shan L, He P, de Vries S, Kemmerling B** (2009) One for all: the receptor-associated kinase BAK1. *Trends Plant Sci* **14**: 535-541
- Chinchilla D, Zipfel C, Robatzek S, Kemmerling B, Nürnberger T, Jones JD, Felix G, Boller T** (2007) A flagellin-induced complex of the receptor FLS2 and BAK1 initiates plant defence. *Nature* **448**: 497-500
- Chisholm ST, Coaker G, Day B, Staskawicz BJ** (2006) Host-microbe interactions: shaping the evolution of the plant immune response. *Cell* **124**: 803-814
- Cho D, Kim SA, Murata Y, Lee S, Jae SK, Nam HG, Kwak JM** (2009) De-regulated expression of the plant glutamate receptor homolog AtGLR3.1 impairs long-term  $Ca^{2+}$ -programmed stomatal closure. *Plant J* **58**: 437-449
- Cigana C, Curcuru L, Leone MR, Ierano T, Lore NI, Bianconi I, Silipo A, Cozzolino F, Lanzetta R, Molinaro A, Bernardini ML, Bragonzi A** (2009) *Pseudomonas aeruginosa* exploits lipid A and muropeptides modification as a strategy to lower innate immunity during cystic fibrosis lung infection. *PLoS One* **4**: e8439
- Clapham DE** (1995) Calcium signaling. *Cell* **80**: 259-268
- Clark RM, Schweikert G, Toomajian C, Ossowski S, Zeller G, Shinn P, Warthmann N, Hu TT, Fu G, Hinds DA, Chen H, Frazer KA, Huson DH, Scholkopf B, Nordborg M, Ratsch G, Ecker JR, Weigel D** (2007) Common sequence polymorphisms shaping genetic diversity in Arabidopsis thaliana. *Science* **317**: 338-342
- Clayton H, Knight MR, Knight H, McAinsh MR, Hetherington AM** (1999) Dissection of the ozone-induced calcium signature. *Plant J* **17**: 575-579
- Clough SJ, Bent AF** (1998) Floral dip: a simplified method for Agrobacterium-mediated transformation of Arabidopsis thaliana. *Plant J* **16**: 735-743
- Clough SJ, Fengler KA, Yu IC, Lippok B, Smith RK, Jr., Bent AF** (2000) The Arabidopsis *dnd1* "defense, no death" gene encodes a mutated cyclic nucleotide-gated ion channel. *Proc Natl Acad Sci U S A* **97**: 9323-9328

- Conn SJ, Gilliam M, Athman A, Schreiber AW, Baumann U, Moller I, Cheng NH, Stancombe MA, Hirschi KD, Webb AA, Burton R, Kaiser BN, Tyerman SD, Leigh RA** (2011) Cell-specific vacuolar calcium storage mediated by CAX1 regulates apoplastic calcium concentration, gas exchange, and plant productivity in Arabidopsis. *Plant Cell* **23**: 240-257
- Coventry HS, Dubery IA** (2001) Lipopolysaccharides from *Burkholderia cepacia* contribute to an enhanced defensive capacity and the induction of pathogenesis-related proteins in *Nicotiana tabacum*. *Physiological and Molecular Plant Pathology* **58**: 149-158
- D'Ovidio R, Mattei B, Roberti S, Bellincampi D** (2004) Polygalacturonases, polygalacturonase-inhibiting proteins and pectic oligomers in plant-pathogen interactions. *Biochim Biophys Acta* **1696**: 237-244
- Dammann C, Ichida A, Hong B, Romanowsky SM, Hrabak EM, Harmon AC, Pickard BG, Harper JF** (2003) Subcellular targeting of nine calcium-dependent protein kinase isoforms from Arabidopsis. *Plant Physiol* **132**: 1840-1848
- Davletova S, Rizhsky L, Liang H, Shengqiang Z, Oliver DJ, Coutu J, Shulaev V, Schlauch K, Mittler R** (2005) Cytosolic ascorbate peroxidase 1 is a central component of the reactive oxygen gene network of Arabidopsis. *Plant Cell* **17**: 268-281
- Day IS, Reddy VS, Shad Ali G, Reddy AS** (2002) Analysis of EF-hand-containing proteins in Arabidopsis. *Genome Biol* **3**: RESEARCH0056
- de Jong CF, Laxalt AM, Bargmann BO, de Wit PJ, Joosten MH, Munnik T** (2004) Phosphatidic acid accumulation is an early response in the Cf-4/Avr4 interaction. *Plant J* **39**: 1-12
- de Jonge R, van Esse HP, Kombrink A, Shinya T, Desaki Y, Bours R, van der Krol S, Shibuya N, Joosten MH, Thomma BP** (2010) Conserved fungal LysM effector Ecp6 prevents chitin-triggered immunity in plants. *Science* **329**: 953-955
- de Pinto MC, Paradiso A, Leonetti P, De Gara L** (2006) Hydrogen peroxide, nitric oxide and cytosolic ascorbate peroxidase at the crossroad between defence and cell death. *Plant J* **48**: 784-795
- DeFalco TA, Bender KW, Snedden WA** (2010) Breaking the code: Ca<sup>2+</sup> sensors in plant signalling. *Biochem J* **425**: 27-40
- Delker C, Pöschl Y, Raschke A, Ullrich K, Ettingshausen S, Hauptmann V, Grosse I, Quint M** (2010) Natural variation of transcriptional auxin response networks in *Arabidopsis thaliana*. *Plant Cell* **22**: 2184-2200
- Delmer DP, Potikha TS** (1997) Structures and functions of annexins in plants. *Cell Mol Life Sci* **53**: 546-553
- Demidchik V, Davenport RJ, Tester M** (2002) Nonselective cation channels in plants. *Annu Rev Plant Biol* **53**: 67-107
- den Hartog M, Verhoef N, Munnik T** (2003) Nod factor and elicitors activate different phospholipid signaling pathways in suspension-cultured alfalfa cells. *Plant Physiol* **132**: 311-317
- Deng WL, Lin YC, Lin RH, Wei CF, Huang YC, Peng HL, Huang HC** (2010) Effects of galU mutation on *Pseudomonas syringae*-plant interactions. *Mol Plant Microbe Interact* **23**: 1184-1196
- Dennison KL, Spalding EP** (2000) Glutamate-gated calcium fluxes in Arabidopsis. *Plant Physiol* **124**: 1511-1514
- Denoux C, Galletti R, Mammarella N, Gopalan S, Werck D, De Lorenzo G, Ferrari S, Ausubel FM, Dewdney J** (2008) Activation of defense response pathways by OGs and Flg22 elicitors in Arabidopsis seedlings. *Mol Plant* **1**: 423-445
- Desaki Y, Miya A, Venkatesh B, Tsuyumu S, Yamane H, Kaku H, Minami E, Shibuya N** (2006) Bacterial lipopolysaccharides induce defense responses associated with programmed cell death in rice cells. *Plant Cell Physiol* **47**: 1530-1540
- Dodd AN, Kudla J, Sanders D** (2010) The language of calcium signaling. *Annu Rev Plant Biol* **61**: 593-620
- Doherty CJ, Van Buskirk HA, Myers SJ, Thomashow MF** (2009) Roles for Arabidopsis CAMTA transcription factors in cold-regulated gene expression and freezing tolerance. *Plant Cell* **21**: 972-984

- Dow JM, Osbourn AE, Wilson TJ, Daniels MJ** (1995) A locus determining pathogenicity of *Xanthomonas campestris* is involved in lipopolysaccharide biosynthesis. *Mol Plant Microbe Interact* **8**: 768-777
- Du L, Ali GS, Simons KA, Hou J, Yang T, Reddy AS, Poovaiah BW** (2009)  $Ca^{2+}$ /calmodulin regulates salicylic-acid-mediated plant immunity. *Nature* **457**: 1154-1158
- Du L, Poovaiah BW** (2004) A novel family of  $Ca^{2+}$ /calmodulin-binding proteins involved in transcriptional regulation: interaction with fsh/Ring3 class transcription activators. *Plant Mol Biol* **54**: 549-569
- Du L, Poovaiah BW** (2005)  $Ca^{2+}$ /calmodulin is critical for brassinosteroid biosynthesis and plant growth. *Nature* **437**: 741-745
- Ehrhardt DW, Wais R, Long SR** (1996) Calcium spiking in plant root hairs responding to Rhizobium nodulation signals. *Cell* **85**: 673-681
- Elbaz M, Avni A, Weil M** (2002) Constitutive caspase-like machinery executes programmed cell death in plant cells. *Cell Death Differ* **9**: 726-733
- Estelle MA, Somerville C** (1987) Auxin-resistant mutants of *Arabidopsis thaliana* with an altered morphology. *Molecular & General Genetics* **206**: 200-206
- Fauth M, Schweizer P, Buchala A, Markstadter C, Riederer M, Kato T, Kauss H** (1998) Cutin monomers and surface wax constituents elicit  $H_2O_2$  in conditioned cucumber hypocotyl segments and enhance the activity of other  $H_2O_2$  elicitors. *Plant Physiol* **117**: 1373-1380
- Felix G, Boller T** (2003) Molecular sensing of bacteria in plants. The highly conserved RNA-binding motif RNP-1 of bacterial cold shock proteins is recognized as an elicitor signal in tobacco. *J Biol Chem* **278**: 6201-6208
- Felix G, Duran JD, Volko S, Boller T** (1999) Plants have a sensitive perception system for the most conserved domain of bacterial flagellin. *Plant J* **18**: 265-276
- Felix G, Regenass M, Boller T** (1993) Specific perception of subnanomolar concentrations of chitin fragments by tomato cells: induction of extracellular alkalization, changes in protein phosphorylation, and establishment of a refractory state. *The Plant Journal* **4**: 307-316
- Felle H** (1988) Auxin causes oscillations of cytosolic free calcium and pH in *Zea mays* coleoptiles. *Planta* **174**: 495-499
- Flor HH** (1942) Inheritance of pathogenicity in *Melampsora lini*. *Phytopathology* **32**: 653-669
- Foreman J, Demidchik V, Bothwell JH, Mylona P, Miedema H, Torres MA, Linstead P, Costa S, Brownlee C, Jones JD, Davies JM, Dolan L** (2003) Reactive oxygen species produced by NADPH oxidase regulate plant cell growth. *Nature* **422**: 442-446
- Franklin-Tong VE, Drobak BK, Allan AC, Watkins P, Trewavas AJ** (1996) Growth of pollen tubes of *Papaver rhoeas* is regulated by a slow-moving calcium wave propagated by inositol 1,4,5-trisphosphate. *Plant Cell* **8**: 1305-1321
- Franklin-Tong VE, Ride JP, Read ND, Trewavas AJ, Franklin FCH** (1993) The self-incompatibility response in *Papaver rhoeas* is mediated by cytosolic free calcium. *The Plant Journal* **4**: 163-177
- Frietsch S, Wang YF, Sladek C, Poulsen LR, Romanowsky SM, Schroeder JI, Harper JF** (2007) A cyclic nucleotide-gated channel is essential for polarized tip growth of pollen. *Proc Natl Acad Sci U S A* **104**: 14531-14536
- Fuchs Y, Saxena A, Gamble HR, Anderson JD** (1989) Ethylene biosynthesis-inducing protein from cellulysin is an endoxylanase. *Plant Physiol* **89**: 138-143
- Furuichi T, Cunningham KW, Muto S** (2001) A putative two pore channel AtTPC1 mediates  $Ca^{2+}$  flux in Arabidopsis leaf cells. *Plant Cell Physiol* **42**: 900-905
- Galon Y, Aloni R, Nachmias D, Snir O, Feldmesser E, Scrase-Field S, Boyce JM, Bouche N, Knight MR, Fromm H** (2010a) Calmodulin-binding transcription activator 1 mediates auxin signaling and responds to stresses in Arabidopsis. *Planta* **232**: 165-178
- Galon Y, Finkler A, Fromm H** (2010b) Calcium-regulated transcription in plants. *Mol Plant* **3**: 653-669

- Galon Y, Nave R, Boyce JM, Nachmias D, Knight MR, Fromm H** (2008) Calmodulin-binding transcription activator (CAMTA) 3 mediates biotic defense responses in Arabidopsis. *FEBS Lett* **582**: 943-948
- Gao M, Wang X, Wang D, Xu F, Ding X, Zhang Z, Bi D, Cheng YT, Chen S, Li X, Zhang Y** (2009) Regulation of cell death and innate immunity by two receptor-like kinases in Arabidopsis. *Cell Host Microbe* **6**: 34-44
- Gerber IB, Dubery IA** (2004) Protein phosphorylation in *Nicotiana tabacum* cells in response to perception of lipopolysaccharides from *Burkholderia cepacia*. *Phytochemistry* **65**: 2957-2966
- Gimenez-Ibanez S, Hann DR, Ntoukakis V, Petutschnig E, Lipka V, Rathjen JP** (2009) AvrPtoB targets the LysM receptor kinase CERK1 to promote bacterial virulence on plants. *Curr Biol* **19**: 423-429
- Gleason C, Chaudhuri S, Yang T, Munoz A, Poovaiah BW, Oldroyd GE** (2006) Nodulation independent of rhizobia induced by a calcium-activated kinase lacking autoinhibition. *Nature* **441**: 1149-1152
- Gobert A, Park G, Amtmann A, Sanders D, Maathuis FJ** (2006) *Arabidopsis thaliana* cyclic nucleotide gated channel 3 forms a non-selective ion transporter involved in germination and cation transport. *J Exp Bot* **57**: 791-800
- Göhre V, Robatzek S** (2008) Breaking the barriers: microbial effector molecules subvert plant immunity. *Annu Rev Phytopathol* **46**: 189-215
- Göhre V, Spallek T, Haweker H, Mersmann S, Mentzel T, Boller T, de Torres M, Mansfield JW, Robatzek S** (2008) Plant pattern-recognition receptor FLS2 is directed for degradation by the bacterial ubiquitin ligase AvrPtoB. *Curr Biol* **18**: 1824-1832
- Gomez-Gomez L, Boller T** (2000) FLS2: an LRR receptor-like kinase involved in the perception of the bacterial elicitor flagellin in Arabidopsis. *Mol Cell* **5**: 1003-1011
- Gomez-Gomez L, Boller T** (2002) Flagellin perception: a paradigm for innate immunity. *Trends Plant Sci* **7**: 251-256
- Gomez-Gomez L, Felix G, Boller T** (1999) A single locus determines sensitivity to bacterial flagellin in *Arabidopsis thaliana*. *Plant J* **18**: 277-284
- Gong M, van der Luit AH, Knight MR, Trewavas AJ** (1998) Heat-shock-induced changes in intracellular  $Ca^{2+}$  level in tobacco seedlings in relation to thermotolerance. *Plant Physiology* **116**: 429-437
- Granado J, Felix G, Boller T** (1995) Perception of fungal sterols in plants (subnanomolar concentrations of ergosterol elicit extracellular alkalization in tomato cells). *Plant Physiol* **107**: 485-490
- Guo KM, Babourina O, Christopher DA, Borsics T, Rengel Z** (2008) The cyclic nucleotide-gated channel, AtCNGC10, influences salt tolerance in Arabidopsis. *Physiol Plant* **134**: 499-507
- Gust AA, Biswas R, Lenz HD, Rauhut T, Ranf S, Kemmerling B, Gotz F, Glawischig E, Lee J, Felix G, Nürnberger T** (2007) Bacteria-derived peptidoglycans constitute pathogen-associated molecular patterns triggering innate immunity in Arabidopsis. *J Biol Chem* **282**: 32338-32348
- Halim VA, Hunger A, Macioszek V, Landgraf P, Nürnberger T, Scheel D, Rosahl S** (2004) The oligopeptide elicitor Pep-13 induces salicylic acid-dependent and -independent defense reactions in potato. *Physiological and Molecular Plant Pathology* **64**: 311-318
- Han S, Tang R, Anderson LK, Woerner TE, Pei ZM** (2003) A cell surface receptor mediates extracellular  $Ca^{2+}$  sensing in guard cells. *Nature* **425**: 196-200
- Harper JF, Harmon A** (2005) Plants, symbiosis and parasites: a calcium signalling connection. *Nat Rev Mol Cell Biol* **6**: 555-566
- Harper JF, Hong B, Hwang I, Guo HQ, Stoddard R, Huang JF, Palmgren MG, Sze H** (1998) A novel calmodulin-regulated  $Ca^{2+}$ -ATPase (ACA2) from Arabidopsis with an N-terminal autoinhibitory domain. *J Biol Chem* **273**: 1099-1106
- He K, Gou X, Powell RA, Yang H, Yuan T, Guo Z, Li J** (2008) Receptor-like protein kinases, BAK1 and BKK1, regulate a light-dependent cell-death control pathway. *Plant Signal Behav* **3**: 813-815

- He K, Gou X, Yuan T, Lin H, Asami T, Yoshida S, Russell SD, Li J** (2007) BAK1 and BKK1 regulate brassinosteroid-dependent growth and brassinosteroid-independent cell-death pathways. *Curr Biol* **17**: 1109-1115
- Hecht V, Vielle-Calzada JP, Hartog MV, Schmidt ED, Boutilier K, Grossniklaus U, de Vries SC** (2001) The Arabidopsis SOMATIC EMBRYOGENESIS RECEPTOR KINASE 1 gene is expressed in developing ovules and embryos and enhances embryogenic competence in culture. *Plant Physiol* **127**: 803-816
- Heese A, Hann DR, Gimenez-Ibanez S, Jones AM, He K, Li J, Schroeder JI, Peck SC, Rathjen JP** (2007) The receptor-like kinase SERK3/BAK1 is a central regulator of innate immunity in plants. *Proc Natl Acad Sci U S A* **104**: 12217-12222
- Hetherington AM, Brownlee C** (2004) The generation of  $Ca^{2+}$  signals in plants. *Annu Rev Plant Biol* **55**: 401-427
- Hirschfeld M, Ma Y, Weis JH, Vogel SN, Weis JJ** (2000) Cutting edge: repurification of lipopolysaccharide eliminates signaling through both human and murine toll-like receptor 2. *J Immunol* **165**: 618-622
- Hirschi KD** (1999) Expression of Arabidopsis CAX1 in tobacco: altered calcium homeostasis and increased stress sensitivity. *Plant Cell* **11**: 2113-2122
- Hirschi KD, Korenkov VD, Wilganowski NL, Wagner GJ** (2000) Expression of arabidopsis CAX2 in tobacco. Altered metal accumulation and increased manganese tolerance. *Plant Physiol* **124**: 125-133
- Hofmann A, Proust J, Dorowski A, Schantz R, Huber R** (2000) Annexin 24 from *Capsicum annum*. X-ray structure and biochemical characterization. *J Biol Chem* **275**: 8072-8082
- Hrabak EM, Chan CW, Gribskov M, Harper JF, Choi JH, Halford N, Kudla J, Luan S, Nimmo HG, Sussman MR, Thomas M, Walker-Simmons K, Zhu JK, Harmon AC** (2003) The Arabidopsis CDPK-SnRK superfamily of protein kinases. *Plant Physiol* **132**: 666-680
- Hsieh HL, Song CJ, Roux SJ** (2000) Regulation of a recombinant pea nuclear apyrase by calmodulin and casein kinase II. *Biochim Biophys Acta* **1494**: 248-255
- Hua B-G, Mercier RW, Zielinski RE, Berkowitz GA** (2003) Functional interaction of calmodulin with a plant cyclic nucleotide gated cation channel. *Plant Physiology and Biochemistry* **41**: 945-954
- Hückelhoven R** (2007) Cell wall-associated mechanisms of disease resistance and susceptibility. *Annu Rev Phytopathol* **45**: 101-127
- Huffaker A, Pearce G, Ryan CA** (2006) An endogenous peptide signal in Arabidopsis activates components of the innate immune response. *Proc Natl Acad Sci U S A* **103**: 10098-10103
- Huffaker A, Ryan CA** (2007) Endogenous peptide defense signals in Arabidopsis differentially amplify signaling for the innate immune response. *Proc Natl Acad Sci U S A* **104**: 10732-10736
- Hwang I, Sze H, Harper JF** (2000) A calcium-dependent protein kinase can inhibit a calmodulin-stimulated  $Ca^{2+}$  pump (ACA2) located in the endoplasmic reticulum of Arabidopsis. *Proc Natl Acad Sci U S A* **97**: 6224-6229
- Iizasa E, Mitsutomi M, Nagano Y** (2010) Direct binding of a plant LysM receptor-like kinase, LysM RLK1/CERK1, to chitin in vitro. *J Biol Chem* **285**: 2996-3004
- Ishibashi K, Suzuki M, Imai M** (2000) Molecular cloning of a novel form (two-repeat) protein related to voltage-gated sodium and calcium channels. *Biochem Biophys Res Commun* **270**: 370-376
- Islam MM, Munemasa S, Hossain MA, Nakamura Y, Mori IC, Murata Y** (2010) Roles of AtTPC1, vacuolar two pore channel 1, in Arabidopsis stomatal closure. *Plant Cell Physiol* **51**: 302-311
- Jabs T, Tschope M, Colling C, Hahlbrock K, Scheel D** (1997) Elicitor-stimulated ion fluxes and  $O_2^-$  from the oxidative burst are essential components in triggering defense gene activation and phytoalexin synthesis in parsley. *Proc Natl Acad Sci U S A* **94**: 4800-4805
- Jacobs AK, Lipka V, Burton RA, Panstruga R, Strizhov N, Schulze-Lefert P, Fincher GB** (2003) An Arabidopsis callose synthase, GSL5, is required for wound and papillary callose formation. *Plant Cell* **15**: 2503-2513

- Jeworutzki E, Roelfsema MR, Anshütz U, Krol E, Elzenga JT, Felix G, Boller T, Hedrich R, Becker D** (2010) Early signaling through the Arabidopsis pattern recognition receptors FLS2 and EFR involves Ca-associated opening of plasma membrane anion channels. *Plant J* **62**: 367-378
- Jia XY, He LH, Jing RL, Li RZ** (2009) Calreticulin: conserved protein and diverse functions in plants. *Physiol Plant* **136**: 127-138
- Johnson CH, Knight MR, Kondo T, Masson P, Sedbrook J, Haley A, Trewavas A** (1995) Circadian oscillations of cytosolic and chloroplastic free calcium in plants. *Science* **269**: 1863-1865
- Jones JD, Dangl JL** (2006) The plant immune system. *Nature* **444**: 323-329
- Kadota Y, Furuichi T, Ogasawara Y, Goh T, Higashi K, Muto S, Kuchitsu K** (2004) Identification of putative voltage-dependent Ca<sup>2+</sup>-permeable channels involved in cryptogein-induced Ca<sup>2+</sup> transients and defense responses in tobacco BY-2 cells. *Biochem Biophys Res Commun* **317**: 823-830
- Kaku H, Nishizawa Y, Ishii-Minami N, Akimoto-Tomiya C, Dohmae N, Takio K, Minami E, Shibuya N** (2006) Plant cells recognize chitin fragments for defense signaling through a plasma membrane receptor. *Proc Natl Acad Sci U S A* **103**: 11086-11091
- Kang J, Mehta S, Turano FJ** (2004) The putative glutamate receptor 1.1 (AtGLR1.1) in Arabidopsis thaliana regulates abscisic acid biosynthesis and signaling to control development and water loss. *Plant Cell Physiol* **45**: 1380-1389
- Kang J, Turano FJ** (2003) The putative glutamate receptor 1.1 (AtGLR1.1) functions as a regulator of carbon and nitrogen metabolism in Arabidopsis thaliana. *Proc Natl Acad Sci U S A* **100**: 6872-6877
- Kannenberg EL, Carlson RW** (2001) Lipid A and O-chain modifications cause Rhizobium lipopolysaccharides to become hydrophobic during bacteroid development. *Mol Microbiol* **39**: 379-391
- Kawano T, Kadono T, Fumoto K, Lapeyrie F, Kuse M, Isobe M, Furuichi T, Muto S** (2004) Aluminum as a specific inhibitor of plant TPC1 Ca<sup>2+</sup> channels. *Biochem Biophys Res Commun* **324**: 40-45
- Kemmerling B, Schwedt A, Rodriguez P, Mazzotta S, Frank M, Qamar SA, Mengiste T, Betsuyaku S, Parker JE, Mussig C, Thomma BP, Albrecht C, de Vries SC, Hirt H, Nürnberger T** (2007) The BRI1-associated kinase 1, BAK1, has a brassinolide-independent role in plant cell-death control. *Curr Biol* **17**: 1116-1122
- Kiegle E, Moore CA, Haseloff J, Tester MA, Knight MR** (2000) Cell-type-specific calcium responses to drought, salt and cold in the Arabidopsis root. *Plant J* **23**: 267-278
- Kim MC, Lee SH, Kim JK, Chun HJ, Choi MS, Chung WS, Moon BC, Kang CH, Park CY, Yoo JH, Kang YH, Koo SC, Koo YD, Jung JC, Kim ST, Schulze-Lefert P, Lee SY, Cho MJ** (2002) Mlo, a modulator of plant defense and cell death, is a novel calmodulin-binding protein. Isolation and characterization of a rice Mlo homologue. *J Biol Chem* **277**: 19304-19314
- Kim SA, Kwak JM, Jae SK, Wang MH, Nam HG** (2001) Overexpression of the *AtGluR2* gene encoding an Arabidopsis homolog of mammalian glutamate receptors impairs calcium utilization and sensitivity to ionic stress in transgenic plants. *Plant Cell Physiol* **42**: 74-84
- Kingsley MT, Gabriel DW, Marlow GC, Roberts PD** (1993) The *opsX* locus of *Xanthomonas campestris* affects host range and biosynthesis of lipopolysaccharide and extracellular polysaccharide. *J Bacteriol* **175**: 5839-5850
- Knight H, Brandt S, Knight MR** (1998) A history of stress alters drought calcium signalling pathways in Arabidopsis. *Plant J* **16**: 681-687
- Knight H, Knight MR** (2000) Imaging spatial and cellular characteristics of low temperature calcium signature after cold acclimation in Arabidopsis. *J Exp Bot* **51**: 1679-1686
- Knight H, Knight MR** (2001) Abiotic stress signalling pathways: specificity and cross-talk. *Trends Plant Sci* **6**: 262-267
- Knight H, Trewavas AJ, Knight MR** (1996) Cold calcium signaling in Arabidopsis involves two cellular pools and a change in calcium signature after acclimation. *Plant Cell* **8**: 489-503

- Knight H, Trewavas AJ, Knight MR** (1997) Calcium signalling in *Arabidopsis thaliana* responding to drought and salinity. *Plant J* **12**: 1067-1078
- Knight MR, Campbell AK, Smith SM, Trewavas AJ** (1991) Transgenic plant aequorin reports the effects of touch and cold-shock and elicitors on cytoplasmic calcium. *Nature* **352**: 524-526
- Knight MR, Smith SM, Trewavas AJ** (1992) Wind-induced plant motion immediately increases cytosolic calcium. *Proc Natl Acad Sci U S A* **89**: 4967-4971
- Knirel YA, Bystrova OV, Kocharova NA, Zähringer U, Pier GB** (2006) Conserved and variable structural features in the lipopolysaccharide of *Pseudomonas aeruginosa*. *J Endotoxin Res* **12**: 324-336
- Knirel YA, Bystrova OV, Shashkov AS, Lindner B, Kocharova NA, Senchenkova SN, Moll H, Zähringer U, Hatano K, Pier GB** (2001) Structural analysis of the lipopolysaccharide core of a rough, cystic fibrosis isolate of *Pseudomonas aeruginosa*. *Eur J Biochem* **268**: 4708-4719
- Knogge W, Scheel D** (2006) LysM receptors recognize friend and foe. *Proc Natl Acad Sci U S A* **103**: 10829-10830
- Kobayashi M, Ohura I, Kawakita K, Yokota N, Fujiwara M, Shimamoto K, Doke N, Yoshioka H** (2007) Calcium-dependent protein kinases regulate the production of reactive oxygen species by potato NADPH oxidase. *Plant Cell* **19**: 1065-1080
- Kobe B, Kajava AV** (2001) The leucine-rich repeat as a protein recognition motif. *Curr Opin Struct Biol* **11**: 725-732
- Kohle H, Jeblick W, Poten F, Blaschek W, Kauss H** (1985) Chitosan-elicited callose synthesis in soybean cells as a Ca-dependent process. *Plant Physiol* **77**: 544-551
- Kolukisaoglu U, Weini S, Blazevic D, Batistic O, Kudla J** (2004) Calcium sensors and their interacting protein kinases: genomics of the Arabidopsis and rice CBL-CIPK signaling networks. *Plant Physiol* **134**: 43-58
- Krol E, Mentzel T, Chinchilla D, Boller T, Felix G, Kemmerling B, Postel S, Arents M, Jeworutzki E, Al-Rasheid KA, Becker D, Hedrich R** (2010) Perception of the Arabidopsis danger signal peptide 1 involves the pattern recognition receptor AtPEPR1 and its close homologue AtPEPR2. *J Biol Chem* **285**: 13471-13479
- Kudla J, Batistic O, Hashimoto K** (2010) Calcium signals: the lead currency of plant information processing. *Plant Cell* **22**: 541-563
- Kudla J, Xu Q, Harter K, Gruissem W, Luan S** (1999) Genes for calcineurin B-like proteins in Arabidopsis are differentially regulated by stress signals. *Proc Natl Acad Sci U S A* **96**: 4718-4723
- Kunze G, Zipfel C, Robatzek S, Niehaus K, Boller T, Felix G** (2004) The N terminus of bacterial elongation factor Tu elicits innate immunity in Arabidopsis plants. *Plant Cell* **16**: 3496-3507
- Kurusu T, Yagala T, Miyao A, Hirochika H, Kuchitsu K** (2005) Identification of a putative voltage-gated Ca<sup>2+</sup> channel as a key regulator of elicitor-induced hypersensitive cell death and mitogen-activated protein kinase activation in rice. *Plant J* **42**: 798-809
- Kushwaha R, Singh A, Chattopadhyay S** (2008) Calmodulin7 plays an important role as transcriptional regulator in Arabidopsis seedling development. *Plant Cell* **20**: 1747-1759
- Kutuzov MA, Bennett N, Andreeva AV** (2001) Interaction of plant protein Ser/Thr phosphatase PP7 with calmodulin. *Biochem Biophys Res Commun* **289**: 634-640
- Lacombe B, Becker D, Hedrich R, DeSalle R, Hollmann M, Kwak JM, Schroeder JI, Le Novere N, Nam HG, Spalding EP, Tester M, Turano FJ, Chiu J, Coruzzi G** (2001) The identity of plant glutamate receptors. *Science* **292**: 1486-1487
- Lacombe S, Rougon-Cardoso A, Sherwood E, Peeters N, Dahlbeck D, van Esse HP, Smoker M, Rallapalli G, Thomma BP, Staskawicz B, Jones JD, Zipfel C** (2010) Interfamily transfer of a plant pattern-recognition receptor confers broad-spectrum bacterial resistance. *Nat Biotechnol* **28**: 365-369
- Lamotte O, Gould K, Lecourieux D, Sequeira-Legrand A, Lebrun-Garcia A, Durner J, Pugin A, Wendehenne D** (2004) Analysis of nitric oxide signaling functions in tobacco cells challenged by the elicitor cryptogein. *Plant Physiol* **135**: 516-529

- Laohavisit A, Davies JM** (2011) Annexins. *New Phytol* **189**: 40-53
- Laohavisit A, Mortimer JC, Demidchik V, Coxon KM, Stancombe MA, Macpherson N, Brownlee C, Hofmann A, Webb AA, Miedema H, Battey NH, Davies JM** (2009) *Zea mays* annexins modulate cytosolic free Ca<sup>2+</sup> and generate a Ca<sup>2+</sup>-permeable conductance. *Plant Cell* **21**: 479-493
- Laquitaine L, Gomes E, Francois J, Marchive C, Pascal S, Hamdi S, Atanassova R, Delrot S, Coutos-Thevenot P** (2006) Molecular basis of ergosterol-induced protection of grape against *botrytis cinerea*: induction of type I LTP promoter activity, WRKY, and stilbene synthase gene expression. *Mol Plant Microbe Interact* **19**: 1103-1112
- Laxalt AM, ter Riet B, Verdonk JC, Parigi L, Tameling WI, Vossen J, Haring M, Musgrave A, Munnik T** (2001) Characterization of five tomato phospholipase D cDNAs: rapid and specific expression of *LePLDbeta1* on elicitation with xylanase. *Plant J* **26**: 237-247
- Lebrun-Garcia A, Bourque S, Binet MN, Ouaked F, Wendehenne D, Chiltz A, Schaffner A, Pugin A** (1999) Involvement of plasma membrane proteins in plant defense responses. Analysis of the cryptogein signal transduction in tobacco. *Biochimie* **81**: 663-668
- Lecourieux D, Lamotte O, Bourque S, Wendehenne D, Mazars C, Ranjeva R, Pugin A** (2005) Proteinaceous and oligosaccharidic elicitors induce different calcium signatures in the nucleus of tobacco cells. *Cell Calcium* **38**: 527-538
- Lecourieux D, Mazars C, Pauly N, Ranjeva R, Pugin A** (2002) Analysis and effects of cytosolic free calcium increases in response to elicitors in *Nicotiana plumbaginifolia* cells. *Plant Cell* **14**: 2627-2641
- Lee J, Rudd JJ, Macioszek VK, Scheel D** (2004) Dynamic changes in the localization of MAPK cascade components controlling pathogenesis-related (PR) gene expression during innate immunity in parsley. *J Biol Chem* **279**: 22440-22448
- Lee SW, Han SW, Sririyannum M, Park CJ, Seo YS, Ronald PC** (2009) A type I-secreted, sulfated peptide triggers XA21-mediated innate immunity. *Science* **326**: 850-853
- Lemtiri-Chlieh F, MacRobbie EA, Webb AA, Manison NF, Brownlee C, Skepper JN, Chen J, Prestwich GD, Brearley CA** (2003) Inositol hexakisphosphate mobilizes an endomembrane store of calcium in guard cells. *Proc Natl Acad Sci U S A* **100**: 10091-10095
- Leulier F, Parquet C, Pili-Floury S, Ryu JH, Caroff M, Lee WJ, Mengin-Lecreulx D, Lemaitre B** (2003) The Drosophila immune system detects bacteria through specific peptidoglycan recognition. *Nat Immunol* **4**: 478-484
- Li J, Wen J, Lease KA, Doke JT, Tax FE, Walker JC** (2002) BAK1, an Arabidopsis LRR receptor-like protein kinase, interacts with BRI1 and modulates brassinosteroid signaling. *Cell* **110**: 213-222
- Li J, Zhao-Hui C, Batoux M, Nekrasov V, Roux M, Chinchilla D, Zipfel C, Jones JD** (2009) Specific ER quality control components required for biogenesis of the plant innate immune receptor EFR. *Proc Natl Acad Sci U S A* **106**: 15973-15978
- Ligterink W, Kroj T, zur Nieden U, Hirt H, Scheel D** (1997) Receptor-mediated activation of a MAP kinase in pathogen defense of plants. *Science* **276**: 2054-2057
- Lin C, Yu Y, Kadono T, Iwata M, Umemura K, Furuichi T, Kuse M, Isobe M, Yamamoto Y, Matsumoto H, Yoshizuka K, Kawano T** (2005) Action of aluminum, novel TPC1-type channel inhibitor, against salicylate-induced and cold-shock-induced calcium influx in tobacco BY-2 cells. *Biochem Biophys Res Commun* **332**: 823-830
- Liu Y, Zhang S** (2004) Phosphorylation of 1-aminocyclopropane-1-carboxylic acid synthase by MPK6, a stress-responsive mitogen-activated protein kinase, induces ethylene biosynthesis in Arabidopsis. *Plant Cell* **16**: 3386-3399
- Livaja M, Zeidler D, von Rad U, Durner J** (2008) Transcriptional responses of *Arabidopsis thaliana* to the bacteria-derived PAMPs harpin and lipopolysaccharide. *Immunobiology* **213**: 161-171
- Lochman J, Mikes V** (2006) Ergosterol treatment leads to the expression of a specific set of defence-related genes in tobacco. *Plant Mol Biol* **62**: 43-51
- Lu D, He P, Shan L** (2010) Bacterial effectors target BAK1-associated receptor complexes: One stone two birds. *Commun Integr Biol* **3**: 80-83

- Lu D, Wu S, Gao X, Zhang Y, Shan L, He P (2010) A receptor-like cytoplasmic kinase, BIK1, associates with a flagellin receptor complex to initiate plant innate immunity. *Proc Natl Acad Sci U S A* **107**: 496-501
- Lu X, Tintor N, Mentzel T, Kombrink E, Boller T, Robatzek S, Schulze-Lefert P, Saijo Y (2009) Uncoupling of sustained MAMP receptor signaling from early outputs in an Arabidopsis endoplasmic reticulum glucosidase II allele. *Proc Natl Acad Sci U S A* **106**: 22522-22527
- Luan S (2009) The CBL-CIPK network in plant calcium signaling. *Trends Plant Sci* **14**: 37-42
- Luna E, Pastor V, Robert J, Flors V, Mauch-Mani B, Ton J (2011) Callose deposition: a multifaceted plant defense response. *Mol Plant Microbe Interact* **24**: 183-193
- Luo GZ, Wang HW, Huang J, Tian AG, Wang YJ, Zhang JS, Chen SY (2005) A putative plasma membrane cation/proton antiporter from soybean confers salt tolerance in Arabidopsis. *Plant Mol Biol* **59**: 809-820
- Ma W, Qi Z, Smigel A, Walker RK, Verma R, Berkowitz GA (2009) Ca<sup>2+</sup>, cAMP, and transduction of non-self perception during plant immune responses. *Proc Natl Acad Sci U S A* **106**: 20995-21000
- Ma W, Smigel A, Tsai YC, Braam J, Berkowitz GA (2008) Innate immunity signaling: cytosolic Ca<sup>2+</sup> elevation is linked to downstream nitric oxide generation through the action of calmodulin or a calmodulin-like protein. *Plant Physiol* **148**: 818-828
- Malho R, Moutinho A, Van der Luit AH, Trewavas AJ (1998) Spatial characteristics of calcium signalling: the calcium wave as a basic unit in plant cell calcium signalling. *Phil Trans R Soc Lond B* **353**: 1463-1473
- Malho R, Trewavas AJ (1996) Localized apical increases of cytosolic free Calcium control pollen tube orientation. *Plant Cell* **8**: 1935-1949
- Martinec J, Feltl T, Scanlon CH, Lumsden PJ, Machackova I (2000) Subcellular localization of a high affinity binding site for D-myo-inositol 1,4,5-trisphosphate from *Chenopodium rubrum*. *Plant Physiol* **124**: 475-483
- Maser P, Thomine S, Schroeder JI, Ward JM, Hirschi K, Sze H, Talke IN, Amtmann A, Maathuis FJ, Sanders D, Harper JF, Tchieu J, Gribskov M, Persans MW, Salt DE, Kim SA, Guerinot ML (2001) Phylogenetic relationships within cation transporter families of Arabidopsis. *Plant Physiol* **126**: 1646-1667
- Matzinger P (2002) The danger model: a renewed sense of self. *Science* **296**: 301-305
- Mazars C, Bourque S, Mithofer A, Pugin A, Ranjeva R (2009) Calcium homeostasis in plant cell nuclei. *New Phytol* **181**: 261-274
- McAinsh MR, Brownlee C, Hetherington AM (1992) Visualizing Changes in Cytosolic-Free Ca<sup>2+</sup> during the Response of Stomatal Guard Cells to Abscisic Acid. *Plant Cell* **4**: 1113-1122
- McAinsh MR, Hetherington AM (1998) Encoding specificity in Ca<sup>2+</sup> signalling systems. *Trends in Plant Science* **3**: 32-36
- McAinsh MR, Webb A, Taylor JE, Hetherington AM (1995) Stimulus-induced oscillations in guard cell cytosolic free calcium. *Plant Cell* **7**: 1207-1219
- McCormack E, Tsai YC, Braam J (2005) Handling calcium signaling: Arabidopsis CaMs and CMLs. *Trends Plant Sci* **10**: 383-389
- McGurl B, Pearce G, Orozco-Cardenas M, Ryan CA (1992) Structure, expression, and antisense inhibition of the systemin precursor gene. *Science* **255**: 1570-1573
- Meindl T, Boller T, Felix G (2000) The bacterial elicitor flagellin activates its receptor in tomato cells according to the address-message concept. *Plant Cell* **12**: 1783-1794
- Melotto M, Underwood W, He SY (2008) Role of stomata in plant innate immunity and foliar bacterial diseases. *Annu Rev Phytopathol* **46**: 101-122
- Melotto M, Underwood W, Koczan J, Nomura K, He SY (2006) Plant stomata function in innate immunity against bacterial invasion. *Cell* **126**: 969-980

- Meneghelli S, Fusca T, Luoni L, De Michelis MI** (2008) Dual mechanism of activation of plant plasma membrane  $\text{Ca}^{2+}$ -ATPase by acidic phospholipids: evidence for a phospholipid binding site which overlaps the calmodulin-binding site. *Mol Membr Biol* **25**: 539-546
- Meng PH, Raynaud C, Tcherkez G, Blanchet S, Massoud K, Domenichini S, Henry Y, Soubigou-Taconnat L, Lelarge-Trouverie C, Saindrenan P, Renou JP, Bergounioux C** (2009) Crosstalks between myo-inositol metabolism, programmed cell death and basal immunity in Arabidopsis. *PLoS One* **4**: e7364
- Mersmann S, Bourdais G, Rietz S, Robatzek S** (2010) Ethylene signaling regulates accumulation of the FLS2 receptor and is required for the oxidative burst contributing to plant immunity. *Plant Physiol* **154**: 391-400
- Meyer A, Puhler A, Niehaus K** (2001) The lipopolysaccharides of the phytopathogen *Xanthomonas campestris* pv. *campestris* induce an oxidative burst reaction in cell cultures of *Nicotiana tabacum*. *Planta* **213**: 214-222
- Meyerhoff O, Muller K, Roelfsema MR, Latz A, Lacombe B, Hedrich R, Dietrich P, Becker D** (2005) AtGLR3.4, a glutamate receptor channel-like gene is sensitive to touch and cold. *Planta* **222**: 418-427
- Michell RH** (2008) Inositol derivatives: evolution and functions. *Nat Rev Mol Cell Biol* **9**: 151-161
- Miller G, Schlauch K, Tam R, Cortes D, Torres MA, Shulaev V, Dangl JL, Mittler R** (2009) The plant NADPH oxidase RBOHD mediates rapid systemic signaling in response to diverse stimuli. *Sci Signal* **2**: ra45
- Miller G, Suzuki N, Rizhsky L, Hegie A, Koussevitzky S, Mittler R** (2007) Double mutants deficient in cytosolic and thylakoid ascorbate peroxidase reveal a complex mode of interaction between reactive oxygen species, plant development, and response to abiotic stresses. *Plant Physiol* **144**: 1777-1785
- Millet YA, Danna CH, Clay NK, Songnuan W, Simon MD, Werck-Reichhart D, Ausubel FM** (2010) Innate immune responses activated in Arabidopsis roots by microbe-associated molecular patterns. *Plant Cell* **22**: 973-990
- Mishina TE, Zeier J** (2007) Pathogen-associated molecular pattern recognition rather than development of tissue necrosis contributes to bacterial induction of systemic acquired resistance in Arabidopsis. *Plant J* **50**: 500-513
- Mithöfer A, Ebel J, Bhagwat AA, Boller T, Neuhaus-Url G** (1999) Transgenic aequorin monitors cytosolic calcium transients in soybean cells challenged with  $\beta$ -glucan or chitin elicitors. *Planta* **207**: 566-574
- Mithöfer A, Mazars C** (2002) Aequorin-based measurements of intracellular  $\text{Ca}^{2+}$ -signatures in plant cells. *Biol Proced Online* **4**: 105-118
- Mitra RM, Gleason CA, Edwards A, Hadfield J, Downie JA, Oldroyd GE, Long SR** (2004) A  $\text{Ca}^{2+}$ /calmodulin-dependent protein kinase required for symbiotic nodule development: Gene identification by transcript-based cloning. *Proc Natl Acad Sci U S A* **101**: 4701-4705
- Miya A, Albert P, Shinya T, Desaki Y, Ichimura K, Shirasu K, Narusaka Y, Kawakami N, Kaku H, Shibuya N** (2007) CERK1, a LysM receptor kinase, is essential for chitin elicitor signaling in Arabidopsis. *Proc Natl Acad Sci U S A* **104**: 19613-19618
- Miyake K** (2004) Innate recognition of lipopolysaccharide by Toll-like receptor 4-MD-2. *Trends Microbiol* **12**: 186-192
- Molinaro A** (2009) The Structures of lipopolysaccharides from plant-associated Gram-negative bacteria. *European Journal of Organic Chemistry* **2009**: 5887-5896
- Monshausen GB, Messerli MA, Gilroy S** (2008) Imaging of the Yellow Cameleon 3.6 indicator reveals that elevations in cytosolic  $\text{Ca}^{2+}$  follow oscillating increases in growth in root hairs of Arabidopsis. *Plant Physiol* **147**: 1690-1698
- Mortimer JC, Laohavisit A, Macpherson N, Webb A, Brownlee C, Battey NH, Davies JM** (2008) Annexins: multifunctional components of growth and adaptation. *J Exp Bot* **59**: 533-544

- Moyen C, Hammond-Kosack KE, Jones J, Knight MR, Johannes E** (1998) Systemin triggers an increase of cytoplasmic calcium in tomato mesophyll cells:  $\text{Ca}^{2+}$  mobilization from intra- and extracellular compartments. *Plant, Cell & Environment* **21**: 1101-1111
- Muir SR, Sanders D** (1996) Pharmacology of  $\text{Ca}^{2+}$  release from red beet microsomes suggests the presence of ryanodine receptor homologs in higher plants. *FEBS Lett* **395**: 39-42
- Müller J, Staehelin C, Xie ZP, Neuhaus-Url G, Boller T** (2000) Nod factors and chitoooligomers elicit an increase in cytosolic calcium in aequorin-expressing soybean cells. *Plant Physiol* **124**: 733-740
- Munnik T, Testerink C** (2009) Plant phospholipid signaling: "in a nutshell". *J Lipid Res* **50 Suppl**: S260-265
- Munnik T, Vermeer JE** (2010) Osmotic stress-induced phosphoinositide and inositol phosphate signalling in plants. *Plant Cell Environ* **33**: 655-669
- Murphy AM, Otto B, Brearley CA, Carr JP, Hanke DE** (2008) A role for inositol hexakisphosphate in the maintenance of basal resistance to plant pathogens. *Plant J* **56**: 638-652
- Naito K, Taguchi F, Suzuki T, Inagaki Y, Toyoda K, Shiraishi T, Ichinose Y** (2008) Amino acid sequence of bacterial microbe-associated molecular pattern flg22 is required for virulence. *Mol Plant Microbe Interact* **21**: 1165-1174
- Nakagawa Y, Katagiri T, Shinozaki K, Qi Z, Tatsumi H, Furuichi T, Kishigami A, Sokabe M, Kojima I, Sato S, Kato T, Tabata S, Iida K, Terashima A, Nakano M, Ikeda M, Yamanaka T, Iida H** (2007) Arabidopsis plasma membrane protein crucial for  $\text{Ca}^{2+}$  influx and touch sensing in roots. *Proc Natl Acad Sci U S A* **104**: 3639-3644
- Nam KH, Li J** (2002) BRI1/BAK1, a receptor kinase pair mediating brassinosteroid signaling. *Cell* **110**: 203-212
- Navarro L, Dunoyer P, Jay F, Arnold B, Dharmasiri N, Estelle M, Voinnet O, Jones JD** (2006) A plant miRNA contributes to antibacterial resistance by repressing auxin signaling. *Science* **312**: 436-439
- Navarro L, Zipfel C, Rowland O, Keller I, Robatzek S, Boller T, Jones JD** (2004) The transcriptional innate immune response to flg22. Interplay and overlap with *Avr* gene-dependent defense responses and bacterial pathogenesis. *Plant Physiol* **135**: 1113-1128
- Navazio L, Bewell MA, Siddiqua A, Dickinson GD, Galione A, Sanders D** (2000) Calcium release from the endoplasmic reticulum of higher plants elicited by the NADP metabolite nicotinic acid adenine dinucleotide phosphate. *Proc Natl Acad Sci U S A* **97**: 8693-8698
- Navazio L, Mariani P** (2008) Calcium opens the dialogue between plants and arbuscular mycorrhizal fungi. *Plant Signal Behav* **3**: 229-230
- Navazio L, Mariani P, Sanders D** (2001) Mobilization of  $\text{Ca}^{2+}$  by cyclic ADP-ribose from the endoplasmic reticulum of cauliflower florets. *Plant Physiol* **125**: 2129-2138
- Navazio L, Moscatiello R, Bellincampi D, Baldan B, Meggio F, Brini M, Bowler C, Mariani P** (2002) The role of calcium in oligogalacturonide-activated signalling in soybean cells. *Planta* **215**: 596-605
- Navazio L, Moscatiello R, Genre A, Novero M, Baldan B, Bonfante P, Mariani P** (2007) A diffusible signal from arbuscular mycorrhizal fungi elicits a transient cytosolic calcium elevation in host plant cells. *Plant Physiol* **144**: 673-681
- Nekrasov V, Li J, Batoux M, Roux M, Chu ZH, Lacombe S, Rougon A, Bittel P, Kiss-Papp M, Chinchilla D, van Esse HP, Jorda L, Schwessinger B, Nicaise V, Thomma BP, Molina A, Jones JD, Zipfel C** (2009) Control of the pattern-recognition receptor EFR by an ER protein complex in plant immunity. *EMBO J* **28**: 3428-3438
- Newman MA, von Roepenack-Lahaye E, Parr A, Daniels MJ, Dow JM** (2001) Induction of hydroxycinnamoyl-tyramine conjugates in pepper by *Xanthomonas campestris*, a plant defense response activated by hrp gene-dependent and hrp gene-independent mechanisms. *Mol Plant Microbe Interact* **14**: 785-792
- Newman MA, von Roepenack-Lahaye E, Parr A, Daniels MJ, Dow JM** (2002) Prior exposure to lipopolysaccharide potentiates expression of plant defenses in response to bacteria. *Plant J* **29**: 487-495

- Ng CK, Carr K, McAinsh MR, Powell B, Hetherington AM** (2001) Drought-induced guard cell signal transduction involves sphingosine-1-phosphate. *Nature* **410**: 596-599
- Niehaus K, Becker A** (1998) The role of microbial surface polysaccharides in the Rhizobium-legume interaction. *Subcell Biochem* **29**: 73-116
- Nomura H, Komori T, Kobori M, Nakahira Y, Shiina T** (2008) Evidence for chloroplast control of external  $\text{Ca}^{2+}$ -induced cytosolic  $\text{Ca}^{2+}$  transients and stomatal closure. *Plant J* **53**: 988-998
- Nürnberg T, Colling C, Hahlbrock K, Jabs T, Renelt A, Sacks WR, Scheel D** (1994a) Perception and transduction of an elicitor signal in cultured parsley cells. *Biochem Soc Symp* **60**: 173-182
- Nürnberg T, Nennstiel D, Jabs T, Sacks WR, Hahlbrock K, Scheel D** (1994b) High affinity binding of a fungal oligopeptide elicitor to parsley plasma membranes triggers multiple defense responses. *Cell* **78**: 449-460
- Ogasawara Y, Kaya H, Hiraoka G, Yumoto F, Kimura S, Kadota Y, Hishinuma H, Senzaki E, Yamagoe S, Nagata K, Nara M, Suzuki K, Tanokura M, Kuchitsu K** (2008) Synergistic activation of the Arabidopsis NADPH oxidase AtrbohD by  $\text{Ca}^{2+}$  and phosphorylation. *J Biol Chem* **283**: 8885-8892
- Oldroyd GE, Downie JA** (2006) Nuclear calcium changes at the core of symbiosis signalling. *Curr Opin Plant Biol* **9**: 351-357
- Park CY, Lee JH, Yoo JH, Moon BC, Choi MS, Kang YH, Lee SM, Kim HS, Kang KY, Chung WS, Lim CO, Cho MJ** (2005) WRKY group IId transcription factors interact with calmodulin. *FEBS Lett* **579**: 1545-1550
- Pauly N, Knight MR, Thuleau P, Graziana A, Muto S, Ranjeva R, Mazars C** (2001) The nucleus together with the cytosol generates patterns of specific cellular calcium signatures in tobacco suspension culture cells. *Cell Calcium* **30**: 413-421
- Pei ZM, Murata Y, Benning G, Thomine S, Klusener B, Allen GJ, Grill E, Schroeder JI** (2000) Calcium channels activated by hydrogen peroxide mediate abscisic acid signalling in guard cells. *Nature* **406**: 731-734
- Peiter E, Maathuis FJ, Mills LN, Knight H, Pelloux J, Hetherington AM, Sanders D** (2005) The vacuolar  $\text{Ca}^{2+}$ -activated channel TPC1 regulates germination and stomatal movement. *Nature* **434**: 404-408
- Persson S, Wyatt SE, Love J, Thompson WF, Robertson D, Boss WF** (2001) The  $\text{Ca}^{2+}$  status of the endoplasmic reticulum is altered by induction of calreticulin expression in transgenic plants. *Plant Physiol* **126**: 1092-1104
- Petersen M, Brodersen P, Naested H, Andreasson E, Lindhart U, Johansen B, Nielsen HB, Lacy M, Austin MJ, Parker JE, Sharma SB, Klässig DF, Martienssen R, Mattsson O, Jensen AB, Mundy J** (2000) Arabidopsis map kinase 4 negatively regulates systemic acquired resistance. *Cell* **103**: 1111-1120
- Petutschnig EK, Jones AM, Serazetdinova L, Lipka U, Lipka V** (2010) The lysin motif receptor-like kinase (LysM-RLK) CERK1 is a major chitin-binding protein in *Arabidopsis thaliana* and subject to chitin-induced phosphorylation. *J Biol Chem* **285**: 28902-28911
- Pieterse CM, van Wees SC, Hoffland E, van Pelt JA, van Loon LC** (1996) Systemic resistance in Arabidopsis induced by biocontrol bacteria is independent of salicylic acid accumulation and pathogenesis-related gene expression. *Plant Cell* **8**: 1225-1237
- Pieterse CM, van Wees SC, van Pelt JA, Knoester M, Laan R, Gerrits H, Weisbeek PJ, van Loon LC** (1998) A novel signaling pathway controlling induced systemic resistance in Arabidopsis. *Plant Cell* **10**: 1571-1580
- Pittman JK, Shigaki T, Cheng NH, Hirschi KD** (2002) Mechanism of N-terminal autoinhibition in the Arabidopsis  $\text{Ca}^{2+}/\text{H}^{+}$  antiporter CAX1. *J Biol Chem* **277**: 26452-26459
- Plieth C** (2001) Plant calcium signaling and monitoring: pros and cons and recent experimental approaches. *Protoplasma* **218**: 1-23
- Postel S, Kemmerling B** (2009) Plant systems for recognition of pathogen-associated molecular patterns. *Semin Cell Dev Biol* **20**: 1025-1031

- Postel S, Kűfner I, Beuter C, Mazzotta S, Schwedt A, Borlotti A, Halter T, Kemmerling B, Nűrnberger T** (2010) The multifunctional leucine-rich repeat receptor kinase BAK1 is implicated in Arabidopsis development and immunity. *Eur J Cell Biol* **89**: 169-174
- Pottosin, II, Schonknecht G** (2007) Vacuolar calcium channels. *J Exp Bot* **58**: 1559-1569
- Price AH, Taylor A, Ripley SJ, Griffiths A, Trewavas AJ, Knight MR** (1994) Oxidative signals in tobacco increase cytosolic calcium. *Plant Cell* **6**: 1301-1310
- Qi Z, Stephens NR, Spalding EP** (2006) Calcium entry mediated by GLR3.3, an Arabidopsis glutamate receptor with a broad agonist profile. *Plant Physiol* **142**: 963-971
- Qi Z, Verma R, Gehring C, Yamaguchi Y, Zhao Y, Ryan CA, Berkowitz GA** (2010) Ca<sup>2+</sup> signaling by plant *Arabidopsis thaliana* Pep peptides depends on AtPepR1, a receptor with guanylyl cyclase activity, and cGMP-activated Ca<sup>2+</sup> channels. *Proc Natl Acad Sci U S A* **107**: 21193-21198
- Qin C, Wang X** (2002) The Arabidopsis phospholipase D family. Characterization of a calcium-independent and phosphatidylcholine-selective PLD zeta 1 with distinct regulatory domains. *Plant Physiol* **128**: 1057-1068
- Ramonell KM, Zhang B, Ewing RM, Chen Y, Xu D, Stacey G, Somerville S** (2002) Microarray analysis of chitin elicitation in Arabidopsis thaliana. *Mol Plant Pathol* **3**: 301-311
- Ranf S, Wűnnenberg P, Lee J, Becker D, Dunkel M, Hedrich R, Scheel D, Dietrich P** (2008) Loss of the vacuolar cation channel, AtTPC1, does not impair Ca<sup>2+</sup> signals induced by abiotic and biotic stresses. *Plant J* **53**: 287-299
- Reddy AS** (2001a) Calcium: silver bullet in signaling. *Plant Sci* **160**: 381-404
- Reddy AS** (2001b) Molecular motors and their functions in plants. *Int Rev Cytol* **204**: 97-178
- Reddy VS, Reddy AS** (1999) A plant calmodulin-binding motor is part kinesin and part myosin. *Bioinformatics* **15**: 1055-1057
- Reddy VS, Safadi F, Zielinski RE, Reddy AS** (1999) Interaction of a kinesin-like protein with calmodulin isoforms from Arabidopsis. *J Biol Chem* **274**: 31727-31733
- Rentel MC, Knight MR** (2004) Oxidative stress-induced calcium signaling in Arabidopsis. *Plant Physiol* **135**: 1471-1479
- Rienmuller F, Beyhl D, Lautner S, Fromm J, Al-Rasheid KA, Ache P, Farmer EE, Marten I, Hedrich R** (2010) Guard cell-specific calcium sensitivity of high density and activity SV/TPC1 channels. *Plant Cell Physiol* **51**: 1548-1554
- Rizhsky L, Davletova S, Liang H, Mittler R** (2004) The zinc finger protein Zat12 is required for cytosolic ascorbate peroxidase 1 expression during oxidative stress in Arabidopsis. *J Biol Chem* **279**: 11736-11743
- Robatzek S, Chinchilla D, Boller T** (2006) Ligand-induced endocytosis of the pattern recognition receptor FLS2 in Arabidopsis. *Genes Dev* **20**: 537-542
- Rodriguez MC, Petersen M, Mundy J** (2010) Mitogen-activated protein kinase signaling in plants. *Annu Rev Plant Biol* **61**: 621-649
- Ron M, Avni A** (2004) The receptor for the fungal elicitor ethylene-inducing xylanase is a member of a resistance-like gene family in tomato. *Plant Cell* **16**: 1604-1615
- Ronald PC, Beutler B** (2010) Plant and animal sensors of conserved microbial signatures. *Science* **330**: 1061-1064
- Rudd JJ, Franklin-Tong VE** (2001) Unravelling response-specificity in Ca<sup>2+</sup> signalling pathways in plant cells. *New Phytologist* **151**: 7-33
- Rudolf R, Mongillo M, Rizzuto R, Pozzan T** (2003) Looking forward to seeing calcium. *Nat Rev Mol Cell Biol* **4**: 579-586
- Rushton PJ, Somssich IE, Ringler P, Shen QJ** (2010) WRKY transcription factors. *Trends Plant Sci* **15**: 247-258
- Ryan CA, Pearce G** (1998) Systemin: a polypeptide signal for plant defensive genes. *Annu Rev Cell Dev Biol* **14**: 1-17

- Saijo Y, Tintor N, Lu X, Rauf P, Pajeroska-Mukhtar K, Haweker H, Dong X, Robatzek S, Schulze-Lefert P** (2009) Receptor quality control in the endoplasmic reticulum for plant innate immunity. *EMBO J* **28**: 3439-3449
- Salomon S, Robatzek S** (2006) Induced Endocytosis of the Receptor Kinase FLS2. *Plant Signal Behav* **1**: 293-295
- Sanders D, Brownlee C, Harper JF** (1999) Communicating with calcium. *Plant Cell* **11**: 691-706
- Sanders D, Pelloux J, Brownlee C, Harper JF** (2002) Calcium at the crossroads of signaling. *Plant Cell* **14 Suppl**: S401-417
- Sang Y, Cui D, Wang X** (2001) Phospholipase D and phosphatidic acid-mediated generation of superoxide in Arabidopsis. *Plant Physiol* **126**: 1449-1458
- Scheel D** (1998) Resistance response physiology and signal transduction. *Curr Opin Plant Biol* **1**: 305-310
- Scheidle H, Gross A, Niehaus K** (2005) The Lipid A substructure of the *Sinorhizobium meliloti* lipopolysaccharides is sufficient to suppress the oxidative burst in host plants. *New Phytol* **165**: 559-565
- Schellenberg B, Ramel C, Dudler R** (2010) Pseudomonas syringae virulence factor syringolin A counteracts stomatal immunity by proteasome inhibition. *Mol Plant Microbe Interact* **23**: 1287-1293
- Schneeberger K, Ossowski S, Lanz C, Juul T, Petersen AH, Nielsen KL, Jorgensen JE, Weigel D, Andersen SU** (2009) SHOREmap: simultaneous mapping and mutation identification by deep sequencing. *Nat Methods* **6**: 550-551
- Schuhegger R, Ihring A, Gantner S, Bahnweg G, Knappe C, Vogg G, Hutzler P, Schmid M, Van Breusegem F, Eberl L, Hartmann A, Langebartels C** (2006) Induction of systemic resistance in tomato by N-acyl-L-homoserine lactone-producing rhizosphere bacteria. *Plant Cell Environ* **29**: 909-918
- Schulze B, Mentzel T, Jehle AK, Mueller K, Beeler S, Boller T, Felix G, Chinchilla D** (2010) Rapid heteromerization and phosphorylation of ligand-activated plant transmembrane receptors and their associated kinase BAK1. *J Biol Chem* **285**: 9444-9451
- Schweizer P, Felix G, Buchala A, Müller C, Métraux J-P** (1996) Perception of free cutin monomers by plant cells. *The Plant Journal* **10**: 331-341
- Schwessinger B, Zipfel C** (2008) News from the frontline: recent insights into PAMP-triggered immunity in plants. *Curr Opin Plant Biol* **11**: 389-395
- Scrase-Field SA, Knight MR** (2003) Calcium: just a chemical switch? *Curr Opin Plant Biol* **6**: 500-506
- Sedbrook JC, Kronebusch PJ, Borisy GG, Trewavas AJ, Masson PH** (1996) Transgenic AEQUORIN reveals organ-specific cytosolic Ca<sup>2+</sup> responses to anoxia and *Arabidopsis thaliana* seedlings. *Plant Physiol* **111**: 243-257
- Shacklock PS, Read ND, Trewavas AJ** (1992) Cytosolic free calcium mediates red light-induced photomorphogenesis. *Nature* **358**: 753-755
- Shan L, He P, Li J, Heese A, Peck SC, Nürnberger T, Martin GB, Sheen J** (2008) Bacterial effectors target the common signaling partner BAK1 to disrupt multiple MAMP receptor-signaling complexes and impede plant immunity. *Cell Host Microbe* **4**: 17-27
- Sharp JK, McNeil M, Albersheim P** (1984) The primary structures of one elicitor-active and seven elicitor-inactive hexa(beta-D-glucopyranosyl)-D-glucitols isolated from the mycelial walls of *Phytophthora megasperma* f. sp. *glycinea*. *J Biol Chem* **259**: 11321-11336
- Shears SB** (2009) Molecular basis for the integration of inositol phosphate signaling pathways via human ITPK1. *Adv Enzyme Regul* **49**: 87-96
- Sherameti I, Tripathi S, Varma A, Oelmüller R** (2008) The root-colonizing endophyte *Piriformospora indica* confers drought tolerance in Arabidopsis by stimulating the expression of drought stress-related genes in leaves. *Mol Plant Microbe Interact* **21**: 799-807
- Shi J, Kim KN, Ritz O, Albrecht V, Gupta R, Harter K, Luan S, Kudla J** (1999) Novel protein kinases associated with calcineurin B-like calcium sensors in Arabidopsis. *Plant Cell* **11**: 2393-2405

- Shigaki T, Cheng NH, Pittman JK, Hirschi K** (2001) Structural determinants of Ca<sup>2+</sup> transport in the Arabidopsis H<sup>+</sup>/Ca<sup>2+</sup> antiporter CAX1. *J Biol Chem* **276**: 43152-43159
- Shigaki T, Hirschi KD** (2006) Diverse functions and molecular properties emerging for CAX cation/H<sup>+</sup> exchangers in plants. *Plant Biol (Stuttg)* **8**: 419-429
- Shigaki T, Rees I, Nakhleh L, Hirschi KD** (2006) Identification of three distinct phylogenetic groups of CAX cation/proton antiporters. *J Mol Evol* **63**: 815-825
- Shimomura O, Musicki B, Kishi Y, Inouye S** (1993) Light-emitting properties of recombinant semi-synthetic aequorins and recombinant fluorescein-conjugated aequorin for measuring cellular calcium. *Cell Calcium* **14**: 373-378
- Silipo A, Erbs G, Shinya T, Dow JM, Parrilli M, Lanzetta R, Shibuya N, Newman MA, Molinaro A** (2010) Glyco-conjugates as elicitors or suppressors of plant innate immunity. *Glycobiology* **20**: 406-419
- Silipo A, Molinaro A, Sturiale L, Dow JM, Erbs G, Lanzetta R, Newman MA, Parrilli M** (2005) The elicitation of plant innate immunity by lipooligosaccharide of *Xanthomonas campestris*. *J Biol Chem* **280**: 33660-33668
- Silipo A, Sturiale L, Garozzo D, Erbs G, Jensen TT, Lanzetta R, Dow JM, Parrilli M, Newman MA, Molinaro A** (2008) The acylation and phosphorylation pattern of lipid A from *Xanthomonas campestris* strongly influence its ability to trigger the innate immune response in Arabidopsis. *Chembiochem* **9**: 896-904
- Sivaguru M, Pike S, Gassmann W, Baskin TI** (2003) Aluminum rapidly depolymerizes cortical microtubules and depolarizes the plasma membrane: evidence that these responses are mediated by a glutamate receptor. *Plant Cell Physiol* **44**: 667-675
- Stab MR, Ebel J** (1987) Effects of Ca<sup>2+</sup> on phytoalexin induction by fungal elicitor in soybean cells. *Arch Biochem Biophys* **257**: 416-423
- Stephens NR, Qi Z, Spalding EP** (2008) Glutamate receptor subtypes evidenced by differences in desensitization and dependence on the GLR3.3 and GLR3.4 genes. *Plant Physiol* **146**: 529-538
- Stevenson-Paulik J, Bastidas RJ, Chiou ST, Frye RA, York JD** (2005) Generation of phytate-free seeds in Arabidopsis through disruption of inositol polyphosphate kinases. *Proc Natl Acad Sci U S A* **102**: 12612-12617
- Sun CW, Callis J** (1997) Independent modulation of *Arabidopsis thaliana* polyubiquitin mRNAs in different organs and in response to environmental changes. *Plant J* **11**: 1017-1027
- Sze H, Liang F, Hwang I, Curran AC, Harper JF** (2000) Diversity and regulation of plant Ca<sup>2+</sup> pumps: insights from expression in yeast. *Annu Rev Plant Physiol Plant Mol Biol* **51**: 433-462
- Takezawa D** (2003) Characterization of a novel plant PP2C-like protein Ser/Thr phosphatase as a calmodulin-binding protein. *J Biol Chem* **278**: 38076-38083
- Tan X, Calderon-Villalobos LI, Sharon M, Zheng C, Robinson CV, Estelle M, Zheng N** (2007) Mechanism of auxin perception by the TIR1 ubiquitin ligase. *Nature* **446**: 640-645
- Tapken D, Hollmann M** (2008) *Arabidopsis thaliana* glutamate receptor ion channel function demonstrated by ion pore transplantation. *J Mol Biol* **383**: 36-48
- Tavernier E, Wendehenne D, Blein JP, Pugin A** (1995) Involvement of free calcium in action of cryptogein, a proteinaceous elicitor of hypersensitive reaction in tobacco Cells. *Plant Physiol* **109**: 1025-1031
- Tellstrom V, Usadel B, Thimm O, Stitt M, Kuster H, Niehaus K** (2007) The lipopolysaccharide of *Sinorhizobium meliloti* suppresses defense-associated gene expression in cell cultures of the host plant *Medicago truncatula*. *Plant Physiol* **143**: 825-837
- Testerink C, Larsen PB, van der Does D, van Himbergen JA, Munnik T** (2007) Phosphatidic acid binds to and inhibits the activity of Arabidopsis CTR1. *J Exp Bot* **58**: 3905-3914
- Thomma BP, Nürnberger T, Joosten MH** (2011) Of PAMPs and effectors: the blurred PTI-ETI dichotomy. *Plant Cell* **23**: 4-15

- Titarenko E, Lopez-Solanilla E, Garcia-Olmedo F, Rodriguez-Palenzuela P** (1997) Mutants of *Ralstonia (Pseudomonas) solanacearum* sensitive to antimicrobial peptides are altered in their lipopolysaccharide structure and are avirulent in tobacco. *J Bacteriol* **179**: 6699-6704
- Torres MA, Dangl JL, Jones JD** (2002) Arabidopsis gp91phox homologues AtrbohD and AtrbohF are required for accumulation of reactive oxygen intermediates in the plant defense response. *Proc Natl Acad Sci U S A* **99**: 517-522
- Torres MA, Jones JD, Dangl JL** (2006) Reactive oxygen species signaling in response to pathogens. *Plant Physiol* **141**: 373-378
- Travassos LH, Girardin SE, Philpott DJ, Blanot D, Nahori MA, Werts C, Boneca IG** (2004) Toll-like receptor 2-dependent bacterial sensing does not occur *via* peptidoglycan recognition. *EMBO Rep* **5**: 1000-1006
- Trewavas A** (1999) Le calcium, C'est la vie: calcium makes waves. *Plant Physiol* **120**: 1-6
- Tsuda K, Katagiri F** (2010) Comparing signaling mechanisms engaged in pattern-triggered and effector-triggered immunity. *Curr Opin Plant Biol* **13**: 459-465
- Umemoto N, Kakitani M, Iwamatsu A, Yoshikawa M, Yamaoka N, Ishida I** (1997) The structure and function of a soybean beta-glucan-elicitor-binding protein. *Proc Natl Acad Sci U S A* **94**: 1029-1034
- Urquhart W, Gunawardena AH, Moeder W, Ali R, Berkowitz GA, Yoshioka K** (2007) The chimeric cyclic nucleotide-gated ion channel ATCNGC11/12 constitutively induces programmed cell death in a Ca<sup>2+</sup> dependent manner. *Plant Mol Biol* **65**: 747-761
- Vadassery J, Ranf S, Drzewiecki C, Mithofer A, Mazars C, Scheel D, Lee J, Oelmüller R** (2009) A cell wall extract from the endophytic fungus *Piriformospora indica* promotes growth of Arabidopsis seedlings and induces intracellular calcium elevation in roots. *Plant J* **59**: 193-206
- van den Burg HA, Harrison SJ, Joosten MH, Vervoort J, de Wit PJ** (2006) *Cladosporium fulvum* Avr4 protects fungal cell walls against hydrolysis by plant chitinases accumulating during infection. *Mol Plant Microbe Interact* **19**: 1420-1430
- van den Burg HA, Spronk CA, Boeren S, Kennedy MA, Vissers JP, Vuister GW, de Wit PJ, Vervoort J** (2004) Binding of the AVR4 elicitor of *Cladosporium fulvum* to chitotriose units is facilitated by positive allosteric protein-protein interactions: the chitin-binding site of AVR4 represents a novel binding site on the folding scaffold shared between the invertebrate and the plant chitin-binding domain. *J Biol Chem* **279**: 16786-16796
- van Der Luit AH, Olivari C, Haley A, Knight MR, Trewavas AJ** (1999) Distinct calcium signaling pathways regulate calmodulin gene expression in tobacco. *Plant Physiol* **121**: 705-714
- van der Luit AH, Piatti T, van Doorn A, Musgrave A, Felix G, Boller T, Munnik T** (2000) Elicitation of suspension-cultured tomato cells triggers the formation of phosphatidic acid and diacylglycerol pyrophosphate. *Plant Physiol* **123**: 1507-1516
- van Loon LC, Bakker PA, Pieterse CM** (1998) Systemic resistance induced by rhizosphere bacteria. *Annu Rev Phytopathol* **36**: 453-483
- Varma A, Savita V, Sudha, Sahay N, Butehorn B, Franken P** (1999) *Piriformospora indica*, a cultivable plant-growth-promoting root endophyte. *Appl Environ Microbiol* **65**: 2741-2744
- Verma S, Varma A, Rexer K-H, Hassel A, Kost G, Sarbhoy A, Bisen P, Butehorn B, Franken P** (1998) *Piriformospora indica*, gen. et sp. nov., a New Root-Colonizing Fungus. *Mycologia* **90**: 896-903
- Verret F, Wheeler G, Taylor AR, Farnham G, Brownlee C** (2010) Calcium channels in photosynthetic eukaryotes: implications for evolution of calcium-based signalling. *New Phytol* **187**: 23-43
- Very AA, Sentenac H** (2002) Cation channels in the Arabidopsis plasma membrane. *Trends Plant Sci* **7**: 168-175
- Vlot AC, Dempsey DA, Klessig DF** (2009) Salicylic Acid, a multifaceted hormone to combat disease. *Annu Rev Phytopathol* **47**: 177-206
- Walter A, Mazars C, Maitrejean M, Hopke J, Ranjeva R, Boland W, Mithofer A** (2007) Structural requirements of jasmonates and synthetic analogues as inducers of Ca<sup>2+</sup> signals in the nucleus and the cytosol of plant cells. *Angew Chem Int Ed Engl* **46**: 4783-4785

- Wan J, Zhang XC, Neece D, Ramonell KM, Clough S, Kim SY, Stacey MG, Stacey G** (2008) A LysM receptor-like kinase plays a critical role in chitin signaling and fungal resistance in Arabidopsis. *Plant Cell* **20**: 471-481
- Wang X** (2001) Plant Phospholipases. *Annu Rev Plant Physiol Plant Mol Biol* **52**: 211-231
- Wang YJ, Yu JN, Chen T, Zhang ZG, Hao YJ, Zhang JS, Chen SY** (2005) Functional analysis of a putative Ca<sup>2+</sup> channel gene *TaTPC1* from wheat. *J Exp Bot* **56**: 3051-3060
- Ward JM, Schroeder JI** (1994) Calcium-activated K<sup>+</sup> Channels and calcium-induced calcium release by slow vacuolar ion channels in guard cell vacuoles implicated in the control of stomatal closure. *Plant Cell* **6**: 669-683
- Webb AAR, McAinsh MR, Taylor JE, Hetherington AM** (1996) Calcium ions as intracellular second messengers in higher plants. In JA Callow, ed, *Advances in Botanical Research*, Vol Volume 22. Academic Press, pp 45-96
- Weinl S, Held K, Schlucking K, Steinhorst L, Kuhlger S, Hippler M, Kudla J** (2008) A plastid protein crucial for Ca<sup>2+</sup>-regulated stomatal responses. *New Phytol* **179**: 675-686
- Weinl S, Kudla J** (2009) The CBL-CIPK Ca<sup>2+</sup>-decoding signaling network: function and perspectives. *New Phytol* **184**: 517-528
- Wheeler GL, Brownlee C** (2008) Ca<sup>2+</sup> signalling in plants and green algae--changing channels. *Trends Plant Sci* **13**: 506-514
- White PJ, Broadley MR** (2003) Calcium in plants. *Ann Bot* **92**: 487-511
- Wyatt SE, Tsou PL, Robertson D** (2002) Expression of the high capacity calcium-binding domain of calreticulin increases bioavailable calcium stores in plants. *Transgenic Res* **11**: 1-10
- Xiang T, Zong N, Zou Y, Wu Y, Zhang J, Xing W, Li Y, Tang X, Zhu L, Chai J, Zhou JM** (2008) *Pseudomonas syringae* effector AvrPto blocks innate immunity by targeting receptor kinases. *Curr Biol* **18**: 74-80
- Yamaguchi T, Minami E, Shibuya N** (2003) Activation of phospholipases by N-acetylchitooligosaccharide elicitor in suspension-cultured rice cells mediates reactive oxygen generation. *Physiologia Plantarum* **118**: 361-370
- Yamaguchi T, Minami E, Ueki J, Shibuya N** (2005) Elicitor-induced activation of phospholipases plays an important role for the induction of defense responses in suspension-cultured rice cells. *Plant Cell Physiol* **46**: 579-587
- Yamaguchi Y, Huffaker A, Bryan AC, Tax FE, Ryan CA** (2010) PEPR2 is a second receptor for the Pep1 and Pep2 peptides and contributes to defense responses in Arabidopsis. *Plant Cell* **22**: 508-522
- Yang T, Poovaiah BW** (2002) Hydrogen peroxide homeostasis: activation of plant catalase by calcium/calmodulin. *Proc Natl Acad Sci U S A* **99**: 4097-4102
- Yang T, Poovaiah BW** (2003) Calcium/calmodulin-mediated signal network in plants. *Trends Plant Sci* **8**: 505-512
- Yang Y, Shah J, Klessig DF** (1997) Signal perception and transduction in plant defense responses. *Genes Dev* **11**: 1621-1639
- Yokoyama T, Kobayashi N, Kouchi H, Minamisawa K, Kaku H, Tsuchiya K** (2000) A lipochitooligosaccharide, Nod factor, induces transient calcium influx in soybean suspension-cultured cells. *Plant J* **22**: 71-78
- Yoo JH, Park CY, Kim JC, Heo WD, Cheong MS, Park HC, Kim MC, Moon BC, Choi MS, Kang YH, Lee JH, Kim HS, Lee SM, Yoon HW, Lim CO, Yun DJ, Lee SY, Chung WS, Cho MJ** (2005) Direct interaction of a divergent CaM isoform and the transcription factor, MYB2, enhances salt tolerance in arabidopsis. *J Biol Chem* **280**: 3697-3706
- Yoo SD, Cho YH, Sheen J** (2007) Arabidopsis mesophyll protoplasts: a versatile cell system for transient gene expression analysis. *Nat Protoc* **2**: 1565-1572
- York JD** (2006) Regulation of nuclear processes by inositol polyphosphates. *Biochim Biophys Acta* **1761**: 552-559

- Yoshioka K, Moeder W, Kang HG, Kachroo P, Masmoudi K, Berkowitz G, Klessig DF** (2006) The chimeric Arabidopsis CYCLIC NUCLEOTIDE-GATED ION CHANNEL11/12 activates multiple pathogen resistance responses. *Plant Cell* **18**: 747-763
- Yu IC, Parker J, Bent AF** (1998) Gene-for-gene disease resistance without the hypersensitive response in Arabidopsis dnd1 mutant. *Proc Natl Acad Sci U S A* **95**: 7819-7824
- Zähringer U, Lindner B, Inamura S, Heine H, Alexander C** (2008) TLR2 - promiscuous or specific? A critical re-evaluation of a receptor expressing apparent broad specificity. *Immunobiology* **213**: 205-224
- Zeidler D, Zähringer U, Gerber I, Dubery I, Hartung T, Bors W, Hutzler P, Durner J** (2004) Innate immunity in *Arabidopsis thaliana*: lipopolysaccharides activate nitric oxide synthase (NOS) and induce defense genes. *Proc Natl Acad Sci U S A* **101**: 15811-15816
- Zeller G, Clark RM, Schneeberger K, Bohlen A, Weigel D, Ratsch G** (2008) Detecting polymorphic regions in *Arabidopsis thaliana* with resequencing microarrays. *Genome Res* **18**: 918-929
- Zeng W, He SY** (2010) A prominent role of the flagellin receptor FLAGELLIN-SENSING2 in mediating stomatal response to *Pseudomonas syringae* pv *tomato* DC3000 in Arabidopsis. *Plant Physiol* **153**: 1188-1198
- Zhang J, Li W, Xiang T, Liu Z, Laluk K, Ding X, Zou Y, Gao M, Zhang X, Chen S, Mengiste T, Zhang Y, Zhou JM** (2010) Receptor-like cytoplasmic kinases integrate signaling from multiple plant immune receptors and are targeted by a *Pseudomonas syringae* effector. *Cell Host Microbe* **7**: 290-301
- Zhang J, Shao F, Li Y, Cui H, Chen L, Li H, Zou Y, Long C, Lan L, Chai J, Chen S, Tang X, Zhou JM** (2007) A *Pseudomonas syringae* effector inactivates MAPKs to suppress PAMP-induced immunity in plants. *Cell Host Microbe* **1**: 175-185
- Zhang W, Qin C, Zhao J, Wang X** (2004) Phospholipase D alpha 1-derived phosphatidic acid interacts with ABI1 phosphatase 2C and regulates abscisic acid signaling. *Proc Natl Acad Sci U S A* **101**: 9508-9513
- Zhang W, Wang C, Qin C, Wood T, Olafsdottir G, Welti R, Wang X** (2003) The oleate-stimulated phospholipase D, PLDdelta, and phosphatidic acid decrease H<sub>2</sub>O<sub>2</sub>-induced cell death in Arabidopsis. *Plant Cell* **15**: 2285-2295
- Zhang Y, Zhu H, Zhang Q, Li M, Yan M, Wang R, Wang L, Welti R, Zhang W, Wang X** (2009) Phospholipase dalpha1 and phosphatidic acid regulate NADPH oxidase activity and production of reactive oxygen species in ABA-mediated stomatal closure in Arabidopsis. *Plant Cell* **21**: 2357-2377
- Zhao J, Shigaki T, Mei H, Guo YQ, Cheng NH, Hirschi KD** (2009) Interaction between Arabidopsis Ca<sup>2+</sup>/H<sup>+</sup> exchangers CAX1 and CAX3. *J Biol Chem* **284**: 4605-4615
- Zhao MG, Tian QY, Zhang WH** (2007) Ethylene activates a plasma membrane Ca<sup>2+</sup>-permeable channel in tobacco suspension cells. *New Phytol* **174**: 507-515
- Zimmermann S, Nürnberger T, Frachisse J-M, Wirtz W, Guern J, Hedrich R, Scheel D** (1997) Receptor-mediated activation of a plant Ca<sup>2+</sup>-permeable ion channel involved in pathogen defense. *Proc Natl Acad Sci U S A* **94**: 2751-2755
- Zipfel C** (2009) Early molecular events in PAMP-triggered immunity. *Curr Opin Plant Biol* **12**: 414-420
- Zipfel C, Felix G** (2005) Plants and animals: a different taste for microbes? *Curr Opin Plant Biol* **8**: 353-360
- Zipfel C, Kunze G, Chinchilla D, Caniard A, Jones JD, Boller T, Felix G** (2006) Perception of the bacterial PAMP EF-Tu by the receptor EFR restricts Agrobacterium-mediated transformation. *Cell* **125**: 749-760
- Zipfel C, Robatzek S, Navarro L, Oakeley EJ, Jones JD, Felix G, Boller T** (2004) Bacterial disease resistance in Arabidopsis through flagellin perception. *Nature* **428**: 764-767

## 5. APPENDIX

### 5.1. Supporting information to 2.2.2

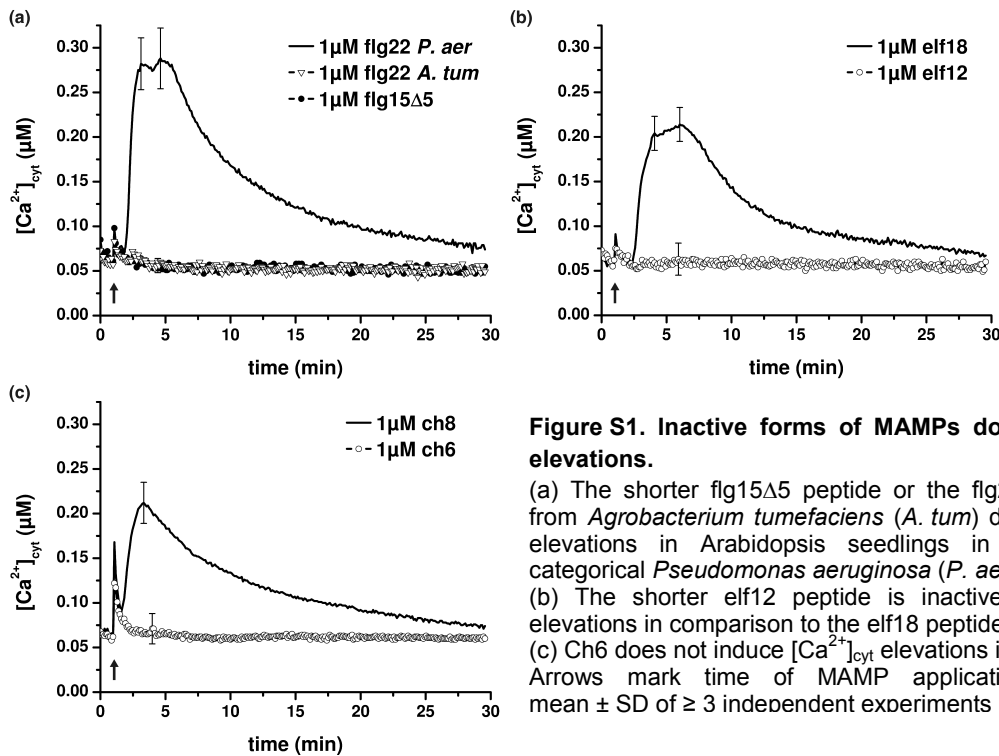


**Figure S1. Inactive forms of MAMPs do not evoke  $[Ca^{2+}]_{cyt}$  elevations.**

(a) The shorter flg15 $\Delta$ 5 peptide or the flg22-analogous peptide from *Agrobacterium tumefaciens* (*A. tum*) do not induce  $[Ca^{2+}]_{cyt}$  elevations in Arabidopsis seedlings in comparison to the categorical *Pseudomonas aeruginosa* (*P. aer*) flg22 peptide. (b) The shorter elf12 peptide is inactive in eliciting  $[Ca^{2+}]_{cyt}$  elevations in comparison to the elf18 peptide. (c) Ch6 does not induce  $[Ca^{2+}]_{cyt}$  elevations in comparison to ch8. Arrows mark time of MAMP application. Data represent mean  $\pm$  SD of  $\geq 3$  independent experiments ( $n \geq 12$ ).

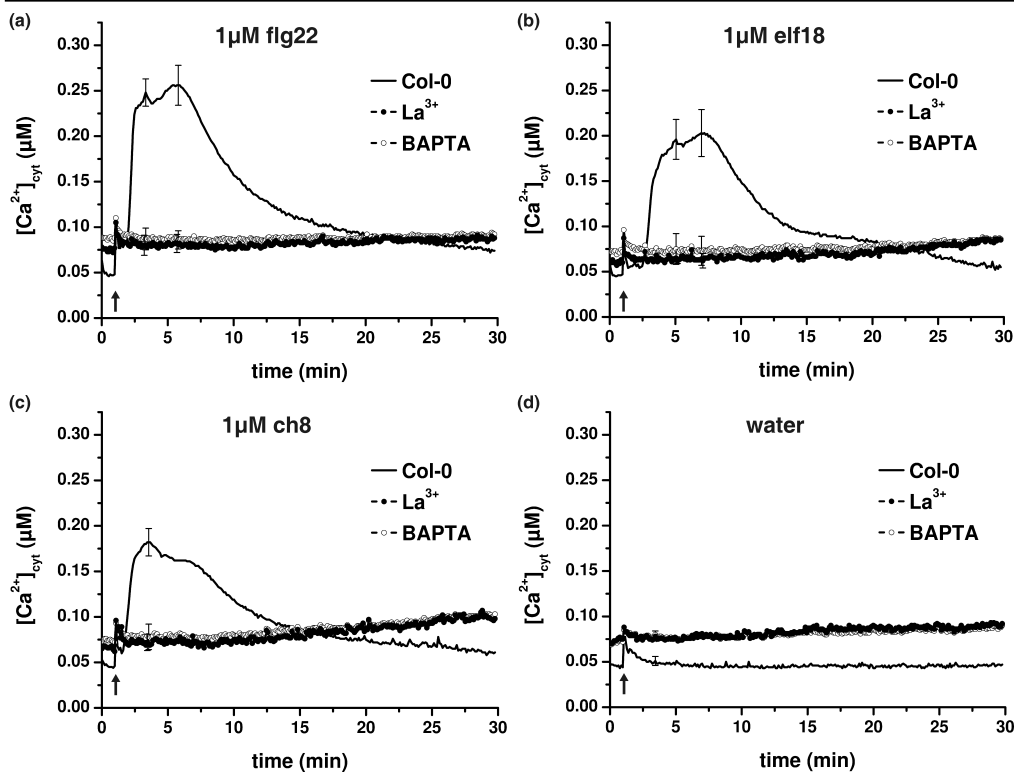


**Figure S2. Pre-treatment with  $LaCl_3$  or BAPTA abolishes MAMP-induced  $[Ca^{2+}]_{cyt}$  elevations.**

(a-c) Pre-treatment of Col-0 seedlings with 10 mM  $LaCl_3$  or 10 mM BAPTA for 30 min inhibits  $[Ca^{2+}]_{cyt}$  elevations induced by the indicated MAMPs.

(d) Both inhibitors slightly raise the  $[Ca^{2+}]_{cyt}$  resting level as observed in the water control.

Arrows mark time of MAMP application. Data represent mean  $\pm$  SD of two independent experiments ( $n \geq 3$ ).

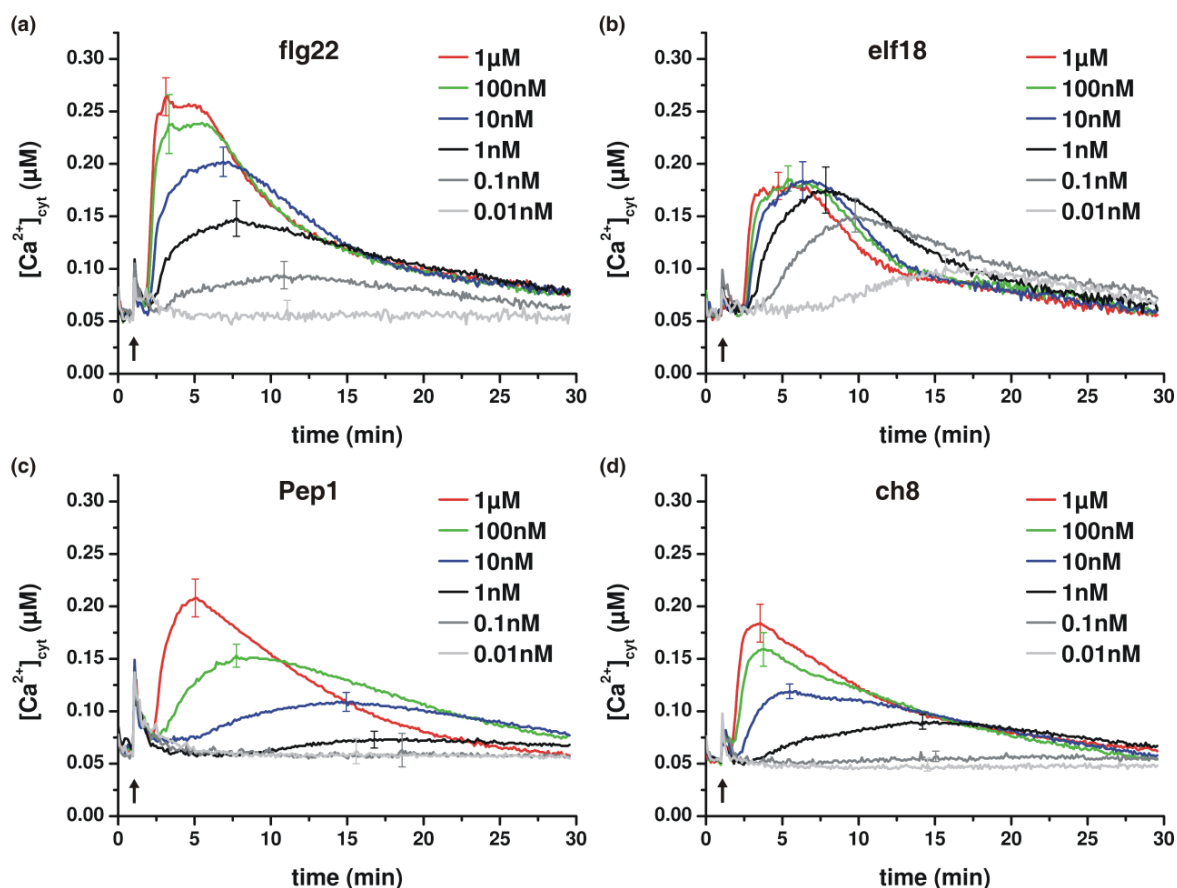


**Figure S3. MAMP/DAMP-induced  $[Ca^{2+}]_{cyt}$  elevations are dose-dependent.**

$[Ca^{2+}]_{cyt}$  elevations in Arabidopsis seedlings induced by the indicated concentrations of (a) flg22, (b) elf18, (c) Pep1 and (d) ch8. Nearly saturating concentrations reveal similar patterns for all the tested MAMPs/DAMPs but distinct  $[Ca^{2+}]_{cyt}$  amplitudes. At lower concentrations, the  $[Ca^{2+}]_{cyt}$  responses were also very similar in shape, but in general the maximum peak heights were lower and the maxima occurred at later times. Arrows mark time of MAMP/DAMP application. Data represent mean  $\pm$  SD of  $\geq 3$  independent experiments ( $n \geq 8$ ).

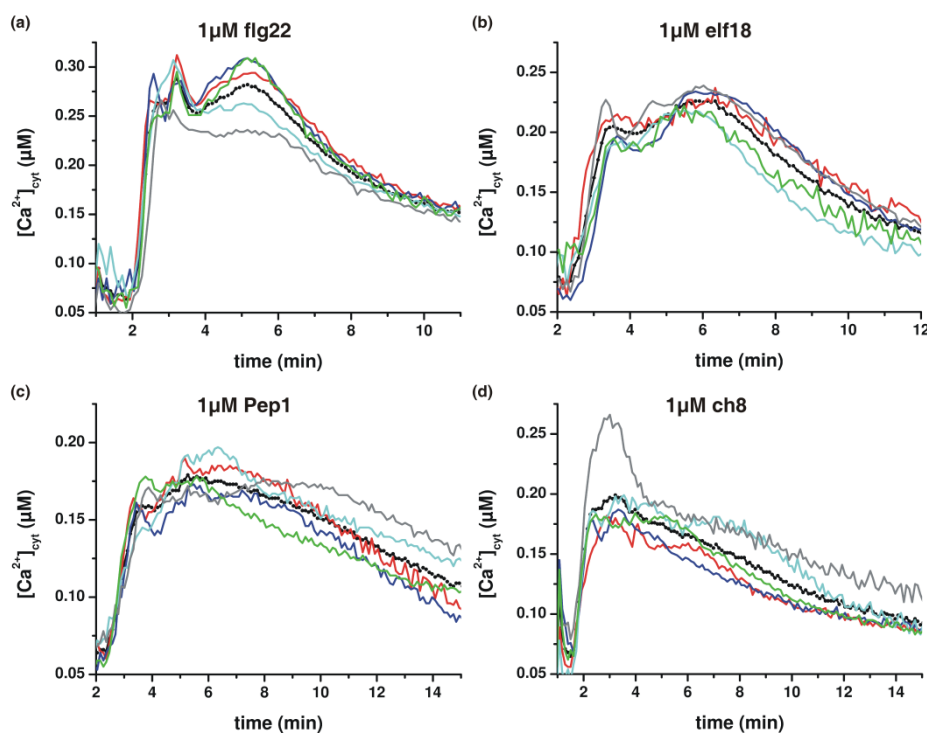


**Figure S4. Individual traces of MAMP/DAMP-induced  $[Ca^{2+}]_{cyt}$  elevations in seedlings.**

Five individual traces (illustrated by different colours) of  $[Ca^{2+}]_{cyt}$  elevations in Col-0 seedlings upon application of the indicated MAMPs/DAMPs. While individual traces illustrate the occurrence of distinct Ca peaks, these "fine structures" are not always visible in average graphs (dotted black line).

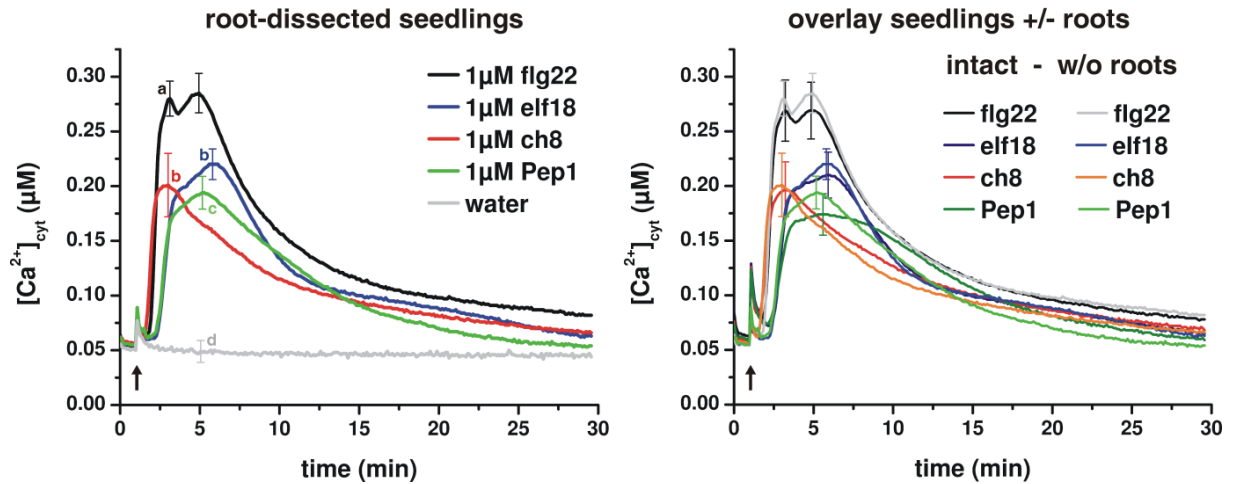


**Figure S5. MAMPs/DAMPs induce comparable  $[Ca^{2+}]_{\text{cyt}}$  elevations in intact and root-dissected Arabidopsis seedlings.**

$[Ca^{2+}]_{\text{cyt}}$  elevations upon application (marked by arrow) of the MAMPs/DAMPs flg22, elf18, ch8 and Pep1 in root-dissected Col-0 seedlings are comparable to intact seedlings (cf. fig. 1a). To facilitate comparison, an overlay of the  $[Ca^{2+}]_{\text{cyt}}$  elevations in intact (shown in figure 1a) and root-dissected (w/o roots) seedlings is included. Thus, the  $[Ca^{2+}]_{\text{cyt}}$  response in intact seedlings mostly originates from the aerial parts, which under the growth conditions used also comprise the bulk of the seedling fresh weight. Water was used as control. Data represent mean  $\pm$  SD of  $\geq 3$  independent experiments ( $n \geq 24$ ).

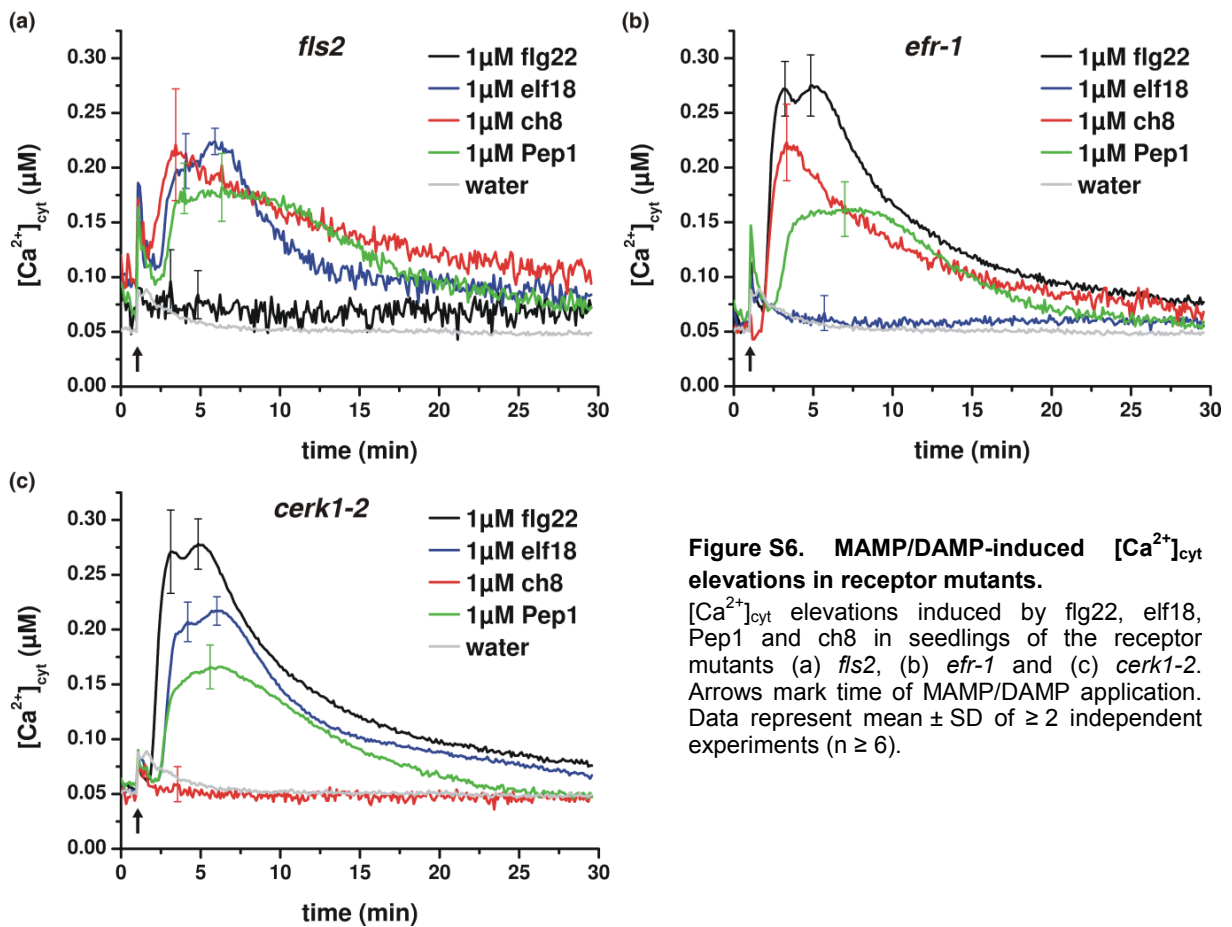


**Figure S6. MAMP/DAMP-induced  $[Ca^{2+}]_{\text{cyt}}$  elevations in receptor mutants.**

$[Ca^{2+}]_{\text{cyt}}$  elevations induced by flg22, elf18, Pep1 and ch8 in seedlings of the receptor mutants (a) *fls2*, (b) *efr-1* and (c) *cerk1-2*. Arrows mark time of MAMP/DAMP application. Data represent mean  $\pm$  SD of  $\geq 2$  independent experiments ( $n \geq 6$ ).

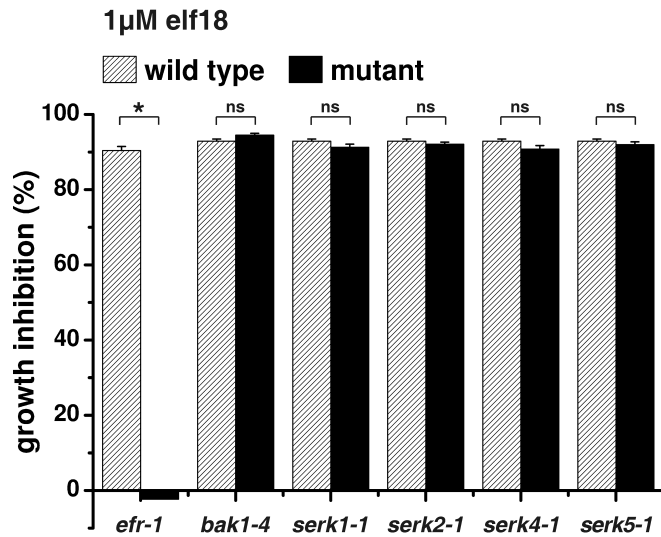


**Figure S7. Elf18-induced growth arrest in *bak1* and *serk* mutants.**

5-days-old seedlings from agar plates were transferred to liquid medium ± 1 μM elf18 and fresh weight was analysed after 15 days. Growth arrest of *bak1*, *serk* and *efr* (control) mutant seedlings (black bars) each compared to its respective wild-type control (shaded bars). Data are given as % inhibition compared to untreated control; mean ± SE of n ≥ 7 seedlings; \* indicates statistical significant difference; ns = not significant (2-way ANOVA genotype x treatment; p < 0.001).

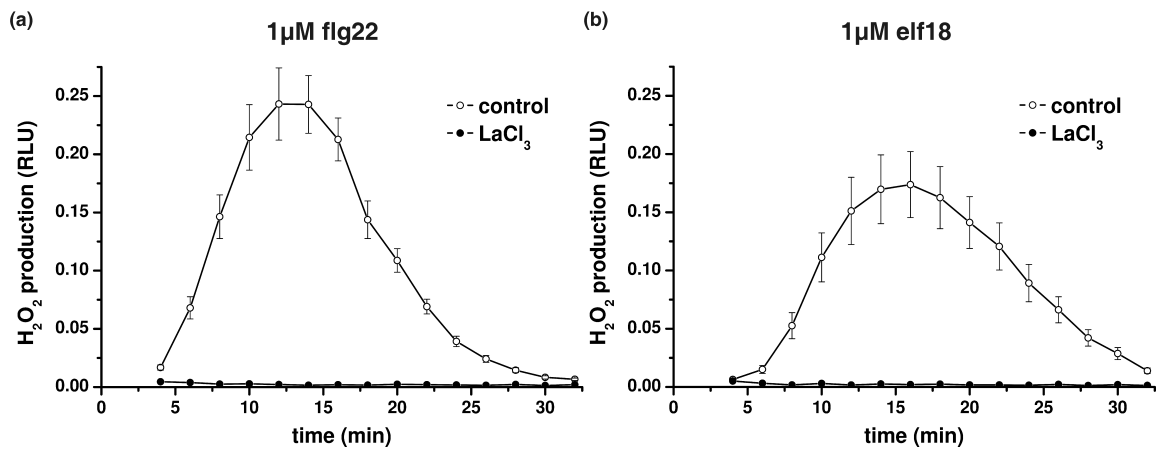


**Figure S8. Flg22- and elf18-induced ROS accumulation is abolished by LaCl<sub>3</sub> pre-treatment.**

(a,b) ROS (H<sub>2</sub>O<sub>2</sub>) production induced by the indicated MAMPs was monitored using a luminol-based assay in Col-0 leaf discs pre-treated with 10 mM LaCl<sub>3</sub> for 30 min. Data are given as relative light units (RLU) and represent mean ± SE of n ≥ 16. Two independent experiments revealed similar results.

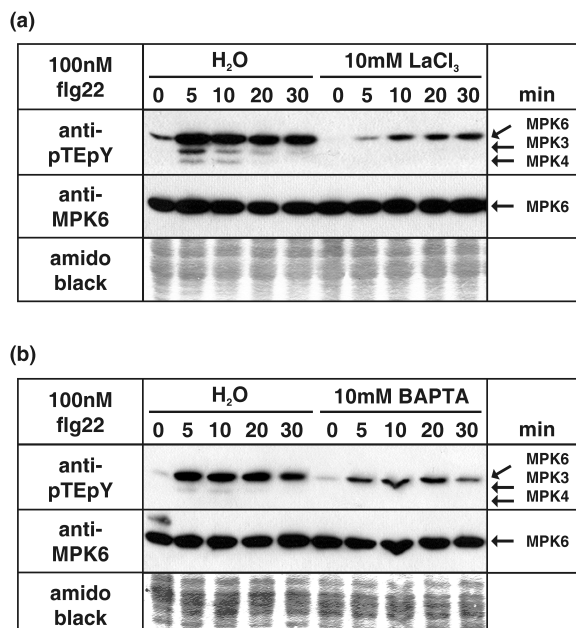


**Figure S9. Flg22-induced MAPK activation is reduced, but not abolished by pre-treatment with LaCl<sub>3</sub> and BAPTA.**

(a,b) MAPK activation upon flg22 application in Arabidopsis suspension-cultured cells was analysed by anti-pTEpY Western blot at indicated time points. Cells were pre-treated with 10 mM LaCl<sub>3</sub>, 10 mM BAPTA or water as control for 2 h. Anti-MPK6 Western blot shows equal amounts of MPK6 protein in untreated and inhibitor pre-treated samples. Amido-black-stained membranes show equal loading. Three independent experiments revealed comparable results.

**Table S1. Mutant lines used in the reverse genetic screen**

Mutant lines used are listed below showing AGI code, identity of insertion line, primers used for genotyping, kind and number of aequorin transgenic lines (T = transformants, C = crossing) and references.

mutant	AGI code	insertion line	genotyping primers	aeq. lines	reference	obtained from
<i>fls2</i>	At5g46330	SALK 062054	fwd: gttgtccggtgatgttcctgag rev: cggtgaaatgattcctcccaa	T (3)		B. Kemmerling
<i>efr-1</i>	At5g20480	SALK 044334	fwd: tccagataaagccggttg rev: tcatttccctcggaatcaag	T (4)	Zipfel <i>et al.</i> , 2006	C. Zipfel
<i>cerk1-2</i>	At3g21630	GABI-KAT 096F09	fwd: ggagaagtgtctgcaaaagtag rev: ctaccggccggacataagactg	T (3)	Wan <i>et al.</i> , 2008	G. Stacey
<i>bak1-3</i>	At4g33430	SALK 034523	fwd: atctgacggaattggtgagc rev: cttgtagcgtcaggacagca	T (3)	Chinchilla <i>et al.</i> , 2007	B. Kemmerling
<i>bak1-4</i>	At4g33430	SALK 116202	fwd: ccggagatattcctgttaatgg rev: acaagcaatctttcggttg	T (3)	Chinchilla <i>et al.</i> , 2007	B. Kemmerling
<i>serk1-1</i>	At1g71830	SALK 044330	fwd: cgtgacaacagcagtcctggcaccatcgg rev: cccttttaatcgaaccatagcac	C	Albrecht <i>et al.</i> , 2008	S. De Vries
<i>serk2-1</i>	At1g34210	SAIL 119-G03	fwd: ctctggtatgggaagatggtaatgtggtctgag rev: cggctagtaactggcccatagatcc	C	Albrecht <i>et al.</i> , 2008	S. De Vries
<i>serk4-1</i>	At2g13790	SALK 057955	fwd: gcagctgaagaagaccaga rev: acgctcaagtggagtaatga	C	Albrecht <i>et al.</i> , 2008	S. De Vries
<i>serk5-1</i>	At2g13800	SALK 147275	fwd: ctgaagaagaccagagg rev: ttgcttaatggaagtggagaga	C	Albrecht <i>et al.</i> , 2008	S. De Vries
<i>rbohD</i>	At5g47910	<i>dSpm</i> transposon	fwd: gtcgcaaaaggaggcggccga rev: ggatactgatcatagcgtggctcca	C + T (1)	Torres <i>et al.</i> , 2002	J. Dangl
<i>mpk3-1</i>	At3g45640	SALK 151594	fwd: atttttgtcaacaatggcctg rev: tctgccttttcacggaatag	T (5)	Wang <i>et al.</i> , 2007	S. Zhang
<i>mpk3-DG</i>	At3g45640	deletion	fwd: atgaacaccggcggtggccaata rev: aaccgtatgttgattgagtgtct	T (3)	Miles <i>et al.</i> , 2005	B. Ellis
<i>mpk6-3</i>	At2g43790	SALK 127507	fwd: tgatacggattgtttcgct rev: atcgctttgcgttttcgttca	T (3)	Bethke <i>et al.</i> , 2009	NASC
			SALK_LBa1: tggttcacgtagtggccatcg			
			SAIL_LB: gccttttcagaaatggataaatagccttgcttcc			
			<i>dSpm</i> transposon: ggtgcagcaaaaccacacttttacttc			
			GABI_T-DNA rev: atattgaccatcactcattgc			

**Table S2. Primers for cloning of promoters**

To clone the *NHL10* and *PHI1* promoters into the *pFRK1-LUC* vector, BamHI and NcoI restriction sites were added to the 5'- and 3'-primers (underlined), respectively, allowing direct exchange of the original *FRK1* promoter.

primer	sequence
pNHL10_5'-BamHI	<u>ggatcc</u> ccaatgacgaccaaagagtg
pNHL10_3'-NcoI	<u>ccatgg</u> gatagtaatttgggagaattatattg
pPHI1_5'-BamHI	<u>ggatcc</u> agtagttggagaaaattggctaagg
pPHI1_3'-NcoI	<u>ccatgg</u> taatttctgtaatgtagaagcaagaaaac

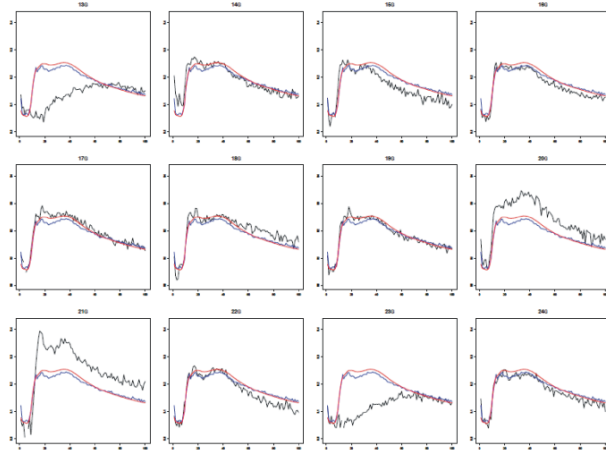
**Supplementary references**

- Albrecht, C., Russinova, E., Kemmerling, B., Kwaaitaal, M. and de Vries, S.C.** (2008) Arabidopsis SOMATIC EMBRYOGENESIS RECEPTOR KINASE proteins serve brassinosteroid-dependent and -independent signaling pathways. *Plant Physiol*, **148**, 611-619.
- Bethke, G., Unthan, T., Uhrig, J.F., Pöschl, Y., Gust, A.A., Scheel, D. and Lee, J.** (2009) Flg22 regulates the release of an ethylene response factor substrate from MAP kinase 6 in *Arabidopsis thaliana* via ethylene signaling. *Proc Natl Acad Sci U S A*, **106**, 8067-8072.
- Chinchilla, D., Zipfel, C., Robatzek, S., Kemmerling, B., Nürnberger, T., Jones, J.D., Felix, G. and Boller, T.** (2007) A flagellin-induced complex of the receptor FLS2 and BAK1 initiates plant defence. *Nature*, **448**, 497-500.
- Miles, G.P., Samuel, M.A., Zhang, Y. and Ellis, B.E.** (2005) RNA interference-based (RNAi) suppression of AtMPK6, an Arabidopsis mitogen-activated protein kinase, results in hypersensitivity to ozone and misregulation of AtMPK3. *Environ Pollut*, **138**, 230-237.
- Torres, M.A., Dangl, J.L. and Jones, J.D.** (2002) Arabidopsis gp91phox homologues AtrbohD and AtrbohF are required for accumulation of reactive oxygen intermediates in the plant defense response. *Proc Natl Acad Sci U S A*, **99**, 517-522.
- Wan, J., Zhang, X.C., Neece, D., Ramonell, K.M., Clough, S., Kim, S.Y., Stacey, M.G. and Stacey, G.** (2008) A LysM receptor-like kinase plays a critical role in chitin signaling and fungal resistance in Arabidopsis. *Plant Cell*, **20**, 471-481.
- Wang, H., Ngwenyama, N., Liu, Y., Walker, J.C. and Zhang, S.** (2007) Stomatal development and patterning are regulated by environmentally responsive mitogen-activated protein kinases in Arabidopsis. *Plant Cell*, **19**, 63-73.
- Zipfel, C., Kunze, G., Chinchilla, D., Caniard, A., Jones, J.D., Boller, T. and Felix, G.** (2006) Perception of the bacterial PAMP EF-Tu by the receptor EFR restricts Agrobacterium-mediated transformation. *Cell*, **125**, 749-760.

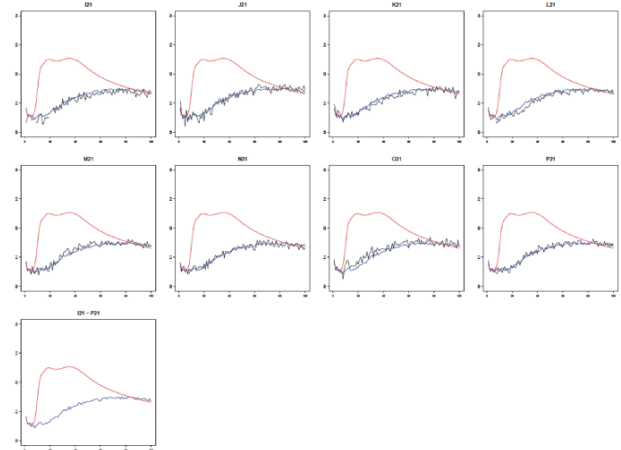
## 5.2. Supporting information to 2.3.2

### A

Screening of 12 M2 seedlings

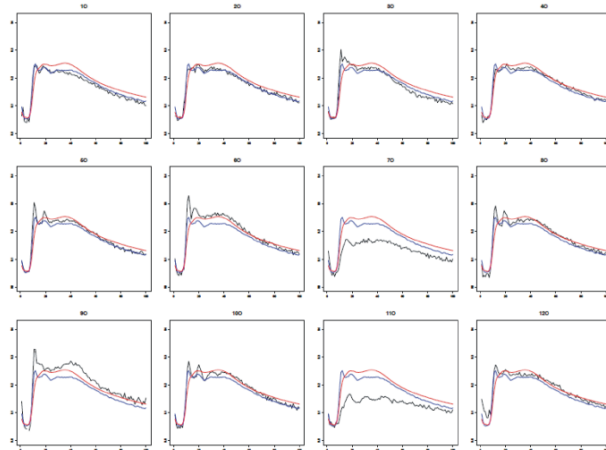


Confirmation in M3 generation



### B

Screening of 12 M2 seedlings



Confirmation in M3 generation

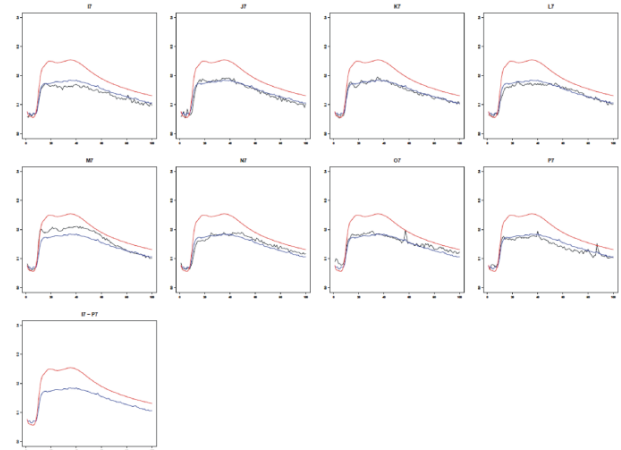


**Figure S1. Output examples of R-based data calibration.**

(A/B) Pdf-output files show the R-based calibration of  $[Ca^{2+}]_{cyt}$  measurements in a 384 well-plate. The left panel shows the screening result (12 segregating M2 seedlings per individual M1 line) and in the right panel, the subsequent validation of the mutant phenotype (8 M3 seedlings). As examples (A) a *bak1* and (B) a *cce* mutant with reduced  $[Ca^{2+}]_{cyt}$  elevation are shown. The black graphs show single seedlings measurements and the blue graph the average of all seedlings per line. A wild-type reference graph is shown in red. Numbers above graphs indicate the well coordinates on the 384 well-plate.

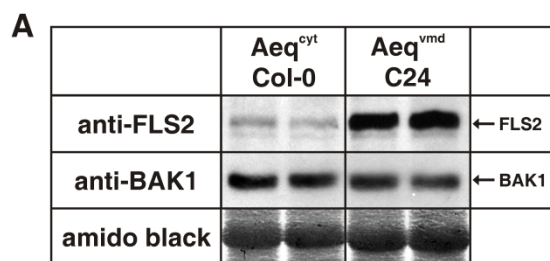


**Figure S2. Col-0 and C24 seedlings show differential expression and accumulation of immune receptors.**

(A) FLS2 and BAK1 protein accumulation in Aeq<sup>cyt</sup>/Col-0 and Aeq<sup>vmd</sup>/C24 seedlings was analysed by immunoblot using specific anti-FLS2 and anti-BAK1 antibodies. Amido-black stained membranes show equal loading. Three independent experiments revealed identical results.

(B) Comparative expression of MAMP/DAMP receptors in Arabidopsis Col-0 and C24 seedlings grown in liquid culture. Data were obtained from public database (Genevestigator v3, AT-407; (Delker *et al.*, 2010).



**Table SI: *fls2* mutants**

<i>fls2</i> -	nucleotide mutation	amino acid mutation
<b>25</b>	- 2981 A (insertion)	frame shift (I 972 N)
<b>26</b>	C 2659 T	Q 865 -
<b>27</b>	G 3340 A	G 1064 R
<b>28</b>	A 2661 x (deletion)	frame shift (A 866 Q)
<b>29</b>	C 3541 T	L 1131 F
<b>30</b>	G 3205 A	exon-intron border
<b>31</b>	C 1376 T	S 437 F
<b>32</b>	G 222 A	W 52 -
<b>33</b>	C 1025 T	S 320 L
<b>34</b>	C 3124 T	R 1020 W

**Table SII: *bak1* mutants**

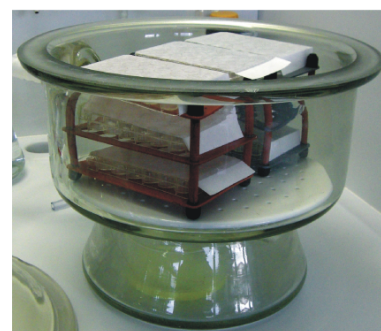
<i>bak1</i> -	nucleotide mutation	amino acid mutation
<b>6</b>	G 3904 A	C 545 Y
<b>7</b>	G 1052 A	exon-intron border
<b>8</b>	C 1415 T	R 138 -
<b>9</b>	G 2762 A	W 249 -
<b>10</b>	G 2334 A	exon-intron border
<b>11</b>	G 3008 A	G 306 R
<b>12</b>	G 3708 A	D 507 N
<b>13</b>	C 3498 T	L 437 F
<b>14</b>	G 2988 A	G 299 D
<b>15</b>	G 3035 A	A 315 T

**Table SIII: Primers for PCR and sequencing**

<b>Gene</b>	<b>PCR primers</b>		<b>Sequencing primers</b>	
<b><i>FLS2</i></b>	FLS2_fwd	5'-TATTGCGTCTTGGCCTTTTC-3'	1)	5'-ATCCGTGACATGATCCCTCA-3'
	FLS2_rev	5'-GGGACAAACGTCATCTCCAT-3'	2)	5'-CCATTAACTGGTTTCGATTCC-3'
			3)	5'-CAAGCCATTAATTGGGAAGC-3'
			4)	5'-TTCCAGAGAGTCTCGCCAAT-3'
			5)	5'-TCCCATCGTTCATTGTGATCT-3'
<b><i>EFR</i></b>	EFR_fwd	5'-TGTTTTGGGTAGCACTTTGC-3'	1)	5'-CACACACGTTTATGTGTTTTGACTG-3'
	EFR_rev	5'-CCCAACATTTGTTCTGTTTCG-3'	2)	5'-AGGCTTCAGTACTTGAACATGAG-3'
			3)	5'-TGGCGAACTGCACTCAATTA-3'
			4)	5'-TTGTTGGACTAGGTGCTTCG-3'
			5)	5'-ACTTTGGGGATGTTCCATGA-3'
			6)	5'-TCAGAGGCACCATTGGCTAT-3'
<b><i>BAK1</i></b>	BAK1_fwd	5'-GGGCTTTTCTCGTATTCTGC-3'	1)	5'-CCTTGTGTGGGTGGTAGCTT-3'
	BAK1_rev	5'-TGGGTTTTAGCTTTCAACAACA-3'	2)	5'-TGTACATGGTTTCATGTTACTTGC-3'
			3)	5'-AATACGTTTTTAATAAGCAGCCTAA-3'
			4)	5'-TTTTAAAGTTTGTATTTTGTCTCA-3'
			5)	5'-TTTGTCTTTGAAATGTTATTCAACTG-3'
			6)	5'-GCAGTTCAGACAGAGGTTGA-3'
			7)	5'-ACCGATGTCTTTGGGTATGG-3'

**Protocol 1: Seed sterilization**

- 1) Around 15 dry M2 seeds per M1 line were put into each well of a 24-well plate and the plate was sealed with a breathable, gas-permeable seal (BREATHseal™, GreinerBioOne).
- 2) Up to 8 plates, means 192 M1 lines, stacked in a plastic rack, were incubated in an exsiccator with a beaker at the bottom filled with NaOCl solution (12% Cl) and hydrochlorid acid (3:1, v/v) to produce chlorine gas.
- 3) After incubation for up to four hours the exsiccator was opened and the chlorine gas allowed to completely evaporate under a proper chemical fume hood over night. This minimized exposure of humans to the toxic chlorine gas.
- 4) As the breathable seal has a mesh width of less than 50µm avoiding contamination by aerial contaminants, sealed plates can be simply removed from the exsiccator. This way, dry sterilized seeds in 24 well plates can also be stored for several days before use, on the shelf.
- 5) Under a clean bench the breathable seal was removed. Plates can be filled with MS medium (2ml/well), covered with a clear sterile lid and sealed with breathable tape.
- 6) Alternatively, dry sterilized seeds can be easily transferred onto agar plates with sterile plastic tips or toothpicks. Resealing of the plate allows sterile storage of seeds for multiple use.
- 7) Plates were stratified for at least two days at 4°C in the dark.
- 8) Plates were transferred to an appropriate growth chamber.



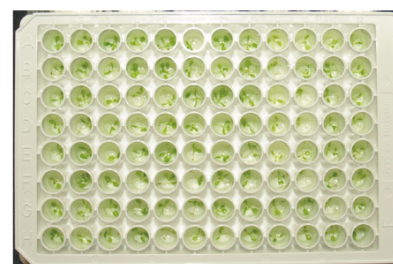
## **Protocol 2: [Ca<sup>2+</sup>] measurements in 96/384 well plates**

### **A) 384 well plates: high-throughput, less accurate**

1) Twelve 8-10 days-old M2 seedlings per M1 line from liquid culture were transferred individually into wells of a 384 well-plate containing 50 $\mu$ l dH<sub>2</sub>O. After transfer of seedlings, 10 $\mu$ l of a 6-fold concentrated coelenterazine solution in dH<sub>2</sub>O were added to yield a final concentration of 2-10 $\mu$ M per well. Seedlings were reconstituted over night in the dark. Coelenterazine stocks were 5mM in MeOH (-20°C, protected from light).

2) Each quarter of the 384-well plate was measured separately:

- a. 24 of the 96 wells (e. g. A1-12/B1-12) were scanned in 10sec intervals for 10min after automatic injection of 30 $\mu$ l of a 3-fold concentrated flg22 solution. This equals 100ms integration time per well per measurement point.
- b. After finishing all 96 wells in 4 groups of 24 wells each, candidate seedlings were rescued (according to raw data RLU peak) or discharged for quantitative analysis. All 96 samples were discharged well by well with 30 $\mu$ l of a two-fold concentrated discharge solution and integrated for at least 1min per well.
- c. After completion of the first 96-well quarter, the other 3 quarters were measured accordingly. Thus, a complete 384 well-plate, corresponding to 32 M1 lines with 12 M2 seedlings each, was measured automatically in less than 10 hours without any additional hands-on time.



### **B) 96 well plates: more accurate quantitative analysis**

1) 8-10 days-old seedlings from liquid culture were transferred individually into wells of a 96 well-plate containing 75 $\mu$ l dH<sub>2</sub>O. After transfer of seedlings 25 $\mu$ l of a 4-fold concentrated coelenterazine solution in dH<sub>2</sub>O were added to yield a final concentration of 2-10 $\mu$ M per well and the seedlings were reconstituted over night in the dark. Coelenterazine stocks were 5mM in MeOH (-20°C, protected from light).

2) Each row of the 96-well plate was measured separately:

- a. The first 12 wells (e. g. A1-12) were scanned in 6sec intervals for 1min to obtain resting level readings. This equals 300ms integration time per well per measurement point.
- b. After automatic injection or manual application of 50 $\mu$ l of a 3-fold concentrated flg22 solution wells were further scanned in 6sec intervals for 30min.
- c. After finishing the first 12 wells/row, wells were discharged for quantitative analysis. All 12 samples were discharged well by well with 150 $\mu$ l of a two-fold concentrated discharge solution and integrated for 3min per well for complete discharge.
- d. After completion of the first row, the remaining rows were measured accordingly row by row. Thus, a complete 96 well-plate can be accurately measured in around 8 hours, which was not feasible with continuous single well measurements.
- e. A wild type control was included in each row for direct comparison and evaluation of the measurement.

## 5.3. Publication and supporting information to 2.5.2

THE JOURNAL OF BIOLOGICAL CHEMISTRY VOL. 282, NO. 44, PP. 32338–32348, NOVEMBER 2, 2007  
© 2007 by The American Society for Biochemistry and Molecular Biology, Inc. Printed in the U.S.A.

## Bacteria-derived Peptidoglycans Constitute Pathogen-associated Molecular Patterns Triggering Innate Immunity in *Arabidopsis*<sup>\*,§</sup>

Received for publication, June 13, 2007, and in revised form, August 29, 2007. Published, JBC Papers in Press, August 30, 2007, DOI 10.1074/jbc.M704886200

Andrea A. Gust<sup>†1</sup>, Raja Biswas<sup>§</sup>, Heike D. Lenz<sup>‡</sup>, Thomas Rauhut<sup>||</sup>, Stefanie Ranf<sup>||</sup>, Birgit Kemmerling<sup>‡</sup>, Friedrich Götz<sup>§</sup>, Erich Glawischnig<sup>||</sup>, Justin Lee<sup>||</sup>, Georg Felix<sup>‡</sup>, and Thorsten Nürnberger<sup>‡</sup>

From the <sup>†</sup>Center for Plant Molecular Biology, Plant Biochemistry, and <sup>§</sup>Microbial Genetics, University of Tübingen, 72076 Tübingen, the <sup>||</sup>Department of Genetics, Technical University Munich, 85350 Freising, and the <sup>||</sup>Department of Stress and Developmental Biology, Leibniz-Institute of Plant Biochemistry, 06120 Halle/Saale, Germany

Pathogen-associated molecular pattern (PAMP)-triggered immunity constitutes the primary plant immune response that has evolved to recognize invariant structures of microbial surfaces. Here we show that Gram-positive bacteria-derived peptidoglycan (PGN) constitutes a novel PAMP of immune responses in *Arabidopsis thaliana*. Treatment with PGN from *Staphylococcus aureus* results in the activation of plant responses, such as medium alkalization, elevation of cytoplasmic calcium concentrations, nitric oxide, and camalexin production and the post-translational induction of MAPK activities. Microarray analysis performed with RNA prepared from PGN-treated *Arabidopsis* leaves revealed enhanced transcript levels for 236 genes, many of which are also altered upon administration of flagellin. Comparison of cellular responses after treatment with bacteria-derived PGN and structurally related fungal chitin indicated that both PAMPs are perceived via different perception systems. PGN-mediated immune stimulation in *Arabidopsis* is based upon recognition of the PGN sugar backbone, while muramyl dipeptide, which is inactive in this plant, triggers immunity-associated responses in animals. PGN adds to the list of PAMPs that induce innate immune programs in both plants and animals. However, we propose that PGN perception systems arose independently in both lineages and are the result of convergent evolution.

The innate immune system is a host defense mechanism that is evolutionarily conserved from insects to human and is mainly involved in the recognition and control of the early stage of infection in all animals (1). Over the last decade, it has become increasingly evident that also plants have acquired the ability to recognize “non self” via sensitive perception systems for components of microorganisms called pathogen-associated molecular patterns (PAMPs)<sup>2</sup> (2–4). As classically defined,

PAMPs are highly characteristic of potentially infectious microbes, but are not present in the host. In addition, such patterns are often vital for microbial survival and are therefore not subject to mutational variation. PAMPs that trigger innate immune responses in various vertebrate and non-vertebrate organisms include lipopolysaccharides (LPS) from Gram-negative bacteria, eubacterial flagellin, viral, and bacterial nucleic acids, fungal cell wall-derived glucans, chitins, mannans, or proteins and peptidoglycans (PGN) from Gram-positive bacteria (5–8).

Peptidoglycan (PGN) is an essential and unique component of the bacterial envelope that provides rigidity and structure to the bacterial cell. Virtually all bacteria contain a layer of PGN, but the amount, location, and specific composition vary. PGN is a polymer of alternating *N*-acetylglucosamine (GlcNAc) and *N*-acetyl-muramic acid (MurNAc) residues in  $\beta$ -1–4 linkage which are cross-linked by short peptides (9, 10). The glycan chains display little variation among different bacterial species while the peptide subunit and the interpeptide bridge reveal species specific differences. PGN from *Staphylococcus aureus* belongs to the *L*-lysine (Lys)-type, which is primarily found in Gram-positive bacteria whereas meso-diaminopimelate (Dap)-type PGN is typical for many Gram-negative bacteria.

As PGNs are located on most bacterial surfaces they constitute excellent targets for recognition by the innate immune system. Indeed, PGN is known for a long time to promote an innate immune response in vertebrates and insects (11–13), and a breakdown product of PGN, muramyl dipeptide (MurNAc-*L*-Ala-*D*-Glu; MDP) was found to be the minimal chemical structure required for PAMP activity in mammals (14). PGN is perceived in animals via various pattern recognition receptors (PRRs), including scavenger receptors, nucleotide-binding oligomerization domain-containing proteins (NODs), a family of peptidoglycan recognition proteins (PGRPs), PGN-lytic enzymes and Toll-like receptor TLR2 (15–19).

Remarkable similarities have been uncovered in the molecular mode of PAMP perception in animals and plants (2, 20, 21). Perception of flagellin in *Arabidopsis* was shown to be depend-

\* The costs of publication of this article were defrayed in part by the payment of page charges. This article must therefore be hereby marked “advertisement” in accordance with 18 U.S.C. Section 1734 solely to indicate this fact.  
§ The on-line version of this article (available at <http://www.jbc.org>) contains supplemental Figs. S1 and S2 and Tables S1 and S2.

<sup>1</sup> To whom correspondence should be addressed: Center for Plant Molecular Biology, Plant Biochemistry, University of Tübingen, Auf der Morgenstelle 5, 72076 Tübingen, Germany. Fax: 49-7071-295226; E-mail: andrea.gust@zmbp.uni-tuebingen.de.

<sup>2</sup> The abbreviations used are: PAMP, pathogen-associated molecular pattern; EFR, EF-Tu receptor; Flg22, 22 amino acid fragment of flagellin; FLS2, flagellin-sensing 2; GUS,  $\beta$ -glucuronidase; LPS, lipopolysaccharides; LRR,

leucine-rich repeat; MAPK/MPK, mitogen-activated protein kinase; MDP, muramyl dipeptide; NLP<sub>pp</sub>, Nep1 (necrosis and ethylene-inducing peptide 1)-like protein; NOD, nucleotide-binding oligomerization domain; PGN, peptidoglycan; PR-1, pathogenesis-related 1; RLK, receptor-like kinase; TLR, toll-like receptor; MBP, myelin basic protein.

ent on FLS2, a plasma membrane-located receptor-like kinase protein with extracellular leucine-rich repeats (LRR-RLKs) (22). The extracytoplasmic LRR-domain of FLS2 thereby resembles the structure of the extracytoplasmic domain of human TLR5, which also recognizes bacterial flagellin as a PAMP (23). Generally, transmembrane LRR proteins appear to be a common element in PAMP perception in animal and plant systems. In mammals, 11 TLRs have been identified so far and a second plant LRR-RLK, EFR, was described to recognize the bacterial elongation factor Tu (EF-Tu) (24, 25). Interestingly, the LRR-containing cytoplasmic PGN receptors NOD1 and NOD2 in mammals (26) are structurally similar to the cytoplasmic LRR-containing pathogen resistance proteins in plants that mediate plant cultivar-specific, effector-triggered immunity (ETI) (2, 4).

Here we present evidence that PGNs mediate the activation of innate defense responses in the model plant *Arabidopsis thaliana* in addition to their well established role as a PAMP in vertebrates and insects. Treatment with PGN from the phytopathogenic Gram-positive bacterium *S. aureus* (27) results in the activation of plant defense responses such as medium alkalization, elevation of cytoplasmic calcium concentrations, NO production, the activation of MAPKs, the accumulation of camalexin and the induction of various defense-related genes. Interestingly, even though a comparison of the defense responses triggered by PGN and the structurally closely related glycan chitin showed a strong overlap, our results indicate that PGN and chitin engage different perception systems. Moreover, we identify the PGN glycan backbone as the PAMP-active part in PGN. This is in contrast to mammals in which MDP was shown to be the minimal structural requirement for PAMP activity (14).

### EXPERIMENTAL PROCEDURES

**Materials**—Flg22 peptide and hydrolyzed chitin fragments were described previously (25). MDP, muramic acid, the pentapeptide Ala-D- $\gamma$ -Glu-Lys-D-Ala-D-Ala, lipoteichoic acid from *S. aureus*, PGN from *Bacillus subtilis* and *Streptomyces* ssp. and LPS from *Pseudomonas aeruginosa* and *Escherichia coli* were obtained from Sigma and dissolved in water at a concentration of 10 mg/ml. PGN from *E. coli* was purchased from InvivoGen (San Diego, CA). LPS from *Burkholderia cepacea* was prepared as described (28). The lipopeptides Pam<sub>3</sub>Cys, Pam<sub>2</sub>Cys, and PamCys were a kind gift from emc microcollections (Tübingen, Germany).

**Plant Growth Conditions**—*PR-1:GUS* transgenic (29), pMAQ2 aequorin-transgenic (30, 31), or wild type *A. thaliana* Columbia-0 (Col-0) plants were grown on soil for 5–6 weeks as described (32). Dark grown cell cultures of *Arabidopsis* Ler were maintained as described (33) and were used for experiments 5–6 days after subculture.

**Peptidoglycan Preparation**—PGN from *S. aureus* SA113 (ATCC 35556) and sortase deletion mutant (SA113 $\Delta$ srtA)<sup>3</sup> was purified as described earlier (34, 35). Briefly, cells from stationary phase cultures were harvested by centrifugation at 3,000  $\times$  g for 30 min, boiled with 5% SDS for 30 min and broken with

glass beads. Insoluble polymeric PGN was harvested by centrifugation at 30,000  $\times$  g for 30 min and washed several times with lukewarm water to remove SDS. Broken cell walls were suspended in 100 mM Tris-HCl, pH 7.2, and treated with 10  $\mu$ g/ml DNase and 50  $\mu$ g/ml RNase A for 2 h and subsequently with 100  $\mu$ g/ml trypsin for 16 h at 37  $^{\circ}$ C. To remove wall teichoic acid, the PGN preparations were incubated with 48% hydrofluoric acid (HFA) for 48 h at 4  $^{\circ}$ C. PGN was harvested by centrifugation at 30,000  $\times$  g for 30 min and washed several times with water for complete removal of HFA. Further treatment of PGN included 8 M LiCl, 100 mM EDTA and acetone to remove residual protein and LPS contamination. PGN was finally washed several times with water and lyophilized. HPLC and mass spectrometry analysis of soluble PGN was carried out as described (34), with following modifications. Purified PGN (1 mg/ml) was suspended in 100 mM sodium phosphate buffer, pH 6.8, and digested with mutanolysin (50  $\mu$ g/ml), lysostaphin (10  $\mu$ g/ml), or both for 16 h at 37  $^{\circ}$ C. Digestion was terminated by boiling the samples at 90  $^{\circ}$ C for 10 min followed by centrifugation. Desalting of soluble muropeptides was performed by reverse phase HPLC using a Reprosil-Pur ODS-3 column (5  $\mu$ m; 250  $\times$  20 mm; Dr. Maisch). Muropeptides were eluted in a step gradient at a flow rate of 10 ml/min starting from water for 10 min to 100% methanol for the next 20 min. Muropeptides were detected at 210 nm. PGN peaks were collected and concentrated in a rotary evaporator to remove excess methanol. Finally, PGN preparations were lyophilized and stored at  $-20^{\circ}$ C.

**Histochemical GUS Detection**—For the histochemical detection of  $\beta$ -glucuronidase (GUS) enzyme activity whole leaves of *PR-1:GUS* transgenic *Arabidopsis* (29) were placed in 1 ml of 50 mM sodium phosphate, pH 7, 0.5 mM potassium ferrocyanide, 0.5 mM potassium ferricyanide, 10 mM EDTA, pH 8, 0.1% Triton X-100, and 0.5 mg/ml 5-bromo-4-chloro-3-indolyl- $\beta$ -D-glucuronide (X-gluc, X-Gluc-DIRECT). After vacuum infiltration, the leaves were incubated at 37  $^{\circ}$ C overnight, and chlorophyll was subsequently removed by several washings in 70% ethanol.

**Medium Alkalinization, NO, and Camalexin Detection**—Medium alkalinization in *A. thaliana* Ler cell suspensions was measured in 2-ml aliquots as described (25). Nitric oxide synthesis in cell cultures was analyzed as described (36). Camalexin production in plants was quantified by reverse phase HPLC (LiChroCART 250–4, RP-18, 5  $\mu$ m, Merck; 1 ml/min; MeOH/H<sub>2</sub>O (1:1) for 2 min, followed by a 10 min linear gradient to 100% MeOH, followed by 3 min 100% MeOH) (37). The peak at 12 min was identified as camalexin by comparison with an authentic standard with respect to retention time and UV spectrum (photodiode array detector, Dionex) and quantified using a Shimadzu F-10AXL fluorescence detector (318 nm excitation, 370 nm emission) and by UV absorption at 318 nm.

**Calcium Measurements**—Cytosolic calcium concentrations were measured by calcium-induced aequorin luminescence using transgenic *Arabidopsis* pMAQ2 plants expressing cytosolic apoaquorin under the control of the CaMV 35S promoter (30, 31). Mature leaves of 5-week-old plants were cut into 1-mm strips and floated on 100  $\mu$ l of water supplemented with 10  $\mu$ M coelenterazine (native coelenterazine, 5 mM stock in methanol,

<sup>3</sup> G. Thumm and F. Götz, unpublished data.

### Peptidoglycans in *Arabidopsis* Immunity

Invitrogen) in a 96-well plate (4 strips/well,  $n > 3$ ). For aequorin reconstitution plates were incubated in the dark for at least 4 h. Luminescence was measured in a Luminoskan Ascent 2.1 luminometer (Labsystems) and recorded in integration intervals of 10 s. After 60 s recording, PAMPs were applied by addition of 50  $\mu$ l of a 3-fold concentrated solution in water and measurements continued for the indicated time. Controls were performed by addition of an equal volume of water. Remaining aequorin was discharged by automatic injection of 1 volume of 2 M  $\text{CaCl}_2$ /20% ethanol and luminescence was recorded for another 8–10 min until values were within 1% of the highest discharge value. Relative luminescence values were calculated and converted into actual  $\text{Ca}^{2+}$  concentrations as described (38).

**MAPK Activity Assay**—After elicitor treatment, leaves were immediately frozen in liquid nitrogen and MAP kinase activity was determined by in-gel kinase assays using myelin basic protein (MBP, Sigma) as substrate as described previously (39).

**RNA Isolation and Reverse Transcription-PCR**—Total RNA from leaves was isolated using the Tri Reagent method according to the manufacturer's recommendations (Sigma). First-strand cDNA was synthesized from 1  $\mu$ g of total RNA using RevertAid<sup>TM</sup> M-MuLV Reverse Transcriptase (Fermentas). RT-PCR was performed as described previously (40) using gene-specific primers (supplemental Table S1). Except for *EF1a*, which was amplified with 25 PCR cycles, all other PCRs were performed with 30 cycles.

**Microarray Experiments**—Microarray experiments were performed on *A. thaliana* Col-0 plants infiltrated with 100  $\mu$ g/ml PGN or water as a control. Affymetrix ATH1 high density oligonucleotide gene arrays were used for triplicate hybridizations of each biological sample. Global analysis of temporal gene expression was performed by subjecting the absolute expression values for scaling using the Affymetrix MAS5.0 software. Scaled mean values of expression were imported into Genespring software (version 7.2, Agilent Technologies, Waldbronn, Germany) using a gcRMA (41) plug-in normalization tool prior to data analysis. Means of three replicate values for each data set were analyzed for stimulus-induced differential gene expression. Data sets with expression levels below 50 were excluded from comparative analyses (noise level of expression cut-off). Genes were considered as up- or down-regulated if their mean expression levels deviated more than 2-fold from that of the non-elicited control samples.

### RESULTS

**Staphylococcal PGN Acts as a PAMP in *Arabidopsis***—Despite the well established role of PGN as a PAMP in animal innate immunity, surprisingly little is known about PGN perception in plants. We thus inquired about the ability of plants to recognize and respond to PGN from the Gram-positive bacterium *S. aureus*, that is found as root-associated bacterium in the rhizosphere of many plants and was recently shown to be pathogenic on *A. thaliana* (27, 42, 43). A typical and well characterized plant response to pathogen infection or treatment with PAMPs is the induction of genes encoding pathogenesis-related (PR) proteins (44), such as PR-1. To facilitate the detection of gene induction, we used a transgenic *PR-1:GUS* reporter line,

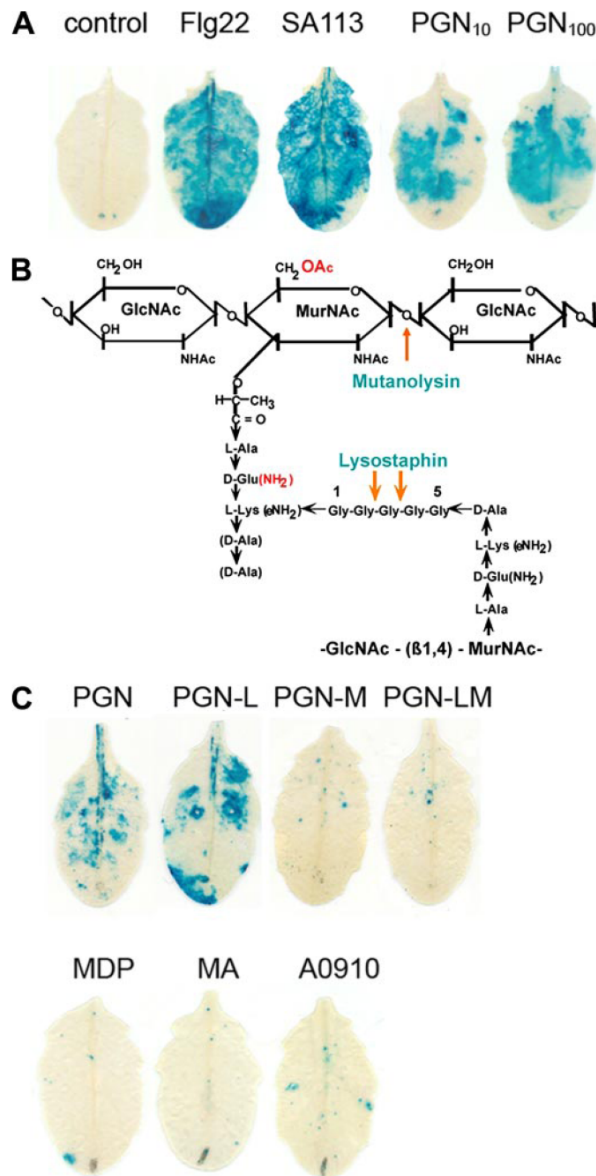


**FIGURE 1. *S. aureus* PGN is perceived in *A. thaliana* plants.** *A*, leaves from 5-week-old *PR1:GUS* transgenic *Arabidopsis* plants were infiltrated with 1  $\mu$ M Flg22, 100  $\mu$ g/ml heat-killed *S. aureus* SA113 cells, 10 or 100  $\mu$ g/ml PGN or water as a control and stained for GUS activity after 24 h. *B*, structure of *S. aureus* PGN, highlighting differences to PGNs from other Gram-positive bacteria (red) and cleavage sites for the enzymes mutanolysin and lysostaphin. *C*, leaves were treated with 100  $\mu$ g/ml of undigested PGN, lysostaphin-digested PGN (PGN-L), mutanolysin-digested PGN (PGN-M), double-digested PGN (PGN-LM), muramyl dipeptide (MDP), muramic acid (MA), or the pentapeptide Ala-D- $\gamma$ -Glu-Lys-D-Ala-D-Ala (A0910) as described in *A*.

in which the *PR-1* promoter is fused to the  $\beta$ -glucuronidase gene from *E. coli* (29, 45). As shown in Fig. 1*A*, treatment with heat-killed *S. aureus* cells or purified PGN resulted in a strong *PR-1:GUS* expression, similar to that observed with the elicitor-active 22 amino acid fragment from bacterial flagellin (Flg22) (46). We have consistently found *PR-1* gene expression with all PGN preparations tested. Quantitative differences in *PR-1* gene

## Peptidoglycans in Arabidopsis Immunity

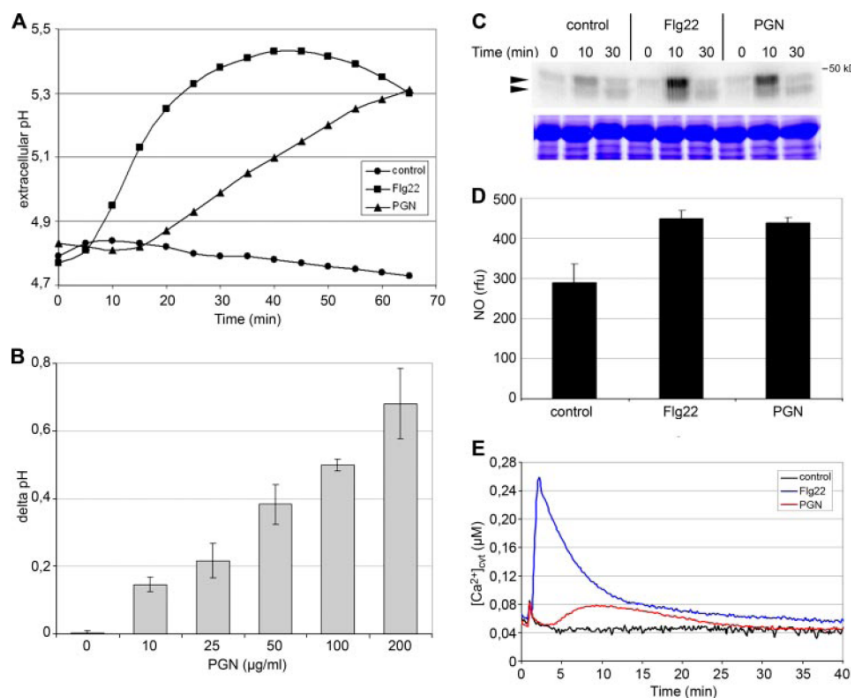


**FIGURE 2. PGN triggers early defense responses.** *A*, extracellular pH was monitored over a time course in 6-day-old *A. thaliana* Ler cell suspension cultures treated with 100 nM Flg22 (squares), 100  $\mu\text{g/ml}$  purified and undigested PGN (triangles) or water as a control (circles). *B*, cell cultures were treated with the indicated PGN concentrations and the extracellular pH was measured at 0 and 60 min to obtain the delta pH. *C*, leaves of 5-week-old *Arabidopsis* plants were infiltrated with 1  $\mu\text{M}$  Flg22, 100  $\mu\text{g/ml}$  PGN or water as a control. At indicated times, leaves were harvested, and MAP kinase activity was analyzed using an in-gel kinase assay with myelin basic protein as a substrate (upper panel). The positions of MAPK activities are indicated by arrowheads. Equal protein loading was confirmed by staining a duplicate gel with Coomassie Brilliant Blue (lower panel). *D*, cell cultures were treated with 1  $\mu\text{M}$  Flg22, 100  $\mu\text{g/ml}$  PGN, or water (control), and NO production was measured as described under "Experimental Procedures." NO production is given as relative fluorescence units. *E*, leaves of 5-week-old aequorin-transgenic *Arabidopsis* plants were cut into strips and  $[\text{Ca}^{2+}]_{\text{cyt}}$  was measured in a luminometer after addition of 1  $\mu\text{M}$  Flg22, 100  $\mu\text{g/ml}$  PGN, or water as a control described under "Experimental Procedures."

expression have only been observed upon infiltration into leaves of different PGN preparations, but not in assays using cultured cells (see below). Thus, these differences are most likely due to variations in the applicability of PGN into different biological samples. We next wanted to investigate which part of PGN is responsible for the induction of *PR-1:GUS*. Purified PGN was digested with either lysostaphin, an enzyme that specifically cleaves pentaglycin interpeptide bridges in staphylococcal PGN, or with mutanolysin, which hydrolyzes glycosidic linkages between disaccharide units of PGN (Fig. 1B). After HPLC purification, soluble muropeptides were infiltrated into *Arabidopsis* leaves, and GUS activity was detected after 24 h. Whereas lysostaphin-digested PGN was able to trigger *PR-1:GUS* expression, no induction was observed with mutanolysin- or mutanolysin/lysostaphin-digested PGN (Fig. 1C). Furthermore, treatment with smaller synthetic PGN components such as MDP, muramic acid or the pentapeptide Ala-D- $\gamma$ -Glu-Lys-D-Ala-D-Ala did not result in any *PR-1:GUS* induction. Taken together, these results indicate that not the protein part of PGN is perceived by *Arabidopsis*. Rather, sugar chains longer than the disaccharide are recognized, which is in contrast to

$\mu\text{g/ml}$  PGN triggered nearly maximal responses in medium alkalization assays (see also Fig. 5D) all further experiments were conducted with this PGN concentration.

Post-translational activation of mitogen-activated protein kinase (MAPK) activity is commonly associated with plant immunity (49). PGN or Flg22 were infiltrated into *Arabidopsis* leaves, and MAPK activity was subsequently analyzed in an in-gel kinase assay using MBP as artificial substrate. As shown in Fig. 2C, hypoosmotic stress because of water infiltration in the control samples caused a rapid, but transient activation of two MAPK species of 44 and 46 kDa, respectively. However, PGN treatment resulted in a much stronger response, which closely resembled that obtained with Flg22, most likely representing activation of MPK3 and MPK6 (50). Another hallmark of immune responses in animals and plants is the production of nitric oxide (NO) (36). Treatment of *Arabidopsis* cells with Flg22 or PGN resulted in a significant increase in NO production within 30 min (Fig. 2D). Calcium is a key second messenger in signal transduction pathways to external stimuli in various organisms (51, 52). We used *Arabidopsis* plants expressing cytoplasmic aequorin (31) to monitor changes of cytoplasmic

PGN perception in vertebrates in which already MDP displays strong immunogenic activity (14).

*PGN Triggers Early Plant Immune Responses*—Medium alkalization, occurring as a consequence of altered ion fluxes across the plasma membrane, is one of the earliest marker responses observed in elicitor-treated plant cells (47). In tobacco cells, addition of lyophilized *Micrococcus lysodeikticus* cells as well as *M. lysodeikticus* PGN induced a strong and rapid increase in extracellular pH (48). Here, we compared PGN-induced changes in extracellular pH in *Arabidopsis* cell suspension cultures with that induced by Flg22 (Fig. 2A). Flg22 treatment resulted in a rapid but transient increase in extracellular pH, reaching a maximum at about 30–40 min. In comparison, PGN induced a somewhat slower but more persistent increase in extracellular pH starting after a lag phase of about 15 min. Similar responses were obtained with commercially available PGN from the Gram-positive bacteria *B. subtilis* and *Streptomyces* ssp. (supplemental Fig. S1) and the Gram-negative bacterium *E. coli* (supplemental Fig. S2). Medium alkalization was dose-dependent with saturating concentrations of 100–200  $\mu\text{g/ml}$  PGN (Fig. 2B). As a concentration of 100

### Peptidoglycans in *Arabidopsis* Immunity

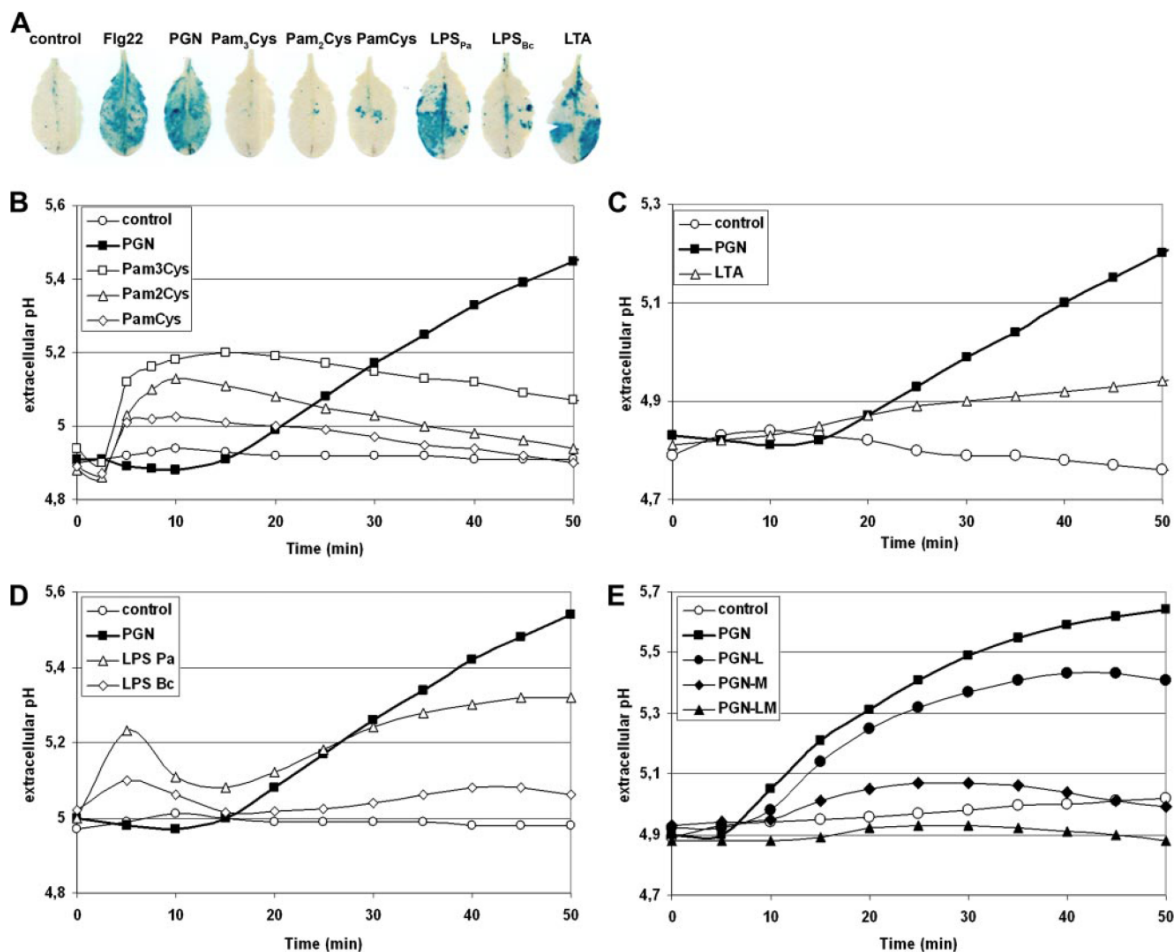


FIGURE 3. PGN elicitation differs from perception of other bacterial cell wall components. *A*, *PR-1:GUS* transgenic *Arabidopsis* leaves were infiltrated with water as control, 1  $\mu\text{M}$  Flg22, or each 100  $\mu\text{g}/\text{ml}$  purified PGN, the lipopeptides Pam<sub>3</sub>Cys, Pam<sub>2</sub>Cys, or PamCys, lipopolysaccharides from *P. aeruginosa* (LPS<sub>Pa</sub>) or *B. cepacea* (LPS<sub>Bc</sub>) and lipoteichoic acid (*LTA*) and stained for GUS activity after 24 h. *B–D*, extracellular pH in *Arabidopsis* cell cultures treated with each 100  $\mu\text{g}/\text{ml}$  of lipopeptides (*B*), lipopolysaccharides (*C*), or lipoteichoic acid (*D*). *E*, *Arabidopsis* cell cultures were treated with each 100  $\mu\text{g}/\text{ml}$  of undigested PGN, lysostaphin-digested PGN (*PGN-L*), mutanolysin-digested PGN (*PGN-M*), or double-digested PGN (*PGN-LM*), and extracellular pH was measured over a time course. All experiments were repeated once with similar results.

$\text{Ca}^{2+}$  levels *in vivo* after PAMP treatment. Luminometry of *Arabidopsis* leaf strips treated with Flg22 revealed a strong and rapid increase in  $[\text{Ca}^{2+}]_{\text{cyt}}$  starting after a 30–40 s lag phase and peaking after  $\sim 2$ –3 min, which was followed by a plateau phase of elevated  $[\text{Ca}^{2+}]_{\text{cyt}}$  (Fig. 2*E*). Likewise, PGN treatment also resulted in a significant elevation of  $[\text{Ca}^{2+}]_{\text{cyt}}$ ; however, as observed for medium alkalization, increase of  $[\text{Ca}^{2+}]_{\text{cyt}}$  occurred more slowly, reaching almost the same  $[\text{Ca}^{2+}]_{\text{cyt}}$  as the flg22-induced plateau phase at about 10 min before a gradual decrease to basal levels (Fig. 2*E*).

As undigested PGN is a very complex molecule, we wanted to rule out that cell wall components tightly associated with PGN act as PAMPs in addition to or instead of PGN. For example, lipopeptides and lipoteichoic acid are ligands for TLR-mediated immunity in animals (6). Lipoteichoic acid, LPS and highly abundant proteins such as flagellin or EF-Tu have also been shown to trigger immune responses in *Arabidopsis* (25, 36, 53). We therefore tested the synthetic lipopeptide analogs

Pam<sub>3</sub>Cys, Pam<sub>2</sub>Cys, and PamCys (54), LPS preparations from *P. aeruginosa* and *B. cepacea* and lipoteichoic acid from *S. aureus* in medium alkalization assays. All tested compounds induced a weak pH shift in *Arabidopsis* cell cultures but with completely different kinetics to that observed with PGN (Fig. 3, *B–D*). Moreover, the lipopeptides Pam<sub>3</sub>Cys, Pam<sub>2</sub>Cys, and PamCys did not trigger *PR-1:GUS* reporter gene expression (Fig. 3*A*). Furthermore, no protein or LPS contamination was detected in PGN preparations using SDS-PAGE followed by silver staining, and proteinase K-digested PGN still induced *PR-1:GUS* expression (data not shown). In addition, PGN preparations from the *S. aureus* sortase mutant  $\Delta\text{srtA}$  still induced *PR-1* expression (data not shown). These mutant bacteria are defective in covalently tethering surface proteins to PGN (55), indicating that *PR-1:GUS* induction was not due to contaminations of PGN preparations with PGN-associated proteins. To rule out that the PGN-induced pH shift was merely a consequence of mechanical stimulation due to the insolubility of

PGN, we also treated cells with a suspension of ground glass pasteur pipettes. This treatment, however, did not induce any medium alkalization (data not shown). Furthermore, we measured medium alkalization after treatment of cell cultures with HPLC-purified lysostaphin-, mutanolysin- or mutanolysin/lysostaphin-digested PGN. Similar to the PR-1:GUS assay (Fig. 1C), only lysostaphin-digested PGN displayed strong PAMP activity while only a marginal pH shift was induced with mutanolysin- or mutanolysin/lysostaphin-digested PGN (Fig. 3E). However, as the response to lysostaphin-digested PGN was somewhat weaker than to undigested PGN, it seems that the sugar backbone accounts for the majority, but not necessarily all, of the PAMP-activity. Altogether, these data indicate that PGN and not putative proteinaceous or other contaminants such as lipopeptides are responsible for the induction of the observed cellular responses.

Inducible PR-1:GUS expression (Fig. 1B) suggested that PGN treatment may have an impact on plant gene expression patterns. To get a comprehensive overview on PGN-induced changes in the *Arabidopsis* transcriptome we performed microarray analyses using plant material harvested 4 h after either PGN or water treatment. For comparative analysis, microarray data for the 4-h time point after Flg22 treatment were obtained from *AtGenExpress* experiments (56). For each treatment versus control condition, genes with an altered expression were assigned based on a one-way analysis of variance test combined with a Benjamini and Hochberg false discovery rate algorithm (cutoff of 0.05). Of the ~23,750 expressed genes represented on the Affymetrix ATH1 full genome array (57), expression of 236 genes (1%) was found to be induced more than 2-fold after PGN treatment (supplemental Table S2). Intriguingly, we observed a strong overlap of genes with altered expression when comparing PGN and Flg22 treatment (Table 1 and Fig. 4). Gene induction for randomly chosen genes was confirmed by RT-PCR analysis and all tested PGN-induced genes showed a similar expression profile after Flg22 treatment (Fig. 4).

A detailed analysis of PGN-induced genes (Table 1 and supplemental Table S2) revealed a considerable number of up-regulated genes that can be classified as being involved in signal perception, such as receptor-like kinases (18 genes) or disease resistance-like proteins (5 genes), and signal transduction, such as protein kinases (17 genes) and phosphatases (1 gene). Moreover, genes coding for typical defense-related proteins were responsive to both PGN and Flg22 treatment including chitinases (5 genes), protease inhibitors (5 genes), peroxidases (1 gene), phenylalanine ammonia lyase 1 (PAL1), and a HIN1-family protein. We also found numerous up-regulated genes with a putative function in protein degradation (U-box or F-box-domain-containing proteins, 5 genes) and transcriptional regulation (WRKY transcription factors, AP2 domain-containing transcription factors, 16 genes).

**PGN Induces Phytoalexin Production without Causing Cell Death**—While medium alkalization, NO production, and MAPK activation are early responses observed after various PAMP treatments, the production of the antimicrobial phytoalexin camalexin (58) occurs at later stages and was shown to be induced after infection with *P. syringae* (59) or upon treatment

with the necrotizing *phytophthora parasitica* toxin NLP<sub>pp</sub> (56) and heat-killed yeast cells (60). No significant increase in camalexin levels could be detected in *Arabidopsis* leaves after Flg22 treatment. However, both PGN and NLP<sub>pp</sub> triggered a strong production of this phytoalexin, reaching up to 155  $\mu\text{g/g}$  dry weight after 4 days of PGN treatment (Fig. 5B). In contrast to NLP<sub>pp</sub>, which triggers cell death (32, 56), infiltration of PGN and Flg22 did not result in any macroscopic tissue damage for up to 5 days (Fig. 5A and data not shown).

**PGN and Chitin Do Not Engage the Same Perception System**—Elicitor activity of PGN depends on an intact glycan backbone (Figs. 1C and 3E), which consists of alternating N-acetylglucosamine and N-acetylmuramic acid residues. This carbohydrate backbone resembles the unbranched  $\beta$ -1-4-linked N-acetylglucosamine chains of chitin. Chitin is a major component of fungal cell walls and has been shown to act as PAMP in many plant species. In *Arabidopsis*, chitin was shown to induce typical PAMP responses such as the activation of MAPK cascades (61) and alterations in protein phosphorylation (62) or gene transcription (63, 64). We compared both elicitors with respect to PR-1 expression by using both the PR-1:GUS reporter line and RT-PCR analysis, but we could not observe any chitin-induced PR-1 expression in concentrations up to 100  $\mu\text{g/ml}$  (Fig. 6, A and B). Interestingly, chitin strongly induced a transient expression of *At2g39530* and *At1g51850*, whereas inducible gene expression after PGN and Flg22 treatment was prolonged and still detectable after 24 h. Furthermore, we measured medium alkalization after PGN or chitin treatment. As shown in Fig. 6C, chitin induced a very rapid and transient pH shift similar to that observed after Flg22 addition (Fig. 2A), but clearly distinguishable from the delayed and prolonged response triggered by PGN. The difference in PGN and chitin induced defense responses suggested that both elicitors were recognized by different perception systems. To corroborate this finding, we investigated whether chitin and PGN are perceived by different perception systems using the alkalization assay. *Arabidopsis* cell cultures treated for 70 min with 100  $\mu\text{g/ml}$  PGN did not show a significant further increase in extracellular pH when treated with a second dose of 1 mg/ml PGN, indicating saturation of these cells for PGN. However, these cells still responded to subsequent treatment with 100  $\mu\text{g/ml}$  chitin, strongly suggesting that PGN and chitin are perceived via different receptors.

## DISCUSSION

PGN from both Gram-positive and Gram-negative bacteria is highly immunogenic in mammals and *Drosophila* (17). Although Gram-positive bacteria have so far not been regarded as important plant pathogens, members of the species *Streptomyces* are known for a long time to cause economically important diseases such as potato scab (65). *Streptomyces* spp. are not host specific and can also infect *Arabidopsis* (66). Similarly, Gram-positive *S. aureus* causes typical bacterial disease symptoms in *in vitro* and soil-grown *Arabidopsis* plants such as water-soaked lesions and chlorosis eventually leading to plant death both upon leaf and root inoculation (27). Here we show that *Arabidopsis* is able to respond to PGN as a PAMP from both Gram-positive and Gram-negative bacteria. Typical plant immunity-associated responses were triggered such as medium alkalization, increase in  $[\text{Ca}^{2+}]_{\text{cyt}}$ , NO production, camalexin

## Peptidoglycans in Arabidopsis Immunity

TABLE 1

### PGN or Flg22-induced genes with known or putative roles in plant innate immune responses

Average relative values from three independent experiments of PGN and Flg22-treated samples were compared to water control samples and adjusted *p* values derived from one-way analysis of variance combined with a Benjamini and Hochberg false discovery rate calculation are given. *p* values greater than the threshold of 0.05 are indicated by >0.05.

AGI number	Gene description	Name	PGN		Flg22	
			Fold change	<i>p</i> value	Fold change	<i>p</i> value
			4 h		4 h	
<b>RLKs</b>						
AT1G07390	Leucine-rich repeat family protein		2.4	0.017	2.8	0.039
AT1G09970	Leucine-rich repeat transmembrane protein kinase		2.6	0.009	3.7	0.022
AT1G51790	Leucine-rich repeat protein kinase		3.3	0.009	14	0.011
AT1G51800	Leucine-rich repeat protein kinase		6.8	0.007	60.3	0.023
AT1G51820	Leucine-rich repeat protein kinase		8.8	0.011	83.9	>0.05
AT1G51850	Leucine-rich repeat protein kinase		15.5	0.007	260	>0.05 <sup>a</sup>
AT1G51890	Leucine-rich repeat protein kinase		5.6	0.011	64.2	>0.05
AT1G53430	Leucine-rich repeat protein kinase		2.1	0.017	3.5	0.019
AT2G02220	Leucine-rich repeat protein kinase		2.3	0.011	13.6	0.012
AT2G19190	Light/senescence-responsive LRR protein kinase	FRK1	4.9	0.011	196.1	>0.05
AT3G02880	Leucine-rich repeat transmembrane protein kinase		2.5	0.017	4.3	0.011
AT4G08850	Leucine-rich repeat protein kinase		2.2	0.017	5.8	0.026
AT2G37710	Lectin protein kinase		2.1	0.027	4.5	0.016
AT5G35370	Lectin protein kinase		2.1	0.019	2.8	0.025
AT1G61360	S-locus lectin protein kinase		3.5	0.016	6.9	0.010
AT1G61380	S-locus lectin protein kinase		3.1	0.017	5.8	0.012
AT4G21390	S-locus lectin protein kinase		3.7	0.035	12.5	>0.05 <sup>a</sup>
AT3G22060	Receptor protein kinase-related		5.3	0.018	21.4	0.008
<b>Other protein kinases</b>						
AT1G18390	Protein kinase family protein		3.9	0.007	10.9	0.010
AT1G25390	Protein kinase family protein		2.2	0.011	4.7	0.012
AT1G28390	Protein kinase family protein		3.7	0.022	6.1	0.021
AT1G51620	Protein kinase family protein		4.6	0.027	34.8	0.031
AT2G01450	Mitogen-activated protein kinase (MPK17)	MPK17	2.4	0.015	3.5	0.019
AT2G28930	Protein kinase APK1b	APK1b	2	0.017	3.2	0.022
AT2G39660	Protein kinase family protein	BIK1	2.8	0.031	5.6	0.004
AT3G46280	Protein kinase related		15.9	0.007	264.4	0.024
AT4G11330	Mitogen-activated protein kinase (MPK5)	MPK5	2.4	0.045	2.5	>0.05 <sup>a</sup>
AT4G23190	Protein kinase family protein		3.4	0.009	7.3	>0.05
AT4G23210	Protein kinase family protein		3.4	0.007	9.1	0.012
AT4G23220	Protein kinase family protein		2.1	0.007	4.7	0.028
AT4G23300	Protein kinase family protein		2.9	0.010	5.6	0.026
AT5G20050	Protein kinase family protein		3.1	0.013	10.2	0.012
AT5G24430	Calcium-dependent protein kinase, CDPK		2.5	0.039	6.5	0.010
AT5G39020	Protein kinase family protein		2.1	0.019	3.9	0.023
AT5G61560	Protein kinase family protein		3	0.017	22.1	0.009
<b>Protein phosphatases</b>						
AT2G40180	Protein phosphatase 2C	PP2C5	6.3	0.019	9	>0.05
<b>Disease resistance-like genes</b>						
AT3G45290	Seven transmembrane MLO family protein 3 (MLO3)	MLO3	2.9	0.035	7.4	0.011
AT2G39200	Seven transmembrane MLO family protein 12 (MLO12)	MLO12	19	0.007	77.4	0.009
AT1G65390	Disease resistance protein (TIR class)	ATPP2-A5	8.8	0.013	51.95	0.005
AT4G09420	Disease resistance protein (TIR-NBS class)		3.5	0.018	6.5	0.037
AT5G44910	TIR domain-containing protein		6.5	0.011	38.7	>0.05
<b>Pathogenesis/defense-related genes</b>						
AT1G02360	Chitinase		2.9	0.011	18.8	0.005
AT2G43620	Chitinase		4.2	0.007	5.1	0.026
AT2G43590	Chitinase		5.1	0.033	2.9	>0.05 <sup>a</sup>
AT3G54420	Class IV chitinase (CHIV)	AtEP3	3.7	0.028	23.5	0.002
AT4G01700	Chitinase		4.3	0.010	24.8	0.019
AT2G35980	Harpin-induced protein (YLS9) / HIN1 family protein	HIN1	2.7	0.043	6.8	>0.05
AT2G37040	Phenylalanine ammonia-lyase 1 (PAL1)	PAL1	3	0.049	6.5	0.013
AT3G02840	Immediate-early fungal elicitor family protein		3.2	0.014	9.7	>0.05 <sup>a</sup>
AT5G64120	Peroxidase		7.5	0.010	25.4	0.003
AT2G38870	Protease inhibitor		3.2	0.011	6.3	0.010
AT4G12470	Protease inhibitor/seed storage/lipid transfer protein (LTP)		3.7	0.007	6.1	0.039
AT4G12480	Protease inhibitor/seed storage/lipid transfer protein (LTP)	PEARL1	3.9	0.011	9.9	0.031
AT4G12500	Protease inhibitor/seed storage/lipid transfer protein (LTP)		46.1	0.028	144.3	0.037
AT4G22470	Protease inhibitor/seed storage/lipid transfer protein (LTP)		11.5	0.011	18.9	0.023
<b>Protein degradation</b>						
AT1G66160	U-box domain-containing protein		4.4	0.007	8.7	0.013
AT2G35930	U-box domain-containing protein		7.5	0.011	63.1	0.039
AT3G52450	U-box domain-containing protein		21.2	0.010	154.8	>0.05 <sup>a</sup>
AT1G15670	Kelch repeat-containing F-box family protein		3.8	0.035	19.1	0.024
AT5G43190	F-box family protein (FBX6)	FBX6	2.2	0.033	3.6	0.035
<b>Transcription factors</b>						
AT1G62300	WRKY family transcription factor	WRKY 6	2.5	0.011	5.7	0.008
AT1G80840	WRKY family transcription factor	WRKY 40	2.2	0.018	8.2	>0.05 <sup>a</sup>
AT2G23320	WRKY family transcription factor	WRKY15	2.3	0.019	5.2	0.046

## Peptidoglycans in Arabidopsis Immunity

TABLE 1—continued

AGI number	Gene description	Name	PGN		Flg22	
			Fold change	<i>p</i> value	Fold change	<i>p</i> value
			4 h		4 h	
AT2G24570	WRKY family transcription factor	WRKY 17	2.5	0.011	20.6	0.015
AT2G38470	WRKY family transcription factor	WRKY 33	2.8	0.023	7	>0.05 <sup>a</sup>
AT4G01720	WRKY family transcription factor	WRKY 47	4.1	0.016	10.7	0.007
AT4G18170	WRKY family transcription factor	WRKY 28	3.6	0.009	7.7	0.020
AT4G23810	WRKY family transcription factor	WRKY 53	3.2	0.011	5.9	>0.05
AT4G24240	WRKY family transcription factor	WRKY 7	3.9	0.019	13.8	0.029
AT4G31550	WRKY family transcription factor	WRKY 11	2.8	0.019	6.8	0.004
AT5G49520	WRKY family transcription factor	WRKY 48	5.3	0.019	12.1	0.012
AT3G23250	Myb family transcription factor	MYB15	5.1	0.028	26.7	0.008
AT1G64380	AP2 domain-containing transcription factor, ERF-family		2.6	0.029	3.7	0.013
AT1G68840	AP2 domain-containing protein	RAV2	4.2	0.013	18	0.006
AT3G50260	AP2 domain-containing transcription factor, ERF-family	CEJ1	2.1	0.025	5.4	0.036
AT5G44210	Ethylene-responsive element-binding factor 9 (ERF9)	ERF9	3.8	0.038	6.2	0.005
AT5G61890	AP2 domain-containing transcription factor, ERF family		5	0.047	11.8	0.018
<b>Others</b>						
AT2G39530	Integral membrane protein		3.5	0.019	288.1	>0.05
AT4G15610	Integral membrane family protein		2.7	0.019	8.6	0.009

<sup>a</sup> Genes with a significant induction after 1 h of Flg22 treatment (56).

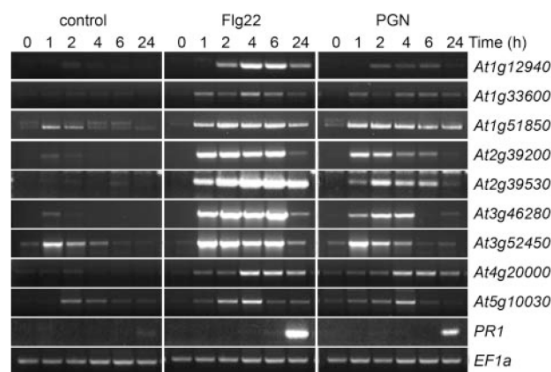


FIGURE 4. PGN activates expression of various genes. *Arabidopsis* leaves were infiltrated with 1  $\mu$ M Flg22, 100  $\mu$ g/ml PGN, or water as a control. Leaves were harvested at the indicated time points and total RNA was isolated and subjected to RT-PCR with specific primers for PGN-induced genes. Equal cDNA amounts were controlled by amplification of the constitutively expressed *EF1a* gene.

accumulation, MAPK activation and extensive reprogramming of the transcriptome (Figs. 2–5). Immune responses were triggered with PGN concentrations of about 100  $\mu$ g/ml, which is in accordance to the amounts that are necessary to stimulate immune responses in mammals and *Drosophila* (16, 67). Although responses to Flg22 were often stronger than those to PGN, the effects of both elicitors were quantitatively similar. In particular, early cellular responses such as medium alkalinization, NO production and MAPK activation were basically indistinguishable upon stimulation with PGN or Flg22 (Fig. 2). More evidence that responses to PGN and Flg22 are comparable is the large overlap of alterations in gene expression observed by microarray analysis (Fig. 4 and Table 1). Importantly, genes encoding proteins implicated in pathogen recognition, such as receptor-like kinases and resistance proteins, resistance signaling like WRKY transcription factors and plant defense execution like PR-proteins were found to be co-induced, suggesting that both signals are perceived as equivalent determinants of microbial non-self by the plant and similarly trigger activation of the plant surveillance system. Altogether, PGN, as a constitutive surface component of many bacterial cells, must be

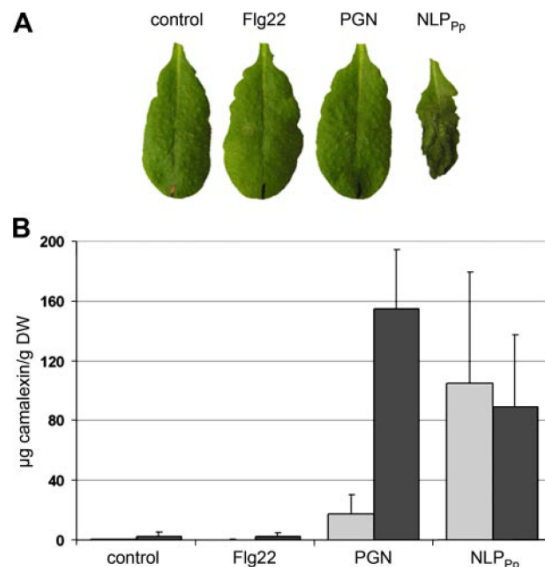
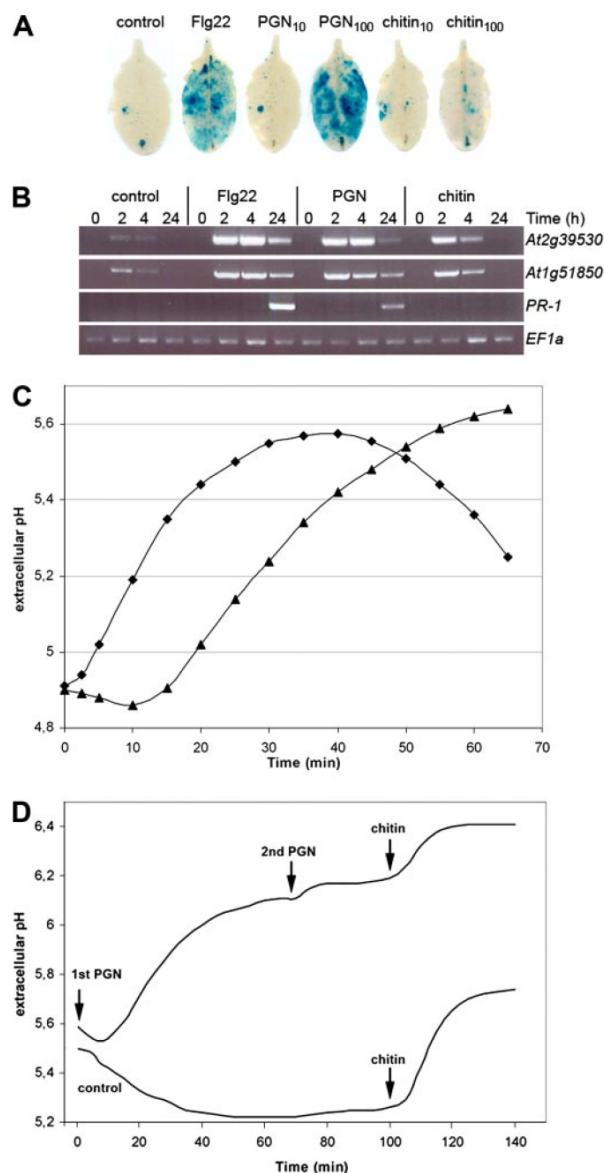


FIGURE 5. PGN induces camalexin production, but no cell death. *A*, *Arabidopsis* leaves were infiltrated with 1  $\mu$ M Flg22, 100  $\mu$ g/ml PGN, 2  $\mu$ M NLP<sub>Pp</sub>, or water as a control and pictures were taken 2 days after infiltration. *B*, camalexin accumulation in six independent leaves was determined at 2 days (gray bars) or 4 days (black bars).

added to the list of PAMPs with immunogenic activity in both plants and animals.

PGN, flagellin, and chitin act as PAMPs inducing largely overlapping response patterns. However, defense responses were not identical as has been proposed for the two proteinaceous elicitors flagellin and EF-Tu (24). PGN treatment resulted for instance in camalexin production whereas application of Flg22 did not (Fig. 5B). Additionally, the pH shift induced by chitin closely resembled that induced by Flg22 (compare Figs. 2A and 6C), but chitin treatment did not result in any *PR-1* transcription (Fig. 6, A and B). Comparison of the microarray data indicated a strong overlap of PGN- and Flg22-responsive genes; however, Flg22 induced approximately three times as many genes as PGN ((56) and supplemental Table S2). Moreover, only 133 of a total of 1168 chitin-induced genes (63)

### Peptidoglycans in *Arabidopsis* Immunity



**FIGURE 6. PGN and chitin do not engage the same perception system.** *A*, *PR-1::GUS* transgenic *Arabidopsis* leaves were infiltrated with 1  $\mu$ M Flg22, 10 or 100  $\mu$ g/ml PGN, 10 or 100  $\mu$ g/ml chitin or water as a control and stained for GUS activity after 24 h. *B*, leaves infiltrated with 1  $\mu$ M Flg22, 100  $\mu$ g/ml PGN, 100  $\mu$ g/ml chitin, or water were harvested at indicated time points and used for RT-PCR analysis with specific primers for *At2g39530*, *At1g51850*, or *PR-1*. Equal cDNA amounts were controlled by amplification of the constitutively expressed *EF1a* gene. *C*, *Arabidopsis* cell cultures were treated with 100  $\mu$ g/ml PGN (triangles) or 100  $\mu$ g/ml chitin (diamonds) and extracellular pH was measured over a time course. *D*, cell cultures were treated with 100  $\mu$ g/ml PGN (1st PGN) and after 70 min with 1 mg/ml PGN (2nd PGN) to reach saturation. Control cells were left untreated. After 100 min 100  $\mu$ g/ml chitin was added to both samples, and the pH was measured for further 40 min.

also showed enhanced transcription after PGN treatment. Likewise, NLP<sub>pp</sub>- and Flg22-induced gene expression is only identical for 50% of the induced genes (56), and NLP<sub>pp</sub> induces a strong cell death response that is not observed after application of Flg22, PGN, or chitin (Fig. 5 and data not shown). Such

differences in PAMP perception have also been described in animals. Differential responses to various TLR ligands was partially attributed to a selective usage of certain adaptor molecules linked to TLRs followed by differential activation of transcription factors (8, 68). It can be assumed that each PAMP triggers specific sets of both individual as well as generic cellular responses with putative cross-talk of the signaling pathways. Another explanation for the observed differences in PAMP-induced downstream responses could be that some late defense-related responses such as *PR-1* induction or camalexin production require a certain threshold of preceding events. Hence, strength, kinetics, and duration of the induction would be important for triggering those late cellular responses. We could for instance observe that PGN triggered a sustained pH shift, whereas the response to Flg22 was stronger and faster, but more transient (Fig. 2A) and thus possibly not lasting long enough to induce camalexin production (Fig. 5). Moreover, different PAMP perception systems might rely on different classes of receptor molecules, each possibly initiating a specific subset of downstream responses. Intriguingly, proteinaceous PAMPs such as flagellin and EF-Tu not only induce nearly identical plant responses but are also perceived by the same kind of receptors, the two LRR-RLKs FLS2 and EFR (22, 24). The identity of the corresponding PGN receptor(s) and its nature are outstanding questions and will be the focus of future research.

In animal systems, it has been shown that compounds that are associated with PGN, such as lipoteichoic acid or lipopeptides, also possess immunostimulatory activity (6). For *S. aureus* it has been shown that lipoproteins play a major role in promoting immune responses in various human cell lines, whereas lipoteichoic acid has, if at all, only a minor role (69, 70). However, we could rule out such PGN contaminations by performing a number of experimental controls: (i) Medium alkalization assays in *Arabidopsis* cell cultures indicated that although lipoteichoic acid, lipopolysaccharides, or lipopeptides induced weak pH shifts, this response showed differences in kinetics compared with PGN (Fig. 3, B–D). (ii) *PR-1::GUS* expression assays revealed LPS and lipopeptides as rather weak inducers of defense gene expression in *Arabidopsis* (Fig. 3A). (iii) Lysostaphin-digested, HPLC-purified PGN retained PAMP-activity (Fig. 3E). (iv) PGN-associated PAMP activity was not lost after heating or protease-digestion, and (v) PGN preparations of *S. aureus* sortase mutants, which lack PGN-associated proteins, were still able to induce *PR-1* gene expression (data not shown). Altogether, these data indicate that the observed responses in *Arabidopsis* must be attributed to the recognition of PGN rather than to factors associated with PGN.

Interestingly, cellular responses in *Arabidopsis* were only induced by whole PGN preparations or PGN that was digested with lysostaphin which creates long PGN glycan chains that are no longer interconnected by peptide stems. In contrast, smaller PGN constituents such as purified fragments after mutanolysin or mutanolysin/lysostaphin digestion, MDP, muramic acid or the cross-linking pentapeptide remained inactive (Figs. 1 and 3E). Our data suggest that *Arabidopsis* has evolved a perception system for the glycan part of PGN, which is highly conserved among all bacteria, rather than for the peptide crosslink, in which the amino acid composition can vary between bacterial

species. This is in contrast to mammals in which MDP as a natural partial structure of PGN was reported to be the minimal structure with immunostimulatory activity (14). However, we could not observe any PAMP activity for MDP in *Arabidopsis* when used to induce medium alkalization or *PR-1:GUS* expression (Fig. 1C and data not shown). Apparently, plants and animals have different structural requirements for PGN recognition. Interestingly, *Drosophila* is also not responsive to MDP (12) although PGN triggers strong immune responses in this insect (71). Rather, the minimal structure required to stimulate *Drosophila* innate immunity is a mucopeptide dimer, and monomers (GlcNAc-MurNAc-dipeptide) were completely inactive and even had an inhibitory effect (67). Moreover, tracheal cytotoxin (TCT), a tetrapeptide containing PGN fragment, was a strong inducer of mouse NOD1 whereas human NOD1 required a tripeptide for efficient sensing of PGN (72), again indicating that PGN detection systems are host-specific. Apparently, even though PGN is recognized in plants, insects, and mammals, the different lineages have evolved perception systems for distinct regions of this complex PAMP. This has also been demonstrated for flagellin, the protein subunit that builds up bacterial flagella: whereas the *Arabidopsis* flagellin receptor FLS2 recognizes the very conserved peptide Flg22, which is part of the so called Spike region of bacterial flagellin, a more central hypervariable peptide in the D1 region acts as PAMP in mammals (7, 73, 74). Moreover, in mammals lipid A as the invariable part of LPS is the most potent stimulator of innate immunity (75, 76), whereas *Arabidopsis* perceives LPS via both the lipid A part as well as synthetic oligosaccharides, which are commonly found in the highly variable O-antigen of LPS (36, 77).

We suggest a model in which PGN was chosen as non-self determinant both in plants and animals because of its characteristics as a typical PAMP: it is widely found in bacteria, structurally stable, displayed on the cell surface and not found in eukaryotic cells. However, our results indicate that plants respond differently to PGN than animals. Therefore, despite obvious conceptual similarities in plant and animal innate immunity, PAMP perception systems in both kingdoms are most likely the result of independent, convergent evolution (3, 7, 20).

*Acknowledgments*—We thank Alan Shapiro (Florida Gulf Coast University) for the *PR-1:GUS* line, Marc Knight (Durham University) for the *pMAQ2 aequorin* line, emc microcollections (Tübingen) for lipopeptides, Isabell Küfner and Frédéric Brunner for NLP<sub>pp</sub> protein, Markus Schmid (MPI for Developmental Biology, Tübingen) for his expertise in microarray analysis, Caterina Brancato for the maintenance of the *A. thaliana* cell culture, Stefan Engelhardt for LPS preparations from *B. cepacia*, and Ulrich Zähringer (Research Center Borstel) for helpful discussions.

## REFERENCES

- Janeway, C. A., Jr., and Medzhitov, R. (2002) *Annu. Rev. Immunol.* **20**, 197–216
- Chisholm, S. T., Coaker, G., Day, B., and Staskawicz, B. J. (2006) *Cell* **124**, 803–814
- Nürnbergger, T., Brunner, F., Kemmerling, B., and Piater, L. (2004) *Immunol. Rev.* **198**, 249–266
- Jones, J. D., and Dangl, J. L. (2006) *Nature* **444**, 323–329
- Jones, D. A., and Takemoto, D. (2004) *Curr. Opin. Immunol.* **16**, 48–62
- Akira, S., Uematsu, S., and Takeuchi, O. (2006) *Cell* **124**, 783–801
- Zipfel, C., and Felix, G. (2005) *Curr. Opin. Plant Biol.* **8**, 353–360
- Kawai, T., and Akira, S. (2006) *Cell Death Differ.* **13**, 816–825
- Glauner, B., Holtje, J. V., and Schwarz, U. (1988) *J. Biol. Chem.* **263**, 10088–10095
- Schleifer, K. H., and Kandler, O. (1972) *Bacteriol. Rev.* **36**, 407–477
- Stewart-Tull, D. E. (1980) *Annu. Rev. Microbiol.* **34**, 311–340
- Leulier, F., Parquet, C., Pili-Floury, S., Ryu, J. H., Caroff, M., Lee, W. J., Mengin-Lecreux, D., and Lemaitre, B. (2003) *Nat. Immunol.* **4**, 478–484
- McDonald, C., Inohara, N., and Nunez, G. (2005) *J. Biol. Chem.* **280**, 20177–20180
- Traub, S., von Aulock, S., Hartung, T., and Hermann, C. (2006) *J. Endotoxin Res.* **12**, 69–85
- Kufer, T. A., Banks, D. J., and Philpott, D. J. (2006) *Ann. N. Y. Acad. Sci.* **1072**, 19–27
- Dziarski, R., and Gupta, D. (2005) *Infect. Immun.* **73**, 5212–5216
- Dziarski, R., and Gupta, D. (2005) *J. Endotoxin Res.* **11**, 304–310
- Girardin, S. E., and Philpott, D. J. (2004) *Eur. J. Immunol.* **34**, 1777–1782
- Royet, J., and Dziarski, R. (2007) *Nat. Rev. Microbiol.* **5**, 264–277
- Ausubel, F. M. (2005) *Nat. Immunol.* **6**, 973–979
- Nürnbergger, T., and Kemmerling, B. (2006) *Trends Plant Sci.* **11**, 519–522
- Gomez-Gomez, L., and Boller, T. (2000) *Mol. Cell* **5**, 1003–1011
- Hayashi, F., Smith, K. D., Ozinsky, A., Hawn, T. R., Yi, E. C., Goodlett, D. R., Eng, J. K., Akira, S., Underhill, D. M., and Aderem, A. (2001) *Nature* **410**, 1099–1103
- Zipfel, C., Kunze, G., Chinchilla, D., Caniard, A., Jones, J. D., Boller, T., and Felix, G. (2006) *Cell* **125**, 749–760
- Kunze, G., Zipfel, C., Robatzek, S., Niehaus, K., Boller, T., and Felix, G. (2004) *Plant Cell* **16**, 3496–3507
- Inohara, N., and Nunez, G. (2003) *Nat. Rev. Immunol.* **3**, 371–382
- Prithiviraj, B., Bais, H. P., Jha, A. K., and Vivanco, J. M. (2005) *Plant J.* **42**, 417–432
- Westphal, O., and Jann, K. (1965) *Methods in Carbohydrate Chemistry* (Whistler, R. L., ed), Vol. 5, pp. 83–91, Academic Press, New York
- Shapiro, A. D., and Zhang, C. (2001) *Plant Physiol.* **127**, 1089–1101
- Knight, M. R., Smith, S. M., and Trewavas, A. J. (1992) *Proc. Natl. Acad. Sci. U. S. A.* **89**, 4967–4971
- Knight, M. R., Campbell, A. K., Smith, S. M., and Trewavas, A. J. (1991) *Nature* **352**, 524–526
- Fellbrich, G., Romanski, A., Varet, A., Blume, B., Brunner, F., Engelhardt, S., Felix, G., Kemmerling, B., Krzymowska, M., and Nürnbergger, T. (2002) *Plant J.* **32**, 375–390
- Fuerst, R. A., Soni, R., Murray, J. A., and Lindsey, K. (1996) *Plant Physiol.* **112**, 1023–1033
- Bera, A., Herbert, S., Jakob, A., Vollmer, W., and Götz, F. (2005) *Mol. Microbiol.* **55**, 778–787
- de Jonge, B. L., Chang, Y. S., Gage, D., and Tomasz, A. (1992) *J. Biol. Chem.* **267**, 11248–11254
- Zeidler, D., Zähringer, U., Gerber, I., Dubery, I., Hartung, T., Bors, W., Hutzler, P., and Durner, J. (2004) *Proc. Natl. Acad. Sci. U. S. A.* **101**, 15811–15816
- Glawischnig, E., Hansen, B. G., Olsen, C. E., and Halkier, B. A. (2004) *Proc. Natl. Acad. Sci. U. S. A.* **101**, 8245–8250
- Rentel, M. C., and Knight, M. R. (2004) *Plant Physiol.* **135**, 1471–1479
- Ludwig, A. A., Saitoh, H., Felix, G., Freymark, G., Miersch, O., Wastermack, C., Boller, T., Jones, J. D., and Romeis, T. (2005) *Proc. Natl. Acad. Sci. U. S. A.* **102**, 10736–10741
- Romeis, T., Ludwig, A. A., Martin, R., and Jones, J. D. (2001) *EMBO J.* **20**, 5556–5567
- Schmid, M., Davison, T. S., Henz, S. R., Pape, U. J., Demar, M., Vingron, M., Scholkopf, B., Weigel, D., and Lohmann, J. U. (2005) *Nat. Genet.* **37**, 501–506
- Berg, G., Eberl, L., and Hartmann, A. (2005) *Environ. Microbiol.* **7**, 1673–1685
- Prithiviraj, B., Weir, T., Bais, H. P., Schweizer, H. P., and Vivanco, J. M.

**Peptidoglycans in Arabidopsis Immunity**

- (2005) *Cell Microbiol.* **7**, 315–324
44. Uknes, S., Mauch-Mani, B., Moyer, M., Potter, S., Williams, S., Dincher, S., Chandler, D., Slusarenko, A., Ward, E., and Ryals, J. (1992) *Plant Cell* **4**, 645–656
45. Laird, J., Armengaud, P., Giuntini, P., Laval, V., and Milner, J. J. (2004) *Planta* **219**, 1089–1092
46. Gomez-Gomez, L., Felix, G., and Boller, T. (1999) *Plant J.* **18**, 277–284
47. Atkinson, M. M., Huang, J. S., and Knopp, J. A. (1985) *Plant Physiol.* **79**, 843–847
48. Felix, G., and Boller, T. (2003) *J. Biol. Chem.* **278**, 6201–6208
49. Pedley, K. F., and Martin, G. B. (2005) *Curr. Opin. Plant Biol.* **8**, 541–547
50. Nühse, T. S., Peck, S. C., Hirt, H., and Boller, T. (2000) *J. Biol. Chem.* **275**, 7521–7526
51. White, P. J., and Broadley, M. R. (2003) *Ann. Bot. (Lond)* **92**, 487–511
52. Hepler, P. K. (2005) *Plant Cell* **17**, 2142–2155
53. Gomez-Gomez, L., and Boller, T. (2002) *Trends Plant Sci.* **7**, 251–256
54. Reutter, F., Jung, G., Baier, W., Treyer, B., Bessler, W. G., and Wiesmüller, K. H. (2005) *J. Pept. Res.* **65**, 375–383
55. Mazmanian, S. K., Liu, G., Ton-That, H., and Schneewind, O. (1999) *Science* **285**, 760–763
56. Qutob, D., Kemmerling, B., Brunner, F., Küfner, I., Engelhardt, S., Gust, A. A., Luberacki, B., Seitz, H. U., Stahl, D., Rauhut, T., Glawischnig, E., Schween, G., Lacombe, B., Watanabe, N., Lam, E., Schlichting, R., Scheel, D., Nau, K., Dodt, G., Hubert, D., Gijzen, M., and Nürnberger, T. (2006) *Plant Cell* **18**, 3721–3744
57. Redman, J. C., Haas, B. J., Tanimoto, G., and Town, C. D. (2004) *Plant J.* **38**, 545–561
58. Glawischnig, E. (2007) *Phytochemistry* **68**, 401–406
59. Hagemeyer, J., Schneider, B., Oldham, N. J., and Hahlbrock, K. (2001) *Proc. Natl. Acad. Sci. U. S. A.* **98**, 753–758
60. Raacke, I. C., von Rad, U., Mueller, M. J., and Berger, S. (2006) *Mol. Plant Microbe Interact.* **19**, 1138–1146
61. Wan, J., Zhang, S., and Stacey, G. (2004) *Mol. Plant Pathol.* **5**, 125–135
62. Peck, S. C., Nühse, T. S., Hess, D., Iglesias, A., Meins, F., and Boller, T. (2001) *Plant Cell* **13**, 1467–1475
63. Ramonell, K., Berrocal-Lobo, M., Koh, S., Wan, J., Edwards, H., Stacey, G., and Somerville, S. (2005) *Plant Physiol.* **138**, 1027–1036
64. Ramonell, K., Zhang, B., Ewing, R. M., Chen, Y., Xu, D., Stacey, G., and Somerville, S. (2002) *Mol. Plant Pathol.* **3**, 301–311
65. Loria, R., Kers, J., and Joshi, M. (2006) *Annu. Rev. Phytopathol.* **44**, 469–487
66. Joshi, M., Rong, X., Moll, S., Kers, J., Franco, C., and Loria, R. (2007) *Mol. Plant Microbe Interact.* **20**, 599–608
67. Filipe, S. R., Tomasz, A., and Ligoxygakis, P. (2005) *EMBO Rep.* **6**, 327–333
68. Akira, S., Yamamoto, M., and Takeda, K. (2003) *Biochem. Soc. Trans.* **31**, 637–642
69. Hashimoto, M., Tawaratsumida, K., Kariya, H., Kiyohara, A., Suda, Y., Krikae, F., Kirikae, T., and Götz, F. (2006) *J. Immunol.* **177**, 3162–3169
70. Stoll, H., Dengjel, J., Nerz, C., and Götz, F. (2005) *Infect. Immun.* **73**, 2411–2423
71. Royet, J., Reichhart, J. M., and Hoffmann, J. A. (2005) *Curr. Opin. Immunol.* **17**, 11–17
72. Magalhaes, J. G., Philpott, D. J., Nahori, M. A., Jehanno, M., Fritz, J., Bourhis, L. L., Viala, J., Hugot, J. P., Giovannini, M., Bertin, J., Lepoivre, M., Mengin-Lecreux, D., Sansonetti, P. J., and Girardin, S. E. (2005) *EMBO Rep.* **6**, 1201–1207
73. Smith, K. D., Andersen-Nissen, E., Hayashi, F., Strobe, K., Bergman, M. A., Barrett, S. L., Cookson, B. T., and Aderem, A. (2003) *Nat. Immunol.* **4**, 1247–1253
74. Felix, G., Duran, J. D., Volko, S., and Boller, T. (1999) *Plant J.* **18**, 265–276
75. Galanos, C., Luderitz, O., Rietschel, E. T., Westphal, O., Brade, H., Brade, L., Freudenberg, M., Schade, U., Imoto, M., and Yoshimura, H. (1985) *Eur. J. Biochem.* **148**, 1–5
76. Raetz, C. R., and Whitfield, C. (2002) *Annu. Rev. Biochem.* **71**, 635–700
77. Bedini, E., De Castro, C., Erbs, G., Mangoni, L., Dow, J. M., Newman, M. A., Parrilli, M., and Unverzagt, C. (2005) *J. Am. Chem. Soc.* **127**, 2414–2416

Supplemental Material can be found at:  
<http://www.jbc.org/content/suppl/2007/08/30/M704886200.DC1.html>

## Supporting information

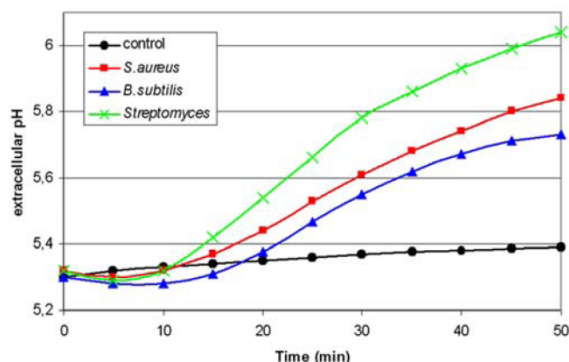


**Figure S1. PGN from various Gram-positive bacteria induces a similar pH-shift.**

Extracellular pH was measured over a time course in *Arabidopsis thaliana* Ler cell suspension cultures treated with 100 µg/ml PGN from *S. aureus* (squares), *B. subtilis* (triangles), *Streptomyces* spp. (crosses) or water as a control (circles).

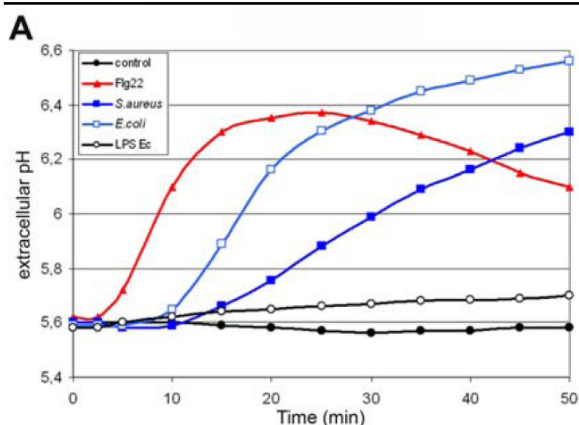


**Figure S2. PGN from the Gram-negative bacterium E. coli triggers early defense responses.**

A. Extracellular pH was monitored over a time course in 6 d old *Arabidopsis thaliana* Ler cell suspension cultures treated with 100 nM Flg22 (triangles), 100 µg/ml PGN from *S. aureus* (solid squares) or *E. coli* (open squares), 100mg/ml *E. coli* LPS (open circles) or water as a control (solid circles).

B. *PR-1:GUS* transgenic *Arabidopsis* leaves were infiltrated with 1 µM Flg22, 10 or 100 µg/ml *S. aureus* PGN, 10 or 100 µg/ml *E. coli* PGN, 10 or 100 µg/ml *E. coli* LPS or water as a control and stained for GUS activity after 24 h.

C. Leaves infiltrated with 1 µM Flg22, 100 µg/ml PGN from *S. aureus* or *E. coli*, 100 µg/ml *E. coli* LPS or water were harvested at indicated time points and used for RT-PCR analysis with specific primers for *At1g51850* or *At2g39200*. Equal cDNA amounts were controlled by amplification of the constitutively expressed *EF1a* gene.

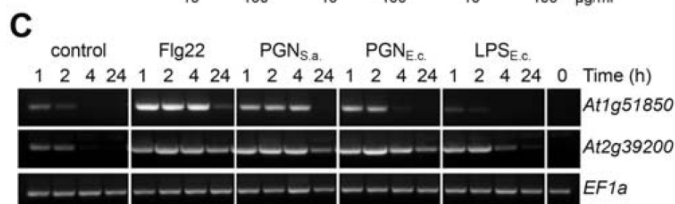
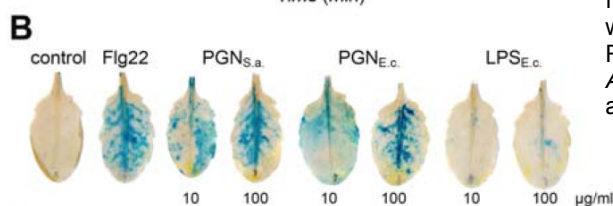


**Table S1: Primers used for RT-PCR analyses**

AGI	Primer name	Sequence 5' → 3'
At1g12940	At1g12940F	ATGGCTATTGTTTTGGAGTAG
	At1g12940R	TCAAGTTTGGGGATGAGTCG
At1g33600	At1g33600F	AATCTCAAGATCTTGTGTC
	At1g33600R	TTAGCCACGGTCATTGGTAC
At1g51850	At1g51850for	TGAATTGGGGAAGACTAGACTGA
	At1g51850R3	AAATCCACGTTACATATGGCG
At2g39200	At2g39200F	AAGGAGATGTGGTTAAAGGAG
	At2g39200R	TCACTTCTTGAACGTAACACTC
At2g39530	At2g39530F	AGTGCTCCTTCTCCT TAGGG
	At2g39530R	GAGACTGGAAGTGGTCGTTT
At3g46280	At3g46280F	ATGATGGAGGCGCTTCTTTATG
	At3g46280R	TCAATGATGCCATCTTCAAC
At3g52450	At3g52450F	TTAGAGGTTGGCTTGATGAG
	At3g52450R	TTAACCTTAAGCGGTCAAC
At4g20000	At4g20000F	ATGAACAACCTAGAGAAGAC
	At4g20000R	TTATAAATCGAGATCTCTCATC
At5g10030	At5g10030F	TTCCACCAGAGAAGGTTTGAAG
	At5g10030R	TTGGTTCACGTTGCCTAGCC
At1g14610 (PR1)	At2g14610F	ATGAATTTTACTGGCTATTTC
	At2g14610R	TTAGTATGGC TTCTCGTTC
At1g07920/30/40 (EF1a)	EF1a-s	TCACATCAACATTGTGGTCATTGG
	EF1a-as	TTGATCTGGTCAAGAGCCTACAG

#### 5.4. Supporting information to 2.6.2

##### Supplementary data (Appendix S1)

###### *Ca<sup>2+</sup> measurements*

One root or leaf disc was transferred into a well of a 96 well plate containing 100  $\mu$ l of reconstitution solution. For leaf measurements, seedlings were grown in MS media for 3 weeks and the leaf disc was incubated overnight with 10  $\mu$ M coelenterazine. Bioluminescence counts in *Arabidopsis* from roots or shoots were recorded at 5 sec intervals for 20 min, recorded as relative light units (RLU/sec) with a microplate luminometer (Luminoscan Ascent, version 2.4, Thermo Fischer Scientific, Germany). After a 1-min background reading, the CWE was added manually to the well and readings in RLU were taken for 20 min. Calibrations were performed by estimating the amount of aequorin remaining at the end of experiment by discharging all remaining aequorin in 0.1 M CaCl<sub>2</sub>, 10 % ethanol, and the counts were recorded for 10 min. The luminescence counts obtained were calibrated using the equation by Rentel *et al.* (2004) that takes into account double logarithmic relationship between concentration of free Ca<sup>2+</sup> present in the cell and the remaining aequorin discharged at any point of time. The calibration equation is:  $pCa = 0.332588(-\log k) + 5.5593$ , where  $k$  is a rate constant equal to luminescence counts per sec divided by total remaining counts. For Ca<sup>2+</sup> measurements in transgenic tobacco (*N. tabacum* L. cv. BY-2) cell lines expressing the Ca<sup>2+</sup> sensing protein apoaequorin either in the cytosol or in the nucleus were used and readings were taken at 1 sec interval for 12 min (Mithöfer and Mazars, 2002).

###### *Comparison of the P. indica CWE activity with known elicitors*

Laminarin, a linear  $\beta$ -1.3-glucan from the brown algae *Laminaria digitata*, stimulates a [Ca<sup>2+</sup>]<sub>cyt</sub> increase and induces defense responses in cell suspension cultures of tobacco (Lecourieux *et al.*, 2002) and grapevine (Aziz *et al.*, 2003). Laminarin (1 mg/ml) induces a [Ca<sup>2+</sup>]<sub>cyt</sub> elevation in the leaves of *Arabidopsis*, but no response was observed in the roots (Supplemental Fig. S5a). Lipopolysaccharides (LPS), a microbe associated molecular pattern (MAMP) found in bacteria, induce a [Ca<sup>2+</sup>]<sub>cyt</sub> elevation in the leaves and a much lower response in the roots. The [Ca<sup>2+</sup>]<sub>cyt</sub> in leaves reached a maximum at 1 min after application of LPS (1 mg/ml), but it induces a second sustained [Ca<sup>2+</sup>]<sub>cyt</sub> increase giving a biphasic peak unlike *P. indica* CWE. The response in the roots showed only a weak parabolic increase and thus differs substantially from the signature obtained with the CWE (Supplemental Fig. S5b). Pathogen-derived chitin elicitors (chitotetraose, CH4 and chitopentaose, CH5) produced no Ca<sup>2+</sup> elevation in the roots (data not shown). Thus, *P. indica* CWE is the only elicitor tested that gave a clear response in the roots.

## Supplementary figures

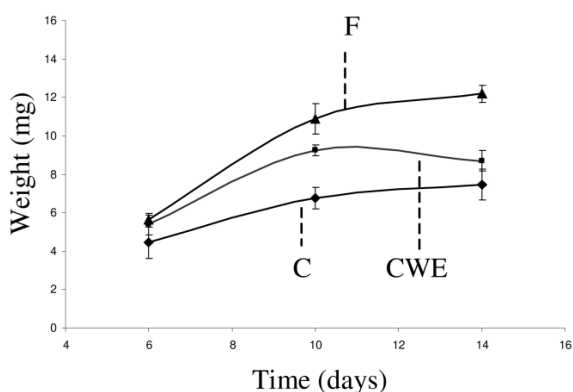


**Figure S1.** The effect of the cell wall extract (CWE) on Arabidopsis growth.

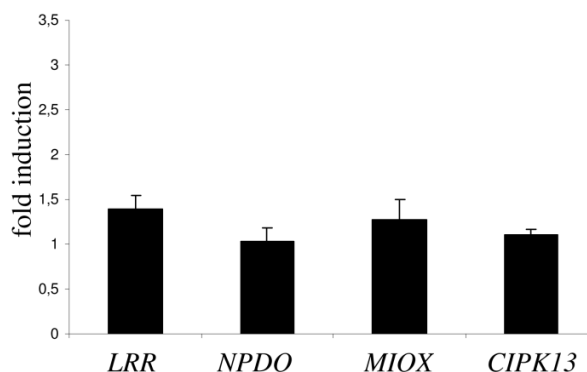


**Figure S2.** Genes which are up-regulated in the wild-type roots after the application of the cell wall extract (CWE) are not up-regulated in the *Piriformospora indica*-insensitive mutant *pij-3*.

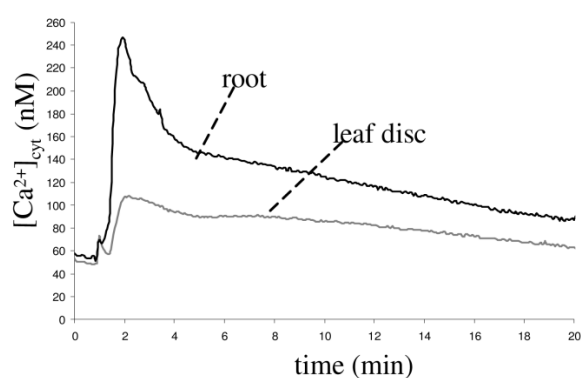


**Figure S3.** *Piriformospora indica* cell wall extract (CWE) induces changes in cytosolic  $\text{Ca}^{2+}$  ( $[\text{Ca}^{2+}]_{\text{cyt}}$ ) in apoaecorin-transformed Arabidopsis seedlings.

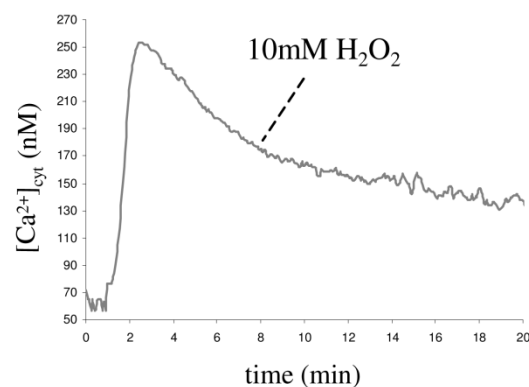


**Figure S4.** Changes in cytosolic  $\text{Ca}^{2+}$  ( $[\text{Ca}^{2+}]_{\text{cyt}}$ ) in Arabidopsis roots on treatment with 10 mM  $\text{H}_2\text{O}_2$ .

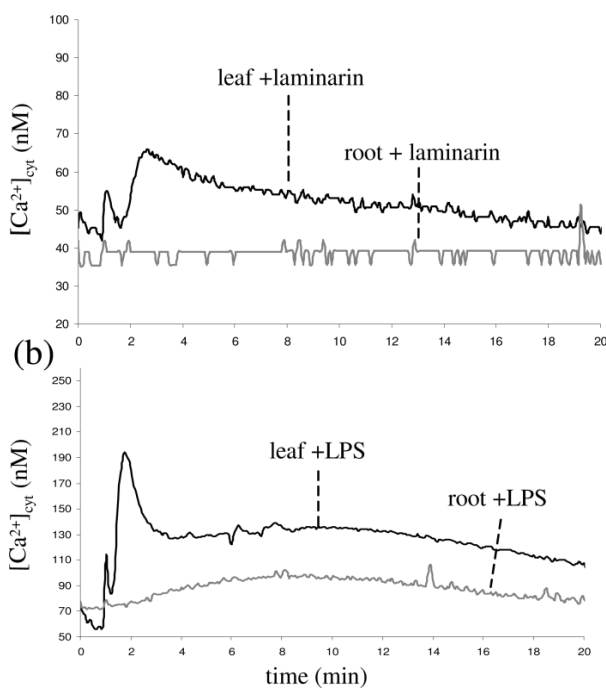


**Figure S5.** Tissue specific ' $\text{Ca}^{2+}$  signatures' of various biotic elicitors in Arabidopsis.

## **EIDESSTATTLICHE ERKLÄRUNG**

Hiermit erkläre ich, dass ich die vorliegende wissenschaftliche Arbeit selbstständig und ohne fremde Hilfe angefertigt habe. Ich erkläre weiterhin, dass ich keine anderen als die von mir angegebenen Quellen und Hilfsmittel benutzt habe und die den Werken wörtlich oder inhaltlich entnommenen Stellen als solche kenntlich gemacht habe.

Mit dieser Arbeit bewerbe ich mich erstmals um die Erlangung des Doktorgrades. Diese Arbeit wurde an keiner anderen Fakultät oder Universität zur Begutachtung eingereicht.

Halle (Saale), den 27.04.2011

Stefanie Ranf

# LEBENS LAUF

## PERSÖNLICHE DATEN

---

Name: Stefanie Ranf  
Anschrift: Hegelstraße 75b  
06114 Halle (Saale)  
Geburtsdatum: 29. November 1978  
Geburtsort: Augsburg  
Geschlecht: weiblich  
Staatsangehörigkeit: deutsch

## AUSBILDUNG

---

1989 bis 1998 Wernher-von-Braun-Gymnasium Friedberg; Abitur  
1998 bis 2002 Studium der Biochemie an der Fakultät Biologie und Vorklinische Medizin der Universität Regensburg, gefördert durch die Studienstiftung des deutschen Volkes (seit SS 2001)  
Mai 2002 bis Februar 2003 Diplomarbeit an der Fakultät Biologie und Vorklinische Medizin der Universität Regensburg in der Gruppe von Herrn PD Dr. Armin Hallmann  
Thema:  
„Charakterisierung eines chitinase-homologen Proteins aus der Grünalge *Chlamydomonas reinhardtii*“  
Abschluss: Diplom-Biochemikerin  
Oktober 2003 bis Dezember 2004 Forschungsaufenthalt bei Prof. Dr. Johannes Stratmann an der Universität von South Carolina, Auslandsstipendium der Studienstiftung des deutschen Volkes  
Seit Januar 2005 Promotionsarbeit am Institut für Pflanzenbiochemie in der Arbeitsgruppe Stress- und Entwicklungsbiologie unter Leitung von Herrn Professor Dr. Dierk Scheel und Dr. Justin Lee  
Fachgebiet: Biologie/Biochemie  
Thema:  
“The role of calcium signalling in innate immunity in *Arabidopsis thaliana*”

Halle (Saale), den 27.04.2011

**Gust AA, Biswas R, Lenz HD, Rauhut T, Ranf S, Kemmerling B, Gotz F, Glawischnig E, Lee J, Felix G, Nürnberger T** (2007) Bacteria-derived peptidoglycans constitute pathogen-associated molecular patterns triggering innate immunity in Arabidopsis.

*J Biol Chem* **282**: 32338-32348

**Kandoth PK, Ranf S, Pancholi SS, Jayanty S, Walla MD, Miller W, Howe GA, Lincoln DE, Stratmann JW** (2007) Tomato MAPKs LeMPK1, LeMPK2, and LeMPK3 function in the systemin-mediated defense response against herbivorous insects.

*Proc Natl Acad Sci U S A* **104**: 12205-12210

**Niller HH, Salamon D, Uhlig J, Ranf S, Granz M, Schwarzmann F, Wolf H, Minarovits J** (2002) Nucleoprotein structure of immediate-early promoters Zp and Rp and of oriLyt of latent Epstein-Barr virus genomes.

*J Virol* **76**: 4113-4118

**Ranf S, Wünnenberg P, Lee J, Becker D, Dunkel M, Hedrich R, Scheel D, Dietrich P** (2008) Loss of the vacuolar cation channel, AtTPC1, does not impair Ca<sup>2+</sup> signals induced by abiotic and biotic stresses.

*Plant J* **53**: 287-299

**Vadassery J, Ranf S, Drzewiecki C, Mithöfer A, Mazars C, Scheel D, Lee J, Oelmüller R** (2009) A cell wall extract from the endophytic fungus *Piriformospora indica* promotes growth of Arabidopsis seedlings and induces intracellular calcium elevation in roots.

*Plant J* **59**: 193-206